

ADMIXTURES TO REDUCE CHLORIDE INGRESS INTO CONCRETE

by

Muthena Abdul Hussain Ibrahim Al Isa, MSc, DIC, BSc

February, 1995

**A Thesis submitted for the degree of Doctor of Philosophy
of the University of London.**

**Department of Civil Engineering
Imperial College
London, S.W. 7**

Title of Thesis : ADMIXTURES TO REDUCE CHLORIDE INGRESS INTO CONCRETE

Author : Muthena Abdul Hussain Ibrahim Al Isa

Abstract

Despite extensive research carried out worldwide to develop methods for protecting new concrete construction against chloride-induced corrosion of the reinforcing steel, the options available to the designer in chloride-rich environments remain very limited. This research deals with an important, but under assessed, approach which involves the use of admixtures to modify conventional concrete such that it becomes more resistant to chloride penetration, so that the onset of corrosion is sufficiently delayed.

A wide range of basic materials (suggested in the literature, or by the author) and several proprietary products were investigated. These fall into the following categories: cement replacement materials, fine particulate materials, water repellents, polymer latices, amino alcohol derivatives, proprietary waterproofers, and miscellaneous materials. The experimental programme was conducted in three phases. The first phase was conducted to identify, from all the potential materials available, those to investigate in detail in Phase 2. Tests were designed to be fast and yet provide information on how well the materials tested can reduce chloride penetration, oxygen permeability, capillary rise, resistivity, and compressive strength testing was undertaken. In Phase 2, transport tests were devised to study the influence of the materials studied on each of the three principal chloride transport processes (characterized by chloride diffusivity, water absorption, and water permeability) separately. These tests included water and oxygen permeability, capillary rise, drying, and accelerated and natural chloride ion diffusion. Other tests included resistivity, carbonation, compressive strength, corrosion testing, and conduction calorimetry. In addition, the Scanning Electron Microscope was used to study the microstructure of the various concretes.

Using cement replacement materials at normal replacement levels was found to be the most effective means of increasing the chloride ion diffusion resistance of OPC concrete. This is due to physical, chemical and electrochemical effects. Addition of 3% or less (by weight of cement) of a material capable of increasing the angle of contact of surfaces with water to more than 90° (water repellent) was found to be the most effective means of reducing water absorption. Most materials investigated increased water permeability. Low water permeability was achieved by

the use of bentonite, cellulose acetate, or silica fume. Results suggested that certain polymer latices (at around 10% polymer solids by weight of cement) are very effective in reducing chloride penetration if the modified concrete is normally cured, dried sufficiently, then immersed in fresh water before exposure; this is due primarily to drying promoting polymer film formation. Two proprietary waterproofers were found effective in reducing absorption, but were bettered in this respect by several water repellents, although they did not increase permeability.

In Phase 3, combinations of the materials tested in Phase 2 were investigated, to produce practical admixtures with the ability to reduce chloride transport in the most commonly encountered chloride-rich exposure environments. In most of these environments, chlorides penetrate the concrete by absorption (during drying and wetting cycles) and then ion diffusion assists in transporting the ions to the depth of the reinforcing steel. Since it was not possible to better the chloride ion diffusion resistance of concretes containing normal replacement levels of GGBS, PFA, or silica fume, by using OPC and an admixture, this phase concentrated on using effective water repellents to improve absorption resistance in cement replaced concrete. The water repellents were found to be compatible with cement replaced concrete in that they improved absorption resistance substantially and did not reduce resistance to chloride ion diffusion. Microstructural examination (SEM) revealed that water repellents render the cement paste less homogeneous, by promoting the formation of areas of relatively high and low porosity.

Based on the available literature and the findings of the experimental work, preliminary specifications are proposed for more durable concrete for construction in the most commonly encountered chloride-rich exposure environments.

*To my Mother and Father,
brothers Zayd, Akeel and Ibrahim, and my sister Nada*

Acknowledgements

This work was undertaken in the Concrete Section, Department of Civil Engineering, Imperial College, and the Materials Department, Imperial College. I am very grateful to my supervisors Dr. N.R. Buenfeld and Dr. K.L. Scrivener for their continued support and guidance.

I am particularly indebted to the following for their financial support:

- The University of London from whom I received the University of London Studentship Award;
- The Arab-British Chamber Charitable Trust from whom I received the Arab-British Chamber Award; and
- The Committee of Vice Principals and Chancellors for the Overseas Research Studentship Award.

I also wish to record my appreciation for the technical staff of the concrete laboratory, and in particular Mr. Roy Baxter, for the assistance I received throughout the experimentation.

Contents

Title Page	1
Abstract	2
Dedication	3
Acknowledgments	4
Contents	5
<u>Chapter 1 Introduction</u>	12
1.1 Background	12
1.2 Objectives	14
1.3 Structure of thesis	15
<u>Chapter 2 Corrosion Chlorides and Carbonation</u>	16
2.1 Background	16
2.1.1 Introduction	16
2.1.2 Electrochemical processes at the reinforcement:concrete interface	16
2.1.2.1 Passivation and depassivation of reinforcement in concrete	16
2.1.2.1.1 The passive state of steel in concrete	16
2.1.2.1.2 Depassivation	17
2.1.2.2 Corrosion propagation	20
2.1.2.2.1 Introduction	20
2.1.2.2.2 Factors influencing corrosion rate	21
2.2 Resistivity of concrete	23
2.2.1 Background	23
2.2.2 Factors influencing the resistivity of concrete	24
2.2.3 Field corrosion rate measurements and resistivity	27
2.3 Chlorides and chloride-induced corrosion	28
2.3.1 Chlorides in concrete	28

2.3.1.1	Introduction	28
2.3.1.2	Sources of chlorides in concrete	28
2.3.1.3	States of chlorides in concrete	29
2.3.2	Chloride-induced corrosion	34
2.3.2.1	Introduction	34
2.3.2.2	Pitting corrosion	34
2.3.2.3	Chloride corrosion threshold	36
2.4	Carbonation and carbonation-induced corrosion	39
2.4.1	Carbonation	39
2.4.1.1	Background	39
2.4.1.2	Factors influencing carbonation in concrete	39
2.4.2	Carbonation-induced corrosion	43
2.5	Cracks and corrosion	46
<u>Chapter 3 Chloride Transport Processes</u>		49
3.1	Introduction	49
3.1.1	General	49
3.1.2	Pore structure of concrete	50
3.1.2.1	Background	50
3.1.2.2	Pore structure influencing factors	50
3.1.3	Transport in concrete	60
3.1.3.1	Definitions	60
3.1.3.2	Principal transport processes in concrete	60
3.1.3.3	Effect of moisture content on transport in concrete	61
3.1.3.3.1	General	61
3.1.3.3.2	Physical nature of pore water in concrete	61
3.1.3.3.3	Factors influencing the moisture state of concrete	63
3.1.3.4	Mechanisms of transport of chlorides in concrete	68
3.2	Chloride ingress through drying and wetting of concrete	69
3.2.1	Introduction	69
3.2.2	Drying of concrete	69

3.2.3	Wetting of concrete	75
3.2.3.1	Background	75
3.2.3.2	Definition of the sorptivity of concrete	77
3.2.3.3	Factors influencing the sorptivity of concrete	79
3.3	Chloride ingress through wick action	81
3.4	Chloride ingress through osmotic effects	83
3.5	Chloride ingress through pressure-induced water flow	87
3.5.1	Background	87
3.5.2	Water permeability of concrete	89
3.5.3	Gas permeability of concrete	93
3.6	Chloride ingress by diffusion	97
3.6.1	Introduction	97
3.6.2	Factors involved in chloride ion diffusion in concrete	97
<u>Chapter 4 Protection Against Chloride-Induced Corrosion in New Construction</u>		107
4.1	Introduction	107
4.1.1	General	107
4.1.2	Accelerated corrosion testing	108
4.2	Methods of increasing corrosion resistance of reinforcement	109
4.2.1	Corrosion inhibitors	109
4.2.2	Corrosion resistant and corrosion protected reinforcement	111
4.2.2.1	Corrosion resistant reinforcement	111
4.2.2.2	Corrosion protected reinforcement	112
4.3	Methods of reducing chloride ingress into concrete	115
4.3.1	General	115
4.3.2	Polymer impregnation	116
4.3.3	Surface treatments	117
4.3.4	Material design and admixtures	119

<u>Chapter 5 Phase 1: Preliminary Testing</u>	120
5.1 Materials	120
5.2 Experimental details	128
5.2.1 Concrete mixes	128
5.2.1.1 General	128
5.2.1.2 Control concrete design	128
5.2.1.3 Design of admixture-modified concretes	130
5.2.1.3.1 General	130
5.2.1.3.2 Cement replacement materials	131
5.2.1.3.3 Fine particulate materials	132
5.2.1.3.4 Water repellents	134
5.2.1.3.5 Polymer latices	137
5.2.1.3.6 Amino alcohol derivatives	138
5.2.1.3.7 Proprietary waterproofers	139
5.2.1.3.8 Miscellaneous	140
5.2.2 Programme of work	144
5.2.2.1 General	144
5.2.2.2 Testing	146
5.2.2.2.1 General	146
5.2.2.2.2 Transport tests	147
5.2.2.2.3 Testing programme	152
5.3 Results and selection of materials for Phase 2	154
5.3.1 General	154
5.3.2 Quality of the control concrete	155
5.3.2.1 Results	155
5.3.2.2 Discussion	157
5.3.3 Modified concrete results	159
5.3.4 Selection of materials for Phase 2	173

<u>Chapter 6 Phase 2: Detailed Investigation</u>	193
6.1 Experimental details	193
6.1.1 Design of concrete mixes	193
6.1.1.1 Control concretes	193
6.1.1.2 Admixture-modified concretes	195
6.1.1.2.1 General	195
6.1.1.2.2 Cement replacement materials	196
6.1.1.2.3 Fine particulate materials	199
6.1.1.2.4 Water repellents	201
6.1.1.2.5 Polymer latices	205
6.1.1.2.6 Amino alcohol derivatives	207
6.1.1.2.7 Proprietary waterproofers	208
6.1.1.2.8 Miscellaneous	210
6.1.1.3 Low paste-volume concretes	211
6.1.2 Programme of work	213
6.1.2.1 Testing	213
6.1.2.1.1 Transport tests	213
6.1.2.1.2 Corrosion-related testing	221
6.1.2.1.3 Compressive strength and related testing	227
6.1.2.1.4 Microstructural examination	229
6.1.2.2 Testing programme	230
6.2 Results	223
6.2.1 General	233
6.2.2 Transport testing	233
6.2.3 Corrosion-related testing	245
6.2.4 Compressive strength and related testing	250
6.2.5 Microstructural examination	253
6.3 Evaluation of experimental results	270
6.3.1 Scope	270
6.3.2 Properties relevant to transport	272
6.3.3 Properties relevant to reinforcement corrosion	310

6.3.4	Compressive strength and early-age hydration rate	317
6.3.5	Microstructure	324
6.3.5.1	General	324
6.3.5.2	Control concretes	326
6.3.5.3	Modified concretes	326
6.4	General discussion	330
<u>Chapter 7 Phase 3: Performance Optimization</u>		348
7.1	Materials and design of concrete mixes	348
7.2	Tests and testing programme	351
7.3	Results	356
7.4	Discussion	381
7.4.1	Acrylic-modified mix	381
7.4.2	Water repellent-modified mixes	385
7.4.2.1	General	385
7.4.2.2	Silica fume concretes	386
7.4.2.3	PFA concretes	391
7.4.2.4	Slag concretes	396
7.5	Summary	401
<u>Chapter 8 Concrete Specification in Chloride-Rich Environments</u>		403
8.1	Introduction	403
8.2	World climate	407
8.3	Specification recommendations	410
8.3.1	General	410
8.3.2	Structures in the marine environment	411
8.3.2.1	Classification of exposure conditions	411
8.3.2.2	Relevant deterioration mechanisms	413
8.3.2.3	Regional climate and deterioration rate of marine structures	416
8.3.2.4	Recommendations	419
8.3.2.4.1	Structures situated in seawater	419

8.3.2.4.2 Coastal structures	421
8.3.3 Structures in chloride-contaminated soils	424
8.3.3.1 Foundations of coastal structures	424
8.3.3.1.1 Background	424
8.3.3.1.2 Recommendations	426
8.3.3.2 Undersea tunnels	429
8.3.4 Structures affected by deicing salts	432
8.4 Summary	436
<u>Chapter 9 Conclusions</u>	440
<u>Chapter 10 Recommendations For Further Research</u>	443
<u>References</u>	445
<u>Appendices</u>	480
Appendix 1 <u>Materials</u>	481
A1.1 General	481
A1.2 Cement replacement materials	484
A1.3 Fine particulate materials	489
A1.4 Water repellents	499
A1.5 Polymer latices	512
A1.6 Amino alcohol derivatives	514
A1.7 Miscellaneous	517
Appendix 2 <u>Details of Concrete Mixes</u>	524
A2.1 Phase 1 mixes	524
A2.1.1 Control mix	524
A2.1.2 Modified mixes	525
A2.2 Phase 2 mixes	531
A2.2.1 Control mixes	531
A2.2.2 Modified mixes	533

A2.3	Phase 3 mixes	537
A2.3.1	Control mix	537
A2.3.2	Modified mixes	538
Appendix 3	<u>Calculations</u>	540
A3.1	Calculation of resistivity	540
A3.2	Calculation of intrinsic (oxygen-based) permeability coefficient	541
Appendix 4	<u>Ordinary Portland cement hydration, development of microstructure, and effect of organics</u>	543
A4.1	OPC hydration and development of microstructure	543
A4.2	Effect of organics on OPC hydration	552

Chapter 1: Introduction

1.1 Background

Concrete is the most widely used construction material, and excellent performance spanning a number of decades has already been achieved by many reinforced and prestressed concrete structures. However, over the last two decades, there has been an increasing number of reports on worldwide deterioration and early failure of reinforced concrete structures caused, in the majority of cases, by reinforcement corrosion (see 8.1).

Steel embedded in concrete is normally in a passive state due to the high alkalinity of the surrounding cement paste, but neutralisation by atmospheric carbon dioxide (carbonation), or depassivation by chloride ions, may initiate corrosion. Once initiated, reinforcement soon causes cracking and then spalling of the concrete cover, which further accelerates deterioration. The specification of an appropriate depth of reasonable quality cover with good workmanship is generally sufficient to ensure that the possibility of carbonation-induced corrosion is eliminated, but chloride-induced corrosion is still a problem. Until approximately fifteen years ago it was common practice to add calcium chloride to accelerate strength development. Furthermore, and particularly the Middle East, chloride-bearing aggregate, unwashed sea-dredged sands and even seawater (as mixing water in the concrete) were used in reinforced concrete. BS8110 (Part 1; 1985) and other design Codes now recommend that chloride-based admixtures should never be added in concrete containing embedded metal and place strict limits on the total percentage of chloride adventitiously introduced as a contaminant of the aggregate or the mixing water. However, chloride may still penetrate from the exterior, particularly in a marine environment, chloride contaminated soils and groundwater, or where deicing salts are used or carried (e.g. roads, runways, bridges, car parks, etc.). Indeed, it is now clear that in such chloride-rich environments conventional concretes may be penetrated to the depth of the reinforcement within a fraction of the design life of the structure.

The serious economic and social implications associated with the rehabilitation of damaged structures has prompted extensive research aimed at developing methods for protecting new construction in chloride-rich environments. However, the options available to the designer in such environments remain very limited, because almost all of the methods devised to date suffer various shortcomings. Indeed, the development of more effective techniques is still a pressing need for the construction industry.

One important but under-assessed approach is the use of admixtures to modify conventional concrete such that it becomes more resistant to chloride penetration, so that the onset of corrosion is sufficiently delayed.

1.2 Objectives

The main purpose of the research reported in this thesis was to identify, assess and explain the effect of admixtures that increase the resistance of concrete to chloride ion penetration, in order to develop more durable concrete for construction in chloride-rich environments. This was broken down into 5 subsidiary objectives:

- (i) to identify basic and proprietary materials thought to reduce chloride ion penetration;
- (ii) to assess the effect of these materials on each of the transport processes responsible for chloride ion penetration into concrete;
- (iii) to explain the influences of the most promising of these materials in terms of their effect on cement paste microstructure;
- (iv) to predict and assess combinations of materials expected to give maximum resistance to the various molecular transport processes; and
- (v) to propose specifications for more durable concretes for particular chloride-rich environments.

1.3 Structure of thesis

The thesis is presented in 10 chapters as outlined below:

- Chapter 2 reviews the current state of knowledge relevant to reinforcement corrosion in concrete.
- Chapter 3 reviews the fundamentals of molecular and ion transport in concrete, placing emphasis on chloride transport processes.
- Chapter 4 presents a critical review of the methods currently available for protecting new construction in chloride-rich environments.
- Chapter 5 provides details of the preliminary phase (Phase 1) of the experimental programme, and deals with objective (i) (outlined in 1.2).
- Chapter 6 describes the detailed investigation phase (Phase 2) of the experimental programme, and deals, primarily, with objectives (ii) and (iii).
- Chapter 7 provides details of the optimization phase (Phase 3) of the experimental programme and deals with objective (iv).
- Chapter 8 deals with objective (v).
- Conclusions are drawn in Chapter 9 and suggestions for future work are made in Chapter 10.

Chapter 2 Corrosion Chlorides and Carbonation

2.1 Background

2.1.1 Introduction

Corrosion of reinforcing steel in concrete structures is a widespread problem, with affected structures frequently showing signs of severe deterioration after only a few years of service. Repair of these structures is very expensive and the costs incurred have imposed a large financial burden on the economics of many countries worldwide (Litvan & Bickley 1987, Al-Rabiah et al. 1988, OECD Scientific Experts Group 1989, Wallbank 1989, Browne 1991, Sedgwick 1991).

Clearly, a pre-condition to guarantee the durability of new structures as well as to guarantee durability of existing structures after repair is the knowledge of the relevant deterioration mechanisms and the rate-determining influencing factors. Hence, extensive research has been carried out and many of the relevant phenomena with respect to reinforcement corrosion are, at present, known and generally accepted. This chapter embodies those points of general agreement and highlights those which require further clarification.

2.1.2 Electrochemical processes at the reinforcement/concrete interface

2.1.2.1 Passivation and depassivation of reinforcement in concrete

2.1.2.1.1 The passive state of steel in concrete

It is now generally accepted that steel embedded in dense uncontaminated concrete is protected by the passivity (chemical stabilisation) induced by the highly alkaline nature of the surrounding concrete and that this passivity persists not in spite of the oxygen and water present, but as a result of water and oxygen. Furthermore, it is because of these inherent protective attributes, corrosion of steel does not occur in the majority of concrete elements or structures.

As a result of many investigations, using scanning electron microscopy, the reinforcement/concrete interface is now generally believed (Leek & Poole 1990) to be composed of an aggregate free zone and an oxide film.

The aggregate free zone is of variable thickness and is composed of a discontinuous layer of portlandite (Ca(OH)_2) with inclusions of Calcium-Silicate-Hydrate (CSH) gel. It also contains, within its pores, an aqueous solution of sodium, potassium, and calcium hydroxides with a pH typically of the order of 13.5. This zone of high alkalinity results in the formation of the oxide film (the second component) on the surface of the reinforcing steel. Additionally, the Ca(OH)_2 and CSH are believed to form a buffering pair to the pore solution keeping its pH value, more or less, above 12 (Sagoe-Crentsil & Glasser 1990).

The oxide film is a tightly adhering film (a spinel iron oxide layer with composition in the Fe_3O_4 : γ - Fe_2O_3 range (Sagoe-Crentsil & Glasser 1990)) about 10^{-3} - 10^{-1} μm thick (Bazant 1979).

2.1.2.1.2 Depassivation

Before corrosion can begin, both the protective barriers mentioned earlier (2.1.2.1.1) must be overcome. The portlandite layer is often incomplete and only provides imperfect protection. Thus, the passive film is the primary protective mechanism (Leek & Poole 1990), and the process by which this film is destroyed, either locally (leading to pitting corrosion) or generally (leading to general corrosion), is termed depassivation.

In practice, depassivation results from either loss of alkalinity through the full depth of cover, or the presence of aggressive salts (generally chlorides) at the reinforcement/concrete interface.

Depassivation by loss of alkalinity

Passivity will be destroyed when the environment in which the steel is embedded is no longer able to stabilise the passive film due to a reduction in its alkalinity (a pH value of 11.5 has been suggested to be the minimum required to maintain the stability of the passive film (Page 1988)).

A reduction in alkalinity at the reinforcement/concrete interface can occur in one of three ways: i) neutralization of concrete to the level of reinforcement caused by penetration of acidic materials, the most important of which is carbon dioxide (carbonation), ii) chemical reactions within the cement paste matrix (mainly by use of cement replacement materials or other admixtures), and iii) water leaching of the alkalies in the cement paste.

Electrochemical role of chlorides in depassivation

It is now universally accepted that, even in the highly alkaline environment surrounding the reinforcing steel, chloride ions possess the capacity to negate the inhibitive action of the oxide film (depassivation) and, in addition, act as a catalyst for metallic dissolution; a clear distinction between the two roles is difficult to establish. This section will, however, concentrate on the depassivation aspect. Among the theories which attempt to explain depassivation are (ACI Committee 222 1985): i) the oxide film theory, ii) the adsorption theory, iii) the transitory complex theory.

i) The oxide film theory

This theory postulates that chloride ions penetrate the oxide film on steel, through pores or defects in the film, easier than do other ions, or alternatively, that chloride ions may colloiddally disperse the oxide film thereby making it easier to penetrate.

(ii) The adsorption theory

The adsorption theory proposes that chloride ions are adsorbed preferentially on the metal surface in competition with dissolved O₂ or hydroxyl ions (both of which contribute to passivation). Furthermore, the chlorides are believed not to remain adsorbed, but form soluble species, thus facilitating anodic dissolution.

iii) The transitory complex theory

According to this theory, chloride ions compete with hydroxyl ions for the ferrous ions produced by anodic dissolution, forming a soluble complex of iron chloride which diffuses away from the anode, to break down releasing chlorides which, in turn, become available to transport more ferrous ions. Additionally, it is asserted (Hime & Erlin 1987) that the complexation of the ferrous ion, in accordance with LeChatelier's law and the anodic reaction equation, results in more metallic iron oxidizing at the anode.

It therefore seems, from the above considerations, that the precise mechanism by which chlorides destroy passivity is still a subject for debate. Indeed, Leek and Poole (1990) suggest that their observations of disbondment of chemically unaltered film support the view that a physical process may also be in operation during depassivation, and that this process contributes to expand the size of the depassivated areas.

2.1.2.2 Corrosion propagation

2.1.2.2.1 Introduction

It is generally recognised that corrosion of reinforcement embedded in concrete is primarily[#] caused by naturally occurring galvanic cells in which separate anodic and cathodic processes occur simultaneously at equal rates. The driving force (emf) for this electrochemical action is created by differences in potential (between active and less active (passive) sites) on the surfaces of the reinforcement resulting from any or a combination of the following:

- i) the use of dissimilar steels as reinforcement;
- ii) inherent inhomogenities of the steel surfaces brought about during manufacture, forming or surface preparation, or possibly during rusting prior to incorporation in the concrete;
- iii) differences in the environment at the steel/cement paste interface possibly as a consequence of differences in exposure conditions, in the penetrability of the cover concrete, and in the actual depth of cover to the reinforcement, which may manifest in:
 - a) differences in oxygen concentration;
 - b) inhomogeneity in the solution present in the pores of the cement paste, due to leaching, evaporation, carbonation or the ingress of salts;
 - c) inhomogeneities of the hydration products possibly aggravated by carbonation, drying, or chemical reaction with salts;
 - d) temperature gradients.

[#] Corrosion of steel in concrete due to stress corrosion, hydrogen embrittlement, or electrolysis due to stray electrical currents have been reported as possible cause of distress much less frequently.

2.1.2.2.2 Factors influencing corrosion rate

Corrosion rate is known to be related to the density of the current flowing in the corrosion cell, which is influenced by:

- i) The value of the driving force (emf) for the corrosion process (2.1.2.2.1): clearly a higher difference between the reversible potentials of the relevant anodic and cathodic processes may lead to a higher corrosion rate (2.3.2.2);
- ii) Anode/cathode area ratio: as the cathode/anode area ratio increases, the density of current at the anode increases, hence the corrosion rate (Fraczek 1987);
- iii) Polarization: three forms of polarization, which may occur simultaneously, are of relevance to corrosion, namely activation polarization, concentration polarization, and ohmic polarization (ACI Committee 222 1985).

Activation polarization, of which passivation is a special case, occurs due to kinetic hindrance of the rate controlling step of an electrode reaction, while concentration polarization occurs when the concentration of ions which contribute to the reactions at the electrode changes, possibly due to limited diffusion. An important example of concentration polarization is the situation where concrete becomes so devoid of oxygen that corrosion becomes cathodically restricted (polarised). On the other hand, ohmic polarization refers to the resistance (R) of the electrolytic path between the anode and cathode which tends to create a potential drop (IR) in accordance with Ohm's law; the resistance is, in turn, determined by: i) the length of electrolytic path, which is primarily of importance in relation to macro corrosion cells, and ii) the resistivity of the concrete (2.2)

- iv) Temperature: An increase in temperature accelerates the corrosion reactions, and thus escalates corrosion if the other conditions for corrosion are satisfied. It has, for instance, been reported (Shalon & Raphael 1964) that the corrosion rate is sharply in

creased by increases in temperature in the range of 20°C to 40°C, especially at high relative humidities.

Other factors which may influence corrosion rate will be referred to later in this chapter (2.3, 2.4).

2.2 Resistivity of concrete

2.2.1 Background

While an understanding of electrical conduction in concrete is of practical importance from many viewpoints, in the context of this work, emphasis will be placed on the relationship between the electrical properties of concrete and the corrosion of embedded metals (particularly reinforcing steels).

It is now firmly established that concrete resistivity is one of the main factors controlling the rate of corrosion of embedded steel once its passivity is destroyed, yet, comparatively little research has been undertaken to elucidate the role of resistivity in this context.

In fact, comparatively little research has been undertaken on the electrical properties of cement pastes and even less on concretes. A survey of the published literature on the electrical resistivity of cement and concrete revealed a wide variety of measuring techniques used with little agreement on which is the most appropriate. Controversy has mainly rested on whether to use of d.c. or a.c. currents in the measurement of the resistivity of concrete.

Several authors (e.g. Schulte et al. 1978, Whittington et al. 1981) have concluded that a.c. rather than d.c. measurements should be used because the d.c. data are influenced by electrochemical factors (polarization at the electrodes is the most prominent), which can be avoided if an alternating current of sufficiently high frequency (1000 Hz (Bhargava & Rehnstrom (1978)) is employed; in situ, using a four electrode system (Stratfull 1968) also serves the same purpose. On the other hand, Hansson and Hansson (1985) have argued that d.c. measurements are far more informative than a.c. measurements if the electrochemical processes, referred to above, are expressed in terms of a variety of parameters which are primarily involved in the current-time relationship (obtained through application of a d.c. current through embedded electrodes), and used these parameters to explain the behaviour of two silica fume

pastes on which they conducted both a.c and d.c. measurements. An interested reader is also referred to earlier work by Hansson and Hansson (1983).

2.2.2 Factors influencing the resistivity of concrete

Several workers (e.g. Whittington et al. 1981) have suggested that concrete may be considered as a composite of particles of aggregate of various sizes in a matrix of portland cement paste, and suggested three paths for the conduction of current: i) through the aggregate and paste in series, ii) through the aggregate particles in contact with each other, and iii) through the paste itself. However, the resistivities of the aggregates commonly used in concrete are (of the order of $1.6 \times 10^3 \Omega\text{m}$ to $7.1 \times 10^9 \Omega\text{m}$, according to Parkhomenko (1967)) extremely high compared to those of moist concrete (typically $50 \Omega\text{m}$) suggesting that most of the current would pass through the path of least resistance, i.e. the cement paste. Moreover, the large increase in resistivity upon removal of evaporable water ($50 \Omega\text{m}$ when moist to $10^9 \Omega\text{m}$ when bone dry) would almost certainly imply that electrical current is conducted through concrete mainly by electrolytic means, that is by ions in the pore solution, with electronic conduction through the solid cement matrix being negligible. Consequently it is not surprising that the following factors are of prime importance in determining concrete resistivity:

- i) volume fraction occupied by pore solution, which is determined by: a) degree of saturation, b) water/cement ratio, c) aggregate/cement ratio, d) the degree of hydration;
- ii) ionic concentration of pore solution, which is dependent upon: a) cement content, b) alkali content of the cement, c) ionic admixtures (e.g. chlorides), d) leaching of pore solution ions or ingress of ions from an external source, e) degree of hydration, f) presence and amount of cement replacement materials;
- iii) temperature (see A3.1).

Many of the above parameters are inter-related, and the following paragraphs will attempt to highlight those of most importance and to explain how they influence resistivity.

The ⁱInfluence of both the water/cement ratio and hydration time (period of moist curing) on the resistivity of an OPC cement paste can be seen in Figure 2.1. The increase in resistivity with the decrease in water/cement ratio, and with curing time can be primarily attributed to a decrease in the volume of pore space. Additionally, Figure 2.1 reveals, at a glance, that at 14 days moist curing a relatively large increase in resistivity appears when the water/cement ratio reduces from 0.6 to 0.5. Since Powers et al. (1959) suggested that 14 days of moist curing are required to segment the capillary space of a 0.5 water/cement ratio cement paste while the corresponding period for a 0.6 water/cement ratio paste is 6 months, it appears that resistivity is not a simple function of the volume of the pore space, but is also related to its connectivity and that, in practice, resistivity may be expected to be limited by the highest resistance of the least resistant path, which may constitute the narrow channels between larger pores.

Figure 2.2 demonstrates that the degree of water saturation has a substantial effect on the electrical resistivity and that its influence is larger than any other parameter. It is also important to mention that the percentage increase in resistivity upon drying exceeds the percentage reduction in moisture content and that this effect is more pronounced the lower the water/cement ratio and the lower the final degree of saturation reached. These observations can be explained, at least in part, by the fact that, upon drying, it is mostly the larger pores which are emptied first, and thus the path responsible for current flow shifts towards the finer porosity and ultimately, if complete segmentation is achieved, electronic conduction may become the controlling factor.

The nature of the ionic species present, their concentrations, mobility, and their interaction with the pore walls are all believed to have an influence on resistivity (Buenfeld 1984).

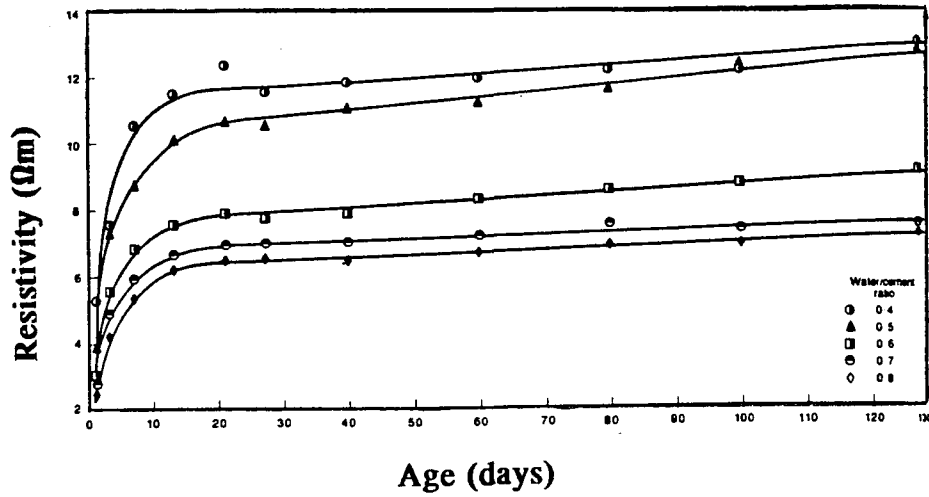


Figure 2.1 Influence of water/cement ratio and age on the resistivity of moist-cured cement pastes (Whittington et al. 1981).

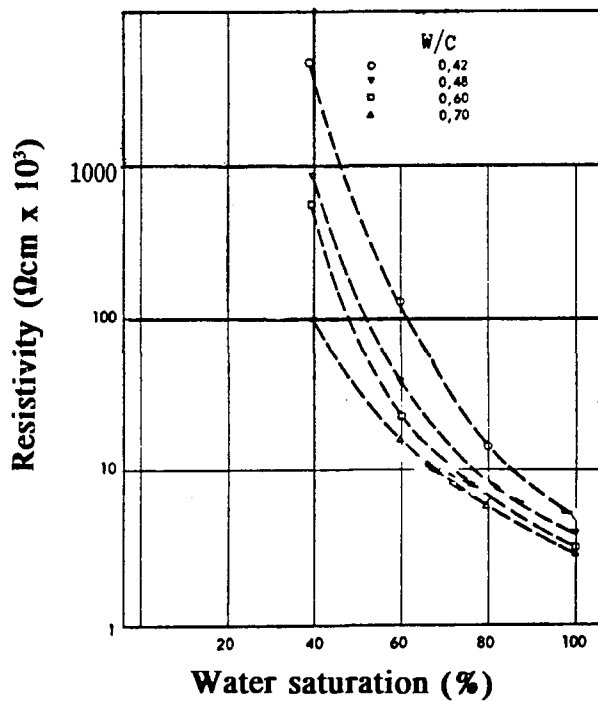


Figure 2.2 Influence of the degree of saturation on resistivity in OPC concrete (Gjørv et al. 1977).

Finally, it is well known that the use of cement replacement materials in concrete results in large increases in resistivity. The reasons for this behaviour will be discussed later (6.1.1.2.2).

2.2.3 Field corrosion rate measurements and resistivity

A number of authors have previously related corrosion and concrete resistivity; Table 2.1 provides a listing of some of the efforts made in this respect.

Table 2.1 Concrete resistivity levels related to the vulnerability of embedded steel to corrosion

Resistivity range (Ωm)	Corrosion (occurrence, degree or rate)	Type of structure	Reference(s)
below 50-100	corrosion occurs	offshore	Browne 1982
below 50 50-120 above 120	certain probable not significant	highway bridge	Cavalier & Vassie 1981
above 200	not significant	outdoor slab, corrosion measured between upper and lower mats	Clear 1982
above 600	not significant	marine	Tremper et al. 1958
below 50 50-100 100-200 above 200	very high high low negligible	structures in general	Browne and Baker 1983

Analysis of the information above shows great variability and, hence, it may only be used as an empirical guide in anticipating the corrosion rate when the resistivity of concrete is known.

2.3 Chlorides and chloride-induced corrosion

2.3.1 Chlorides in concrete

2.3.1.1 Introduction

Although a relationship involving the presence of chlorides in concrete and the corrosion of embedded reinforcing steel is now firmly established, the corrosion risk that chlorides pose to the reinforcement embedded in concrete was found to be strongly influenced by their source and state, hence the need for the distinction.

2.3.1.2 Sources of chlorides in concrete

Chlorides in concrete may be classified, depending on their source, into internal chlorides and external chlorides.

Internal chlorides are those which are introduced into concrete during mixing either intentionally, as chloride based admixtures (CaCl_2 accelerator, polyvinylidene chloride latex (which was found to decompose, over a period of years, liberating chloride and causing extensive corrosion (Erlin & Hime 1985))), or adventitiously as contaminants of the aggregate or mixing water.

External chlorides are derived from an external source such as sea-water, deicing salts, contaminated ground water, and chemicals industrial plants.

Naturally, internal chlorides are involved in the early hydration reactions, while external chlorides may only contribute to later hydration.

2.3.1.3 States of chlorides in concrete

Chlorides may be present in concrete in several forms: loosely bound (immobilised), strongly bound, or free.

Loosely bound chloride

The term loosely bound has been used in reference to chloride ions which reside both in the interlayer positions and on the surface (adsorbed or chemisorbed) of the CSH sheets.

Ramachandran (1971) argued that the CSH product has a large surface area and has both electrostatic (resulting from it having a positively-charged surface) and van der Waal's forces, and that this should encourage the adsorption of chloride ions. In a later publication, Beaudoin, Ramachandran, and Feldman (Beaudoin et al. 1990) suggested that chlorides may also interact with Ca^{2+} ions and OH^- groups to form oxychloride complexes which can be leached by water and that interlayer regions may be relatively inaccessible to water and thus extended leaching periods may be required before all adsorbed chlorides can dissociate and desorb. Their work also revealed a direct linear relationship between the amount of loosely bound chloride and the C/S and H/S ratios of synthetic CSH preparations. Interestingly, Beaudoin et al. argued that, in support of their results, the Feldman and Taylor models for CSH feature missing tetrahedra in the silica chain which are replaced by hydroxyl groups and, since these are potential sites for oxychloride complex formation, at low C/S ratios there would be fewer OH^- sites for chloride complexing to occur as the degree of polymerization is higher.

It is important to mention here that Arya, Buenfeld, and Newman (Arya et al. 1987) contested the above mentioned, and stipulated that the results of their work cast doubt on the existence of loosely bound chloride. They argued that NaCl and KCl, and not CaCl_2 as suggested by Ramachandran (1971), would be present in the powdered samples on which leaching tests are performed, and that NaCl and KCl while highly

soluble in water are only slightly soluble in ethanol and, consequently, it is only natural for the relatively mild leaching techniques employed by Ramachandran et al. that the water leached chloride would exceed that leached by ethanol.

In any case, the amount of chloride which can be adsorbed would be expected to depend on the existence of competing ions (e.g. OH^- (Tritthart 1989), SO_4^{2-}) and, additionally, adsorbed chlorides are expected to exist in equilibrium with the free chlorides present in the pore solution.

Strongly bound chloride

There is almost universal agreement that chlorides can react with calcium aluminates and to a lesser extent with calcium aluminoferrites in cement pastes to form chloroaluminate and chloroferrite hydrates. A proportion of the chloride present in concrete thus becomes strongly bound; the predominant reaction being that of the formation of the chloroaluminate hydrate known as Friedel's salt ($3\text{CaO} \cdot \text{Al}_2\text{O}_3 \cdot \text{CaCl}_2 \cdot 10\text{H}_2\text{O}$) (Bakker 1988).

In concrete, the amount of chloride bound is dependent upon the cement content of the concrete and the chloride binding capacity of the cement. The chloride binding capacity of the cement is usually expressed in terms of the ratio of the amount of chloride bound to the total chloride present.

Much of the research work done to elucidate the factors which determine the chloride binding capacity of cement has been performed on test specimens with internal chloride, mainly because of the ease with which chlorides can be introduced (in the mix water). However, the use of internal chlorides in concrete in which metal is embedded is strictly restricted by most codes of practice (BS8110 (1985): Part 1 "Code of practice for design and construction"). Moreover, it has been demonstrated by Arya, Buenfeld, and Newman (Arya et al. 1990) that chloride binding capacity is dependent on whether the chlorides are internal or external and, in fact, to elucidate external chloride binding

capacity, it would be erroneous to extrapolate trends which are obtained through measurements on internal chlorides. Consequently, in the context of this work, this discussion will focus mainly on the binding of external chlorides.

In contrast to the findings of Tuutti (1982), who reported that the free chloride concentrations show rectilinear dependence on total chloride from the origin, linear relationships, with very high correlation coefficients, between total chloride and free chloride concentration in the pore solution were observed in tests carried out by Page, Lambert, and Vassie (Page (1) et al. 1991). They also observed that the straight lines were all characterized by positive intercepts on the horizontal axis, corresponding to total chloride contents in the range 0.6-1.0% , which implies that, at total chloride contents below about 1.0 percent, the cement hydrates bind a substantial proportion of the chloride in an insoluble form but beyond this point binding capacity is largely exhausted.

The factors which influence the binding capacity of cement can best be discussed with reference to the work carried out by Arya et al. (1990). Their work suggested that the two principal factors that control the degree of binding of external chlorides are: the source of chloride ions (i.e. the associated cation) and the chloride concentration of the penetrating solution. They discovered a 75% increase in binding when OPC specimens were exposed to a CaCl_2 rather than an NaCl solution, and thought it likely to be due to chloroaluminate forming more readily in the presence of CaCl_2 than NaCl . As for the concentration of the external solution they found that the bound chloride increases with increasing the concentration of the exposure solution, but there is a decrease in the bound/total chloride ratio; this is in agreement with the work reported in the preceding paragraph (Page (1) et al. 1991).

As mentioned earlier, chlorides are mainly bound by C_3A and it, therefore, seems likely that the C_3A content of the cement will influence binding (a direct relationship). Surprisingly, however, OPC and SRPC pastes were found to have remarkably similar binding capacities, suggesting that C_3A content has little effect on the binding of

external chlorides (Arya et al. 1990). This may be attributed to the consumption of C_3A , in the early stages of hydration, upon reaction with gypsum to form sulphoaluminates, and the fact that much of the C_3A remaining after such reaction will be present in hydrated form by the time external chlorides penetrate to the potential reaction sites; according to Mehta (1977), significant chemical binding of external chlorides cannot be expected unless the C_3A content is higher than about 8 percent.

Another factor which influences binding is concerned with the stability of the products formed upon binding (Friedel's salt), and, in this respect, it is known that the solubility of this product increases as the pore solution pH decreases. It is, therefore, not surprising that Arya et al. (1990) found that increasing the alkali content of cement increased its binding capacity. Additionally, it would be expected that any factor which may reduce alkalinity (2.1.2.1.2) would increase the solubility of Friedel's salt and hence decrease the amount of chloride bound. Temperature also seems to influence the stability of Friedel's salt. According to Roberts (1962), chloride bound by C_3A is likely to be released at temperatures around 40°C to 50°C , as the chloroaluminates decompose.

At this stage, it should certainly be pointed out that, in the work done by Arya et al. (1990) and that done by Page(1) et al. (1991), a pore press has been used to establish the amount of free chloride in the pore solution. Consequently, according to Beadoin et al. (1990), who remarked that pore pressing is unlikely to release adsorbed chloride, it can be argued that the bound chloride referred to by the former authors is likely to entail both the loosely bound, and the strongly bound chloride.

The binding capacity of concrete in which OPC is replaced by any of the cement replacement materials is yet to be fully clarified. Silica fume is known to reduce the binding capacity for internal chlorides (compared to plain OPC), and many attribute this to the increased solubility of Friedel's salt resulting from a reduction in the pH of the pore solution (Page & Vennesland 1983). Beaudoin et al (1990) proposed that, according to their findings (as mentioned earlier), the reduction in the C/S ratio of the

CSH upon OPC replacement by silica fume also played a part. For external chlorides, the binding capacity of the silica fume cement was found to be the lower than that of the control (plain OPC) although this was partially ascribed to the chloride concentration in pore solution being below that of the external chloride solution at the time of pressing (Arya et al. 1990). Blended cements containing PFA or GGBS were found (Arya et al. 1990) to be able to bind greater proportions of chloride ions than 100% OPC mixes, and the reasons for this are yet far from established. In the case of GGBS, Brodersen indicates that this increase is due to a substantial increase in the amount of adsorbed chloride, with the formation of compounds with the aluminate phases in cement only playing a minor part in this process (Arya et al. 1990). It was also suggested (Dhir et al. 1991) that chloride ions may be bound in physio-chemical adsorption form by unreacted PFA particles and that only a minor part of the chloride ions bound in this way could be released by any form of water dissolution. Finally, concerning the binding capacity of blended cements, it should be mentioned that the differences in binding capacity, compared to 100% OPC, are considerably less pronounced in mixes containing external chloride than in those containing internal chloride (Arya et al. 1990).

Finally, the chemical nature of the pore solution is expected to play a role in binding. For example, it is widely believed that chloride that is tied up in the form of chloroaluminates will not stay tied up if sulphates penetrate into concrete; sulphate changes calcium chloroaluminate to calcium sulphoaluminate, thus liberating chloride (e.g. ACI Forum 1987).

2.3.2 Chloride-induced corrosion

2.3.2.1 Introduction

Chloride-induced corrosion usually manifests itself in localised attack in what is known as pitting corrosion. However, very high concentrations of chloride in the pore liquid can generate such active pitting attack that the pitting sites coalesce and give rise to a more general form of corrosion occurring at a high rate.

2.3.2.2 Pitting corrosion

The electrochemical theory of pitting corrosion is still the subject of much research and discussion. Nevertheless, some principles of the process are now generally agreed upon and the following sections focus on those points of general agreement.

As discussed earlier, the passivity of steel in an alkaline environment may be destroyed by the presence of chloride ions, thus promoting pitting corrosion; a process which is believed to be characterised by galvanic action between relatively large areas of passive steel acting as a cathode and small anodic pits where the local environment develops high chloride concentrations.

The process by which pitting propagates, as can be seen in Figure 2.3, has been briefly described earlier (2.1.2.1.2). Clearly, the propagation of this process requires continuing activity at the anodic sites; this is believed to be controlled by maintenance of the $[Cl^-]/[OH^-]$ ratio above the critical value for initiation (2.3.2.3).

As pitting continues, anodic activity develops as a result of hydrolysis of the corrosion product so liberating hydrogen ions. At the same time, hydroxyl ions are produced as the consequence of the cathodic reactions. Thus, pitting becomes self-supporting by lowering the pH at anodic sites while increasing the pH at adjacent cathodic areas, so reducing the chances of attack at these areas.

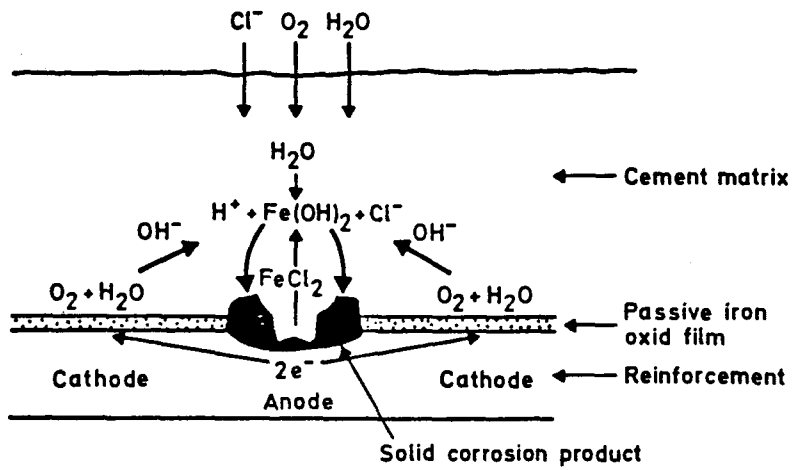


Figure 2.3 Reactions involved in pitting corrosion (Treadaway 1988).

Two key factors are expected to influence the propagation of pitting in chloride-bearing concrete:

i) the availability of chloride ions, which will be influenced by: a) the concentration of chloride ions at the pit, b) the recycling of chloride ions (see Figure 2.3), and c) the diffusion of chloride ions to the pit;

ii) the availability of hydroxyl ions, which will be influenced by: a) see 2.1.2.1.2, b) rate of hydrolysis, and c) diffusion of hydroxyl ions to active sites.

It is also important to realise that cathodic processes are also required to be maintained if pitting is to propagate. In this context, oxygen availability is of major importance (2.1.2.2.2). Furthermore, concrete resistivity is of major importance as it may control the size of the available cathode for a given anodic site (2.1.2.2.2). However, if the concrete is of low resistivity, the total cathodic process can still stimulate intense anodic activity and hence significant corrosion.

2.3.2.3 Chloride corrosion threshold

Much research has been directed at attempting to define the chloride corrosion threshold, the chloride content of concrete (at the level of the steel) below which the risk of corrosion is negligible. Furthermore, while most investigators suggest that it is only the free chloride that contributes to the corrosion process, some workers consider that, since bound chloride can decompose to release chloride into the pore solution, all chlorides present a potential risk to corrosion. Another complicating factor arises because the threshold value is dependent upon a number of factors including mix ingredients and exposure conditions, and so it is not possible to give a single value which is applicable in all cases. Nevertheless, much work has been done in this area; for example, on the basis of visual and chemical examinations of structures and components containing internal chloride, the Building Research Establishment (Everett & Treadaway 1980) proposed that a total chloride content of less than 0.4% (by weight

of cement) produces a low risk of corrosion, between 0.4% and 1% produces a medium risk, and greater than 1% produces a high risk. However, in the case of external chlorides, work at the Federal Highway Administration (Clear 1976) has shown that, even in the absence of significant carbonation, chlorides penetrating from an external source can initiate corrosion at acid-soluble (i.e. total) chloride levels as low as 0.2 percent (by weight of cement), since a larger proportion of the total chloride present remains free within the pore solution and the inevitable gradients in concentration also encourage corrosion.

On the other hand, other workers consider it advisable to assess corrosion risk in terms of not only the free chloride content but also the hydroxyl ion concentration in the pore solution, since the latter influences passivity. They, therefore, propose that the corrosion threshold should be expressed in terms of the ratio of the concentration of free chloride ions to that of the of hydroxyl ions in the pore solution, i.e. the critical $[Cl^-]/[OH^-]$ ratio, and it is above this ratio that depassivation takes place and corrosion may propagate (2.3.2.2).

Based on work conducted on electrolytic solutions of hydroxides and chloride, various workers have suggested relatively similar values for the critical $[Cl^-]/[OH^-]$ ratio (0.25-0.8 (Gofni & Andrade 1990); 0.5-1.08 with 0.63 from a statistical treatment of the probability of corrosion (Hausmann 1967); a limiting value of 0.83 derived from a logarithmic relationship between $[Cl^-]$ and pH (Gouda 1970)). However, work conducted on concretes (pastes or mortars) which were exposed to external chlorides suggested for the critical threshold ratio to be an order of magnitude higher (a value of 3 was suggested (Page(2) et al. 1991)) than that reported using electrolytic solutions. This may, at least in part, be due to the electrolytes employed not representing mass transfer in porous media.

The work done by Page et al. ((2) 1991) also presents some interesting observations. Firstly, there was considerable scatter in the corrosion current versus $[\text{Cl}^-]/[\text{OH}^-]$ ratio plot when $[\text{Cl}^-]/[\text{OH}^-]$ ratio exceeds the threshold value, and there were instances in which no significant corrosion was observed even at $[\text{Cl}^-]/[\text{OH}^-]$ values as high as 15 to 20. Secondly, concerning the chloride (total) corrosion threshold, Page found it to be of the order of 1.5%, which is substantially higher than that proposed by analysis of real structures; clearly an observation which reveals the danger of using experimental values with the intention of predicting the behaviour of real structures.

2.4 Carbonation and carbonation-induced corrosion

2.4.1 Carbonation

2.4.1.1 Background

Carbonation refers to the chemical reactions in which the calcium silicate hydrates, calcium hydroxide and various calcium aluminate or ferro-aluminate hydrates react with atmospheric carbon dioxide to produce calcium carbonate, silica gel, hydrated aluminium, and iron oxides. Additionally, in this process, the sulphate originally present in the cement reverts to gypsum. The unhydrated cement compounds are also known to react, where carbon dioxide is present at high concentrations, but under normal atmospheric conditions they may be regarded as unreactive (Parrott 1987).

It has long been advocated that carbonation advances into concrete as a distinct front separating two distinct zones, namely, the fully carbonated and the uncarbonated. However, it is now agreed that this approach is simplistic and a carbonating layer has been proposed to separate these two zones (Ying-yu & Qui-dong 1987). Indeed Parrott (1987) reported that the zone in which carbonation takes place, i.e. the carbonating zone, has been found, in some instances, to be fairly narrow, while in others, to extend over a distance some times greater than the depth of fully carbonated concrete. The same author also reports that there is some evidence that the carbonating zone is wider in drier concrete.

2.4.1.2 Factors influencing carbonation in concrete

The capacity of concrete to hinder the advance of the carbonation front is dependent on the amount of alkaline hydration products per unit volume (binding capacity), which depends on the cement content and type. In a Building Research Establishment report (1978), it was suggested that, in practice, increasing the cement content above about 15% in OPC concrete has only a marginal effect on the concrete's resistance to carbonation, but that concretes produced with cement contents lower than 15% are likely to be more susceptible to carbonation. As for the cement type, it has been

frequently reported that the use of cement replacement materials (e.g. GGBS, PFA, Silica fume) in concrete, in direct replacement (by weight) of OPC, results in increased rates of carbonation in comparison to concretes with 100% OPC. This increase can be accounted for, at least partly, by a reduction in the alkaline hydration products available in concrete upon the partial replacement of OPC.

Despite the importance of the above mentioned factors, it is now widely accepted that carbonation of concrete or mortar is a chemical reaction controlled primarily by diffusion of carbon dioxide within its pore system (Ying-yu & Qui-dong 1987) which, in turn, depends on the nature of the exposure environment (the concentration of carbon dioxide in the atmosphere, relative humidity, temperature), and the pore structure and porosity of concrete; the latter being dependent upon the particular binder, the water/binder ratio and the conditions (type, duration) of curing.

Figure 2.4 demonstrates that the rate of carbonation increases as the carbon dioxide concentration of the exposure environment increases, with the increase being more pronounced the lower the quality of concrete. However, it has been reported (Parrott 1987) that the increase in carbonation rate is small beyond 1% of carbon dioxide by volume.

Ying-yi and Qui-dong (1987) investigated the influence of the equilibrium relative humidity and pore size distribution on the rate of carbonation in mortar. Employing scanning electron microscopy, they examined carbonated mortars and observed dense CaCO_3 growth on some pore walls; they referred to these pores as active pores. They then carried out porosimetry studies and observed that, in an OPC mortar, the total porosity decreased upon carbonation. However, they observed that this was largely due to a decrease in the porosity of those pores with radii less than 630 \AA , with the volume of pores larger than 1000 \AA remaining almost the same. They, thus, concluded that the active pores are mainly those whose radii are smaller than 630 \AA , and that the formation of CaCO_3 upon carbonation has resulted in a remarkable decrease in the porosity of these pores. As for the pores with radii over 1000 \AA , they stipulated that

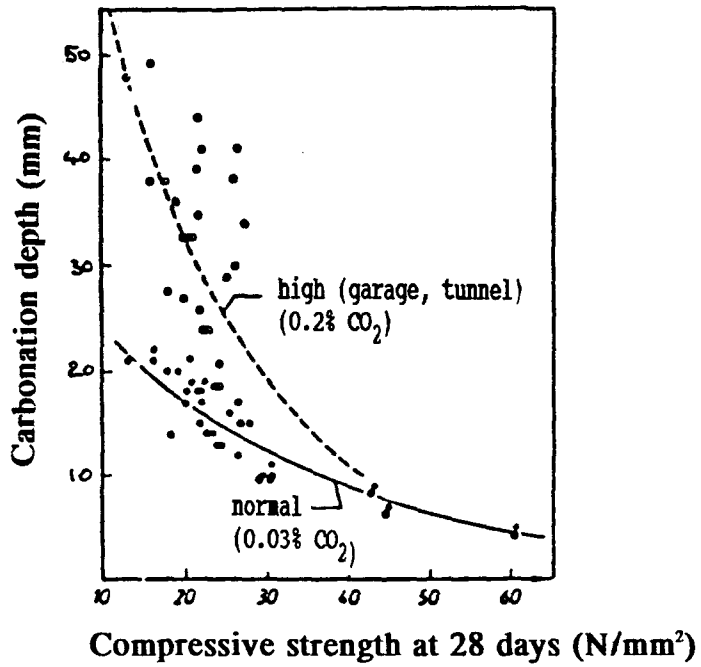


Figure 2.4 Carbonation depth as a function of the CO₂ concentration of the exposure environment and the quality of OPC mortar (Parrott 1987).

these are relatively inactive and mainly act as a diffusion path for CO₂ and, thus, decreasing the volume of these pores would increase the carbonation resistance of mortar. Furthermore, since it is generally known that there is a drop, by a factor of 10⁴, in the diffusion coefficient of gases when they diffuse in a liquid media instead of gaseous media, it is the equilibrium relative humidity and temperature, which will determine the moisture condition of these pores (see Chapter 3), that controls the diffusion rate of carbon dioxide.

While the above analysis provides a convincing explanation for observations by many (e.g. Calleja 1981) that carbonation advances at very high rates for relative humidities in the range 50-70%, but much slower for RH in the range 75-100%, the slow rate of carbonation at low (0-45%) relative humidity levels may seem to contradict it. It should, however, be remembered that the presence of water is essential for the chemical reactions involved in carbonation and, thus, while low relative humidity levels would allow more rapid diffusion of carbon dioxide, depletion of water would result in the rate of carbonation being controlled by the kinetics of the carbonation reactions, which are expected to be hindered at these low relative humidities.

Finally, it is worth mentioning that, in environments which are exposed to frequent wetting and drying, the rate of carbonation will be very low. In fact, it can be deduced from what is known as the Eindhoven model (Bakker 1988) that in such environments, carbonation will reach a limit which is determined by the rate of water vapour diffusion, i.e. the speed of drying of concrete; the factors influencing water vapour diffusion will be discussed later (Chapter 3).

2.4.2 Carbonation-induced corrosion

The neutralisation of the alkali hydration products in concrete as a consequence of carbonation results in the pH of the pore fluid dropping from a value greater than 12.6 (13.5 in OPC) in the uncarbonated region, to a value of around 8.0 in the region of complete carbonation (Hobbs 1988). The passivity of reinforcement will thus be lost and a general (uniform) form of corrosion is initiated.

While factors that affect the rate of carbonation of concrete are well documented, this is not true of those that influence the rate of carbonation-induced corrosion. Variables such as temperature, relative humidity, and the presence of chloride salts are known to influence corrosion rates in carbonated concrete (Short et al. 1991).

Figure 2.5 demonstrates the influence of temperature, and relative humidity upon the rust formation of a carbonated mortar, from which it is apparent that corrosion rates in carbonated mortar (or similarly concrete) are minimal below 75% relative humidity and are high at 95% relative humidity. It is also apparent that corrosion increases substantially with an increase in temperature above 20°C (2.1.2.2.2) with the effect being slightly more pronounced at higher relative humidity levels. Upon close examination of the foregoing, it seems that it is unlikely that oxygen availability will have a decisive effect on the corrosion rate since, at 95% relative humidity, oxygen diffusion should be more restricted than at 50% RH. So the decisive parameters influencing carbonation-induced corrosion are likely to be those associated with the resistivity of the electrolyte in the carbonated pore structure and, in the absence of chloride, this is likely to be associated with moisture content (2.2.2).

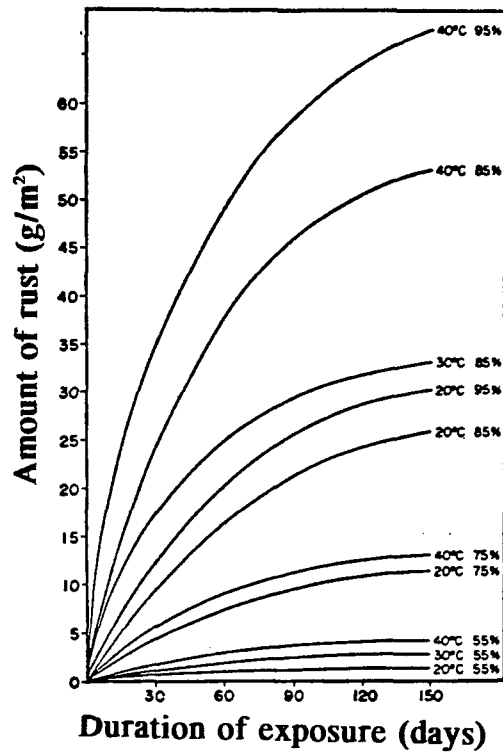


Figure 2.5 Effect of temperature and relative humidity on rust formation in carbonated concrete (Parrott 1987).

Concerning the role of chlorides (except for internal chlorides), in most circumstances, it is likely that they will have penetrated concrete to the reinforcement level well before the fully carbonated, or even the carbonating, front reaches that level. The presence of chlorides is known to contribute in reducing the resistivity of concrete and, upon the arrival of the carbonating front, bound chlorides are released (2.3.1.3), thus contributing to a further reduction in resistivity. A further consequence would be a certain increase in the $[\text{Cl}^-]/[\text{OH}^-]$ ratio, and if the increase is such that the critical $[\text{Cl}^-]/[\text{OH}^-]$ is breached, pitting corrosion may result (2.3.2.3). This apparent synergetic effect has been observed by Roper and Baweja (1991), although they point out that the presence of chlorides may retard the drying of concrete, hence hinder the advance of the carbonation front.

2.5 Cracks and corrosion

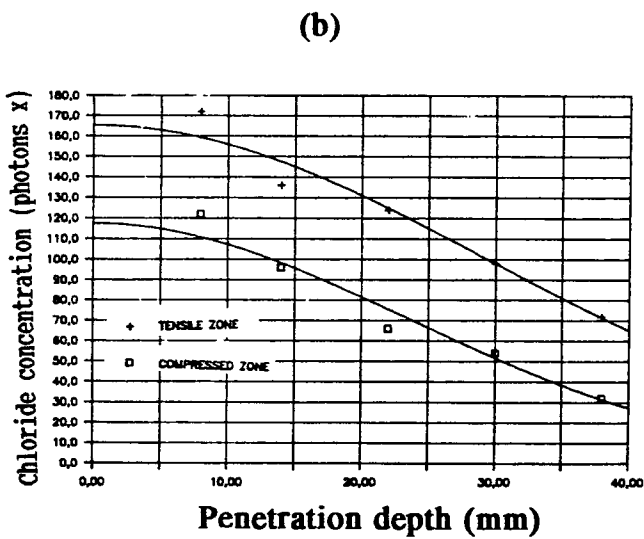
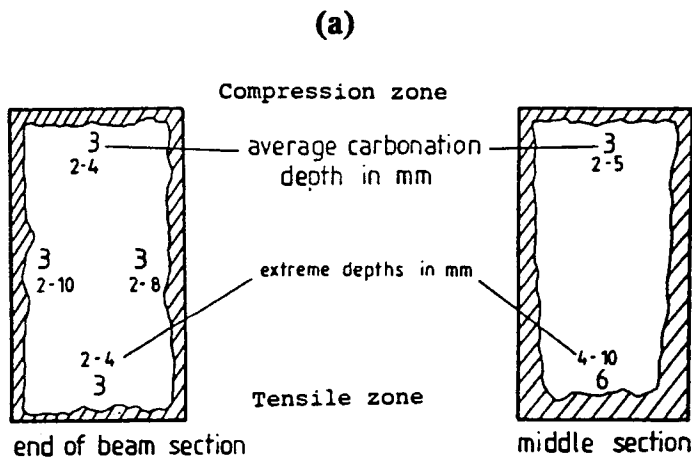
It is universally accepted that the presence of cracks in reinforced concrete promotes the ingress of harmful substances to the level of reinforcement, and it may, thus, be argued that to restrain the ingress of harmful substances through the use of admixtures would be much undermined by the presence of cracks. It is, therefore, the intention of this section to clarify the role played by cracks in corrosion initiation and propagation.

One of the most controversial subjects which concerns reinforcement corrosion is the role of cracks. The role of cracks on corrosion initiation seems to be easily comprehended. Intuitively, if a crack intersects the reinforcing steel then there is a comparatively easy path for aggressive substances (Cl^- and CO_2) to penetrate to the level of the reinforcing steel (see Figure 2.6), initiating corrosion. The commonly questioned roles of the cracks are: whether there is a relationship between their presence and the rate of corrosion and if the crack width also has a role to play, and if so, to what extent.

Before the role of cracks can be clarified it is important to point out that the orientation of cracks with respect to the reinforcement plays an important role in determining their influence on corrosion; where the crack is perpendicular to the reinforcement, the corroded length of the intercepted bars is believed to be no more than three bar diameters (Beeby 1978), whereas when cracks follow the line of a reinforcing bar (as might be the case with a plastic shrinkage crack, for example) they are expected to be much more damaging because the corroded length of the bar would be much greater.

Suzuki et al. (1990) carried out a thorough investigation into the influence of flexural cracks on corrosion. They observed that steel at every crack of singly-cracked specimens corroded. On the other hand, in multi-crack specimens, they observed a tendency for the widest crack, the crack width measured at the level of reinforcing steel, in the specimen to induce corrosion earliest, and a consequent delay or suppression of corrosion at the other cracks; they referred to the crack which induces

Figure 2.6 (a): Influence of cracking on depth of carbonation in a beam section subjected to flexure;
(b): Influence of cracking on chloride penetration in a beam section subjected to flexure (Francois & Arliguie 1991).



corrosion first as a major crack, while others were referred to as minor cracks. They then argued that since it is clear that steel corrosion at the minor cracks was delayed and suppressed by the presence of major cracks, if all cracks were used to analyze the relationship between the width of cracks and the measured degree of corrosion, as is often the case, no correlation would be found. They, therefore, sought to relate only the width of major cracks to the corrosion rate. The results were that, while a larger width of major cracks increased the corrosion rate during the early age of exposure, corrosion rate at the latter age was unaffected by crack width. The reasons for this behaviour can be explained by the fact that after depassivation anodic dissolution takes place in the region of the cracks, whereas the steel surface besides the depassivated area between the cracks acts as the cathode. Thus, it is clear that, in this case, it is the efficiency of this cathode that would determine the corrosion rate, with the consequence of crack widths having no influence on corrosion rate especially in good quality concrete (if the thickness of cover is adequate to restrict the flow of oxygen and moisture, or the resistivity of the concrete is high enough, then the corrosion processes initiated at cracks can be slowed down and eventually stopped).

Chapter 3 Chloride Transport Processes

3.1 Introduction

3.1.1 General

The previous chapter demonstrated that the initiation and propagation of the corrosion of reinforcing steel is strongly dependent upon the rate of transport of various species within and into concrete. It is essential, therefore, that an understanding of the mechanisms of transport of all the species involved in corrosion is developed. This chapter focuses on chloride transport processes, since resisting chloride transport is the subject of this thesis.

It should also be mentioned that, unfortunately, the conditions under which chloride transport mechanisms have been investigated have been so various that it is often very difficult to establish precisely the influence of changes in concrete parameters on the rate of chloride ion transport in concrete via these mechanisms. The discussion in this chapter will, therefore, emphasise the principles which govern the effects of concrete parameter changes on chloride ion transport.

3.1.2 Pore structure of concrete

3.1.2.1 Background

Voids present in concrete vary in size from several millimetres to less than 20 Å (see Figure 3.1), and can be classified as: i) air voids, ii) aggregate voids, iii) cement paste voids, and iv) other voids. The voids referred to as "other voids" include internal cracks, voids under aggregate particles, and "honeycomb" voids.

POWERS			
GEL	CAPILLARY	AIR VOIDS	
2.5	50	10,000	PORE DIA
	10		(nm)
IUPAC			
MICRO	MESO	MACRO	AIR VOIDS

Figure 3.1 Pore size classification for cement paste (Young 1988).

3.1.2.2 Pore structure influencing factors

Various strongly inter-related parameters collectively determine the pore structure of normal weight concrete. These include: type of cement, water/cement ratio, aggregate content, grading of aggregate, use of cement replacement materials and admixtures, curing (method, duration, temperature) and exposure conditions.

Understanding the influence of changes in any of the parameters listed above on the pore size distributions of cement pastes has been aided greatly by the application of mercury intrusion porosimetry. Figure 3.2, for instance, shows the effect of varying the water/cement ratio of OPC paste on the pore size distribution.

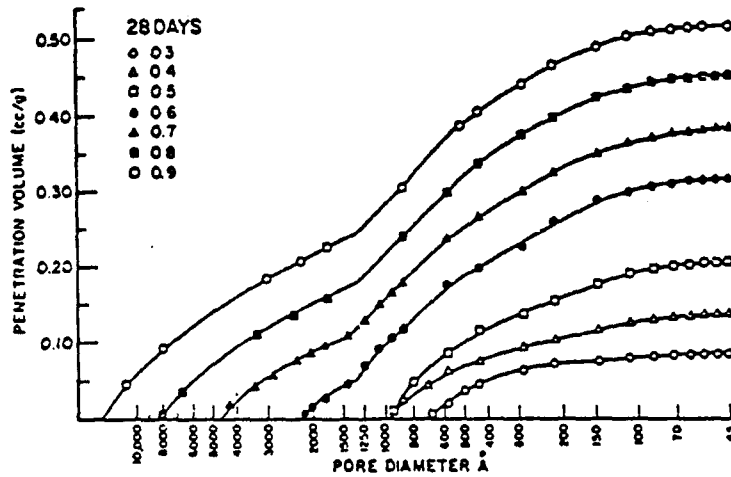


Figure 3.2 The effect of varying the water/cement ratio on the pore size distribution of cement paste cured in lime water for 28 days (Mehta & Manmohan 1980)

Many workers have attempted to relate pore structure to transport and postulated that the penetrability of concrete is mainly affected by the presence of continuous capillary channels. In relation to this, the pioneering work by Powers et al. (1959) is of interest. They demonstrated that continued hydration results in a progressive decrease in the capillary pore volume (see Figure 3.3) with the consequence of the capillaries eventually becoming blocked by gel and segmented, i.e. they become interconnected solely by the gel pores. The degree of hydration, for pastes of various water/cement ratios, required to produce this effect can be gauged from Figure 3.4, which demonstrates that the lower the water/cement ratio, the lower the degree of hydration required to segment the capillaries, hence the information in Table 3.1 has been derived (Powers et al. 1959).

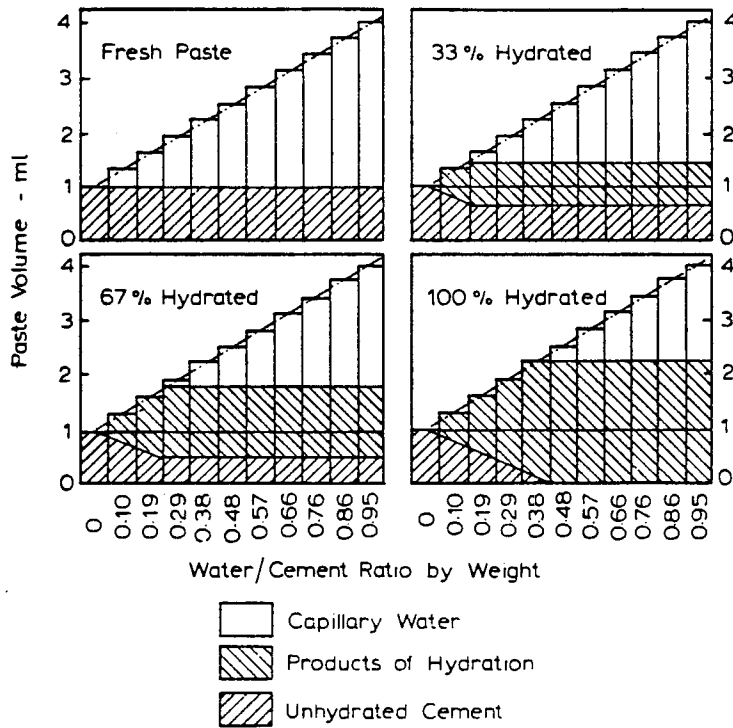


Figure 3.3 Composition of cement pastes at different ages; applicable to pastes with enough water-filled space to accommodate the hydration products at the degree of hydration indicated.

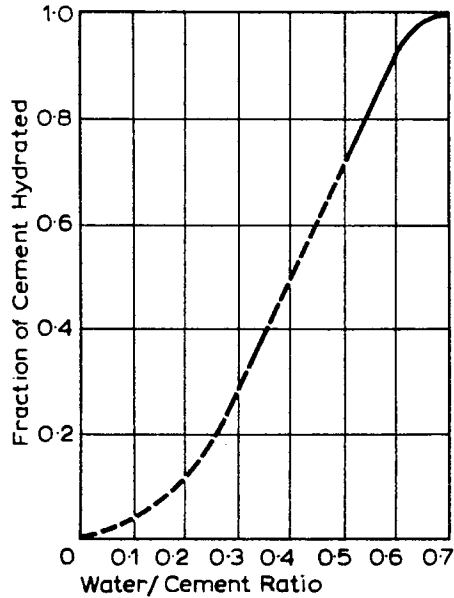


Figure 3.4 Relation between the water/cement ratio and the degree of hydration at which the capillaries cease to be continuous.

Table 3.1 Approximate period of moist curing required to achieve capillary discontinuity

Water/cement ratio (by weight)	0.4	0.45	0.5	0.6	0.7	over 0.7
Time to produce discontinuity	3 days	7 days	14 days	6 months	1 year	impossible

Other workers analyzed the data produced through application of mercury porosimetry and suggested that pore structure can be characterised by parameters which, in turn, can be employed in understanding pore structure-transport relations. Two such parameters are of importance and will now be discussed, namely the critical pore radius r_c and the maximum continuous pore radius r_{∞} . Katz and Thompson (Garboczi 1990) defined the critical pore radius r_c as the pore radius corresponding to the inflection point when the total intruded volume is plotted against the intrusion pressure. This is essentially the same as the threshold diameter which, according to Winslow and Diamond, represents the minimum diameter of pores which are geometrically continuous throughout all regions of hydrated cement paste (Garboczi 1990). On the other hand, the pore radius which represents the grouping of the largest fraction of interconnected pores, corresponding to the highest frequency of occurrence on a frequency of occurrence versus pore size plot, according to Nyame and Illston (1980), is the maximum continuous pore radius r_{∞} ; according to Garboczi (1990), the value r_{∞} is approximately half that of r_c .

It is clear from the definitions above that both r_c and r_{∞} are of great importance to the penetrability of cement systems and it would, therefore, be desirable to express variations in the pore structure of concrete in terms of these parameters. In relation to this, attention is drawn to Figure 3.5 which considers the combined influence of varying the water/cement ratio of pastes, and the time of moist curing on r_{∞} . Figure 3.5a shows r_{∞} , for all water/cement ratios excluding 1.0, decreasing with increasing moist curing periods up to 28 days, but remaining essentially constant thereafter.

Additionally, expressing porosimetry results as shown in Figure 3.5b may be advantageous, as it reveals that the lower the water/cement ratio of pastes, the more r_w becomes important to transport in pastes: this is because the plots narrow and the frequency of occurrence at r_w increases, as the water/cement ratio is decreased. Finally, Figures 3.5c, d, and e are in slight disagreement with Figure 3.5a in that they suggest, perhaps more realistically, that the point at which r_w becomes constant comes about at lower degrees of hydration the lower the water/cement ratio.

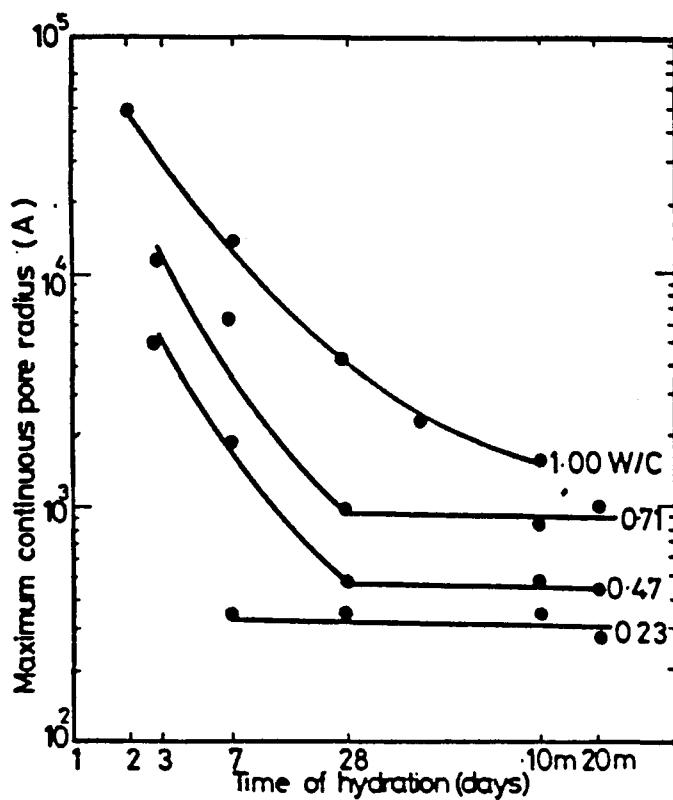


Figure 3.5a Effect of water/cement ratio and time of hydration on the maximum continuous pore radius of hydrated cement paste (Nyame & Illston 1980).

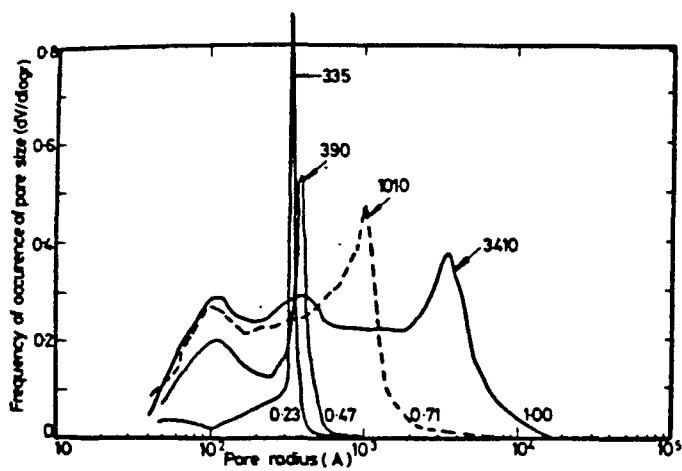


Figure 3.5b Effect of water/cement ratio on the differential pore size distributions of hardened cement pastes hydrated in water for 28 days (Nyame & Illston 1980).

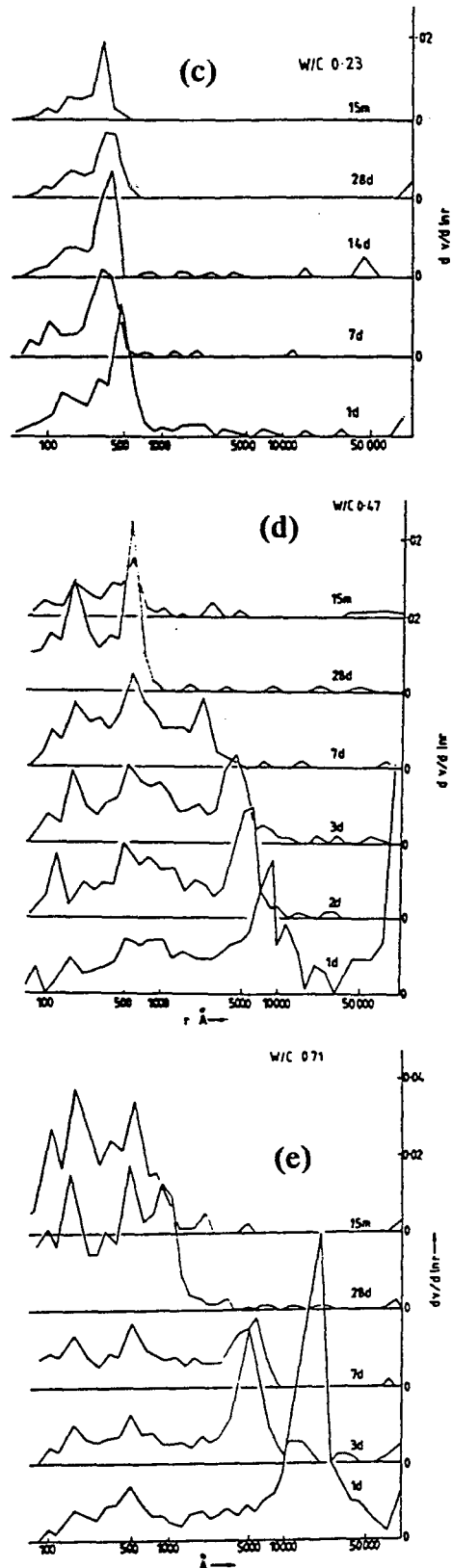


Figure 3.5c, d, e Pore size distribution plots for cement pastes of differing water/cement ratios (Midgley & Illston 1983).

Regarding pore size determinations, the following points should be remembered. Firstly, in well compacted normal weight concretes, essentially all forms of molecular and ion transport are believed to take place within the paste pore fraction, hence, many investigators have chosen to carry out their work on pastes rather than concretes. However, in assessing the influence of the cement paste pore structure on transport in concrete, pore structure determinations made on pastes, rather than concretes, are now believed to be of little practical significance. This is because of the strong evidence (e.g. Maso 1980, Winslow & Liu 1990) that the presence of aggregate results in an increase in the volume of pores in the large size range (see Figure 3.6), i.e. the pores which are expected, as will be seen later, to strongly influence the penetrability of concrete. Secondly, it is feared that the measured pore size distributions may not entirely correspond to the actual pore structures that are responsible for transport in concrete, because of the following:

i) the possibility of the measured pore structure rendered not corresponding entirely to the actual pore structures:

a) since some form of drying is employed before porosity measurements can be made (to remove the resident pore water), with many of the drying techniques usually employed often being harsher than those which may be present in practice, unrealistic damage may be induced even before pore structure determinations are made (3.2.2, see also: Feldman 1986, Day & Marsh 1988),

b) unrealistic damage may also be caused by the high mercury intrusion pressures employed, especially when characterizing the relatively fine pores; damage also manifests in opening new channels for mercury flow by breaking the hydration products responsible for pore blocking as is the case when mercury porosimetry is conducted on well hydrated pfa and ggbs pastes, and on some silica fume pastes (Feldman & Cheng-yi 1985, Feldman 1986, Day & Marsh 1988, Young 1988); and

ii) the assumptions relevant to pore structure characterization by mercury porosimetry (the value of the contact angle of mercury to pore walls, the assumption of cylindrical pores) being not entirely accurate, and possibly varying according to the material tested or the testing conditions.

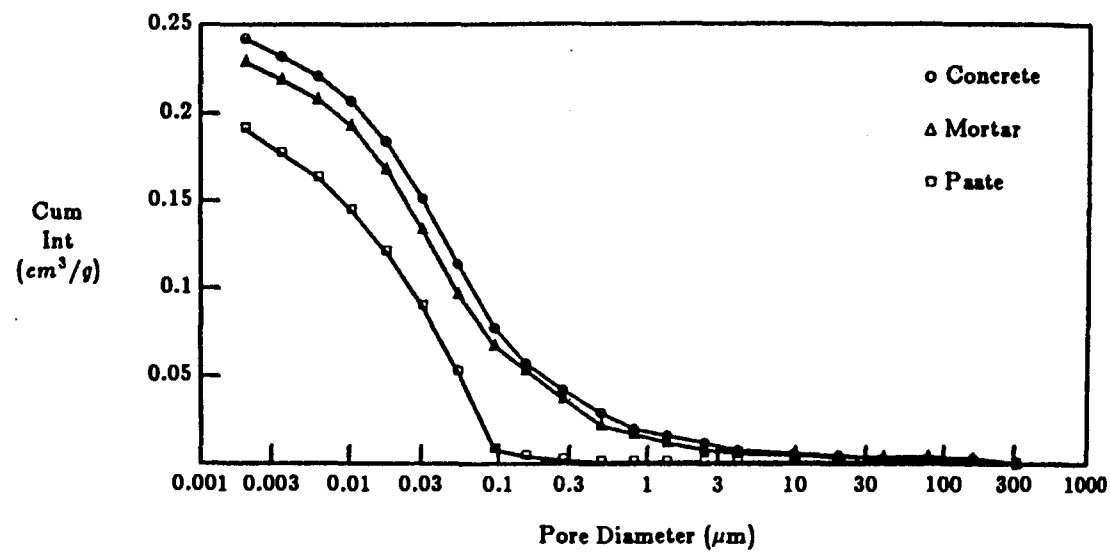


Figure 3.6 Pore size distribution plots for a 0.45 water/cement ratio concrete, the corresponding mortar and paste (Winslow & Liu 1990).

Finally, it should be remembered that increasing the volume fraction of normal weight aggregate in concrete has essentially two effects on pore structure: i) in relation to decreasing the paste volume, the volume of pores available for transport decreases: this is because normal weight aggregates are of little significance to transport as they are enveloped by pastes in properly compacted concrete (Ben-Othman 1994), ii) the coarsening of pore structure at aggregate-paste interfaces, as discussed above.

3.1.3 Transport in concrete

3.1.3.1 Definitions

- Adsorption is the process by which molecules adhere to the surface of pores in concrete. It can be attributed to chemical as well as physical effects.
- Capillary absorption is the process whereby concrete, by virtue of capillary suction forces, takes in a fluid to fill empty spaces within its pores.
- Diffusion is the process by which a liquid, gas, or ion passes through concrete under the action of a concentration gradient.
- Pressure-induced flow is the process by which a fluid passes through concrete under the action of a pressure gradient.

Finally, penetrability is a general term which indicates the ease of movement of liquids, gases, or ions through concrete.

3.1.3.2 Principal transport processes in concrete

The transport processes relevant to the durability behaviour of concrete and concrete structures are:

- i) water vapour diffusion;
- ii) capillary absorption;
- iii) wick action;
- iv) osmosis;
- v) pressure-induced water flow;
- vi) ion diffusion;
- vii) oxygen diffusion.

3.1.3.3 Effect of moisture content on transport in concrete

3.1.3.3.1 General

Figure 3.7 illustrates the various stages by which water moves within concrete (the connected voidage being idealised as a single pore with a neck at each end) as the relative humidity increases. After initial surface adsorption, water vapour movement is via diffusion. As relative humidity increases (stages (c) and (d)), water condenses within the pore necks which, consequently, act as short circuits for vapour movement by shortening the effective path length for vapour diffusion. Flow thus occurs in the liquid films and is therefore termed "liquid-assisted" vapour transfer (Rose(1) 1963). Once a meniscus forms within a capillary, due to either increasing relative humidity or an external source of water, forces arise as a result of the pressure differential across the meniscus and induce flow through the capillary. When the pore system becomes completely saturated, water may flow as a fluid if a sufficiently high pressure head exists. Additionally, superimposed upon bulk fluid movement, ionic species can diffuse through the free water within the concrete pore structure.

3.1.3.3.2 Physical nature of pore water in concrete

Water in concrete is held with varying degrees of firmness. First, there is the chemically combined water which forms part of the hydrated compounds. Next, there is the adsorbed water, i.e. water held by surface forces in the form of films on the pore walls. Finally, there is free water which is held beyond the influence of surface forces.

The distribution of water within these categories is dependent upon a variety of parameters, some of which will be discussed in the following section.

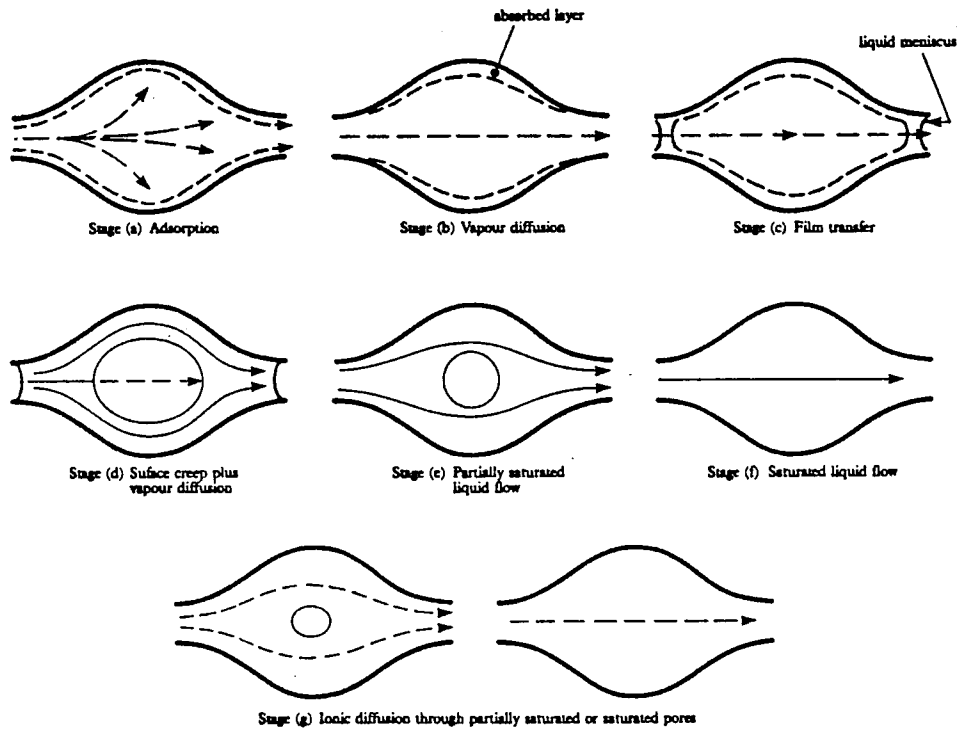


Figure 3.7 Idealised model of movement of water and ions within concrete (Rose(2) 1963).

3.1.3.3.3 Factors influencing the moisture state of concrete

The discussion earlier (3.1.3.3.1) implies that the mechanism by which fluids and ions migrate through concrete, and the rate of migration, are strongly dependent on the moisture condition of concrete, hence the importance of factors which govern the moisture state of concrete.

The moisture state of concrete can be expressed in terms of the degree of saturation of its pores with water (m) defined as the fraction of pore volume filled with water.

Molecules of water vapour are attracted by pore-surface forces forming adsorbed layers (Hudec 1987). The thickness of these layers increases as the pore relative humidity increases, as illustrated in Figure 3.8 for a micro pore of variable diameter. Furthermore, providing the thickness of the pore allows it (pore size greater than 26 Å (Horrigmoe 1985)), and the relative humidity is sufficiently high, water vapour condenses in the pore, and a certain amount of water will reside in the pore. Mathematical models which relate the moisture state of pores to their size, relative humidity and to temperature have been formulated; these are addressed next.

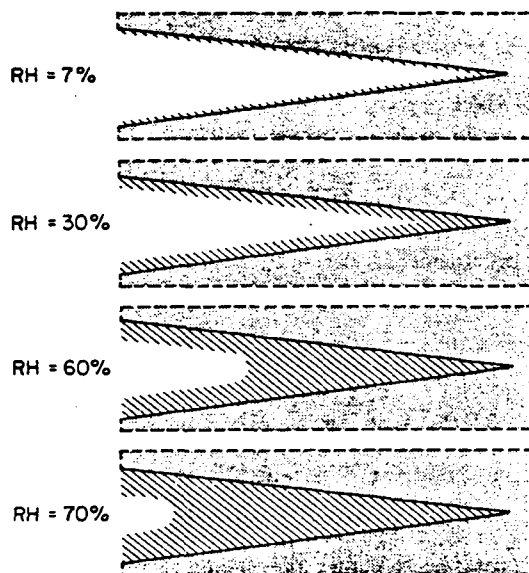


Figure 3.8 Gradual filling of a micropore due to adsorption and capillary condensation (Horrigmoe 1985).

Under conditions of hygrothermal equilibrium between the pores in concrete and the environment, all pores with diameter less than the Kelvin diameter (d_k) would be filled with water, while the pores with diameters exceeding d_k would only have a water film on their surface, of thickness (w). The values of w and d_k (both in μm) can be obtained from the following expressions (Gregg & Sing 1982, Mikhail 1983):

$$w = \frac{C \times d_w}{[1 + (C - 1) x] (1 - x)} (1 - x^{d/2d_w}) \quad (3.1)$$

$$d_k = 2w + \frac{A}{T \ln(1/x)} \quad (3.2)$$

in which: T is the absolute temperature, $x = \text{RH}/100$; RH is the relative humidity (percent), the constant A being equal to 0.6323 for non carbonated material (OPC paste) and 0.2968 for carbonated material, with C representing the BET constant for the particular temperature and the water vapour-solid surface system, and d_w is the molecular diameter of water ($3 \times 10^{-4} \mu\text{m}$).

It is not difficult to imagine that knowing w , d_k , and the pore size distribution of concrete, theoretical predictions can be made for the fraction of pore volume completely filled with water as well as the fraction of pore volume occupied by aqueous films (Papadakis et al. 1991), and the degree of saturation can be estimated as the sum of these two fractions.

The approach above has been tested by Papadakis et al. (1991) and the data are presented in Figure 3.9, in which the degree of saturation of pores at a given relative humidity are presented for concretes of different water/cement ratios. The data plotted in this figure were experimentally obtained from desorption, adsorption measurements, and also predicted from theoretical considerations. It can be seen that, at a given relative humidity level, the value of m obtained during desorption exceeds that obtained

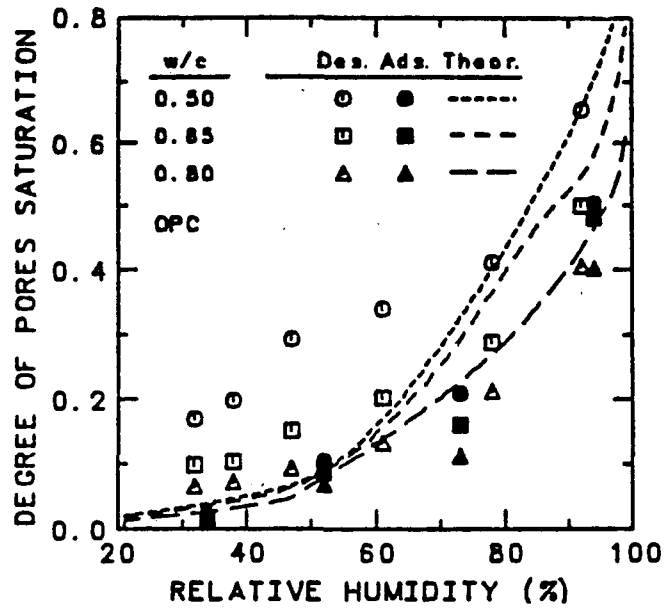


Figure 3.9 The relation between equilibrium relative humidity and moisture content of concrete of different water/cement ratios (Papadakis et al. 1991)

during adsorption, a phenomenon which the authors explained by either the extremely slow rate at which ultimate hygral equilibrium is established, or by the ink-bottle shape of the pores. The latter explanation may, however, be contrary to the liquid-assisted vapour transfer phenomenon which asserts a favourable influence of pore necks on water vapour flow (3.1.3.3.1). A more plausible explanation may rest on the former hypothesis together with the influence of drying which is believed to induce effects which coarsen the cement paste pore structure (3.1.2.2) thus causing the moisture content to be lower at a certain relative humidity. Noteworthy, also, is the observation by Papadakis et al. (1991), which they believe to be consistent with the effect of pore necks, that the theoretical values of m lie close to the adsorption data for low relative humidities and the desorption ones for high RH levels, and are in between for intermediate relative humidities (see Figure 3.9).

Despite these shortcomings, it can be deduced from Figure 3.9 that, at a given equilibrium relative humidity, the degree of saturation of concrete is higher the lower the water/cement ratio, and that this effect is more pronounced at high relative humidity levels; this is almost certainly due to the increase in the proportion of small pores as the water/cement ratio is lowered.

3.1.3.4 Mechanisms of transport of chlorides in concrete

Chlorides from a variety of exposure environments can penetrate concrete through any of the following processes:

i) bulk movement of water containing chlorides into concrete, via the following distinct transport processes: a) absorption in the form of wetting and drying, b) wick action, c) osmotic effects, d) pressure induced flow;

ii) diffusion through the pore solution of concrete.

The following sections provide a description of these transport processes, as well as an analysis of some of the primary factors which influence the rate at which they contribute to chloride ingress.

Common to all processes listed under category (i), except osmosis, is the fact that chlorides are essentially carried with water. Thus, when discussing these processes, emphasis will be given to the transport of water, while highlighting any effects arising from the presence of chlorides.

Before proceeding, it should be pointed out that the discussions in the rest of this chapter should, unless otherwise stated, be understood to relate to plain OPC concrete.

3.2 Chloride ingress through drying and wetting of concrete

3.2.1 Introduction

When concrete is exposed to conditions wherein the relative humidity of the surroundings is lower than that of its pores, water vapour diffuses out of these pores leaving empty spaces. Subsequently, upon exposure to moisture, the empty pore space refills with water, which may contain chlorides, and it is the repeated action of these drying and wetting cycles which may constitute a mechanism whereby large amounts of chlorides penetrate into concrete.

Additionally, wetting and drying may result in salt crystallisation, possibly causing microcracking, which, in turn, is thought to further facilitate the ingress of chlorides into concrete.

3.2.2 Drying of concrete

Movement of water vapour from concrete during drying has been described by Bazant and Najjar (1971) to be a non-linear diffusion process characterised by a water vapour diffusion coefficient (C) which decreases as drying progresses: as the pore relative humidity dropped from 90% to 60%, C dropped from 2.2×10^{-10} to 5.5×10^{-11} m²/s, but remained constant below a relative humidity of 60%. Additionally, in agreement with the above, Lowe et al. (1971) monitored the drying of concrete spheres, and concluded that the diffusion coefficient of water vapour was strongly influenced by the concentration of evaporable water (Figure 3.10). An explanation of these results lies in the fact that water is held in concrete with various degrees of firmness (3.1.3.3.2, see also Table 3.2), making it likely that the removal of water will become more difficult as drying proceeds. Bazant and Najjar (1971), for example, attributed the very slow rate of drying when 60% pore RH was reached to the very slow flow of firmly held water molecules along the strongly adsorbed water layers.

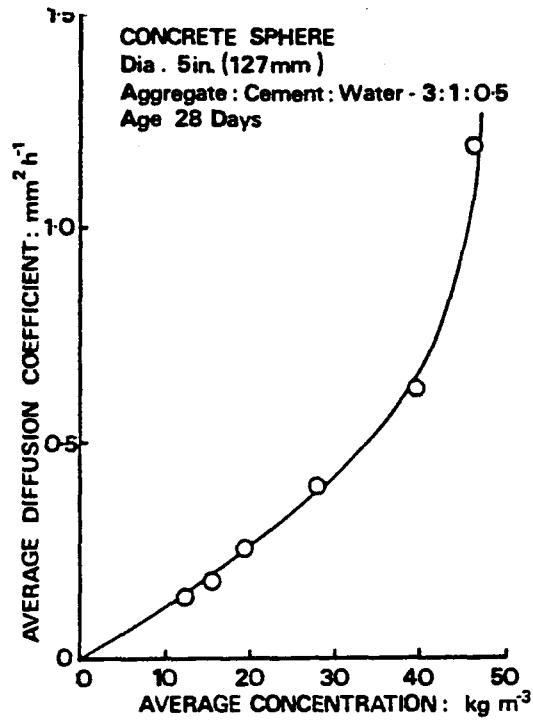


Figure 3.10 Dependence of water vapour diffusion coefficient on concentration of evaporable water (Lowe et al. 1971).

Another factor which is known to influence the rate of drying is temperature, and it is well known that increasing temperature accelerates drying (Figure 3.11). Figure 3.11 reveals an upwards jump in diffusivity as 100°C is exceeded; this can be explained by the change in the mode of moisture transfer when water transforms into vaporised steam above its boiling point. Interestingly, while Figure 3.11 implies that diffusivity increases along a smooth curve with the increase in temperature up to 100°C , the work of Glover and Raask (1972) proposed the presence of a fairly clear inflection point at approximately 50°C which, in their opinion, indicates that water vapour diffusion in hydrated OPC pastes is a structure sensitive process, and that some form of structural re-arrangement occurs upon drying above 50°C .

It seems, therefore, that drying of concrete may result in secondary effects which manifest in an alteration of the paste pore structure and/or microcracking. Also noteworthy, at this point, is that it is generally agreed upon that drying which results in loss of free water results in no shrinkage, hence little microcracking, and its only upon further drying, which removes adsorbed water, that shrinkage occurs fuelling microcracking. Furthermore, it is important to realise that, in practice, the occurrence and severity of microcracking is determined not only by the severity of drying, but also by carbonation shrinkage, creep, and temperature effects.

According to Bazant and Raftshol (1982), cracking almost certainly occurs in most cases of drying of concrete. They argued that for a typical 15 cm concrete wall, a humidity decrease from 100% to 50% would have to gradually take place over 23 years in order to be sure of avoiding cracking and microcracking. Furthermore, they suggested that this cracking takes the form of discontinuous microcracks which, despite their discontinuity, may cause the rate of drying of concrete to increase. More work is, however, required to elucidate the parameters which determine the intensity of this increase.

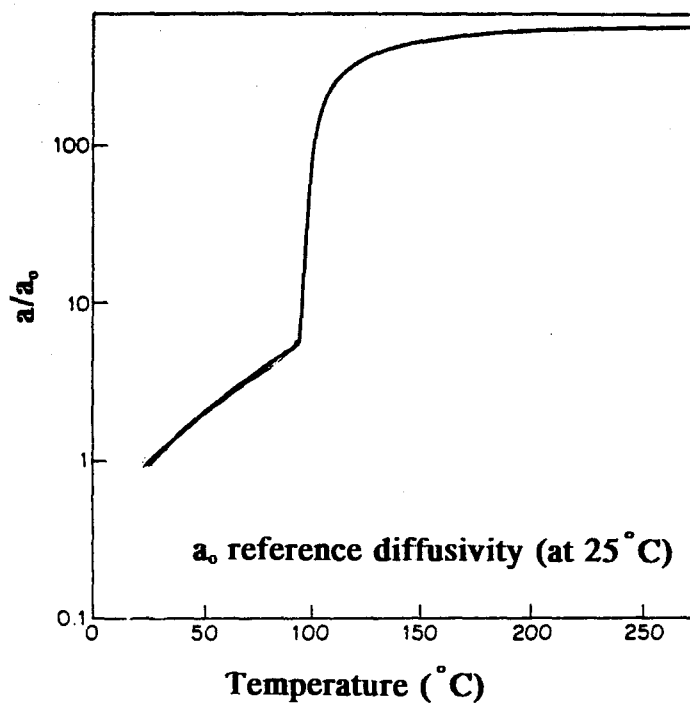


Figure 3.11 Water vapour diffusion as a function of temperature.

Changes in the pore structure of concrete induced by drying can be associated with the phenomenon of irreversible shrinkage; a phenomenon wherein a part of the shrinkage induced by drying remains still unrecovered upon re-wetting, hence thought to be associated with the collapse of parts of the pore system. It is generally accepted that it is only those pores which hold water with some degree of firmness that experience collapse upon the removal of water. This can be illustrated with reference to Table 3.2, which reveals that water is held more strongly in smaller pores.

Table 3.2 The relative humidity below which drying of pore water occurs (Czernin 1980).

	Relative Humidity %			
	99.9	99.0	89.9	34.8
Pore Radius (Å)	10000	1000	100	10

While the precise nature and extent of pore structure damage induced by drying has not been fully clarified to date, it is advocated that the effect is, in general terms, as if the total pore volume is reduced, and the pore structure coarsened. Much information is available concerning the influence of 105 °C drying in OPC and blended cement pastes and concretes, because of the importance of this drying temperature to various durability related tests. For example, Moukwa and Aitcin (1988) suggested that oven dried OPC cement pastes exhibited an increase in the volume of pores between 0.2 μm and 0.1 μm, and that this was more pronounced the lower the water/cement ratio. Further evidence on pore structure collapse with oven drying has been obtained when pore structure measurements were made using both alcohol and water, separately (Day & Marsh 1988). The results showed that, as commonly reported in the literature, porosity values obtained by alcohol re-saturation (after drying to equilibrium at 105 °C) were considerably lower than those obtained by water, and explained this by the inability of alcohol to penetrate those parts of the pore structure which collapsed due to drying. Also, interestingly, they showed that the effect of drying was more

pronounced in the case of well hydrated pfa and also the silica fume pastes. Considering the size range of pores which experience damage upon drying, Midgley and Illston (1983) dried pastes for mercury intrusion measurements in vacuum at 105°C and for electron microscopy by solvent replacement with ether, compared the pore radii obtained by these two techniques, to find a surprising equivalence of pores above 100 Å, suggesting that different drying techniques may, in essence, effect only those pores with radii less than 100 Å; the pores in this size range are of little significance to penetrability.

The comparatively larger collapse in pore structure upon drying in the lower water/cement ratio pastes is easily comprehended when considering that as the water/cement ratio is decreased, the pores generally become of smaller size, causing a larger proportion of pores to experience damage (see Table 3.2 and associated discussion). It is possible that similar considerations also apply in the case of silica fume mixes, as well as in well hydrated pfa mixes; for a more comprehensive treatment, an interested reader is referred to the excellent work by Day and Marsh (1988).

Finally, it should be emphasized that much of the discussion above may not be exactly applicable to the drying of concrete which contains chloride salts. This is because the pore structure-moisture content characteristics already discussed may be altered, and also because the drying of concrete is known to be hindered when chloride salts are present possibly due to the hygroscopic properties of chloride salt solutions. Unfortunately, no work, in relation to cement pastes, which quantifies these effects can be traced in the literature.

3.2.3 Wetting of concrete

3.2.3.1 Background

It is a common observation that if water is brought into contact with unsaturated concrete it will, even in the absence of an imposed pressure, be absorbed into the concrete, because concrete possesses a fine fraction of pores (10 Å to 14000 Å) which have the capacity to absorb water by virtue of capillarity.

In order to establish an understanding of the various parameters involved in water uptake by concrete via capillarity, the simple case, in which concrete may be represented by a mass of straight cylindrical capillary tubes of differing radii and with a mean pore radius (r), is considered.

The suction force F (N) acting in a single capillary of radius r (m), open at both ends and subject to atmospheric pressure P_0 (Pa), is defined by the following equation:

$$F = 2\pi r\sigma \cos\theta \quad (3.3)$$

Where

σ : is the surface tension of the fluid (N/m); and

θ : is the angle of contact of the fluid with the pore wall (degrees).

It is seen from equation 3.3 that the suction force is positive, i.e. the fluid will rise in the capillary, as long as θ is less than 90° . In uncarbonated concrete the capillaries are hydrophillic, i.e. they have very small contact angles to water ($\theta = 0^\circ$ being a reasonable assumption). The maximum height of fluid h_{\max} (m) that can be supported by capillary forces can be calculated as follows:

$$h_{\max} = \frac{2\sigma}{r\rho g} \quad (3.4)$$

where:

ρ : is the density of the fluid; and

g : is the acceleration of gravity (m/s^2)

It is important to realise that, while h_{\max} increases as the diameter of the capillary decreases this is only the case up to a head of fluid equivalent to atmospheric pressure; this is because for surface forces to support a maximum head greater than this value would require the fluid to be under tension, which is theoretically impossible to achieve. Hence, $r_0 = 2\sigma/P_0$ is the capillary size below which a ceiling on the maximum capillary rise is sustained ($h_{\max} = P_0/(\rho g)$) and, for radii larger than r_0 , h_{\max} progressively decreases, according to equation 3.4.

When a capillary is brought into contact with water, the maximum capillary rise does not occur instantaneously, for it is time dependent, and the rise of the fluid (viscosity μ (Pa.s)) with time may be represented by the following expressions:

For $r < r_0$,

$$h = \frac{r}{2} \left(\frac{P_0 t}{\mu} \right)^{\frac{1}{2}} \quad (3.5)$$

and for $r > r_0$,

$$h = \left(\frac{\sigma r t}{2\mu} \right)^{\frac{1}{2}} \quad (3.6)$$

3.2.3.2 Definition of the sorptivity of concrete

Sorptivity is an easily measured property which is often used to characterize the tendency of concrete to absorb and transmit water by capillarity.

Despite the considerable differences in the manner with which many researchers have presented their sorptivity results (e.g. Hall 1981, Fagerlund 1982, Bamforth et al. 1985, Ho & Lewis 1987, Kelham 1988), one common finding does emerge; the early stage of absorption is governed by the square root of time. It is also clear from Equations 3.5 and 3.6, as well as from a review of the literature referred to above, that there exists a linear relationship between the square root of time and the weight gain of a concrete specimen, or the height of penetration of water, or the volume of the absorbed water per unit area of the absorbing surface. One of the mathematical definitions of sorptivity is described below.

According to Kelham (1988), for a cylindrical specimen of concrete of cross sectional area A (mm^2), length l (mm), sealed on its curved surface, placed in contact with water at one end and left open to the air at the other end (Figure 3.12), a plot of the mass M (g) of the specimen against the square root of time takes the form shown in Figure 3.13, and sorptivity S ($\text{mm}/\text{h}^{1/2}$) can be calculated from the slope of the line of phase I, i.e.:

$$S = 10^5 \frac{\text{slope}}{Az} \quad (3.7)$$

in which z can be obtained from the second phase of Figure 3.13, as follows:

$$z = 10^5 \frac{(M_{\text{sat}} - M_0)}{AL} \quad (3.8)$$

where: z represents the effective empty porosity, M_{sat} is the mass of the specimen at saturation, and M_0 is the mass of the specimen at the start of the test.

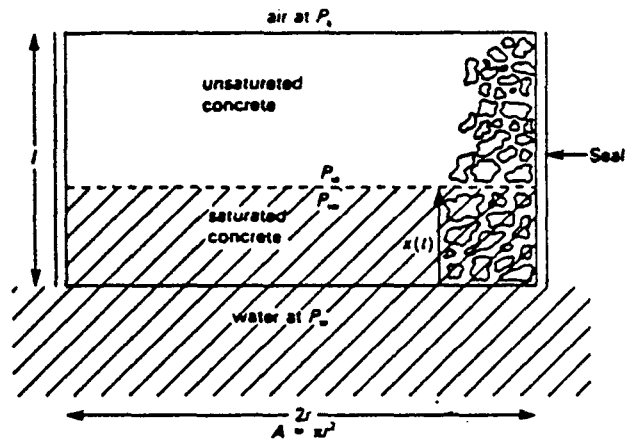


Figure 3.12 Cross section of concrete cylinder considered in analysis.

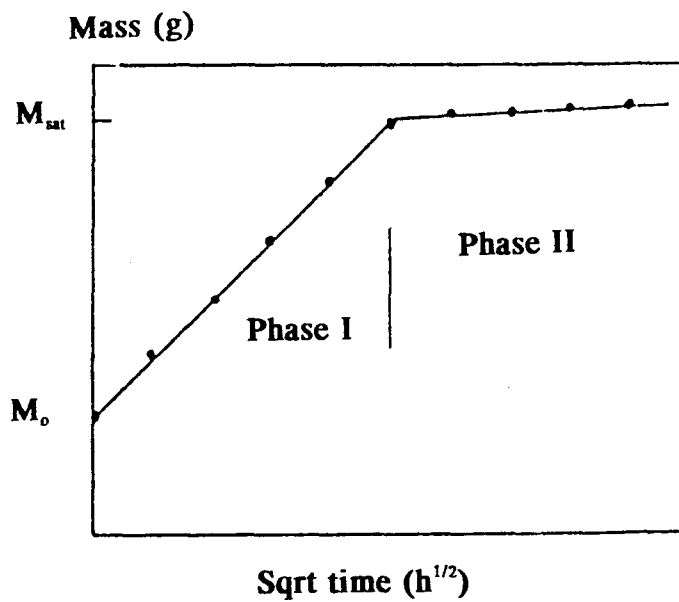


Figure 3.13 Typical capillary rise test output.

3.2.3.3 Factors influencing the sorptivity of concrete

This section focuses on the main parameters which determine the sorptivity of concrete, namely: temperature, presence of chemical impurities in the permeating water, moisture content, porosity, pore size distribution and connectivity of pore space. These parameters are largely inter-related and collectively determine the sorptivity of concrete through their influence on the nature (size fraction) of the pore space available for absorption, and the strength of the capillary forces.

Both temperature and the presence of chemical impurities in the permeating water (e.g. chloride salts, chemicals in sea water) influence sorptivity proportionally through changes in $(\sigma/\mu)^{1/2}$. The changes in the quantity $(\sigma/\mu)^{1/2}$ brought about by moderate changes in temperature are, however, relatively small ($(\sigma/\mu)^{1/2}$ increases from about $7 \text{ m}^{1/2}/\text{s}^{1/2}$ at 5°C to about $10 \text{ m}^{1/2}/\text{s}^{1/2}$ at 35°C), and so are changes resulting from the presence of chemical impurities in water (Macinnes & Nathawad 1980).

Before considering the other factors which influence sorptivity it is useful to refer back to Figure 3.13 which shows the process of absorption of water in concrete occurring in two phases. The first phase is thought to be associated with water being absorbed by the relatively large pores in concrete, while the second phase would probably be dominated by much slower absorption through the relatively small pores, and also by a process involving water vapour diffusion/condensation.

Naturally, for concrete to absorb water, empty pore space must be available to accommodate it. Furthermore, although not directly applicable to concrete, it has been reported (Kirkham & Powers 1972) that capillary suction forces increase dramatically as the degree of saturation of soils decreases from 100 to 20%. It is not surprising, therefore, that sorptivity is often found to be greatly influenced by the moisture state of concrete, and mathematical representations of this relationship have been proposed (Hall 1989, Peer 1990). Additionally, if the concepts of a maximum continuous pore radius or critical pore diameter (3.1.2.2) are assumed to be applicable to absorption in

concrete, then it is the size of such pores and their volume fraction in concrete together with their moisture state (3.1.3.3.3) which should determine the slope of the line in phase I (Figure 3.13). It should be pointed out that adsorption of water to pore surfaces also takes place during absorption (3.1.3.3.1), and the pore should therefore be taken as the effective pore size remaining for liquid flow after adsorption. It has been reported that the thickness of the adsorbed layer is of the order of five water molecules (Horrigmoe 1985)(i.e. 26 \AA should be subtracted from the pore size to obtain the effective pore size); in the case of concrete equilibrated at a certain moisture state before water absorption takes place, the capillary size may be adjusted by calculating the thickness of the resident water layer, using equation 3.1.

Finally, work by McCarter et al. (1992) on the absorption of chloride contaminated water into concrete, revealed that, although little difference is often observed (Macinnis & Nathawad 1980) between the values of sorptivity, based on weight gain measurements, when water or chloride solutions of various concentrations are used, the chloride front moves into concrete at a slightly lower rate than the water in which the chloride is dissolved (although it should be noted that only chloride levels greater than 60 ppm could be detected in these measurements); the reasons for the filtering of chlorides from absorbed water are probably associated with the binding of chlorides by concrete (2.3.1.3). The significance of these observations becomes apparent when considering that the depth of penetration of chlorides would be overestimated if it were calculated using sorptivity values obtained through cumulative weight gain measurements even if chloride solutions were used as the permeating solutions.

3.3 Chloride ingress through wick action

Wick action in concrete denotes the transport of water (and any species it contains, possibly chlorides) from the saturated face of a concrete element to a drying face (Figure 3.14). It may be thought of as a combination of water absorption and water vapour diffusion, where, water vapour leaving the system at the drying face, creates a condition for the water at the saturated face to migrate through the capillaries to replace the lost water.

When chlorides, or any other salts, are present in the permeating water, they crystallise at the location of evaporation and may lead to microstructural disruption and high salt concentrations in the immediate pore solutions; if the moisture condition changes, the crystallised salts may dissolve into the pore solution and diffuse within the concrete.

Despite an established strong relationship between the deterioration of concrete structures in many environments and the transport of aggressive species into concrete by means of wick action, very little research effort has been made to understand the precise nature of wick action in concrete, and even less on the concrete and environmental parameters which govern the rate at which wick action occurs; relevant work is now in progress at Imperial College (Buenfeld & S-Daoudi 1994).

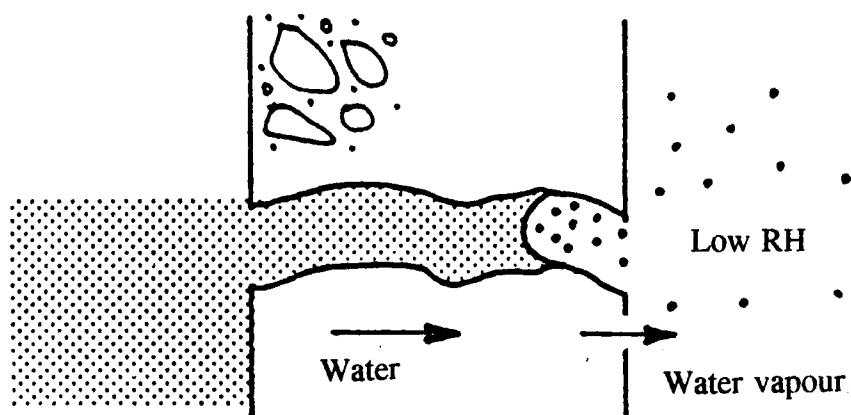


Figure 3.14 Wick action process.

3.4 Chloride ingress through osmotic effects

Osmosis refers to the process whereby water moves through a semi-permeable membrane separating two solutions: a solution of high concentration (ionic or molecular) and a solution of low concentration, from the low concentration side to the high concentration side until both sides equilibrate at an equal intermediate concentration.

The definition of a barrier as a semi-permeable membrane requires that it allows the through movement of water molecules, but not that of soluble species. Bakker (1983) demonstrated, through the arrangement shown in Figure 3.15, that a cement mortar may act as a semi-permeable membrane, with the direction and rate of water movement being dependent on the nature (Figure 3.16) and the concentrations (Figure 3.17) of the solutions involved.

The relative importance of osmotic effects in chloride-laden water transport is difficult to establish since cement pastes are not completely impermeable to ions. In fact, the diffusion of ions through concrete usually takes place in conditions where ionic concentration differences exist (the same conditions which fuel osmosis), relieving somewhat the osmotic pressures. In addition, Figures 3.16 and 3.17 demonstrate that it is only the solutions of relatively high ionic concentrations that can stimulate appreciable osmotic effects (for example in Figure 3.17 it was only at a 120 g/l KOH concentration that flow against a 400 mm water head occurred). Nevertheless, osmosis has been reported to occur in concrete structures under certain conditions: osmosis has been identified (Warlow & Pye 1978) as the cause of blistering of in situ resin flooring on wet concrete, implying that water movement had actually arisen from osmotic pressures.

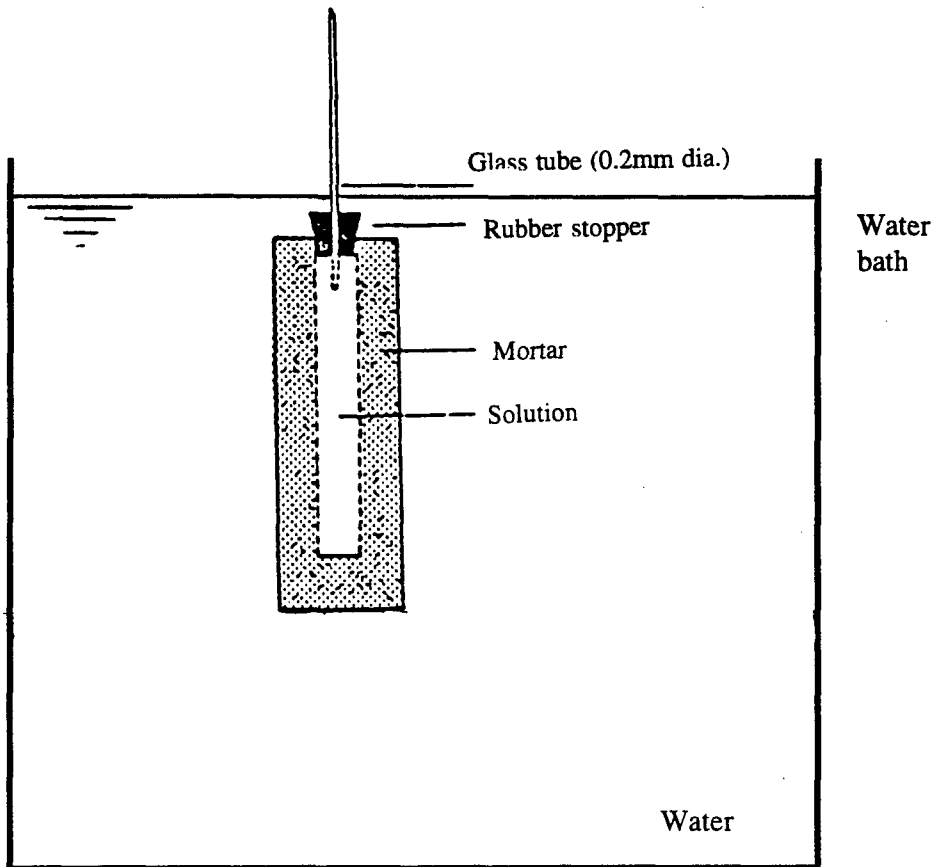


Figure 3.15 Experimental setup for osmosis studies (Bakker 1983).

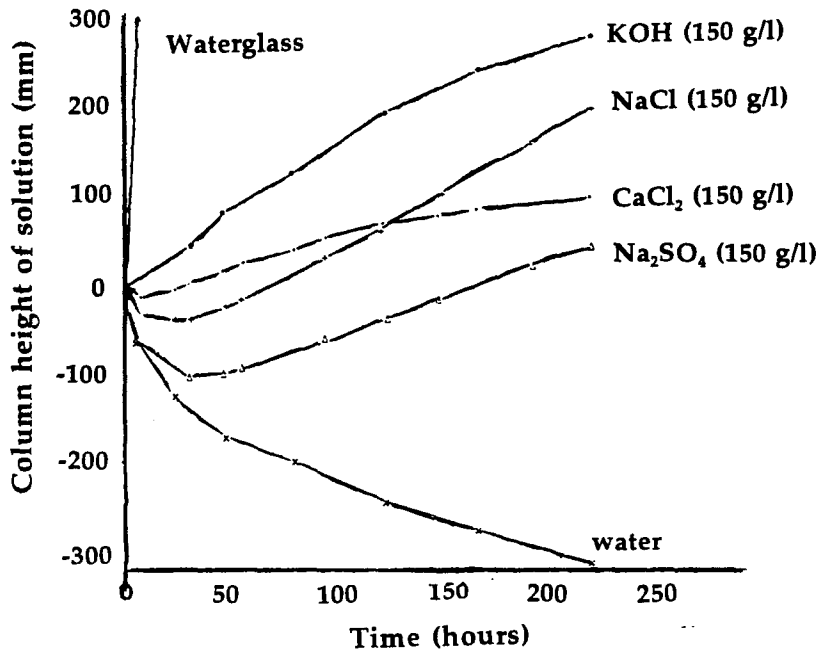


Figure 3.16 Osmotic effect of different solutions on 7-day old OPC mortar (Bakker 1983).

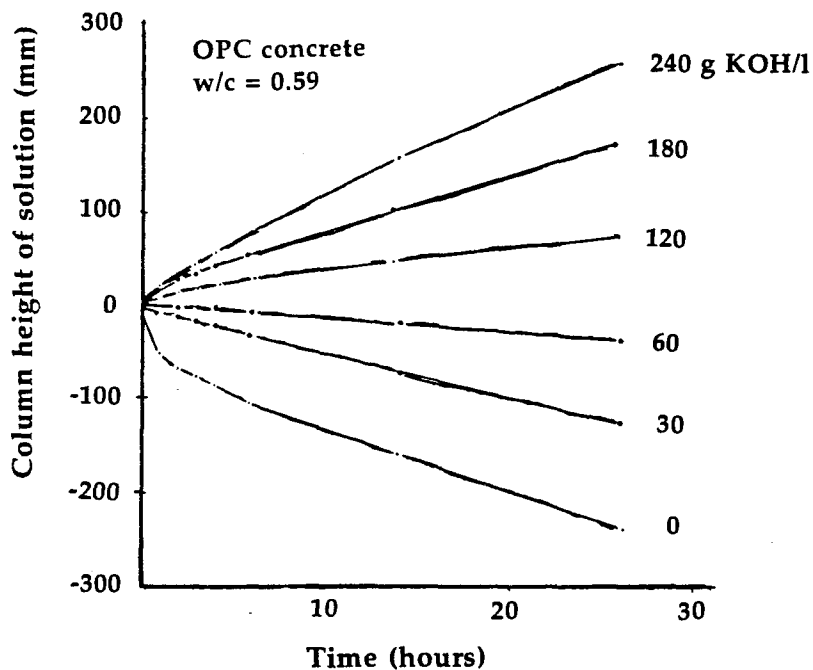


Figure 3.17 The osmotic effect of KOH solution of different concentrations (Bakker 1983).

While the above discussion casts some doubts on the relevance of osmotic effects to chloride transport in concrete, there are suggestions that the influence of osmosis must not be totally ignored (Bakker 1983). Bakker's work demonstrated the fact that the ability of cement mortars to behave as a semi-permeable membranes increases as their pore structure becomes less interconnected, and in a later publication (1985) he argued that while cement pastes are not fully impermeable to ions, they are, though, much less permeable to ions than water, and that under such conditions, osmotic pressures would be generated, possibly leading to the development of microcracking, which can facilitate the ingress of ions.

3.5 Chloride ingress through pressure-induced water flow

3.5.1 Background

Permeability is a flow property, which characterises the ease with which a fluid will pass through porous media under the action of pressure differentials.

A mathematical representation of the volumetric rate of flow Q (m^3/s) of a fluid passing through a saturated porous medium under the action of a hydraulic gradient dh/dl (dh is the hydraulic head loss (m) along the length dl (m)) can be expressed in terms of D'Arcy's law:

$$Q = K_D A \frac{dh}{dl} \quad (3.9)$$

in which A is the cross-sectional area of flow, and K_D (m/s) is termed the coefficient of permeability.

The application of D'Arcy's law to represent the pressure-induced flow of water (or water contaminated with salts), through concrete is subject to disadvantages as it is only applicable to: i) fully saturated concrete, and ii) steady state flow conditions; both of which rarely eventuate in most high quality concretes. Consequently, the modified Valenta equation (Valenta 1970) has been proposed, in which the coefficient of water permeability of concrete K_v (m/s) is expressed in terms of the depth of water penetration d (m) into concrete, the applied head of water h (m), the duration of application t (s), as follows:

$$K_v = \frac{d^2 v}{2ht} \quad (3.10)$$

where the parameter v represents the volume of voids which become filled by water ingress into the initially unsaturated concrete. It should be pointed out, however, that

determining the coefficient of permeability by the Valenta equation is also subject to disadvantages, most important of these is concerned with the fact that, since the concrete tested is not fully saturated, water penetration would be influenced by sorption effects as well as those of the applied pressure, and corrections will have to be made if accurate determinations are sought.

It may be considered disadvantageous that the parameters $K_{(D \text{ or } v)}$ are dependent on the properties of both the permeating fluid and the porous medium. Permeability, however, may be defined in terms of another parameter, which is dependent purely on the properties of the porous medium, namely the intrinsic permeability k (m^2), defined by:

$$k = \kappa \frac{\mu}{\rho g} \quad (3.11)$$

Equation 3.11 is of great importance since it implies that the permeability of concrete to a given fluid (e.g. water, water contaminated with salts (sea water salts, chloride salts), gases) can be predicted provided the permeability coefficient of any other fluid is known. Unfortunately, this is not necessarily true in practice, as will be seen through discussions on the permeability of concrete to gas, water, chloride-contaminated water, and the relationships between the various permeability coefficients.

3.5.2 Water permeability of concrete

As mentioned earlier (3.5.1), pressure-induced water flow in concrete can be characterised by the coefficient of water permeability. It is therefore advantageous, from many viewpoints, to investigate the main factors which influence the water permeability of concrete.

While a discussion of the whole set of factors influencing water permeability is outside the scope of this chapter, it has been observed that the effect of many of these factors may be evaluated in terms of their influence on concrete pore structure characteristics, and it is the principal aim of this section to illustrate this.

Much of the experimental work on the water permeability of cement pastes has been accompanied by pore size distribution determinations employing mercury intrusion porosimetry and, despite the shortcomings of the latter method (3.1.2.2), the literature abounds with suggestions that a strong relationship exists between the volume fraction of the relatively large pores and water permeability coefficients.

It has been firmly established (Mehta & Manmohan 1980, Nyame & Illiston 1980, Goto & Roy 1981, Young 1988) that permeability of pastes and concretes to water decreases as the water/cement ratio decreases and with increased cement hydration. Mehta & Manmohan (1980) related the sharp increase in the water permeability of cement pastes as their water/cement ratios increased from 0.5 to 0.7 to the volume of pores in the 1320 Å range (see Figure 3.2). Admittedly, this finding is of little significance to the behaviour of low (0.5 and less) water/cement ratio pastes, since pores of this order are almost absent in these pastes. Nevertheless, it is important to the permeability behaviour of the corresponding concretes (see Figure 3.6, and accompanying discussion in 3.1.2.2). In other work, Goto and Roy (1981) noted a substantial rise in the permeability of OPC pastes when cured at 60°C, rather than 20°C, and ascribed this behaviour to the presence of pores in the range from 750 Å to 2300 Å in radius in the case of the 60°C cured mixes. Marsh et al. (1985) also reported results for hardened

cement pastes, with and without fly ash, moist cured over a temperature range of 20°C to 65°C, for periods ranging from seven days to one year. These experiments revealed (see Figure 3.18) that none of the low permeability pastes had more than 8% of their bulk-volume in pores greater than 500 Å (the 500 Å value was chosen arbitrarily). Finally, applying an analogy between the flow of mercury under pressure and pressure-induced water flow (3.1.2.2), mathematical relationships, with high correlation coefficients, have been derived, relating the critical pore radius (Mehta & Manmohan 1981), or the primary continuous pore radius (Nyame & Illston 1980), to the coefficient of water permeability.

Changes brought about by the conditions of long exposure to water under pressure may result in the pore structure of test specimens undergoing significant and wide ranging changes, owing to, for example, continuing hydration and autogenous healing, silting of fine particulate material, dissolution, transportation and reprecipitation of $\text{Ca}(\text{OH})_2$, and crystallization (Hearn 1992). These factors, together with the variable test techniques and instrumentation employed, could be partly responsible for the large scatter often encountered with the permeability results reported in the literature.

It could be suggested that, measuring the water permeability coefficient for a particular concrete, the coefficient of permeability of the same concrete relevant to a chloride solution would then be predicted, and the extent and magnitude of chloride ingress resulting from pressure induced flow could be estimated. Unfortunately, there are several complicating factors. Firstly, when a chloride solution penetrates concrete under pressure, a fraction of the chloride is bound, and the advance of the chloride lags behind that of the carrying water; similar observations have been made earlier (3.2.3.3). Under these conditions, chloride ingress has been shown (Wood et al. 1989) to be characterized by chloride concentrations decreasing with the penetration depth. Secondly, the presence of chloride is known to alter the pore structure of concrete probably as a consequence of chloroaluminate formation, or the precipitation of salts: Midgley and Illston (1984) suggested that CaCl_2 formation on the surfaces of the C-S-H was responsible for pore blocking. This is further supported by observations (Kayyali

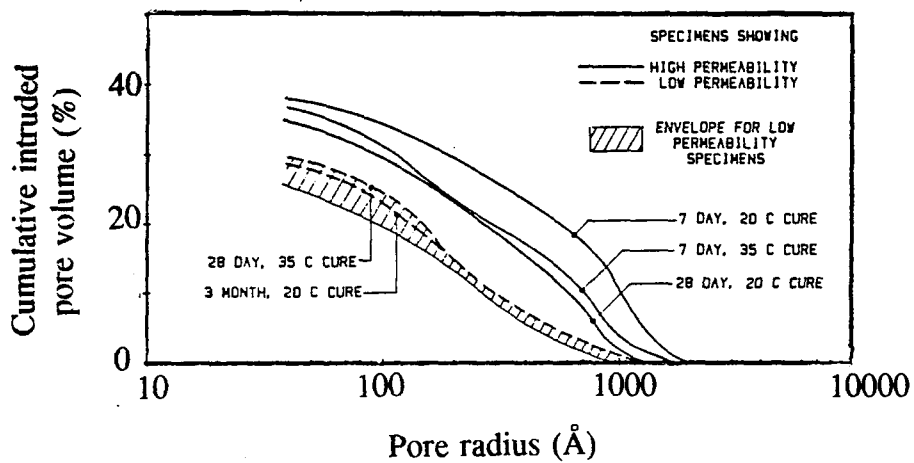


Figure 3.18 Relation between the mercury pore size distribution of pastes and water permeability (Marsh et al. 1985).

& Haque 1988) that, in contrast with specimens cured in saturated air, great difficulty was experienced in expressing pore solutions (by pore pressing) from specimens which were immersed in sodium chloride solution (23400 ppm Cl⁻) for 90 days. Clearly, such behaviour can only be attributed to pore structure refinement which occurred during exposure to the chloride solution. These factors should certainly be taken into consideration if the approach suggested above is to yield results which may be of practical significance.

3.5.3 Gas permeability of concrete

Pressure-induced gas flow in concrete can be characterized by a permeability coefficient, derived from the following expression:

$$Q = \frac{k_{g(D)} A (P_1^2 - P_2^2)}{2\mu L P_2} \quad (3.12)$$

Where P_1 and P_2 are the gas pressures measured at the inlet and outlet faces, respectively, and other parameters are as defined earlier.

Permeability measurements using a variety of flow techniques (Kollek 1989) in which a relatively neutral gas (non reactant, such as oxygen or nitrogen) is employed as the permeating fluid are, compared to water permeability measurements, relatively fast and easy to carry out. Thus, they are considered practical for estimating the intrinsic permeability of concrete. It would be advantageous to derive experimentally, using gas, intrinsic permeability coefficients, and, employing Equation 3.11, predict the corresponding coefficients of water permeability.

Unfortunately, the limited published data comparing water-derived and gas-derived intrinsic permeabilities for concrete indicate that their values may differ significantly (Bamforth 1987, Dhir et al. 1989). One known complicating factor is the occurrence of gas slippage; a phenomenon which results in gas flow being affected by pressure, which, in turn, affects the mean free path of gas molecules, with the consequence of gas flow in concrete being larger than what would be predicted by the Poiseuille formula (the formula from which equation 3.12 has been derived). Bamforth (1987), relying on previous work (on various porous materials other than concrete) by Klinkenberg (1941) and the American Petroleum Institute (1952), derived an expression which can be employed to correct for gas slippage effects. Caution should, however, be raised that the derived expression is likely to be applicable only for the concretes used, and for the particular testing conditions. Dhir et al. (1989) suggested a probably

better approach to correct for gas slippage, and the attraction of their approach is that they did not depend on water permeability results in correcting for gas slippage. Instead, they gradually increased the pressure at which the permeating air was applied and measured the respective permeability coefficients. Constructing a plot of the permeability coefficients versus the reciprocal of the mean applied pressure ($1/P_m$, where $P_m = (P_1 + P_2)/2$), they then extrapolated the straight line portion of this plot to infinite mean pressure ($1/P_m = 0$) to deduce the corrected permeability value. Following this approach, they then compared the water and air permeability coefficients for specimens conditioned, to equilibrium, in two different ways: i) at 20°C and 55% RH, ii) 105°C dried (for water permeability testing the specimens were vacuum saturated after conditioning), as can be seen in Figure 3.19. Two interesting points arise from this figure: i) intrinsic permeability coefficients were generally lower for water, compared to air, under all conditions, and for all mixes, ii) for the less harsh drying technique (20°C and 55% RH), the deviation between the intrinsic permeabilities derived using water and air was wider, especially for low permeability concretes. Explaining their results, they proposed that the swelling of cement hydrates which occurs during water permeability testing is partly responsible. However, it is known that, in addition to the difficulties connected with water permeability testing (3.5.2), gas permeability testing presents additional problems.

It is a well known fact that gas permeability of concrete is strongly influenced by its moisture state (inverse relationship). Attempting to eliminate the effect of moisture, many investigators (Dhir et al. 1989) preferred to completely dry their test specimens often employing harsh drying techniques (105°C to equilibrium). These techniques, however, result in pore structure alterations and microcracking (3.1.2.2, 3.2.2), manifesting in unrealistically high gas permeabilities. Others, therefore, tried less harsh drying techniques (Feldman 1986) which involved equilibrating all their test specimens to the same relative humidity. Such an approach, would not, however, result in attaining the same moisture content since concretes with fine pore structures would equilibrate at greater moisture contents than those with coarser pore structures (3.1.3.3.3). The work of Grube and Lawrence (1984) may, however, provide a

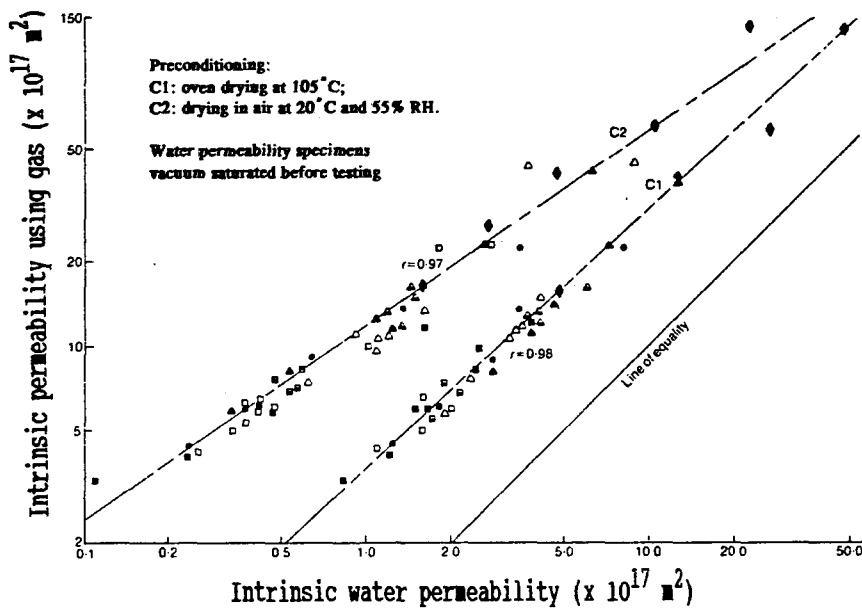


Figure 3.19 Relation between intrinsic water and gas permeability coefficients obtained for concretes conditioned in two different ways (Dhir et al. 1989).

possible solution to these difficulties. They used a wide range of mixes and different curing conditions followed by drying at 55% RH, and observed that once a certain degree of drying had been achieved, the diffusivity of oxygen remained reasonably unaffected by further drying. Similar considerations may, therefore, apply to gas permeability (Lawrence 1984), and common sense dictates that specimens should be equilibrated by employing the least destructive drying techniques, yet achieving a degree of drying such that those pores most responsible for gas transport (see 3.1.2.2) are relatively free of moisture. This approach, while appearing very promising, still faces serious drawbacks: firstly, since differing degrees of drying would be required for different concretes, it follows that differing degrees of microstructural damage may be brought about, distorting the oxygen permeability results. Secondly, in any case, there is little relevant information available, making it impossible to accurately predict the extent of drying required for any given concrete.

3.6 Chloride ingress by diffusion

3.6.1 Introduction

The diffusion of external chlorides into concrete is usually characterised by concentration profiles similar to those shown in Figure 3.20, with chloride concentrations decreasing with the penetration depth and increasing with exposure time. Moreover, throughout the vast literature relevant to ion diffusion in concrete, Fick's second diffusion law (Crank 1975) has often been accepted as a mathematical representation of the process described above (Browne 1982, Raharinaivo et al. 1986, Smolczyk 1984, Buenfeld & Newman 1987, Sergi et al. 1992).

3.6.2 Factors involved in chloride ion diffusion in concrete

Since it is known that most chemical species present in aqueous solutions experience some kind of interaction with any solids with which they come into contact, it is not surprising that ion diffusion in concrete is now known to be influenced by various factors including those involved in physical transport (pore structure and pore size distribution), chemical reactions, and electrochemical interactions.

However, despite the extensive amount of research carried out in order to better the understanding of ion diffusion in cement pastes and concretes, the exact nature and relative importance of the physical, chemical and electrochemical processes involved in ion diffusion, are far from being fully elucidated. This is possibly, at least in part, due to the complex and varied interactions between these processes. Nevertheless, a review of the information available on these processes would be beneficial since it is certainly essential to our understanding of the influence of alterations in concrete and exposure parameters on ion diffusion.

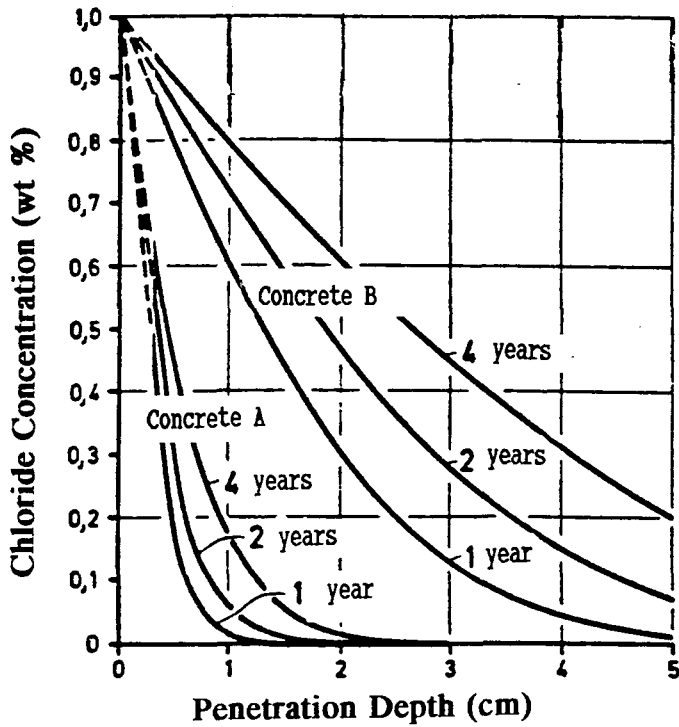


Figure 3.20 Diffusion of external chloride into concrete.

Common to the transport of many species in concrete, many researchers suggested that the pore structure of concrete has an important effect on the diffusion rate of chloride and other ions. Indeed, the effects on ion diffusion induced by changes to concrete parameters have often been discussed in relation to the pore structure changes induced, particularly, to the volume fraction of the relatively large pores. Page et al. (1981), for instance, attributed the larger diffusion coefficients in 0.6 water/cement ratio pastes, compared to those in 0.5 and 0.4 water/cement ratio pastes, to chloride diffusion occurring most readily within the large continuous pore channels (pores with minimum effective neck diameter greater than 1000 \AA) of which a substantial volume was found in the former pastes, while minimal porosity in this range was found in the latter pastes. Another example is the work of Moukwa (1989) wherein he observed a reduction in chloride penetration in mortars with 8% silica fume replacement, and an increase in chloride penetration in mortars with 20% addition of a limestone filler (both compared to a reference plain mortar), and attributed this behaviour to the reduction in the initial volume fraction of pores with radius greater than 300 \AA in the case of the former mortar, and an increase in the volume fraction of these pores in the latter. Additionally, it has been proposed that the increase in the chloride diffusion coefficients, which has often been observed when OPC concrete was cured at elevated temperatures (for example in the case of steam curing), compared to 20°C curing, can be attributed to the coarsening of the pore structure which usually occurs upon curing at elevated temperatures (Detwiler et al. 1991).

Despite these examples, no simple relationship has been established between any of the pore structure parameters and ion diffusion in concrete. This is in contrast to the case of pressure induced water flow where pore structure was closely linked to the coefficient of water permeability (3.5.2), or even to that of molecular diffusion where simple relationships have been suggested: Parrott (Killoh et al. 1989), for example, suggested a relationship of the form l^2/p^4 (l is the concrete layer thickness and p is the large diameter porosity) as a measure of the diffusion resistance of a concrete layer. Indeed, it has been frequently reported that the very low diffusion rates of chlorides and other ions in blended cement pastes could not be explained simply in terms of their

refined pore structures (Gjørv & Vennesland 1979, Page et al. 1981, Smolczyk 1984, Li & Roy 1986). Moreover, in some cases, pore structure determinations indicated trends which were in stark contrast to those of the experimentally measured diffusivities. For example, Page et al. (1981) found an OPC paste containing pfa, in 30% replacement, exhibiting lower chloride diffusivities than the parent OPC paste despite being substantially more porous than the latter. Diab et al. (1988) presented another similar example in observing that, in the cement pastes and mortars which were modified with a polymer (Vinylsulfonic acid), the pore structure was coarser than that of the corresponding portland cement systems, the larger differences in the pore structure actually manifesting in the range of the relatively large pores, and, in spite of these characteristics, the diffusion coefficients of the former pastes and mortars were smaller than those of the latter, by more than one order of magnitude.

Chloride binding (2.3.1.3) is thought to influence the rate of diffusion of chlorides in concrete. The significance of chloroaluminate formation remains the subject of contention. It would, however, be useful to mention some of the views held on this subject. Page et al. (1981) postulated that sulphate resisting cement pastes had a coarser pore structure than that of the corresponding OPC pastes, and thus concluded that, in so far as diffusion kinetics are concerned, the effects of chloroaluminate formation may be of secondary importance compared with the influence of factors determined by pore structure. It should however be pointed out that these conclusions are not surprising since they were made based on diffusion coefficients which were measured under steady state conditions, i.e. chloroaluminate formation could not have contributed to these determinations since (as will be explained later) much of it would have already taken place during the transient state. Nevertheless, Figure 3.21 demonstrates the relatively small effect of chloroaluminate formation since an increase in C_3A content of concretes, from 3.7% to 12.6%, had little influence effect on the chloride profiles; the elevated penetration exhibited by 0% C_3A concretes can be attributed to their coarser pore structure, as demonstrated by Page et al. (1981). Concerning the case of loose binding of chlorides, this falls into the electrochemical factors which will be discussed next.

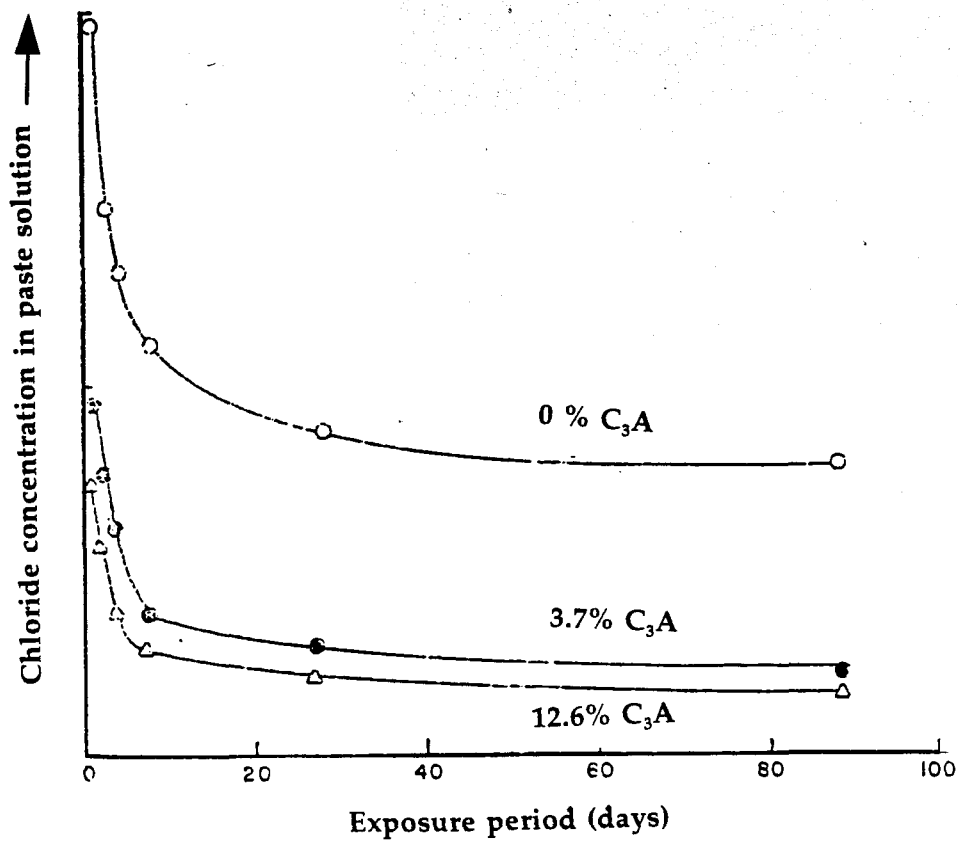


Figure 3.21 The effect of C₃A content of cement on chloride concentration in pore solutions of cement paste after various periods of exposure to a chloride solution (Monfore & Verbeck 1960).

The adsorptive binding of external chlorides by the C-S-H hydrates at the pore walls (2.3.1.3) and the reports of activation energy values for ions diffusing within cement pastes being much greater than those characteristic of the same ions diffusing in dilute solutions (Goto & Roy 1981, Page et al. 1981, Atkinson & Nickerson 1984) lead to suggestions that the interaction between the hydrates at pore wall surfaces and the diffusing ions should impose restrictions on ion diffusion in concrete. Moreover, it has often been reported that when cement pastes were exposed to a salt solution, the diffusion coefficients were higher and the values of the activation energy for diffusion were lower for anions, compared to those of the co-diffusing cations (Ushiyama & Goto 1974, Atkinson & Nickerson 1984, Goto & Roy 1981, Kumar et al. 1987); this behaviour which was observed in cement pastes, whether blended or not, has been taken as evidence that the pore walls in cement pastes may actually be positively charged, possibly because of Ca^{2+} adsorption (Ushiyama & Goto 1974, Kumar et al. 1987). In verification of these phenomenon the work of Yu and Page (1991) is of great significance. They compared the steady state molecular diffusion of dissolved oxygen and that of chloride ions in hydrated OPC and OPC pastes with 20% pfa replacements (Figure 3.22). Dissolved oxygen has a diffusion coefficient in infinitely dilute solutions which is very similar to that of the chloride ion. Moreover, oxygen diffusion is considered not to be affected by electrochemical interactions since oxygen molecules are neutral and possess no dipolar charge. Based on these considerations, the results in Figure 3.22 conclusively ascertain the presence of electrochemical interactions influencing the diffusion of chloride, and other ions in cement pastes.

The question would then arise concerning the relative importance of the hindering effect of these electrochemical forces on ion diffusion in relation to the pore structure considerations (i.e. the physical factors). This may not be so difficult to establish since it is known that electrochemical surface forces become of more significance as the thickness of the double layer increases and also as the pore size decreases. To illustrate this, a value of the order of 100 Å (Goto & Roy 1981) is assumed for the thickness of the electrical double layer (the thickness of the double layer may actually vary depending on the type of pore solution and its ionic strength (Shaw 1966)). It can then

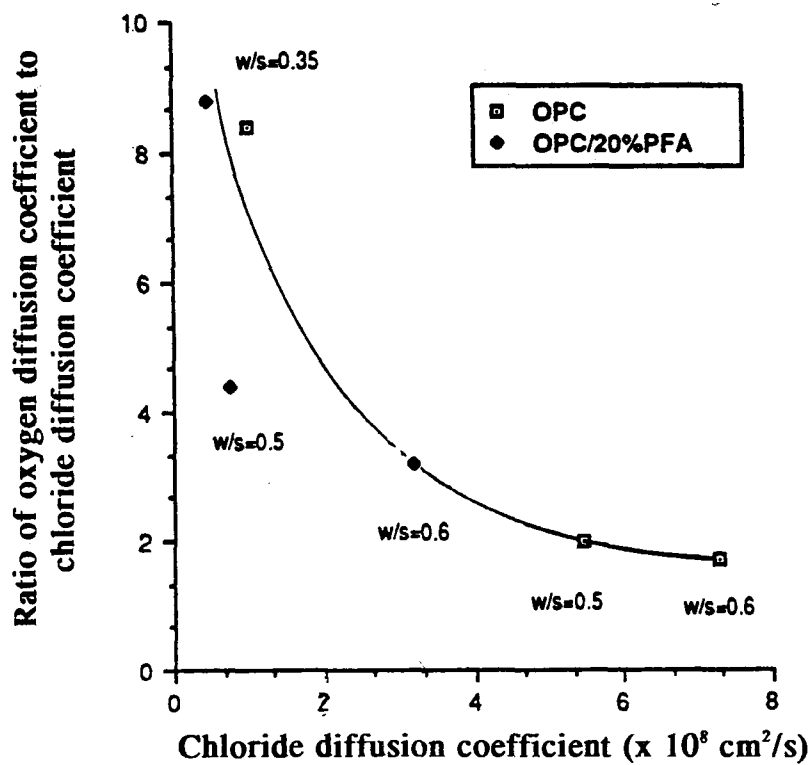


Figure 3.22 Variation of the ratio (oxygen:chloride diffusion coefficients) with chloride diffusion coefficient.

be demonstrated, according to Goto and Roy (1981), that 75% of the volume of the pores which have a 200 Å radius and 44 % of the volume of pores which have 400 Å radius may be affected by the pore-surface forces. This example has important implications since it means that fine pores act to hinder ion transport not only by virtue of their small size but also, more predominantly, by means of surface forces. It also follows that large reductions in the rate of ion diffusion through pastes would be observed as their fine volume fraction increases since ion diffusion paths would, as a consequence, become more tortuous. It is, hence, not surprising that Yu and Page (1991) found the hinderance exerted on chloride ion diffusion, relative to oxygen diffusion, progressively increasing as pastes became denser (see Figure 3.22). Moreover, it affirms the view that ion diffusion may only occur readily if large continuous pore channels exist in abundance, since diffusing ions will then be able to by-pass the fine pore fraction (Page et al. 1981, Atkinson and Nickerson 1988). In connection with this, the observations made by the latter authors are worthy of mention: they examined Cs^+ diffusion profiles in 0.4 water/cement ratio pastes made with sulphate resisting Portland cement, and proposed that the concentration profiles revealed: i) a deep penetrating front which corresponded to fast Cs^+ diffusion occurring in large pore channels with little surface interactions experienced with the surfaces of these pores, and ii) a shallow penetrating part which was indicative of slow Cs^+ diffusion occurring under the action of high surface interactions.

It has often been reported (Kondo et al. 1974, Theissing et al. 1975, Al-Qaser et al. 1990) that the rate of chloride diffusion into concrete, from various chloride solutions having the same chloride concentration, may be considerably affected by the type of cation associated with the chloride, as follows: $D_{\text{Cl}^-}(\text{MgCl}_2) > D_{\text{Cl}^-}(\text{CaCl}_2) > D_{\text{Cl}^-}(\text{LiCl}) > D_{\text{Cl}^-}(\text{KCl}) > D_{\text{Cl}^-}(\text{NaCl})$. Moreover, it has been reported that external chloride ingress accelerates the leaching of $\text{Ca}(\text{OH})_2$ from concrete (Hoffmann 1984, Gégout et al. 1992). These findings suggest that electrochemical factors other than surface interactions may be in action when ions diffuse in concrete. While precise explanations for these phenomenon could not be furnished in the light of existing knowledge, it would be advantageous to review the related literature. Firstly it is important to

emphasize the fact that the exposure of concretes to chloride solutions results in the generation of concentration gradients for all the ions which are present in the system (i.e. the ions of the external solution as well as those already present in the pore solution), hence promoting the diffusion of these ions, possibly in different directions and at different rates (Haufmann 1984, Sergi et al. 1992, Tritthart 1992). It then follows that, since it is imperative that electrical neutrality (charge balance) in the system (concrete+exposure solution) must be in existence and also because of the possible occurrence of charge interactions in the relatively small sized pores present in concrete, the rate of movement of any ion in this system should be affected by the movement of the other ions in the system (Schiessl 1987). Indeed, suggestions which are in accord with these hypotheses have been made; these are covered next.

Li and Roy (1986) proposed that the higher, in comparison to plain OPC mixes, resistance to Cl⁻ ion diffusion exhibited by OPC/fly ash pastes could be partially attributed to a combination of the following:

- i) the increase in the total concentration of cations which, in view of their low mobility, resist chloride diffusion, namely Ca²⁺, Al³⁺, and Si⁴⁺ (the Al probably exists as a complex ion such as AlOH²⁺, and the Si as a complex ion or multimetric species); and
- ii) the reduced K⁺ ion concentration, since K⁺ is known to increase Cl⁻ ion mobility.

According to GjØrv (1968), great amounts of chloride ions can penetrate into concrete from fresh circulating sea water without the penetration of equivalent amounts of sodium ions. Furthermore, it has already been mentioned that the diffusion rate of chlorides was found to be higher than that of the co-existing cations, and that chloride ingress into concrete accelerates Ca(OH)₂ leaching. Collectively, these findings strongly suggest that the exchange of anions between salt solutions and the pore solution of the concrete is an important mechanism which contributes to accelerate chloride diffusion. This can be realised when considering that blended cement pastes exhibit lower chloride diffusion rates, compared to the corresponding OPC pastes, partly because their pore solutions have lower concentrations of hydroxyl ions, which, in turn, implies a lower capacity for exchanging anions with the permeating solution (GjØrv & Vennesland

1979). In another case, Moukwa (1989) regarded the increased chloride penetration when mortars were exposed to sea water at -1°C (see Figure 3.23), compared with that of exposure at 20°C , to be probably due to the increased dissolution of calcium hydroxide at low temperatures. Moreover, it has been frequently reported (Hoffmann 1984, Gégout et al. 1992) that $\text{Ca}(\text{OH})_2$ leaching would manifest in the creation of residual porosity with the effect of increasing the volume of macro porosity; this would further encourage chloride diffusion.

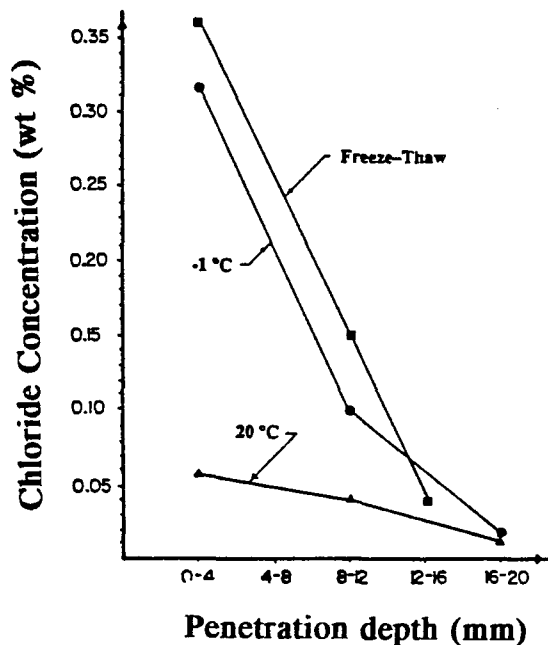


Figure 3.23 Chloride ion entration profiles for an OPC mortar immersed in chloride solutions under three different conditions: -1°C storage temperature; 20°C storage temperature; freeze-thaw cycling.

Chapter 4 Protection Against Chloride-Induced Corrosion in New Construction

4.1 Introduction

4.1.1 General

The increasing instances, over the past two decades, of severe deterioration caused by chloride-induced reinforcement corrosion has prompted considerable interest in research aimed at developing means of reducing the risk of unacceptable distress occurring within the design lives of concrete structures (reinforced and prestressed) exposed to chloride-rich environments. Various methods have since been explored. These broadly fall into three categories:

- methods for retarding the ingress of chloride into concrete;
- methods for reducing the rate at which corrosion proceeds when threshold levels of chloride eventually reach the reinforcing steel;
- optimising design (architectural and structural) and construction practices;

The first two methods are often referred to in the literature as "protective" or "preventative" methods.

This chapter presents a general, but by no means exhaustive, account of protective methods, based on a review of relevant research and field experience. The discussion is focused on providing a general description of the manner by which protective methods counteract chloride-induced corrosion, and the principal advantages and disadvantages inherent in their use.

4.1.2 Accelerated corrosion testing

This section is primarily concerned with the consequences of using accelerated corrosion testing, as has often been the case, in evaluating the performance of protected concretes; for a more detailed discussion on the advantages and disadvantages of accelerated corrosion testing, the CRC Technical Committee (1974) provides an excellent review.

Anticipating that reinforcement corrosion would take place at very slow rates in protected concretes, researchers have often resorted to accelerate the onset of corrosion, by performing their tests under conditions which, along with other effects, cause large amounts of chloride to reach the level of reinforcement within practically acceptable test durations (1-3 years). These conditions involved, usually, combinations of the following: i) accelerating the ingress of chloride salts by subjecting test specimens to many cycles of severe (relatively high temperature and very low RH) drying followed by wetting with a chloride solution, ii) using test solutions with relatively high chloride concentrations, iii) using small depths (10-30 mm) of relatively low quality concrete (water/cement ratio greater than 0.55, and cement content lower than 300 kg/m³) to provide cover to the embedded reinforcement. Such conditions are evidently much harsher than those encountered in real situations, and inevitably give rise to unrealistic damage in test specimens. A consequence of that would be that whilst it may be possible to recommend the use of a protective measure based on test results which show excellent performance, it would, on the other hand, be difficult to arrive at definite conclusions when test results reveal bad, or even average, levels of protection. Moreover, while such tests can help establish whether the use of a given protective technique would provide an advantage as against low quality unprotected concrete, the information so obtained would be of little benefit in predicting the extent of extra benefit that would be provided by such measures in circumstances of actual practice, where much better quality concretes with high cover depths are used under long-term normal exposure conditions.

4.2 Methods of increasing corrosion resistance of reinforcement

4.2.1 Corrosion inhibitors

Corrosion inhibitors have been used extensively and successfully in various industries for nearly 100 years, and the use of such materials in concrete is an extension of this concept. Although a wide range of materials have been found to be effective in corrosion inhibition in concrete, interest has recently been focused on calcium nitrate primarily because, unlike the other materials of the class, it has no adverse effects on the mechanical properties of concrete (Berke et al. 1988).

Extensive laboratory research involving accelerated corrosion testing revealed that calcium nitrate, when added in sufficient quantities, not only largely delays corrosion initiation, but also considerably retards the rate of corrosion as corrosion propagates (Virmani et al. 1983, Berke et al. 1988, Hope & Ip 1989, El-Jazairi et al. 1990).

Calcium nitrate counteracts reinforcement corrosion by virtue of a chemical reaction whereby the ferrous ions produced at anodic sites are removed by the nitrates and converted into stable passive products. In the presence of chlorides, the nitrates compete with the chloride ions for the ferrous ions and, consequently, it is the relative concentration of chloride and nitrate present in the vicinity of the reinforcing steel which determines the type of reaction which would eventually take place. It is not surprising, therefore, that the protective benefits of calcium nitrate have been found to increase as the addition dose is increased, and that recommendations for effective calcium doses have often been expressed in terms of threshold nitrate/chloride ratios (Berke et al. 1988, El-Jazairi et al. 1990). It is to be recalled, however, that these ratios have been derived through accelerated corrosion testing and it is possible, therefore (see 4.1.2), that they would overestimate the nitrate dose required at a given chloride level, because they tend not to take account of the favourable effects (in limiting corrosion rates) of the nitrate action being supported, as would be the case in practice, by the use of high reinforcement cover of good quality concrete. Nevertheless,

adopting such high levels of addition is desirable for two reasons. Firstly, it is often very difficult to predict the chloride concentrations against which protection is required. Secondly, there have been some suggestions (Hope & Ip 1989, Nurenberger 1988) that nitrates are not suitable for conditions of continuous exposure to chlorides since they are consumed during inhibition and may leach.

The performance of calcium nitrate at crack locations is also a subject of debate. Collepari et al. (1990) maintain that their experiments show that corrosion inhibitors (sodium nitrate being used) lead to more severe (compared to unmodified concrete) pitting corrosion at crack locations. They explain that the inhibitor ceases to be effective at crack locations (because very high concentrations of chloride relative to nitrates eventuate at crack locations) while remaining effective in the neighbouring sound concrete and can thereby lead to high potential differences and result in intense macro-cell action (see 2.1.2.2.2). Others (Berke & Rosenberg 1990, El Jazairi et al. 1990), however, maintain that calcium nitrate is effective even when cracks are present. In any case, it should be recalled that cracks generally become of less significance to the corrosion behaviour of structural members the higher the quality of the concrete used (see 2.5), and this probably explains the conclusions that El-Jazairi et al. (1990) arrived at.

Reports on field performance of structures where calcium nitrate has been used are scarce. It is worth noting, however, that to date, and after more than 10 years of commercial use in the USA, no instances of corrosion-induced deterioration have been reported. Noteworthy also is that, as reported by El-Jazairi et al. (1990), analysis of nitrate levels in a bridge deck after 8 years in service revealed that nitrate levels at the reinforcing bars remained high. For more recent developments, involving the use of calcium nitrate in concrete containing cement replacement materials (Florida bridges), the interested reader is referred to Armaghani et al. (1993).

4.2.2 Corrosion resistant and corrosion protected reinforcement

4.2.2.1 Corrosion resistant reinforcement

Widespread research has not been undertaken on the performance of corrosion resistant (alloy) steel. Treadaway et al. (1989) investigated various alloy steels as part of a wider investigation and found that austenitic stainless steels have a very high resistance to pitting even in concrete heavily contaminated with chloride (3% internal chloride by weight of cement), but that ferretic stainless steels, with lesser degrees of alloying, display substantially inferior corrosion resistance under similar circumstances. It is noteworthy also that the performance of austenitic stainless steels has been found (Sørensen & Jensen 1990) to be undermined by welding, and that in any case they are unlikely to find wide application in concrete construction as they are very expensive.

4.2.2.2 Corrosion protected reinforcement

Reinforcement can be protected against corrosion by physically isolating it from harmful substances through the use of inert coatings, and/or by coating with materials of sacrificial nature (Schiessl 1987).

Two types of corrosion protected reinforcement which have received considerable attention, both in laboratory research and field applications, are galvanised reinforcement and epoxy coated reinforcement.

Galvanizing has been used for over a century and a half as a means of protecting steel against corrosion. The technique results in the formation of complex coating layers (of zinc and zinc-iron alloys) metallurgically bonded to the steel base. The coating layer thus functions as an integral barrier and also provides sacrificial protection against corrosion. When embedded in concrete, certain chemical reactions between the zinc coating and the pore solution alkalis cause a reduction in bond strength between the galvanized bars and the concrete (Swamy 1990). Fortunately, this weakness can be remedied through chromate treatment of galvanized bars. In fact, it has been reported (Sarja et al. 1984) that chromate treatment results in galvanized bars displaying even better bond compared with normal reinforcement. Unfortunately, the literature abounds with contradictory information regarding the performance of galvanized steel in chloride-contaminated concrete. Accelerated corrosion studies (Shimada & Nishi 1983, ACI Committee 222 1985, Swamy et al. 1988, Treadaway et al. 1989, Swamy 1990) on small-scale laboratory made specimens revealed that galvanizing steel considerably delays the onset of corrosion; however, as concrete becomes heavily contaminated with chloride, galvanized bars, despite displaying less intense corrosion compared with normal unprotected steels, still show signs of appreciable corrosion in the form of extensive zinc loss, pitting, and cracking (of test specimens). As for field performance, examination of bridge decks and marine structures (Cornet & Bresler 1981, Swamy 1990) in which chloride concentrations were found to be well in excess of the threshold value needed to cause corrosion of untreated steel revealed no evidence of corrosion or

impaired performance of the concrete. There are, however, cases (Sopler 1973) where the use of galvanized reinforcement in marine structures delayed the onset of delamination and spalling, but did not prevent them.

The main impetus for the development of organic (inert) coatings has come from the USA. Amongst a wide range of different coatings examined, electrostatically applied epoxy coatings were generally found to perform best and hence major developments have been centred around them. The performance of epoxy-coated reinforcing steels has been the subject of extensive laboratory testing (primarily accelerated corrosion testing). The work reveals almost conclusively that even in concrete heavily contaminated with chloride undamaged epoxy coated reinforcement suffers substantially less corrosion than normal reinforcing steels (ACI Workshop Committee 1988, Swamy et al. 1988, Salparanta 1990, Yeomans 1991). In field applications (mostly bridge decks), epoxy coated reinforcement has also been found to perform substantially better than normal reinforcing steels (Weyers & Cady 1987, Babaei & Hawkins 1988). However, there are adverse effects associated with the use of epoxy reinforcement that should not be overlooked. The inert nature of the epoxy coating and its smooth surface reduces the bond strength with concrete by as much as 20%, in comparison with uncoated steel bars (Treece & Jirsa 1989, Yeomans 1991). It has also been reported (Al-Sulaimani 1989) that increasing the thickness of the epoxy coating, which is known to have a favourable effect in terms of corrosion protection, exacerbates the adverse effects of the coating on bond strength. New bridge and parking garage decks constructed using epoxy-coated reinforcing bars have been observed to develop an excessive amount of deep cracks during the early stages of curing, and it was suggested (ACI Workshop Committee 1988) that this phenomenon results from the interactive influence of: i) greater shrinkage of concretes (high cement contents) and the high concrete strength, ii) large cover over the reinforcement (epoxy-coated rebars not as effective in restraining cracking at the surface), and iii) lower "in-and-out" bond strength (transfer of tensile thrust in to the reinforcing bar at cracks and away from cracks) of epoxy-coated rebars. Nevertheless, it is now thought (Cairns & Abdullah 1989, Yeomans 1991) that the use of deformed epoxy-coated reinforcement (instead of plain reinforcement) can help

alleviate the problems associated with bond strength. Another perhaps more serious problem facing the use of epoxy-coated reinforcement is related to loss of protection as a consequence of damage to the protective epoxy coating. Although epoxy coatings are quite flexible and have good adhesion to steel, they can be easily damaged during storage (due, for example, to exposure to salts, severe temperature cycling, ultraviolet exposure (Dickie 1986, Leidheiser 1987, Funke 1988)), handling, transportation, fabrication, and fixing. Epoxy coatings have also been shown to sustain damage during service, as they tend to flow away from high stress locations (ACI Workshop Committee 1988). It is not surprising, in view of the above, that extensive research has been carried out to assess the performance of damaged (artificially) coatings. The results of this work were generally favourable, for they reveal that whilst the protection provided by epoxy-coating is impaired by damage, especially when cracks coincide with the damaged locations, epoxy-coated rebars still experience substantially reduced corrosion when compared with unprotected reinforcement (Swamy et al. 1988, Salparanta 1990, Yeomans 1991). Unfortunately, however, testing (accelerated corrosion testing) was mostly performed on small-scale laboratory made specimens and, therefore, does not investigate the possibility, as may be the case in practice, of electrochemical coupling occurring between a damaged location on the protected reinforcement (small anode) and large parts of unprotected steel (large cathode); such conditions raise much concern since they may lead to severe pitting (2.1.2.2.2). It has indeed been suggested (Sagues et al. 1990) that such phenomena partly explain why epoxy-coated reinforcement in the substructures of several bridges exposed in the subtropical marine environment of Florida suffered rapid (in less than 10 years) and extensive corrosion; it is worth noting that following this experience the Florida Department of Transport decided to stop the use of epoxy-coated rebars in new bridges (Armaghani et al. 1993)(it should be noted that these are bridges exposed to a hot wet (8.2) marine environment, not to deicing salts).

The aforementioned raises concern regarding the use of any protective technique which may suffer damage or interruptions. An obvious solution to this problem is to apply protection to all parts of a structure whose reinforcement is electrically interconnected.

4.3 Methods of reducing chloride ingress into concrete

4.3.1 General

The principal function of protective methods in this category is to reduce the rate of ingress of chloride into concrete. Moreover, since the ingress of other species which are necessary for corrosion propagation (e.g. oxygen, water) may be also retarded, the net effect will be that the initiation of corrosion is delayed and its propagation suppressed.

The mechanism(s) responsible for chloride transport vary according to the exposure environment (Chapter 8). To be effective a protective method should be capable of reducing the ingress of chlorides via all the relevant transport mechanisms. A review of published literature revealed, rather surprisingly, that much of the research carried out on the protective techniques belonging to this category employed accelerated corrosion testing (see 4.1.2) and, as a consequence, information on how the various methods affect the individual chloride transport processes is often unavailable.

4.3.2 Polymer impregnation

In this method, concrete is subjected to drying (by application of heat) before being impregnated with a monomer, which is then polymerized using heat or radiation. The object of this treatment is to seal with polymer a large proportion of the pores which allow chloride ingress. Since a substantial portion of the pore space which is filled by polymer is obtained by removing, by means of drying, free water from pores in concrete, the extent to which concrete is impregnated (i.e. whether concrete is partially or fully impregnated) and the thickness of the impregnated layer is largely dependent on the degree and the depth to which concrete is dried. Under laboratory conditions, or the carefully controlled conditions of precast concrete production, impregnation results in an appreciable proportion of pores being sealed by polymer along with any cracks induced by drying (polymer impregnation is often performed by application of pressure), and the resulting composite material has been found to be of substantially lower penetrability than the parent concrete (Fowler & Paul 1978, Shindou et al. 1986, ACI Committee 548 1986). However, the results of field applications have not been so impressive. A report published by the Bureau of Reclamation and Federal Highway Administration (based on an investigation of a number of impregnated bridge decks) indicates that the principal deficiency with polymer impregnation has been the tendency of the concrete to crack as a consequence of the heat treatment (ACI Committee 548 1986). Therefore, and also due to numerous practical difficulties and financial considerations, polymer impregnation in the field has often been limited to small depths (about 25mm) below the surface of concrete members, and it is widely reported (Smoak 1976, ACI Committee 548 1986) that the resistance to chloride penetration of such treatments, though still better than that of the parent concrete, has not been particularly impressive. It is perhaps worth noting that in small-scale field trails (Cady et al. 1987) the impregnated layer was extended to encapsulate the reinforcing steel (3/4 in. depth), and the result was a huge improvement over adjacent untreated concrete, both in terms of retarding chloride ingress and corrosion protection.

4.3.3 Surface treatments

The technology associated with surface treatments is rapidly expanding and many new products are constantly being developed. Unfortunately, to date, there are various factors which erode confidence in the ability of surface treatments to fulfil their intended function; these are summarized below.

- Although many surface treatments have been variously evaluated and shown to be very effective, being of a specific generic type does not guarantee effectiveness: there are many reported cases (Hankins 1985, Aitken & Litvan 1989, Hansen & Villasden 1989) of surface treatments of similar generic types exhibiting considerably different degrees of performance.
- It is often difficult to ensure that no poorly protected areas are present after treatment (see 4.2.2.2). Poorly protected areas can arise from: i) inherent faults, ii) damage during installation, iii) difficulty of application at some locations, iv) exposure (Babaei & Hawkins 1988, Oshiro & Tanigawa 1988, Wei et al. 1990, Carter 1991), and also from v) incompatibility with the underlying concrete in terms of the moduli of elasticity and thermal expansion (Swamy & Tanikawa 1990). It is not surprising, therefore, that surface treatments have generally been found (ACI Committee 222 1985) to display impressive protective qualities when carefully applied in the laboratory, yet display variable performance (ranging from excellent to bad) when applied in the field, depending on the quality of the workmanship, weather conditions at the time of installation, design details, and the nature of the service environment.
- The majority of surface treatments are themselves of limited durability and require reapplication in, usually, less than, say, 20 years. Reapplication may be difficult in some cases and is simply impossible under some conditions of exposure.

There are in general three types of protective surface treatments: barrier coatings, impregnants, and overlays.

Barrier coatings comprise preformed sheet systems and liquid applied materials. The purpose of such treatments is to provide a protective barrier physically limiting ingress of water and chloride ions.

The majority of impregnants, usually supplied in solution form or as a suspension in a solvent, derive their protective property from physically blocking the capillary pore system to varying depths (usually only a few millimetres) from the concrete surface. Silane and siloxane-based impregnants, which are currently attracting considerable interest (Perenchio 1988), are, however, an exception: these, by virtue of a series of chemical reactions, render the capillary pore surfaces in the treated concrete water repelling (Wong et al. 1983), thus, primarily function to hinder the absorption of chloride-containing water.

Overlays, of varying thicknesses, are usually made from cementitious systems known to have high resistance to chloride penetration. Examples of widely used systems are: polymer concretes, polymer modified mortar and concretes, OPC concretes with high cement content and low (0.35 or lower) water/cement ratio.

4.3.4 Material design and admixtures

It is universally accepted that designing durable concrete structures for service in chloride-rich environments requires that careful attention be given first to the selection and proportioning of the basic concrete constituents (cement, aggregates, and mix water), to maximize the inherent resistance of the resulting concrete to chloride penetration. However, it is now widely accepted that the severity of the conditions of exposure in many chloride-rich environments is such that additional protection is required. The preceding sections revealed that substantial benefits can be gained by applying various protective techniques. However, the majority of these methods were also found to suffer from various, in some cases serious, shortcomings, and there would seem to be great potential for developing admixtures (mineral, chemical) to modify concrete such that it becomes more resistant to chloride penetration.

Chapter 5 Phase 1: Preliminary Testing

5.1 Materials

A thorough literature and product survey was undertaken to identify basic materials and proprietary products which have the potential to modify concrete such that it becomes more resistant to the ingress of chlorides via any of the transport mechanisms discussed earlier (3.1.3.4).

A huge variety of materials were found to exhibit the potential to satisfy the criteria outlined above. They were found to fall into two groups, according to whether they:

- i) reduce bulk movement of chloride-containing waters, or
- ii) reduce chloride ion diffusion.

I) Admixtures to reduce bulk movement of chloride-laden water into concrete

Concrete admixtures with the principal function of reducing the penetration of water into hardened concrete have been available for many years, and their use and applications have often been reviewed (Fulton 1969, Lea 1970, Rixon & Mailvaganam 1986, Hewlett et al. 1988, ACI Committee 212 1989). Such admixtures have usually been referred to as "integral waterproofers"; however, it may be of interest to note that, since the use of the name "waterproofer" implies prevention or stoppage of water transmission, which has not been found to be brought about by inclusion of these admixtures, the term "integral waterproofer" has been deprecated in the British Standard Glossary of Building and Civil Engineering Terms (BS6100; Section 6.4) and the term recommended instead is "water-resisting" admixtures.

Water penetration can take place via a variety of transport mechanisms (Chapter 3). Admixtures, however, were found to have been developed to target only two of these mechanisms, namely pressure-induced water flow and water absorption by capillary action. Indeed, the term "integral waterproofer" has been used in reference to any

material (powder, liquid, or suspension) that when intimately mixed with fresh concrete results in:

- (i) reduction in the hydraulic permeability of the cured concrete mass; and/or
- (ii) a water repelling or hydrophobic property being imparted to the set concrete.

Admixtures which can impart the first function have often been referred to as "permeability reducers", while the terms "water repellents", "hydrophobers", or "dampproofers" have been used in reference to those capable of imparting the second function.

The history of waterproofing admixtures can best be described as sparse and full of generalisations, and their performance is uncertain. Most of the work done on their use as integral waterproofers was performed in the early part of the century (White & Bateman 1926, Jumper 1931), and, throughout, they have received little attention in comparison with other classes of admixtures. This can be attributed partly to a general disbelief in their efficacy as waterproofers, which might have stemmed from various factors, some of which are listed below:

- inclusion of many waterproofers in concrete often caused large reductions in compressive strength, and this was considered to be a major disadvantage, for two reasons: i) earlier cements were slow, relative to modern cements, in attaining strength, and ii) earlier in the century, emphasis in concrete mix design was mainly focused on achieving high compressive strengths as an assurance of the attainment of good quality concrete.
- many waterproofers were marketed under proprietary names as potential waterproofers. They were formulated from mixtures of several materials and makers rarely disclosed their composition.

- partly because of the difficulties encountered in reliably demonstrating the imparted property of waterproofness, and their complex nature, the use of the majority of waterproofers seems to have preceded any detailed understanding of their mode of action. This has, in many cases, led to them being used in applications where they were unsuitable. As a consequence, vast variations in their short and long-term performance have been reported; indeed, conflicting accounts of their performance are often encountered.

It was also evident from the review that very little reference has been made to the use of these materials as a means to reduce the risk of chloride-induced corrosion. Indeed, many of the formulations developed had inclusions of chloride salts (especially calcium chloride as an accelerating agent). Moreover, they have often been employed to generally low quality concretes; concretes which would not be used normally in structures subjected to chloride-rich environments.

II) Admixtures to reduce chloride diffusion in concrete

Chloride diffusion in concrete has received considerable attention, yet the factors which determine this process remain only partly elucidated and the subject of considerable contention (3.6). It is, therefore, not surprising that little effort has been directed at developing admixtures to reduce chloride diffusion in concrete; nonetheless, some materials have been experimentally shown to retard this process appreciably.

The preceding discussions highlight the limited relevance of past research and experience to this work. Therefore, a decision was made to adopt a fresh approach, i.e. to carry out a preliminary investigation, to identify the materials that merit subsequent detailed consideration, and their dose levels.

A decision was made to investigate, as far as practically possible, all basic materials which have been reported or appeared to be useful. Given the preliminary nature of the investigation, it was decided to exclude admixtures reported in the literature to be made of more than one basic material. Proprietary waterproofers were included in the investigation only when recommended by their manufacturers for this application.

It was found convenient to group all the potential materials into seven classes as follows:

- cement replacement materials;
- fine particulate materials;
- water repellents;
- polymer latices;
- amino alcohol derivatives;
- proprietary waterproofers;
- miscellaneous.

Table 5.1 provides a listing of the materials which fall into each class. It also encompasses other additional relevant information, viz.:

- the principal transport mechanism(s) which have been reported (or are hoped) to be affected by their inclusion (principal function);
- whether a particular material was selected to be investigated, and if not the reasons for its rejection;
- other important comments which pertain to all materials within the class in question, or to a specific material within the class.
- reference is made to sections of Appendix 1, in which the materials are characterized in terms of their physical and chemical properties and the literature regarding the use of the materials in concrete is reviewed.

Table 5.1 Selection of potential materials

Class	Materials	Principal function	Selected or Rejected	Reason not selected	Comments	Review	
Cement replacement materials	Ground granulated blastfurnace slag (GGBS)	(1)(3)	S		(10)	(14)	
	Pulverized fuel ash (PFA)		S				
	Silica fume (SF)		S				
Fine particulate materials	Kieselguhr	(1)	S			(15)	
	Bentonite		S				
	Whiting		S				
	Talc		S				
	Pumice powder		S				
	Hydrated lime		S				
	Mortar sand		S				
Iron oxide powder	S						
Water repellents	Soaps and Butyl stearate	(2)	S	(5)		(16)	
			Sodium oleate				S
			Calcium stearate				R
			Ammonium stearate				S
			Magnesium stearate				S
			Aluminum stearate				S
			Calcium oleate				R
			Ammonium oleate				R
			Butyl stearate				S
	Fatty acids		Stearic acid	R	(6)		
			Oleic acid	S			
			Caprylic acid	S			
	Oils		Soyabean oil	S			
			Corn oil	S			
			linseed oil	S			
			Mineral oil	S			
Tar and Asphalt emulsions	Tar emulsion	S					
	Asphalt emulsion	S					

table 5.1
continued

Class	Materials	Principal Function	Selected or Rejected	Reason not selected	Comments	Review
Polymer latices	EVA		S			
	PVA	(1)(2)	R	(7)	(11)	(17)
	PAE	(3)	R	(8)		
	SBR		S			
	Acrylic		S			
Amino alcohol derivatives	Diethyl ethanolamine	(4)	S			(18)
	Dimethyl ethanolamine		S			
Proprietary waterproofers	Caltite	(1)(2)	S			
	Conplast prolapin	(2)	S		(12)	
	Sikal	(1)(2)	S			
	Setcrete I	(1)(2)	S			
Miscellaneous	Iron powder		S			
	Sodium silicate		S			
	Potassium silicate		S			
	Cellulose acetate fibres	(4)	S			
	Aluminum powder		S			
	Plaster of paris		R	(9)	(13)	(19)
	Calcium sulphate anhydride		R	(9)		
	Gypsum		R	(9)		
	Magnesium carbonate		S			
	Triethanolamine		S			

Table definitions

• **Principal function (in relation to a corresponding unmodified OPC concrete):**

(1): reduction in water permeability;

(2): reduction in water absorption;

(3): reduction in chloride diffusion;

(4): other; will be discussed later.

- **Selected or Rejected**

S: selected; **R:** rejected.

- **Reason not selected**

- (5): could not be obtained from chemical or other suppliers in the UK.
- (6): was not available in readily usable form.
- (7): unsuitable for use in moist environments (Hosek 1966, Frondistou-Yannas & Shah 1972, ACI Committee 548 1986).
- (8): could not be obtained from suppliers in the UK; widely used in Japan (Ohama 1987), and in some parts of Europe (Semerad et al. 1987).
- (9): may increase sulphate content beyond code-recommended allowable limits; such limits are imposed to limit the risk of swelling due to sulphoaluminate formation.

- **Comments**

- (10): there has been extensive interest in cement replacement materials and the literature abounds with information concerning a wide variety of applications. However, as the name implies, these materials are not admixtures in the true sense, but cementitious materials often used in concrete to replace a fraction of the Ordinary Portland Cement.
- (11): of the wide variety of polymers which have been investigated for use as admixtures, latex polymers, in general, and the selected latexes, in particular, have been the most widely used and accepted (ACI Committee 548 1986).
- (12): these are often composed of mixtures of materials from the different groups above. To compile a list of such materials, the seven main admixture suppliers in the UK together with a number of specialist companies were invited to submit their admixtures for inclusion in the study and the 4 materials listed in the table were submitted. It is noteworthy that, as anticipated, most were unable to offer admixtures other than water-reducing admixtures for this application. Although water-reducing agents are believed (ACI Committee 212 1989) to give rise to some modifications to the hydration reaction and concrete microstructure, they are principally used, in applications which are similar to those of interest, to allow the water/cement ratio of concrete mixtures to be reduced to very low levels (0.28 can be practically produced) while maintaining a reasonable workability.

(13): most of these materials have often been used in combination with other materials. They have little in common with each other, except that their benefits in relation to this work are doubtful, or as yet unclear.

• **Review**

(14): refer to A1.2.

(15): refer to A1.3.

(16): refer to A1.4.

(17): refer to A1.5.

(18): refer to A1.6.

(19): refer to A1.7.

5.2 Experimental details

5.2.1 Concrete mixes

5.2.1.1 General

Having identified the potential admixtures available (5.1), the experimental work was focused on evaluating their performance, chiefly in terms of the changes, if any, that their inclusion in Ordinary Portland Cement (OPC) concrete impart to chloride transport.

Clearly, all aspects of the experimental work had to be devised to allow for alterations in chloride transport due to admixtures to be readily isolated from those induced by other effects. All concrete mixes were therefore designed such that they corresponded to a suitable unmodified OPC concrete, referred to hereafter as the "Control mix". Realising that complete correspondence was unattainable, it was decided to maintain the parameter most important to chloride transport, i.e. the ratio of water to cementitious material (Chapter 3), constant for all mixtures. With this approach adopted, it was considered justifiable to assume that unless admixtures are added in large proportions (relative to the other concrete ingredients) modified mixes would have essentially similar aggregate and cementitious material contents.

5.2.1.2 Control concrete design

The water/cement ratio and proportions of the Control mix were selected in compliance with the minimum code requirements pertaining to the design of concrete mixes for use in structures subjected to chloride-rich environments. It was also judged essential that the Control mix should be sufficiently workable such that it would be able to accommodate, without the need to resort to the use of plasticizing admixtures, materials which were anticipated to give rise to large reductions in workability. Despite being unfavourable from the viewpoint of workability, it was viewed essential to restrict the size of aggregates used to a maximum of 10mm. This was done in order to avoid the case wherein the relatively porous aggregate-paste interfaces short-circuit transport

of species through the relatively small thickness of test specimens (50mm), and to ensure that relatively small replicate test specimens are essentially similar in composition.

Reviewing code requirements, it was felt appropriate to test the feasibility of using, as a Control, a concrete mix having a free water/cement ratio of 0.4 and a cement content of 400 kg/m^3 . A series of trials were conducted using the materials available at Imperial College with little success; stiff mixes having slump values of no more than 20mm were obtained. Trials were hence made with similar concretes but with the water/cement ratio raised to the maximum allowable level (according to code requirements) of 0.45, but again to no avail; mixes remained stiff and slump did not exceed 30mm. A common feature of all mixes made was that they seemed, despite the relatively high cement contents used, to be harsh and to have poor cohesion due to, apparently, a deficiency in fines. Tests were hence conducted to establish the grading of the aggregates used. Analysis of the fine aggregates revealed no irregularities, and the problem seemed to arise from the manner in which the coarse aggregate fraction was prepared: it was sieved to discard particles smaller than 5mm, whilst common practice was to retain particles down to 2.36mm. To correct this, the 10mm aggregate was prepared to include particles down to 2.36mm as their inclusion was believed to alleviate the workability problems encountered earlier. Using the new 10mm aggregate, 0.4 water/cement ratio (400 kg/m^3 cement) formulations exhibited improved workability, with slump values up to 35mm. Nevertheless, better workability was desired and raising the water/cement ratio to 0.45 (400 kg/m^3 cement) seemed to provide the best practically attainable mix (55mm slump), and was therefore chosen to be the Control mix; complete details of this mix are included in A2.1.1.

5.2.1.3 Design of admixture-modified concretes

5.2.1.3.1 General

According to an earlier discussion (5.2.1.1), all admixture-modified concretes were designed to have the same free water/cement ratio as the Control concrete. They were therefore formulated from the Control concrete by simply incorporating the admixture and, where an admixture contained a significant amount of water (see Appendix 1), the amount of water used in the mix was reduced by an equal amount.

Whilst every effort was made to introduce admixtures singly, it was found imperative or advantageous in some cases to introduce other accompanying materials, which shall be referred to hereafter as "secondary materials". These include circumstances where it would have been impossible to introduce the main admixture without including the secondary materials (mainly because of workability problems), or others where secondary admixtures were used to facilitate the introduction of the main admixture in a specific fashion, for instance, in emulsion form.

An earlier discussion (5.1) underlines the difficulty of establishing from the literature, for most of the admixtures to be tested, the dose at which they would perform best. This was thought to be best revealed by using admixtures at 2 or 3 levels, which were chosen on the basis of the relevant literature and/or an understanding of the mode of action of the materials in question (see Appendix 1). For most of the admixtures used, it was found convenient to express the dose employed as a weight percentage of the cementitious material (OPC content). Others were, however, introduced at a volume ratio expressed as litres of the admixture per cubic meter of concrete.

The mixes tested are shown in Tables 5.2 to 5.8 of the following sections and more comprehensive information is given in A2.1.2.

5.2.1.3.2 Cement replacement materials

Cement replacement materials were introduced, as reported in Table 5.2, at the levels commonly used in practice and also widely recommended for applications where hindering chloride transport is important. For further details of these materials, refer to A1.2.

Table 5.2 Mixes tested (cement replacement materials)

Material	Mix reference	Dose' (%)	Secondary materials
GGBS	GGBS40	40	---
	GGBS70	70	---
PFA	PFA30	30	---
SF	SF5	5	---
	SF10	10	---

all were introduced as replacements by weight of Ordinary Portland cement.

--- not introduced to mix.

5.2.1.3.3 Fine particulate materials

It was generally difficult to establish, from the available literature, the appropriate addition levels for fine particulate materials. It was nevertheless judged that, for the purposes of this application, dose rates should not exceed 10%, although it was thought useful to investigate the performance of the commonly used material, namely hydrated lime, at higher levels, viz. 15% and 30%, respectively. Most materials were, as shown in Table 5.3, added at levels varying from 2% to 10% w/w_{cement}. To weigh the benefits, if any, of using fine particulate materials against those associated with increasing the content of the fine fraction of aggregate (see A1.3), mixes containing mortar sand, i.e. the type of sand (sieved for this work to contain no particles larger than 300 micron) often used in preparing cement mortars, were investigated.

Table 5.3 Mixes tested (fine particulate materials)

Material	Mix reference	Dose (% by cement)	Secondary materials
Kieselguhr	KIES5	5	---
	KIES10	10	---
Bentonite	BEN2	2	---
	BEN5	5	---
	BEN10	10	(1)
Whiting	WHIT5	5	---
	WHIT10	10	---
Talc	TALC5	5	---
	TALC10	10	---
Pumice	PUM2	2	---
	PUM5	5	---
Hydrated lime	LIME5	5	---
	LIME15	15	---
	LIME30	30	---
Mortar sand	MSAND5	5	---
	MSAND10	10	---
Iron oxide	IRO0.125	0.125	---
	IRO0.25	0.25	---
	IRO2	2	---

Secondary materials

(1): as predicted, adding bentonite at 10% resulted in the mix being unworkable (bentonite, being a clay, absorbed a considerable amount of the mix water (see A1.3)). It was found possible to produce a mix that can be properly compacted under laboratory conditions by addition of a superplasticizer (based on a blend of sulphonated melamine formaldehyde condensate and selected lignosulphonate (SP-450)) at a relatively high rate (2.0 w/w_{cement}).

5.2.1.3.4 Water repellents

All water repellents were used in direct addition expressed as a percentage by weight of the cementitious material; asphalt and tar emulsions, being an exception, were more conveniently added in volume ratios expressed as litres of material per cubic meter of concrete.

The literature revealed three factors closely linked to the dosing levels of water repellents: i) improved performance, in terms of the principal function, with increasing dose levels (Aldred 1989), ii) recommendations to increase dose levels so as to counteract the loss due to leaching of hydrophobic material (the admixture, or the products formed from its reaction with the cement hydration products/pore solution (see A1.4), which may occur under long-term exposure (Aldred 1988, Aldred 1989), and finally iii) the reported (see references in 5.1) detrimental effects, in terms of loss of compressive strength (compared to corresponding unmodified concretes), associated with increasing dose levels. To accommodate these apparently conflicting requirements, dose levels were generally chosen in an attempt to investigate performance at two extremes: high levels to satisfy requirements (i) and (ii) and low doses to satisfy (iii), and/or at intermediate levels. Admittedly, considerable judgment was employed in selecting these levels (Table 5.4).

Water-soluble soaps (sodium stearate, sodium oleate) were added, as recommended in most publications (see references in 5.1), at a rate of 0.2%, and the effects of higher additions were also investigated (SO0.4). Insoluble soaps were added at levels ranging between 0.25% and 3%. Butyl stearate was added at rates of 2% and 3%. Oils and fatty acids were generally introduced at rates ranging from 0.5% to 3%, although unusually high rates of 5% and 10% were also employed. It was felt that introducing oils in the form of emulsions would improve their distribution within concrete, hence enhancing their performance, and suitable "secondary materials" were used to facilitate this. Finally, the tar and asphalt emulsions were introduced in rates ranging from 10 l/m³ to 50 l/m³.

Table 5.4 Mixes tested (water repellents)

Material	Mix reference	Dose (% by cement)	Secondary materials
Sodium stearate	SODST0.2	0.2	---
Calcium stearate	CALST1	1	---
	CALST3	3	---
Magnesium stearate	MAGST0.5	0.5	---
	MAGST1.0	1	---
	MAGST3.0	3	---
Aluminum stearate	ALST0.25	0.25	---
	ALST0.5	0.5	---
	ALST1.0	1	---
Sodium oleate	SODOL0.2	0.2	---
	SODOL0.4	0.4	---
Butyl stearate	BUTSTS2	2	---
	BUTSTS3	3	---
Oleic acid	OLEICA1	1	---
	OLEICA2	2	---
Caprylic acid	CAPA0.5	0.5	---
	CAPA2.0	2	---
Soyabean oil	SOYO1	1	---
	SOYO5	5	---
	SOYOE0.5	0.5	(1)
	SOYOE1.0	1	(1)
	SOYOE3.0	3	(2)
	SOYOE10.0	10	(3)
Corn oil	CORNO1	1	---
	CORNO5	5	---
linseed oil	LINSO0.5	0.5	---
	LINSO1.0	1	---
	LINSO2.0	2	---
Mineral oil	MINO0.5	0.5	(4)
	MINO1.0	1	(4)
Tar emulsion	TAR10	10#	---
	TAR20	20#	---
	TAR50	50#	---
Asphalt emulsion	ASPH15	15#	---
	ASPH30	30#	---

l/m³ of concrete

Secondary materials

- (1): kieselguhr at 0.25% w/w_{cement} was used to facilitate the emulsification of the oil.
- (2): kieselguhr at 0.5% w/w_{cement} was used to facilitate the emulsification of the oil.
- (3): kieselguhr at 1% w/w_{cement} was used to facilitate the emulsification of the oil.
- (4): sodium oleate at 0.013% w/w_{cement} was used to facilitate emulsification of oil.

5.2.1.3.5 Polymer latices

The use of polymer latices in concrete with the object of improving the performance of structures in chloride-rich exposure has been the subject of considerable research. Recommended dose levels vary between 5% to 20%, the percentage being based on the weight of polymer solids to that of the cementitious material (ACI Committee 548 1986, Ohama 1987, Lavelle 1988, Kuhlmann 1990, see also A1.5). Latices were, however, seldom employed to concretes of such relatively high water/cement ratios, especially at the high range of dose levels. Executing several trials with the polymer latices available, it appeared that concretes made with high additions (more than 10%) were subject to high rates of bleeding and to floatation of the polymer solids. It was decided, therefore, to limit dose levels at this stage to no more than 10%. As shown in Table 5.5, dose levels were also chosen to be no less than 5%, as this level is considered as the minimum dose at which polymers would be of benefit in relation to the intended function(s) (Pomeroy 1976, Semerad et al. 1987).

Table 5.5 Mixes tested (polymer latices)

Material	Mix reference	Dose (% by cement)	Secondary materials
EVA	EVA5	5	(1)
SBR	SBR5	5	---
Acrylic	ACR5	5	---
	ACR10	10	---

Secondary materials

(1): silicone anti-foaming agent was added to the emulsion at a rate of 0.2% weight to the weight of polymer solids, with the object of counteracting the tendency of the polymer to cause, as is well established, huge air entrainment. The dose of detraining agent was in accordance with common practice.

5.2.1.3.6 Amino alcohol derivatives

In the preceding two chapters, it was revealed that chloride binding is beneficial in the sense that it may retard chloride ingress, and reduces the amount of chloride which is readily available to participate in the corrosion process (free chloride).

Sakuta et al. (1987) reported that amino alcohol derivatives possess the capacity to bind chloride ions and thereby retard their ingress. They also maintained that these materials are capable also of binding carbon dioxide and hence retard carbonation (as seen in 2.4 carbonation can also cause reinforcement to corrode). A more comprehensive discussion is given in A1.6

Table 5.6 Mixes tested (amino alcohol derivatives)

Material	Mix reference	Dose (% by cement)	Secondary materials
Diethyl ethanolamine	AMINO13	3	---
Dimethyl ethanolamine	AMINO23	3	---

5.2.1.3.7 Proprietary waterproofers

Proprietary products were introduced as recommended by their respective manufacturers (Table 5.7). The effects of high dosage levels were also thought of interest, and they were investigated for two materials (mixes SIK18 and SET15). Except for Conplast Prolapin, which was added as w/w_{cement} , all products were added as l/m^3 of concrete.

Table 5.7 Mixes tested (proprietary waterproofers)

Material	Mix reference	Dose		Secondary materials
		Level	Remarks	
Everdure Caltite	CAL30	30	(1)	---
Conplast prolapin	CONP1	1		---
	CONP3	3		---
Sika1	SIK9	9		---
	SIK18	18	(2)	---
Setcrete1	SET6	6		---
	SET15	15	(3)	---

Dose (Remarks)

- (1): the dosing rate was as recommended by the manufacturers. Noteworthy, however, is that the manufacturers recommend that their product be used with lower (0.35) w/c concretes and always in conjunction with a purpose provided superplasticizer.
- (2): double the recommended dose.
- (3): slightly more than double the recommended dose.

5.2.1.3.8 Miscellaneous

As has earlier been mentioned, materials whose function(s) appeared uncertain comprise this group (for a review of literature concerning their use and behaviour in concrete, see A1.7). Understandably, therefore, considerable difficulty was encountered in establishing the appropriate dosing levels. All materials were added as w/w_{cement} .

i) Iron powder

When introduced in concrete, iron powder acts as an inert filler. In some proprietary products (Lea 1970), however, iron powder has been used in conjunction with agents (commonly ammonium chloride) which promote its rusting, giving rise to the formation of voluminous iron oxides thereby blocking concrete pores. For obvious reasons, chlorides, in any form, could not be introduced into concrete; however, it was hoped that intruding chlorides would promote the rusting of the iron fillings, possibly producing some form of pore blocking or, perhaps, at least, causing the advance of chlorides to be stalled. Owing to the uncertainties involved, it was thought best to test the performance of iron fillings at two dose levels: a relatively low level of 2% and a high level of 10%.

ii) Sodium and potassium silicate

Sodium silicate introduced in OPC concrete is believed to react, primarily with the Ca(OH)_2 produced by the hydration of cement, forming calcium silicates which, being insoluble in pore water, precipitate thereby giving rise to pore blocking. A detrimental aspect of this reaction is, however, known to exist: it is related to the consumption of Ca(OH)_2 which encourages C_3S hydration (see A4.1), and the consequent formation of sodium hydroxide which, in turn, further accelerates setting (Jawed & Skalny 1978). When sodium silicate was introduced at the level of 1%, a stiffening of the mix was observed, indicating an instant reaction of the silicate. This was thought undesirable, since calcium silicates would then precipitate before the cement paste matrix has

formed, hence producing no pore blocking. To counteract the instant reaction of silicates, especially when high (5% and 10%) levels were used, retarders were employed (sugar/zinc sulphate (Lea 1970, Neville 1981)). Potassium silicate was investigated because it was found to cost less than sodium silicate.

iii) Cellulose acetate

The cellulose acetate employed was in the form of fibres. Since fibres are normally introduced in concrete at levels ranging from 1% to 5% (Pomeroy 1976), these levels were adopted.

vi) Aluminum powder

Aluminum powder was firstly added at levels (0.1% and 0.2%) much higher than those reported (ACI Committee 212 1989) as commonly used. A high level of expansion was observed to take place owing to the gas-forming action of the aluminum powder. Since such expansion would result in the creation of a rather porous concrete matrix, it was considered undesirable. A more realistic addition level of 0.05% was, therefore, adopted, and an attempt was made to restrain the resulting expansion. Moreover, a second mix with 0.2% aluminum powder was employed and an attempt was also made to restrain expansion. In this case expansion could not be entirely restrained and excessive bleeding of mix water occurred.

v) Magnesium carbonate and Iron sulphate-Calcium carbonate

These materials were introduced as it was anticipated they would react with the pore solution constituents to deposit precipitates thereby giving rise to pore blocking. It was found impossible to introduce magnesium carbonate at doses greater than 2% because of the considerable stiffening that occurred when this level was exceeded. The iron sulphate-calcium carbonate mixes were chosen arbitrarily. However, consideration was given to limit the amount of iron sulphate added: i) to avoid the possibility of later

expansion, and ii) to avoid the formation of iron hydroxide in amounts that can seriously delay, or even prohibit, hydration.

vi) Triethanolamine

It was anticipated that a non-chloride-based accelerator may be required to counteract the retarding action exhibited by many of the materials tested, hence, triethanolamine was investigated. Since the mode of action of triethanolamine is reported (see A1.7) to vary according to mix constituents and proportions, between that of an accelerator and that of a retarder, it was introduced at four distinct levels.

Table 5.8 Mixes tested (miscellaneous materials)

Material	Mix reference	Dose			Secondary materials
		Level (% by cement)	Type	Remarks	
Iron powder	IRON2	2			---
	IRON10	10			---
Sodium silicate	SODSIL1	1			---
	SODSIL5	5			(1)
	SODSIL10S	10			(2)
	SODSIL10ZS	10			(3)
Potassium silicate	POTSIL1	1			---
	POTSIL3	3			---
Cellulose acetate	CEL1	1			---
	CEL5	5			---
Aluminum powder	AL0.1	0.1			---
	AL0.2	0.2			---
	ALR0.05	0.05		(1)	---
	ALR0.2	0.2		(1)	---
Magnesium carbonate	MAGC1	1			---
	MAGC2	2			---
Iron sulphate + Calcium carbonate	FORM1	1	FeSO ₄		---
		2	CaCO ₃		---
	FORM2	0.5	FeSO ₄		---
		2	CaCO ₃		---
	FORM3	2	FeSO ₄		---
		3	CaCO ₃		---
Triethanolamine	TEA0.025	0.025			---
	TEA0.1	0.1			---
	TEA0.25	0.25			---
	TEA10.5	0.5			---

Dose (remarks)

(1): expansion restrained.

Secondary materials(1): 0.05% w/w_{cement} sugar added.(2): sugar addition of 0.15% w/w_{cement}.(3): zinc sulphate powder added at 2% w/w_{cement}.

5.2.2 Programme of work

5.2.2.1 General

All concrete mixes were prepared in the same small pan mixer, the mixing procedure being essentially that prescribed by BS1881: Part 125: 1986. The aggregates were mixed for 2 minutes, first in the dry state and then with approximately half of the mix water added. They were then allowed to stand for 5 minutes with the mixer pan covered. The cement was introduced and mixed with the aggregates for 30 seconds. At this point, the remaining water was added during the next 30 seconds, and the whole was mixed for a further 2-3 minutes.

Care was taken to introduce admixtures in a manner such that ultimate performance and maximum distribution was attained, as follows:

- fine particulate materials and other materials which are not miscible with water were introduced immediately after the second half of mix water was added;
- materials which are miscible or dissolve in water were mixed with the second half of the mix water;
- where retarders (secondary materials) were employed, they were introduced first, followed by the material in question;
- materials which were received as emulsions were introduced immediately after the second half of mix water was added;
- where a material was to be emulsified, it was first mixed with the second half of the mix water, together with the emulsifying aids, then the mixture was stirred by means of a magnetic stirrer before being introduced;

- sodium stearate was supplied in the form of relatively large (1mm) granules which did not readily dissolve in water (see A1.4). To dissolve sodium stearate a magnetic stirrer was used (the mixture (second half of mix water + sodium stearate) was stirred for 20 minutes at approximately 50°C). The mixture was thereafter allowed to cool down to its original temperature before being introduced. It is also worth mentioning that sodium stearate levels higher than 0.2% were found impossible to dissolve fully, and this explains why levels higher than 0.2% were not investigated.

Immediately after the completion of mixing, slump testing was performed. The required specimens were then cast and compacted on a vibrating table. As soon as the small amount of bleed water had evaporated, specimens were stored under wet burlap and polythene sheets, for over night curing. The following day, specimens were released from moulds, marked, and those prepared for transport measurements were kept in sealed condition until required for testing. Sealing was performed by wrapping specimens with ample cling film, inserting them into plastic bags, which, in turn, were sealed. It is worth noting that preliminary testing indicated that weight loss from specimens thus sealed was negligible.

5.2.2.2 Testing

5.2.2.2.1 General

Considering the preliminary nature of this phase, the limited duration and resources allocated to this project, and the large number (96) of mixes to be investigated, it was judged essential to carry out this investigation using testing methods which are fast, yet provide adequate indications on how well the materials tested can help reduce chloride ingress. It was felt that these indications would be provided by investigating the following transport mechanisms: pressure induced water flow, water absorption, and diffusion.

In addition to transport testing, the 28 day cube (100mm) strength was measured (in accordance with standard practice prescribed by BS1881: Part 3: 1970), due to the suspicion that many of the materials used may cause a substantial reduction in compressive strength (Hewlett et al. 1988). Before cubes were crushed, they were weighed, both in air and in water, in order to allow an estimate of the bulk density of the hardened concretes to be determined. This was done as it was felt that bulk density constitutes a simple non-destructive means which could help identify air entrainment suspected to occur in mixes with water repellents (see A1.4); these materials were introduced in such small doses that bulk density was thought unlikely to be significantly affected by their inclusion unless they caused entrainment of large amounts of air.

5.2.2.2.2 Transport tests

I) Testing to characterize resistance to pressure-induced water flow

Resistance to pressure-induced water flow is usually measured by permeability testing. To undertake water permeability testing on all specimens of interest, using all the rigs available at IC, would have taken years to complete. Attention was, therefore, focused on a faster method, namely oxygen permeability testing.

An earlier discussion (3.6.3) revealed the need to condition specimens (drying) prior to oxygen permeability testing and uncovered the problems encountered when interpreting test results. Such problems pertain to all conditioning alternatives; admittedly, however, in varying degrees. Conditioning other than that involving drying at 105 °C was expected to take months to complete. Consequently, a decision was made to oven dry specimens until equilibrium at 105 °C; equilibrium was considered achieved at the point when the weight loss in 24 hours did not exceed 0.1% of the weight of a specimen (Dhir et al. 1989). Arguably, such harsh and unrealistic treatment would make it almost impossible to derive intrinsic permeability coefficients which can be used in practice (3.6.3); however, the object of testing was to establish relative rather than absolute performance. Possible distorting factors were, nonetheless, identified, these are:

- i) different concretes may sustain varying degrees of microstructural damage upon drying (3.2.2);
- ii) the admixtures, or the materials which result from their reaction in concrete, may be altered by drying at 105 °C (e.g. water repellents (see A1.4), polymer latices (see 6.4)), and
- iii) some admixtures may affect water flow in a manner completely different to that by which they affect oxygen flow. One example is bentonite which swells when in contact with water, but shrinks on drying (see A1.3). Another example is a material introduced

in liquid form and remains, at least in part, in liquid form in the concrete pores. The material can thus offer resistance to oxygen flow, but not to water flow (it is simply leached).

Oxygen permeability testing involved inserting a disk specimen (101.6mm diameter and 50mm nominal thickness) into a cell which seals the curved surface, allowing oxygen flow only through the length of the specimen. Oxygen was then applied (under pressure) to the as cast surface and its flow rate was measured on the down-stream side by means of a series of bubble flow meters. Flow rates were measured, for each specimen, at three distinct gauge pressure levels (0.5, 1.5, and 2.5 bars), which were applied consecutively, and the permeability coefficient was calculated as shown in A3.2.

II) Testing to characterize absorption resistance

As explained earlier (Chapter 3), capillarity plays a principal role in the absorption of chloride-containing water in concrete.

Capillary absorption in concrete has been investigated by many means (Bamforth et al. 1985), of which, capillary rise testing is the most widely used, mainly because of it being most informative, and its relative simplicity. Capillary rise testing was therefore adopted as the principal test by which resistance to water absorption is evaluated. However, where it was necessary to hasten, without the application of pressure, the saturation of test specimens a modified form of testing, which will be referred to hereafter as MAT, was employed.

Capillary rise testing involves monitoring the weight gain of specimens held with their as-cast face in contact with water. To simulate absorption into site concrete, testing was performed in trays sealed such that the relative humidity in the air surrounding the specimens remained close to 100%. Ideally, specimens would be conditioned to a relatively low, but realistic, relative humidity prior to testing. Unfortunately, this

process takes many weeks for the representatively large specimens (101.6mm dia. and 50mm thick disks) of low penetrability concretes. Specimens were therefore tested after oven drying at 105 °C to constant weight. Such treatment is obviously disadvantageous, in that: i) different concretes may sustain varying degrees of microstructural damage upon drying (3.2.2), ii) some admixtures, or the materials which result from their reaction with concrete, may be altered by drying at 105 °C (this may cause a material to show worse, or better, resistance to water absorption than would be revealed under more realistic drying conditions). This necessitated carrying out similar tests on unconditioned specimens, i.e. specimens as-received. The relatively short sealed-curing period allowed before testing was thought to result in mixes which hydrate at different rates showing varying degrees of self desiccation, and a consequent variation in moisture state. From the viewpoint of comparing absorption behaviour, and considering that absorption is sensitive to moisture state (3.2.3.3), this was clearly disadvantageous; nevertheless, as anticipated, this test proved useful in providing a "feel" for the influence of damage sustained by 105 °C drying on the results of subsequent tests.

Modified absorption testing (MAT) involved subjecting specimens to water such that all surfaces except the top surface were exposed to water. The top surface was left unexposed to allow trapped air to escape as it became replaced by absorbed water. The test was carried out in the capillary rise trays by pouring water into the trays until the curved surface of specimens was covered.

III) Testing to characterize resistance to chloride diffusion

In the context of the duration of this project, ion diffusion in concrete is an extremely slow process. A test which would help "get a feel" for the effect of an admixture on chloride ion diffusivity was therefore sought.

There have been reports (Atkinson & Nickerson 1984) of studies on the transport properties of porous rocks where measurements of electrical conductivity on specimens saturated with an aqueous electrolyte have proven useful as a rapid substitute for diffusion testing. Indeed, it has often been suggested that, provided the solid phase of a porous medium is effectively an insulator, diffusion and ionic conductivity are controlled by the same process, and connected by the renowned Nernst-Einstein relation. It appears, therefore, that an essentially similar analogy can be applied to concrete: electrical conduction in concrete is electrolytic in nature and hence in saturated concrete, at constant temperature, the electrical resistivity of concrete is a function of the conductivity of its pore solution and the mobility of the ions present (2.2.2). It was therefore felt that resistivity testing would provide a rapid means of diffusion assessment, although it was appreciated that conductivity will be dependent upon the mobility of all the ions present in the pore solution (i.e. Na^+ , K^+ , OH^- etc.) rather than a specific ion (e.g. Cl^-), and that many of the admixtures investigated certainly have an effect on pore solution composition, hence its conductivity. Ideally, corrections would be made by determining the conductivity of pore solutions expressed from specimens identical to those resistivity tested. Such analysis was, however, ruled out as it was impossible to undertake on all specimens in the duration allocated to this phase.

Resistivity testing was performed on concrete disk (101.6mm dia. and 50mm thick) specimens. It involved inserting a specimen in a cell such that it was housed between two compartments which were later filled with an electrolyte (0.3M NaOH solution). The cell had an electrode mounted at the far end of each of its two compartments. Resistance was measured between these electrodes using a Universal Bridge; an

alternating current at 1000Hz and 9V was employed to eliminate polarization at the electrodes (2.2.1). The measured resistance was corrected to take account of the resistivity of the NaOH solution, converted to an equivalent concrete resistance at a predetermined temperature (20 °C), and resistivity was calculated; all calculations involved are illustrated in A3.1.

Before resistivity testing, care was taken to dry the curved surface of specimens thoroughly; this was done in order to avoid the case where water films present on the curved surface form a conductive path, short-circuiting the test specimen.

5.2.2.2.3 Testing programme

In the context of the duration of the project, priority was given to the completion of this phase in the shortest possible duration. Given the large number of mixes involved, it was therefore regarded essential to devise a testing plan which would require a minimum number of specimens, of each mix, to be cast.

The testing programme was designed to require only the following specimens be cast from each mix: 4 disks (101.6 mm diameter and 50mm nominal length), and 2 100mm cubes; the disk specimens were employed in transport testing, and the cubes in compressive strength determinations.

Transport testing commenced at 28 days, in the following sequence:

Disk specimens (1 & 2)

Specimens were unsealed and tested under capillary rise conditions for a period of 24 hours, after which they were subjected to MAT testing for a further 8 days. At the end of that period, they were removed from their trays, and for some mixes the specimens were resistivity tested. Immediately following resistivity testing, all specimens were rinsed with distilled water and vacuum saturated, then returned to their trays to be totally immersed in water for a period of 2 days (the process consisting of vacuum saturation and the two days water immersion will be referred to hereafter as "saturation"). Finally, specimens were removed from the water tanks, surface dried, weighed, and resistivity tested.

For reasons explained earlier, it was important to bring specimens to near saturation prior to resistivity testing. As anticipated, water uptake for some mixes (primarily mixes with water repellents) was so low that it was thought impractical to rely on capillary rise conditions to achieve saturation. Capillary rise testing was therefore aborted, to be succeeded by MAT testing, which also seemed not to bring about the

desired degree of saturation (even after 8 days of such testing water uptake was less than 50% of that of the control specimens), leaving the saturation procedure, which was undesirable (see 5.3.4), as the only practical option.

Vacuum saturation was performed in existing purpose built cells. The specimens were firstly surface dried, inserted into a vacuum cell and subjected to vacuum for 2 hours in order to facilitate removal of air from concrete voids. Thereafter, while maintaining the vacuum, water was gradually allowed into the vacuum cell and the specimens were left under vacuum for a further 2 hours (Fagerlund 1975).

Disk specimens (3 & 4)

Specimens were unsealed and inserted into a large preheated oven (at 105°C). Sufficient silica gel was used in the oven so as to absorb moisture thereby helping to maintain the relative humidity close to nil. When equilibrated, specimens were placed in desiccators (at laboratory temperature) for at least 1 day prior to being oxygen permeability tested. Capillary rise testing was then performed for a period of 28 days, after which specimens were saturated. Immediately afterwards, they were surface dried and their weight was recorded; this was performed in order to obtain an estimate of the effective (penetrable under the given conditions of exposure) porosity of the concretes.

5.3 Results and selection of materials for Phase 2

5.3.1 General

The purpose of the following sections is to present the results of the experimental work, and to illustrate how materials were evaluated for inclusion in the second phase of the experimental work.

Ideally, the results from each test would have been projected onto classification systems, allowing the performance of the control concrete and the modified concretes to be readily established. Unfortunately, it was found impossible to do so as most such classification systems were found to be unreliable; this is primarily because they tend to be based on collections of test results without due allowance for variations in specimen conditioning methods and testing techniques. Materials were therefore selected, or rejected, principally on the basis of the performance of their respective concretes in relation to the Control mix.

Since the performance of the Control concrete represented the basis of all evaluations, it was necessary to ensure that it fell within expectations.

5.3.2 Quality of the Control concrete

5.3.2.1 Results

In the fresh state, the Control concrete appeared to have excellent cohesion and sufficient workability (55mm slump).

The compressive strength and bulk density were found to be of the order of 50.3 MPa and 2347 Kg/m³, respectively.

The control concrete had an intrinsic (oxygen-based) permeability coefficient k_g of the order of 6×10^{-16} m². Resistivity before saturation (RS_{bs}) was calculated to be 68.0 Ω m, and 66.0 Ω m after saturation (RS_{ss}). Shown in Table 5.9 are the results of absorption testing, both for the as-received and 105°C dried specimens. Also shown is the weight gain after saturation.

The effective porosity (5.2.2.2.3) was found to be of the order of 15.8%.

All results represent an average value for the two specimens tested.

Table 5.9 Absorption testing results (Control concrete)

OVEN DRIED SPECIMENS (105° C)								
Time ^a	15min	1hr	4hr	1d	4d	12d	28d	30d ^c
Weight Gain ^b (g)	6.75	13.2	21.9	51.1	58.3	60.3	62.0	63.6
AS-RECEIVED SPECIMENS								
Time	1hr	1d	3d	9d	11d ^c			
Weight Gain (g)	0.6	3.55	10.3	11.15	12.25			

a: time after testing commenced.

b: weight gain relative to the initial weight of specimens.

c: after saturation.

min:- minutes; hr:- hours; d:- days.

Double lines are used in the table to emphasise points after which the mode of testing was altered (5.2.2.2.3):

- departure from capillary rise to MAT (all faces of specimen, except top face, are exposed to water);
- departure from MAT to saturation (vacuum saturation followed by two days immersion in water).

5.3.2.2 Discussion

The results are, in general, typical of an average quality concrete. The intrinsic coefficient of permeability can be classified as average according to a Concrete Society Technical Report (1988). RS_{∞} is roughly comparable to resistivity values determined by others (Gjørv et al. 1979), using a similar testing technique, for saturated concretes of the same water/cement ratio. Little difference was found in resistivity before and after saturation; this was not surprising since the bulk of the effective porosity had already been filled by absorption (saturation resulted in filling a mere 1.75% of the effective porosity of the specimens). As can be seen from Figure 5.1, capillary absorption behaviour (105°C dried specimens) was in good accord with normally observed trends (3.2.3.2).

Moreover, it is immediately obvious (Table 5.9) that the amount and rate of water uptake of as-received specimens are much lower than those pertaining to 105°C dried specimens; this can be attributed primarily to capillary absorption being strongly influenced by the moisture state of concrete.

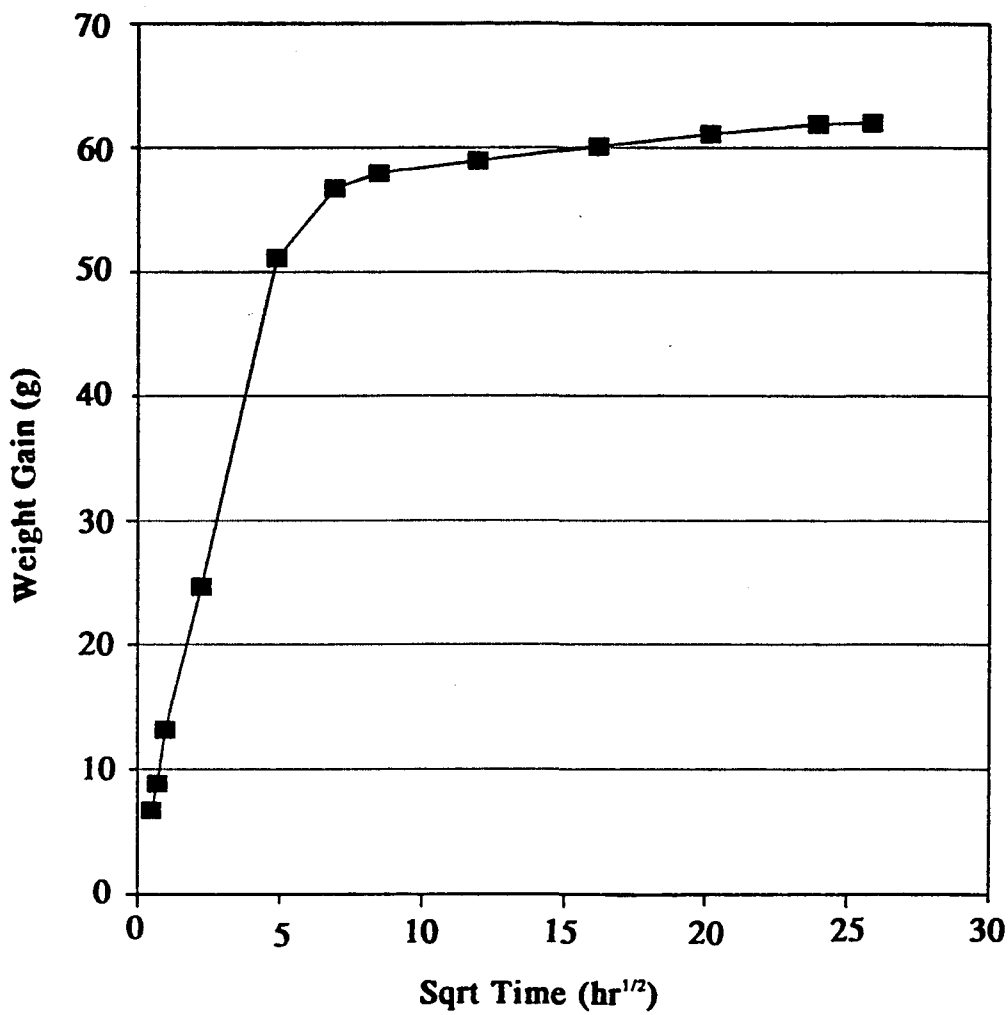


Figure 5.1 Absorption behaviour of Control concrete.

5.3.3 Modified concrete results

To allow the performance of modified concretes to be readily compared with those of the Control concrete, results for all modified mixes, listed in Tables 5.10 to 5.19, are presented as percentage ratios of the corresponding results, displayed earlier (5.3.2.1), of the Control mix.

Listed in Table 5.10 are the oxygen-derived intrinsic permeability percentage ratios.

Tables 5.11 to 5.17 show the percentage weight gain ratios at various times from the start of capillary rise testing; included are results for the 105° C dried specimens, and the as received specimens. Also shown, for the as-received specimens, are the percentage weight gain ratios after saturation. Double lines in the tables emphasise the points after which the mode of testing was altered (departure from capillary rise testing to MAT or to saturation, see 5.2.2.2.3).

Presented in Table 5.18 are resistivity percentage ratios.

Finally, Table 5.19 presents the compressive strength, density, and effective porosity ratios.

All results represent an average value for the two specimens tested.

Table 5.10 Intrinsic permeability (oxygen-derived) relative to the Control

Mix ref.	kr _(g) [#]	Mix ref.	kr _(g)	Mix ref.	kr _(g)
GGBS40	143	SODOL0.2*	422*	AMINO13	49
GGBS70*	217*	SODOL0.4*	569*	<u>AMINO23</u>	<u>31</u>
PFA30	85	BUTST2	80		
SF5	55	BUTST3	87		
SF10	58				
		OLEICA1	116	CAL30	128
		OLEICA2	177	<u>CONP1</u>	<u>20</u>
		CAPA0.5	42	<u>CONP3</u>	<u>30</u>
KIES5	58	CAPA2	104	<u>SIK9</u>	<u>34</u>
KIES10	51			SIK18	54
BEN2	116	SOYO1	116	<u>SET6</u>	<u>33</u>
BEN5	152	SOYO5	91	SET15	65
BEN10	48	SOYOE0.5	69		
<u>WHIT5</u>	<u>31</u>	SOYOE1	43		
WHIT10	95	<u>SOYOE3</u>	<u>33</u>		
TALC5	88	SOYOE10	46	IRON2	77
TALC10	82	CORNO1	133	IRON10	54
PUM2	48	CORNO5	46	SODSIL1	46
PUM5	45	LINSO0.5	91	SODSIL5	59
LIME5	67	LINSO1	49	SODSIL10S	111
LIME15	48	LINSO2	49	SSI10SZ	83
LIME30	80	MINO0.5	91	POTSIL1	62
<u>MSAND5</u>	<u>34</u>	MINO1*	245*	POTSIL3	110
MSAND10	47			<u>CEL1</u>	<u>34</u>
IRO0.125	49	TAR10	57	CEL5	51
IRO0.25	<u>32</u>	TAR20	47	AL0.1*	283*
IRO2	<u>33</u>	<u>TAR50</u>	<u>37</u>	AL 0.2*	955*
		<u>ASPH15</u>	<u>36</u>	ALR0.05	84
		<u>ASPH30</u>	<u>20</u>	ALR0.2*	434*
SODST0.2	44			MAGC1	171
CALST1	173			MAGC2*	191
CALST3	105			FORM1	48
MAGST0.5	72	EVA5	175	<u>FORM2</u>	<u>37</u>
MAGST1	64	SBR5	61	FORM3	61
MAGST3	63	ACR5	45	<u>TRI0.025</u>	<u>25</u>
ALST0.25	139	<u>ACR10</u>	<u>38</u>	<u>TRI0.1</u>	<u>25</u>
ALST0.5	85			<u>TRI0.25</u>	<u>27</u>
ALST1	105			<u>TRI0.5</u>	<u>28</u>

percentage ratio of the permeability coefficient of a given mix relative to that of the Control.

kr_(g) values lower than roughly 33% are presented in **highlighted** underlined text (see 5.3.4).

kr_(g) values higher than roughly 200% are followed by a **highlighted** asterisk (see 5.3.4).

Table 5.11 Percentage ratio of weight gain relative to the Control (cement replacement materials)

105°C DRIED SPECIMENS								
Mix ref.	Time							Band [@]
	15min	1hr	4hr	1d	4d	12d	28d	
GGBS40	69	66	78	81	105	105	102	N
GGBS70	89	83	94	103	117	113	109	N
PFA30	68	80	82	90	108	107	102	N
SF5	82	94	95	102	102	102	100	N
SF10	79	86	87	98	104	103	99	N
AS-RECEIVED SPECIMENS								
Mix ref.	Time					Band		
	1hr	1d	3d	9d	11d#			
GGBS40	125	111	96	112	107	A		
GGBS70	675*	404*	181	177	178	?		
PFA30	142	108	141	144	138	A		
SF5	142	125	120	126	120	A		
SF10	100	77	82	85	89	A		

after saturation.

@ for definition of Bands, see 5.3.4.

? absorption does not conform to any trend; refer to numerical results.

Weight gain ratio values higher than roughly 150% are followed by a **highlighted** asterisk (see 5.3.4).

Table 5.12 Percentage ratio of weight gain relative to the Control (fine particulate materials)

105°C DRIED SPECIMENS								
Mix ref.	Time							Band ®
	15min	1hr	4hr	1d	4d	12d	28d	
KIES5	87	94	98	103	101	100	99	N
KIES10	69	70	88	81	96	96	95	N
BEN2	84	88	71	96	100	100	98	N
BEN5	81	86	67	92	105	106	105	N
BEN10	<u>35</u>	65	53	67	91	92	89	?
WHIT5	79	86	92	101	99	99	99	N
WHIT10	116	114	109	107	103	104	103	N
TALC5	100	105	104	101	102	102	101	N
TALC10	82	94	96	103	105	104	103	N
PUM2	73	86	89	98	98	97	96	N
PUM5	73	87	90	99	101	99	98	N
LIME5	86	84	104	100	98	98	96	N
LIME15	88	85	101	96	98	98	97	N
LIME30	92	91	113	111	110	112	110	N
MSAND5	64	71	67	91	95	94	93	N
MSAND10	72	78	71	93	97	97	95	N
IRO0.125	82	80	71	99	99	99	99	N
IRO0.25	69	69	63	86	92	93	93	N
IRO2	70	70	71	111	96	97	97	N

table 5.12 continued

AS-RECEIVED SPECIMENS						
Mix ref.	Time					Band [@]
	1hr	1d	3d	9d	11d [#]	
KIES5	37	<u>32</u>	<u>32</u>	46	44	C-D
KIES10	45	62	70	92	91	B-C
BEN2	60	75	102	116	115	A
BEN5	142	85	88	106	113	A
<u>BEN10</u>	<u>0</u>	<u>8</u>	<u>16</u>	<u>22</u>	38	E
WHIT5	<u>17</u>	<u>20</u>	45	56	62	D-E
WHIT10	167	134	135	140	131	A
TALC5	183*	139	170	167	155	A
TALC10	133	106	146	145	137	A
PUM2	133	94	117	131	145	A
PUM5	100	93	117	126	139	A
LIME5	125	79	68	78	90	?
LIME15	55	58	57	73	82	B-C
LIME30	150	76	90	107	143	A
MSAND5	75	85	75	91	94	A
MSAND10	55	54	74	96	109	B-C
IRO0.125	42	38	47	50	82	C-D
IRO0.25	<u>25</u>	<u>30</u>	<u>36</u>	49	69	D-E
IRO2	<u>17</u>	<u>30</u>	<u>37</u>	57	111	D-E

after saturation.

@ for definition of Bands, see 5.3.4.

? absorption not in conformity with any trend; refer to numerical results.

Weight gain ratio values lower than roughly 33% are presented in **highlighted** underlined text (see 5.3.4).

Weight gain ratio values higher than roughly 150% are followed by a **highlighted** asterisk (see 5.3.4).

Table 5.13 Percentage ratio of weight gain relative to the Control (water repellents)

105°C DRIED SPECIMENS								
Mix ref.	Time							Band ®
	15min	1hr	4hr	1d	4d	12d	28d	
SODST0.2	57	47	46	41	57	73	76	1-2
CALST1	<u>19</u>	<u>17</u>	<u>17</u>	<u>14</u>	<u>19</u>	<u>33</u>	<u>32</u>	3-4
CALST3	<u>18</u>	<u>14</u>	<u>14</u>	<u>11</u>	<u>15</u>	<u>21</u>	<u>28</u>	3-4
MAGST0.5	<u>35</u>	<u>28</u>	<u>27</u>	<u>22</u>	<u>28</u>	<u>36</u>	43	2-3
MAGST1	<u>28</u>	<u>22</u>	<u>15</u>	<u>15</u>	<u>20</u>	<u>25</u>	<u>30</u>	3-4
MAGST3	<u>8</u>	<u>8</u>	<u>5</u>	<u>9</u>	<u>13</u>	<u>19</u>	<u>24</u>	4
ALST0.25	54	45	46	36	48	59	63	1-2
ALST0.5	45	<u>35</u>	<u>26</u>	<u>25</u>	<u>33</u>	41	46	2-3
ALST1	<u>21</u>	<u>17</u>	<u>16</u>	<u>13</u>	<u>18</u>	<u>24</u>	<u>29</u>	3-4
SODOL0.2	39	<u>34</u>	<u>36</u>	<u>31</u>	43	53	58	2-3
SODOL0.4	<u>33</u>	<u>28</u>	<u>27</u>	<u>23</u>	<u>32</u>	41	47	2-3
BUTST2	<u>6</u>	<u>8</u>	<u>10</u>	<u>8</u>	<u>12</u>	<u>17</u>	<u>22</u>	4
BUTST3	<u>7</u>	<u>8</u>	<u>9</u>	<u>8</u>	<u>11</u>	<u>16</u>	<u>21</u>	4
OLEICA1	<u>25</u>	<u>20</u>	<u>21</u>	<u>20</u>	<u>31</u>	44	53	2-3
OLEICA2	<u>16</u>	<u>14</u>	<u>15</u>	<u>12</u>	<u>18</u>	<u>25</u>	<u>32</u>	3-4
CAPA0.5	<u>16</u>	<u>15</u>	<u>16</u>	<u>12</u>	<u>17</u>	<u>23</u>	<u>29</u>	3-4
CAPA2	<u>7</u>	<u>8</u>	<u>10</u>	<u>9</u>	<u>12</u>	<u>17</u>	<u>23</u>	4
SOYO1	<u>27</u>	<u>25</u>	<u>23</u>	<u>22</u>	<u>35</u>	46	51	2-3
SOYO5	<u>11</u>	<u>9</u>	<u>10</u>	<u>8</u>	<u>12</u>	<u>17</u>	<u>23</u>	4
SOYOE0.5	<u>33</u>	<u>28</u>	<u>34</u>	<u>32</u>	49	61	67	1-2
SOYOE1	<u>30</u>	<u>23</u>	<u>26</u>	<u>23</u>	<u>37</u>	49	55	2-3
SOYOE3	<u>23</u>	<u>17</u>	<u>16</u>	<u>12</u>	<u>17</u>	<u>26</u>	<u>33</u>	3-4
SOYOE10	<u>6</u>	<u>5</u>	<u>6</u>	<u>6</u>	<u>10</u>	<u>15</u>	<u>19</u>	4
CORNO1	<u>30</u>	<u>24</u>	<u>23</u>	<u>21</u>	<u>30</u>	41	49	2-3
CORNO5	<u>13</u>	<u>12</u>	<u>11</u>	<u>9</u>	<u>12</u>	<u>18</u>	<u>23</u>	4
LINSO0.5	40	37	<u>34</u>	39	58	73	76	1-2
LINSO1	40	<u>31</u>	<u>26</u>	<u>29</u>	46	61	66	1-2
LINSO2	<u>30</u>	<u>23</u>	<u>19</u>	<u>19</u>	<u>32</u>	<u>36</u>	54	2-3
MINO0.5	55	47	53	41	60	73	77	1-2
MINO1	47	<u>33</u>	46	<u>31</u>	42	52	56	2-3
TAR10	73	66	77	61	87	91	91	N
TAR20	64	57	67	53	78	86	87	N
TAR50	51	41	45	36	54	70	77	1-2
ASPH15	50	44	41	57	74	83	84	N
ASPH30	61	56	55	82	94	97	97	?

table 5.13 continued

AS-RECEIVED SPECIMENS							
Mix	ref.	Time					Band @
		1hr	1d	3d	9d	11d#	
SODST0.2		67	49	76	88	113	B-C
CALST1		50	63	70	85	216	B-C
CALST3		<u>33</u>	49	57	71	224	B-C
<u>MAGST0.5</u>		<u>0</u>	<u>4</u>	<u>13</u>	<u>19</u>	174	E
<u>MAGST1</u>		<u>17</u>	<u>3</u>	<u>15</u>	<u>22</u>	134	E
<u>MAGST3</u>		<u>0</u>	<u>1</u>	<u>2</u>	<u>16</u>	105	E
<u>ALST0.25</u>		<u>8</u>	<u>13</u>	<u>18</u>	<u>26</u>	169	D-E
<u>ALST0.5</u>		<u>17</u>	<u>10</u>	<u>17</u>	<u>24</u>	134	D-E
<u>ALST1</u>		<u>8</u>	<u>3</u>	<u>2</u>	<u>13</u>	153	E
SODOL0.2		42	<u>35</u>	52	67	444	C-D
SODOL0.4		42	<u>32</u>	44	58	462	C-D
<u>BUTST2</u>		<u>26</u>	<u>21</u>	<u>16</u>	<u>26</u>	147	D-E
<u>BUTST3</u>		<u>17</u>	<u>4</u>	<u>10</u>	<u>17</u>	111	E
<u>OLEICA1</u>		<u>17</u>	<u>9</u>	<u>18</u>	<u>27</u>	247	D-E
<u>OLEICA2</u>		<u>17</u>	<u>9</u>	<u>17</u>	<u>25</u>	45	D-E
<u>CAPA0.5</u>		<u>0</u>	<u>12</u>	<u>19</u>	<u>32</u>	42	D-E
<u>CAPA2</u>		<u>25</u>	<u>13</u>	<u>20</u>	<u>28</u>	58	D-E
<u>SOYO1</u>		<u>17</u>	<u>8</u>	<u>17</u>	<u>24</u>	140	D-E
<u>SOYO5</u>		<u>17</u>	<u>11</u>	<u>18</u>	<u>27</u>	210	D-E
<u>SOYOE0.5</u>		<u>0</u>	<u>0</u>	<u>6</u>	<u>12</u>	119	E
<u>SOYOE1</u>		<u>0</u>	<u>0</u>	<u>5</u>	<u>12</u>	98	E
<u>SOYOE3</u>		<u>0</u>	<u>0</u>	<u>1</u>	<u>6</u>	95	E
<u>SOYOE10</u>		<u>0</u>	<u>0</u>	<u>0</u>	<u>1</u>	65	E
<u>CORNO1</u>		<u>25</u>	<u>17</u>	<u>22</u>	<u>27</u>	222	D-E
<u>CORNO5</u>		<u>8</u>	<u>10</u>	<u>18</u>	<u>24</u>	181	D-E
<u>LINSO0.5</u>		<u>0</u>	<u>0</u>	<u>8</u>	<u>10</u>	181	E
<u>LINSO1</u>		<u>0</u>	<u>0</u>	<u>5</u>	<u>8</u>	40	E
<u>LINSO2</u>		<u>0</u>	<u>6</u>	<u>15</u>	<u>22</u>	115	E
<u>MINO0.5</u>		<u>8</u>	<u>18</u>	<u>35</u>	40	125	D-E
MINO1		42	75	118	127	217	?
TAR10		46	38	46	57	67	D
<u>TAR20</u>		<u>15</u>	<u>8</u>	<u>15</u>	<u>21</u>	59	E
<u>TAR50</u>		<u>16</u>	<u>12</u>	<u>10</u>	<u>19</u>	36	E
<u>ASPH15</u>		<u>18</u>	<u>8</u>	<u>21</u>	<u>31</u>	44	D-E
<u>ASPH30</u>		<u>0</u>	<u>0</u>	<u>14</u>	<u>23</u>	39	E

after saturation.

@ for definition of Bands, see 5.3.4.

? absorption not in conformity with any trend; refer to numerical results.

Weight gain ratio values lower than roughly 33% are presented in **highlighted** underlined text (see 5.3.4).

Table 5.14 Percentage ratio of weight gain relative to the Control (polymer latices)

105°C DRIED SPECIMENS								
Mix ref.	Time							Band ®
	15min	1hr	4hr	1d	4d	12d	28d	
EVA5	56	44	<u>36</u>	<u>33</u>	48	64	75	1-2
SBR5	<u>28</u>	<u>26</u>	<u>27</u>	<u>25</u>	<u>38</u>	55	64	2-3
ACR5	56	51	46	50	76	89	91	?
ACR10	<u>36</u>	<u>30</u>	<u>37</u>	<u>31</u>	51	72	81	?

AS-RECEIVED SPECIMENS						
Mix ref.	Time					Band ®
	1hr	1d	3d	9d	11d [#]	
EVA5	50	38	<u>36</u>	51	256	C-D
SBR5	100	58	51	64	89	?
ACR5	---	---	---	---	---	---
ACR10	150	158	63	72	85	?

after saturation.

--- result not available.

@ for definition of Bands, see 5.3.4.

? absorption not in conformity with any trend; refer to numerical results.

Weight gain ratio values lower than roughly 33% are presented in **highlighted** underlined text (see 5.3.4).

Table 5.15 Percentage ratio of weight gain relative to the Control (amino alcohol derivatives)

105°C DRIED SPECIMENS								
Mix ref.	Time							Band [®]
	15min	1hr	4hr	1d	4d	12d	28d	
AMINO13	56	51	50	64	93	91	93	N
AMINO23	73	69	73	91	102	101	102	N
AS-RECEIVED SPECIMENS								
Mix ref.	Time					Band [®]		
	1hr	1d	3d	9d	11d [#]			
<u>AMINO13</u>	<u>0</u>	<u>11</u>	<u>22</u>	<u>35</u>	49	D-E		
<u>AMINO23</u>	<u>30</u>	<u>30</u>	<u>34</u>	39	63	D-E		

after saturation.

@ for definition of Bands, see 5.3.4.

Weight gain ratio values lower than roughly 33% are presented in **highlighted** underlined text (see 5.3.4).

Table 5.16 Percentage ratio of weight gain relative to the Control (proprietary waterproofers)

105°C DRIED SPECIMENS								
Mix ref.	Time							Band [@]
	15min	1hr	4hr	1d	4d	12d	28d	
CAL30	38	24	23	18	26	34	39	2-3
CONP1	56	54	61	67	94	94	95	N
CONP3	41	37	33	35	51	65	71	1-2
SIK9	77	77	56	91	97	97	97	N
SIK18	91	85	84	99	104	101	104	N
SET6	81	78	99	83	96	95	94	N
SET15	70	67	78	74	95	96	96	N

AS-RECEIVED SPECIMENS						
Mix ref.	Time					Band [@]
	1hr	1d	3d	9d	11d [#]	
CAL30	67	46	54	66	147	B-C
CONP1	0	0	13	22	39	E
CONP3	17	10	18	28	58	D-E
SIK9	25	27	31	38	76	D-E
SIK18	0	3	17	20	56	E
SET6	8	6	14	20	46	E
SET15	17	11	16	21	45	E

after saturation.

@ for definition of Bands, see 5.3.4.

Weight gain ratio values lower than roughly 33% are presented in **highlighted** underlined text (see 5.3.4).

Table 5.17 Percentage ratio of weight gain relative to the Control (miscellaneous)

105°C DRIED SPECIMENS								
Mix ref.	Time							Band ®
	15min	1hr	4hr	1d	4d	12d	28d	
IRON2	93	93	80	100	99	99	98	N
IRON10	73	78	71	98	100	100	98	N
SODSIL1	87	86	104	96	102	101	101	N
SODSIL5	104	103	131	114	109	108	108	N
SODSIL10S	104	105	129	129	122	120	119	N
SODSIL10SZ	99	104	101	119	109	108	108	N
POTSIL1	83	83	101	99	101	100	100	N
POTSIL3	102	98	115	107	108	107	108	N
CEL1	73	71	84	77	95	94	97	N
CEL5	63	54	56	43	57	71	83	1-2
AL0.1	80	80	92	85	103	105	102	N
AL0.2	108	95	92	80	99	102	99	N
ALR0.05	85	82	77	93	98	98	97	N
ALR0.2	98	87	79	85	96	97	97	N
MAGC1	104	95	102	86	96	96	96	N
MAGC2	104	98	110	101	104	105	106	N
FORM1	76	80	77	93	103	103	101	N
FORM2	77	79	76	89	102	102	102	N
FORM3	95	93	87	97	103	103	102	N
TEA0.025	68	65	62	82	89	88	88	N
TEA0.1	76	98	92	103	100	100	100	N
TEA0.25	76	78	96	104	100	99	100	N
TEA0.5	69	67	81	88	94	93	94	N

table 5.17 continued

AS-RECEIVED SPECIMENS						
Mix ref.	Time					Band [®]
	1hr	1d	3d	9d	11d [#]	
IRON2	142	266*	105	109	113	?
IRON10	<u>25</u>	<u>31</u>	<u>32</u>	43	58	D-E
SODSIL1	175*	99	69	97	93	?
SODSIL5	158*	94	60	66	76	?
<u>SODSIL10S</u>	<u>0</u>	<u>7</u>	<u>10</u>	<u>16</u>	44	E
<u>SODSIL10SZ</u>	<u>25</u>	<u>24</u>	<u>33</u>	39	46	D-E
POTSIL1	125	73	69	78	79	?
POTSIL3	158*	86	79	94	102	?
CEL1	67	73	78	97	99	A
CEL5	83	73	82	110	111	A
AL0.1	217*	118	143*	158*	241	?
AL0.2	242*	100	175*	189*	252	?
ALR0.05	42	61	76	80	103	B-C
ALR0.2	75	70	102	102	167	A
MAGC1	45	46	66	84	199	B-C
MAGC2	<u>33</u>	44	67	91	116	?
FORM1	<u>25</u>	<u>31</u>	46	51	71	D-E
FORM2	<u>33</u>	38	55	60	90	C-D
FORM3	45	62	71	78	88	B-C
<u>TEA0.025</u>	<u>0</u>	<u>15</u>	<u>22</u>	<u>33</u>	49	D-E
<u>TEA0.1</u>	<u>0</u>	<u>0</u>	<u>16</u>	<u>24</u>	41	E
<u>TEA0.25</u>	<u>0</u>	<u>0</u>	<u>11</u>	<u>22</u>	38	E
<u>TEA0.5</u>	<u>0</u>	<u>15</u>	<u>26</u>	<u>38</u>	51	D-E

after saturation.

? absorption does not conform to any trend; refer to numerical results.

@ for definition of Bands, see 5.3.4.

? absorption not in conformity with any trend; refer to numerical results.

Weight gain ratio values lower than roughly 33% are presented in **highlighted** underlined text (see 5.3.4).

Weight gain ratio values higher than roughly 150% are followed by a **highlighted** asterisk (see 5.3.4).

Table 5.18 Resistivity relative to the Control

Mix Ref.	RSR [#] _{bs}	RSR ^{\$} _{bs}	Mix	RSR _{bs}	RSR _{as}	Mix	RSR _{bs}	RSR _{as}
GGBS40	132	100	SODOL0.2	162	53	AMINO13	---	73
GGBS70	316	359	SODOL0.4	156	53	AMINO23	---	108
PFA30	126	130	BUTST2	---	102			
SF5	138	140	BUTST3	---	111			
SF10	292	285						69
			OLEICA1	155	87	CAL30	---	95
			OLEICA2	---	70	CONP1	---	105
			CAPA0.5	---	150	CONP3	---	88
KIES5	99	99	CAPA2	---	142	SIK9	---	78
KIES10	123	126				SIK18	---	90
BEN2	---	92	SOYO1	190	101	SET6	---	81
BEN5	---	80	SOYO5	292	167	SET15		
BEN10	---	82	SOYOE0.5	---	84			
WHIT5	---	109	SOYOE1	---	89			
WHIT10	114	88	SOYOE3	---	102			86
TALC5	89	90	SOYOE10	---	179	IRON2	---	81
TALC10	---	87	CORNO1	209	92	IRON10	---	99
PUM2	---	97	CORNO5	350	153	SODSIL1	---	84
PUM5	---	98	LINSO0.5	---	78	SODSIL5	---	65
LIME5	---	88	LINSO1	---	132	SODSIL10S	---	76
LIME15	---	91	LINSO2	---	110	SODSIL10SZ	91	95
LIME30	---	73	MINO0.5	---	85	POTSIL1	79	84
MSAND5	---	101	MINO1	---	77	POTSIL3	---	114
MSAND10	---	96				CEL1	---	113
IRO2	---	104	TAR10	---	91	CEL5	---	93
IRO0.25	---	99	TAR20	---	82	AL0.1	---	91
IRO0.125	---	95	TAR50	---	84	AL0.2	---	87
			ASPH15	---	93	ALR0.05	---	74
			ASPH30	---	82	ALR0.2	---	82
SODST0.2	109	104				MAGC1	---	73
CALST1	143	87				MAGC2	---	93
CALST3	152	87				FORM1	---	87
MAGST0.5	---	72	EVA5	---	63	FORM2	---	95
MAGST1	---	84	SBR5	---	91	FORM3	---	103
MAGST3	---	82	ACR5	---	---	TRI0.025	---	73
ALST0.25	---	66	ACR10	---	93	TRI0.1	---	65
ALST0.5	---	73				TRI0.25	---	72
ALST1	---	73				TRI0.5		

percentage ratio of resistivity before saturation of mix relative to Control.

\$ percentage ratio of resistivity after saturation of mix relative to Control.

--- not measured.

Table 5.19 Strength, density and effective porosity relative to the Control

Mix ref.	SR [#]	DR ^{\$}	PR [@]	Mix ref.	SR	DR	PR	Mix ref.	SR	DR	PR
GGBS40	91	98	108	SODOL0.2	48	89	125	AMINO13	77	99	95
GGBS70	68	98	113	SODOL0.4	40	90	168	AMINO23	97	100	104
PFA30	84	99	107	BUTST2	83	99	76				
SF5	108	99	101	BUTST3	82	98	62				
SF10	116	99	103								
				OLEICA1	62	93	109	CAL30	83	99	89
				OLEICA2	44	91	146	CONP1	93	99	101
				CAPA0.5	53	93	102	CONP3	93	99	105
				CAPA2	66	97	86	SIK9	90	99	99
KIES5	106	100	99					SIK18	78	98	106
KIES10	111	99	97	SOYO1	77	99	107	SET6	88	98	100
BEN2	89	100	104	SOYO5	55	97	100	SET15	70	96	108
BEN5	85	99	108	SOYOE0.5	82	99	103				
BEN10	79	99	96	SOYOE1	72	99	97				
WHIT5	103	100	98	SOYOE3	60	97	87				
WHIT10	101	100	102	SOYOE10	32	96	62	IRON2	99	100	100
TALC5	99	100	100	CORNO1	60	96	118	IRON10	97	147	104
TALC10	89	100	102	CORNO5	50	97	81	SODSIL1	94	101	101
PUM2	103	100	97	LINSO0.5	68	97	120	SODSIL5	88	99	108
PUM5	105	100	99	LINSO1	59	96	120	SODSIL10S	73	98	120
LIME5	95	99	100	LINSO2	58	96	120	SODSIL10SZ	95	99	107
LIME15	93	98	98	MINO0.5	72	95	134	POTSIL1	93	100	102
LIME30	87	98	114	MINO1	55	92	140	POTSIL3	83	101	107
MSAND5	84	100	95					CEL1	95	99	98
MSAND10	99	99	100	TAR10	86	98	101	CEL5	84	98	96
IRO2	101	99	100	TAR20	73	96	107	AL0.1	80	97	118
IRO0.25	104	100	96	TAR50	58	94	120	AL0.2	79	96	130
IRO0.125	97	99	102	ASPH15	93	99	101	ALR0.05	90	99	100
				ASPH30	83	98	105	ALR0.2	86	96	123
SODST0.2	88	100	97					MAGC1	88	99	102
CALST1	98	99	99	EVA5	61	92	130	MAGC2	83	99	107
CALST3	86	99	86	SBR5	67	98	97	FORM1	98	100	100
MAGST0.5	92	99	102	ACR5	90	99	97	FORM2	101	99	100
MAGST1	81	98	80	ACR10	73	100	104	FORM3	108	98	103
MAGST3	71	97	55					TEA0.025	104	100	93
ALST0.25	92	99	101					TEA0.1	95	99	104
ALST0.5	84	99	107					TEA0.25	100	100	104
ALST1	80	97	82					TEA0.5	100	99	97

percentage ratio of the compressive strength of a given mix to that of the Control.

\$ percentage ratio of the bulk density of given mix to that of the Control.

@ percentage ratio of the effective porosity of given mix to that of the Control.

5.3.4 Selection of materials for Phase 2

Before materials could be selected for the next phase it was necessary to identify those results which suggest a worthwhile (large), and statistically significant, reduction in chloride transport. In connection with this, contrasting the benefits imparted to the control concrete by introduction of an admixture to those associated with a large reduction in water/cement ratio (from 0.45 pertaining to the Control to, say, 0.26) would have been ideal. This would have required a plain OPC concrete of 0.26 water/cement ratio to be additionally cast and tested. Unfortunately, this was not done, and an alternative approach, to which the rest of this section is devoted, was followed.

Graphical illustrations are included in this section to allow easy assimilation of important results. For convenience, numbers from 1 to 96 are used in the graphs to identify mixes (see Table 5.20).

Before proceeding, it is important to point out that throughout the rest of this chapter statements on the performance of modified concretes should be, unless otherwise stated, implicitly understood to indicate performance relative to the Control. It is also worth remembering (see 5.3.3) that the term "ratio" (e.g. in "weight gain ratio") refers to the percentage ratio of the result for a given mix relative to the corresponding result of the Control.

An earlier discussion (3.5.3) revealed that gas-derived intrinsic permeability coefficients tend to hugely overestimate water-derived intrinsic permeability, the effect being more pronounced in low permeability concretes. This has been substantiated by research at IC (Denno 1990): when oxygen was used, lowering the water/cement ratio of concrete from 0.4 to 0.26 resulted in the intrinsic permeability coefficient being reduced by only 2-fold (105° C dried specimens); the corresponding reduction (specimens were vacuum saturated before testing) was larger when water was used (8-fold). Table 5.10 shows some of the materials investigated capable of reducing intrinsic permeability by up to 5-fold. On average, results on supposedly similar specimens were observed to exhibit

Table 5.20 Mix identification numbers (Phase 1 mixes)

Mix Ref.	Mix identification number	Mix ref.	Mix identification number	Mix ref.	Mix identification number
C	1	SODOL0.2	35	AMINO13	65
		SODOL0.4	36	AMINO23	66
GGBS40	2	BUTST2	37		
GGBS70	3	BUTST3	38		
PFA30	4			CAL30	67
SF5	5	OLEICA1	39	CONP1	68
SF10	6	OLEICA2	40	CONP3	69
		CAPA0.5	41	SIK9	70
		CAPA2	42	SIK18	71
				SET6	72
				SET15	73
KIES5	7	SOYO1	43		
KIES10	8	SOYO5	44		
BEN2	9	SOYOE0.5	45		
BEN5	10	SOYOE1	46		
BEN10	11	SOYOE3	47	IRON2	74
WHIT5	12	SOYOE10	48	IRON10	75
WHIT10	13	CORNO1	49	SODSIL1	76
TALC5	14	CORNO5	50	SODSIL5	77
TALC10	15	LINSO0.5	51	SODSIL10S	78
PUM2	16	LINSO1	52	SODSIL10SZ	79
PUM5	17	LINSO2	53	POTSIL1	80
LIME5	18	MINO0.5	54	POTSIL3	81
LIME15	19	MINO1	55	CEL1	82
LIME30	20			CEL5	83
MSAND5	21	TAR10	56	AL0.1	84
MSAND10	22	TAR20	57	AL0.2	85
IRO0.125	23	TAR50	58	ALR0.05	86
IRO0.25	24	ASPH15	59	ALR0.2	87
IRO2	25	ASPH30	60	MAGC1	88
				MAGC2	89
				FORM1	90
				FORM2	91
SODST0.2	26	EVA5	61	FORM3	92
CALST1	27	SBR5	62	TEA0.025	93
CALST3	28	ACR5	63	TEA0.1	94
MAGST0.5	29	ACR10	64	TEA0.25	95
MAGST1	30			TEA0.5	96
MAGST3	31				
ALST0.25	32				
ALST0.5	33				
ALST1	34				

up to 25% variations (relative to the average value for the two specimens tested). Based on these considerations, it was felt that a large improvement in resistance to pressure-induced flow can be associated with $kr_{(w)}$ values lower than roughly 33% (indicated in Table 5.10 by **highlighted** underlined text); conversely, adverse behaviour was considered indicated by $kr_{(w)}$ larger than approximately 200% (indicated by a highlighted asterisk).

Capillary rise testing, on 105° C dried specimens, revealed trends different to those normally observed for most concretes (3.2.3.2, see also Figure 5.1). These unusual trends seem to pertain particularly to water repellent-modified mixes, although were observed in others (mixes with proprietary products or polymers). Figure 5.2 shows five weight gain versus square root time trends which, respectively, indicate increasing absorption resistance: the normal trend (Trend N), characterized by two distinct absorption stages (3.2.3.2), and four unusual trends (Trend 1, Trend 2, Trend 3, Trend 4). It is of course conceivable that in Trends 1, 2, 3 and 4, respectively, a process involving water vapour diffusion/condensation plays an increasing role in water uptake[#]. Porosity results (Table 5.19) indicate that Trend N mixes become nearly completely saturated at the completion of stage I (1-2 days), indicating large continuous pores to represent a sizable portion of their effective porosity after drying (3.2.3.2). Trends 1, 2, 3, and 4, respectively, show a progressive disappearance of stage I which may, therefore, appear to have arisen from the materials involved giving rise to considerable refinement in pore structure and a consequent decrease in pore continuity. However, as will be seen next, oxygen permeability testing suggests that these effects play a rather limited, or at least secondary, role.

[#] The conditions under which capillary rise testing was performed (5.2.2.2.2,(II)) allow water vapour to diffuse into the largely unsaturated specimens not only from the surface exposed to free water, but also through surfaces exposed to nearly saturated air.

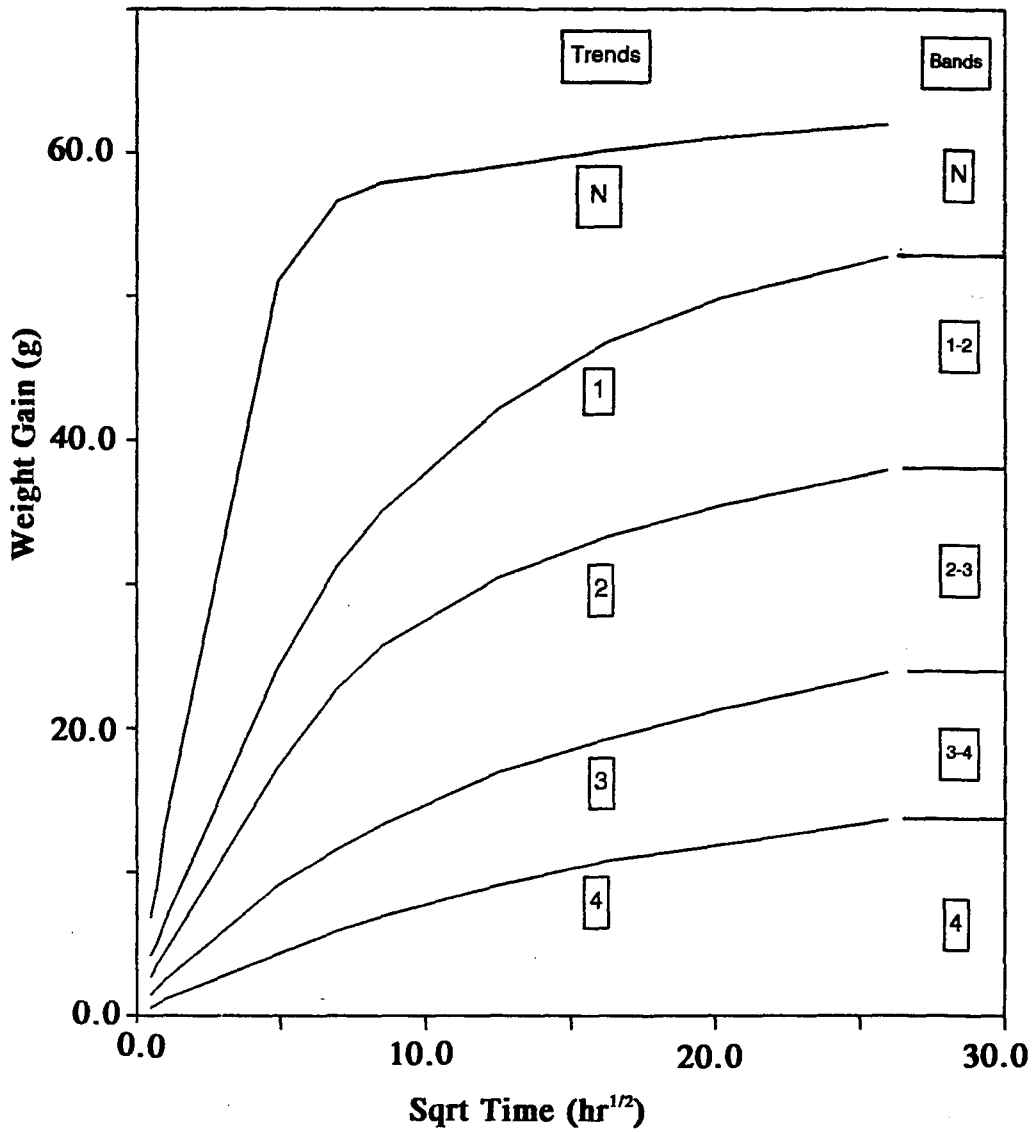


Figure 5.2 Absorption trends and bands (105°C-dried specimens).

This can best be explained with reference to Figures 5.3a, b and c. It is immediately obvious that many of the mixes showing pronounced reductions in absorption are nearly as permeable as the Control (e.g. mixes: 27 (CALST1), 34 (ALST1), 37 (BUTST2), 42 (CAPA2), 43 (SOYO1), 44 (SOYO5), 51 (LINSO0.5), 67 (CAL30), etc.), and, remarkably, a few (27 (CALST1), 35 (SODOL0.2), 36 (SODOL0.4), 40 (OLEICA2), 55 (MINO1), 61 (EVA5)), in fact, exhibit increased permeability. Admittedly, several of the materials responsible for unusual behaviour (e.g. in mixes: 47 (SOYOE3), 48 (SOYOE10), 58 (TAR50), 69 (CONP3), etc.) are found to have decreased permeability by 2-fold or more; however, it should be emphasised that materials from other classes (e.g. in mixes: 12 (WHIT5), 25 (IRO2), 93 (TEA0.025), etc.) give rise to a decrease in oxygen permeability to an extent similar or greater than that associated with the former materials, yet cause no departure from the normal trend, with changes in absorption being unimportant.

All mixes which exhibit a more than 2-fold increase in permeability (mixes: 35 (SODOL0.2), 36 (SODOL0.4), 55 (MINO1), 84 (A10.1), 85 (A10.2), 87 (A1R0.2)) appear, as indicated by bulk density determinations (see 5.2.2.2.1 and Table 5.19), to contain varying amounts of entrained air. This would suggest that the presence of entrained air has to some extent contributed to the increase in permeability. Indeed, it is conceivable that, because specimens are severely (105°C) dried prior to testing, the originally isolated air voids become interconnected by microcracks. The resulting network of air bubbles and microcracks thus allows easy permeation of gas, short-circuiting areas of less permeable paste. The question would then arise as to why an admixture belonging to the miscellaneous group and capable of generating gas bubbles in concrete (in mix 85 (A10.2), see A1.7) should cause a more than 9-fold increase in permeability, yet, instead of showing a parallel increase in absorption, shows a marginal decrease. This may be explained as follows. Air voids are relatively large (see 3.1.2.1) and are thus capable of generating fairly modest capillary suction forces in comparison with capillary pores. Thus, despite being interconnected by microcracks, they cannot compete for water with capillary pores and fill only very slowly.

Figure 5.3a Weight gain ratio after 1 day capillary rise testing versus corresponding oxygen permeability ratio for each mix.

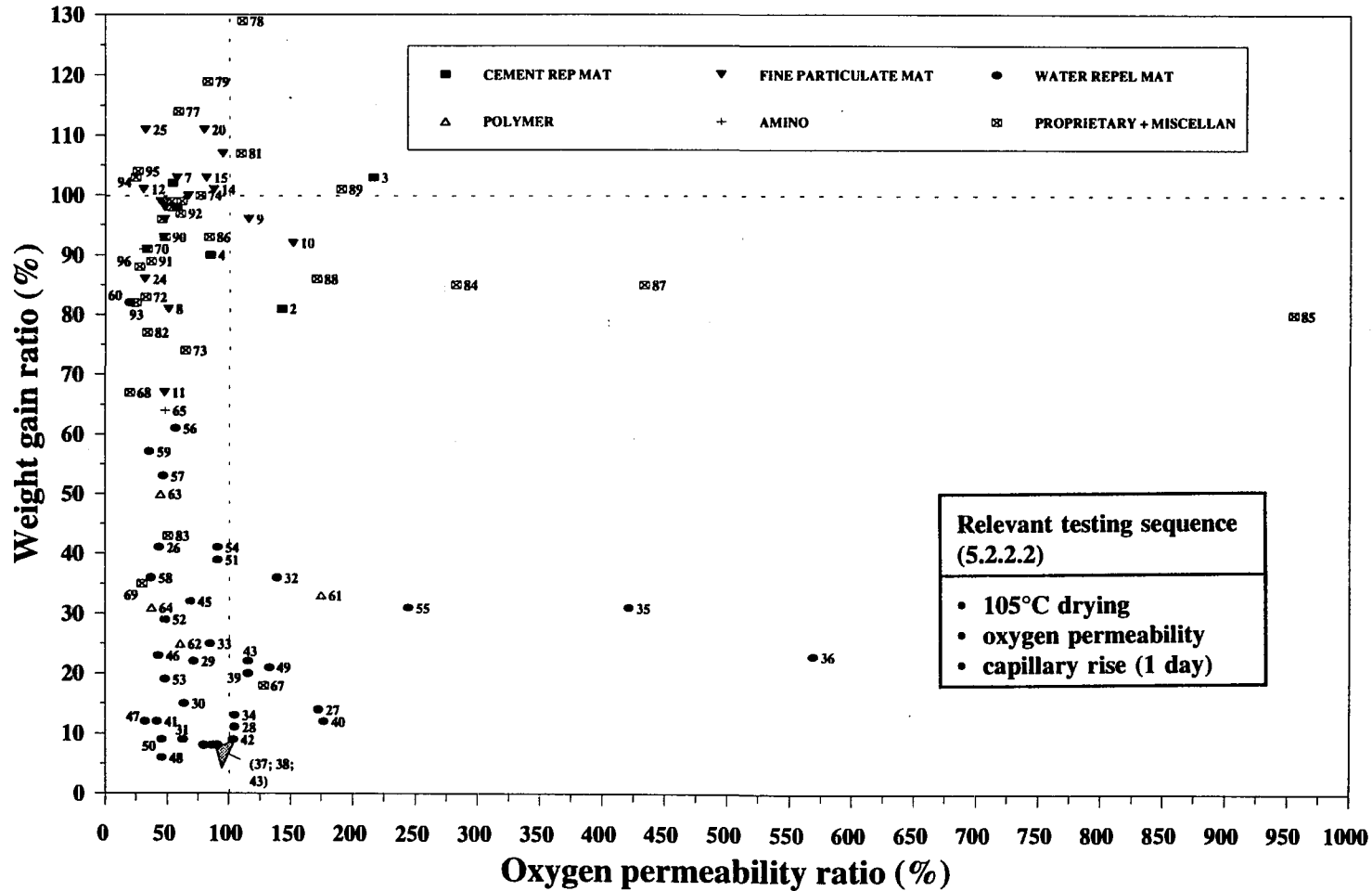


Figure 5.3b Expanded version of Figure 5.3a.

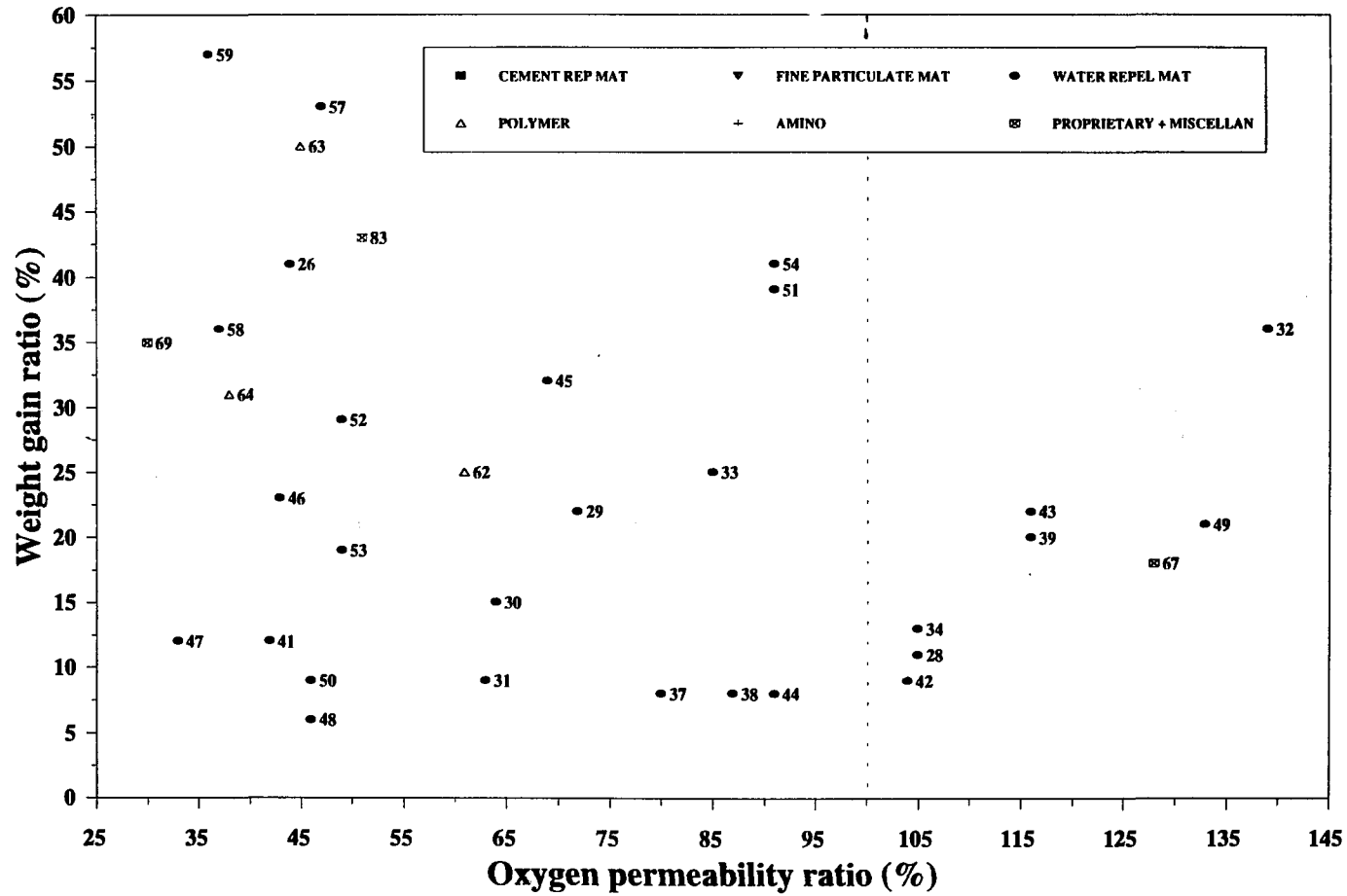
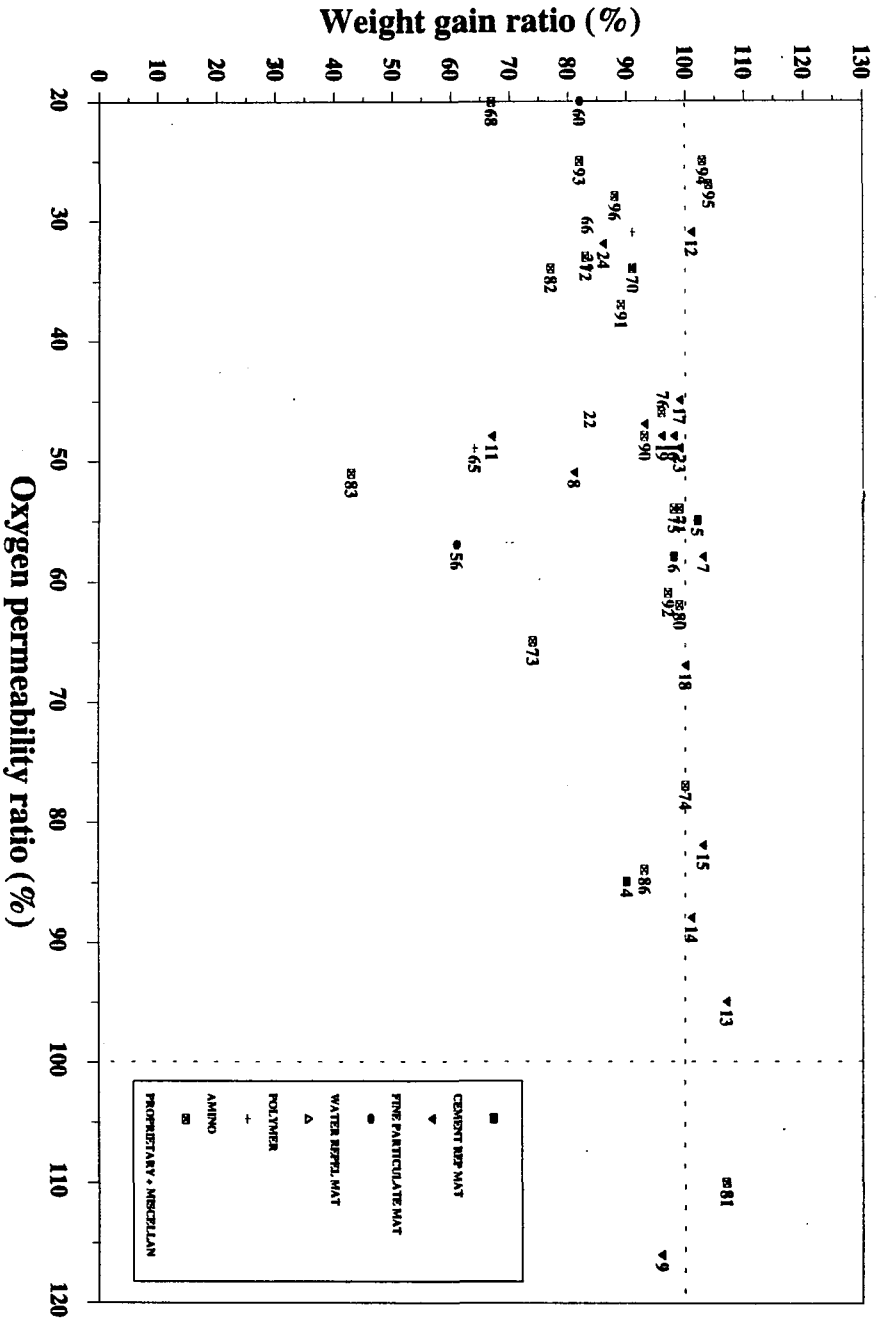


Figure 5.3c Expanded version of Figure 5.3a.



It is also interesting to observe, as seen in Figure 5.4, how mixes which appear effective in reducing water absorption exhibit much less favourable performance after being subjected to saturation (5.2.2.2.3). Indeed, some of these mixes show nearly similar (e.g. mixes: 27 (CALST1), 33 (ALST0.5), 41 (CAPA0.5), 69 (CONP3), etc.), or even higher (e.g. mixes: 35 (SODOL0.2), 36 (SODOL0.4), 49 (CORNO1), 55 (MINO1), etc.), water uptake compared to the Control after saturation. It seems that large parts of the porosity are not capable of generating sufficiently strong capillary suction forces and are thus not accessible to water unless pressure is applied. It is envisaged that two kinds of such porosity may be relevant, viz.: pores with walls coated with water repelling material (see A1.4 and 6.4), and large (air) pores (note that some, if not all, air is expelled by vacuum saturation).

Testing on as-received specimens uncovered five trends (Figure 5.5): Trend A to which the Control mix conforms, and four other trends (Trend B, Trend C, Trend D, Trend E), which, respectively, indicate increasing absorption resistance. In Trend A, water uptake during the early stages of testing (up to 3 days) is rapid, indicating capillary absorption control; thereafter the trend is evidently that of diffusion control. Trend E, on the other hand, appears to be almost entirely diffusion controlled.

Figure 5.6 shows that, as in the case of testing on oven-dried specimens, many of the mixes which are effective in reducing capillary absorption show nearly similar (e.g. mixes: 31 (MAGST3), 43 (SOYO1), 53 (LINSO2), etc.) or even higher (e.g. mixes: 29 (MAGST0.5), 36 (SODOL0.4), 49 (CORNO1), etc.) water uptake compared to the Control after being subjected to saturation.

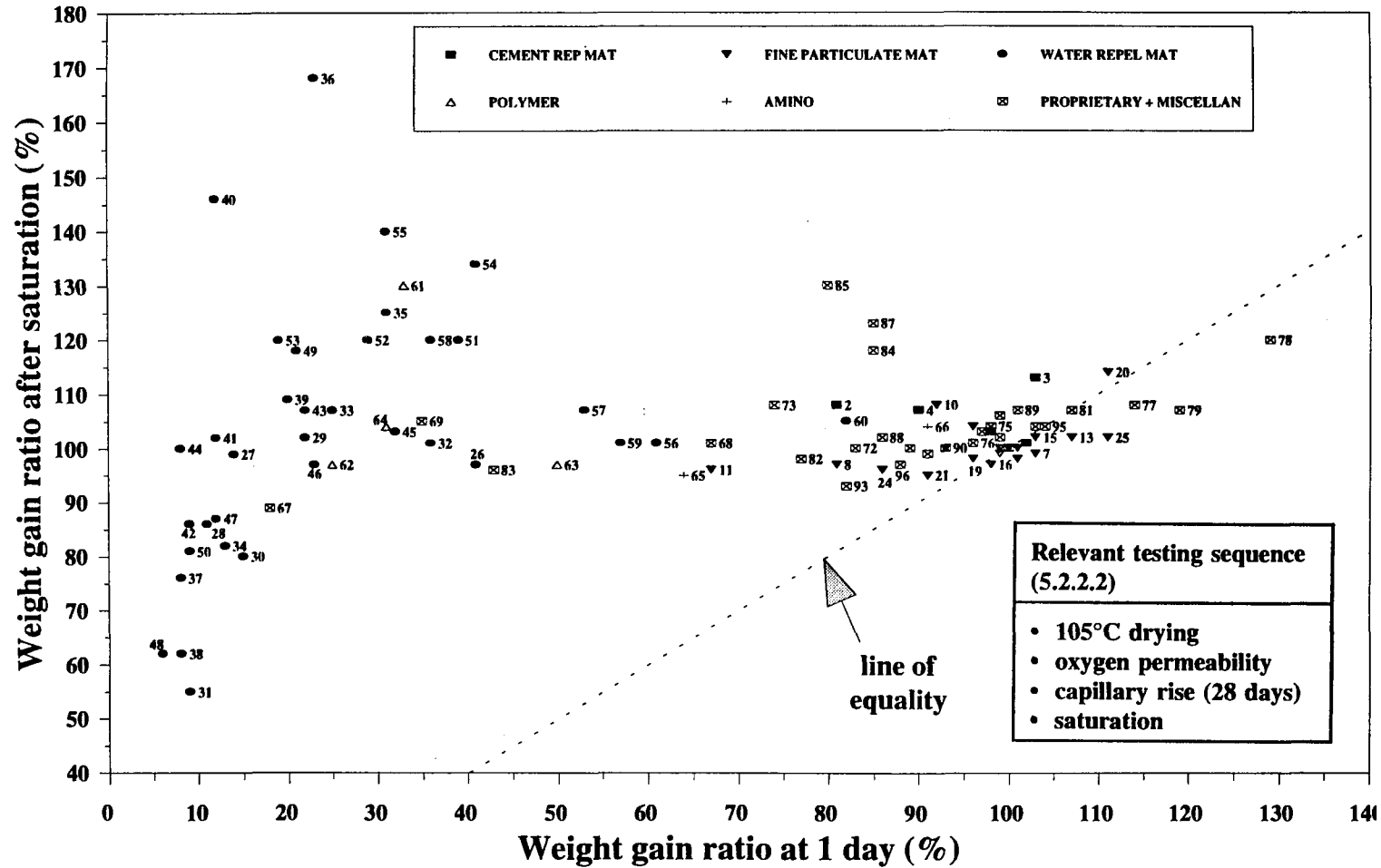


Figure 5.4 Weight gain ratio for each mix after specimens are subjected to saturation (effective porosity) versus corresponding ratio after 1 day capillary rise testing.

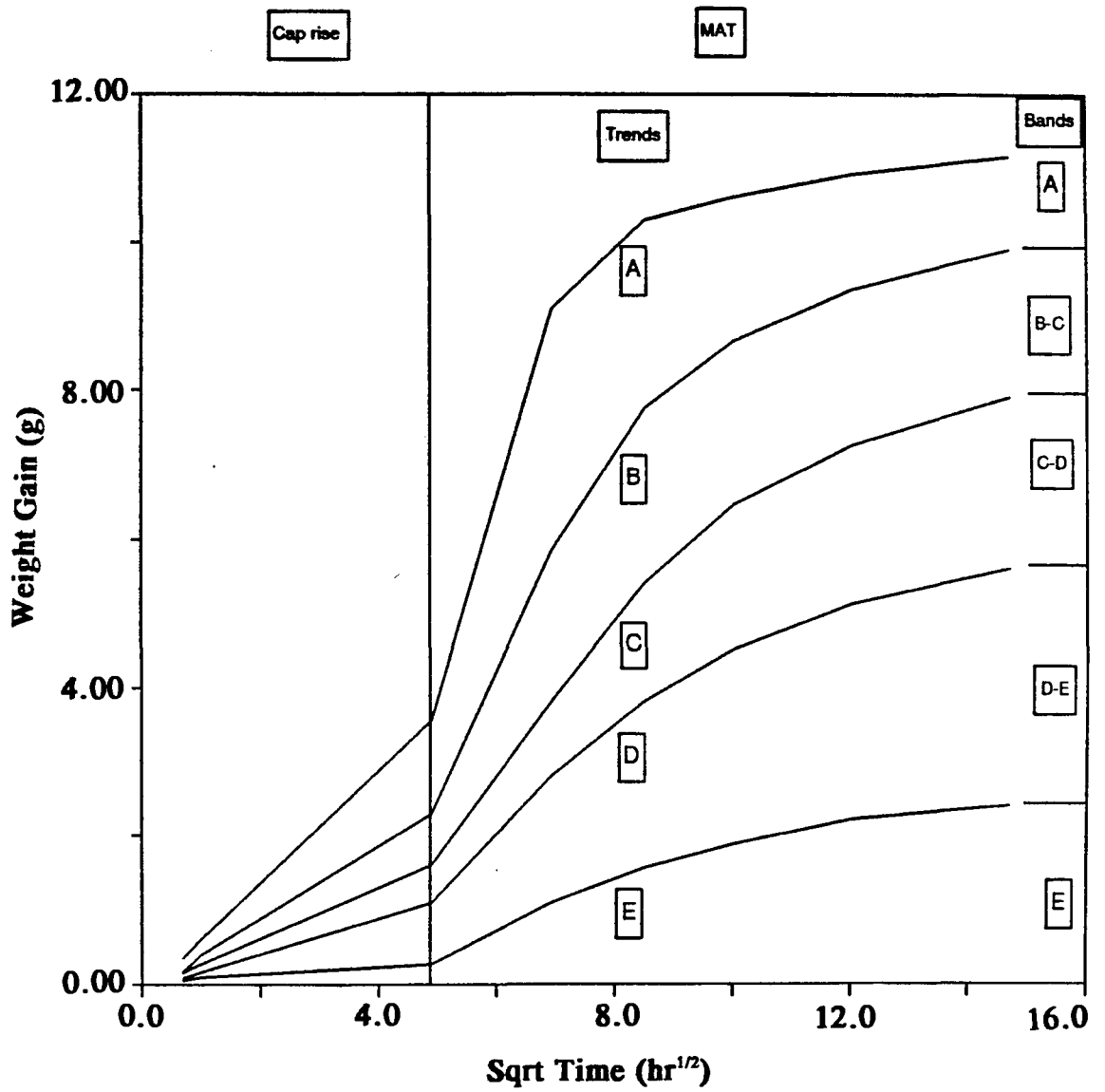


Figure 5.5 Absorption trends and bands (as-received specimens).

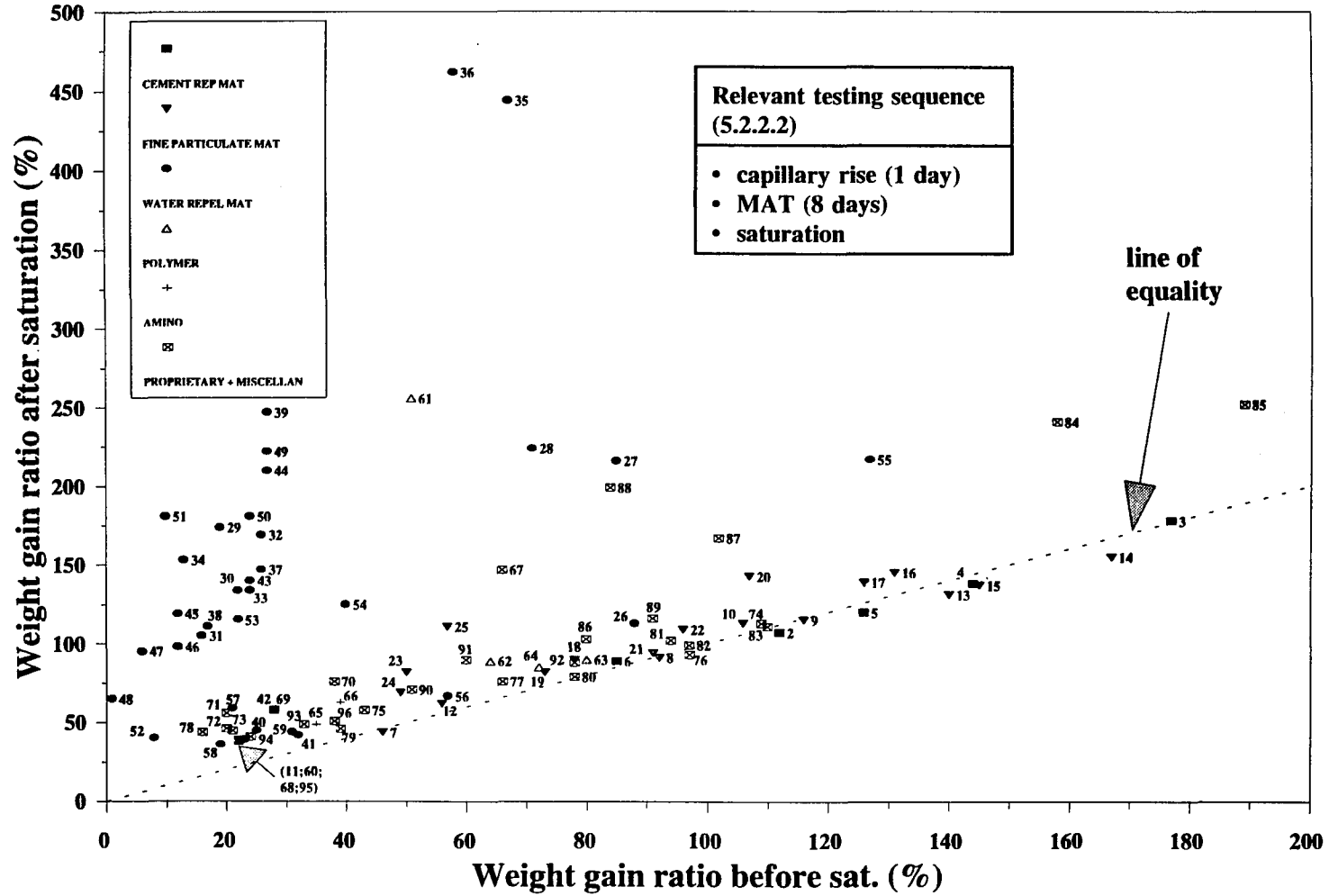


Figure 5.6 Weight gain ratio for each mix after specimens are subjected to saturation versus corresponding ratio before saturation.

Relative to the observed trends, bands were formulated to which mixes were allocated, as shown in Tables 5.11 to 5.17; these bands, shown in Figures 5.2 and 5.5, indicate, towards the bottom of the figures, increasing absorption resistance. Mix performance was then classed according to the bands into "average", "good", "very good", and "excellent" (see Table 5.21). Also, in Tables 5.11 to 5.17, data which indicate a percentage weight ratio below about 33% are highlighted and underlined; those which correspond to absorption resistance being substantially reduced are followed by a highlighted asterisk.

Table 5.21 Absorption resistance classification and bands

105° C-dried specimens		As-received specimens	
Band	Class	Band	Class
N		A	
1-2	average	B-C	average
2-3	good	C-D	good
3-4	very good	D-E	very good
4	excellent	E	excellent

In light of the foregoing, it first seemed reasonable to associate a large improvement in absorption resistance with "very good" or "excellent" performance pertaining in both the 105° C-dried and as-received states. There were, however, cases of materials which, in tests on as-received specimens, showed "good" (e.g. in mixes: 7 (KIES5), 91 (FORM2), etc.), "very good" (e.g. in mixes: 12 (WHIT5), 23 (IRO0.25), 25 (IRO2), 54 (MINO0.5), 59 (ASPH15), 69 (CONP3), 70 (SIK9), 65 (AMINO13), 66 (AMINO23), 90 (FORM1), 93 (TEA0.025), etc.), or even "excellent" (e.g. in mixes: 11 (BEN10), 52 (LINSO1), 57 (TAR20), 60 (ASPH30), 68 (CONP1), 71 (SIK18), 78 (SODSIL10S), 94 (TEA0.1)) absorption resistance, yet exhibited much inferior performance on oven-dried specimens (see also Figure 5.7). One explanation

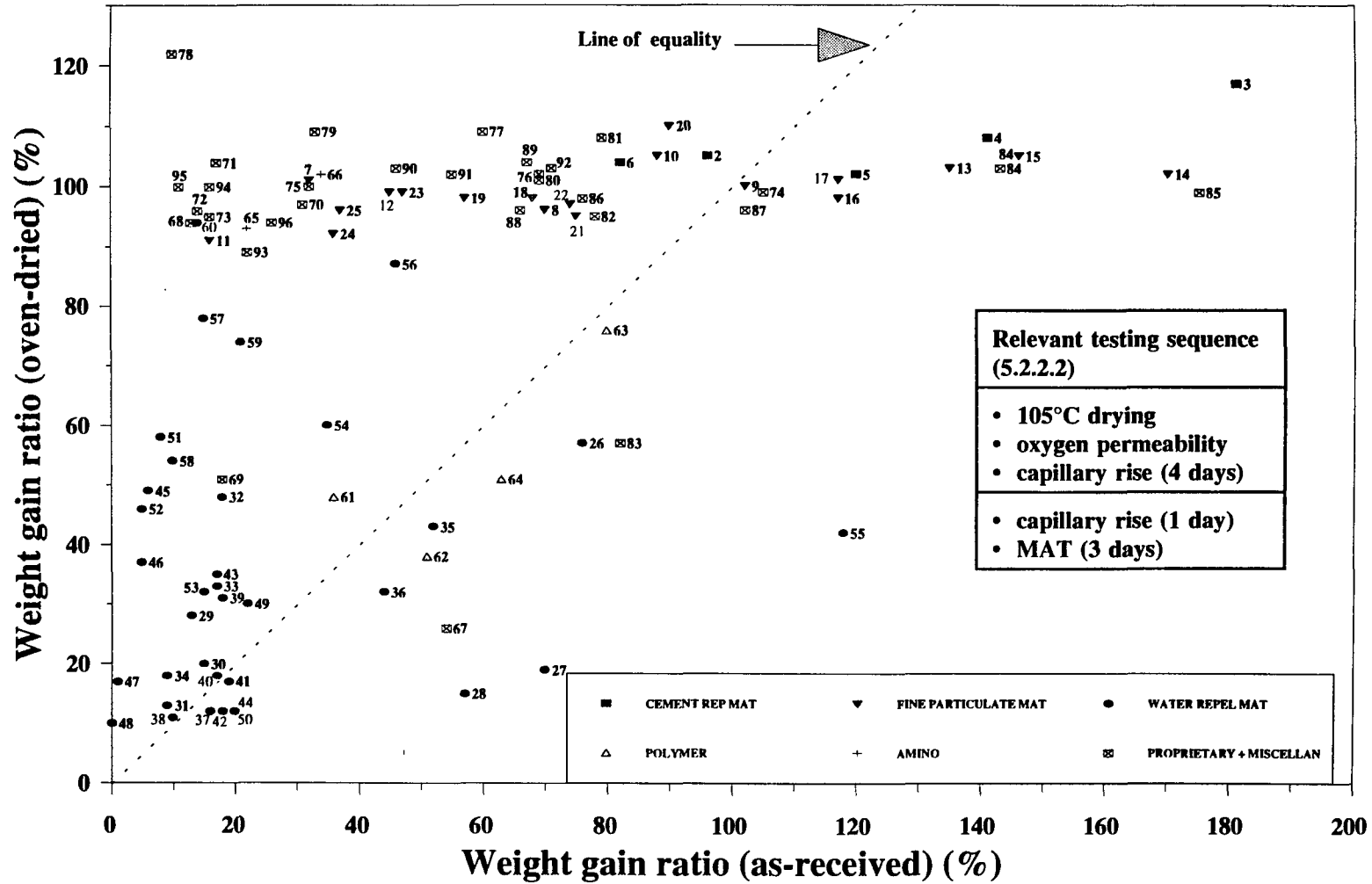


Figure 5.7 Weight gain ratio for each mix after 4 days capillary rise testing (105°C dried specimens) versus corresponding ratio after 3 days testing on as-received specimens.

may be that, before being tested in the as-received state, these mixes had a much higher moisture content than the Control (5.2.2.2.2). However, a much more likely explanation may be laid on the destructive influence of oven drying (5.2.2.2.2), implying that better absorption resistance may have been experienced had less harsh, and more realistic, conditioning been employed. This meant that, for these materials, less stringent selection criteria may be applied where oven drying was employed: "average" absorption resistance being acceptable, and good resistance to pressure-induced flow being indicated by $kr_{(g)}$ less than roughly 50%, rather than 33%.

The majority of resistivity testing was performed after saturation. Such treatment may, in addition to filling unsaturated voids, fill pore space emptied by expulsion of some, if not all, entrained air. This means that resistivity may be artificially depressed, the effect being more pronounced the higher the air entrainment. Bulk density determinations (Table 5.19) which suggest varying degrees of air entrainment, with high levels pertaining to several concretes (mixes: 35 (SODOL0.2), 36 (SODOL0.4), 39 (OLEICA1), 40 (OLEICA2), 41 (CAPA0.5)), therefore, raise some concern that results may have been to some extent distorted. Despite this weakness, some resistivity measurements taken before and after saturation (on mixes: 27 (CALST1), 28 (CALST3), 43 (SOYO1), 44 (SOYO5), 49 (CORNO1), 50 (CORNO5), see Table 5.18) substantiate beyond doubt that it was imperative to employ saturation (they reveal that, unlike the Control mix, some of the modified concretes experience a sharp drop in resistivity after being subjected to saturation).

Variations in resistivity (after saturation) between supposedly identical specimens were found to range from 5% to 10%. It is therefore likely that most RSR_{ω} values ranging roughly from 80% to 120% indicate insignificant, or small, variations from the Control. The results in Table 5.18 (see also Figure 5.8) therefore suggest that except for a few mixes (3 (GGBS70), 4 (PFA30), 5 (SF5), 6 (SF10), 41 (CAPA0.5), 42 (CAPA2), 44 (SOYO5), 48 (SOYOE10), 50 (CORNO5), 52 (LINSO1)) no increase in resistance to ion diffusion can be anticipated. It is also noteworthy that there seems to be a poor correlation between resistivity and effective porosity (Figure 5.8).

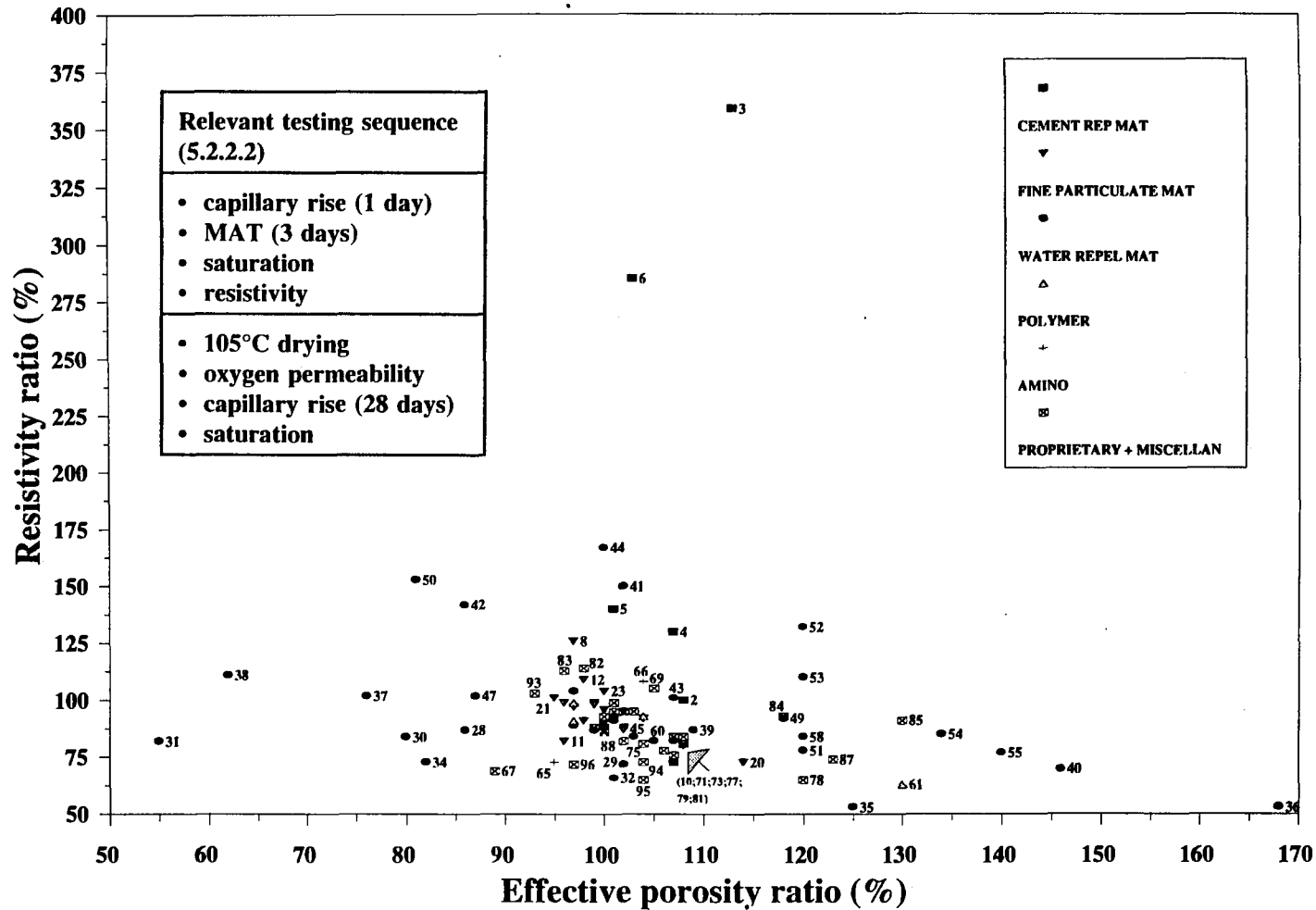


Figure 5.8 Resistivity ratio for each mix after specimens are subjected to saturation (as-received specimens) versus corresponding effective porosity ratio (105°C dried).

Table 5.22 presents the materials selected and those rejected, in accordance with the criteria outlined below. All materials for which at least one mix showed good performance in connection with at least one transport process were listed for selection, within their respective classes and subclasses. Detailed testing of the kind anticipated for Phase 2 could, however, only be performed on a limited number of mixes. Therefore, a decision was made to exclude any material which, at all dose levels used, caused seriously adverse behaviour in connection with any of the other transport processes. It is important to emphasise at this point that, in practice, adverse behaviour pertaining to a transport process would only preclude the use of the admixture responsible in environments where the transport process in question is relevant (Chapter 8), even then, consideration should be given to the possibility of counteracting adverse behaviour by simultaneous inclusion of other admixtures. Finally, some materials were rejected simply because others showed better performance; at this stage compressive strength results were taken into consideration.

Table 5.22 Selection of Materials for Phase 2

Class		Materials	Selected or rejected	Comments
Cement replacement materials		Ground granulated blastfurnace slag (GGBS)	S	(1)
		Pulverized fuel ash (PFA)	S	(1)
		Silica fume (SF)	S	
Fine particulate materials		Kieselguhr	S	
		Bentonite	S	
		Whiting	S	
		Talc	R	
		Pumice powder	R	
		Hydrated lime	R	
		Mortar sand	R	
		Iron oxide powder	S	
Water repellents	Soaps and Butyl stearate	Sodium stearate	R	
		Calcium stearate	R	
		Magnesium stearate	S	
		Aluminum stearate	S	
		Sodium oleate	R	
		Butyl stearate	S	
	Fatty acids	Oleic acid	R	
		Caprylic acid	S	
	Oils	Soyabean oil	S	
		Corn oil	R	
		Linseed oil	S	
		Mineral oil	R	
	Tar and Asphalt emulsions	Tar emulsion	S	
Asphalt emulsion		S		

table 5.22
continued

Class	Materials	Selected or Rejected	Comments
Polymer latices	EVA	S	(2)
	SBR	S	(2)
	Acrylic	S	(2)
Proprietary waterproofers	Caltite	S	
	Conplast prolapin	S	
	Sika1	S	
	Setcrete1	S	
Amino alcohol derivatives	Diethyl ethanolamine	R	(3)
	Dimethyl ethanolamine	S	(3)
Miscellaneous	Iron powder	S	(4)
	Sodium silicate	S	
	Potassium silicate	R	
	Cellulose acetate	S	(5)
	Aluminum powder	R	
	Magnesium carbonate	R	
	Iron sulphate + Calcium carbonate	S	
	Triethanolamine	S	

Table definitions

- **Selected or Rejected**

S: selected; R: rejected.

- **Comments**

(1): generally, the performance of mixes made with ggbs or pfa is known to be sensitive to the degree and efficiency of curing (Concrete Society 1990); therefore, better performance is expected when testing is performed after a longer curing period;

(2): refer to discussion on 5.2.1.3.5;

- (3): in relation to the desired function (5.2.1.3.6), performance cannot be established from the tests in Phase 1 (the dimethyl derivative was selected in preference to the diethyl derivative on account of its better performance as revealed by the tests performed).
- (4): in relation to the desired function (5.2.1.3.8), performance cannot be established from the tests in Phase 1;
- (5): it was felt interesting to carry out more testing to verify the performance of fibres.

Chapter 6 Phase 2: Detailed Investigation

6.1 Experimental details

6.1.1 Design of concrete mixes

6.1.1.1 Control concretes

Three OPC concretes, with water/cement ratios of 0.3, 0.35, and 0.4, were proportioned for use as control concretes, so that admixtures could be introduced to the concrete at the most appropriate water/cement ratio. This approach was also considered desirable as it would allow the performance of a modified concrete to be judged not only in relation to the respective control concrete (i.e. the control concrete with the same water/cement ratio (see 5.3.1)), but also against the other OPC concretes (see 5.3.4). In order to facilitate comparison between the performance of mixes having different water/cement ratios, the control concretes were proportioned on the basis of a common volume fraction of paste (see 3.1.2.2). As seen in Table 6.1, this was accomplished by using higher cement contents the lower the water/cement ratio; more details are given in A2.2.1.

Table 6.1 General details of the control concretes

Mix ref.	W/C	Cement content (kg/m ³)	Secondary materials
C(0.4)	0.4	397	---
C(0.35)	0.35	427	---
C(0.3)+	0.3	456	(1)

- **Mix ref.**

C : identifies the mix as a control mix.

(0.35) : indicates the free water/cement ratio of the mix.

+ : indicates that a secondary material was introduced.

- **Secondary materials**

(1): 1% superplasticizer (SP-450) was used to produce a sufficiently workable mix that could be properly compacted.

6.1.1.2 Admixture-modified concretes

6.1.1.2.1 General

Admixture-modified mixes were proportioned to have the same free water/cement ratio as the selected control. Each mix was formulated from the corresponding control mix by simply incorporating the admixture in question, and where an admixture contained a significant amount of water (see Appendix 1) the amount of water used in the mix was reduced by an equal amount.

At the outset, it was recognised that the limited duration and resources allocated to this project would dictate that the selected admixtures (Table 5.22) could only be investigated at this stage at a single dose level. This was, as will be seen in the following sections, determined largely on the basis of the experimental results of Phase 1.

General details of the mixes tested are given in Tables 6.2 through 6.9 of the following sections, and more comprehensive information is given in A2.2.2.

To allow easy identification of modified mixes, the mix reference will follow the format exemplified below:

Mix reference: LINSO1(0.35)+

where,

- LINSO** : abbreviation which identifies the material used (linseed oil in the case of this example)(the same abbreviations were used in Chapter 5);
- 1** : indicates the dose level at which the material was introduced;
- (0.35)** : indicates the free water/cement ratio;
- +** : indicates that a secondary material was introduced.

6.1.1.2.2 Cement replacement materials

Cement replacement materials were used in replacement (by weight) of the Ordinary Portland Cement (see Table 6.2).

Two mixes, with GGBS replacement levels of 40% (mix 2 (GGBS40)) and 70% (mix 3 (GGBS70)), were investigated in Phase 1.

Oxygen permeability testing showed that inclusion of GGBS increased permeability, and that the effect was much more pronounced at the high replacement level (see Table 5.20 and Figure 5.3a). Capillary rise testing (on as-received specimens) suggests that capillary absorption is also increased markedly in the case of GGBS70 (see Figure 5.7). It may be argued that the reduction in absorption in the case of the as-received specimens is attributable to GGBS70 specimens having a much lower amount of residual pore water than the Control (see 5.2.2.2.2,(II)). This, however, is unlikely to occur since it would imply that a mix with 70% GGBS undergoes more rapid early-age hydration than a corresponding unmodified OPC mix. Moreover, even when well hydrated, slag binds lower amounts of water than OPC and hence it would be expected that the residual moisture in the GGBS mix is higher; Taylor (1990) reports that "non-evaporable water contents of 2-year-old pastes of w/c ratio of 0.5 typically decrease with slag content from around 23% for pure Portland cements to 10-13% for cements with 90% slag". Thus, it can only be concluded that the inclusion of GGBS at high replacement levels increases porosity and renders it more interconnected. However, it is well established that unless well-cured, concrete having high GGBS replacement will allow more rapid molecular transport than comparable OPC concrete (Concrete Society 1990) and, in that context, the poor performance of GGBS can be attributed to the inadequacy of curing (method/duration, or both).

At 40%, GGBS was found to have no effect on electrical resistivity, whereas at 70% it increased resistivity by more than 3-fold (see Figure 5.8). That GGBS70 showed substantially higher resistivity than the control despite having a coarser pore structure

can only be seen (see 2.2.2, also 5.2.2.2.2,(III)) to emphasise the principal role of two effects: i) an increase in the resistivity of the cement paste pore solution, and/or ii) a decrease in ion mobility. Although it is difficult to establish the relative contributions of these two effects, it is well established that the use of GGBS in OPC concrete reduces ion (including chloride) mobility substantially, especially at high replacement levels (Gjørv & Vennesland 1979, Decker et al. 1989, Concrete Society 1990).

Finally, since resistivity testing suggested that only a few of the materials investigated can reduce chloride diffusion (see Figure 5.8), it was felt desirable that GGBS be tested at a high (65%) replacement level.

PFA was investigated in Phase 1 at a single replacement level (30%), and this level was also considered appropriate at this stage (see 5.2.1.3.2).

Silica fume was investigated (Table 5.2) at two levels, 5% (mix 5 (SF5)) and 10% (mix 6 (SF10)).

Little difference was detected in oxygen permeability between the two mixes (see Figure 5.3c). This may seem surprising since it is widely reported that permeability (in OPC concrete) can be lowered substantially by increasing the silica fume replacement level. This discrepancy may be explained by the effects of specimen pre-conditioning (5.2.2.2.2, (I)): oven drying resulted in the SF10 specimens sustaining a greater degree of microstructural damage than the SF5 specimens. This may also explain why capillary rise testing (on oven-dried specimens) revealed little difference between specimens from SF5 and SF10 mixes, particularly when considering that testing performed on as-received specimens showed SF10 to have a higher absorption resistance than SF5 (see Figure 5.7, refer also to 5.2.2.2.2, (II)).

At 5%, silica fume is found to increase electrical resistivity by 40%, whereas at 10% the increase is much more dramatic (Figure 5.8). Although the increase is likely to have been influenced by a decrease in pore solution resistivity (the pozzolanic reaction

of silica fume alters the pore solution chemistry), the inclusion of silica fume in OPC concrete is widely reported to have a substantial retarding effect on chloride ion diffusion (Byfors 1987, Gautefall & Havdahl 1989, Zhang & GjØrv 1991), particularly with increased silica fume contents. It is hence very likely that the increase in resistivity reflects also an increase in resistance to ion mobility.

Based on the above considerations, the inclusion of silica fume at 10% seemed more appropriate than at 5%.

Table 6.2 General details of mixes tested (cement replacement materials)

Material	Mix ref.	W/C	Dose level (% by cement)	Secondary materials
GGBS	GGBS65(0.4)	0.4	65	---
PFA	PFA30(0.4)	0.4	30	---
SF	SF10(0.4)+	0.4	10	(1)

(1): 1% superplasticizer (SP-450) was used to produce a sufficiently workable mix that could be properly compacted.

6.1.1.2.3 Fine particulate materials

It was mentioned before (5.2.1.3.3) that mixes with finely sieved mortar sand (mixes: 21 (MSAND5) and 22 (MSAND10)) were investigated so that the benefits, if any, of introducing fine particulate materials can be gauged against increasing the content (in concrete) of the fine fraction of aggregate. As seen in Table 5.10, mortar sand at 5% brings about a reduction in permeability which is roughly comparable to that of the best performing mixes in the group (mixes: 12 (WHIT5), 24 (IRO0.25), 25 (IRO2)). Similarly, with the exception of BEN10 (mix 11), MSAND5 appeared to offer comparable, or even better, resistance to capillary absorption than the majority of fine particulate mixes, when specimens were tested in the oven-dry state (see Figure 5.3c). However, when testing was performed on specimens as received, several materials (in mixes: 11 (BEN10), 12 (WHIT5), 19 (LIME15), 23 (IRO0.125), 24 (IRO0.25), 25 (IRO2)) are found to yield an absorption resistance much superior to that of the mortar sand mixes. Hence, the results furnished from Phase 1 appeared inconclusive. In a review of relevant literature (see A1.3), it was found that there is almost universal agreement that fine particulate materials, in their role as permeability reducers (see 5.1), would only be of benefit when used in mixes deficient in fines or cement. In such mixes, however, increasing the fine/coarse aggregate ratio might prove a successful remedy (Neville 1981). In the light of the foregoing, it was considered best to proceed by investigating fine particulate materials in concrete having a greater proportion of fines (i.e. fine aggregate) than that of the mixes of Phase 1 (this explains why the control mixes were designed to have a 40:60 fine to coarse aggregate ratio as against a 35:65 ratio for the Phase 1 Control).

All fine particulate materials were used in direct addition, as a percentage weight ratio of the cement content (Table 6.3). Dose levels were selected on the basis of oxygen permeability and capillary rise (on as-received specimens) test results. This was because capillary rise (on oven-dried specimens) and electrical resistivity testing revealed only marginal differences between the modified mixes and the control.

Kieselguhr, whiting, and bentonite, were all selected (for inclusion in this phase) primarily on account of their effectiveness in reducing capillary absorption in as-received specimens (see Figure 5.7 and discussion in 5.3.4). Kieselguhr and whiting were tested at 5% (mixes: 7 (KIES5) and 12 (WHIT5)) and 10% (mixes: 8 (KIES10) and 13 (WHIT10)) dose levels, and performance was found to be better at the lower dose. However, on preparation of the mixes, kieselguhr at 5% rendered the concrete mix entirely unworkable (kieselguhr has a high water absorption capacity (see A1.3)), and a sufficiently workable mix was obtained, without the need for a superplasticizer, when the dose rate was lowered to 3%. As for bentonite, 10% was selected as bentonite was found to yield appreciable benefits (in regard to both permeability and water absorption) consistently only when used at this level (mix 11 (BEN10), see Figures 5.3c, 5.6 and 5.7).

The optimum iron oxide dose rate seemed to lie in the range 0.25% to 2%.

Table 6.3 General details of mixes tested (fine particulate materials)

Material	Mix ref.	W/C	Dose level (% by cement)	Secondary materials
Kieselguhr	KIES3(0.4)	0.4	3	---
Bentonite	BEN10(0.4)+	0.4	10	(1)
Whiting	WHIT5(0.4)	0.4	5	---
Iron oxide	IRO2(0.4)	0.4	2	---

(1): Superplasticizer (SP-450) added at a rate of 1% w/w_{cement} to ensure adequate compaction.

6.1.1.2.4 Water repellents

All water repellents were used in direct addition, as a weight percentage ratio of the cement; asphalt and tar emulsions were, however, added in volume ratios expressed as litres of material per cubic meter of concrete.

It was mentioned before (5.2.1.3.4) that three factors should be considered when selecting appropriate dosing levels for water repellent materials. Two of these factors ((i) and (iii)) appeared later (see Table 6.4) to be in large measure valid. This meant that for the majority of water repellent materials, the dose levels required to bring about a worthwhile increase in absorption resistance would require that a 20%, or even greater, reduction in compressive strength to be tolerated, the actual strength levels obtained being lower than those currently in use by the industry (see Table 5.19 and 5.3.2.1). Consideration was therefore given to introducing those water repellent materials which showed a tendency to cause appreciable reductions in strength at as low a water/cement ratio as practically possible (mix being sufficiently workable without the need for a superplasticizer). It was felt that this approach would also help in accommodating the conflicting dosing requirements outlined above, since:

- reducing the water/cement ratio should bring about a decrease in the volume of conducting pores (large continuous pores), hence, it was anticipated based on relevant literature, a lower dose of water repellent would be required to achieve a given degree of improvement in absorption resistance;
- higher compressive strengths may be achieved by lowering the water/cement ratio, especially since lower water repellent dose levels would then be adopted; and finally
- it would be sensible to reduce the water/cement ratio in order to hinder leaching of water repellent material.

Details of water repellent mixes, proportioned in light of the foregoing, are given in Table 6.5.

That many water repellent materials (i.e. oils, fatty acids, and their soaps) entrain air when used in concrete is abundantly in evidence in the literature (Orchard 1979, Neville 1981, Rixon & Mailvaganam 1986, ACI Committee 212 1989; see also A1.4). It was therefore felt that the reduction in compressive strength, associated with the introduction of water repellents, may be, at least in part, due to air entrainment, and this appeared to be supported by the results of bulk density and compressive strength testing (of Phase 1, see Table 5.19). To investigate whether air entrainment accompanies the inclusion, at the selected dose levels, of the water repellents concerned, trial fresh density determinations were performed (in accordance with BS 1881: Part 107: "Method for determination of density of compacted fresh concrete"). The results confirmed that air was entrained in several mixes (the measured density was distinctly lower than the theoretically calculated density). Accordingly, it was considered important to investigate whether compressive strength loss can be avoided by eliminating entrained air. Towards this end, air-detraining agents (also referred to in the literature as anti-foaming agents) were introduced with the mix water; tri-*n*-butyl phosphate and silicone emulsion were employed as they have been widely used in concrete (Maslow 1974). Finally, the dosing levels of air-detraining agent were determined on the basis of trial tests in which the air-detraining agent was introduced at increasing dose levels until the measured fresh density was brought to a level roughly equal to the theoretically calculated density; it was felt that this would ensure that entrained air is largely eliminated.

Table 6.4 The influence of dose rate on the water absorption resistance and compressive strength of water repellent-modified concretes (Phase 1)

Material	Dose level (% by cement)	Absorption resistance ^a		Compressive strength ratio ^b (%)
		As-received	Oven-dried	
Magnesium stearate	0.5	excellent	good	92
	1	excellent	very good	81
	3	excellent	excellent	71
Aluminum stearate	0.25	very good	average	92
	0.5	very good	good	84
	1	excellent	very good	80
Butyl stearate	2	very good	excellent	83
	3	excellent	excellent	82
Caprylic acid	0.5	very good	very good	53
	2	very good	excellent	66
Soyabean oil	1	very good	good	77
	5	very good	excellent	55
	0.5@	excellent	average	82
	1@	excellent	good	72
	3@	excellent	very good	60
	10@	excellent	excellent	32
linseed oil	0.5	excellent	average	68
	1	excellent	average	59
	2	excellent	good	58
Tar emulsion	10#	good	\$	86
	20#	excellent	\$	73
	50#	excellent	average	58
Asphalt emulsion	15#	very good	\$	93
	30#	excellent	\$	83

a see 5.3.4

b see Table 5.19.

@ see 5.2.1.3.4.

introduced as l/m^3 of concrete.

\$ see Table 5.13

Table 6.5 General details of mixes tested (water repellents)

Material	Mix ref.	W/C	Dose level (% by cement)	Secondary materials
Magnesium stearate	MAGST2(0.35)+	0.35	2	(1)
Aluminum stearate	ALST0.5(0.35)+	0.35	0.5	(1)
Butyl stearate	BUTST3(0.4)	0.4	3	---
Caprylic acid	CAPA0.25(0.35)+	0.35	0.25	(1)
Soyabean oil	SOYO1(0.35)+	0.35	1	(2)
Linseed oil	LINSO(0.35)+	0.35	1	(3)
Tar emulsion	TAR25(0.35)+	0.35	25#	(4)
Asphalt emulsion	ASPH20(0.35)+	0.35	20#	---

introduced as l/m^3 of concrete.

(1): 0.05% w/w_{cement} air detrainng agent (tri-*n*-butyl phosphate).

(2): 0.5% w/w_{cement} emulsification aid (kieselguhr); also, 0.375% w/w_{cement} air detrainng agent (silicone).

(3): 0.07% w/w_{cement} air detrainng agent (tri-*n*-butyl phosphate).

(4): 0.131% w/w_{cement} air detrainng agent (tri-*n*-butyl phosphate).

6.1.1.2.5 Polymer latices

The use of polymer latices in concrete, at conventional dose levels (5.2.1.3.5), is known to improve workability substantially, and slumps in excess of 100mm at a water/cement ratio of less than 0.4 are not uncommon (Kuhlmann 1990). This improvement is believed (Chorinsky 1987, Semerad et al. 1987, Dennis 1988, Lavelle 1988, Justnes et al. 1990, Kuhlmann 1990) to be largely due to the combined influence of the following: i) the surface-active agents (surfactants) present on the latex particles (these are introduced in polymer latex mixes to prevent coagulation (A1.5)) which function as water-reducing admixtures, improving the wetting properties of the mix water and, additionally, causing air-entrainment (air entrainment improves workability), ii) the lubricating effect of the polymer solids, iii) the retarding effect that polymer latices have on cement hydration.

Polymer latices are widely reported to reduce substantially the penetrability of OPC concrete. In many publications, however, the performance of latex-modified concretes was assessed in comparison with unmodified OPC concrete at the same consistency, the water/cement ratio of the polymer mix thus being substantially lower than that of the control (e.g. 0.3 as against 0.45). Clearly, in such cases it is often difficult to establish the exact cause of the improvement in the property investigated. It is therefore desirable, from a research point of view, to introduce polymer latices at as low a water/cement ratio as would be permitted by workability requirements and to compare their performance against a control concrete of the same water/cement ratio, using a superplasticizer in the latter if necessary.

The mixes shown in Table 6.6 were proportioned based on the above, and such that their workability would not be substantially higher than that of the other concretes tested. Air detrainng agents were also used, to eliminate air entrainment, where necessary (whether or not they were necessary, and the required dose of air-detraining agent, was established in a similar fashion to water repellent mixes).

Table 6.6 General details of mixes tested (polymer latices)

Material	Mix ref.	W/C	Dose level (% by cement)	Secondary materials
EVA	EVA10(0.3)+	0.3	10	(1)
SBR	SBR5(0.35)+	0.35	5	(2)
	SBR10(0.3)+	0.3	10	(3)
Acrylic	ACR10(0.3)+	0.3	10	(2)

(1): air detrainng agents (0.18% w/w_{cement} tri-*n*-butyl phosphate and 0.09% w/w_{cement} silicone).

(2): air detrainng agent (0.15% w/w_{cement} silicone).

(3): air detrainng agents (0.15% w/w_{cement} tri-*n*-butyl phosphate and 0.3% w/w_{cement} silicone).

6.1.1.2.6 Amino alcohol derivatives

As Table 6.7 shows, the amino alcohol derivative dimethyl ethanolamine was introduced at this stage to the control at 0.35 water/cement ratio, at a dose level lower than that of Phase 1. Admittedly, Phase 1 testing did not shed any light on the performance of amino alcohol derivatives in the context of their intended function (5.2.1.3.6). Nonetheless, the approach was considered reasonable on the basis that: i) a reduction in water/cement ratio would lead to a reduction in the volume fraction of the relatively large continuous pores, which constitute the main channels through which chlorides diffuse (3.6.2) yet exhibit a comparatively low capacity to bind chloride, and ii) it is in this porosity that the amino alcohol derivative (which is completely miscible with water (see A1.6)) will be mainly present.

Table 6.7 General details of mix tested (amino alcohol derivatives)

Material	Mix ref.	W/C	Dose level (% by cement)	Secondary materials
Dimethyl ethanolamine	AMINO22(0.35) #	0.35	2	---

the first "2" in "22" identifies the amino alcohol derivative as the dimethyl derivative, as in 5.2.1.3.6.

6.1.1.2.7 Proprietary waterproofers

The products Everdure Caltite, Sika 1, and Setcretel were all introduced at the dose levels (see Table 6.8) recommended by their respective manufacturers. Conplast Prolapin, on the other hand, was introduced at 3%, after consideration of Phase 1 results.

Conplast Prolapin was tested at two dose levels, viz. 1% (mix 68 (CONP1)) and 3% (mix 69 (CONP3)). The results in Table 5.10 show that Conplast Prolapin decreases permeability substantially, the effect being somewhat more pronounced at the low (1%) dose level. On as-received specimens, Conplast also appears to give rise to a substantial increase in absorption resistance, with better performance pertaining to CONP1 (see Figures 5.6 and 5.7). On oven-dried specimens, however, results were disappointing (see Figure 5.7 and Table 5.16). At first, it was thought this discrepancy may have been a consequence of the effects of oven-drying (as discussed in 5.3.4). However, observing that increasing the dose level (from 1% to 3%) improved absorption resistance, it seemed also viable to presume that Conplast Prolapin comprises an amount of water repellent material which is merely sufficient to retard low rate water absorption, e.g. in as-received specimens. It was therefore felt appropriate that Conplast Prolapin be tested at the 3% level.

Table 6.8 General details of mixes tested (proprietary waterproofers)

Material	Mix ref.	W/C	Dose level	Secondary materials
Everdure Caltite	CAL30(0.35)+	0.35	30#	(1)
Conplast prolapin	CONP3(0.35)	0.35	3\$	---
Sika1	SIK9(0.4)	0.4	9#	---
Setcrete1	SET6(0.4)	0.4	6#	---

introduced as l/m^3 of concrete

\$ introduced as w/w_{cement}

(1): superlasticizer (Superplastet) used at 1% w/w_{cement} , in accordance with the manufacturer's recommendations.

6.1.1.2.8 Miscellaneous

Iron powder, sodium silicate, a blend of calcium carbonate and iron sulphate, cellulose acetate, and triethanolamine were all selected for inclusion in this phase (Table 5.22). However, it was later decided that sodium silicate should not be investigated because it was unclear whether the beneficial effects associated with its inclusion (primarily related to mix 78 (SODSIL10S)) can be attributed to its presence or that of the sugar used in conjunction with it.

Despite the benefits disclosed, when the miscellaneous materials were tested in Phase 1, testing failed to uncover the nature of the mechanism(s) responsible for these beneficial effects. This made it difficult to anticipate the appropriate dosing levels particularly since the water/cement ratio was lowered at this stage; the levels shown in Table 6.9, all expressed as percentage weight ratios of the cement content, were generally selected to be within range of levels used in the previous phase.

Table 6.9 General details of mixes tested (miscellaneous materials)

Material	Mix ref.	W/C	Dose	
			Level (% by cement)	Type
Iron powder	IRON10(0.4)	0.4	10	
Cellulose acetate	CEL2(0.4)	0.4	2	
Iron sulphate + Calcium carbonate	FORM2	0.4	0.5 2	FeSO ₄ CaCO ₃
Triethanolamine	TEA0.025(0.4) TEA0.1(0.4)	0.4 0.4	0.025 0.1	

6.1.1.3 Low paste-volume concretes

In an earlier discussion, on the pore structure of normal-weight concretes (3.1.2.2), it was suggested that since it is the paste fraction which accommodates chloride transport, there may be scope for retarding chloride ingress if the paste fraction was reduced to the minimum practical volume (which would be dictated primarily by workability requirements). However, the benefits of this approach, which was earlier brought to light through research at IC (Denno 1991), may be called into question by the argument that, given the same aggregates are used and the proportion of fine to coarse aggregate is maintained constant, an increase in the volume fraction of aggregate would most certainly lead to an increase in the volume fraction of paste located at the interface region with the aggregate, the effect of which may be to counteract the beneficial effects associated with the decrease in paste content.

As it is always recommended that when admixtures are considered for use in concrete, attention should be given first to achieving the best quality possible for the base concrete, it was considered necessary to carry out an investigation into the benefits and drawbacks, primarily in relation to chloride transport, of the approach outlined above. Towards this end, the two mixes listed in Table 6.10 were produced.

Starting with a certain base concrete, the control mix C(0.4), two options were considered for proportioning mixes with decreased paste volume, viz.: i) decreasing the water/cement ratio whilst maintaining the cement content constant, or ii) maintaining the water/cement ratio constant whilst decreasing the cement content, and using a superplasticizer if necessary; the second approach was adopted on the basis that the first approach would introduce complicating effects which would defeat the purpose of the study: reducing the water/cement would bring about pore structure refinement (3.1.2.2).

Table 6.10 General details of mixes tested (low paste volume group)

Mix ref.	Cement content (kg/m ³)	W/C	Secondary materials
LPV325(0.4)	325	0.4	---
LPV245(0.4)+	245	0.4	(1)

• **Mix ref.**

LPV : low paste volume group mix.

325 : cement content.

() : free w/c ratio.

+ : secondary material was used.

• **Secondary material**

(1): superplasticizer (SP-450) used at a rate of 2.4% w/w_{cement}.

6.1.2 Programme of work

6.1.2.1 Testing

6.1.2.1.1 Transport tests

I) Testing to characterize resistance to pressure-induced water flow

Methods commonly employed in characterizing the water permeability of concrete can be grouped into two main categories (Concrete Society 1988): i) output methods, where the rate of water flow (inflow or outflow, or both) through a test specimen is monitored, and ii) input methods, which rely on registering the depth of water penetration in concrete.

Apparatus available at Imperial College was designed primarily for measuring permeability based on the output method (essentially that originally developed by the Cement and Concrete Association (Concrete Society 1988)). At the outset, it was suspected that the apparatus available may not be suitable at least for some of the concretes under study due, primarily, to (Concrete Society 1988, Bamforth 1987): i) the difficulty of ensuring that specimens are fully saturated before testing (specimen saturation is considered vital if satisfactory results are to be obtained (3.5.1)), ii) the difficulty of detecting the extremely low water flow rates expected, and iii) the difficulty of ensuring that no significant leakage occurs around the sealing. Trials were therefore conducted to establish the suitability of the apparatus, using specimens from the control concrete C(0.3)+. The results were anomalous, for they seemed to suggest water flow to occur in a direction opposite to that of the applied pressure (the water meniscus at the outflow side, which would normally exhibit a gradual rise, showed instead a gradual drop, which continued until the test was aborted, at 5 days). This was not completely unexpected since similar tests carried out by another worker (Denno 1991) at IC, on concretes of more or less similar quality, also revealed similar tendencies. As no explanation was then found for these tendencies, a decision was made not to use the apparatus in any further investigations, to abandon the output technique, and to resort alternatively to oxygen permeability testing.

It is perhaps worth mentioning that later research at Cambridge University (Hearn 1992) revealed that positive flow through very low permeability concrete cannot be established unless a threshold pressure of the order of about 20 Bar is applied, and that below this pressure negative flow will occur.

In an earlier discussion (5.3.4, see also 5.2.2.2.2,(I)), it was suggested that the difficulties experienced when interpreting oxygen permeability results (of Phase 1) are most likely to have arisen because of harsh specimen preconditioning. Therefore, it was decided that less severe drying should be used in bringing test specimens to equilibrium (i.e. approximately constant weight). As it was difficult to elect, as most suited for this application (see 3.5.3), a particular drying regime, it was felt that it would be prudent to employ several drying regimes, as follows:

- Regime 1 (RG1)- 30 °C & 75% RH;
- Regime 2 (RG2)- 30 °C & 55% RH; and
- Regime 3 (RG3)- 50 °C & 10-14% RH.

The intrinsic permeability coefficients thus derived will be hereafter termed $k_{(g)RG1}$, $k_{(g)RG2}$, and $k_{(g)RG3}$, respectively.

Later on, it was possible to measure water permeability by an input method, when a testing assembly (with 14 test cells) which was earlier set up for use in another project at IC became available. Testing was performed on 150mm cubes in which embedded were a pair of electrodes (these were used earlier in electrical resistance measurements (Table 6.13)), as these were then the only available specimens fit for use in the apparatus. Testing was carried out as follows. The specimens, which were kept in sealed condition for approximately 11 months, were removed from their plastic bags and the cling film wrapping was cut off to expose the face which was to be injected with water. Plastic insulation tape was then applied to the now exposed parts of the injected face in order to prevent drying of specimens during testing. Specimens were weighed, then assembled in the test cells; the cell arrangement is shown in Figure 6.1. Immediately after measuring the electrical resistance (across the embedded electrodes), water was applied, the water pressure being gradually raised (during 1 hour) up to 7

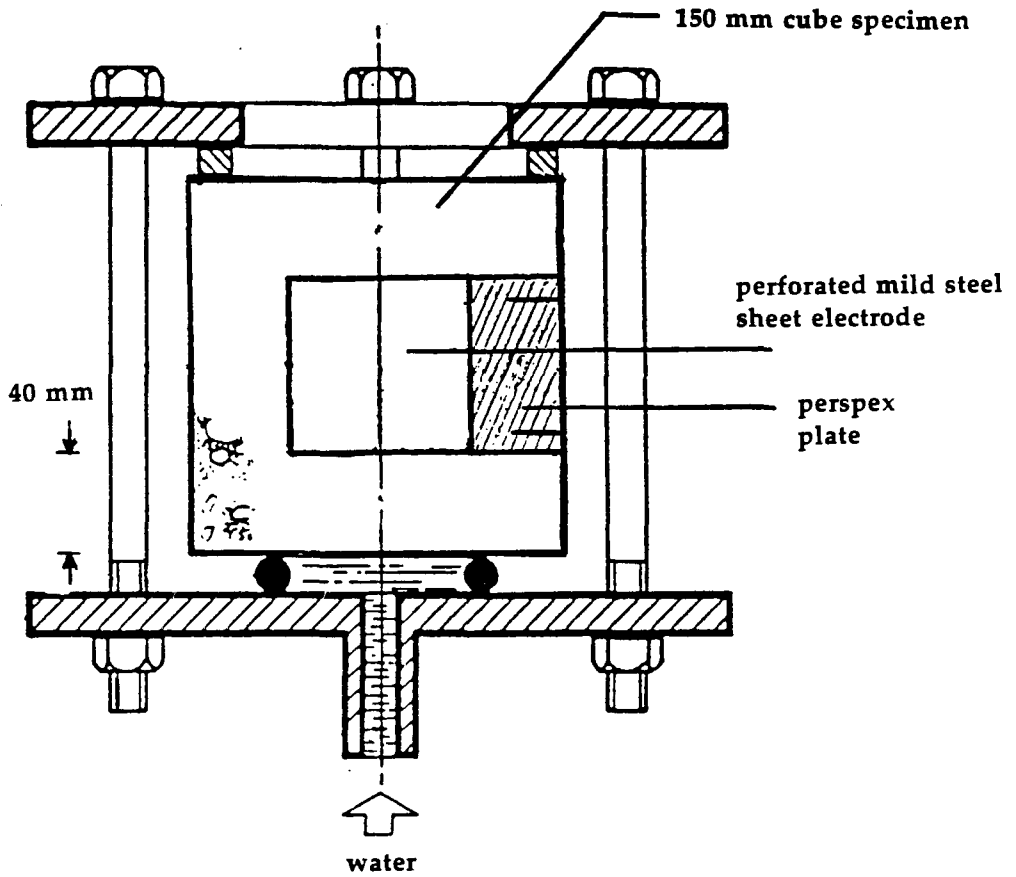


Figure 6.1 Cell arrangement (water permeability test).

bar and maintained at this level for the entire test duration (9 days). At the end of that period, specimens were removed from test cells, surface dried, weighed, then split, perpendicular to the injected face, so that the water penetration front could be visually detected. Moreover, electrical resistance was monitored regularly during the 9-day period of testing, as it was felt that the advance of water into specimens would be indirectly monitored (if advancing water was to reach the area between the electrodes, this would certainly be accompanied by a fall in resistance (2.2.2)).

II) Testing to characterize absorption resistance

The resistance afforded by concrete to absorption of chloride-containing water was evaluated before (5.2.2.2.2,(II)) using distilled water, instead of a chloride solution, on the grounds that the chemical composition of the permeating solution should have little influence on the absorption rate (3.2.3.3). However, at this stage, and in view of the unconventional nature of many of the concretes investigated, it was considered essential to explore whether the approach was justified before proceeding with large-scale testing. Towards this end, a preliminary investigation was carried out. This involved 17 different mixes chosen to be representative of the range of concretes tested. Due to time constraints, a rapid form of testing, namely MAT (5.2.2.2.2,(II)), was applied to 105 °C oven-dried specimens. Two parallel series of tests were conducted on two groups of replicate disk specimens (101mm diameter and 50mm thick). On one group of specimens, water was used as the permeating solution, and on the other a 0.5M NaCl solution. The results of these tests, shown in Figure 6.2, appeared to lend unequivocal support to the earlier approach, hence justifying the use of distilled water in subsequent testing.

Capillary rise testing was primarily used in assessing absorption resistance (5.2.2.2.2, (II)). However, it was considered desirable at this stage to employ a relatively milder preconditioning regime, involving oven drying to constant weight at 50 °C and 11-14% RH. Parallel testing was also conducted on unconditioned specimens, i.e. specimens as-received, in order to "get a feel" for any possible negative influences associated with the conditioning of specimens.

Finally, since water absorption usually occurs as part of wet/dry cycling (3.2.1), the rate of weight loss of specimens subjected to two different drying regimes was investigated, viz. i) mild drying, at 30 °C & 75% RH, and ii) severe drying, at 50 °C & 11-14% RH.

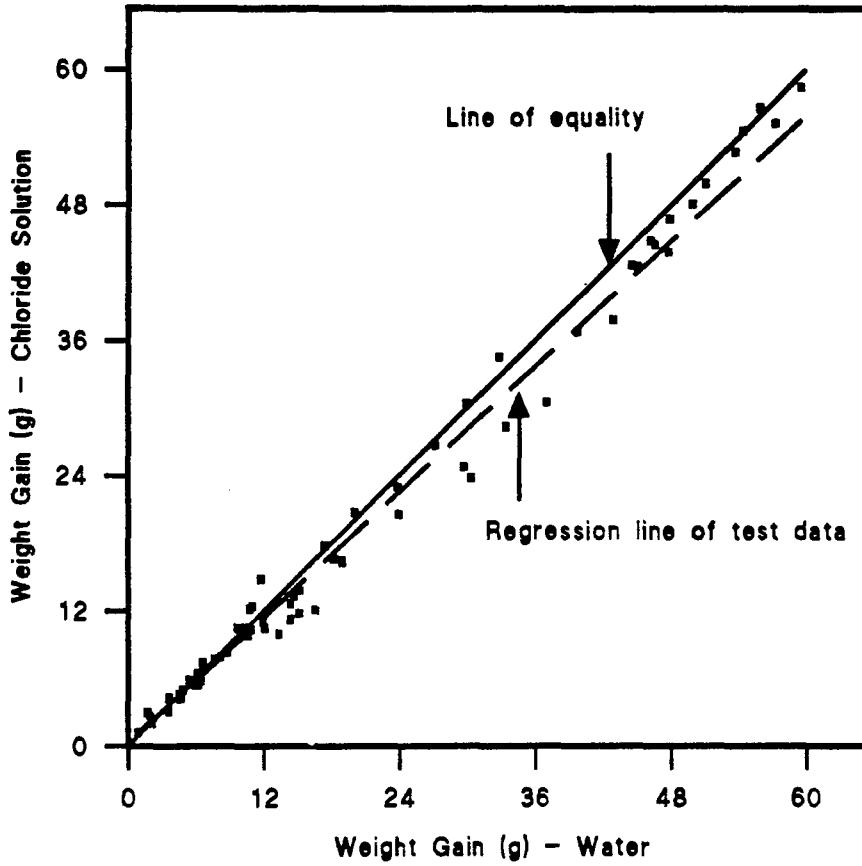


Figure 6.2 Effect of chloride on capillary absorption rate (data represent the average weight gain, measured throughout the 10-day test period, for all the concretes tested).

III) Testing to characterize resistance to chloride diffusion

Chloride ion diffusion has been investigated using various techniques, of which two techniques, namely the penetration profile and diffusion cell, are the most widely used. An important advantage of the first method is that it is directly applicable to concrete exposed in the field. Unfortunately, however, the method also has various shortcomings (Buenfeld & Newman 1987, Atkinson & Nickerson 1988) which would render the results furnished ambiguous unless several penetration profiles (for each mix tested) are constructed after various periods of exposure, possibly spanning a test period of at least 3 years. The second technique also requires a very long test duration if applied to representative specimens of concrete (specimen thickness of 25mm or more for 10mm aggregates), especially in the case of high quality mixes (El-Belbol 1991). In an attempt to reduce the test duration, many researchers have resorted to using thin (usually < 15mm) specimens of mortar or cement paste. This approach was, however, ruled out as it was felt that the influence of the coarse aggregate, which could be important, would be overlooked. Consideration was also given to accelerating the chloride ion diffusion process by increasing the testing temperature "Cell temperature"; Page et al. (1981), for instance, reported that the effective diffusion coefficient in a 0.4 water/cement ratio OPC paste can be increased by approximately 4-fold when the cell temperature is increased from 25 °C to 44 °C. Unfortunately, the apparent temperature dependence of ion diffusion in cement pastes has been shown (Atkinson & Nickerson 1984) to have a contribution not only from the temperature dependence of the diffusion mechanism, which would be governed by the well known Arrhenius Equation, but also from irreversible temperature-induced changes in pore structure. Moreover, and perhaps more to the disadvantage of this approach, the temperature dependence of ion diffusion has been observed to vary from one type of cement to another (Page et al. 1981). Another alternative to the diffusion cell technique, which is currently attracting considerable attention (Whiting 1981, El-Belbol & Buenfeld 1988, Dhir et al. 1990), lies in driving chloride ion diffusion by an electrical potential difference rather than by a concentration gradient. Indeed, a test method (the Accelerated Chloride Ion Diffusion (ACID) test) based on this technique has been recently developed at IC (El-Belbol

1991), and evidence was presented (using a range of concretes at different water/cement ratios, some containing cement replacement materials) of the ionic transport process in the ACID test being representative of ionic diffusion under a concentration gradient (i.e. in a diffusion cell). Because the ACID test is not widely documented, and since it was by no means certain that the method would be equally applicable to the range of concretes, some of which are unconventional, to be investigated, it was considered necessary to employ, in addition to the ACID test, the penetration profile method. However, the latter was employed only in a limited way (see Table 6.13).

Penetration profiles determinations were conducted on 101.6mm dia. and 50mm thick disk specimens which were immersed for a period of 8 months in a 0.5M sodium chloride solution, at 20° C. Specimens were subjected to saturation (5.2.2.2.2, (II)) before being immersed in the chloride solution in an attempt to eliminate absorption-driven chloride ingress. Concrete powder sampled at various distances (2mm increments) from the exposed surface were then analyzed for chloride (total) content by potentiometric titration.

ACID testing involved placing a previously saturated concrete disk specimen (101.6mm dia. and 50mm thick) to form a partition between two liquid-filled compartments, one containing a 1M NaCl solution and the other a neutral solution (0.3M NaOH). A constant voltage (40V d.c.) was then applied via plate electrodes immersed in the two solutions such that chloride ions were driven through the specimen towards the electrode immersed in the neutral solution. Potentiometric titration was carried out regularly on small samples taken from the neutral solution in order to monitor the chloride concentration.

6.1.2.1.2 Corrosion-related testing

The ability of an admixture to reduce chloride ion penetration does not necessarily imply enhanced resistance to corrosion (Chapter 2). To identify any possible negative influences on the corrosion resistance of embedded steel associated with the use of the tested admixtures, several supplementary studies were undertaken. These included: i) electrical resistivity testing, ii) carbonation testing, and iii) corrosion testing.

I) Electrical resistivity testing

An admixture may alter the electrical resistivity of the respective control concrete in two ways: i) directly, by virtue of induced alterations in porosity, pore size distribution, or pore solution resistivity, and ii) indirectly, by altering response to exposure (e.g. the rate of drying, wetting, ingress/leaching of ions). Since the latter can be, to some extent, elucidated from the results of the transport tests, this study focused on measuring changes in resistivity not related to exposure. Towards this end, electrical resistance was monitored (measurements were made using a Universal Bridge at 9V and a frequency of 1000Hz, see 2.2.1) over a period of 140 days across a pair of perforated mild steel sheet electrodes embedded in 150mm concrete cubes, which were kept in sealed condition throughout the test duration. It was anticipated that the resistance measured would be affected by self-desiccation of the concrete, but this was not considered as a cause for concern since the phenomenon of self-desiccation is a natural manifestation of cement paste hydration.

II) Carbonation resistance

Carbonation resistance was characterized by means of accelerated carbonation testing. This involved conditioning 100mm cube specimens at 75% RH for 1 month, exposing the specimens to 5% CO₂ at 55% RH & 30° C for a further 5 months, then splitting and spraying with phenolphthalein solution to determine the carbonation depth. Additionally, electrical resistance was measured (before cubes were split) across two parallel as-cast faces of the cubes, using external plate electrodes; the purpose of these measurements will become apparent later (6.3.3). Initially, the electrodes were simply clamped to the surface of the cubes, but this was found to give erratic results due, presumably, to the non-uniform contact between the concrete and the electrode over the complete electrode area. A conducting medium (graphite paste) was therefore adopted for use between the concrete and electrode surfaces.

III) Corrosion testing

The main purpose of corrosion testing was to investigate the influence of the unconventional admixtures under investigation (those for which no relevant literature was available) on the corrosion of embedded steel; for comparison purposes, several materials for which abundant literature was found available were also investigated. Details of the mixes tested are given in Table 6.11. For simplicity, all mixes were fabricated from the same control concrete, which was chosen to be mix C(0.4).

Testing involved visually observing the condition of mild steel coupons embedded in concrete specimens of the form shown in Figure 6.3. The specimens were oven-dried until equilibrium at 50° C & 11-14% RH. Thereafter, they were saturated under vacuum with 1.0M sodium chloride solution, in which they were kept immersed for 7 days. Finally, specimens were stored for 1 month in an environmentally controlled chamber, at 30° C & 75% RH; further important details are given below.

Table 6.11 Details of mixes used in corrosion testing

Material	Mix Ref.	Admixture	
		Dose level	Mode
---	CRC	---	---
PFA	CR1	30	A
Silica fume	CR2	10	A
Magnesium stearate	CR3	2	B
Aluminum stearate	CR4	1	B
Butyl stearate	CR5	3	B
Caprylic acid	CR6	2	B
Soyabean oil	CR7	1	B
	CR8	5	B
Linseed oil	CR9	1	B
Tar emulsion	CR10	20	C
Asphalt emulsion	CR11	20	C

..... table 6.11 continued

Material	Mix Ref.	Admixture	
		Dose level	Mode
EVA	CR12	10	D
SBR	CR13	10	D
Acrylic	CR14	10	D
Dimethyl ethanolamine	CR15	2	B
Caltite	CR16	30	C
Iron powder	CR17	10	B
Triethanolamine	CR18	0.25	B

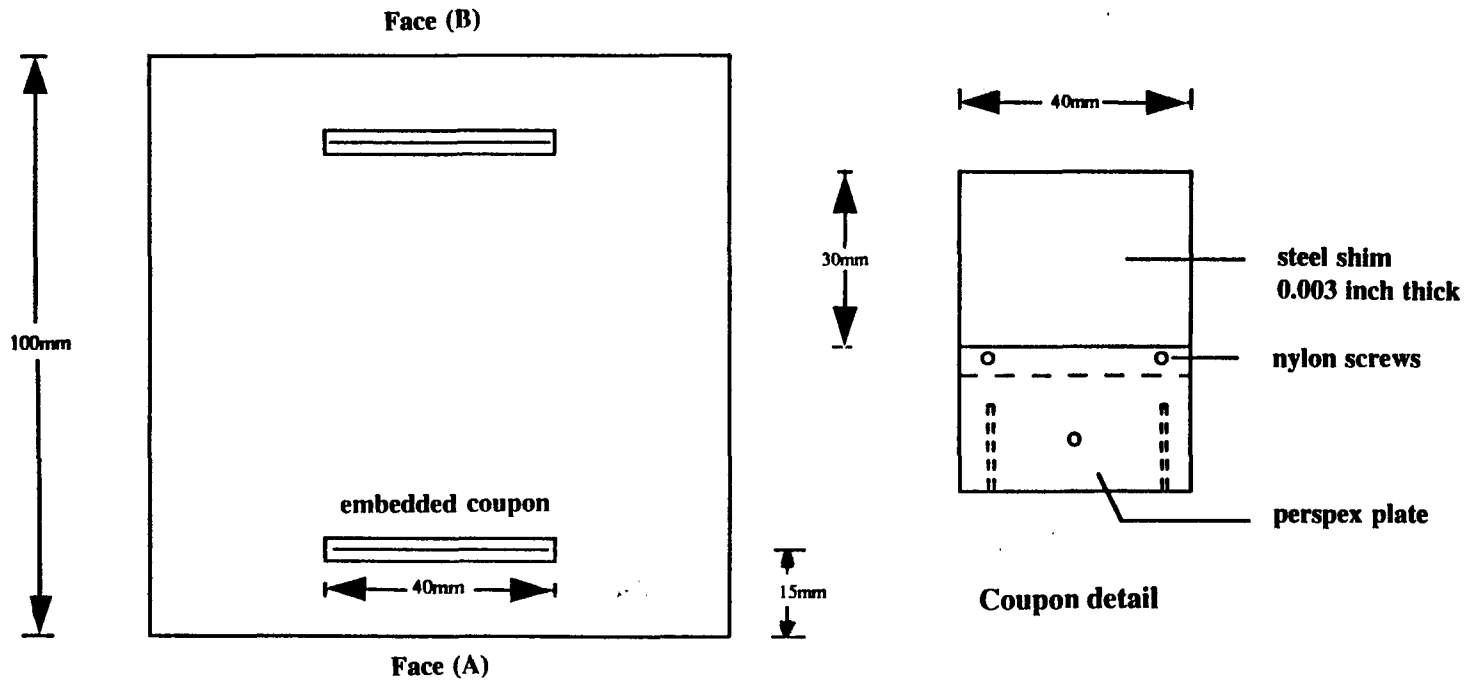
Admixture (Mode)

A: introduced in replacement, as weight percentage of cement.

B: introduced in addition, as weight percentage of cement.

C: introduced in addition, as litres of material per cubic meter of concrete.

D: introduced in addition, as weight percentage of polymer solids relative to weight of cement.



Test specimen (Top view)

Figure 6.3 Corrosion test cube with embedded coupons.

- Specimen conditioning: i) ideally, specimens would be conditioned at a relatively low, but realistic, relative humidity, prior to saturation. Unfortunately, and because of time constraints, this was impossible to undertake (the process was anticipated to take many weeks for the 100mm cubes of the relatively good quality concretes under investigation), ii) an undesirable manifestation of specimen conditioning was the development of visible cracks; these are likely to have arisen because of the discrepancy between the coefficients of thermal expansion of the concrete and the perspex plate.
- Chloride ion concentration in the test solution: in order to facilitate visual comparison between the performance of control concrete and that of the modified concretes, which was to be made in terms of the percentage area of the coupons corroded (PACOR), it was considered desirable that PACOR of the control specimen lie in the range 40 to 60%. A preliminary study was undertaken, in which control concrete specimens were used and three solutions of 0.5M, 1.0M, and 1.5M sodium chloride were employed, based on which the 1.0M solution was selected.
- Chloride content: it is well known that the chloride content of the concrete in the neighbourhood of embedded steel can have a critical influence on the corrosion process (Chapter 2). Hence, after a cube was cut open, a drill was used to obtain a concrete powder sample in the immediate vicinity of the embedded coupons. Samples were stored in air-tight plastic containers until later analyzed, by potentiometric titration, for the total (acid soluble) chloride content.

6.1.2.1.3 Compressive strength and related testing

The results of compressive strength tests (Table 5.19) revealed a tendency for some of the materials under investigation in this phase to cause large strength reductions. Tests were therefore devised, at this stage, to help elucidate the reasons for this behaviour, as follows: i) the effects of some admixtures, see Table 6.12, on the early age hydration in 0.4 water/cement ratio pastes was investigated using conduction calorimetry (details of the test are as described elsewhere (Forrester 1970)), ii) the compressive strength of all concretes was monitored up to the age of 6 months (100mm cubes stored in water at 20°C were tested at 7 days, 28 days, and 6 months); this would reveal whether the rate of strength development is such that the strength reduction (observed at early-age) will diminish with age.

Table 6.12 Details of mixes used in calorimetry

Material	Mix Ref.	Admixture	
		Dose level	Mode
---	CLC	---	---
GGBS	CL1	65	A
PFA	CL2	30	A
Whiting	CL3	5	B
Iron oxide	CL4	2	B
Iron powder	CL5	5	B
Magnesium stearate	CL6	0.5	B
	CL7	2	B
Butyl stearate	CL8	1	B
	CL9	3	B
Soyabean oil	CL10	1	B
	CL11	3	B
SBR	CL12	5	D
	CL13	10	D
Acrylic	CL14	10	D
Dimethyl ethanolamine	CL15	1	B
	CL16	3	B

• Admixture (Mode)

A: introduced in weight percentage replacement of cement.

B: introduced in addition, as weight percentage of cement.

C: introduced in addition, as litres of material per cubic meter of concrete.

D: introduced in addition, as weight percentage of polymer solids relative to weight of cement.

6.1.2.1.4 Microstructural examination

Scanning electron microscopy (SEM) was used in the backscattered electron (bse) imaging mode. This technique was selected in preference to other methods (e.g. mercury intrusion porosimetry, nitrogen adsorption, methanol exchange/adsorption) for three reasons:

- i) a mercury intrusion porosimeter was not then available at IC;
- ii) it was unclear whether the methanol (or propan-2-ol) exchange/adsorption method would be applicable on concretes modified with water repellents (or indeed the proprietary products) as it was suspected, based on a review of the literature (see A1.4) and the results of capillary rise testing in Phase 1 (5.3.4), that these materials alter the surface properties of the cement paste pores; and
- iii) bse imaging has the merit of providing information on not only the pore structure (mainly porosity) of the cement paste but also the morphology and distribution of its phases, hence, any dramatic changes in relation to these properties brought about by the introduction of an admixture can be readily (by visual comparison with images for the control concretes) identified.

6.1.2.2 Testing programme

Mixes were all prepared using the same pan mixer, the mixing procedure and the manner in which admixtures were introduced being as described before (5.2.2.1). Immediately following the completion of mixing, tests for slump and fresh density were performed. The required specimens from each mix (20 disks (101.6mm diameter and 50mm thick), 6 100mm cubes, and 1 150mm cube with embedded electrodes) were then cast and compacted on a vibrating table. As soon as the small amount of bleed water had evaporated, specimens were stored under wet burlap and polythene sheets until the following day, when they were released from moulds, marked, then all stored, with the exception of the 6 100mm cubes which were stored in water at 20°C (see 5.2.2.2.1), in sealed condition until required for testing. Immediately following the completion of this casting phase, cubes with embedded coupons were fabricated for use in corrosion testing (1 100mm cube for each of the mixes shown in Table 6.11, with the exception of mix CRC for which 6 cubes were prepared); specimens were then stored in sealed conditions until required for testing.

The testing programme consisted of 10 separate series of tests (A to J) details of which are summarised in Table 6.13, in which further details of the individual tests are also presented.

Table 6.13 Testing programme

Test Series	Specimens			Test(s)	Additional details
	Type	No. ^a	Age ^b (days)		
A	Disk	2	90	<ul style="list-style-type: none"> • Mild drying (6.1.2.1.1,(II)) • Oxygen permeability (6.1.2.1.1,(I)) 	(1)
B	Disk	3	90	<ul style="list-style-type: none"> • Severe drying (6.1.2.1.1,(II)) • Capillary rise (6.1.2.1.1,(II)) 	(2)
C	Disk	3	90	<ul style="list-style-type: none"> • Capillary rise (6.1.2.1.1,(II)) • MAT (6.1.2.1.1,(II)) • Porosity 	(3)
D	Disk	2	90	<ul style="list-style-type: none"> • ACID (6.1.2.1.1,(III)) 	
E	Disk	1	75	<ul style="list-style-type: none"> • Penetration profile (6.1.2.1.1,(III)) 	(4)
F	150mm cube with embedded electrodes	1	1	<ul style="list-style-type: none"> • Electrical resistivity (6.1.2.1.2,(I)) • Water permeability (6.1.2.1.1,(I)) 	(5)
G	100mm cube	1	75	<ul style="list-style-type: none"> • Carbonation (6.1.2.1.2,(II)) • Resistivity (6.1.2.1.2,(II)) 	
H	100mm cube with embedded coupons	1	75	<ul style="list-style-type: none"> • Corrosion (6.1.2.1.2,(III)) 	(6)
I	100mm cube	2 2 2	7 28 180	<ul style="list-style-type: none"> • Compressive strength (6.1.2.1.3) 	
J	disk	1	90	<ul style="list-style-type: none"> • Microstructural examination (6.1.2.1.4) 	(7)

- a number of specimens tested.
- b age (days) of specimens at the commencement of testing.

Additional details

(1): First, the curved surface of test specimens was carefully sealed, by application of plastic insulation tape. Specimens were then weighed and immediately afterwards they were inserted into an incubator in which the climate was controlled at 30°C and 75% RH. The weight of specimens was monitored regularly for a period of 56 days. Following 5 months of storage, at which time specimens reached near steady weight, oxygen permeability testing was performed. Afterwards, tape was carefully removed from the curved surface of specimens (to allow more rapid drying), and specimens were again inserted in the incubator, this time the climate was controlled at 30°C and 55% RH. After four months of storage, specimens were oxygen permeability tested. Finally, specimens were dried to equilibrium in a large pre-heated oven, at 50°C and 11-14% RH, then subjected to oxygen permeability testing.

(2): Specimens were weighed initially, then inserted into a large pre-heated oven (50°C & 11-14% RH) and weighed regularly until they reached steady weight (a total duration of 56 days). Capillary rise testing was then performed for a period of 28 days, and on some specimens (those with a weight gain at 28 days of less than 60% of that of the respective control) testing was continued for a further 85 days.

(3): Specimens were weighed initially, then tested under capillary rise conditions for a period of 7 days, after which they were subjected to MAT for a further 21 days. Thereafter, specimens were saturated, then weighed, before being inserted into a large preheated (at 105°C) oven. When equilibrated, specimens were placed in desiccators (at laboratory temperature) for 1 day, then weighed; the steps following MAT were performed in order to obtain an estimate of the total porosity of the concretes.

(4): First, specimens were saturated, then carefully wrapped in plastic insulation tape leaving only the as-cast surface exposed, before being immersed in a 0.5M sodium chloride solution. After 8 months designated period, specimens were removed from the tank, rinsed with distilled water, then split approximately in half perpendicular to the flat faces. One half was subsequently used to obtain powdered samples which were stored in airtight plastic containers until later analyzed, by potentiometric titration, for total chloride content.

(5): Electrical resistance was monitored for a period of 140 days, after which period specimens were stored in their sealed condition until they were prepared for water permeability testing.

(6): Following the designated exposure period, the shim plates were exposed by diamond sawing the top and two side faces of the test cube to a depth of 25mm along the horizontal plane of the steel shim, and cracking open the cube using a bolster chisel and club hammer.

(7): Concrete prisms (25mm square base and 10mm thick) were cut from the centre of specimens, then immediately immersed in a freezing mixture of methanol and solid carbon dioxide (-80°C). The prisms were then freeze dried at -35°C for three days, increasing the temperature to 0°C over the next 3 days. Afterwards, specimens were vacuum impregnated with an epoxy resin. Slices of 1-2mm were then cut from the prisms using a diamond slitting wheel with a non aqueous lubricant. The slices were lapped with 14µm diamond paste and polished with 6µ, 3µ, 1µ, 1/4µ diamond paste, for about 2 hours with each grade. Finally, the polished slices were mounted on SEM stubs and coated with carbon.

6.2 Results

6.2.1 General

It was found convenient, as it was in the previous chapter (5.3), to present results for the control concretes as absolute values, and to express the majority of results for the modified concretes relative to the corresponding results of the respective control, as percentage ratios.

Results are mainly presented in tabular form (Tables 6.14 through 6.24). Graphical illustrations are also presented where necessary for easy assimilation of important results.

All results presented represent an average value for the specimens tested.

6.2.2 Transport testing

Presented in Table 6.14 are the results acquired from pressure-induced water flow testing; oxygen permeability test results are all reported in Table 6.15.

Results of capillary rise testing (on Series B specimens) are presented in Table 6.16. The results of tests in Series C are all reported in Table 6.17; double lines emphasise the points after which the mode of testing was altered.

Reported in Tables 6.18 and 6.19 are the results of the mild drying and severe drying tests, respectively.

Results obtained from chloride ion diffusion studies are all presented in Table 6.20.

Table 6.14 Results of testing relevant to pressure-induced water flow (Series F)

Mix ref.	d ^a (cm)	WG ^b (g)	k _{(w)v} (m ² x10 ²⁰)	PDR ^d						Band [@]
				Time ^c						
				2hr	1d	2d	4d	6d	9d	
C(0.4)	7.9	93	67@	9	29	39	43	51	63	5
C(0.35)	8.5	94	62@	9	34	43	45	52	67	5
C(0.3)+	3.5	23	7.9	3	3	2	6	8	29	2
GGBS65(0.4)	13.5	135	89@	30	58	62	65	63	62	6
PFA30(0.4)	9.2	89	98@	11	41	49	58	62	68	5
SF10(0.4)+	2.9	13	3.4	4	6	5	11	6	9	1
KIES3(0.4)	10.7	199	122@	9	36	46	63	65	68	5
BEN10(0.4)+	1.5	8	2.6	7	10	5	8	11	12	1
WHIT5(0.4)	12.2	142	91@	9	38	49	54	64	72	5
IRO2(0.4)	10.9	118	70@	8	40	47	51	58	68	5
MAGST2(0.35)+	11.3	120	104@	17	46	56	61	64	66	6
ALST0.5(0.35)+	9.3	83	86@	3	33	38	45	47	58	5
BUTST3(0.4)	5.6	58	31@	8	6	17	28	36	49	4
CAPA0.25(0.35)+	6.8	88	67@	13	35	45	49	53	58	5
SOYO1(0.35)+	12.8	150	120@	27	57	61	65	65	66	6
LINSO1(0.35)+	11.4	126	90@	16	46	53	58	59	60	6
TAR25(0.35)+	13.1	136	87@	20	50	57	61	61	63	6
ASPH20(0.35)	9.3	83	69@	10	30	38	50	53	59	5
EVA10(0.3)+	3.9	29	12	5	9	11	17	26	44	3
SBR5(0.35)+	6.9	63	40@	13	38	43	50	51	60	5
SBR10(0.3)+	1.9	14	4.7	6	10	11	10	15	25	2
ACR10(0.3)+	5.1	14	7.1@	3	4	6	14	18	21	2
AMINO22(0.35)	6.2	51	39@	6	16	19	24	25	34	5
CAL30(0.35)+	2.8	29	11	3	3	2	6	11	22	2
CONP3(0.35)	10.6	93	80@	14	38	45	50	54	66	5
SIK9(0.4)	7.4	64	32@	6	10	19	24	35	55	5
SET6(0.4)	10.2	108	70@	11	26	35	41	51	60	5
IRON10(0.4)	11.4	68	50@	8	34	44	48	56	65	5
CEL2(0.4)	1.9	28	8.3	9	7	12	15	29	35	3
FORM2(0.4)	8.6	70	41@	5	7	15	23	35	49	4
TEA0.025(0.4)	3.4	18	6.9	6	7	13	14	22	25	3
TEA0.1(0.4)	2.1	31	10	9	11	14	17	20	35	3
LPV325(0.4)	3.3	21	10	2	9	5	15	17	25	3
LPV245(0.4)+	2.8	20	6.7	1	9	4	13	18	27	3

a average of 16 penetration depth measurements.

b weight gain with respect to the initial weight of specimen.

c time after application of water pressure.

d percentage depression in electrical resistance, relative to the value measured before water pressure was applied.

@ see 6.3.2

Table 6.15 Oxygen permeability test results (Series A)

Mix ref.	Conditioning regime ^a			$k_{(g)RG3} / k_{(g)RG2}$	$k_{(g)RG3} / k_{(g)RG1}$
	RG3	RG2	RG1		
	$k_{(g)} \text{ (m}^2\text{)}$				
C(0.4)	4.79E-17	1.28E-17	4.98E-18	3.7	9.6
C(0.35)	5.79E-17	1.03E-17	4.74E-18	5.6	12.2
C(0.3)+	3.88E-17	5.11E-18	2.70E-18	7.6	14.4
	$kr_{(g)} \text{ }^b$				
GGBS65(0.4)	553*	1016*	1284*	2.0	4.1
PFA30(0.4)	294*	583*	1077*	1.9	2.6*
SF10(0.4)+	73	<u>21</u>	<u>9</u>	<u>12.9</u>	<u>77.7</u>
KIES3(0.4)	293*	227	497*	4.0	5.7
BEN10(0.4)+	102	76	60	5.0	16.3
WHIT5(0.4)	206*	280*	447*	2.7	4.4
IRO2(0.4)	124	138	174	3.4	6.9
MAGST2(0.35)+	235*	608*	895*	2.2*	3.2*
ALST0.5(0.35)+	136	208	382*	3.7	4.4*
BUTST3(0.4)	60	<u>32</u>	<u>20</u>	<u>7.0</u>	<u>28.8</u>
CAPA0.25(0.35)+	216*	584*	860*	2.1*	3.1*
SOYO1(0.35)+	156	428*	652*	2.1*	2.9*
LINSO1(0.35)+	182	777*	1113*	1.3*	2.0*
TAR25(0.35)+	85	328*	695*	1.5*	1.5*
ASPH20(0.35)	136	176	504*	4.3	3.3*
EVA10(0.3)+	<u>33</u>	<u>24</u>	81	10.2#	5.8#
SBR5(0.35)+	75	96	156	4.4	5.8
SBR10(0.3)+	<u>20</u>	<u>23</u>	56	6.7#	5.0#
ACR10(0.3)+	<u>9</u>	81	121	0.8#	1.1#
AMINO22(0.35)	50	50	46	5.6	13.2
CAL30(0.35)+	81	<u>30</u>	41	<u>15.3</u>	<u>24.1</u>
CONP3(0.35)	83	158	66	3.0	15.2
SIK9(0.4)	155	508*	1018*	1.1*	1.5*
SET6(0.4)	130	438*	570*	1.1*	2.2*
IRON10(0.4)	176	196	364*	3.4	4.7
CEL2(0.4)	135	95	62	5.3	21.0
FORM2(0.4)	163	493*	621*	1.2*	2.5*
TEA0.025(0.4)	135	158	174	3.2	7.4
TEA0.1(0.4)	131	193	190	2.5	6.6
LPV325(0.4)	84	65	46	4.8	17.7
LPV245(0.4)+	64	57	69	4.2	9.0

^a RG1: 30°C & 75% RH; RG2: 30°C & 55% RH; and RG3: 50°C & 11-14% RH.

^b percentage ratio of the permeability coefficient of mix relative to that of the respective control.

see 6.3.2, and 6.4.

- Results are discussed in 6.3.2.
- Results which suggest a worthwhile improvement in performance are presented in **highlighted** underlined text.
- Results which suggest unfavourable performance are followed by a **highlighted** asterisk.

Table 6.16a Results of capillary rise testing (Series B) - (control concretes)

Mix ref.	Weight gain ^a (g)							
	Time ^b							
	1hr	5hr	1d	2d	4d	14d	28d	113d
C(0.4)	4.8	10.9	22.9	29.2	35.4	39.4	40.7	43.2
C(0.35)	4.1	9.6	19.7	24.8	30.1	35.8	37.4	38.9
C(0.3)+	4.1	8.8	16.5	19.8	23.1	27.8	30.3	37.6

a weight gain relative to the initial weight of specimens.

b time after testing commenced.

hr:- hours; **d:-** days.

Testing performed on specimens dried to equilibrium at 50°C & 11-14% (see Table 6.13).

Table 6.16b Results of capillary rise testing (Series B) - (modified concretes)

Mix ref.	WGR ^a							
	Time							
	1hr	5hr	1d	2d	4d	14d	28d	113d
GGBS65(0.4)	99	97	88	83	79	81	85	---
PFA30(0.4)	118	106	95	91	87	84	86	---
SF10(0.4)+	86	79	66	<u>59</u>	<u>55</u>	<u>57</u>	<u>59</u>	71
KIES3(0.4)	132	125	121	119	111	108	106	---
BEN10(0.4)+	96	86	88	89	94	101	106	---
WHIT5(0.4)	124	122	121	117	110	107	107	---
IRO2(0.4)	112	113	115	113	107	104	105	---
MAGST2(0.35)+	<u>36</u>	<u>26</u>	<u>20</u>	<u>19</u>	<u>20</u>	<u>24</u>	<u>28</u>	<u>42</u>
ALST0.5(0.35)+	<u>56</u>	<u>40</u>	<u>31</u>	<u>29</u>	<u>29</u>	<u>33</u>	<u>37</u>	<u>53</u>
BUTST3(0.4)	<u>29</u>	<u>21</u>	<u>16</u>	<u>15</u>	<u>16</u>	<u>21</u>	<u>25</u>	<u>39</u>
CAPA0.25(0.35)+	<u>56</u>	<u>44</u>	<u>35</u>	<u>32</u>	<u>31</u>	<u>35</u>	<u>37</u>	<u>55</u>
SOYO1(0.35)+	<u>60</u>	<u>43</u>	<u>34</u>	<u>32</u>	<u>31</u>	<u>34</u>	<u>37</u>	<u>52</u>
LINSO1(0.35)+	<u>57</u>	<u>46</u>	<u>36</u>	<u>33</u>	<u>32</u>	<u>35</u>	<u>38</u>	<u>56</u>
TAR25(0.35)+	83	<u>69</u>	<u>59</u>	<u>57</u>	<u>55</u>	<u>54</u>	<u>57</u>	71
ASPH20(0.35)	109	103	109	114	119	109	108	---
EVA10(0.3)+	<u>36</u>	<u>28</u>	<u>25</u>	<u>25</u>	<u>28</u>	<u>38</u>	<u>45</u>	<u>60</u>
SBR5(0.35)+	<u>43</u>	<u>46</u>	<u>44</u>	<u>45</u>	<u>49</u>	<u>54</u>	<u>59</u>	84
SBR10(0.3)+	<u>9</u>	<u>13</u>	<u>16</u>	<u>19</u>	<u>25</u>	<u>30</u>	<u>34</u>	<u>42</u>
ACR10(0.3)+	<u>36</u>	<u>22</u>	<u>22</u>	<u>23</u>	<u>25</u>	<u>28</u>	<u>31</u>	<u>43</u>
AMINO22(0.35)	84	<u>59</u>	<u>51</u>	<u>50</u>	<u>58</u>	<u>58</u>	<u>64</u>	89
CAL30(0.35)+	63	<u>52</u>	<u>41</u>	<u>37</u>	<u>36</u>	<u>39</u>	<u>43</u>	<u>55</u>
CONP3(0.35)	<u>60</u>	<u>40</u>	<u>29</u>	<u>26</u>	<u>26</u>	<u>30</u>	<u>34</u>	<u>49</u>
SIK9(0.4)	132	129	128	124	116	115	113	---
SET6(0.4)	99	95	91	87	85	92	96	---
IRON10(0.4)	121	122	124	127	111	107	107	---
CEL2(0.4)	88	78	67	64	64	76	85	---
FORM2(0.4)	131	129	125	119	112	108	105	---
TEA0.025(0.4)	111	110	116	117	113	110	110	---
TEA0.1(0.4)	103	87	93	109	112	109	109	---
LPV325(0.4)	87	79	81	81	83	90	95	---
LPV245(0.4)+	65	65	66	67	70	82	87	---

a percentage ratio of weight gain relative to respective control.

- Results are discussed in 6.3.2.
- Results which suggest a worthwhile improvement in performance are presented in **highlighted** underlined text.
- Results which suggest unfavourable performance are followed by a **highlighted** asterisk.

Table 6.17a Results of Series C testing (control concretes)

Mix ref.	Weight gain ^a (g)								Porosity ^c (%)
	Time ^b								
	h	h	d	d	d	d	d	d [#]	
C(0.4)	0.45	0.80	1.70	3.75	4.70	5.35	7.20	8.45	12.8
C(0.35)	0.35	0.61	1.37	3.23	4.13	4.97	6.73	7.93	12.6
C(0.3)+	0.30	0.63	1.27	2.97	3.67	4.27	7.20	7.20	11.3

a weight gain relative to the initial weight of specimens.

b time after testing commenced.

c total porosity.

after saturation.

- Testing was performed on as-received specimens.
- Test sequence (Table 6.13):
 - 7 days capillary rise;
 - 21 days MAT;
 - saturation.

Table 6.17b Results of Series C testing (modified concretes)

Mix ref.	WGR ^a								PR ^b
	Time								
	1hr	5hr	1d	7d	8d	10d	28d	30d	
GGBS65(0.4)	77	85	83	85	80	83	82	145*	135*
PFA30(0.4)	126	96	88	74	97	102	81	148*	104
SF10(0.4)+	<u>37</u>	<u>38</u>	<u>37</u>	<u>34</u>	<u>33</u>	<u>32</u>	<u>34</u>	<u>49</u>	<u>86</u>
KIES3(0.4)	67	71	84	102	106	103	103	143*	115*
BEN10(0.4)+	<u>57</u>	<u>50</u>	<u>43</u>	59	60	63	64	70	107
WHIT5(0.4)	104	142	137	134	138	138	136	157*	108
IRO2(0.4)	67	104	114	117	121	123	118	151*	111*
MAGST2(0.35)+	<u>38</u>	<u>38</u>	<u>44</u>	<u>49</u>	<u>44</u>	<u>38</u>	<u>42</u>	157*	114*
ALST0.5(0.35)+	70	65	66	60	<u>55</u>	<u>57</u>	<u>52</u>	202*	121*
BUTST3(0.4)	<u>15</u>	<u>21</u>	<u>22</u>	<u>32</u>	<u>26</u>	<u>25</u>	<u>28</u>	<u>39</u>	101
CAPA0.25(0.35)+	76	87	63	68	65	<u>57</u>	<u>56</u>	181*	126*
SOYO1(0.35)+	<u>23</u>	<u>41</u>	<u>44</u>	<u>48</u>	<u>44</u>	<u>42</u>	<u>46</u>	131	118*
LINSO1(0.35)+	<u>46</u>	66	62	78	76	72	72	217*	131*
TAR25(0.35)+	<u>36</u>	<u>44</u>	<u>56</u>	74	75	74	78	114	106
ASPH20(0.35)	229*	191*	147*	135	148*	138	131	145*	117*
EVA10(0.3)+	156*	126	116	118	105	99	99	106	103
SBR5(0.35)+	114	114	107	107	111	102	104	121	111*
SBR10(0.3)+	100	114	121	109	121	114	111	125	97
ACR10(0.3)+	111	126	129	103	101	96	97	97	75#
AMINO22(0.35)	76	104	88	103	84	72	78	85	108
CAL30(0.35)+	<u>48</u>	<u>66</u>	<u>58</u>	67	<u>52</u>	<u>52</u>	<u>59</u>	121	98
CONP3(0.35)	<u>33</u>	<u>47</u>	<u>45</u>	<u>58</u>	<u>53</u>	<u>49</u>	<u>56</u>	73	107
SIK9(0.4)	<u>38</u>	<u>54</u>	<u>55</u>	73	68	67	66	93	110*
SET6(0.4)	<u>44</u>	<u>54</u>	<u>63</u>	80	73	74	73	96	108
IRON10(0.4)	104	117	110	109	108	111	112	128	106
CEL2(0.4)	89	83	80	80	84	85	81	96	103
FORM2(0.4)	<u>57</u>	82	105	134	123	121	114	137	114*
TEA0.025(0.4)	67	67	61	64	64	66	66	93	105
TEA0.1(0.4)	96	75	65	84	84	91	93	108	102
LPV325(0.4)	<u>22</u>	<u>56</u>	<u>53</u>	76	74	72	78	101	96
LPV245(0.4)+	<u>33</u>	<u>50</u>	<u>53</u>	73	78	83	93	107	<u>88</u>

a percentage ratio of weight gain relative to respective control.

b percentage ratio of total porosity of mix relative to that of the control.

see 6.4.

- Results are discussed in 6.3.2.
- Results which suggest a worthwhile improvement in performance are presented in **highlighted** underlined text.
- Results which suggest unfavourable performance are followed by a **highlighted** asterisk.

Table 6.18a Results of mild drying test (Series A) - (control concretes)

Mix Ref.	Weight Loss ^a (g)							
	Time ^b							
	5hr	1d	2d	4d	7d	14d	28d	56d
C(0.4)	0.15	0.40	0.60	0.90	1.45	2.30	3.50	4.95
C(0.35)	0.15	0.35	0.50	0.85	1.30	2.00	3.15	4.50
C(0.3)+	0.00	0.00	0.30	0.30	0.55	1.00	1.75	2.70

a weight loss relative to the initial weight of specimens.

b time after testing commenced.

- Tests were performed on as received specimens (Table 6.13): drying at 30°C & 75% RH.

Table 6.18b Results of mild drying test (Series A) - (modified concretes)

Mix ref.	WLR ^a							
	Time							
	5hr	1d	2d	4d	7d	14d	28d	56d
GGBS65(0.4)	133	163*	175*	172*	152*	133	117	115
PFA30(0.4)	100	138	158*	161*	138	124	107	112
SF10(0.4)+	100	67	72	72	59	54	54	61
KIES3(0.4)	133	137	133	139	117	111	119	119
BEN10(0.4)+	300*	250*	258*	250*	210*	185*	160*	156*
WHIT5(0.4)	100	112	117	94	93	89	90	89
IRO2(0.4)	100	138	142	122	107	111	108	102
MAGST2(0.35)+	200*	186*	210*	182*	165*	150*	135	134
ALST0.5(0.35)+	100	71	170*	141*	131	125	116	114
BUTST3(0.4)	200*	225*	233*	222*	190*	176*	167*	164*
CAPA0.25(0.35)+	233*	214*	210*	206*	169*	153*	138	133
SOYO1(0.35)+	---	---	180*	141*	135	123	114	112
LINSO1(0.35)+	133*	188*	170*	171*	138	133	125	121
TAR25(0.35)+	200*	186*	200*	165*	143	135	124	118
ASPH20(0.35)	133*	171*	180*	159*	146*	138	116	123
EVA10(0.3)+	(0.0)	(0.1)	133*	117	91	80	74	69
SBR5(0.35)+	133*	286*	160*	135	119	120	105	110
SBR10(0.3)+	(0.1)	(0.35)	267*	183*	155*	135	109	115
ACR10(0.3)+	(0.1)	(0.25)	333*	250*	182*	180*	134	126
AMINO22(0.35)	67	100	110	94	85	88	76	83
CAL30(0.35)+	67	129	130	118	108	105	97	93
CONP3(0.35)	33	100	110	106	96	95	89	88
SIK9(0.4)	133	125	125	128	110	111	116	117
SET6(0.4)	167*	213*	200*	194*	166*	154*	151*	143
IRON10(0.4)	200*	137	142	117	103	100	107	98
CEL2(0.4)	167*	175*	183*	178*	159*	137	127	121
FORM2(0.4)	167*	188*	192*	172*	148*	148*	144*	137
TEA0.025(0.4)	233*	250*	267*	250*	217*	183*	179*	164*
TEA0.1(0.4)	167*	157*	158*	156*	134	124	111	115
LPV325(0.4)	---	---	192*	161*	141*	124	116	113
LPV245(0.4)+	---	---	333*	294*	245*	204*	177*	160*

^a percentage ratio of weight loss relative to respective control.

() absolute value is reported since control exhibited no weight loss.

- Results are discussed in 6.3.2.
- Results which suggest a worthwhile improvement in performance are presented in **highlighted** underlined text.
- Results which suggest unfavourable performance are followed by a **highlighted** asterisk.

Table 6.19a Results of severe drying test (Series B) - (control concretes)

Mix Ref.	Weight Loss ^a (g)							
	Time ^b							
	5hr	1d	2d	4d	7d	14d	28d	56d
C(0.4)	3.25	6.35	8.45	11.65	14.80	19.30	24.50	29.50
C(0.35)	2.83	5.67	7.73	10.70	13.70	19.03	23.10	28.40
C(0.3)+	2.10	4.33	5.90	8.33	10.83	14.47	18.97	23.80

a weight loss relative to the initial weight of specimens.

b time after testing commenced.

- Tests performed on as received specimens (Table 6.13): drying at 50°C & 11-14% RH.

Table 6.19b Results of severe drying test (Series B) - (modified concretes)

Mix ref.	WLR ^a							
	Time							
	5hr	1d	2d	4d	7d	14d	28d	56d
GGBS65(0.4)	119	130*	133*	130*	128*	126*	130*	134*
PFA30(0.4)	100	108	110	109	108	107	107	107
SF10(0.4)+	---	82	88	88	89	91	94	103
KIES3(0.4)	113	126*	124*	125*	122	115	118	117
BEN10(0.4)+	106	124*	124*	122	120	119	116	114
WHIT5(0.4)	93	97	101	96	97	99	101	101
IRO2(0.4)	97	104	104	102	102	104	104	104
MAGST2(0.35)+	---	109	107	---	108	100	103	102
ALST0.5(0.35)+	89	98	103	102	102	121	100	100
BUTST3(0.4)	110	109	110	106	106	106	107	108
CAPA0.25(0.35)+	106	115	116	123	114	108	111	108
SOYO1(0.35)+	---	---	111	107	106	101	106	104
LINSO1(0.35)+	95	105	107	107	107	102	106	103
TAR25(0.35)+	---	101	122	104	103	97	102	104
ASPH20(0.35)	93	109	109	109	110	104	109	107
EVA10(0.3)+	<u>79</u>	81	80	78	78	<u>76</u>	<u>76</u>	<u>74</u>
SBR5(0.35)+	86	92	91	90	90	87	94	95
SBR10(0.3)+	<u>57</u>	<u>71</u>	<u>73</u>	<u>72</u>	<u>72</u>	<u>74</u>	<u>74</u>	<u>76</u>
ACR10(0.3)+	---	<u>25</u>	<u>41</u>	<u>50</u>	<u>56</u>	<u>60</u>	<u>63</u>	<u>68</u>
AMINO22(0.35)	84	88	87	86	86	82	86	87
CAL30(0.35)+	91	95	96	94	93	88	92	91
CONP3(0.35)	101	99	99	95	94	89	93	93
SIK9(0.4)	103	110	114	114	112	113	114	113
SET6(0.4)	109	115	118	118	113	113	120	115
IRON10(0.4)	95	99	100	98	99	101	103	101
CEL2(0.4)	<u>77</u>	101	110	109	109	108	105	104
FORM2(0.4)	109	113	116	117	114	109	115	113
TEA0.025(0.4)	93	120	127*	126*	126*	125*	121	119
TEA0.1(0.4)	90	117	108	109	109	108	106	103
LPV325(0.4)	---	---	115	109	108	109	107	104
LPV245(0.4)+	---	---	117	112	109	108	104	96

a percentage ratio of weight loss relative to respective control.

- Results are discussed in 6.3.2.
- Results which suggest a worthwhile improvement in performance are presented in **highlighted** underlined text.
- Results which suggest unfavourable performance are followed by a **highlighted** asterisk.

Table 6.20 Results of chloride ion diffusion studies

Mix ref.	ACID testing (Series D)		Concentration Profile tests (Series E)				
	T _o (hours)	g (mMole/m ² .hr)	Cl ⁻ in PPM of concrete				
			Penetration depth interval (mm)				
			0-2	4-6	8-10	14-16	22-24
C(0.4)	63	139	4981	3338	1617	217	150
C(0.35)	95	120	4450	3570	1822	152	100
C(0.3)+	107	112	5002	2644	1241	85	100
	RT _o ^a	Rg ^a	Cl ⁻ R ^a				
GGBS65(0.4)	217	35	117	77	19	000	000
PFA30(0.4)	133	43	92	64	57	16	000
SF10(0.4)+	224	17	79	44	16	000	000
KIES3(0.4)	56*	149*	170	155	235*	273*	221*
BEN10(0.4)+	103	127*	109	113	176*	209*	150*
WHIT5(0.4)	87	139*	83	116	173*	166*	133*
IRO2(0.4)	70*	103	152	104	168*	212*	108
MAGST2(0.35)+	71*	140*	92	96	170*	335*	279*
ALST0.5(0.35)+	42*	126*	75	67	95	157*	144*
BUTST3(0.4)	137	93	132	84	79	47	55
CAPA0.25(0.35)+	62*	120*	135	106	166*	159*	140*
SOYO1(0.35)+	87	71	76	67	114	203*	000
LINSO1(0.35)+	75*	97	123	110	85	243*	240*
TAR25(0.35)+	67*	103	94	107	145*	325*	208*
ASPH20(0.35)	56*	123*	133	101	170*	420*	220*
EVA10(0.3)+	65*	66	102	127	141*	545*	150*
SBR5(0.35)+	64*	148*	140	90	169*	337*	344*
SBR10(0.3)+	82*	106	120	203	116	304*	108
ACR10(0.3)+	106	47	74	80	57	49	000
AMINO22(0.35)	68*	78	228	198	209*	390*	344*
CAL30(0.35)+	65*	114	144	106	133*	230*	128
CONP3(0.35)	60*	106	95	90	122	194*	124
SIK9(0.4)	46*	155*	136	147	178*	539*	516*
SET6(0.4)	51*	178*	150	122	154*	382*	356*
IRON10(0.4)	63*	125*	94	91	117	155*	244*
CEL2(0.4)	91	111	81	79	163*	251*	000
FORM2(0.4)	38*	132*	128	143	200*	368*	397*
TEA0.025(0.4)	---	---	80	92	131	188*	120*
TEA0.1(0.4)	86	140*	92	105	134*	320*	179*
LPV325(0.4)	87	101	70	78	78	153*	198*
LPV245(0.4)+	38*	134*	60	53	83	173*	697*

a percentage ratio of result for a modified mix relative to the corresponding result of the respective control.

000 no chloride detected.

- Test details are given in Table 6.13, and results are discussed in 6.3.2.
- Results which suggest a worthwhile improvement in performance are presented in **highlighted** underlined text.
- Results which suggest unfavourable performance are followed by a **highlighted** asterisk.

6.2.3 Corrosion-related testing

Results obtained from electrical resistance testing are presented in Table 6.21. Each measurement represents the average value of three determinations (converted to an equivalent concrete resistance at 20° C (A3.1)) taken at roughly 1 hour intervals.

Presented in Table 6.22 are the results of carbonation testing, expressed in terms of both the mean and maximum carbonation depths detected on the split cubes. Also reported are the results from associated resistivity measurements (resistance converted to equivalent value at 20° C (A3.1)).

Finally, the results of corrosion testing are presented in Table 6.23.

Table 6.21a Results of testing for electrical resistance (Series F) - (control concretes)

Mix Ref.	Resistance (Ω)							
	Age (days)							
	1d	3d	7d	14d	28d	56d	84d	140d
C(0.4)	78.5	167	208	229	267	408	456	607
C(0.35)	93.7	196	246	278	349	504	570	749
C(0.3)+	114	205	253	315	389	523	602	786

Table 6.21b Results of testing for electrical resistance (Series F) - (modified concretes)

Mix ref.	RR ^a							
	Age							
	1d	3d	7d	14d	28d	56d	84d	140d
GGBS65(0.4)	68*	65*	<u>156</u>	<u>287</u>	<u>396</u>	<u>432</u>	<u>485</u>	<u>429</u>
PFA30(0.4)	68*	67*	68*	77	103	<u>202</u>	<u>330</u>	<u>445</u>
SF10(0.4)+	76	80	105	<u>248</u>	<u>649</u>	<u>697</u>	<u>687</u>	<u>520</u>
KIES3(0.4)	91	89	103	108	121	93	111	125
BEN10(0.4)+	81	75	79	85	100	77	84	85
WHIT5(0.4)	102	110	111	121	114	112	123	124
IRO2(0.4)	100	81	93	94	100	86	93	97
MAGST2(0.35)+	95	85	101	111	97	96	92	90
ALST0.5(0.35)+	90	83	97	104	92	91	88	88
BUTST3(0.4)	<u>151</u>	98	102	123	123	121	126	124
CAPA0.25(0.35)+	101	108	98	101	104	98	100	89
SOYO1(0.35)+	105	95	108	124	121	115	116	106
LINSO1(0.35)+	103	111	100	104	110	109	119	111
TAR25(0.35)+	89	78	81	93	104	91	98	91
ASPH20(0.35)	85	79	90	98	96	80	83	81
EVA10(0.3)+	91	<u>135</u>	<u>149</u>	<u>186</u>	<u>231</u>	<u>275</u>	<u>295</u>	<u>400</u>
SBR5(0.35)+	87	61	104	121	119	98	103	101
SBR10(0.3)+	85	87	<u>141</u>	<u>140</u>	<u>143</u>	<u>127</u>	<u>131</u>	<u>130</u>
ACR10(0.3)+	78	<u>139</u>	<u>157</u>	<u>162</u>	<u>195</u>	<u>185</u>	<u>191</u>	<u>177</u>
AMINO22(0.35)	66*	59*	63*	73*	82	69*	80	90
CAL30(0.35)+	74	82	82	103	106	93	94	98
CONP3(0.35)	<u>150</u>	96	96	113	105	92	96	102
SIK9(0.4)	80	79	86	99	109	76	85	90
SET6(0.4)	82	78	85	97	117	78	88	89
IRON10(0.4)	102	101	99	104	105	91	97	98
CEL2(0.4)	89	87	85	101	103	113	120	121
FORM2(0.4)	95	95	112	119	134	102	119	126
TEA0.025(0.4)	90	85	79	89	86	84	85	82
TEA0.1(0.4)	95	82	76	87	82	75	83	82
LPV325(0.4)	97	106	106	126	122	116	120	120
LPV245(0.4)+	110	126	127	<u>150</u>	<u>147</u>	<u>147</u>	<u>155</u>	<u>160</u>

^a percentage ratio of resistance for a modified mix relative to the corresponding result of the respective control.

- Test details are given in Table 6.13, and results are discussed in 6.3.3.
- Results which suggest a worthwhile improvement in performance are presented in **highlighted** underlined text.
- Results which suggest unfavourable performance are followed by a **highlighted** asterisk.

Table 6.22 Results of carbonation testing and resistivity measurements (Series G)

Mix ref.	Carbonation depth (mm)		Resistivity (kΩ.m)
	Mean	Maximum	
C(0.4)	5.9	10.0	8.0
C(0.35)	4.8	7.5	6.3
C(0.3)+	0.0	0.0	3.6
	CR ^a		
GGBS65(0.4)	386*	280*	10.0
PFA30(0.4)	271*	220*	17.8
SF10(0.4)+	129	100	5.3
KIES3(0.4)	115	100	11.0
BEN10(0.4)+	69	<u>55</u>	5.4
WHIT5(0.4)	131	110	10.2
IRO2(0.4)	80	100	12.2
MAGST2(0.35)+	225*	200*	18.7
ALST0.5(0.35)+	71	<u>60</u>	7.4
BUTST3(0.4)	134	120	32.3
CAPA0.25(0.35)+	90	107	8.9
SOYO1(0.35)+	213*	150*	31.5
LINSO1(0.35)+	206*	153*	22.6
TAR25(0.35)+	<u>59</u>	<u>57</u>	4.1
ASPH20(0.35)	96	100	5.7
EVA10(0.3)+	***	***	---
SBR5(0.35)+	100	140	23.3
SBR10(0.3)+	(0.9)	(4.0)	15.7
ACR10(0.3)+	***	***	12.0
AMINO22(0.35)	<u>0.0</u>	<u>0.0</u>	8.5
CAL30(0.35)+	<u>44</u>	<u>53</u>	18.7
CONP3(0.35)	---	---	---
SIK9(0.4)	102	75	11.3
SET6(0.4)	131	110	12.7
IRON10(0.4)	120	125	10.3
CEL2(0.4)	<u>63</u>	75	4.4
FORM2(0.4)	144*	135	8.8
TEA0.025(0.4)	<u>49</u>	<u>45</u>	7.4
TEA0.1(0.4)	95	95	8.0
LPV325(0.4)	119	100	5.5
LPV245(0.4)+	259*	195	9.9

^a percentage ratio of carbonation depth relative to respective control.

*** carbonation depth for both the control and modified concretes amounts to nil; a longer duration of carbonation would be required to reveal relative trends.

() absolute value displayed since control exhibits zero carbonation depth.

- Test details are given in Table 6.13, and results are discussed in 6.3.3.
- Results which suggest a worthwhile improvement in performance are presented in **highlighted** underlined text.
- Results which suggest unfavourable performance are followed by a **highlighted** asterisk.

Table 6.23 Results of corrosion testing (Series H)

Mix Ref.	Face A		Face B	
	Chloride level	Corrosion level	Chloride level	Corrosion level
	w/w _{concrete} (%)		w/w _{concrete} (%)	
CRC	0.26	++++	0.19	++++
CR1	0.17	+	0.18	+
CR2	0.15	+	0.16	+
CR3	0.16	+	0.17	++++
CR4	0.22	+++	0.19	+++
CR5	0.17	+	0.19	+++
CR6	0.18	+++	0.22	+++
CR7	0.12	+	0.21	+++
CR8	0.13	+++	0.19	++
CR9	0.23	++	0.24	+
CR10	0.22	++++	0.36	++++
CR11	0.19	+++	0.21	++++
CR12	0.30	+	0.25	++
CR13	0.17	+	0.18	+
CR14	0.15	+	0.17	+
CR15	0.25	+	0.30	+
CR16	0.20	+++	0.19	+++
CR17	0.17	+++	0.23	++
CR18	0.21	++++	0.23	+++

- Test details are given in Table 6.13, and results are discussed in 6.3.3

- **Key**

PACOR **Corrosion level**
(%)

0-20	+
20-40	++
40-60	+++
60-80	++++
80-100	+++++

6.2.4 Compressive strength and related testing

Presented in Table 6.24 are the results obtained from compressive strength testing (Series I), along with the air content (estimated from fresh density measurements, 6.1.2.2).

Reported in Figure 6.4 are the results obtained from calorimetry studies (see 6.3.4 for definition and significance of RQ_{max} and $R(1/t_{max})$). Each point corresponds to one mix (Table 6.12); the associated number represents the mix number: e.g. 1 represents CL1, 2 represents CL2, etc.

Table 6.24 Results of compressive strength testing and air content determinations

Mix ref.	Compressive strength (N/mm ²)			Air content (%)
	7d	28d	6 month	
C(0.4)	48.9	61.2	69.6	1.2
C(0.35)	52.5	62.6	68.5	1.3
C(0.3)+	60.7	67.0	72.6	2.1
	SR ^a			
GGBS65(0.4)	40*	58*	71*	1.0
PFA30(0.4)	74*	73*	94	1.0
SF10(0.4)+	98	108	103	2.5
KIES3(0.4)	99	92	101	1.1
BEN10(0.4)+	81*	81*	89	2.8
WHIT5(0.4)	97	89	88	1.1
IRO2(0.4)	99	91	95	1.2
MAGST2(0.35)+	75*	72*	78*	1.8
ALST0.5(0.35)+	89	90	95	1.2
BUTST3(0.4)	73*	67*	73*	2.3
CAPA0.25(0.35)+	80*	82*	89	1.0
SOYO1(0.35)+	76*	70*	69*	1.2
LINSO1(0.35)+	79*	80*	80*	1.3
TAR25(0.35)+	82*	83*	80*	1.9
ASPH20(0.35)	94	87	103	3.2
EVA10(0.3)+	64*	59*	61*	2.3
SBR5(0.35)+	59*	65*	70*	1.3
SBR10(0.3)+	61*	57*	62*	1.5
ACR10(0.3)+	64*	67*	78*	0.9
AMINO22(0.35)	76*	73*	66*	1.5
CAL30(0.35)+	92	93	91	1.2
CONP3(0.35)	89	90	97	2.4
SIK9(0.4)	88	93	86	1.0
SET6(0.4)	83	81	88	1.8
IRON10(0.4)	100	93	94	1.1
CEL2(0.4)	104	94	89	1.6
FORM2(0.4)	102	94	98	1.1
TEA0.025(0.4)	100	89	91	2.0
TEA0.1(0.4)	98	88	90	1.2
LPV325(0.4)	98	96	93	1.1
LPV245(0.4)+	82*	79*	80*	1.7

^a percentage ratio of the compressive strength relative to respective control.

- Test details are given in Table 6.13, and results are discussed in 6.3.4.
- Results which suggest unfavourable performance are followed by a **highlighted** asterisk.

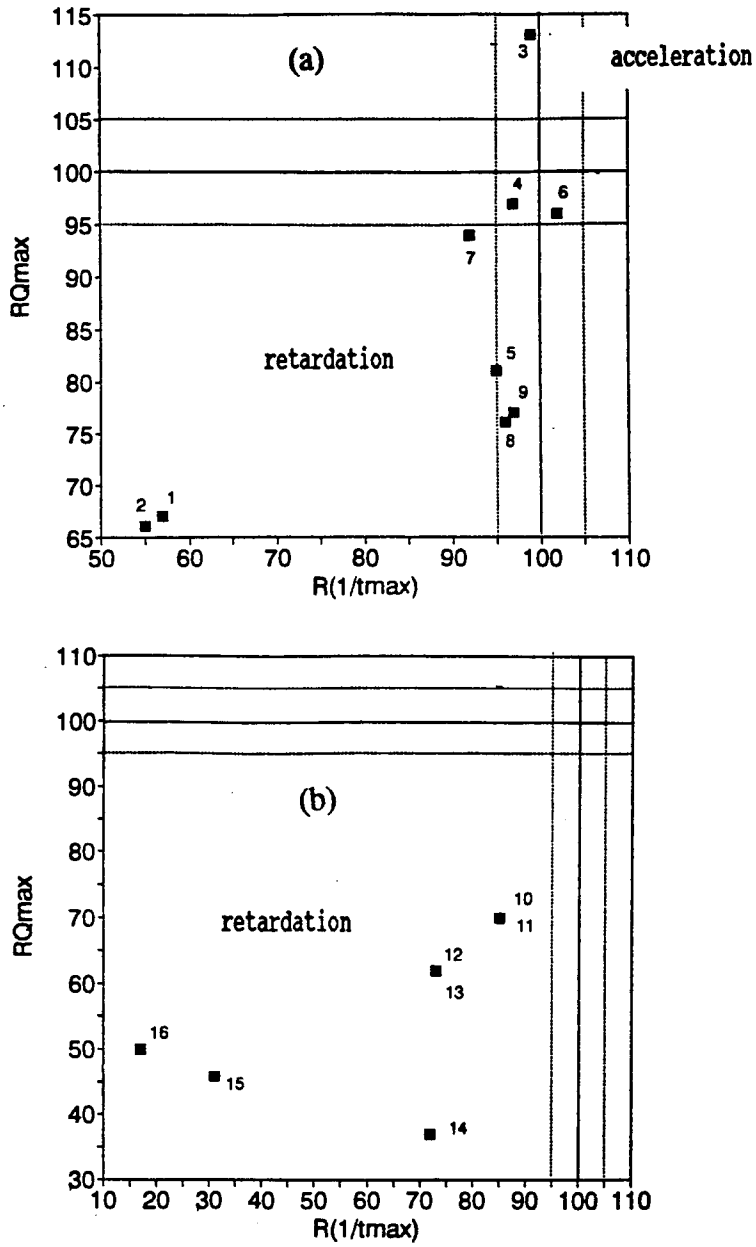
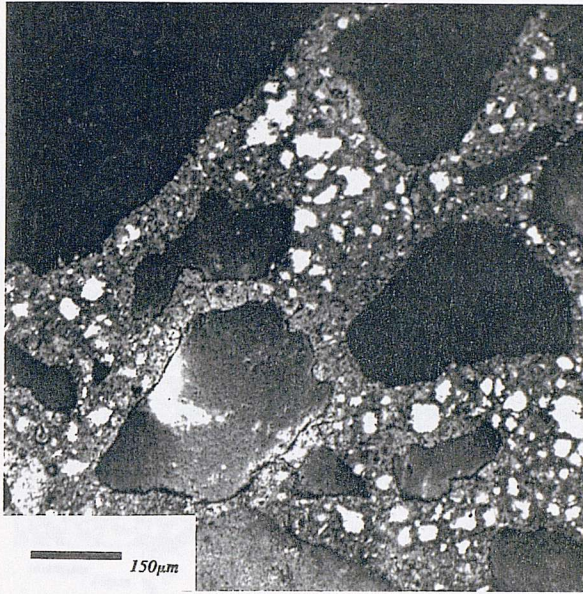


Figure 6.4 Calorimetry results.

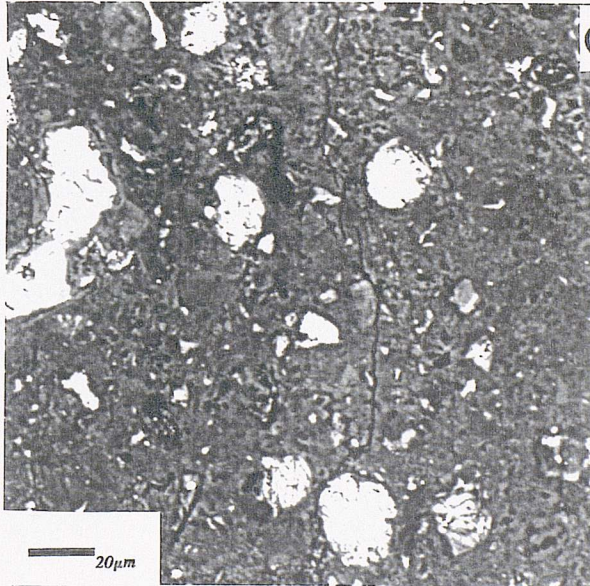
6.2.5 Microstructural examination

Application of the bse technique allowed large areas of the test specimens to be examined. A selection of bse images obtained at various magnifications are displayed in Figures 6.5 to 6.14 (see Table 6.13); the micrographs presented show, unless otherwise stated, features which could be seen throughout the microstructure (at least 20 fields were examined at each magnification level).

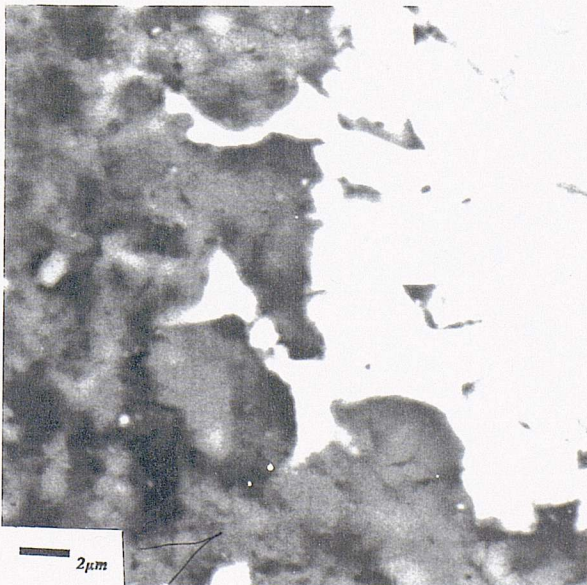
Figure 6.5 Bse images (control mix "C(0.4)")



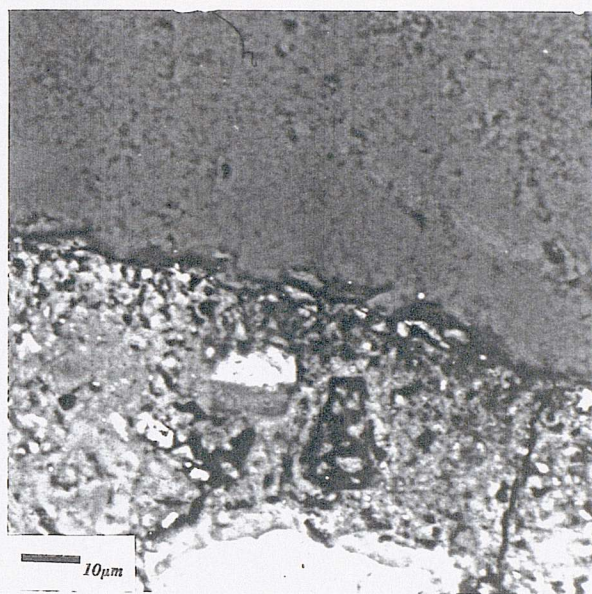
(a) general view of microstructure



(b) microstructure at low magnification

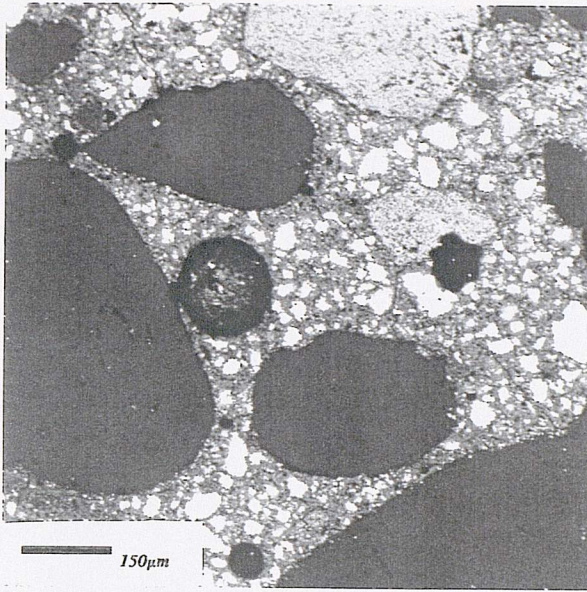


(c) microstructure at high magnification

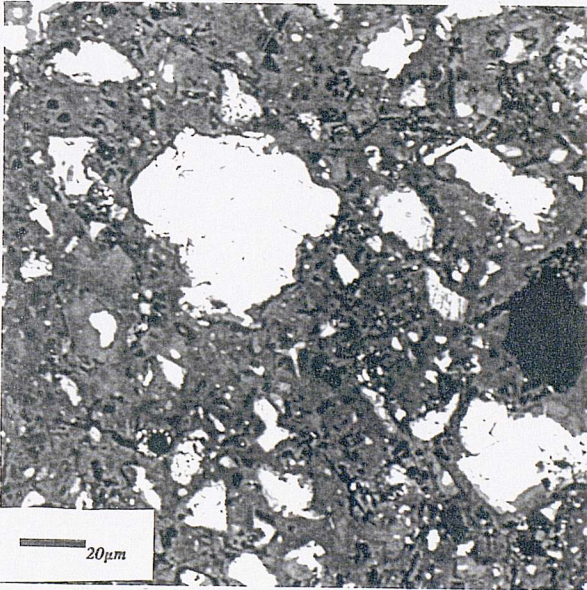


(d) aggregate/paste
interface

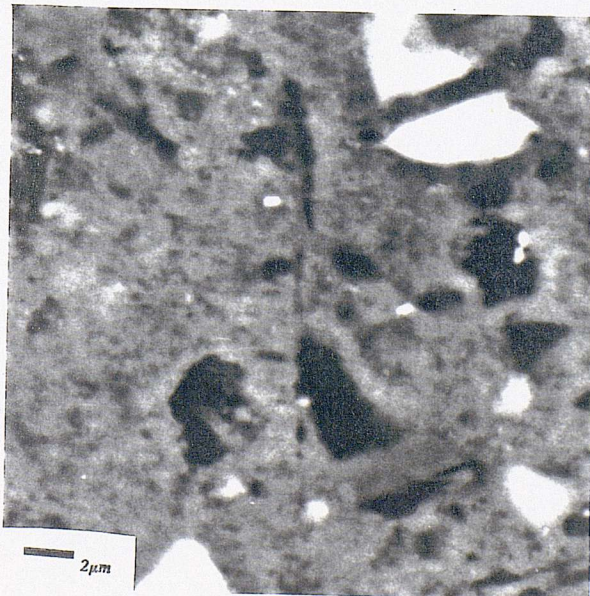
Figure 6.6 Bse images (control mix "C(0.3)+")



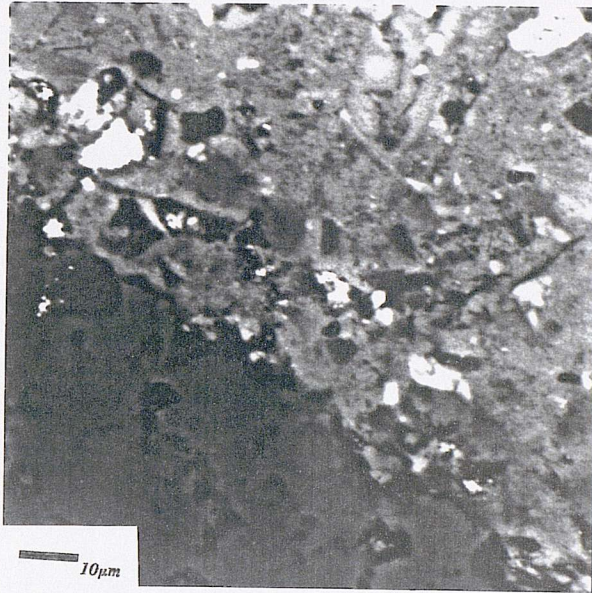
(a) general view of microstructure



(b) microstructure at low magnification

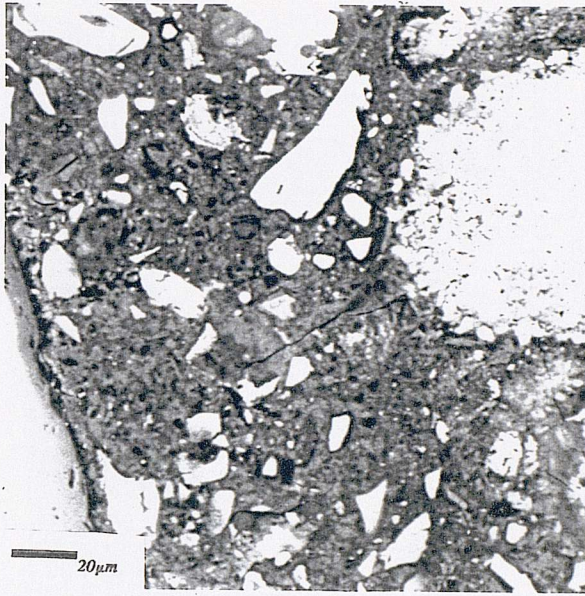


(c) microstructure at high magnification

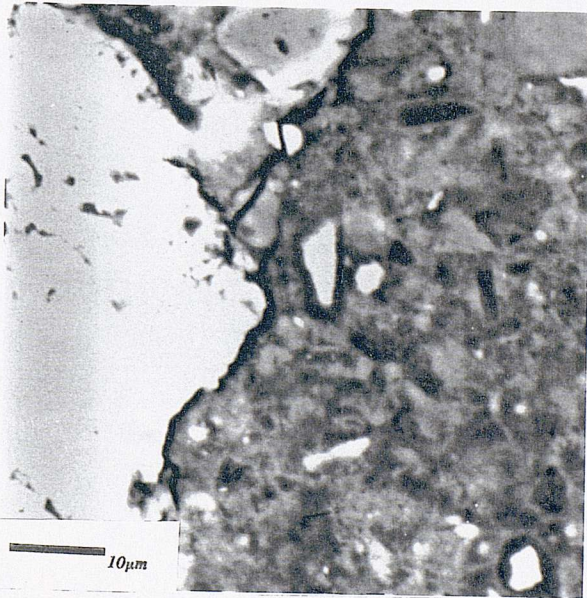


(d) aggregate/paste interface

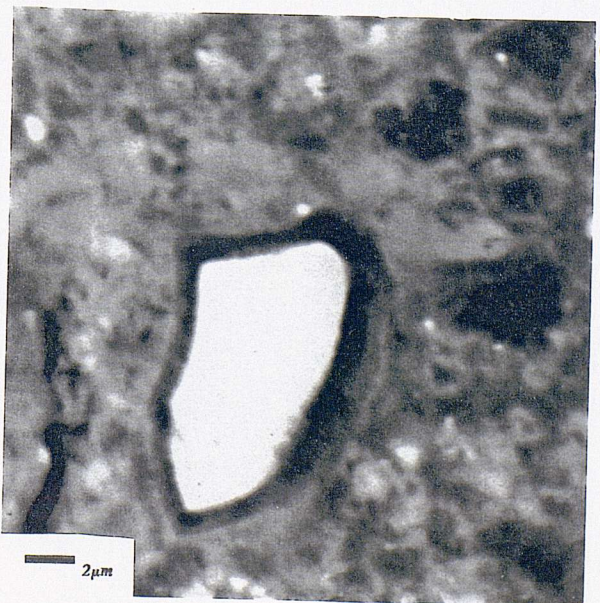
Figure 6.7 Bse images (mix "GGBS65(0.4)")



(a) microstructure at low magnification



(b) microstructure at high magnification



(c) pore structure in the neighbourhood of well hydrated slag grain (high magnification)

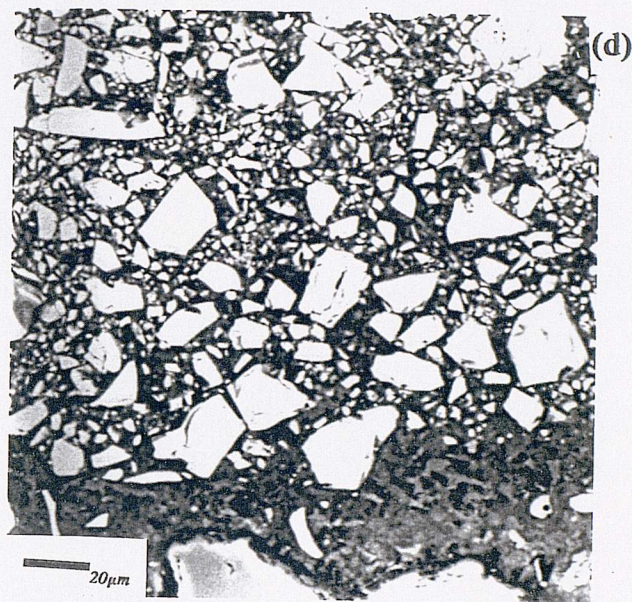
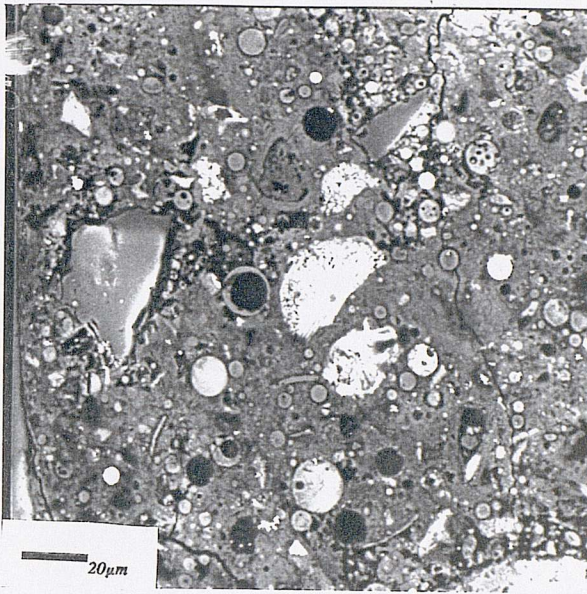
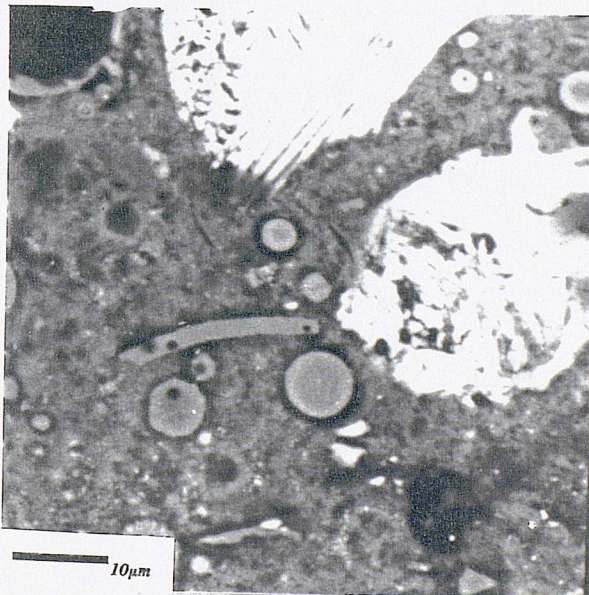


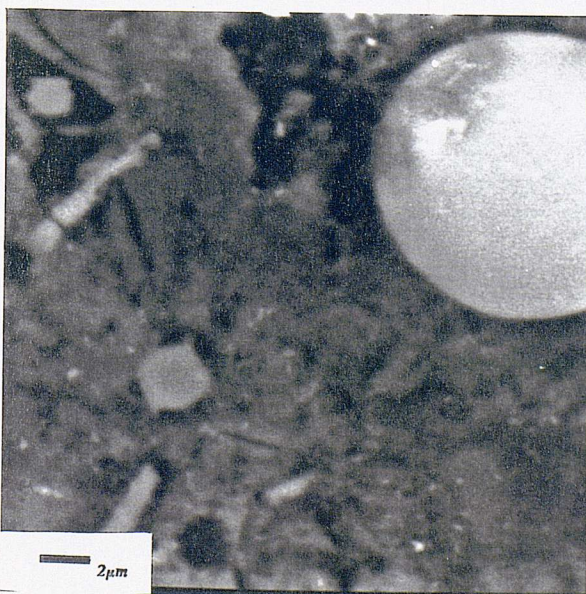
Figure 6.8 Bse images (mix "PFA30(0.4)")



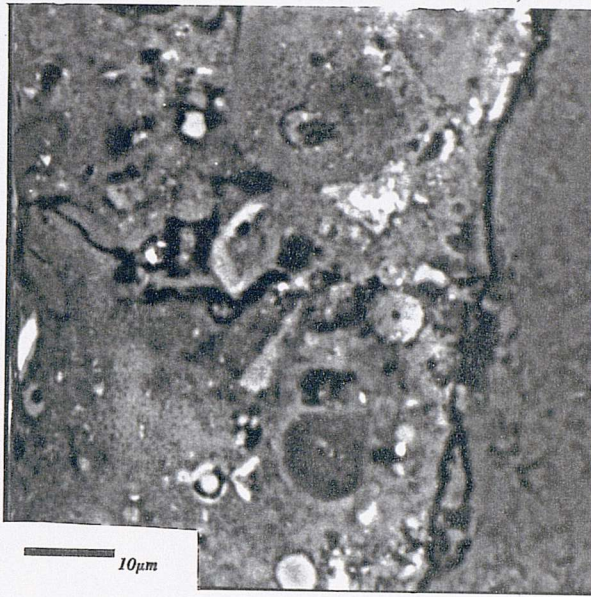
(a) microstructure at low magnification



(b) PFA particles hydrated to varying extents

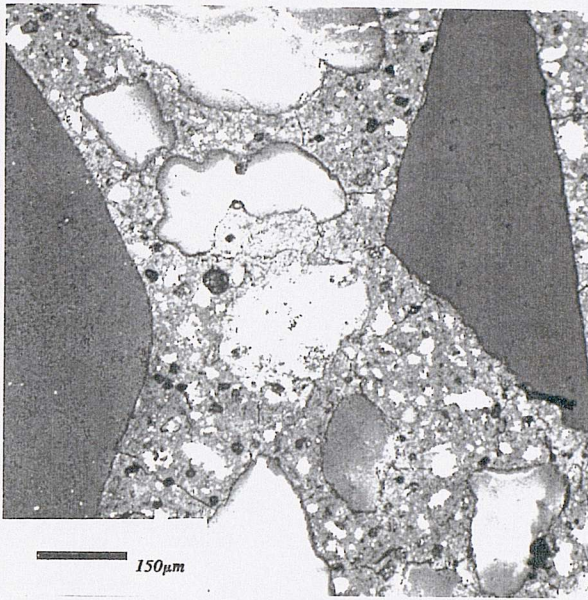


(c) microstructure at high magnification

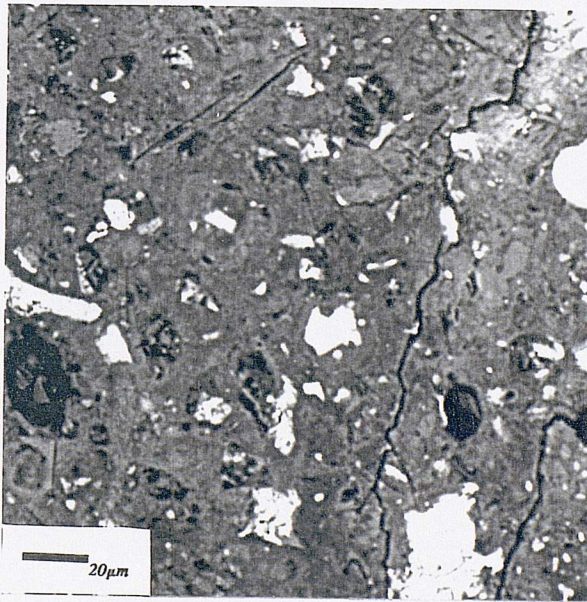


(d) aggregate/paste
interface

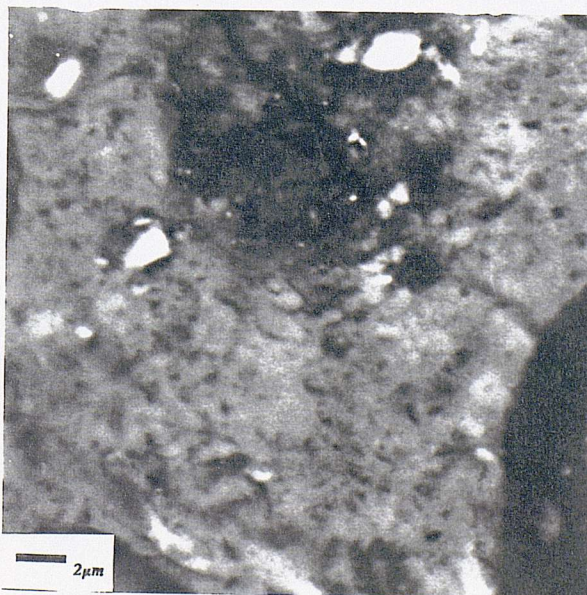
Figure 6.9 Bse images (mix "SF10(0.4)+")



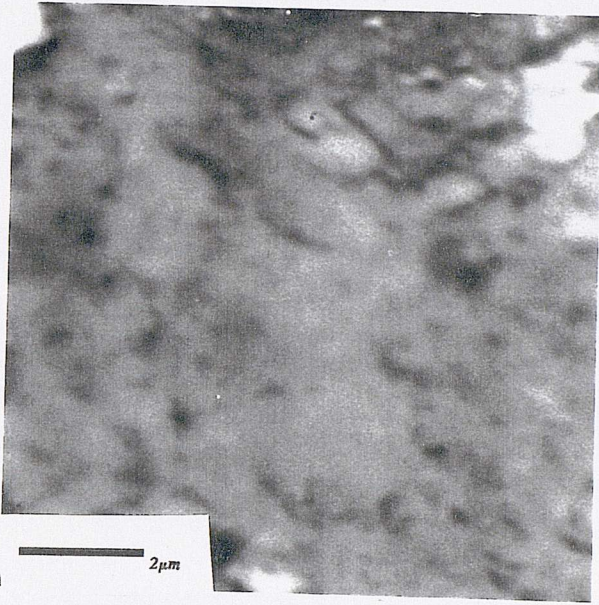
(a) general view of microstructure



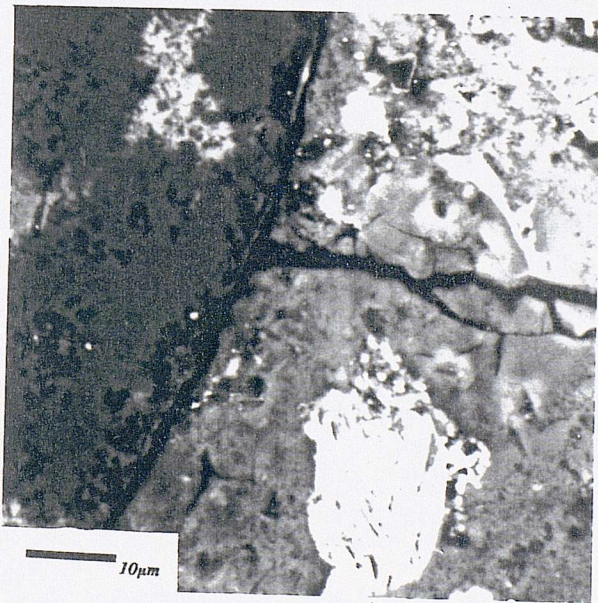
(b) microstructure at low magnification



(c) microstructure at high magnification

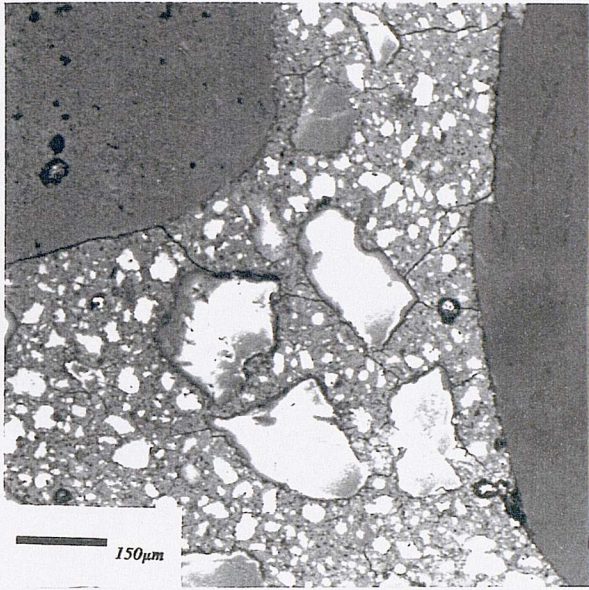


(d) dense microstructure
at fairly high
magnification

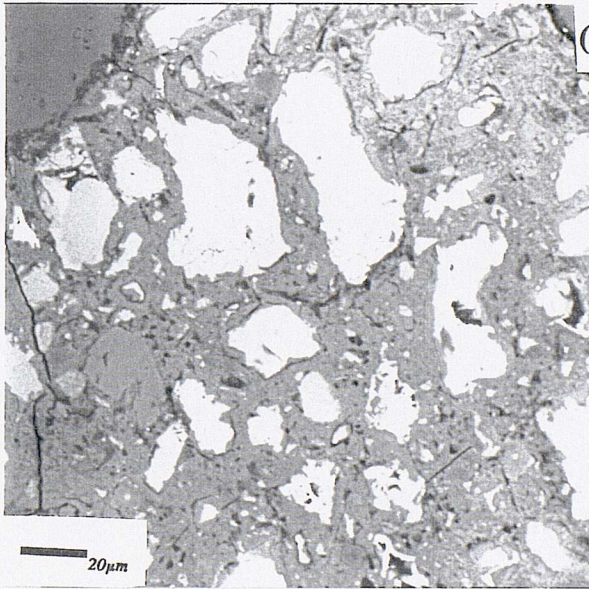


(e) aggregate/paste
interface

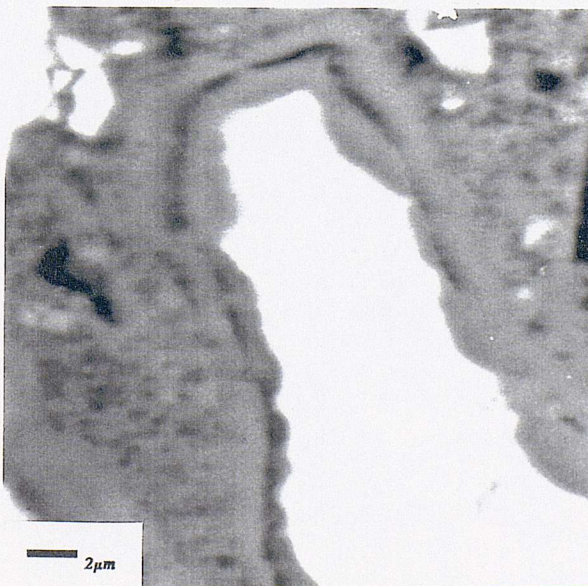
Figure 6.10 Bse images (mix "BUTST3(0.4)")



(a) general view of
microstructure

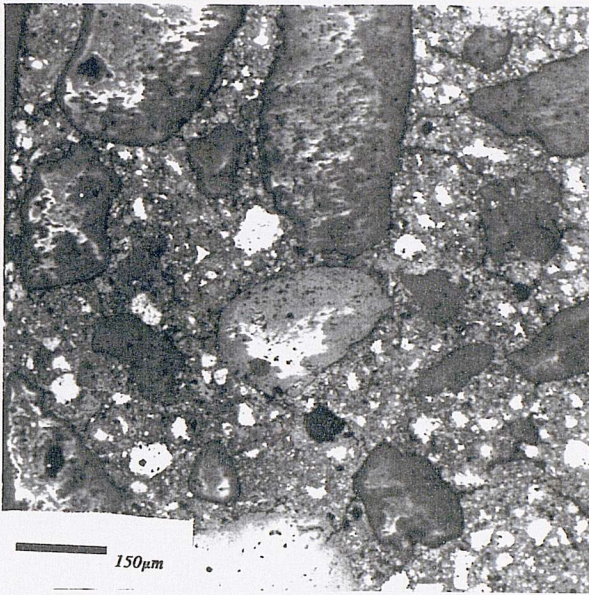


(b) microstructure at
low magnification

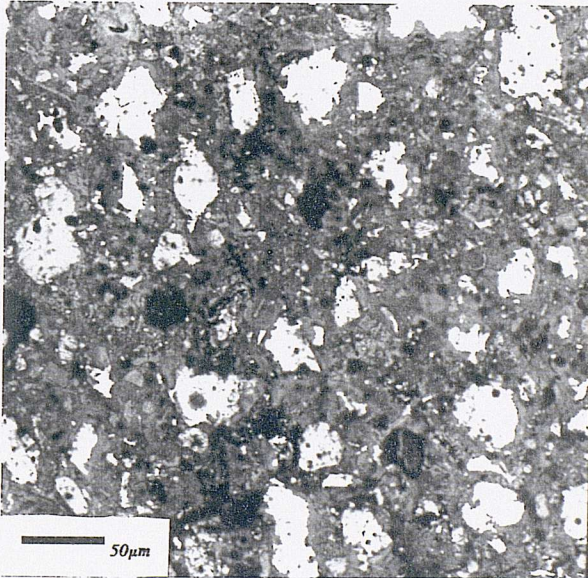


(c) microstructure at
high magnification

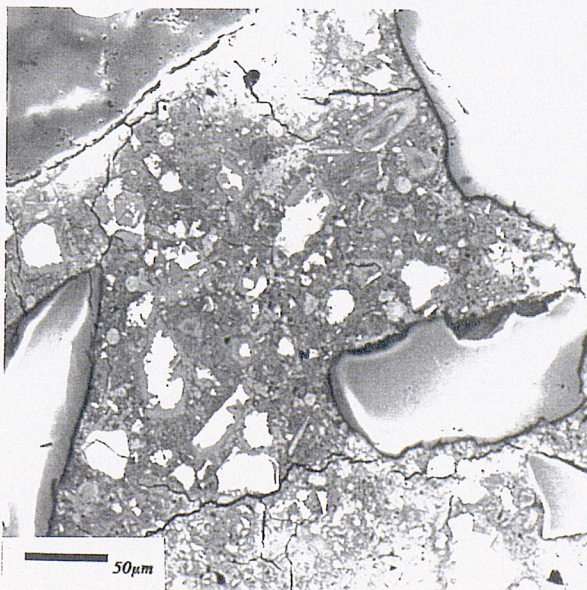
Figure 6.11 Bse images (mix "SOYO1(0.35)+")



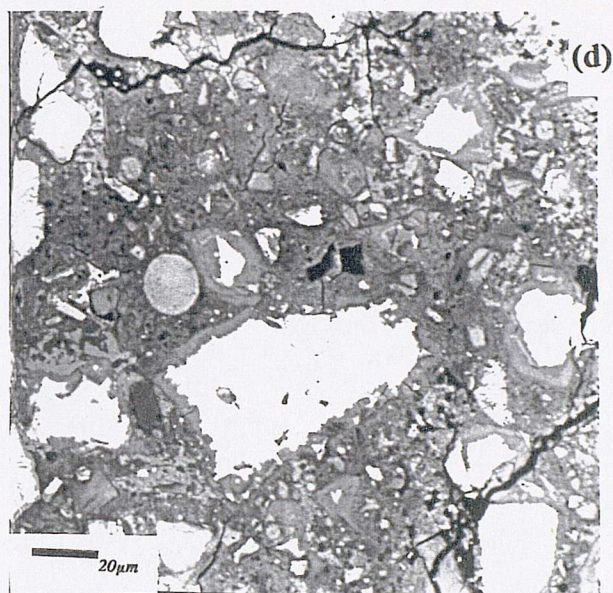
(a) general view of
microstructure



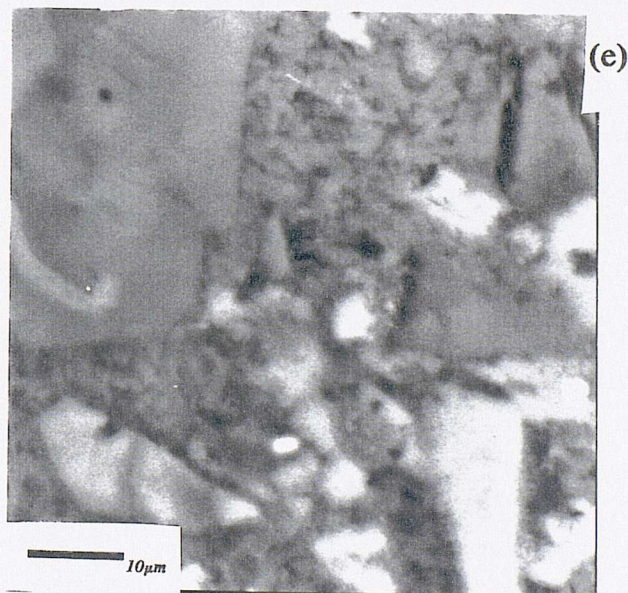
(b) high porosity
area



(c) low porosity
area

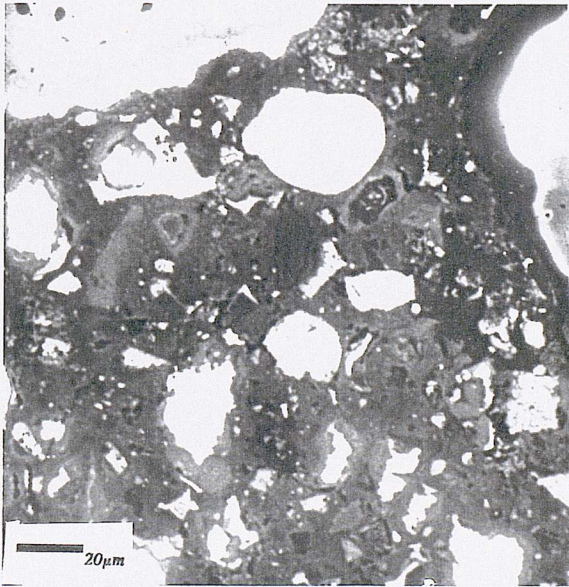


microstructure at
low magnification
(low porosity area)

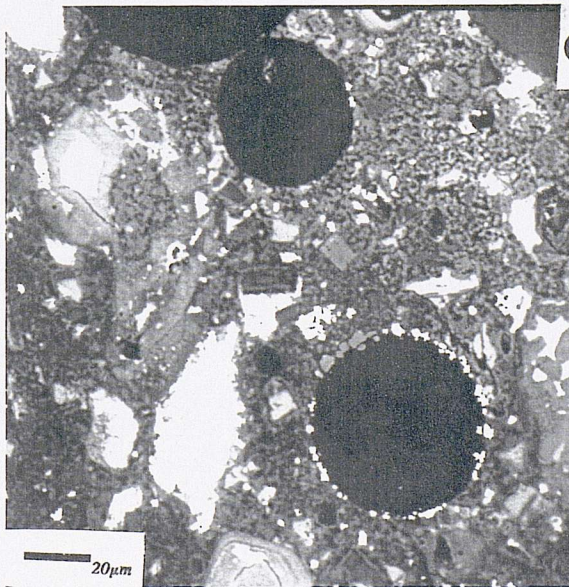


microstructure at
high magnification
(low porosity area)

Figure 6.12 Bse images (mix "ALST0.5(0.35)+")

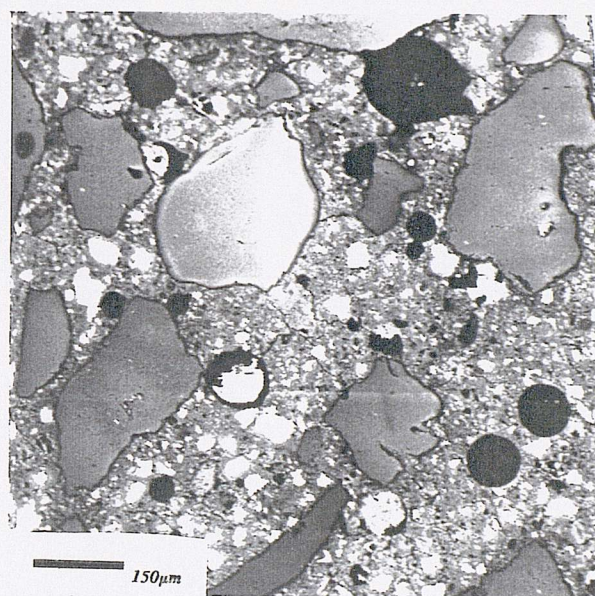


(a) low porosity
area

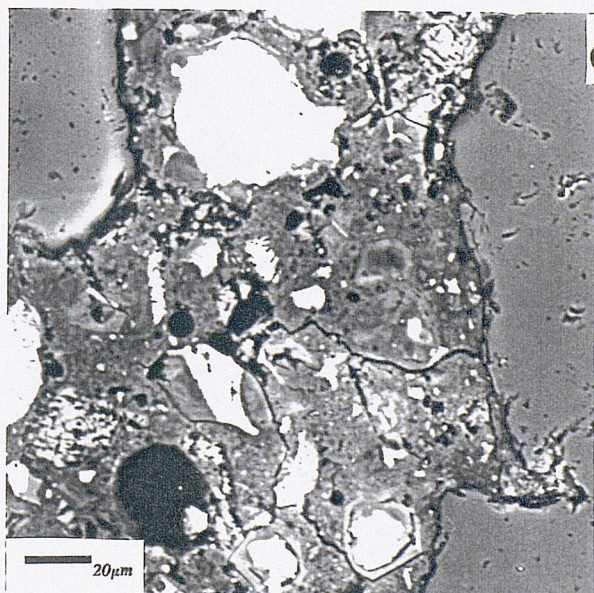


(b) high porosity
area

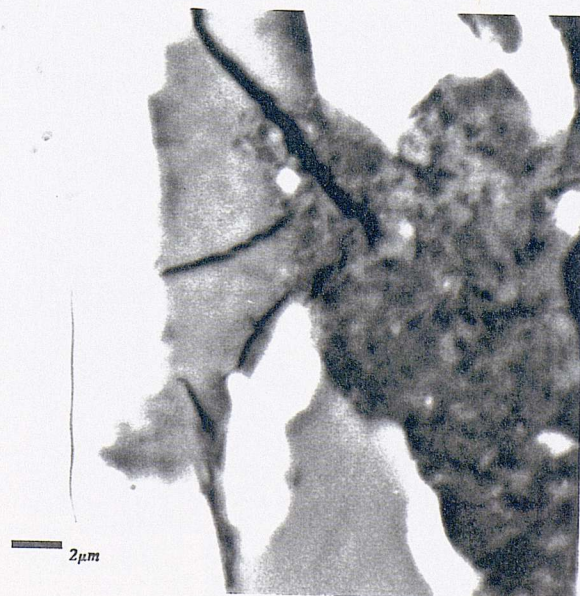
Figure 6.13 Bse images (mix "CAL30(0.35)+")



(a) general view of
microstructure

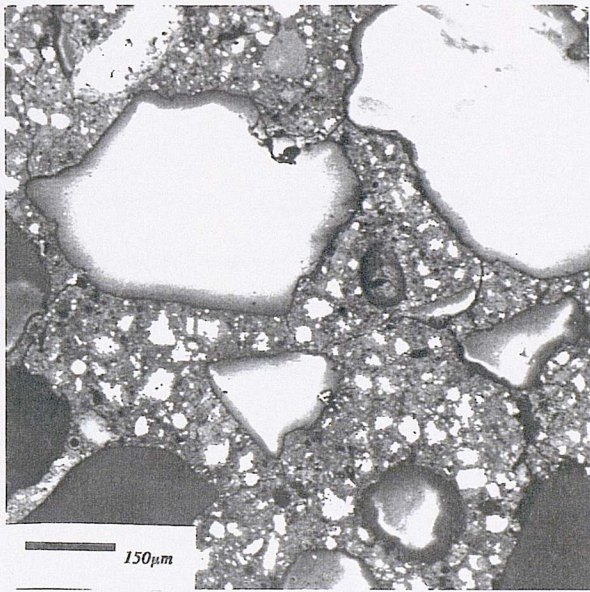


(b) microstructure at
low magnification

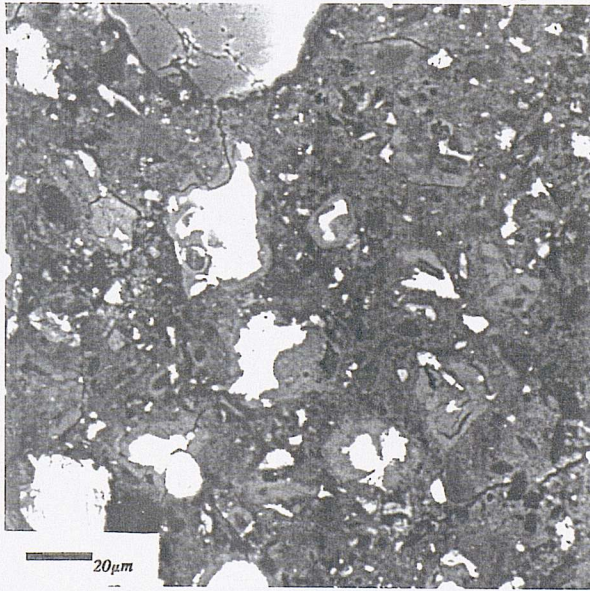


(c) microstructure at
high magnification

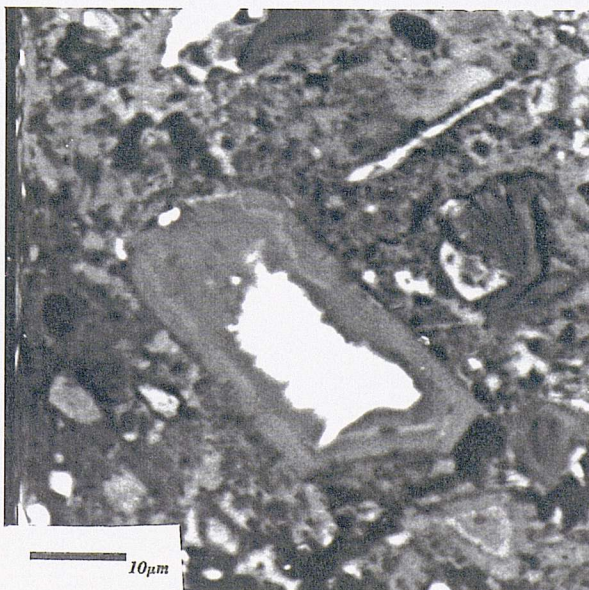
Figure 6.14 Bse images (mix "ACR10(0.3)+")



(a) general view of microstructure



(b) microstructure at low magnification



(c) microstructure at high magnification

6.3 Evaluation of experimental results

6.3.1 Scope

This section broadly examines the results of the experimental work which relate to control concretes and the modified concretes, the aim being to identify those results which indicate favourable performance (with respect to the particular property under consideration) for a modified concrete and those which suggest adverse behaviour in relation to the respective control; in Tables 6.14 to 6.24, the latter are emphasised by a highlighted asterisk, and the former by highlighted underlined text.

Graphical illustrations are included in this section to allow easy assimilation of important results. For convenience, numbers from 4 to 34 are used in the graphs to identify modified mixes (see Table 6.25).

It is worth remembering (see 6.2.1) that the term "ratio" (e.g. in "weight gain ratio") refers to the percentage ratio of the result for a given mix relative to the corresponding result of the respective control.

Table 6.25 Mix identification in graphical illustrations (Phase 2 mixes)

Mix ref.	Mix identification
C(0.4)	C1
C(0.35)	C2
C(0.3)+	C3
GGBS65(0.4)	4
PFA30(0.4)	5
SF10(0.4)+	6
KIES3(0.4)	7
BEN10(0.4)+	8
WHIT5(0.4)	9
IRO2(0.4)	10
MAGST2(0.35)+	11
ALST0.5(0.35)+	12
BUTST3(0.4)	13
CAPA0.25(0.35)+	14
SOYO1(0.35)+	15
LINSO1(0.35)+	16
TAR25(0.35)+	17
ASPH20(0.35)	18
EVA10(0.3)+	19
SBR5(0.35)+	20
SBR10(0.3)+	21
ACR10(0.3)+	22
AMINO22(0.35)	23
CAL30(0.35)+	24
CONP3(0.35)	25
SIK9(0.4)	26
SET6(0.4)	27
IRON10(0.4)	28
CEL2(0.4)	29
FORM2(0.4)	30
TEA0.025(0.4)	31
TEA0.1(0.4)	32
LPV325(0.4)	33
LPV245(0.4)+	34

Details of mixes are given in 6.1.1.

6.3.2 Properties relevant to transport

Permeability

It is perhaps worth recalling first that permeability testing was performed immediately (without prior immersion in water or saturation) on specimens stored for a relatively long period in sealed conditions (Table 6.13). Therefore, the specimens would most certainly exhibit higher permeability than comparable specimens tested after storage in water, or initially sealed cured but subjected to vacuum saturation, or even water immersion, prior to testing. Indeed, Bamforth et al. (1985) reported that about an order of magnitude difference in the permeability coefficient was detected between sealed cured and water cured specimens from a range of concretes. The reason for this difference, it is believed, is associated primarily with the phenomenon of self-desiccation, and may be considered three-fold. First, microcracking and pore collapse which normally accompanies the self-desiccation of concrete (Chatterji 1982, Killoh et al. 1989) would almost certainly bring about an increase in water permeability (Powers et al. 1954, Vuorinen 1985). Storage of the concrete specimens in a moist environment, in contrast, can lead to autogenous healing of microcracks (Neville 1981) and also to swelling of the cement paste hydrates, the latter phenomenon has often been considered (e.g. Dhir et al. 1989, Hearn 1992) to contribute to decreasing the permeability of concrete to water. Second, water tends to penetrate self-desiccated concrete, which is partially saturated, due to capillary absorption as well as in response to the applied pressure. Thirdly, the degree of hydration attained, at a given age, in self-desiccated concrete is likely to be lower than in comparable moist-cured concrete (Copeland & Bragg 1955).

According to the Valenta equation (3.5.1), an approximate value of the water permeability coefficient can be calculated from the average depth of water penetration and the weight gain of test specimens. Water permeability coefficients hence derived are reported in Table 6.14; some (those marked with a "@" sign), however, were judged to be over estimated due to the presence of electrodes influencing penetration depths exceeding approximately 40mm. This is because test cubes, when split, tended

to fracture along the surface of either of the electrodes, therefore, the detected penetration depth tends not to reflect accurately the permeability in the bulk concrete since water flow at the concrete/electrode interface area is likely to be accelerated due to the presence of additional flow channels.

As anticipated (6.1.2.1.1, (I)), electrical resistivity monitoring was found useful. Arguably, the extent of the decline in resistivity (if any) would be governed by a multitude of factors, some of which bear no direct relevance to permeability, and are difficult to quantify. It would appear imprudent, therefore, to employ such data in ranking mixes in order of increasing/decreasing water permeability. Nevertheless, for any particular mix, it seemed reasonable to consider PDR higher than 15% to be evidence of some water ingress into the concrete mass between the electrodes; based on this, the bands shown in Table 6.26 were formulated.

Table 6.26 Water penetration bands

Band	Time water first penetrates the zone between electrodes
1	no penetration
2	> 6 days
3	4 to 6 days
4	1 to 4 days
5	2 hours to 1 day
6	less than 2 hours

Based on the classification system described above, each mix was allocated to the appropriate band (Table 6.14). When the information displayed on both sides of Table 6.14 (i.e. d , WG, and $k_{(w)v}$ on the one hand and the Band class on the other) are compared broad agreement is revealed, though anomalies exist (see Figures 6.15 and 6.16). Strict agreement, is found to pertain merely to the lowest permeability mixes, 6 (SF10(0.4)+) and 8 (BEN10(0.4)+). The most notable discrepancy lies in the penetration depth data indicating no water ingress into the zone between the electrodes whilst the corresponding mixes (e.g. C3 (C(0.3)+), 21 (SBR10(0.3)+), 29 (CEL2(0.4)), 34 (LPV245(0.4)+), etc.) appear in bands which suggest the contrary (Figure 6.16). Moreover, Bands 5 and 6 would appear to suggest appreciably higher permeability than that indicated by the calculated water permeability coefficients (note also how a relatively wide range of permeability values correspond to Band 5). These anomalies might appear, at first sight, to deprecate the results furnished; however, the discussion to follow will demonstrate the contrary, that the two modes of testing yield results which, in effect, complement each other.

First, the penetration depth at any one location within the test specimen may, due to the variation in permeability within the specimen, vary quite markedly from the average value reported in Table 6.14, this being illustrated quite remarkably in Figure 6.17, which depicts the observed wet area in the specimen from mix 22 (ACR10(0.3)+). Secondly, that the visually detected front accurately represents the actual water penetration front is suspect. On a split specimen, the water penetration depth is defined by the visually observed boundary line of the wet area. When the test specimen is split, water present under some pressure in the concrete pores travels to the split surface, where the pressure is atmospheric, and the rate of flow will naturally depend on the pressure difference and the permeability of the specimen. Moreover, the penetration front will only become visible when the rate of arrival of water at the split surface balances the rate of evaporation from it. Therefore, since the pressure difference at the end of the penetration zone cannot be expected to be large (see Figure 6.18), it is conceivable that the water front cannot be accurately detected by visual means in low permeability concretes. Moreover, the water penetration front cannot be defined by a

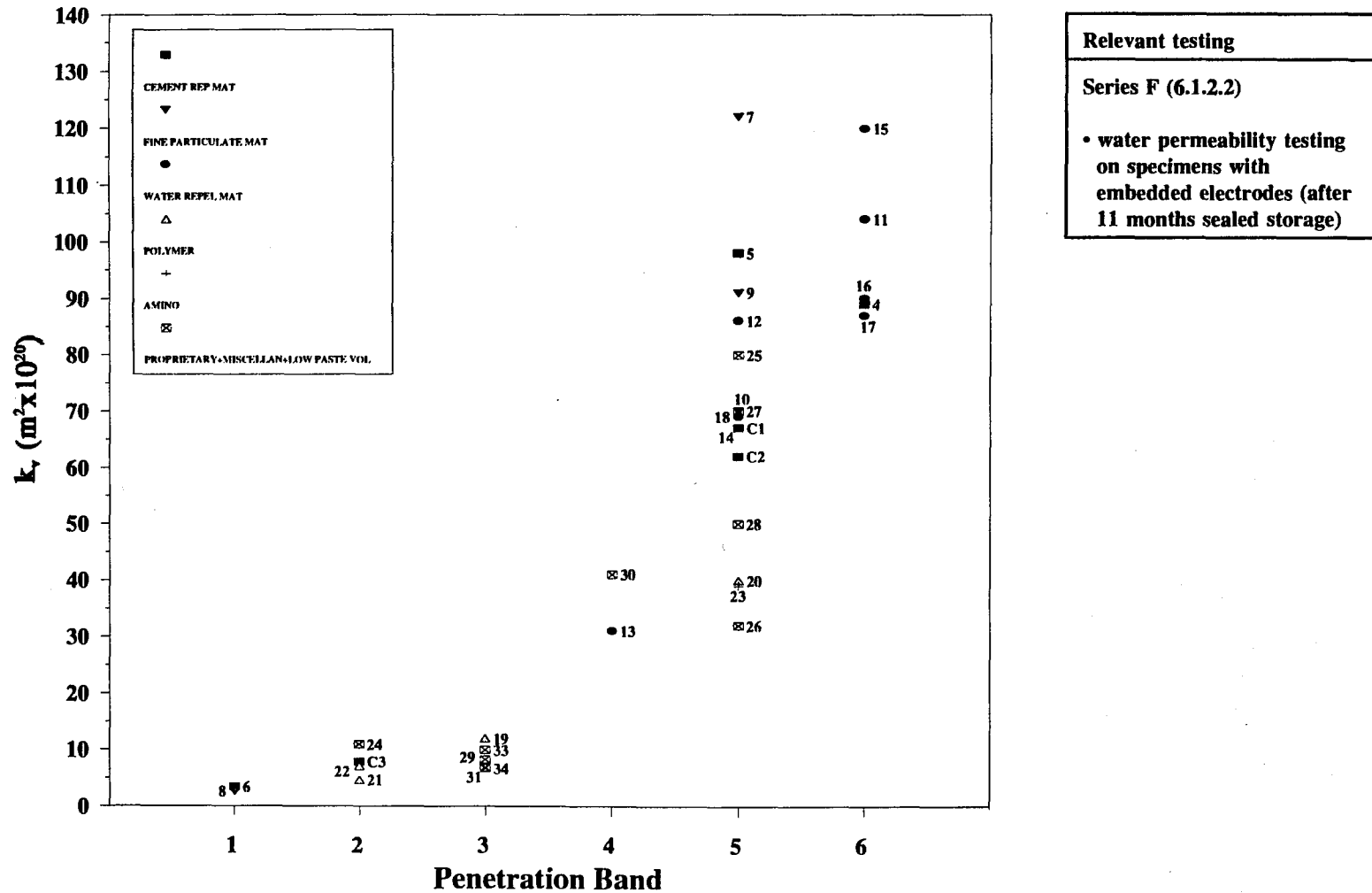
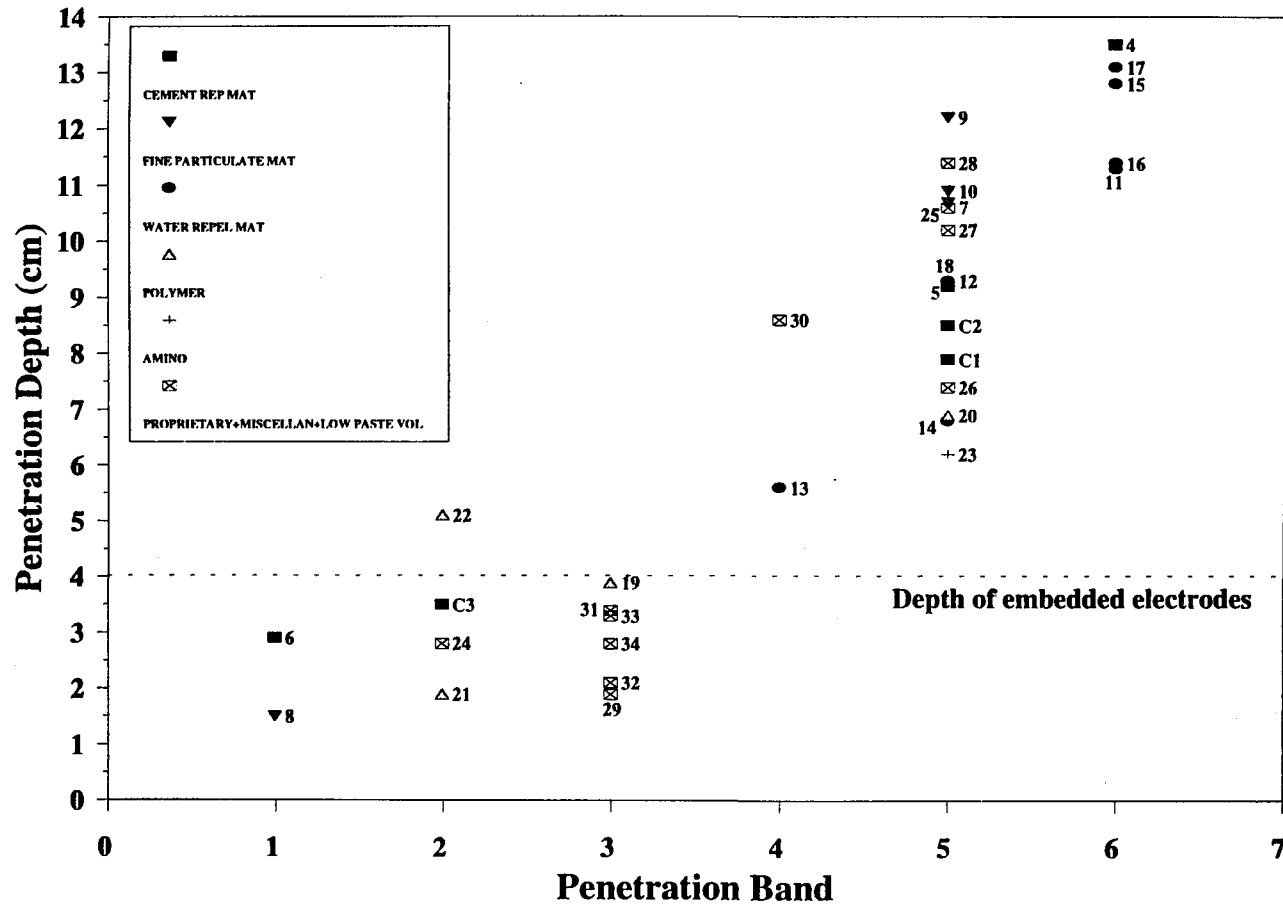


Figure 6.15 Water permeability coefficient for each mix versus corresponding water penetration band.



Relevant testing

Series F (6.1.2.2)

- water permeability testing on specimens with embedded electrodes (after 11 months sealed storage)

Figure 6.16 Water penetration depth for each mix versus corresponding water penetration Band.

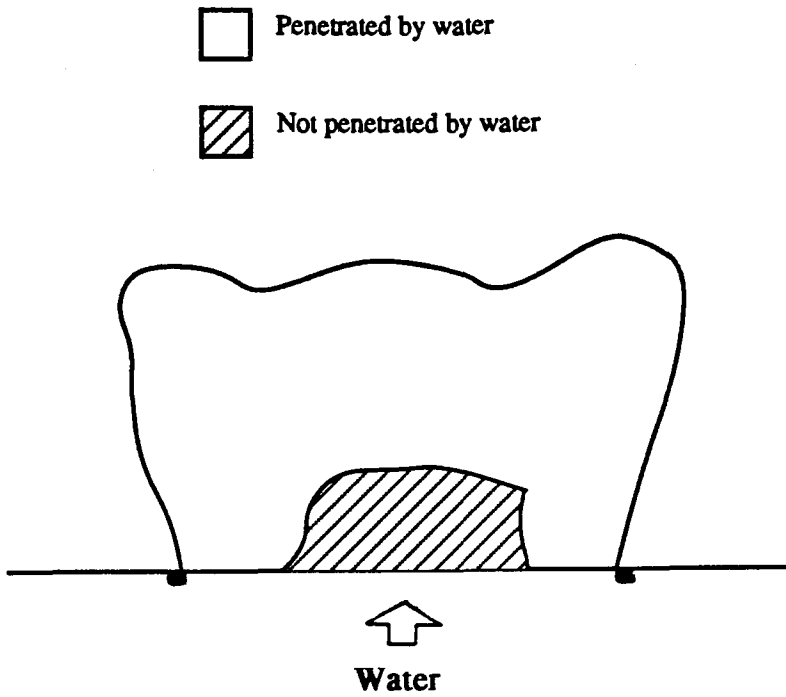


Figure 6.17 Water penetration in acrylic specimen.

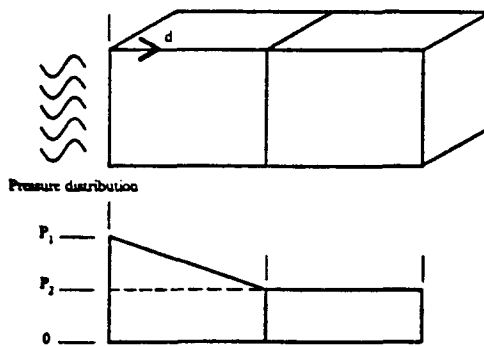
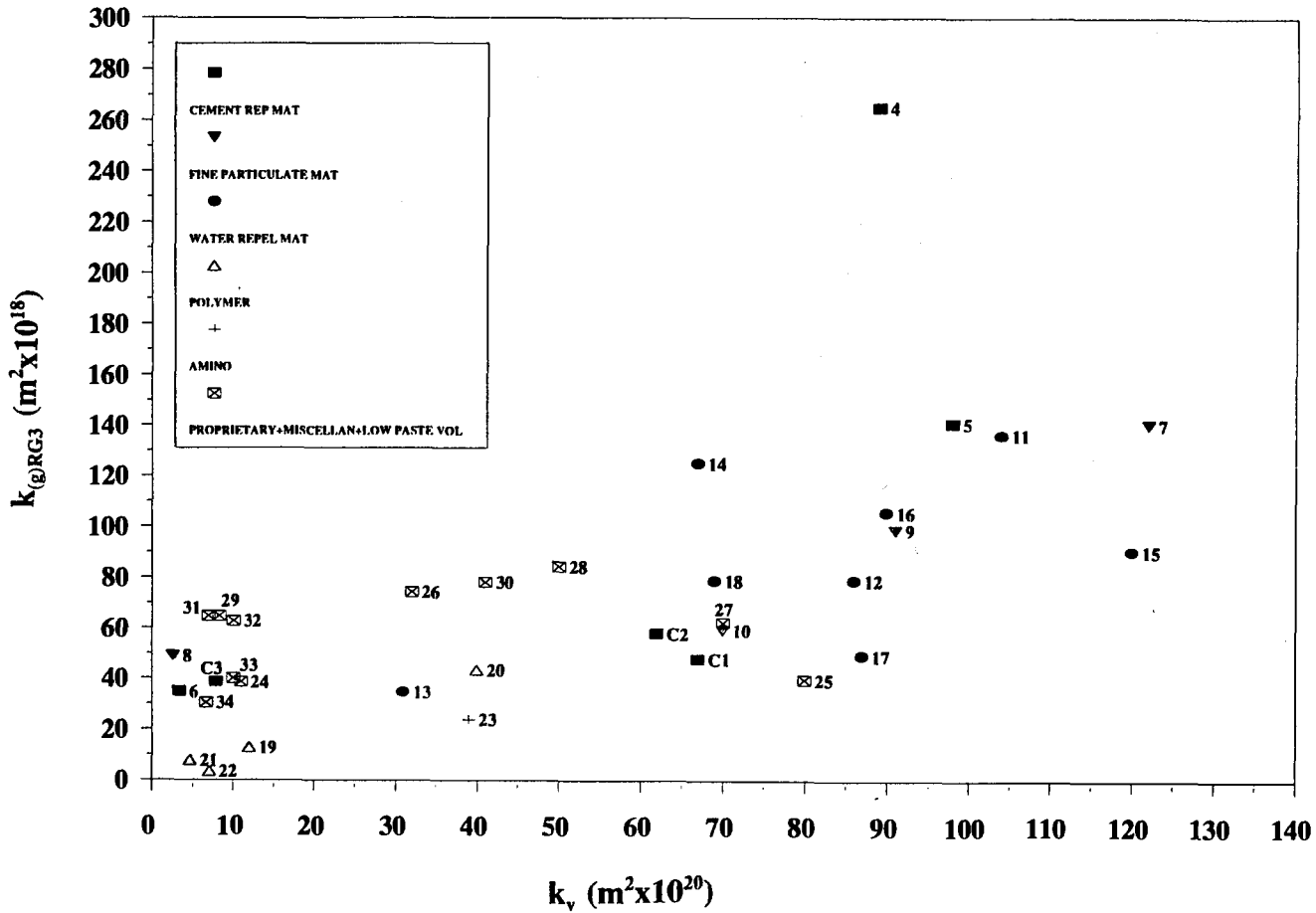


Figure 6.18 Pressure distribution of penetrating water.

distinct boundary, since water may penetrate through large pores and microcracks ahead of the boundaries of the visibly detected water front. The anomalous behaviour exhibited by a range of mixes (C3 (C(0.3)+), 19 (EVA10(0.3)+), 21 (SBR10(0.3)+), 24 (CAL30(0.35)+), 29 (CEL2(0.4)), 31 (TEA0.025(0.4)), 32 (TEA0.1(0.4)), 33 (LPV325(0.4)), 34 (LPV245(0.4)+)) is probably explicable in terms of the above combined. Furthermore, it will become apparent later (6.4) that the anomalous behaviour of mixes belonging to Band 6 can be explained, at least partly, by the presence of areas of high porosity paste. It was also found interesting to examine the oxygen permeability test results. Indeed, the following discussion will display some evidence corroborating earlier mentioned views regarding the influence of specimen preconditioning on oxygen permeability results and the extent to which those results reflect water permeability in concrete.

Supposedly identical specimens were found to exhibit variations in $k_{(g)RG3}$ (drying regime: 50°C & 11-14% RH, see 6.1.2.1.1, (I)) of the order of 25%, on average. As would be anticipated, the control concretes yield $k_{(g)RG3}$ an order of magnitude lower than $k_{(g)}$ relating to the control concrete of Phase 1 (mix C). In contrast, however, the control mixes C1 (C(0.4)) and C3 (C(0.3)+) are found to exhibit merely marginal differences in permeability, this being notably at variance with the corresponding water permeability results. Further similar discrepancies emerge when the relevant data appearing in Tables 6.14 and 6.15 are compared (see Figure 6.19), in connection with a wide range of mixes (e.g. mixes: 6 (SF10(0.4)+), 25 (CONP3(0.35)), 31 (TEA0.025(0.4)), 32 (TEA0.1(0.4)), 33 (LPV325(0.4)), etc.). Results relating to $k_{(g)RG1}$ (drying regime: 30°C & 75% RH) and also $k_{(g)RG2}$ (drying regime: 30°C & 55% RH), measured on supposedly identical specimens, were found to vary by 30%, on average. Figures 6.20 and 6.21 show that the parameters $kr_{(g)RG2}$ and $kr_{(g)RG1}$ indicate trends (of modified mix vs. respective control) which broadly parallel the trends indicated by $kr_{(g)RG3}$. Another interesting feature of the results is that of $kr_{(g)RG2}$ and $kr_{(g)RG1}$ generally tending, respectively, to indicate progressively wider differences in permeability between mixes (e.g. mixes: 4 (GGBS65(0.4)), 5 (PFA30(0.4)), 6 (SF10(0.4)+), 9 (WHIT5(0.4)), 16 (LINSO1(0.35)+), 28 (IRON10(0.4)), etc.) and their respective



Relevant testing sequence
Series A (6.1.2.2) <ul style="list-style-type: none"> • drying at 30°C & 75% RH (5 months) • drying at 30°C & 55% RH (4 months) • drying at 50°C & 11-14% RH (56 days) • oxygen permeability
Series F (6.1.2.2) <ul style="list-style-type: none"> • water permeability testing on specimens with embedded electrodes (after 11 months sealed storage)

Figure 6.19 Oxygen permeability coefficient for each mix versus corresponding water permeability coefficient.

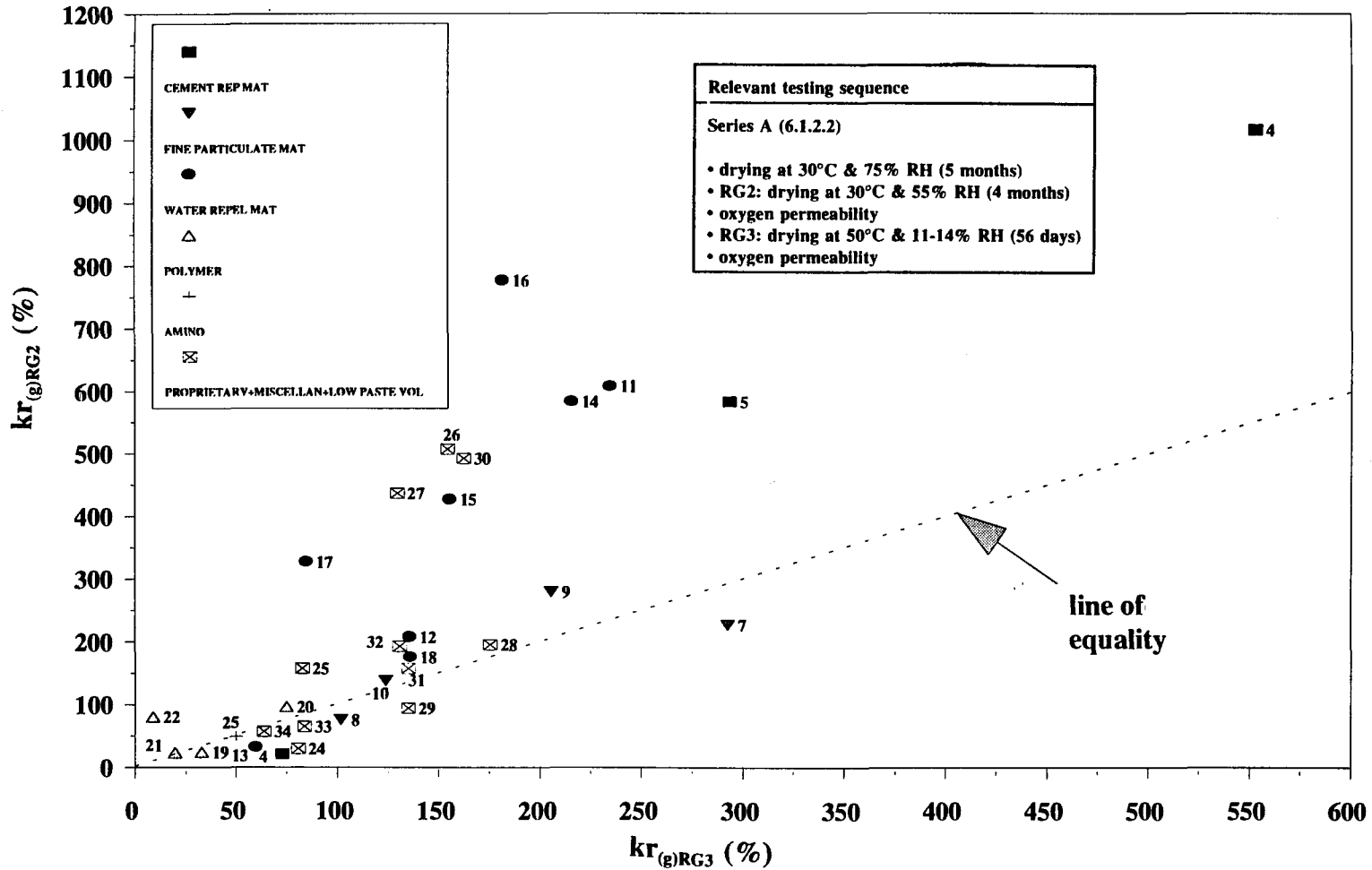


Figure 6.20a Oxygen permeability ratio for each mix (RG2-dried specimens) versus corresponding ratio for RG3-dried specimens.

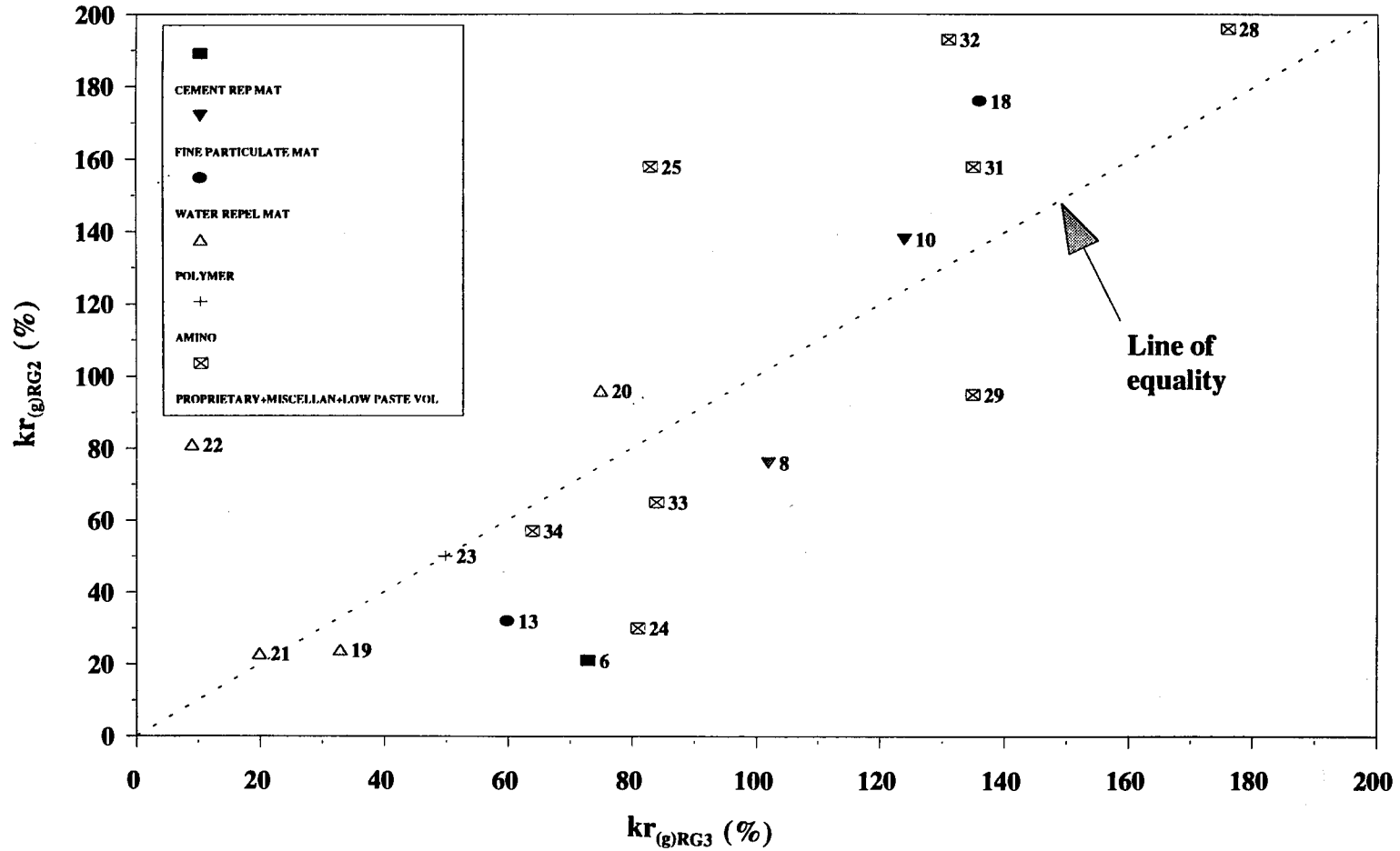


Figure 6.20b Expanded version of Figure 6.20a.

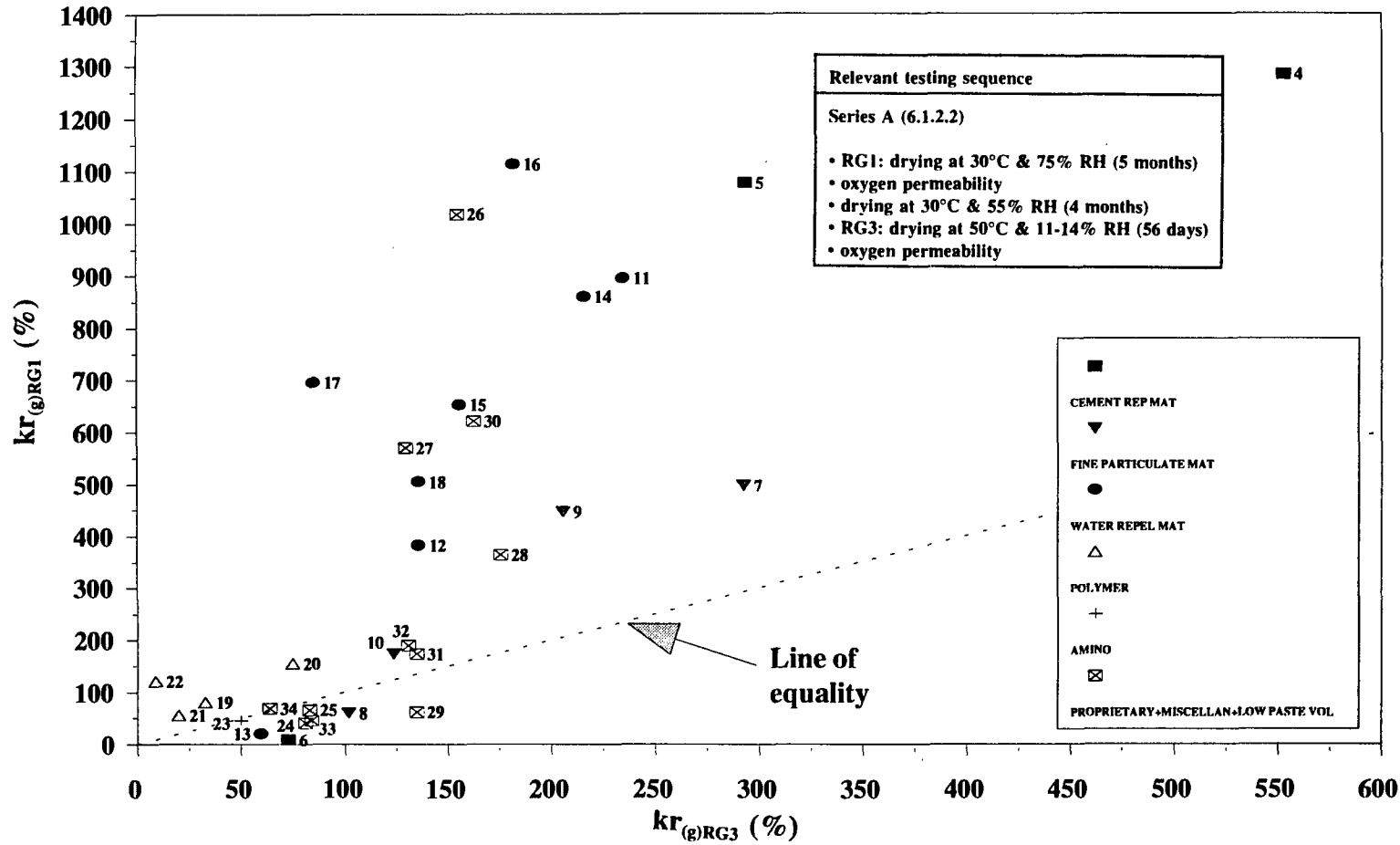


Figure 6.21a Oxygen permeability ratio for each mix (RG1-dried specimens) versus corresponding ratio for RG3-dried specimens.

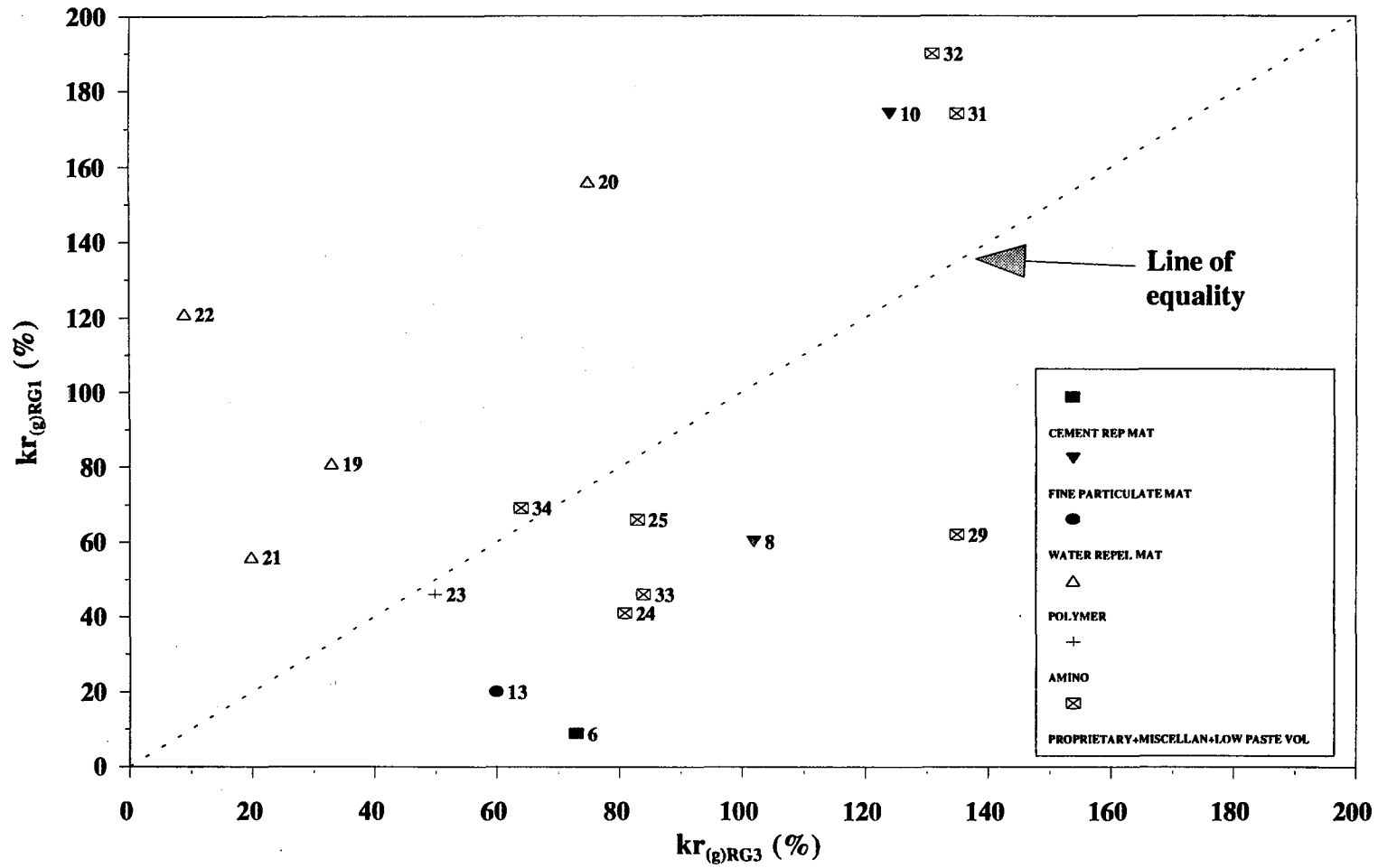


Figure 6.21b Expanded version of Figure 6.21a.

control (see Table 6.15 and Figures 6.20 and 6.21).

In the light of the aforementioned the following general conclusion seemed warranted: the finer the pore structure of the test specimen, the more likely $k_{(g)RG3}$ values will tend to overestimate the true intrinsic permeability, and the more $k_{(g)RG2}$, and to a larger extent $k_{(g)RG1}$, will tend to become depressed due, in part, to residual moisture, and vice versa. Accordingly, it was felt that by expressing results for each mix collectively in terms of the ratios $k_{(g)RG3}/k_{(g)RG1}$ and $k_{(g)RG3}/k_{(g)RG2}$, as shown in Table 6.15, it may be possible to contrast readily the pore structure of a modified concrete with that of the respective control, the concrete having higher ratios being of a finer pore structure, and vice versa. Comparing the relevant data in Tables 6.14 and 6.15 (see Figure 6.22), it becomes apparent that the approach does in fact lead to somewhat better correspondence between oxygen and water permeability results (e.g. mixes: 5 (PFA30(0.4)), 6 (SF10(0.4)+), 24 (CAL30(0.35)+), etc.), though fails to account for the behaviour of a wide range of other mixes (e.g. mixes: 7 (KIES3(0.4)), 8 (BEN10(0.4)+), 19 (EVA10(0.3)+), 21 (SBR10(0.3)+), 22 (ACR10(0.3)+), etc.); it will become apparent later (6.4) that for some of these mixes (mixes: 8 (BEN10(0.4)+), 19 (EVA10(0.3)+), 21 (SBR10(0.3)+), 22 (ACR10(0.3)+)) an explanation for the anomalous behaviour can be found by considering other factors at play (also refer to 5.2.2.2.2). It should also be noted that oxygen permeability results were not corrected to take account of gas slippage, for corrections as described by Dhir et al. (1989) were considered wholly impractical due to the large number of test specimens (see 3.5.3, also A3.2). It would be interesting to examine whether better correspondence between $k_{(g)RG3}/k_{(g)RG1}$ and permeability would have resulted had an even milder drying regime (drying at, say, 30°C and 85% RH instead of 30°C & 75% RH) been adopted for RG1.

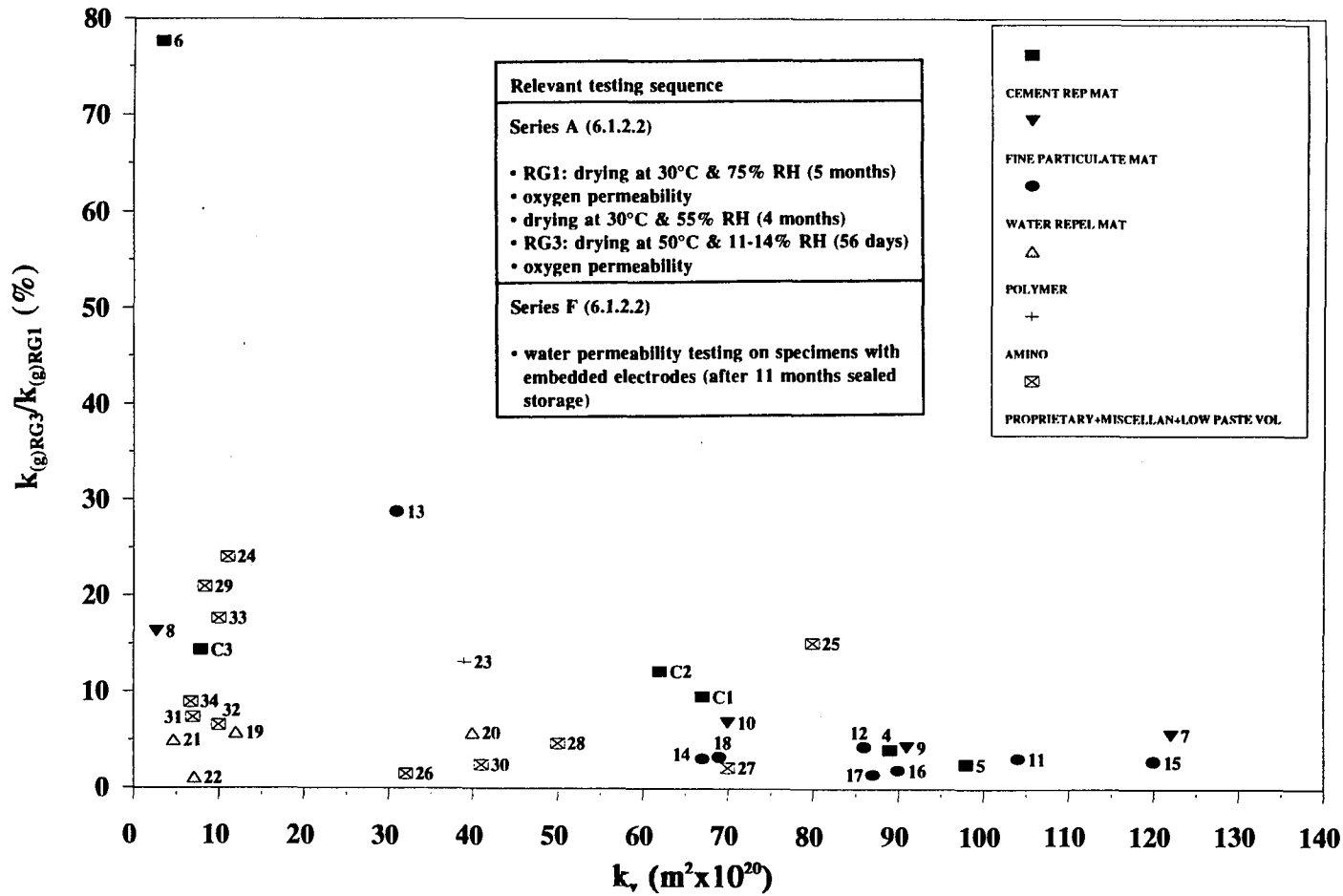


Figure 6.22 The ratio $k_{(g)RG3}/k_{(g)RG1}$ for each mix versus the corresponding water permeability coefficient.

Wetting

The absorption behaviour of the control concretes (Series B specimens; 50 °C & 11-14% RH dried) is illustrated in Figure 6.23a; that of the control mix of Phase 1 (mix C; 0.45 water/cement ratio) is also reported for comparison. It is immediately obvious that graphs relating to the Phase 2 mixes lay well below that of mix C. Such differences are thought to reflect not only the reduction in water/cement ratio, but also the relatively harsher preconditioning of mix C specimens (105 °C as against 50 °C and 11-14% RH), as well as the difference in the age of specimens at testing (28 days as against 90 days). Comparing the early absorption behaviour of C(0.4), C(0.35), and C(0.3)+, as shown more clearly in Figure 6.23b, reveals that initial absorption becomes increasingly characterized by a curve with an ever decreasing gradient, rather than a straight line (which is indicative of flow in relatively large and continuous capillaries (see 3.2.3.3)), which, presumably, reflects a process involving slow capillary-driven water absorption together with condensation of water vapour in the smaller pores; this trend clearly illustrates the effect of the reduction in water/cement ratio, and the associated decrease in pore continuity.

Sorptivity values for mixes C and C(0.4), calculated as described before (3.2.3.2), are of the order of 8.5 mm/h^{1/2} and 5.9 mm/h^{1/2}, respectively; these values are of the correct order of magnitude, considering similar results obtained for roughly comparable systems at IC (Denno 1992). It is worth mentioning at this point that sorptivity, as defined in Equations 3.7 and 3.8, would not reflect fully, nor accurately, the absorption behaviour in concretes which exhibit departure from the normal trend; therefore, to derive sorptivity values for these concretes would be misleading.

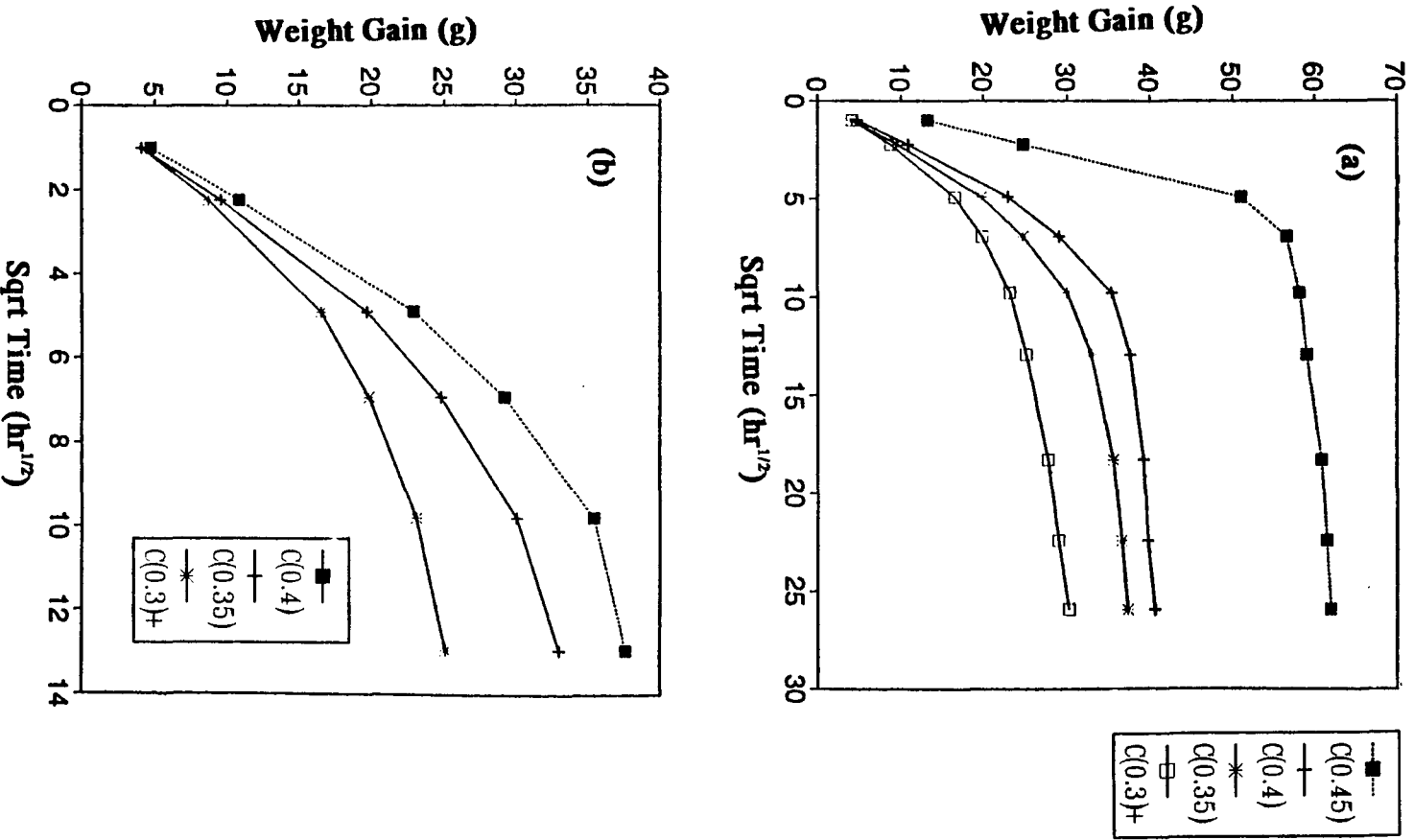
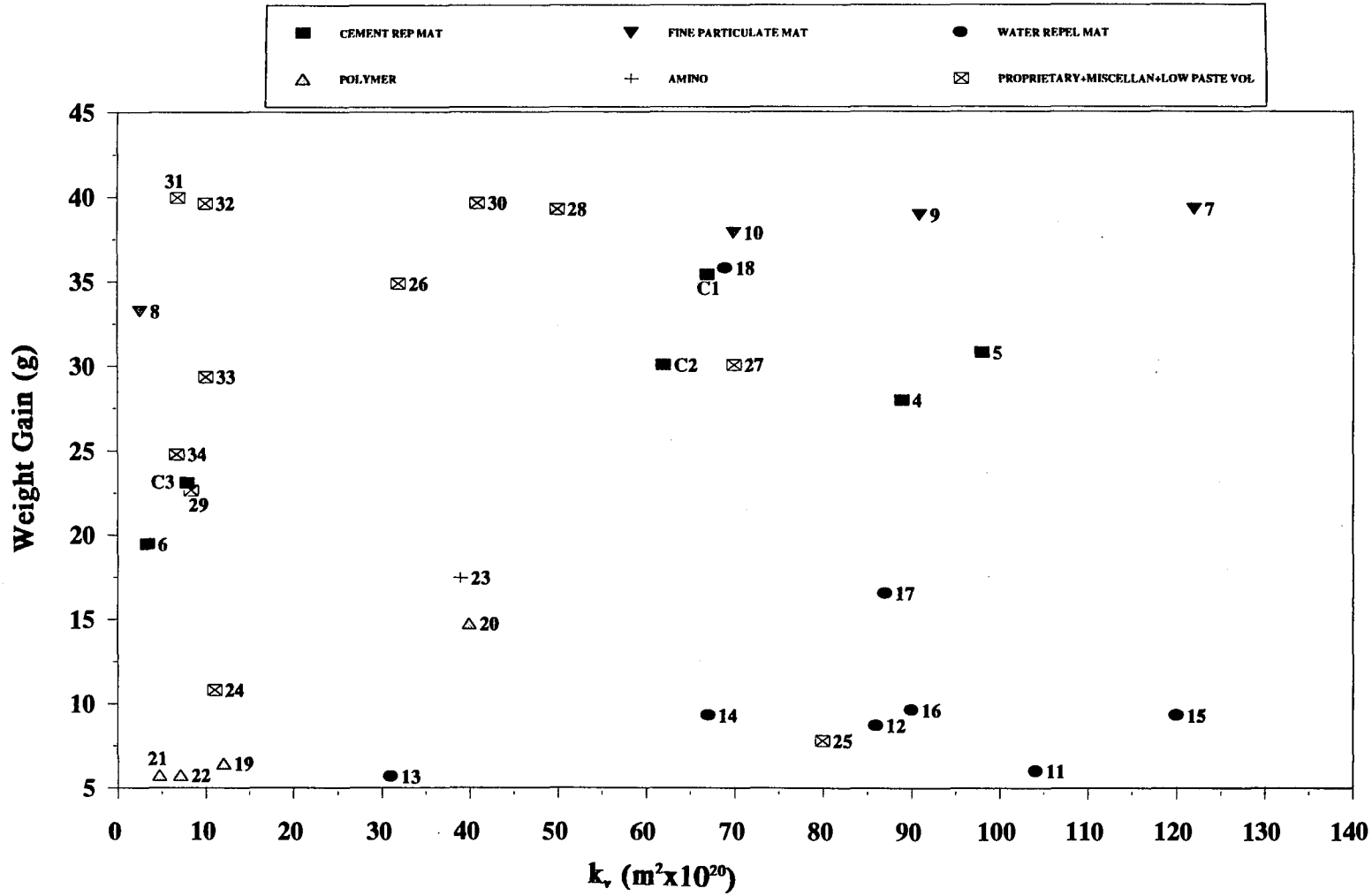


Figure 6.23 Absorption behaviour of control concretes.

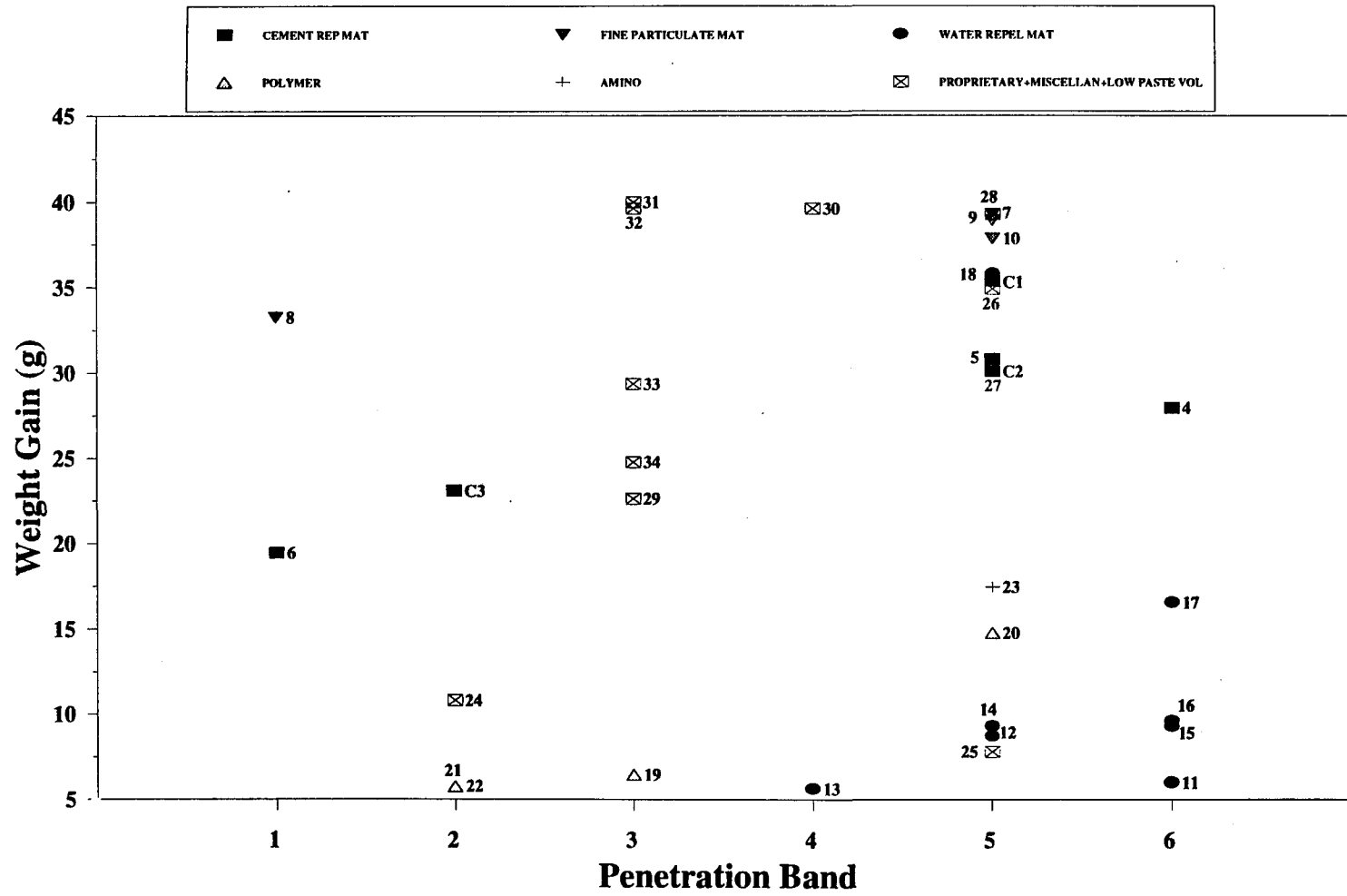
Overall, supposedly identical specimens were found to exhibit weight gain variations amounting to no more than 10%. As seen in Table 6.16, a wide range of modified concretes (e.g. mixes: 11 (MAGST2(0.35)+), 12 (ALST0.5(0.35)+), 15 (SOYO1(0.35)+), 22 (ACR10(0.3)+), etc.) have an absorption resistance much superior to that of the respective control. It may seem, at first sight, that the favourable performance is a manifestation of pore structure refinement and/or decreased pore connectivity. Figures 6.24, 6.25, and 6.26, however, strongly deprecate this proposition; a more comprehensive discussion will appear in 6.4.

Illustrated in Figure 6.27 is the absorption behaviour of Series C specimens (tested as-received) relating to the control concretes; the vertical lines indicate points of departure between the three modes of testing. It is immediately obvious that water uptake in the first stage of testing is extremely slow. This is believed to be principally due to the fact that specimens were tested as-received (sealed cured for 90 days), since residual moisture, which will be present in the capillary pores (Copeland & Brag 1955), will have the effect of not only reducing the pore space through which water absorption can take place, but also of reducing dramatically the capillary suction forces (3.2.3.3); naturally, these effects will become more pronounced as the test proceeds. Moreover, it is important to remember that capillary suction forces are not entirely responsible for water uptake since it is conceivable that a process involving water vapour diffusion/condensation may also have some contribution (5.3.4, (II)). Interestingly, Figure 6.27 reveals a rapid rise in the rate of water uptake upon the commencement of MAT, this being almost entirely due to water being drawn into specimens through the curved surface by virtue of capillary suction forces (curved surfaces were already exposed to near saturated air in the trays before MAT commenced). This observation is obviously of significance, for it reveals that a sizable portion (nearly 40%) of the effective (empty pore space) porosity in specimens remained empty despite the 7 days of capillary rise testing. It is therefore suggested that Series C results are of secondary importance, in so far as indicating capillary absorption resistance is concerned, to those obtained from Series B tests.



Relevant testing sequence
Series B (6.1.2.2)
• drying at 50°C & 11-14% RH (56 days)
• capillary rise (4 days)
Series F (6.1.2.2)
• water permeability testing on specimens with embedded electrodes (after 11 months sealed storage)

Figure 6.24 Weight gain for each mix after 4 days capillary rise testing versus corresponding water permeability coefficient.



Relevant testing sequence

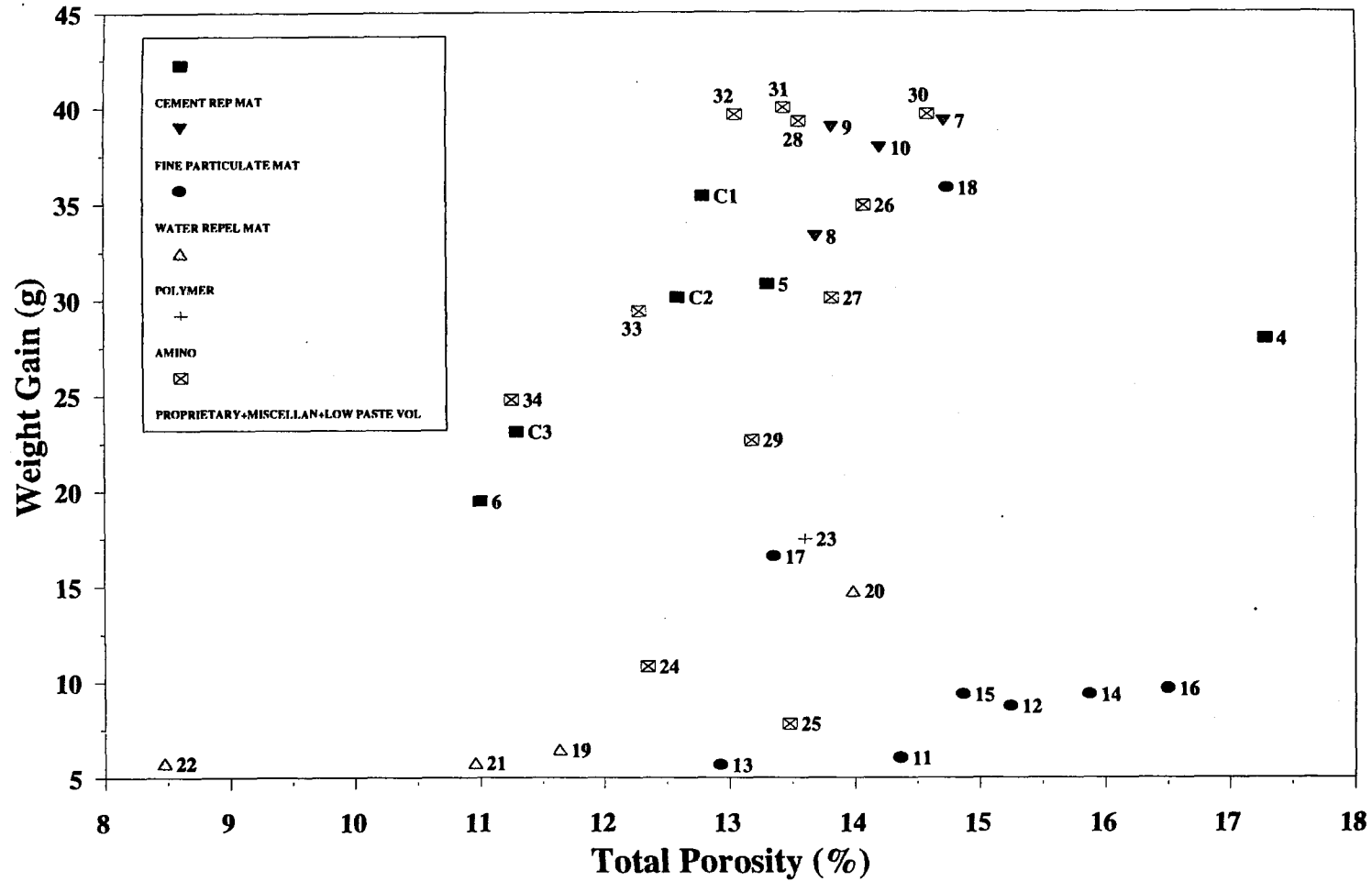
Series B (6.1.2.2)

- drying at 50°C & 11-14% RH (56 days)
- capillary rise (4 days)

Series F (6.1.2.2)

- water permeability testing on specimens with embedded electrodes (after 11 months sealed storage)

Figure 6.25 Weight gain for each mix after 4 days capillary rise testing versus corresponding water penetration Band.



Relevant testing sequence
Series B (6.1.2.2)
• drying at 50°C & 11-14% RH (56 days)
• capillary rise (4 days)
Series C (6.1.2.2)
• capillary rise (7 days)
• MAT (21 days)
• saturation
• oven drying to equilibrium at 105°C

Figure 6.26 Weight gain for each mix after 4 days capillary rise testing versus corresponding total porosity.

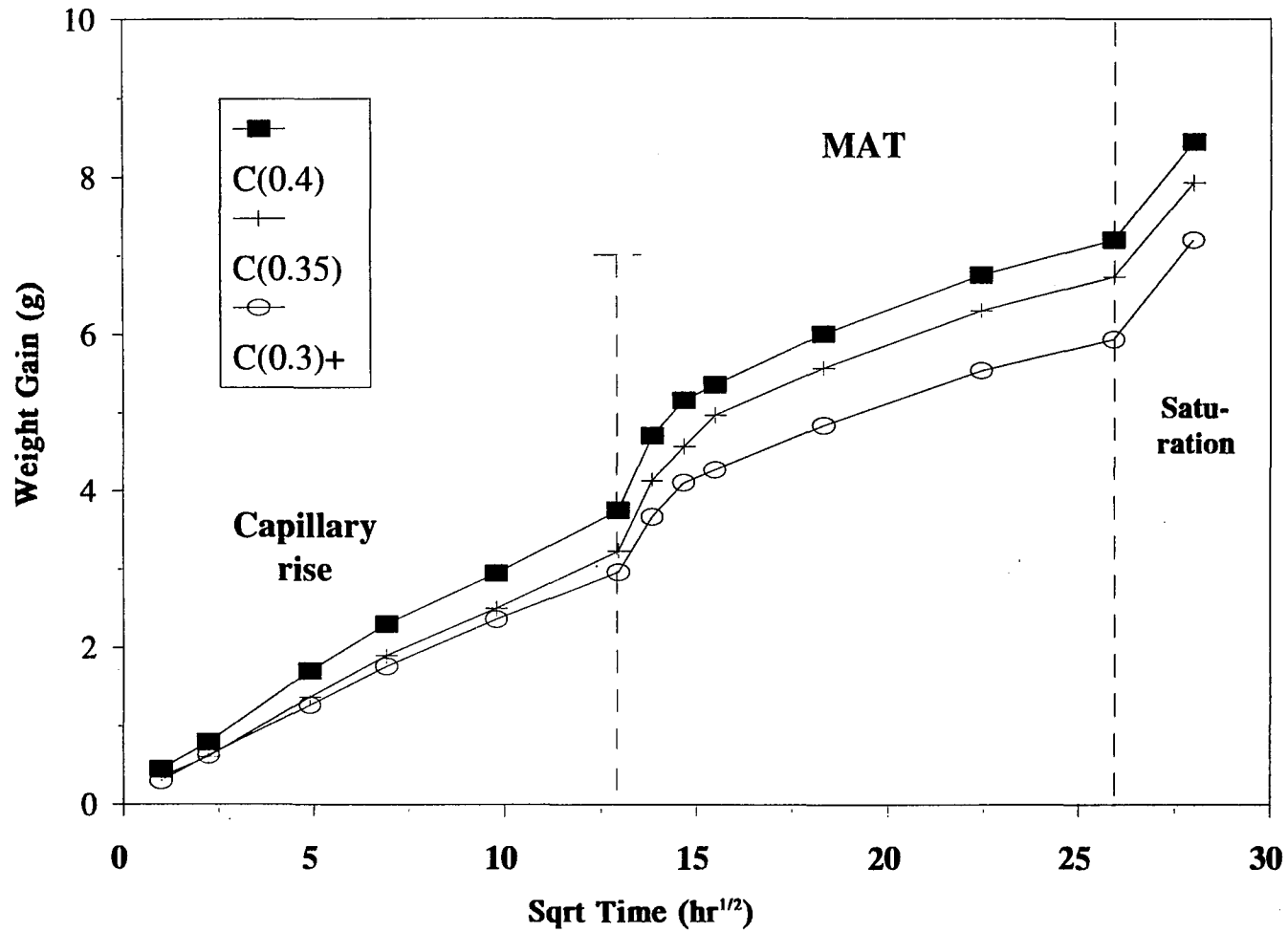


Figure 6.27 Water uptake of control concretes (Testing Series C).

Series C testing was performed on unconditioned specimens originally sealed for 90 days. The relatively short period allowed before testing may result in mixes which hydrate at different rates showing varying degrees of self desiccation, and a consequent variation in moisture state. Even for the same degree of hydration, variations in moisture state can arise from variations in the amount of water bound by the cement hydration products (g/g_{cement}). From the viewpoint of comparing absorption behaviour, and considering that absorption is sensitive to moisture state (3.2.3.3), this would clearly be disadvantageous. According to Taylor (1990), the amount of water lost on drying to equilibrium at 11% RH and ordinary temperature provides a good estimate of the amount of residual pore water. Figures 6.28a and b, and Figure 6.29 show that the majority of modified mixes exhibit either insignificant or marginal variations in the amount of residual moisture relative to the respective control mixes (note that with the exception of mixes 19 (EVA10(0.3)+), 21 (SBR10(0.3)+), and 22 (ACR10(0.3)+), all modified mixes correspond to C1 (C(0.4)) and C2 (C(0.35))), and, moreover, that these variations cannot possibly account for the wide variations in water absorption; see, for example, how mix 15 (SOYO1(0.35)+), which has an amount of residual moisture roughly comparable to that of the corresponding control C2 (C(0.35)), shows a pronounced reduction in water absorption during capillary rise and MAT testing (Figure 6.28), but an increase after specimens are subjected to saturation (Figure 6.29).

That the majority of mixes which exhibit a pronounced reduction in absorption during capillary rise and MAT testing (e.g. mixes: 11 (MAGST2(0.35)+), 15 (SOYO1(0.35)+), etc.) are found to take up much more water during vacuum saturation is shown more clearly in Figure 6.30. It would thus seem that a large proportion of the porosity of these mixes is inaccessible to water without the application of pressure. This can only be explained by the porosity being rendered water repellent by the inclusion of the admixture (see 5.3.4 and note that, because air detraining agents were used, mixes do not exhibit more than 1% increase in the volume of entrained air (Table 6.24)). In the case of mix 6 (SF10(0.4)+), the increase is likely to be due, at least partly, to vacuum saturation resulting in water filling entrained air voidage.

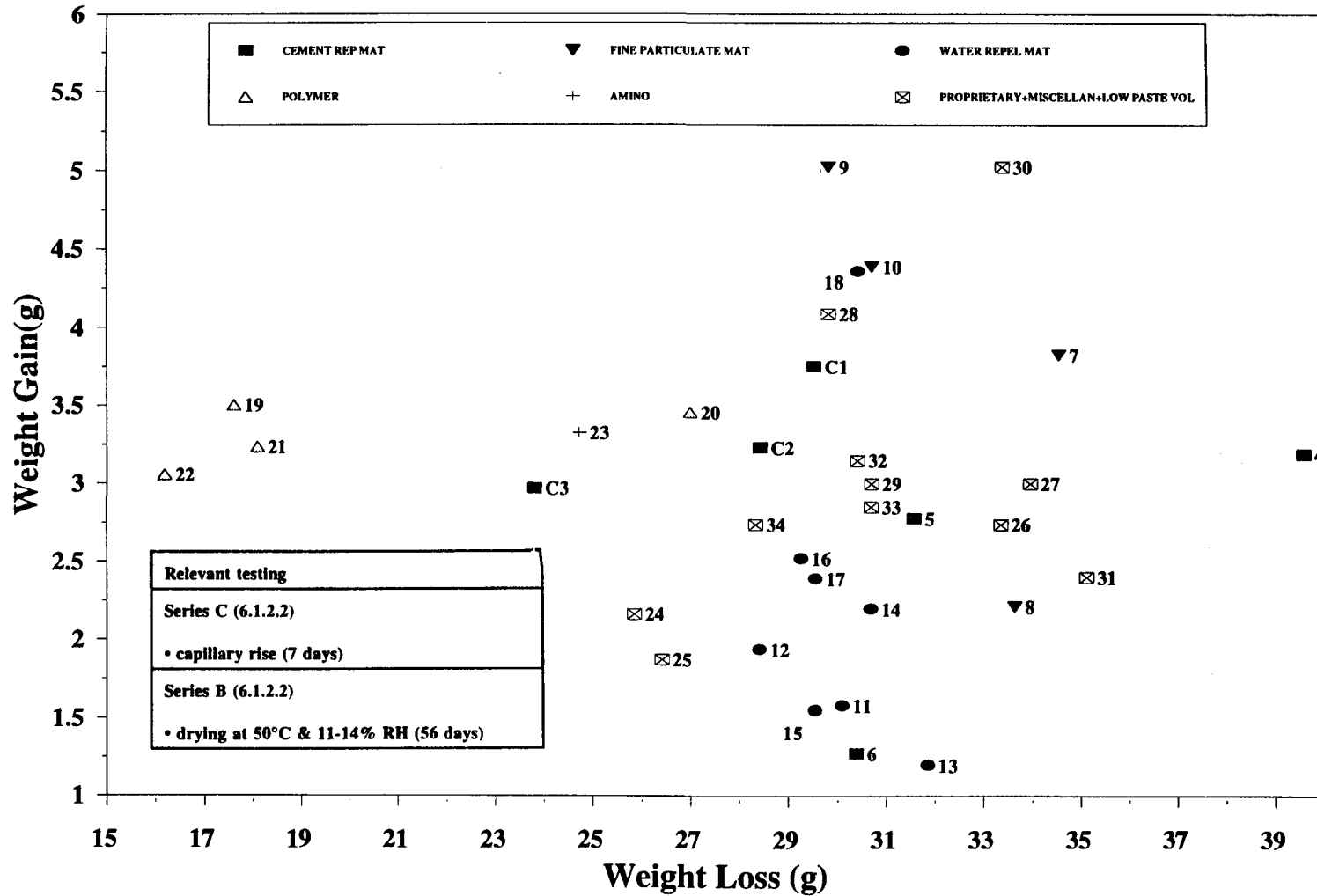


Figure 6.28a Weight gain for each mix after 7 days capillary rise testing on as-received specimens versus corresponding weight loss on drying at 50°C & 11-14% RH to equilibrium.

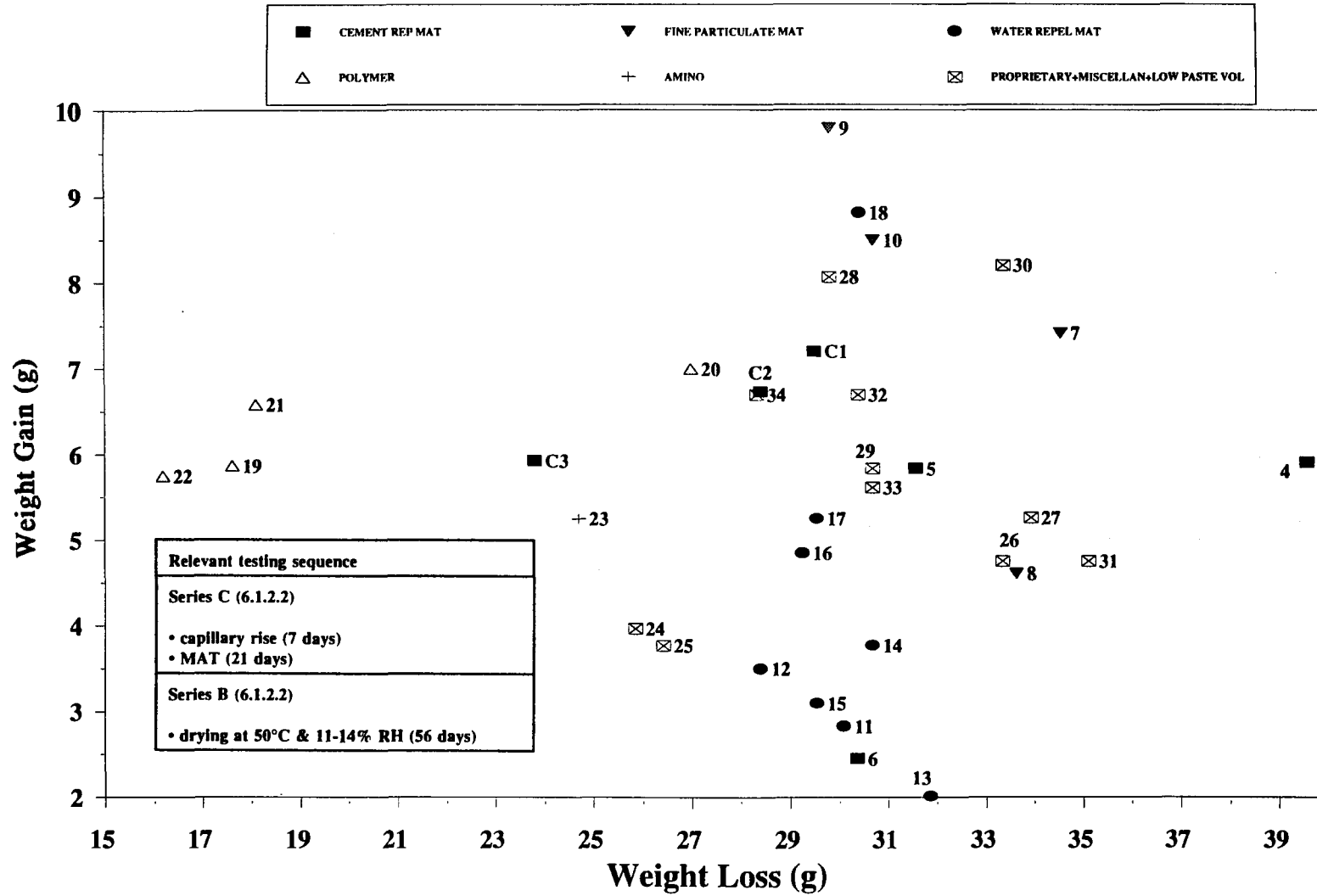
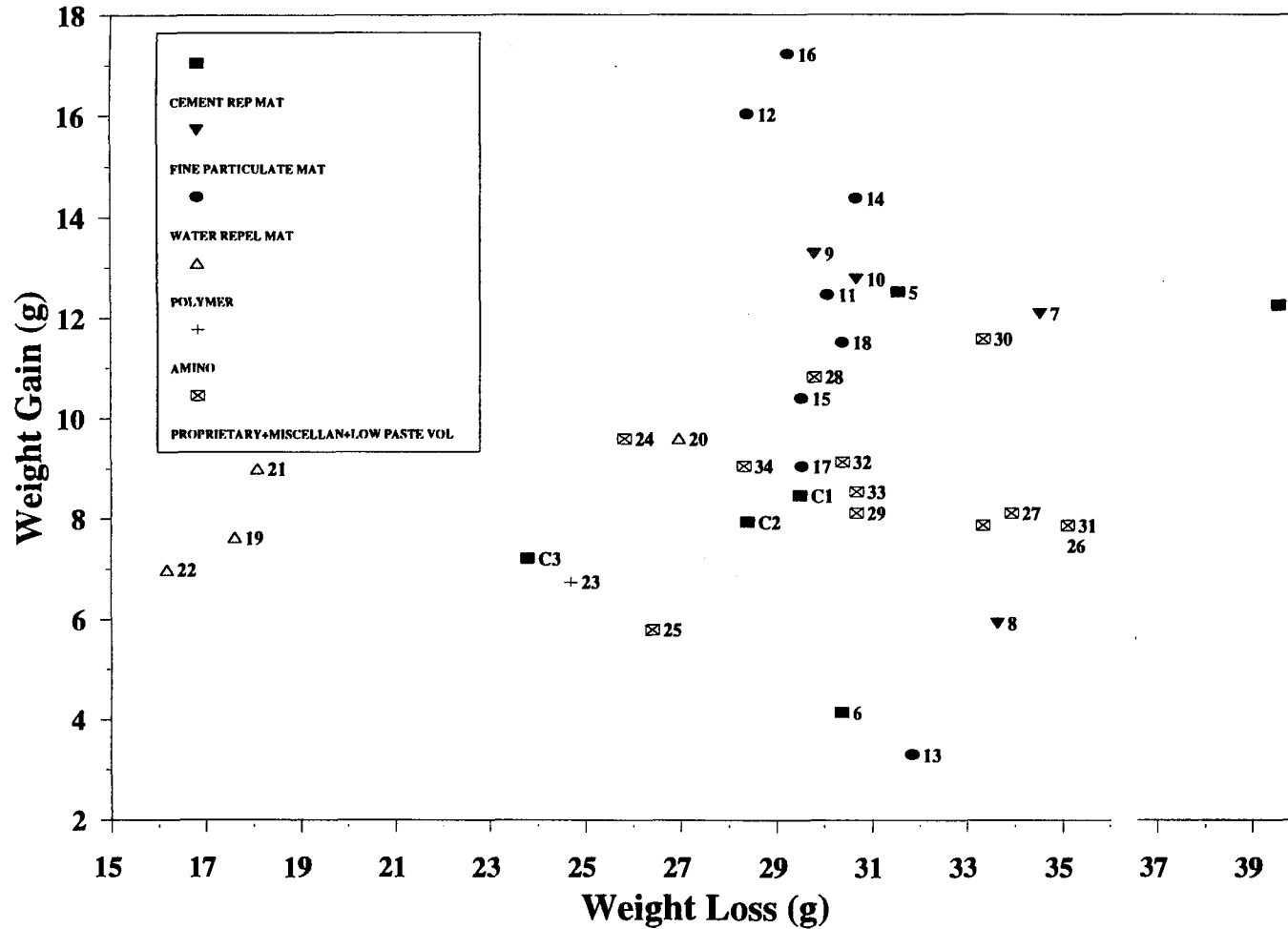


Figure 6.28b Weight gain for each mix after 28 days testing on as-received specimens (Series C) versus corresponding weight loss on drying to equilibrium at 50°C & 11-14% RH.



Relevant testing sequence
Series C (6.1.2.2)
• capillary rise (7 days)
• MAT (21 days)
• saturation
Series B (6.1.2.2)
• drying at 50°C & 11-14% RH (56 days)

Figure 6.29 Weight gain for each mix after specimens are subjected to saturation (Series C) versus corresponding weight loss on drying to equilibrium at 50°C & 11-14% RH.

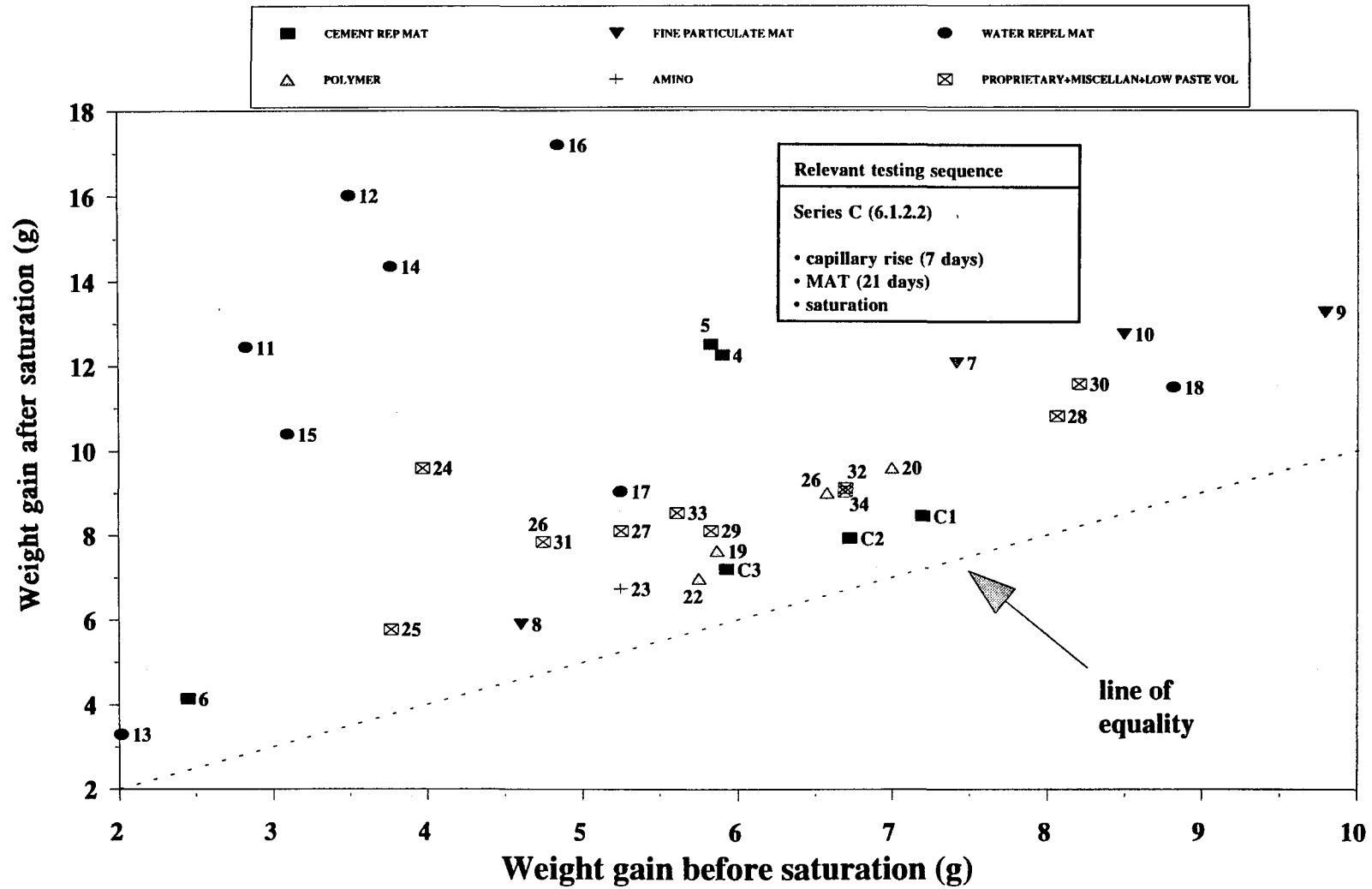


Figure 6.30 Weight gain for each mix after specimens are subjected to saturation versus corresponding result before saturation.

It may be recalled that testing on as-received specimens (Series C) was conducted in order to "get a feel" for any possible distorting effects on the results of Series B capillary rise testing associated with the relatively harsh (50°C & 11-14% RH) preconditioning of specimens (6.1.2.1.1, II). Figure 6.31 shows that the majority of mixes displayed broadly similar performance under both conditions, with the exception of a few mixes (e.g. mixes: 6 (SF10(0.4)+), 8 (BEN10(0.4)+), 26 (SIK9(0.4)), 21 (SBR10(0.3)+), 22 (ACR10(0.3)+), etc.). A more detailed discussion regarding the behaviour of these mixes will appear in 6.4.

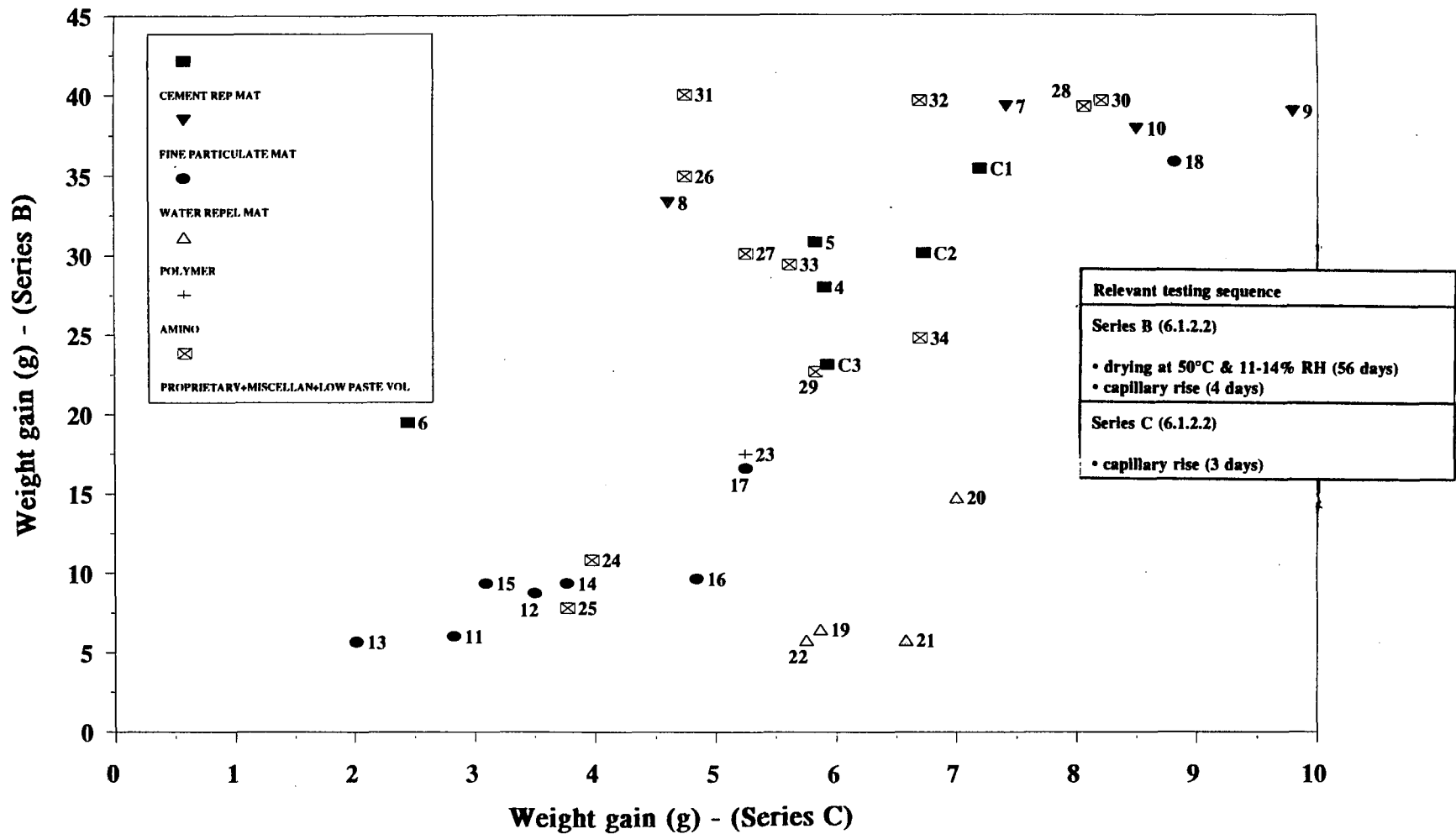


Figure 6.31 Weight gain for each mix after 4 days capillary rise testing (Series B) versus corresponding result after 3 days capillary rise testing on as-received specimens.

Drying

Tables 6.18 and 6.19 present the extent to which the rate of moisture loss from a modified concrete differs from that of the respective control under each of the drying conditions investigated. Drying tests may also be used to give a rapid, though approximate, indication of changes in the rate of water vapour diffusion in concrete, which is of relevance to water uptake (by virtue of water vapour diffusion and condensation) as well as water loss. Accordingly, based on the results of mild drying (see Table 6.18 and Figure 6.32), a range modified concretes (e.g. mixes: 8 (BEN10(0.4)+), 11 (MAGST2(0.35)+), 13 (BUTST3(0.4)), 14 (CAPA0.25(0.35)+), 18 (ASPH20(0.35)), 22 (ACR10(0.3)+), etc.) can be regarded as allowing much more rapid water vapour diffusion, in comparison with the corresponding control. When the severe drying results are examined (see Table 6.19 and Figure 6.32), however, such differences appear to be generally much less pronounced (e.g. mixes: 8 (BEN10(0.4)+), 11 (MAGST2(0.35)+), 13 (BUTST3(0.4)), 14 (CAPA0.25(0.35)+), etc.). It is suggested, therefore, that these observations lend support to the view (Glover & Raask 1972, see 3.2.2) that harsh drying alters the water vapour diffusion process in concrete, this being, primarily, because of increasing microcracking and pore collapse. It is also worth noting that several modified mixes (in particular mixes: 19 (EVA10(0.3)+), 21 (SBR10(0.3)+), 22 (ACR10(0.3)+)) show opposite trends in relation to the control (see 6.4 for possible explanation). Finally, it should be emphasised that vapour diffusion behaviour in concrete may well alter after chloride penetration (3.2.2), that is, the results are only applicable to the drying of concrete before exposure. Drying tests may yield more applicable information if performed on thin (say 10mm thick) mortar specimens after they have been equilibrated for relatively long periods (at least 6 months) in a suitable chloride solution.

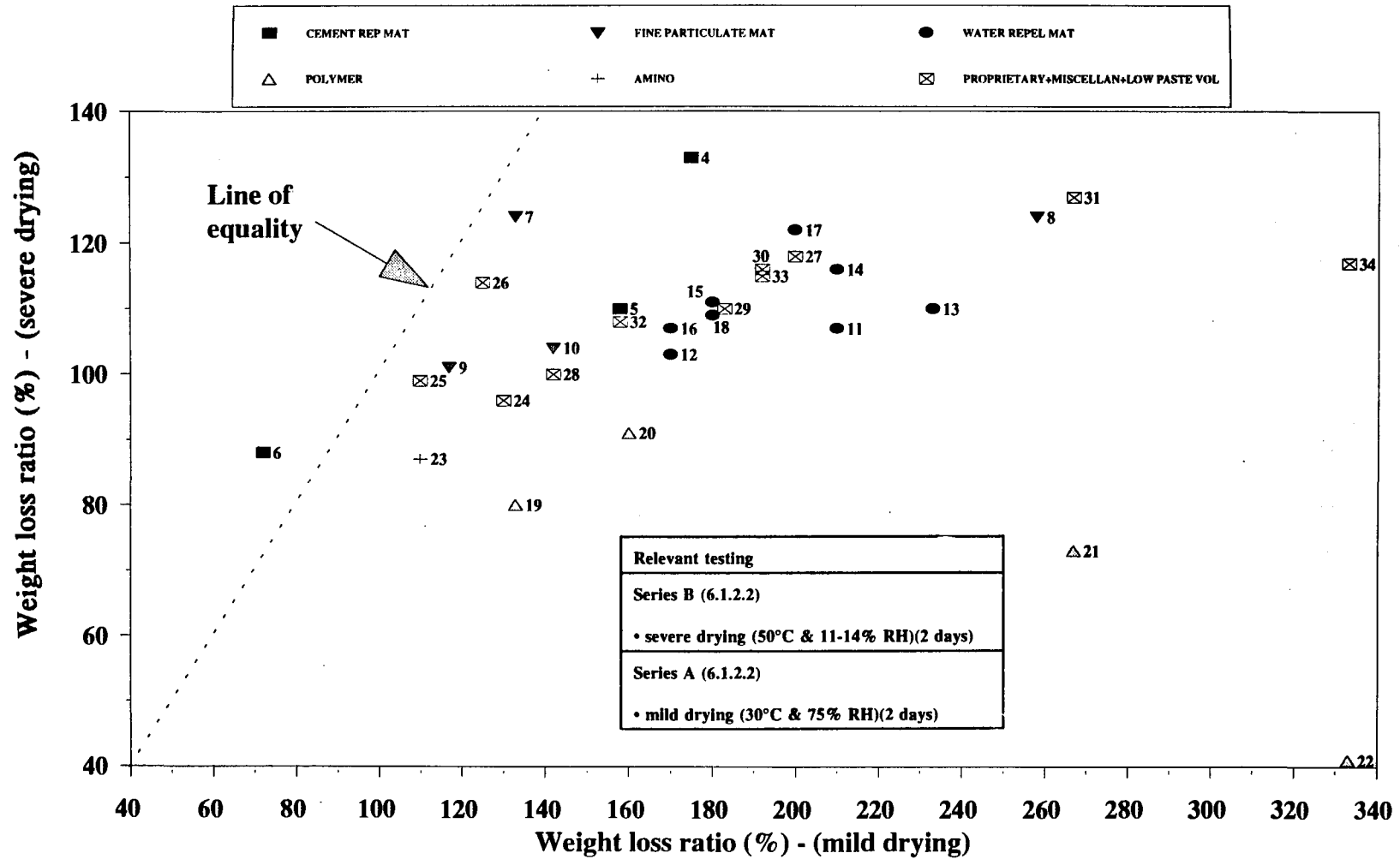


Figure 6.32 Weight loss ratio for each mix after 2 days severe drying versus corresponding result after 2 days mild drying.

Chloride diffusion

Clearly, proper assessment of the relative performance of the modified concretes should involve evaluating the test results with the object of determining the extent to which they can describe chloride ion diffusion in field concrete.

Before proceeding, it is necessary to explain the terms "relatively more/less penetrable/accessible porosity". In connection with chloride ion diffusion, these subjective terms should be understood, in the absence of a clear theory which describes ion diffusion in concrete, within the context of the general principles set out in section 3.6.2.

The chloride ion diffusion process in a conventional diffusion cell (diffusion driven by a concentration gradient) ideally follows the pattern shown in Figure 6.33, with the cumulative amount of chloride having passed through a unit area of the specimen plotted against the diffusion time; linear regression analysis of the linear part of the graph shown yields the two defining parameters, t_0 and r_0 . During the transient period, which is characterized by t_0 , chloride diffuses into the specimen filling accessible pores, the chloride concentrations in the solid and liquid come into equilibrium (probably by virtue of ion sorption onto hydrate surfaces and chloroaluminate formation, see 2.3.1.3), and a linear concentration gradient becomes established through the specimen. Once this is established, the concentration of chloride in the sink side of the cell begins to increase linearly with time, indicating steady-state diffusion, at a rate given by r_0 . As for the ACID test, El-Belbol (1991) found that chloride diffusion follows a form analogous to that of the diffusion cell (see Figure 6.34), and expressed the test results in terms of two defining parameters T_0 and g , which parallel, respectively, t_0 and r_0 . El-Belbol also found that T_0 and g correlate linearly with t_0 and r_0 , respectively, and concluded that the ionic transport in the ACID test is representative of ionic diffusion under a concentration gradient.

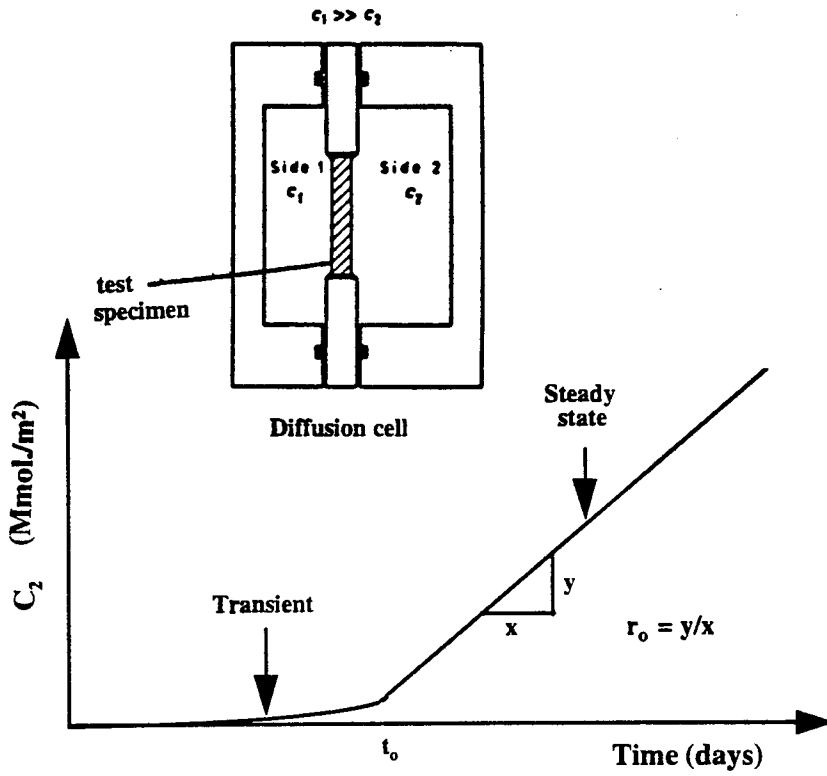


Figure 6.33 Chloride diffusion pattern (diffusion cell).

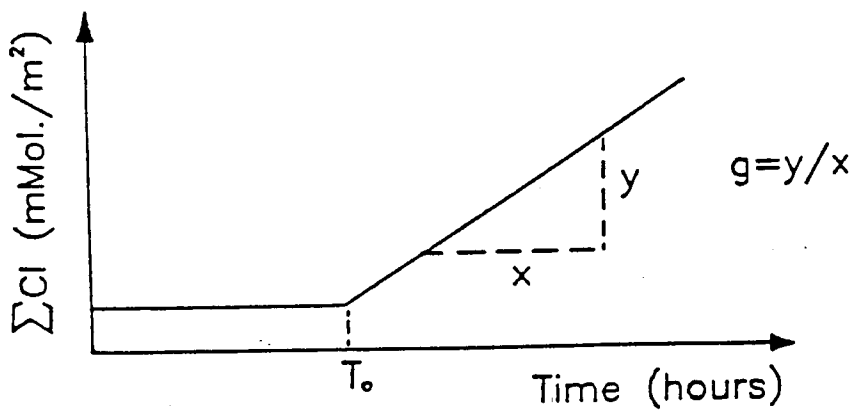


Figure 6.34 Presentation of results (ACID test).

Being a measure of processes involved in the transient stage, it may appear prudent, at first sight, to regard t_0 as providing a rapid means of measuring the non-steady state diffusion of chloride as it would occur in saturated concrete in the field (the effect of differences in the composition of the chloride solution being excluded). Experimental evidence, however, strongly deprecates this approach. For it has been observed (Atkinson and Nickerson 1988) that in a diffusion cell ions (I^- , Cs^+ , and Sr^{2+} were studied) will tend to become sorbed (onto hydrate surfaces) to a much lesser extent than when parallel specimens are immersed for the same duration in an identical solution (i.e. in diffusion profile experiments). This behaviour may be due to variations in pore solution composition between the relatively penetrable and less penetrable porosity. Another reason may be that in the diffusion cell a concentration gradient becomes established relatively quickly through the thin specimen (usually) used, interrupting the binding of ions within the relatively less penetrable fraction of porosity, for the ions would then tend to simply by-pass the less accessible porosity (3.6.2). Accordingly, it is anticipated that the aforementioned effects will be more pronounced in an ACID cell, since steady-state chloride diffusion becomes established at a much faster rate than in a diffusion cell (T_0 is much smaller than t_0).

Based on the foregoing, the parameter r_0 , hence g probably, may be considered to be, in the main, indicative of the rate of diffusion of chloride through the relatively more accessible fraction of porosity in the test specimen. It was mentioned before (3.6.2) that this form of diffusion may also be responsible for the deep penetrating part of the diffusion profile. This being the case, the performance of the modified mixes, in relation to the respective control, should display consistent trends when evaluation is carried out according to g values on the one hand and on the basis of the deep penetrating part of diffusion profiles, on the other. Examination of relevant data (Table 6.20, g versus the chloride concentration relating to the last two depth bands) reveals this to be generally the case (see also Figure 6.35), though, admittedly, a range of mixes (e.g. mixes: 19 (EVA10(0.3)+), 23 (AMINO22(0.35)), 29 (CEL2(0.4)), 34 (LPV245(0.4)+)) show no clear conformity. It should be emphasised at this point that such discrepancy is not particularly surprising because the diffusion process is far more

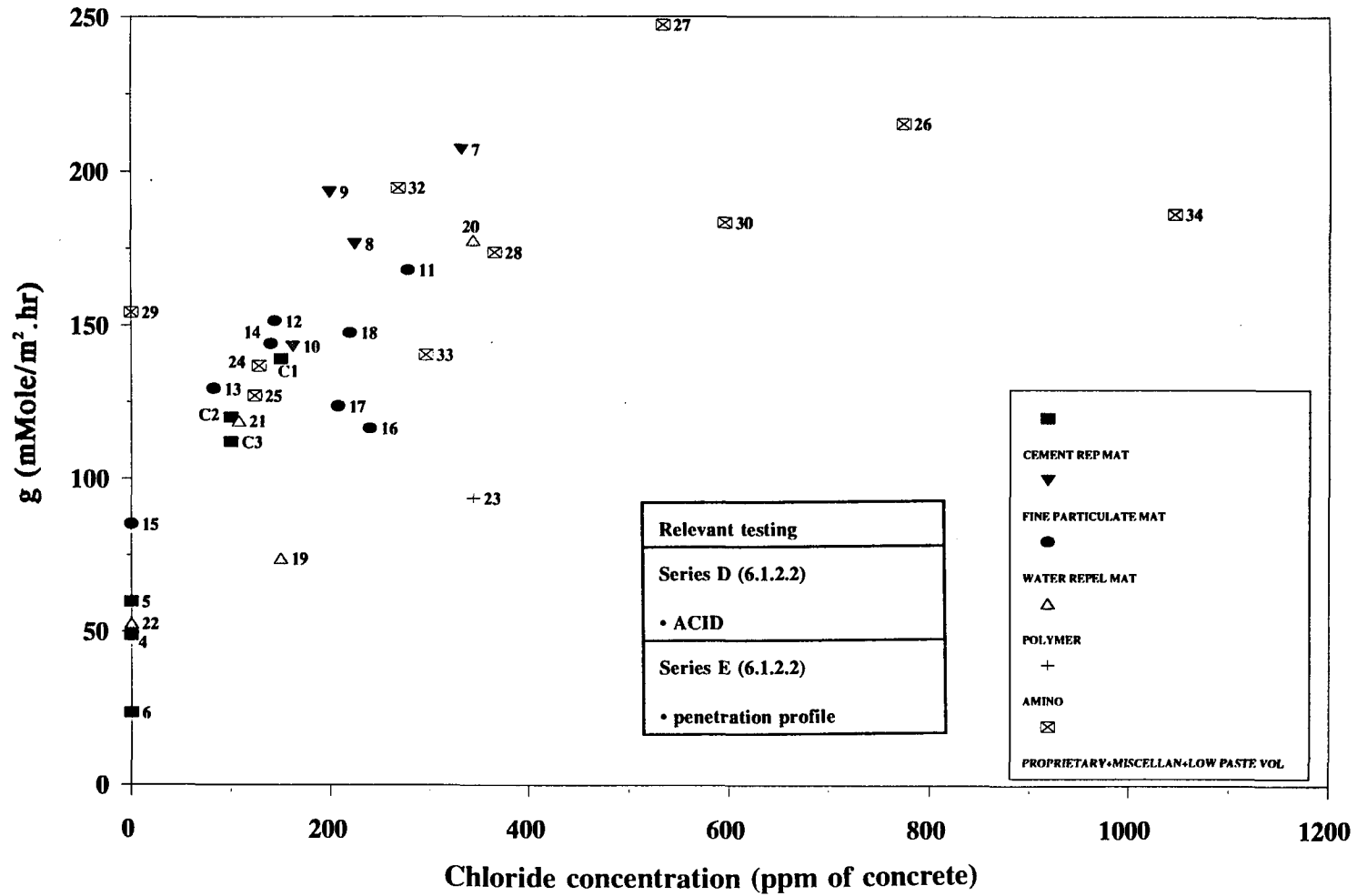


Figure 6.35 The defining parameter g for each mix versus corresponding chloride concentration in the 22 to 24 mm depth interval.

complex than the hypotheses above would tend to imply.

Moreover, it should be noted that the analysis does not take account of long-term effects (in specimens subjected to penetration profile testing), such as pore structure development with continued hydration, leaching (see 6.4), etc..

Figure 6.36 reveals that the parameters g and T_0 are, in general, inversely related. This is to be expected. It would therefore appear anomalous that T_0 may vary (see mixes 11 (MAGST2(0.35)+) and 19 (EVA10(0.3)+)) over a fairly wide range for the same g , and vice versa (see mixes 25 (CONP3(0.35)) and C3 (C(0.3)+)). Indeed, as Figure 6.37 shows, several mixes would be seen, on the basis of R_g (ratio of g for mix relative to that of respective control), to perform better than their respective control mixes (mixes: 19 (EVA10(0.3)+), 23 (AMINO22(0.35))), or similar (mixes: 10 (IRO2(0.4)), 17 (TAR25(0.35)+), 25 (CONP3(0.35))), but appear to perform unfavourably when comparison is made on the basis of RT_0 . The foregoing may be explained by postulating that areas of relatively high and low porosity are present in the test specimen, for it is perfectly conceivable that areas of high porosity would allow the passage of sufficient chloride through the specimen, thereby reducing the time (T_0) before chlorides are first detected in the sink side of the cell. As for g , since this value represents the average diffusion rate over the entire area of the specimen, the effect of the porous areas would certainly be less pronounced, to an extent governed by the proportion of the high porosity areas in relation to the entire penetrable porosity in the paste.

Finally, it is interesting, but not surprising (see 3.6), to observe that diffusion and permeability are poorly correlated (see Figure 6.38).

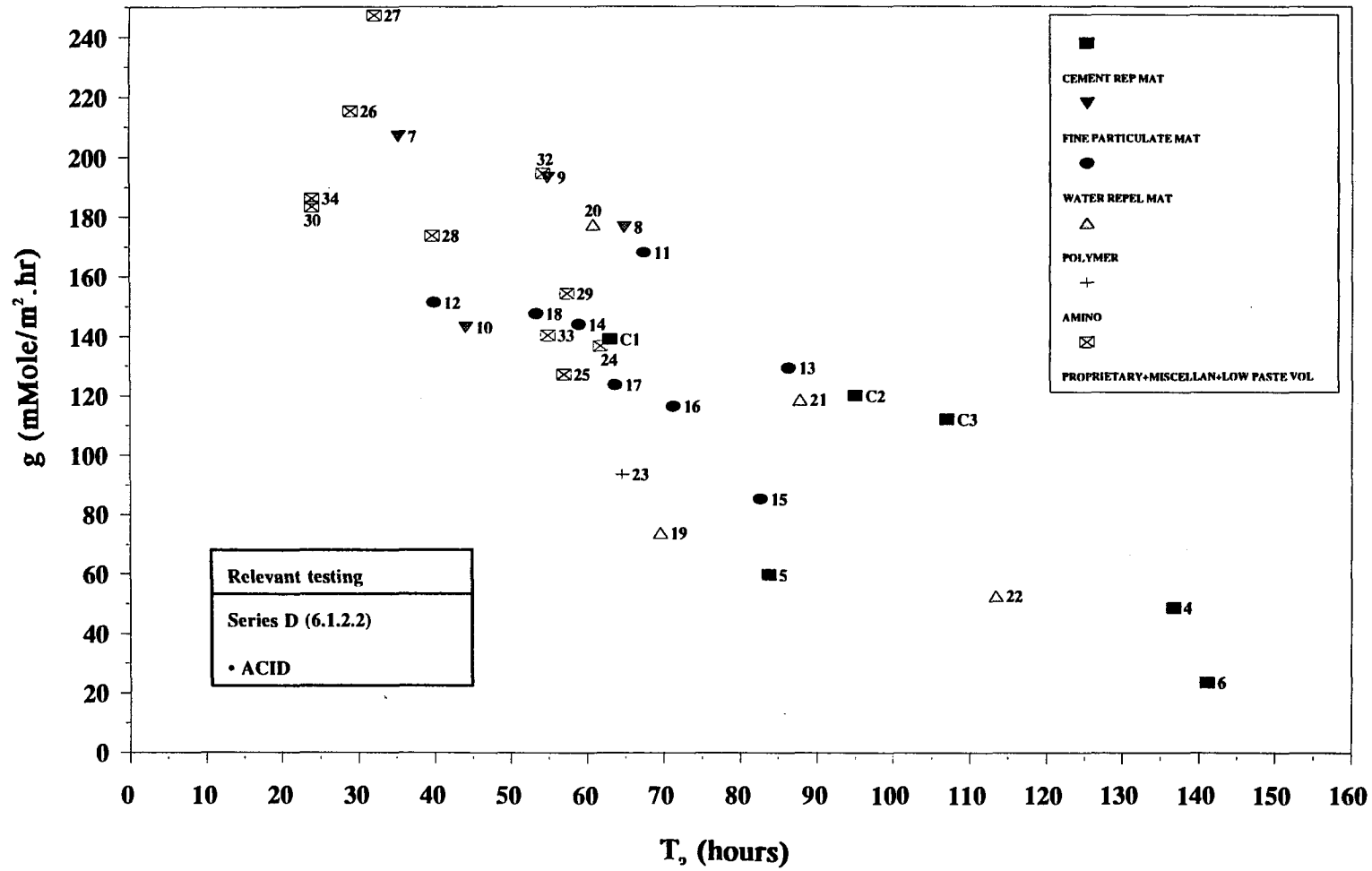


Figure 6.36 The defining parameter g for each mix versus the corresponding parameter T_0 .

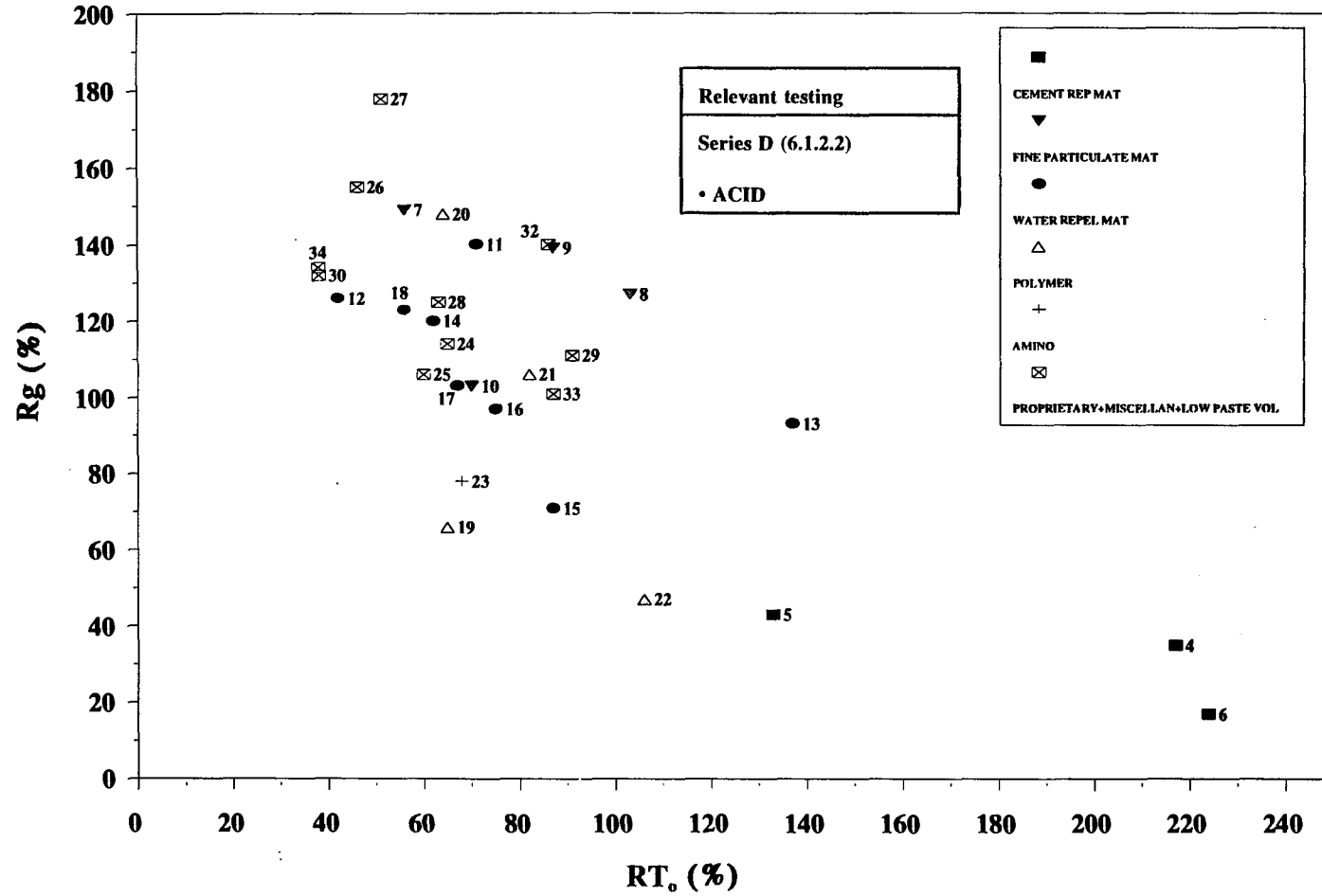
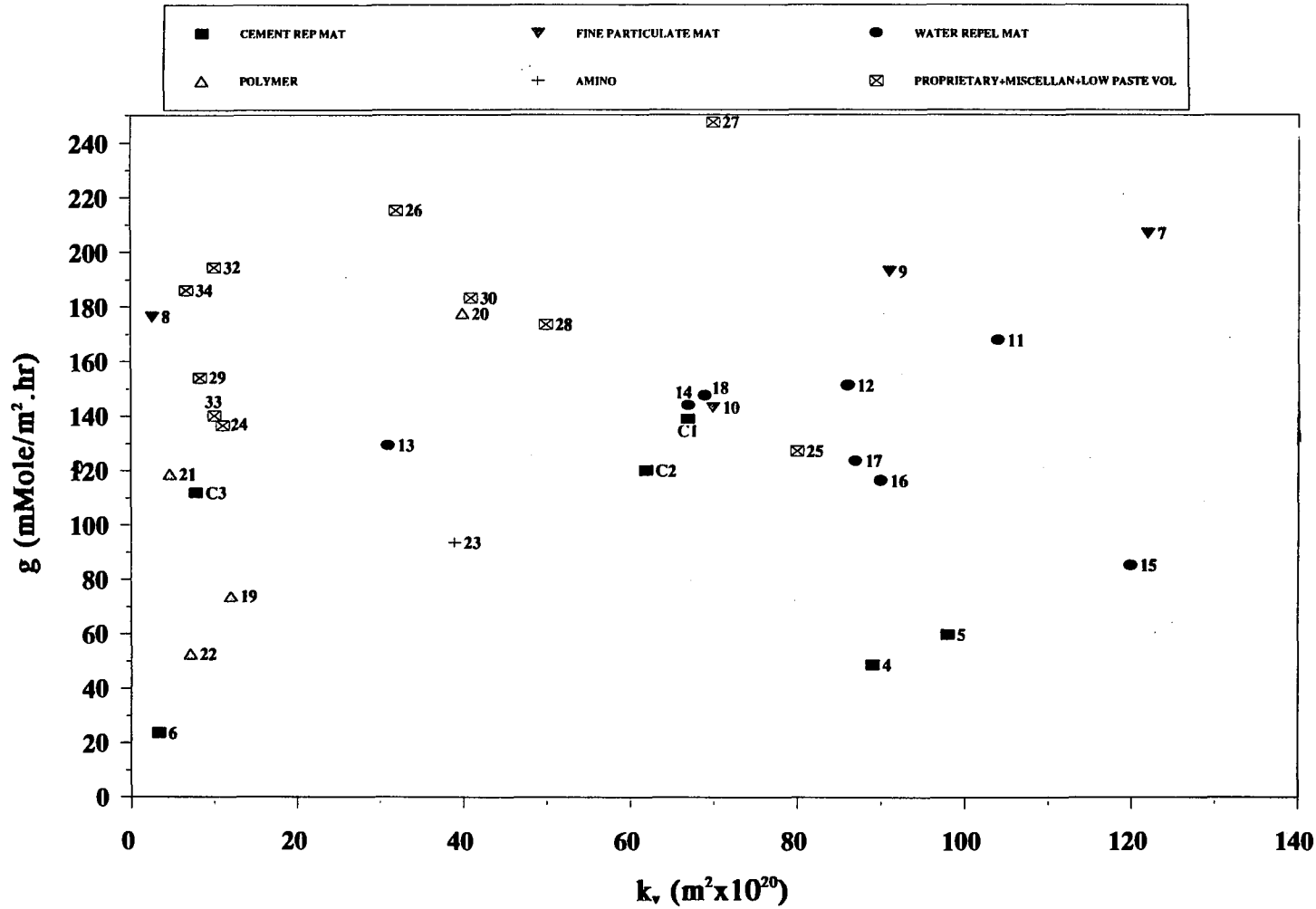


Figure 6.37 The ratio R_g for each mix versus the corresponding ratio RT₀.



Relevant testing
Series D (6.1.2.2)
• ACID
Series F (6.1.2.2)
• water permeability testing on specimens with embedded electrodes (after 11 months sealed storage)

Figure 6.38 The defining parameter g for each mix versus the corresponding water permeability coefficient.

6.3.3 Properties relevant to reinforcement corrosion

Electrical resistance

The variation of measured resistance with age in the control concrete specimens is shown in Figure 6.39. The graphs shown follow predictable trends. Initially (approximately up to the age of 60 days), the increase in resistance is gradual and reflects the reduction in pore space and continuity (2.2.2). At later ages, continued hydration leads to self-desiccation and the increase in resistivity becomes more rapid; broadly similar trends are also found to manifest in all but three (mixes: 4 (GGBS65(0.4)), 5 (PFA30(0.4)), 6 (SF10(0.4)+)) of the modified concretes.

Variations in resistance measured at any one time were observed to range between 5% and 10%; it is likely, therefore, that RR values roughly in the range 75% to 125% indicate merely marginal variations from the respective control.

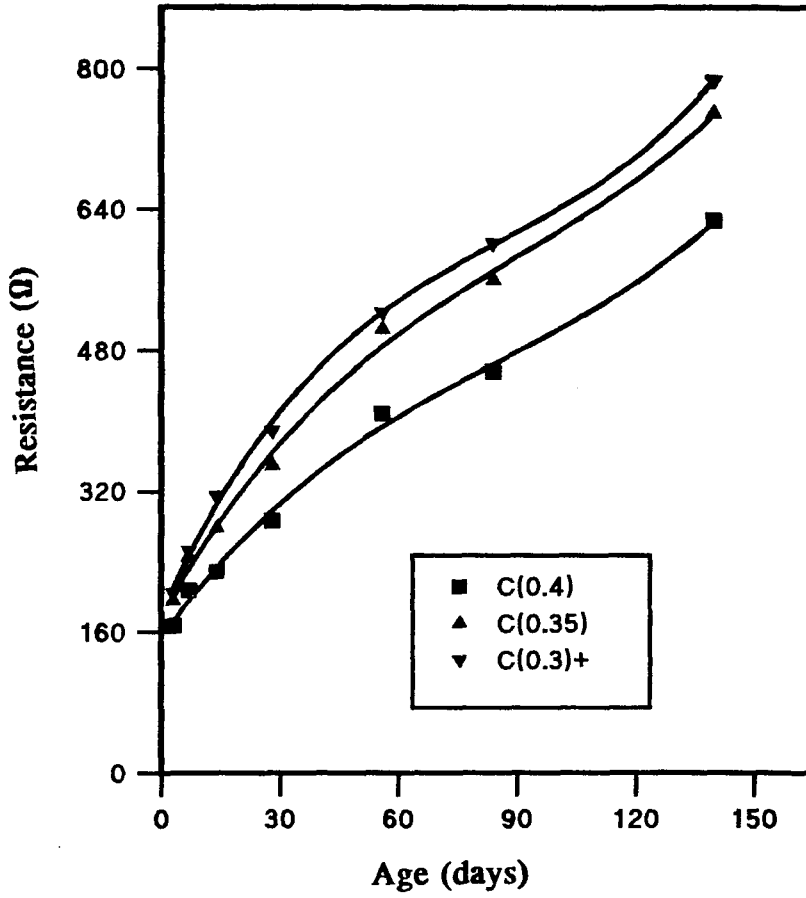


Figure 6.39 Variation in electrical resistance with age (control concretes)

Carbonation

In their present form, accelerated carbonation test results bear little significance to the carbonation of concrete in the field. Fortunately, it is possible to calibrate such results since researchers have found a broad correlation between carbonation depths obtained from accelerated carbonation tests and those obtained after exposure to normal levels of carbon dioxide (all tests carried out at similar relative humidity levels). For instance, Dhir et al. (1989) proposed, on the basis of their studies and those of others, that 1 week of exposure under a typical accelerated test (4% CO₂; 50% RH; 20°C) provides a depth of carbonation approximately equivalent to that produced by 15 months of normal protected (from rain) exposure. Based on these figures, the data displayed in Table 6.22 can be considered to correspond to a period of protected field exposure roughly in the range 20 to 30 years. The resistance of all carbonated cubes (Table 6.22) was extremely high, primarily due to drying, though also attributable in part to carbonation of the pore solution constituents (in both the carbonated and carbonating zones). Hence, even when carbonation advances at the rate detected, eventually causing depassivation, the propagation of reinforcement corrosion will proceed at a negligible rate (2.2.3, see also Figure 2.5). Obviously, had the carbonation test been carried out in an environment of higher relative humidity, resistivity would have been reduced, but the rate of carbonation would also have been greatly depressed.

The foregoing warrants the conclusion that, for the majority of structures in chloride-rich environments where carbonation is relevant (see 2.4), the increase in carbonation rate of the order exhibited by some of the modified mixes is unlikely to be a problem in so far as carbonation-induced corrosion is concerned if adequate cover is provided.

The phenolphthalein indicator method was employed because it is well documented, convenient to use, and gives reproducible results. It is, however, important to point out one of its most serious shortcomings. Whilst a reduction in pH to about 11 may be sufficient to initiate corrosion, phenolphthalein indicates a pH of about 9, which does not necessarily correspond to either the boundary between uncarbonated and partially

carbonated concrete, or the boundary between partially carbonated and fully carbonated concrete (Parrott 1987). Therefore, corrosion can occur in the region classified as uncarbonated by a phenolphthalein indicator. Indeed, it is this discrepancy which explains cases of gradual corrosion occurring despite the detected phenolphthalein front being at about 20mm away from the reinforcing steel, followed by pitting when the detected front advanced merely a further 12mm (Parrott 1987). It is also worth remembering that concrete cast in situ would inevitably be of inferior quality to equivalent laboratory-made concrete. It may thus be argued that the mixes which exhibited the highest increases in carbonation rate (mixes: 4 (GGBS65(0.4)), 5 (PFA30(0.4)), 34 (LPV245(0.4)+)) may not provide reinforcement in sheltered structural elements with adequate protection against carbonation-induced corrosion when a fairly long service life is required (bridges are normally designed for a service life of 120 years (8.1)).

Corrosion protection

Examination of the corroded coupons revealed a roughly common corrosion pattern (see Figure 6.40), and it seemed as though corrosion had initially originated at the contact area with the perspex plate, then spread upwards. This pattern is not surprising, however, for it is conceivable that part of the embedded steel coupon (approximately 10% by area), which is not embedded in concrete (coupons were fitted directly onto the perspex plate), would begin, upon exposure to chloride, to corrode rapidly forming an anode, and forcing the remainder of the coupon to act as the cathode of a macro-corrosion cell.

When corrosion levels are examined along with the corresponding chloride contents (see Table 6.23 and Figure 6.41), no clear correlation appears: the two supposedly identical coupon faces (A and B) appear in some cases (e.g. in mixes: CR3, CR5, CR7, etc.) to have suffered distinctly different degrees of corrosion even at nearly similar chloride levels, and in other cases (e.g. in mixes: CRC, CR10, etc.) essentially equal corrosion levels manifest despite marked differences in chloride levels. It is recognised, of course, that visual comparison provides a rather crude measure of corrosion, PACOR (percentage area corroded of coupon) reflecting primarily the resistance afforded by the concrete to the spread of corrosion on a coupon. Moreover, in light of the forgoing, the chloride content data reported in Table 6.23 cannot be expected to show good correlation with corresponding PACOR, since they merely represent average chloride levels obtained over the whole area of the coupons, rather than differential chloride levels (obtained by determining the chloride level at the corroded and uncorroded areas separately). It also important to remember that variations in PACOR of up to 40%, due to natural variability within the same specimen, would not be considered unusual.

Admittedly, the aforementioned should seriously deprecate the results displayed in Table 6.23. The test results, nonetheless, are considered adequate in the context of the objective sought (6.1.2.1.2, (III)), warranting the following conclusions: i) compared to the control concrete, several modified concretes (CR1 (PFA at 30%), CR2 (SF at

10%), CR12 (EVA at 10%), CR13 (SBR at 10%), CR14 (acrylic at 10%), CR15 (dimethyl ethanolamine at 2%)) are likely to offer distinctly better protection against corrosion of embedded reinforcement, ii) no evidence is found that any admixture would, due perhaps to its chemical or physical nature, adversely affect the protection afforded by OPC concrete against reinforcement corrosion.

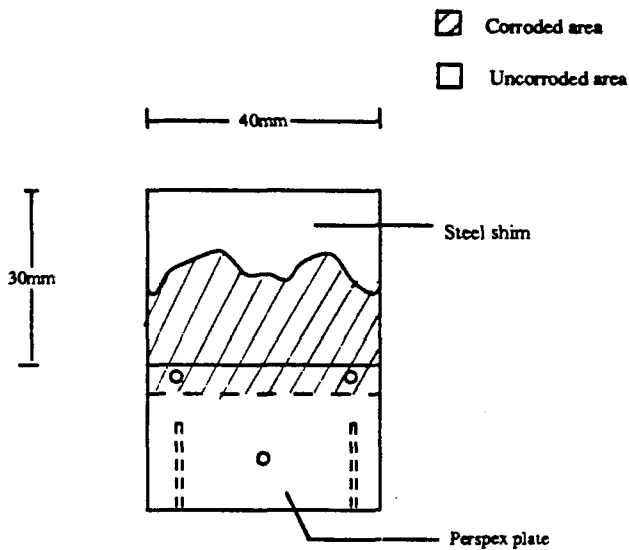


Figure 6.40 Typical corrosion pattern of coupons.

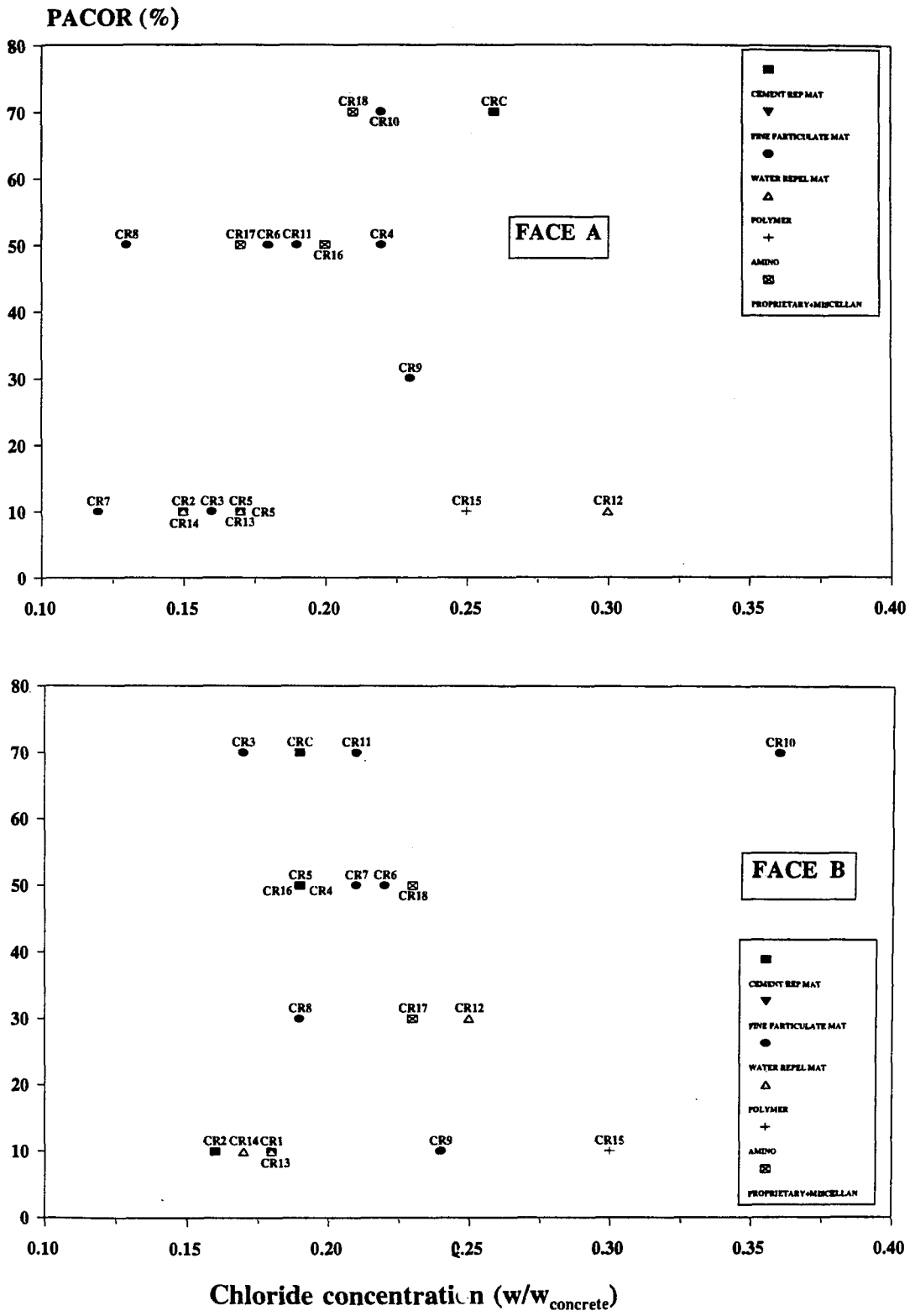


Figure 6.41 Percentage area corroded for each mix versus corresponding chloride concentration.

6.3.4 Compressive strength and early-age hydration rate

Calorimetric output in the control paste is depicted in Figure 6.42. The graph shown apparently follows predictable trends (see Appendix 4), showing an exotherm within the first 10 minutes of hydration, followed by an induction period, then an acceleration stage, which reaches a maximum (Q_{\max}) after about 11 hours (t_{\max}) and decreases slowly thereafter. Although admixtures can affect the curve in various ways, it is a fairly common observation that admixtures which accelerate hydration shorten the induction period, and produce an earlier heat peak (i.e. reduces t_{\max}), with a corresponding increase in Q_{\max} ; retarding admixtures, on the other hand, are usually observed to have the reverse effect (see Figure 6.43). Accordingly, it was felt that it would be adequate, in the context of this study, to assess admixtures on the basis of the extent to which they effect Q_{\max} and t_{\max} , in relation to the control paste. This is illustrated, based on the method proposed by Wilding et al. (1984), in Figures 6.4a and b. In the figures, the abscissa present Q_{\max} and $1/t_{\max}$ as percentage ratios (for a modified paste) relative to the control paste. The solid lines, naturally, relate to the control paste; dashed lines are also plotted to indicate the range of significance of results. This method of presentation was adopted as it has the clear merit of being convenient yet informative, classifying admixtures along a diagonal relationship according to their accelerating (top right) or retarding (bottom left) capacity. Most of the materials tested (GGBS, PFA, iron powder, butyl stearate, soyabean oil, SBR, acrylic, dimethyl ethanolamine) appear to have a retarding effect on OPC hydration, with acrylic and dimethyl ethanolamine having the most dramatic effect. The mechanisms which may be responsible for retardation are discussed in Appendix 4.

Supposedly identical cubes were found to exhibit about 7.5% variations in compressive strength, on average; therefore, SR values (Table 6.24) ranging between around 85% and 115% can be considered to indicate insignificant, or small, variations from the respective control.

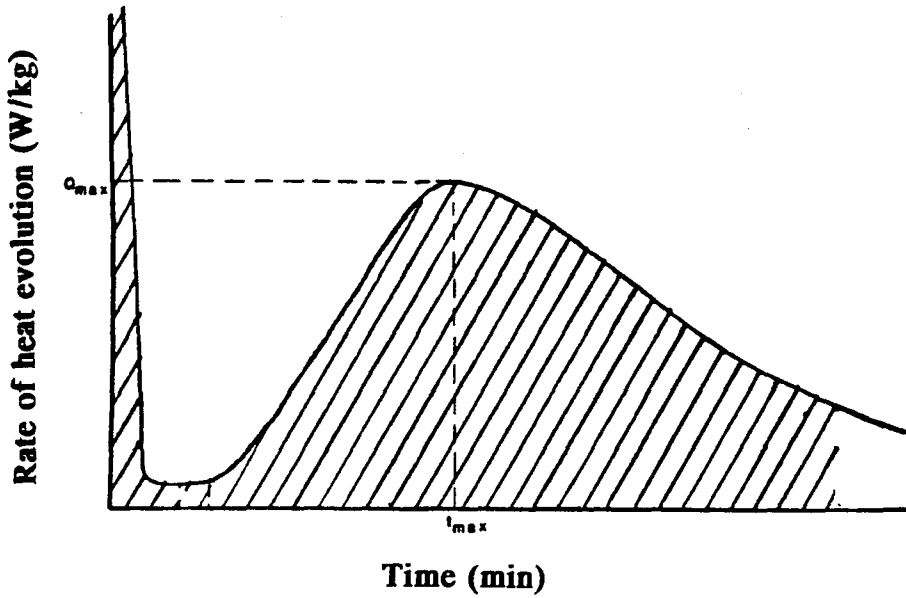


Figure 6.42 Schematic representation of calorimetric output in control paste.

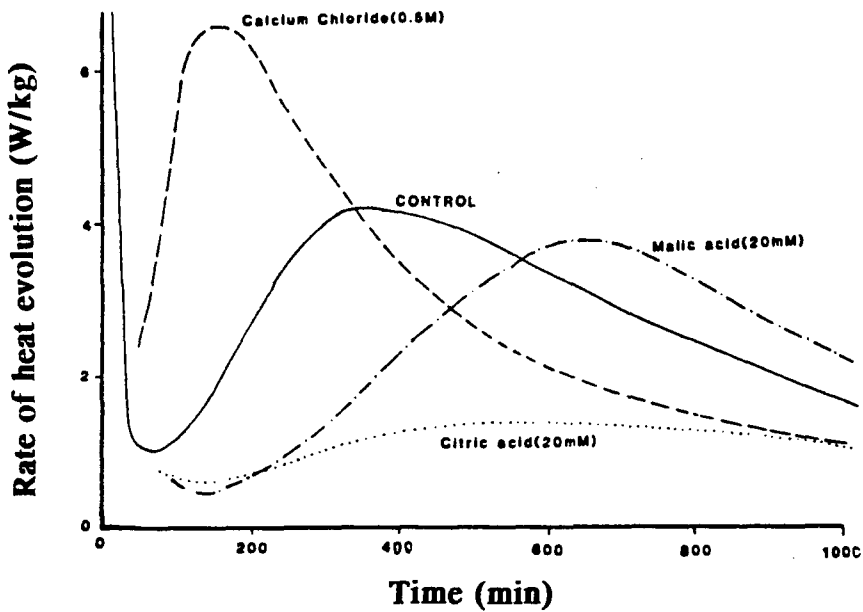


Figure 4.43 Effect of accelerating and retarding agents on the calorimetric output of OPC paste (Wilding et al. 1984).

The pattern of strength development with age for the control concretes, depicted (roughly) in Figure 6.44, is apparently characteristic of medium-strength and high-strength concretes: strength gain is rapid at early ages, and becomes relatively small at later ages. It is notable, however, that the control concretes, having differing water/cement ratios, yield roughly comparable strengths (except at early ages). More remarkable is the behaviour of mix 6 (SF10(0.4)+), showing a 10% silica fume replacement resulting in virtually no increase in strength. One possible explanation for these anomalies is the entrainment of air in mixes C3 (C(0.3)+) and 6 (SF10(0.4)+) (see Table 6.24), brought about by the introduction of the superplasticizer. Table 6.27 presents the strength ratio values of Table 6.24 adjusted so that all mixes are assumed to have 1% air (based on the general rule that a 1% increase in entrained air gives rise to approximately 5.5% loss in compressive strength (Neville 1981)). It is immediately obvious that air entrainment does not account fully for the anomalous behaviour described above. Another more plausible explanation lies in the unsuitability of the coarse aggregate used for the production of high-strength concrete. On visual examination of crushed cubes, numerous coarse aggregate particles appeared to have fractured in specimens with strengths exceeding roughly 60 MPa and, since it is known that the compressive strength of concrete cannot significantly exceed that of the major part of the aggregate contained therein, this would suggest that the strength of the coarse aggregate used may be such that it imposes a ceiling on achievable concrete strength.

As seen in Table 6.24, a wide range of admixtures (e.g. in mixes: : 4 (GGBS65(0.4)), 5 (PFA30(0.4)), 11 (MAGST2(0.35)+), 13 (BUTST3(0.4)), 15 (SOYO1(0.35)+), 16 (LINSO1(0.35)+), 19 (EVA10(0.3)+), 22 (ACR10(0.3)+), 23 (AMINO22(0.35)), etc.), caused more than 15% reduction in compressive strength, even after 6 months of moist curing. The factors connected with this behaviour are considered in Table 6.28.

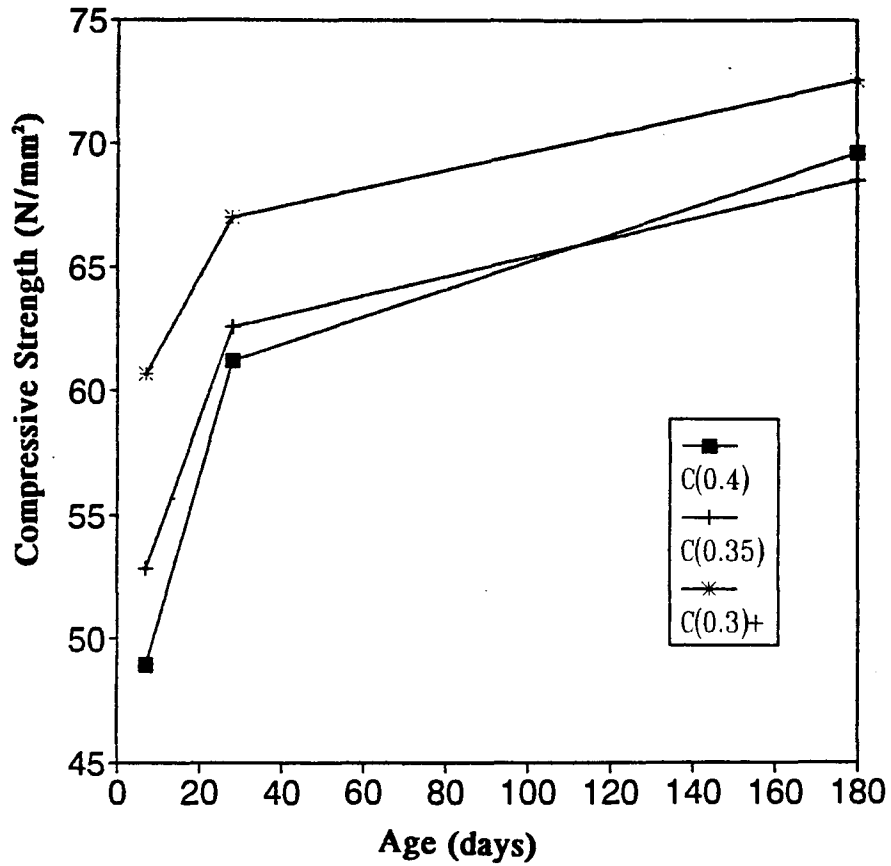


Figure 6.44 Variation in compressive strength with age (control concretes).

Table 6.27 Adjusted compressive strength results

Mix ref.	Compressive strength (N/mm ²)			Air content (%)
	7d	28d	6 month	
C(0.4)	49.4	61.9	70.4	1.2
C(0.35)	53.4	63.6	69.6	1.3
C(0.3)+	64.4	71.1	77.0	2.1
SR ^a				
GGBS65(0.4)	40*	57*	70*	1.0
PFA30(0.4)	73*	72*	93	1.0
SF10(0.4)+	105	116	110	2.5
KIES3(0.4)	98	91	100	1.1
BEN10(0.4)+	88	88*	97	2.8
WHIT5(0.4)	96	89	88	1.1
IRO2(0.4)	99	91	95	1.2
MAGST2(0.35)+	77*	74*	80*	1.8
ALST0.5(0.35)+	89	90	94	1.2
BUTST3(0.4)	77*	71*	77*	2.3
CAPA0.25(0.35)+	79*	81*	88	1.0
SOYO1(0.35)+	76*	70*	69*	1.2
LINSO1(0.35)+	79*	80*	80*	1.3
TAR25(0.35)+	85*	86*	83*	1.9
ASPH20(0.35)	104	96	114	3.2
EVA10(0.3)+	65*	60*	62*	2.3
SBR5(0.35)+	59*	65*	70*	1.3
SBR10(0.3)+	59*	55*	60*	1.5
ACR10(0.3)+	60*	63*	73*	0.9
AMINO22(0.35)	77*	74*	67*	1.5
CAL30(0.35)+	92	92	91	1.2
CONP3(0.35)	94	95	103	2.4
SIK9(0.4)	87	92	85	1.0
SET6(0.4)	86	84	91	1.8
IRON10(0.4)	99	92	93	1.1
CEL2(0.4)	106	96	91	1.6
FORM2(0.4)	101	93	97	1.1
TEA0.025(0.4)	104	93	95	2.0
TEA0.1(0.4)	98	88	90	1.2
LPV325(0.4)	97	95	92	1.1
LPV245(0.4)+	84*	81*	82*	1.7

^a percentage ratio of the compressive strength relative to respective control.

Table 6.28 Evaluation of factors relevant to compressive strength results

Mix	Factor considered		
	(i)	(ii)	(iii)
4 (GGBS70(0.4))	P	N/R	Y
5 (PFA30(0.4))	P	N/R	Y
11 (MAGST2(0.35)+)	S	P	N
13 (BUTST3(0.4))	M	P	N
14 (CAPA0.25(0.35)+)	N/A	N/R	Y
15 (SOYO1(0.35)+)	M	N/R	N
16 (LINSO1(0.35)+)	N/A	N/R	N
17 (TAR25(0.35)+)	N/A	P	N
19 (EVA10(0.3)+)	N/A	N/R	N
21 (SBR10(0.3)+)	M	N/R	N
22 (ACR10(0.3)+)	VP	N/R	Y
23 (AMINO22(0.35))	VP	N/R	N
25 (CONP3(0.35))	N/A	F	Y

• Factor considered

(i) Extent to which early-age hydration is retarded (based on conduction calorimetry results):

- S: slight;
- M: modest;
- P: pronounced;
- VP: very pronounced;
- N/A: result not available.

(ii) Extent to which air entrainment accounts for loss of strength (based on comparison of Tables 6.24 and 6.27):

- F: fully;
- P: partly;
- N/R: not relevant (mix has roughly same air content as respective control).

(iii) Whether strength loss shows signs of diminishing with age (Table 6.25):

- Y: yes;
- N: no.

It is immediately obvious that the behaviour of several mixes cannot be fully explained in terms of retardation of early-age hydration or air entrainment. One example is mix 15 (SOYO1(0.35)+). It will be seen later that the mix contains areas of unusually high porosity (6.3.5.3). These can play an important role in reducing compressive strength, according to the "Weibull Weakest Link Theory". Mehta and Aitcin (1990) explain that whilst brittle materials can fail in tension by rapid propagation of a single flaw or microcrack, a number of microcracks must coalesce together to cause failure in compression, and thus much more energy is needed for the formation and extension of the microcrack system. They explain further that **strength and fracture depend critically on microstructural extremes rather than averages**, or, in other words, fracture, especially in compression is a weak-link type process. As an example they cite the ceramic literature which "contains numerous examples of fracture origins definitely initiating from regions of unusually high porosity".

Finally, it must be stressed that, whilst strength reductions are unwelcome, the majority of adversely affected modified concretes still yielded strength values, at 28 days, in excess of 40 MPa.

6.3.5 Microstructure

6.3.5.1 General

Contrast in bse images is produced by variations in atomic number, the higher the atomic number in a given region, the greater the intensity of backscattered electrons, and the brighter that region appears. In bse images of OPC systems, therefore, anhydrous grains appear bright, calcium hydroxide light grey, C-S-H and other hydration products as various shades of darker grey. The pores, on the other hand, do not scatter electrons and hence appear uniformly black.

Microstructural examination was carried out in the hope that the method would help in elucidating the mechanism(s) by which a particular admixture causes a change in a particular chloride transport process (as indicated by transport testing), or indeed any of the other properties investigated. In this respect, it is worth noting the following: i) bse images merely provide a two dimensional image, and this means that pore connectivity, which is known to govern virtually all modes of transport in concrete (Chapter 3), cannot be assessed except subjectively, ii) ideally, specimens used in the SEM would be conditioned to correspond as closely as possible to the specimens used in transport testing (for example, oven dried specimens would be used to parallel specimens used in Series B capillary rise testing), and examination would be performed before and after testing. Unfortunately this was found impractical to undertake and the simplistic approach outlined in Table 6.13 was adopted.

Initially, it was intended to investigate all modified concretes regardless of performance. This, however, was later found very impractical, and it was decided to limit the investigation to a small number of modified mixes, and the control concretes. Unfortunately, the C2 specimen was damaged during preparation and could not be replaced.

The pore structure of concrete may be characterised through quantitative analysis of bse images (Scrivener & Pratt 1987). There are, however, difficulties which rendered the approach very impractical. As the microstructure of cement paste is not homogeneous, a sufficient number of fields (images) must be analyzed such that the average area fraction of each component is representative of its volume fraction in the bulk paste. Scrivener & Pratt (1987) investigated several cement pastes at a magnification of 400x and found that measurement of the area fraction of pores over eight fields gives values with relatively small errors (about $\pm 1\%$). In concrete, the cement paste is less homogeneous, and analysis would have to be performed over a larger number of fields. Several modified concretes were found to be much less homogeneous than the control (6.3.5.3), hence would have required a still larger number of images. More important, is that at a magnification of 400x the size of the smallest feature that can be identified is about 5000\AA , i.e. the analysis would only provide an estimate of the volume fraction of pores larger than 5000\AA . Pores in the region of 1000\AA , which are widely believed to govern concrete penetrability (Chapter 3), can only be identified at much higher magnifications ($> 2000x$). At such magnification levels, however, the analysis would have to be carried out over a very large number of fields (the greater the magnification used, the greater will be the natural variation between fields so more fields must be measured to obtain a representative result).

6.3.5.2 Control concretes

The micrographs shown in Figures 6.5b and 6.6b are typical of bse images obtained for relatively mature OPC concretes. It is obvious that in both C1 (C(0.4)) and C3 (C(0.3)+) a considerable amount of clinker reaction has taken place. It is also apparent that the hydration products are not distributed evenly within the interstitial space between the cement grains, this leading to the formation of a large number of irregularly-shaped pores. At these magnification levels, these pores appear largely isolated, and differences in porosity between C1 and C3 cannot be distinguished. At higher magnifications, however, a different picture emerges (Figure 6.5c and Figure 6.6c). In C1, the large irregular pores appear to be interconnected by somewhat smaller capillaries, whereas in C3 they seem fully isolated by hydration products comprising much finer porosity.

6.3.5.3 Modified concretes

The effect of GGBS (in mix 4 (GGBS65(0.4))) on the concrete microstructure can be gauged by comparing Figures 6.5 and 6.7. It is apparent that, despite considerable OPC hydration, the total amount of hydration product formed in the GGBS mix is less than in the control, resulting in higher porosity. Thick hydration rims can be seen on some slag particles (Figures 6.7a, b and c). Comparison of Figures 6.5c and 6.7c shows that the pozzolanic reaction has altered the pore structure in the proximity of the slag particle: the pores generally appear smaller, and the larger pores seem isolated by hydration product having much finer porosity. Another interesting feature found throughout the test specimen is shown in Figure 6.7d: a slag clump and an area of relatively high porosity lying immediately below the clump. It is worth noting that the slag was stored in a dry environment, and on visual examination before use there were no signs of an unusually high proportion of slag clumps. This finding highlights the difficulty of achieving uniform distribution of slag, which can result in less homogeneous paste matrix.

The effect of PFA (in mix 5 (PFA30(0.4))) on the concrete microstructure can be gauged by comparing Figures 6.5 and 6.8. It can be seen in Figure 6.8a that a considerable amount of hydration has taken place in the PFA mix, and that the hydration products are distributed more uniformly than in the control, this resulting in the disappearance of the large irregular pores seen in the control images. Distributed throughout this mass of hydrations products are, however, many highly porous areas, which probably result from non-uniform dispersion of the PFA (Jun-yuan et al. 1984). The porous areas seem to form more frequently in close proximity to the aggregate (Figure 6.8a); however, where the PFA is uniformly spread, the aggregate/paste interface appears to be less porous than in the control (Figure 6.8d). Regarding the PFA particles, some are found to be completely encapsulated by hydration products, others appear only partially encapsulated, whilst a few seem almost completely detached from the paste matrix (see Figures 6.8b). The encapsulated particles are seen to have irregular surfaces indicating that they have undergone some degree of pozzolanic reaction, whereas the separated particles seem largely unreacted; this implies that these particles are only weakly bound to the surrounding hydrates, as this would explain why they become separated during specimen preparation. That the fly ash particles have hydrated to varying extents, it should be emphasised, is not surprising, for PFA hydration, even in moist-cured concretes, is known (Sarkar 1991) to occur on a more or less particle-by-particle basis, governed primarily by the particle chemistry. Finally, it is worth noting the presence of large voids in the vicinity of the relatively unreacted PFA particles (Figure 6.8c).

The effect of silica fume (in mix 6 (SF10(0.4)+)) on the concrete microstructure can be gauged by comparing Figures 6.9, 6.5 and 6.6. That the hydrates in the silica fume mix are very evenly distributed throughout the interstitial space between the cement grains is apparent in low and high magnification images. At all magnification levels, the silica fume mix appears much less porous, when comparison is made with the respective control (C(0.4)) and indeed with C(0.3)+, this also being clearly in evidence at the interfacial zone with the aggregate (see Figure 6.9e). The above supports the commonly held view (Cheng-yi & Feldman 1985, Detwiler & Mehta 1989) that silica

fume particles act first as nucleation sites for the OPC hydration products thereby producing a much more uniform distribution of the hydrates (Figure 6.9b), and that subsequent pozzolanic reaction results in filling the fine porosity (Figures 6.9c and d). Isolated dark patches can be seen spread throughout the paste: some are clearly agglomerates of unreacted silica fume (see Figure 6.9b), and others are air voids (see Figure 6.9a).

The effect of incorporating butyl stearate (in mix 13 (BUTST3(0.4))), soyabean oil (in mix 15 (SOYO1(0.35)+)), aluminum stearate (in mix 12 (ALST0.5(0.35)+)), and Everdure Caltite (in mix 24 (CAL30(0.35)+)) on the concrete microstructure can be gauged by comparing Figures 6.10, 6.11, 6.12, and 6.13, respectively, with Figures 6.5, and 6.6.

At low magnification levels, the butyl stearate mix appears to have a denser microstructure, when compared against both C1 (C(0.4)) and C3 (C(0.3)+). At higher magnification levels (Figures 6.10c), the mix appears to have finer and more discontinuous porosity than C1, to an extent more or less paralleled by C3.

A general view of the microstructure of the soyabean oil mix is given in Figures 6.11a, b and c. It is immediately apparent that the cement paste is much less homogeneous than in C1 and C3, this being due to the presence of areas of relatively high (Figure 6.11b) and low (Figure 6.11c) porosity. It is also observed that the high porosity areas tend to concentrate more at, or rather in close proximity to, the interfacial zone with the aggregate (Figure 6.11a). This porosity possibly contains(ed) soyabean oil (see A1.4), and this would suggest non uniform distribution of the oil within the paste matrix. As seen in Figures 6.11d and e, the low porosity areas are of much finer and more segmented porosity compared to C1. However, when comparison is made against C3, the soyabean mix appears to have somewhat coarser and less segmented porosity. As seen in Figures 6.12a and b, the aluminum stearate mix also possesses areas of relatively high and low porosity; the presence of entrained air voids is also worth noting.

A general view of the microstructure of the Everdure Caltite mix is shown in Figure 6.13a; numerous voids of entrained air are apparent. Figure 6.13b shows that the mix has a denser microstructure than both C1 and C3. At higher magnifications (Figures 6.13c), the porosity seems to be finer and more isolated than in C1, but somewhat coarser than that of C3.

The effect of the acrylic latex on the concrete microstructure can be gauged by comparing Figures 6.6 and 6.14. As seen in Figure 6.14c, many of the irregularly shaped pores found in C3 have disappeared, and instead relatively large and small rounded pores are found dispersed throughout the hydration product. However, differences in porosity between the acrylic mix and C3 cannot be distinguished.

6.4 General discussion

The use of ground granulated blastfurnace slag and pulverised fuel ash as cement replacement materials with the object of improving the performance of concrete structures in chloride-rich environments has been the subject of considerable research. One universally reported finding (Concrete Society 1990) is that both materials can, when used at conventional replacement levels, increase resistance to chloride ingress substantially when the concrete is well cured. The term "well-cured" is found to be mostly used in reference to storage for relatively long (usually 28 days or much more) periods in water; sometimes in a saturated lime solution. Curing in saturated lime water is, however, a method only suitable for small-scale specimens prepared for laboratory testing. Moreover, prolonged moist curing (before exposure) is often considered impractical in practice. Indeed, attention is currently shifting to preventing loss of moisture from concrete, by use of curing membranes. Sealed curing in the laboratory provides a good indication of the performance potential of membrane-cured concrete. A review of the literature revealed, surprisingly, a lack of information relating to the performance of GGBS and PFA concrete, which can address the specific question: Can OPC concrete containing conventional replacement levels of GGBS or PFA be regarded as "well-cured" under sealed conditions? The results in Tables 6.14 through 6.19 (see 6.3.2) all seem to indicate that, in so far as resistance to molecular transport is concerned, the answer is "no". This, however, is not true of chloride ion diffusion resistance, as seen in Figures 6.35 to 6.37 (mixes 4 (GGBS65(0.4)) and 5 (PFA30(0.4))). Furthermore, it is interesting to observe that the slag and pfa mixes also have lower diffusion rates (g) when compared with C3 (C(0.3)+), which is found to have much higher resistance to molecular transport (Figure 6.38). That T_0 reflects an opposite trend (in relation to C3) in the case of PFA30(0.4) would appear anomalous, however. According to an earlier discussion (6.3.2), this may be explained by the areas of relatively high porosity identified by SEM (6.3.5.3). In the light of the above, the results can only be seen to confirm the important role that chemical and electrochemical effects play in hindering chloride diffusion in concretes incorporating cement replacement materials (3.6.2, 6.1.1.2.2). The effectiveness of the GGBS and PFA

mixes in suppressing chloride diffusion is also confirmed by penetration profiling (Figure 6.35). Finally, it is worth noting that despite 11 months of sealed storage, both the GGBS and PFA are found (6.3.2) to be more permeable to water than the control.

The silica fume containing mix (mix 6 (SF10(0.4)+)) is found to perform substantially better than the control in respect of most of the properties considered, outperforming even C(0.3)+. These results are not at all surprising considering the SEM findings (6.3.5.3). In fact, the results in Table 6.20 (see Figures 6.35 to 6.38) reveal that the silica fume mix is the most resistive of all mixes considered to chloride ion diffusion, though this is also due, in part, to electrochemical effects (see 3.6.2). In resisting pressure-induced water flow, as Table 6.14 shows (see also Figures 6.15 and 6.16), the silica fume mix was only bettered, slightly, by the bentonite containing mix (8 (BEN10(0.4)+)).

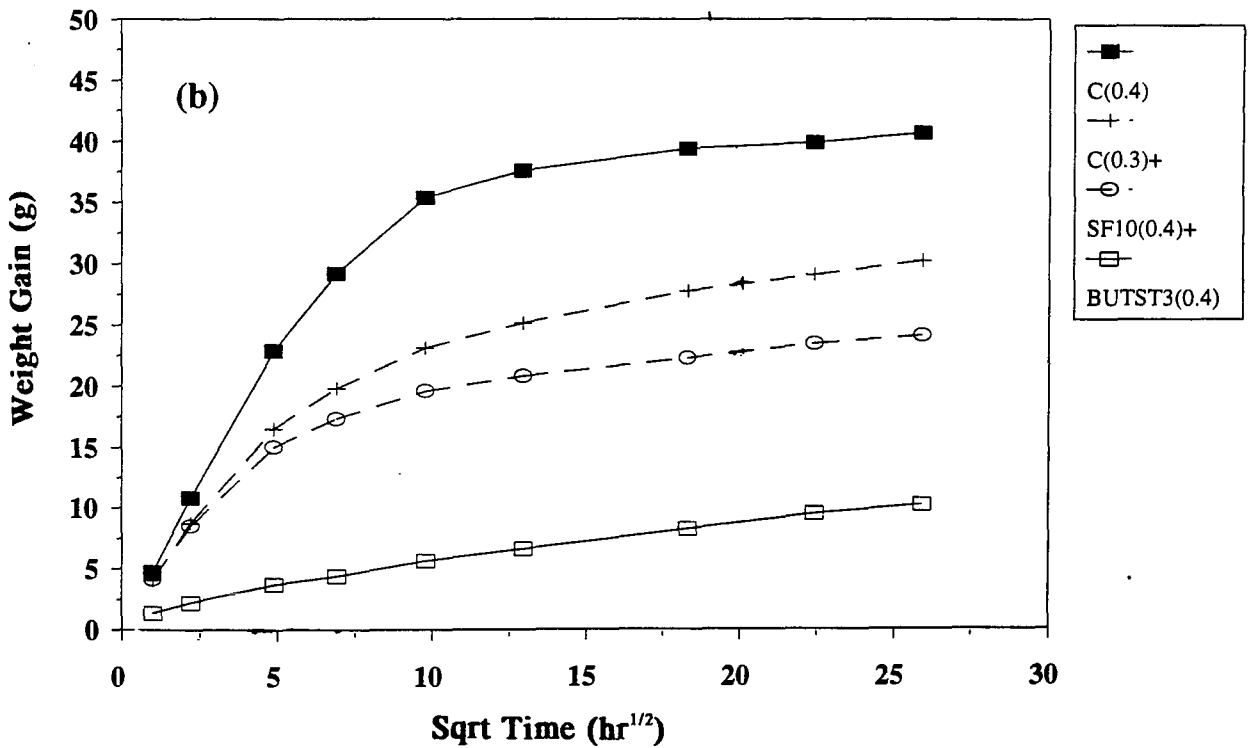
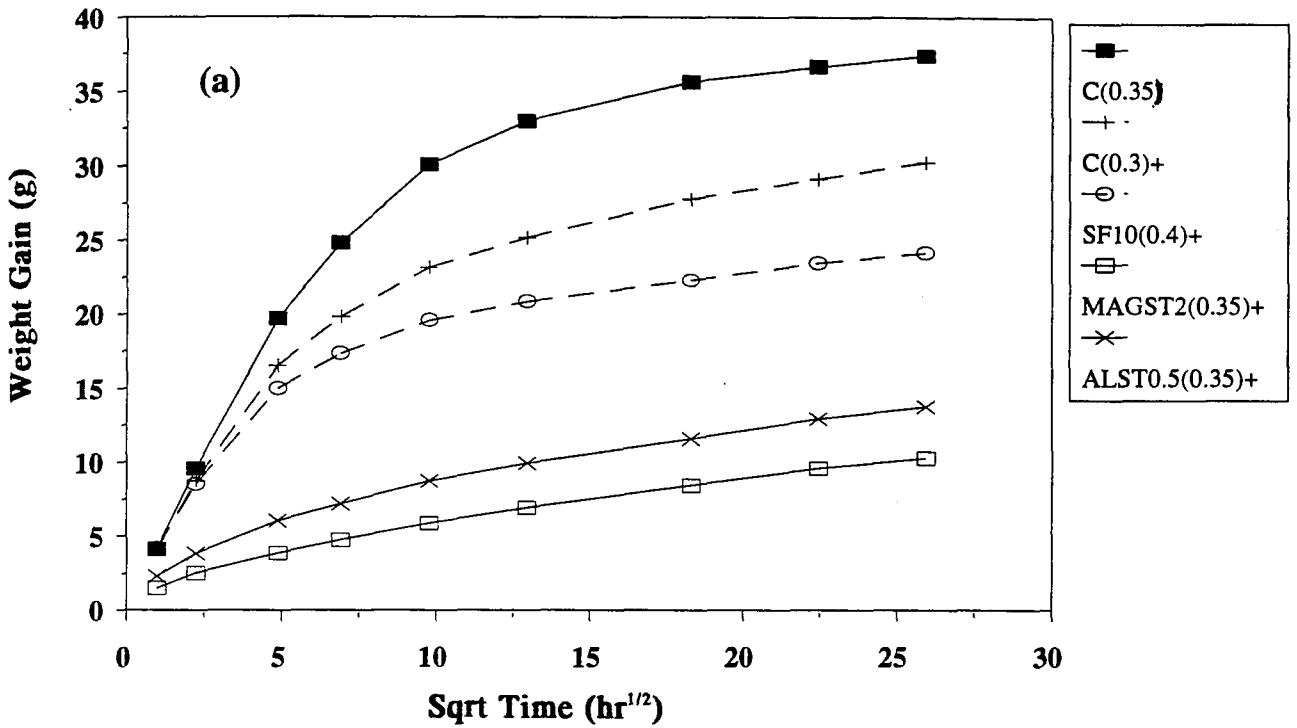
Bentonite (at 10%), however, was found to reduce workability substantially, and even with 1% superplasticizer, the mix was only just workable (A2.2.2). Bentonite absorbs water, swells when wet and shrinks when dry (see A1.3). On mixing, it absorbs a proportion of the mix water, bringing about a reduction in the free water/cement ratio. Bentonite may also help in alleviating the unfavourable effects associated with self-desiccation (6.3.2). This is because it is likely that some of the water initially absorbed by bentonite would be released into the concrete pores as they dry with the progress of hydration; in this respect the behaviour of bentonite is similar to that of some lightweight aggregates (Ben-Othman & Buenfeld 1990). It is anticipated that the effect would be more apparent the more the susceptibility of the concrete to self-desiccation, and with relatively long periods of sealed storage. On exposure to water in the permeability test, bentonite also absorbs water, swells, thereby causing pore blockage. It is thought that a combination of the above effects explain why the bentonite mix exhibited exceptional performance in the water permeability test.

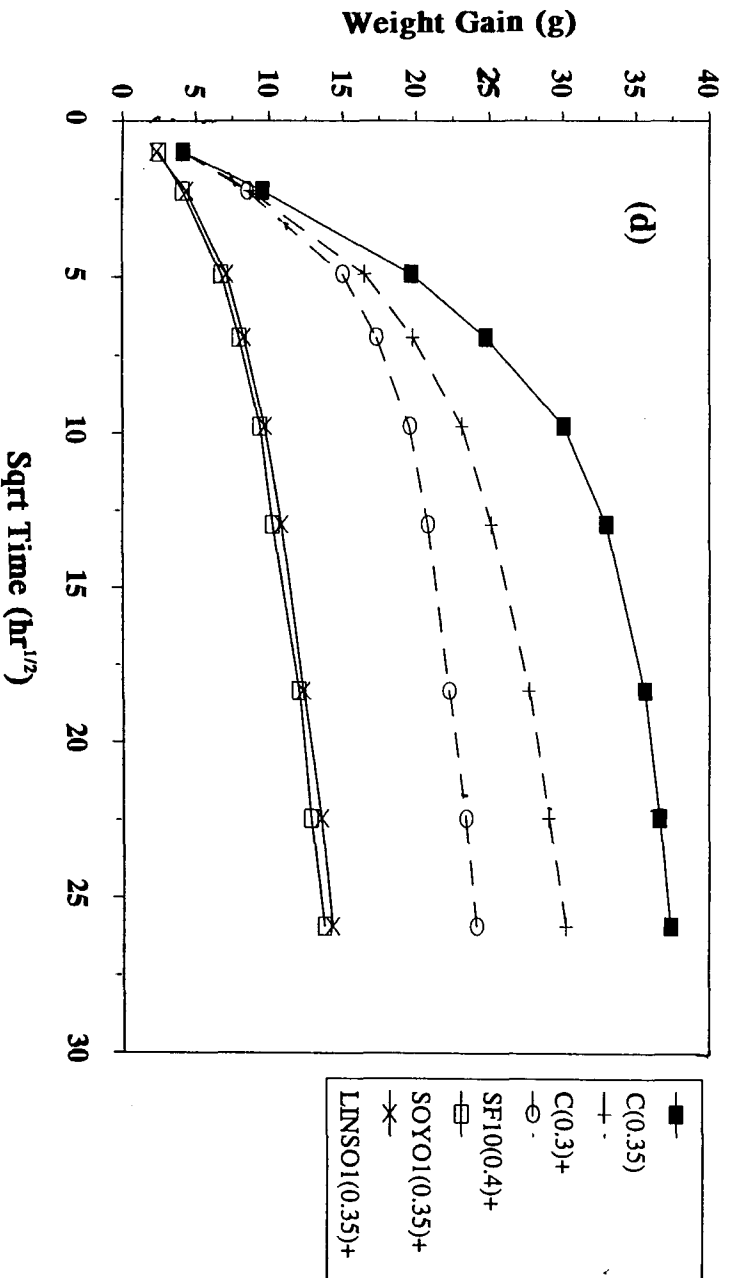
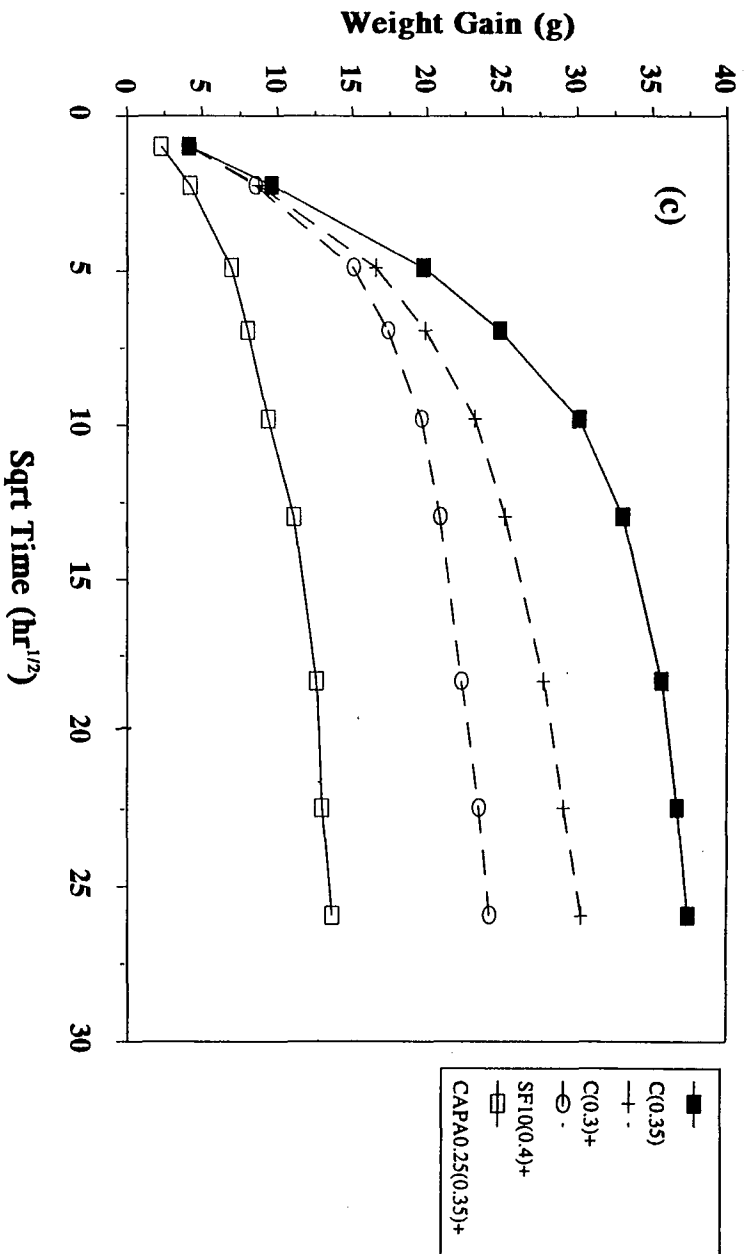
There are, however, adverse effects associated with the use of bentonite that should not be overlooked. Chloride ion diffusion and drying are both accelerated, as seen in Tables 6.20 and 6.18, respectively (see also: Figures 6.35 to 6.38 and Figure 6.32). This behaviour is particularly surprising since, as mentioned above, the bentonite mix is, in effect, of lower water/cement ratio than the control. In the case of chloride diffusion, the increase hence can only be explained in terms of changes in the pore solution composition, relating, perhaps, to the base exchange capacity of the bentonite (bentonite can absorb positive ions selectively from the solution in polar liquids, and release an equivalent quantity of exchangeable ions at the same time (see A1.3)). As for the drying rate, it is thought that the increase is too large to be explicable solely in terms of moisture content variations, if any, and it is suggested that it may be due to the bentonite undergoing considerable shrinkage on drying, hence, aggravating microcracking (see A3.1); if this view is accepted, it follows that bentonite would not be suited for use in environments where concrete is subjected to drying. Clearly more work is required on this topic.

Water repellent materials are again (see 5.3.4) found to have a dramatic effect on capillary absorption. Remarkably, as clearly seen in Figure 6.45, the majority of water repellent-modified mixes (11 (MAGST2(0.35)+), 12 (ALST0.5(0.35)+), 13 (BUTST3(0.4)), 14 (CAPA0.25(0.35)+), 15 (SOYO1(0.35)+), 16 (LINSO1(0.35)+)) outperformed by a huge margin not only the corresponding control, but also mixes C3 (C(0.3)+) and 6 (SF10(0.4)+)(differences in microstructural damage on severe drying not taken into account). This clearly refutes the claim (ACI Committee 212 1989) that water repellents are only effective when incorporated in low quality badly cured concrete.

Microstructural examination (6.3.5.3) carried out on the most effective of all the water repellent mixes (13 (BUTST3(0.4))) identified no characteristic of the cement paste microstructure that could result in pronounced differences in absorption resistance as against C3. Moreover, other mixes examined (12 (ALST0.5(0.35)+), 15 (SOYO1(0.35)+)) were found to have a pore structure which is very unlikely to lead

Figure 4.45 Absorption behaviour of concretes modified with effective water repellents.

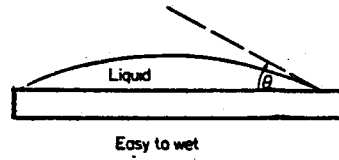
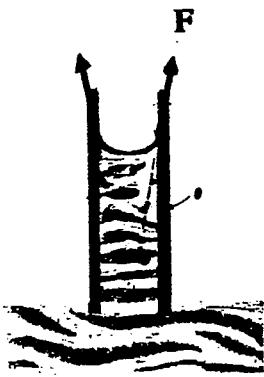




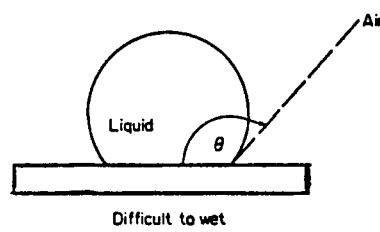
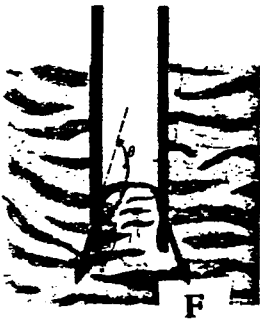
to an absorption resistance higher than even that of the respective control (see 6.3.5.3). These considerations support the idea (Rixon & Mailvaganam 1986, Hewlett et al. 1988, Aldred 1989) that the principal effect of water repellents is to provide a hydrophobic (water repelling) lining to pore walls, since this is one possible form of modification that would not be expected to have produced effects visible in the SEM.

Water-insoluble soaps in finely divided form (calcium stearate, aluminum stearate, magnesium stearate) impart water repellency to surfaces on which they are applied because they are inherently water repellent (see A1.4). Oils (soyabean oil, linseed oil, etc.) and liquid fatty acids (caprylic acid, oleic acid, etc.) impart water repellency by virtue of their inherent water repellent nature, as well as by reacting with the alkalis in concrete to precipitate water-insoluble calcium soaps (A1.4). Butyl stearate, and water-soluble soaps (e.g. sodium stearate, sodium oleate, ammonium stearate, etc.), on the other hand, are not inherently water repellent, but react with the calcium ions in the pore solution and so precipitate out as insoluble water repelling calcium soaps (see A1.4).

The principle of water repellency can be explained by considering the simple example of a capillary glass tube, one end of which is left open to the atmosphere and the other is dipped in water. Water rises in the tube if the walls are clean, but when oil is applied to the internal surfaces of the tube, water does not rise. Water is drawn into the capillary because the angle of contact of glass with water is lower than 90° , therefore, according to Equation 3.3, the suction force F assumes a positive value (Figure 6.46a). Oil, on the other hand, increases the angle of contact of the glass wall with water to above 90° hence F assumes a negative value. This means that not only is the influence of the suction force negated, but also that a force of magnitude F will have to be overcome if water is to enter the capillary (see Figure 6.46b). In theory, a similar situation can occur in a concrete. In practice, however, water repellents can only be introduced at relatively small dose levels (5.2.1.3.4), so it is likely that even the most effective admixture would neither render all the capillaries in concrete water repellent, nor produce a perfect hydrophobic lining on all capillaries (Hosek & Sereda 1968).



(a) $\theta < 90^\circ$



(b) $\theta > 90^\circ$

Figure 6.46 Capillary forces and contact angle.

Hence, it would reduce substantially, but not eliminate, water absorption.

Table 6.16 along with Figure 6.45 shows that the majority of water repellent materials (in mixes: 11 (MAGST2(0.35)+), 12 (ALST0.5(0.35)+), 13 (BUTST3(0.4)), 14 (CAPA0.25(0.35)+), 15 (SOYO1(0.35)+), 16 (LINSO1(0.35)+); these will be termed "effective water repellent mixes") not only reduce the rate of water uptake substantially, but also reduce the total amount absorbed after relatively long exposure periods; this emphasises the slowness of capillarity-driven absorption in these mixes, particularly since a slow process involving water vapour diffusion/condensation would have also had some role in the water uptake of specimens (5.3.4).

The same mixes are also found to exhibit reduced water uptake when specimens are tested as received (under capillary rise and MAT conditions (see Figure 6.31)), though differences, in relation to the corresponding control, seem to be generally less pronounced, particularly under capillary rise conditions; this is not entirely surprising (see 6.3.2).

All effective water repellent mixes, with the exception of the butyl stearate containing mix, are found to exhibit more or less similar, or substantially higher, water uptake compared to the control when the specimens are subjected to saturation (see 6.3.2). This shows that the water repellents involved did not bring about effects capable of increasing resistance to water ingress when even a relatively small pressure is applied. Broadly similar trends are also found to pertain to porosity results (see Figure 6.26). It is to be recalled that two of the mixes referred to above, namely mixes 12 (ALST0.5(0.35)+) and 15 (SOYO1(0.35)+), were found to contain areas of unusually high porosity (6.3.5.3). In the light of all of the above, it is suggested that the areas of unusually high porosity are probably manifest in the other mixes (i.e. mixes: 11 (MAGST2(0.35)+), 14 (CAPA0.25(0.35)+), 16 (LINSO1(0.35)+)). Furthermore, the results furnished from water permeability testing suggest that the presence of these areas of high porosity facilitates water permeation (see 6.3.2). Finally, it is worth noting that the only effective water repellent mix found not to have the adverse effects described

above, namely mix 13 (BUTST3(0.4)), displays a uniformly dense microstructure in the SEM (6.3.5.3).

Two of the four proprietary waterproofers investigated, namely Everdure Caltite (in mix 24 (CAL30(0.35)+)) and Conplast Prolapin (in mix 25 (CONP3(0.35))), are found to have a dramatic effect on water absorption. Everdure Caltite produced by Cementaid, is the most widely specified proprietary waterproofer (Aldred 1988). This is a combination of a suspension of very fine asphaltic globules and ammonium stearate and is recommended for use with a superplasticiser (Superplastet) at a water/cement ratio of around 0.35. Conplast Prolapin is, according to the manufacturers (Fosroc): "a free flowing white powder formulated from a blend of long-chain fatty acids and other hydrophobic raw materials, which together form a matrix of insoluble water resistant material within the cement paste"; the recommended dose is between 1% to 3%.

As seen in Table 6.16 and Figure 6.47, both admixtures produced large reductions in the rate of water absorption and in the long-term amount of water uptake, but Everdure Caltite was bettered in these respects by several water repellents (in mixes: 11 (MAGST2(0.35)+), 13 (BUTST3(0.4))). However, in contrast with the majority of water repellents materials, Conplast Prolapin and Everdure Caltite are found not to influence permeability (water and oxygen) adversely. Indeed, the Everdure Caltite mix displays roughly comparable permeability to C3 (C(0.3)+); this together with the SEM study of this mix (6.3.5.3), in some measure supports the manufacturers claim that the asphaltic material (organic and therefore undetectable in the SEM) physically blocks pores.

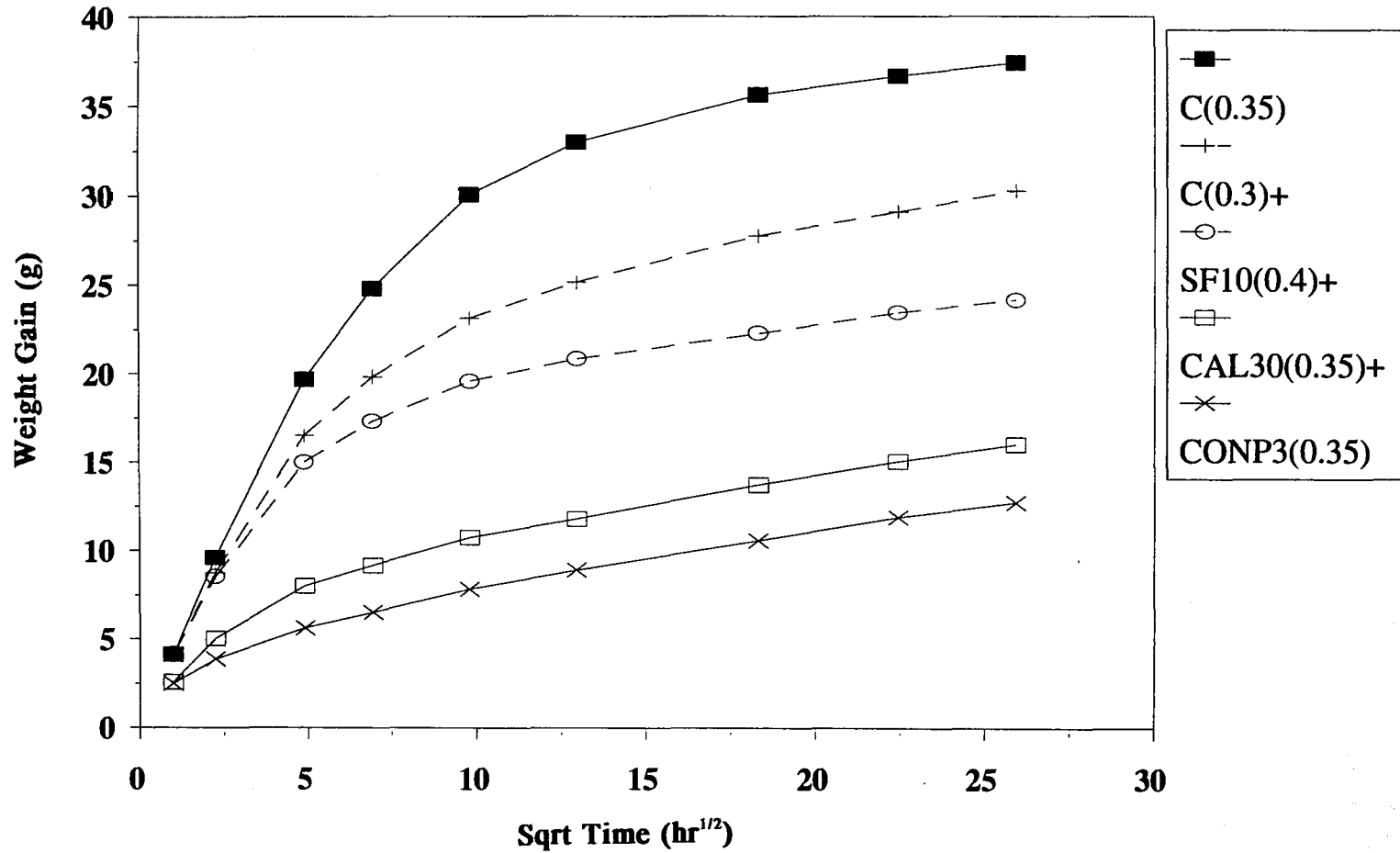


Figure 6.47 Absorption behaviour of concretes modified with effective proprietary waterprooferers.

Interesting aspects of the absorption performance of effective water repellents and proprietary waterproofers are also brought to light when capillary rise test results (on oven dried specimens) relating to the mixes of Phases 1 and 2 are collectively examined (see Table 6.29); compressive strength results are also displayed. For simplicity, absorption behaviour is represented by the absolute and percentage ratio weight gain at 1 day and 28 days; these indicate, respectively, resistance to water uptake under short-term and relatively long-term exposure.

Before proceeding, it is necessary to recall that Phase 1 specimens were tested at an earlier age than those of Phase 2 (28 days as against 90 days), and were subjected to harsher drying (105°C as opposed to 50°C and 11-14% RH); the relative importance of these effects is established in 7.4.2.2.

Comparing mixes belonging to Phase 1 with mix C(0.3)+, shows clearly that, under short-term exposure, the majority of the admixtures considered can, when used in 0.45 water/cement ratio concrete (in mixes: MAGST1, MAGST3, ALSTS1, BUTST2, BUTST3, CAPA0.5, CAPA2, SOYOE3), improve absorption resistance to an extent much higher than that associated with reducing the water/cement ratio from 0.45 to 0.3 with the aid of a superplasticizer (at 1% w/w_{cement}).

It is also apparent that the majority of the admixtures tested exhibit better relative performance (i.e. based on WGR data at 1 day) when tested under the conditions of Phase 1. This implies that these materials yield greater improvements the lower the absorption resistance of the base concrete, or, in other words, where they are required most. This view is supported by others (Aldred 1989). In a study which involved 9 proprietary products (with water repelling properties), used in 0.63 water/cement ratio concrete, Aldred observed that modified mixes effective in resisting capillary absorption were far less sensitive than the control concrete to the quality of curing (three methods were investigated: following 1 day at near 100% RH: 7 days air curing (20°C & 60% RH), or 2 days water curing then 14 days in air, or 27 days in water then 14 days in air), and attributed this effect to "the significant change in contact angle which inhibits

Table 6.29 Performance of effective water repellents and proprietary waterproofers (Phases 1 & 2)

Material	Mix ref.	W/C	Weight Gain ^a (g)		WGR ^b		S ^c (N/mm ²)	SR ^d
			1d	28d	1d	28d		
---	C	0.45	51.1	62.0			50.3	
	C(0.4)	0.40	22.9	40.7			61.2	
	C(0.35)	0.35	19.7	37.4			62.6	
	C(0.3)+	0.30	16.5	30.3			67.0	
Magnesium stearate	MAGST0.5	0.45	11.2	26.7	22	43	46.3	92
	MAGST1	0.45	7.7	18.6	15	30	40.7	81
	MAGST3	0.45	4.6	14.8	9	24	35.7	71
	MAGST2(0.35)+	0.35	3.9	10.3	20	28	45.1	72
Aluminum stearate	ALST0.25	0.45	18.4	39.1	36	63	46.3	92
	ALST0.5	0.45	12.8	28.5	25	46	42.3	84
	ALST1	0.45	6.6	18.0	13	29	40.2	80
	ALST0.5(0.35)+	0.35	6.0	13.8	31	37	56.3	90
Butyl stearate	BUTST2	0.45	4.1	13.6	8	22	41.8	83
	BUTST3	0.45	4.1	13.0	8	21	43.5	82
	BUTST3(0.4)	0.40	3.7	10.2	16	25	41.0	67
Caprylic acid	CAPA0.5	0.45	6.1	18.0	12	29	26.7	53
	CAPA2	0.45	4.6	14.3	9	23	33.2	66
	CAPA0.25(0.35)+	0.35	6.9	13.7	35	37	51.3	82
Soyabean oil	SOYOE0.5	0.45	16.4	41.5	32	67	41.2	82
	SOYOE1	0.45	11.8	34.0	23	55	37.7	72
	SOYOE3	0.45	6.1	20.5	12	33	32.0	60
	SOYOE10	0.45	3.1	11.8	6	19	17.1	32
	SOYO1(0.35)+	0.35	6.8	13.8	34	37	43.9	70
Linseed oil	LINSO0.5	0.45	19.9	47.1	39	76	34.0	68
	LINSO1	0.45	14.8	40.9	29	66	29.7	59
	LINSO2	0.45	9.7	33.5	19	54	29.2	58
	LINSO1(0.35)+	0.35	7.1	14.3	36	38	50.1	80
Everdure * Caltite	CAL30	0.45	9.2	24.2	18	39	41.7	83
	CAL30(0.35)+	0.35	8.0	16.0	41	43	58.2	93
Conplast Prolapin	CONP1	0.45	34.2	59.0	67	95	46.8	93
	CONP3	0.45	17.9	44.0	35	71	46.8	93
	CONP3(0.35)	0.35	5.4	12.7	29	34	56.3	90

* used as l/m³ of concrete.

a weight gain in oven-dried specimens.

b percentage ratio of weight gain relative to respective control.

c compressive strength at 28 days.

d percentage ratio of compressive strength relative to respective control.

water penetration irrespective of the degree of hydration and consequent pore size distribution", and added further "this effect would be very beneficial under actual site conditions where 1 day in the form may be the only protection the concrete receives". It is therefore not surprising that the effectiveness of several water repellents (magnesium stearate, aluminum stearate, butyl stearate, soyabean oil) is found to be less sensitive to variations in water/cement ratio, age, and severity of drying as against the dose rate (of the admixture); the performance of Everdure Caltite also seems insensitive to such variations. This, however, is not true of all water repelling admixtures: Conplast Prolapin, for example, is found to be more effective under the conditions of Phase 2 (see also 6.1.1.2.7). At this point, it also is important to emphasise that in absolute terms, i.e. based on weight gain data, the majority of admixtures tested are found to perform better (when comparison is made at nearly the same dose level) under the conditions of Phase 2, particularly under long-term exposure.

Different types of polymers have been in use in concrete. These can be broadly divided into three groups: latices, liquid resins, and water soluble polymers. This study was concerned with latices as they are the most widely used. Latices are basically dispersed suspensions of solid polymer microparticles (usually 0.05 to 5.0 μm in diameter) held in water by the use of surface-active agents (see A1.5).

The development of microstructure in latex-modified concretes is widely believed (Ohama 1987, Semerad 1987, Dennis 1988, Lavelle 1988, Khulmann 1990) to be the result of two inter-related processes, viz cement hydration and polymer film formation. Under appropriate conditions, these processes lead to the formation of a monolithic matrix phase with a network structure in which the hydrated cement phase and polymer films interpenetrate into each other (see Figures 6.48a, b, and c), together with the aggregates (Figure 6.48d). It is postulated that it is primarily this structure which is responsible for the superior (in comparison with unmodified concrete) physical and durability properties displayed by latex-modified mortars and concretes.

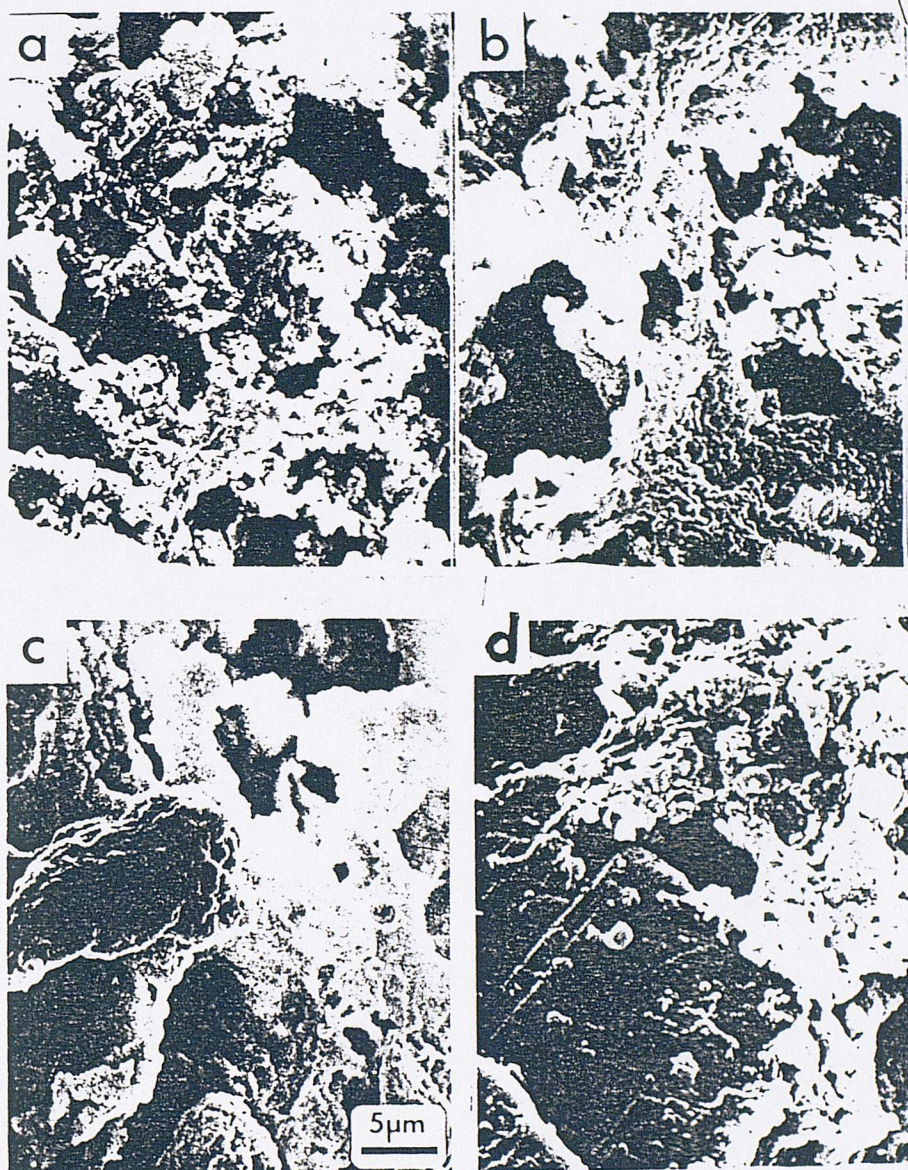


Figure 6.48 SEM images on etched fracture surfaces showing the formation of coherent polymer frame in OPC mortars modified with EVA latex cured for 3 days under moist conditions then air-dry cured for 14 days (Semerad et al. 1987);

- a) 2% EVA;
- b) 8% EVA;
- c) 16% EVA;
- d) 10% EVA (contact with sand grain).

Polymer film formation is dependent on many factors (Jenkins 1972, Lavelle 1988). For the purposes of this work, however, it suffices to mention here that the two essential requirements for polymer film formation are: i) the removal of water separating the polymer particles, usually by drying (this is shown in Figure 6.49), and ii) that a minimum temperature, commonly referred to as the Minimum Film Formation Temperature (MFFT), is exceeded (for the EVA, SBR, and Acrylic latices used, MFFT is 0 °C, 1-4 °C, 10-12 °C, respectively).

It is therefore not surprising to find that, and in order to ensure that maximum benefit is obtained from latices, the widely adopted practice with latex modified mortar and concrete has been (Ohama 1987, Popovics 1987, Dennis 1988, Lavelle 1988) to cure first under moist conditions (up to 7 days), so as to achieve a reasonable degree of cement hydration, then to expose the modified concrete to dry conditions in order to promote the formation of polymer films. This, however, has been mostly done on a more or less ad hoc basis, and a review of available literature revealed that no research has been undertaken to establish the optimum, in regard to the various transport processes, periods of moist and air curing required when a particular latex is used, and the most effective conditions of air drying (i.e. temperature, relative humidity, extent of drying, etc.).

The results of oxygen permeability testing (see 6.3.2) show only marginal differences between latex-modified (mixes: 19 (EVA10(0.3)+), 20 (SBR5(0.35)+), 21 (SBR10(0.3)+), 22 (ACR10(0.3)+)) and control specimens when all are dried at 75% RH & 30 °C. Further drying (at 55% RH & 30 °C) is found to result in mixes 19 and 21 performing appreciably better than the corresponding control. The acrylic-modified mix (22), however, was only marginally better than the control, but drying at 50 °C & 11-14% RH improved its performance substantially; indeed, the acrylic mix was at this stage the least permeable of all mixes (modified and control) tested. Drying is found to have a similar effect on absorption resistance: mixes 19, 21, and 22 exhibit substantially higher absorption resistance than the control when testing is performed on severely dried (50 °C & 11-14% RH) specimens, but show no favourable performance

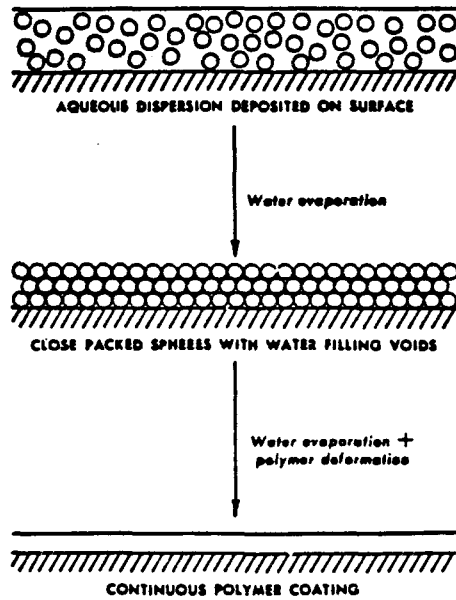


Figure 6.49 Process of polymer film formation (Lavelle 1988).

on as received specimens (Figure 6.31). Finally, the results in Table 6.14 (see also Figure 6.15) reveal that even a relatively long period of sealed curing, despite some degree of drying due to self-desiccation, does not promote polymer film formation sufficiently to cause the modified concretes to be markedly less permeable than the control concrete.

This tendency of the latex-modified concretes to experience substantial improvements in resistance to molecular transport after severe drying starkly contrasts the behaviour of all other concretes tested (see, for example, 6.3.2), and is almost certainly due to the fact that film formation is promoted by severe drying. SEM of the acrylic mix (6.3.5.3) furnishes indirect support for this proposition: no feature of the cement paste microstructure that could bring about a substantial change in any molecular transport process could be identified (note that polymer films would not be visible in bse images; they are detectable, however, on fracture and etched fracture surfaces (Figure 6.48)).

It worth noting at this point that at the 5% dose level (mix 20), which is regarded as the threshold level for polymer latices to be effective (5.2.1.3.5), the SBR latex, even on severely dried specimens, is found to bring about only a modest improvement in absorption resistance, and to have a marginal effect on oxygen permeability.

Based on ACID testing, two latices, namely EVA and acrylic (in mixes: 19 (EVA10(0.3)+) and 22 (ACR10(0.3)+)) are found to produce a modest improvement in chloride diffusion resistance. Diffusion profiling results, however, show a similar trend in the case of the acrylic mix, but not the EVA mix, which actually exhibits an opposite trend (see 6.3). This is believed to be associated with alkaline (pore solution) hydrolysis of the EVA polymer, resulting in water soluble substances being formed which are, in turn, leached from the paste matrix, rendering the matrix more porous. Indeed, evidence of leaching (a white residue spread on the surface) was found on removal of the EVA specimen from the exposure tank, and also the 100mm cubes used in measuring compressive strength at 180 days. In this connection, it is important to emphasise that whilst it is reported in the literature that EVA may be susceptible to

alkaline hydrolysis, it is well known that SBR and acrylic latices are not (A1.5)

The polymer-modified mixes exhibit pronounced reductions in compressive strength even at the age of 6 months (6.3.2). This is partly due to the continuous submersion of the test specimens in water (6.1.2.2), which greatly hinders polymer film formation. Indeed, it is often reported in the literature (e.g. Semerad et al. 1987, Ohama 1988) that polymer-modified concretes exhibit improved compressive strength (in relation to parallel continuously submerged specimens) if allowed to dry in laboratory air at some stage.

Chapter 7 Phase 3: Performance Optimization

7.1 Materials and design of concrete mixes

The purpose of this experimental phase was to predict and assess combinations of the materials tested in Phase 2 expected to give maximum resistance to chloride ingress in a variety of exposure environments.

A review of the literature (Chapter 8) revealed that in most exposure environments where chloride-induced corrosion is a problem, chlorides penetrate the concrete by absorption (during drying and wetting cycles) and then ion diffusion assists in transporting the ions to the depth of the reinforcing steel. Testing in Phase 2 revealed that it was not possible to better the chloride ion diffusion resistance of concretes containing normal replacement levels of silica fume, GGBS, or PFA by using OPC and an admixture. It appears that the relatively small additions of admixtures do not have sufficient influence on the amount of porosity, the continuity of pores or pore solution chemistry to substantially influence chloride ion diffusion. Consequently, Phase 3 concentrated on using admixtures to improve absorption resistance in cement replaced concrete. Several materials belonging to the water repellent group were found effective in reducing water absorption (see 6.4). Of those, butyl stearate and soyabean oil were selected. Butyl stearate was selected because it was found to be the most effective of all water repellents. Soyabean oil was preferred to other effective water repellents because it is a very inexpensive and widely available material and, unlike the other materials, did not affect chloride ion diffusion resistance adversely (see Table 6.20).

Acrylic was also investigated, because it was considered worthwhile to investigate further (see 6.4) the effect of polymer latex modification and polymer film formation on chloride transport in concrete.

General details of the mixes tested are given in Table 7.1, and more comprehensive information is given in A2.3. The base (Control) concrete was chosen to be mix C2 of the previous phase, with the exception that a plasticizer was used at this stage to improve workability. Cement replacement materials were used in direct replacement (by weight) of the Ordinary Portland Cement (in mix CN). The standard GGBS tested in Phases 1 & 2 was at this stage used in combination with the same slag ground to a much greater fineness: FGGBS had a surface area of $550 \text{ m}^2/\text{kg}$ compared with that of the standard GGBS of $390 \text{ m}^2/\text{kg}$. Increasing the slag fineness is one commonly used method of improving its reactivity in OPC concrete. It was therefore felt that the approach would help improve the molecular transport properties and compressive strength of the slag concretes and further increase their resistance to chloride ion diffusion; it is interesting to note in this connection that in Europe slag is normally ground to the same fineness ($380 \text{ m}^2/\text{kg}$) as the Ordinary Portland Cement, whereas it is standard practice in the USA (Mehta & Monteiro 1993) to use much finer slag ($500 \text{ m}^2/\text{kg}$ or even more). The acrylic latex was introduced in addition, expressed as percentage weight of polymer solids relative to that of the cement (the water contained in the latex was considered as part of the mix water). Finally, butyl stearate and the soyabean oil were used in direct addition, expressed as percentage by weight of the cement.

It may be noted at this point that the term "cement" is used here, as before, in reference to the total cementitious material content.

Table 7.1 General details of mixes tested (Phase 3)

Mix ref.	Dose level (% by cement)							
	SF	PFA	GGBS	FGGBS	Acrylic	Soyabean oil	Butyl stearate	Superplasticizer (SP-450) (% w/w _{cement})
CN	---	---	---	---	---	---	---	1
R1	5	---	---	---	10	---	---	---
R2	10	---	---	---	---	---	2	1.5
R3	10	---	---	---	---	1	1	1.5
R4	---	30	---	---	---	1	---	1
R5	5	20	---	---	---	1	---	1
R6	---	---	---	65	---	1	---	1
R7	---	---	65	---	---	---	2	1
R8	---	---	35	30	---	---	2	1
R9	---	---	35	30	---	---	---	1

7.2 Tests and testing programme

All concrete mixes were prepared in the same pan mixer, the mixing procedure and the manner in which the various admixtures were introduced being essentially similar to that employed in the previous phases (see 5.2.2.1). Immediately following the completion of mixing, slump testing was performed. The required specimens from each mix (8 disks (101.6mm diameter and 50mm thick), 2 150mm cubes, and 4 100mm cubes; for mix R1 the number of specimens in each category, except the last, was doubled) were then cast and compacted on a vibrating table. As soon as the small amount of bleed water had evaporated, specimens were stored under wet burlap and polythene sheets. The following day, specimens were released from the moulds and stored, until required for testing, as described below.

- All 100mm cubes were kept immersed in water at 20 °C.
- Specimens from mix R1 were divided equally into two groups. One group of specimens was stored in sealed conditions (at 20 °C); these will be referred to hereafter as the R1 specimens. Specimens from the other group, which will be denoted the R1D specimens, were initially sealed until the age of 7 days, then unsealed and left standing in laboratory air (20 °C average temperature and 60% average relative humidity). The latter method will be referred to as "dry curing".
- Specimens from all other mixes were stored in sealed conditions (at 20 °C).

The testing programme comprised six separate series of tests (Table 7.2).

Table 7.2 Details of testing programme

Test Series	Specimens			Test(s)
	Type	No. ^a	Age ^b	
I	Disk	1	28	• Penetration profile
II	Disk	2	28	• Capillary rise • Porosity
IIIA	Disk	2	28	• Capillary rise • MAT
IIIB				• Capillary rise • MAT • Resistivity • Severe drying
IV	150mm cube	2	90	• Permeability
V	100mm cube	2 2	3 28	• Compressive strength
VI	Disk	1	180	• Microstructural examination

a number of specimens tested.

b age of specimens at the commencement of testing.

Details of tests

Series I

Test details are as indicated before (6.1.2.2), with the exception that the test duration was limited to 75 days, and the temperature of the chloride solution was maintained at a higher (30°C) level.

Series II

Testing under capillary rise conditions was performed for a period of 21 days on oven-dried (until equilibrium at 105°C) specimens. Immediately afterwards, specimens were subjected to saturation (5.2.2.2.3). Finally, specimens were removed from the water tanks, surface dried, then weighed.

Series III (A and B)

Specimens were tested as received under capillary rise conditions for a period of 14 days, after which they were subjected to MAT for a further 7 days (Series IIIA). The specimens were then removed from the test trays, surface dried, and left standing in laboratory air (average temperature and relative humidity being 20°C and 60%, respectively), until they reverted to their original weight (that measured just before testing commenced). Afterwards, specimens were tested under capillary rise (for 14 days) and MAT (for 7 days) conditions. Immediately afterwards, specimens were resistivity tested (the method is described in 5.2.2.2.2, (III)), subjected to saturation, then resistivity tested again. Next, specimens were rinsed with distilled water, surface dried, weighed, then inserted into a large preheated (at 50°C and 11-14% RH) oven and weighed regularly during a period of 35 days.

Series IV

Evaluation of concrete permeability through detection of the depth of water penetration was shown in the previous phase (6.3.2) to be somewhat unreliable, primarily because of the limited accuracy with which the actual water penetration front can be located on the face of a split specimen, particularly in high-quality concrete specimens; it is noteworthy that it is for this reason that input methods have not, as yet, been implemented as a British Standard. However, it was also demonstrated (6.3.2), that by monitoring the variation in electrical resistance between a pair of embedded electrodes this weakness can be largely eradicated. This technique, however, requires further development, particularly in regard to the number, location, size, and spacing of the electrode pairs, and this was impossible to undertake within the short duration allocated to Phase 3. An alternative approach was therefore adopted. This involved direct measurement of pressure-induced chloride ingress. Specimens were assembled in test cells (of the type used in Phase 2 testing (6.1.2.1.1)) and their as cast face was pressurised with a 0.5M NaCl solution gradually (during a period of 1 hour) until a pressure of 7 Bar was reached, and the pressure was maintained at this level for 14 days. At the end of that period, all specimens were removed from the test cells, rinsed with distilled water, then split (roughly in half) perpendicular to the injected surface. One half was subsequently used to obtain powder samples at various depths from the injected face. These were stored in air-tight plastic containers and analyzed later (by potentiometric titration) for total chloride content, to produce a chloride penetration profile.

In an attempt to eliminate absorption-induced chloride ingress, specimens were subjected to saturation before being tested. Initially, it was intended to use the 150mm cubes (2 from each mix) as test specimens. However, in an attempt to facilitate saturation, the cube specimens (only 1 from each mix) were cut (using a diamond saw) approximately in half perpendicular to the trowelled surface, producing two roughly identical prisms (150mm square base and 75 ± 3 mm high), which were then saturated.

Series VI

Specimens were prepared as described before (6.1.2.2), then examined using SEM in the bse mode. The primary purpose of this examination was to determine whether the admixtures used alter the microstructural aspects which are characteristic of cement replaced concretes (as seen in 6.3.5.3). Therefore, it was considered desirable that the examination be carried out on relatively old specimens.

7.3 Results

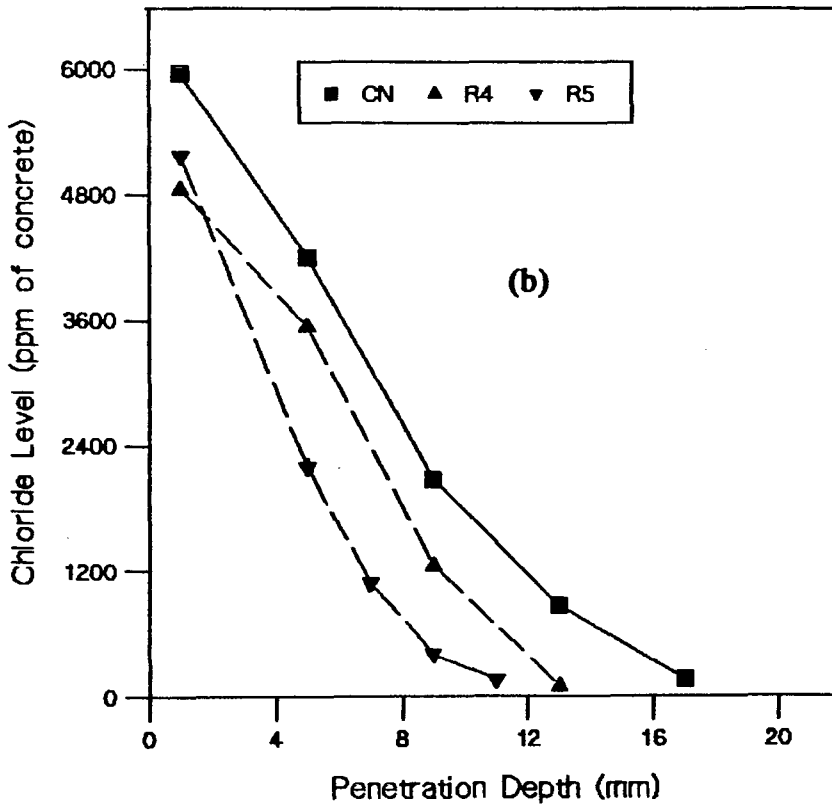
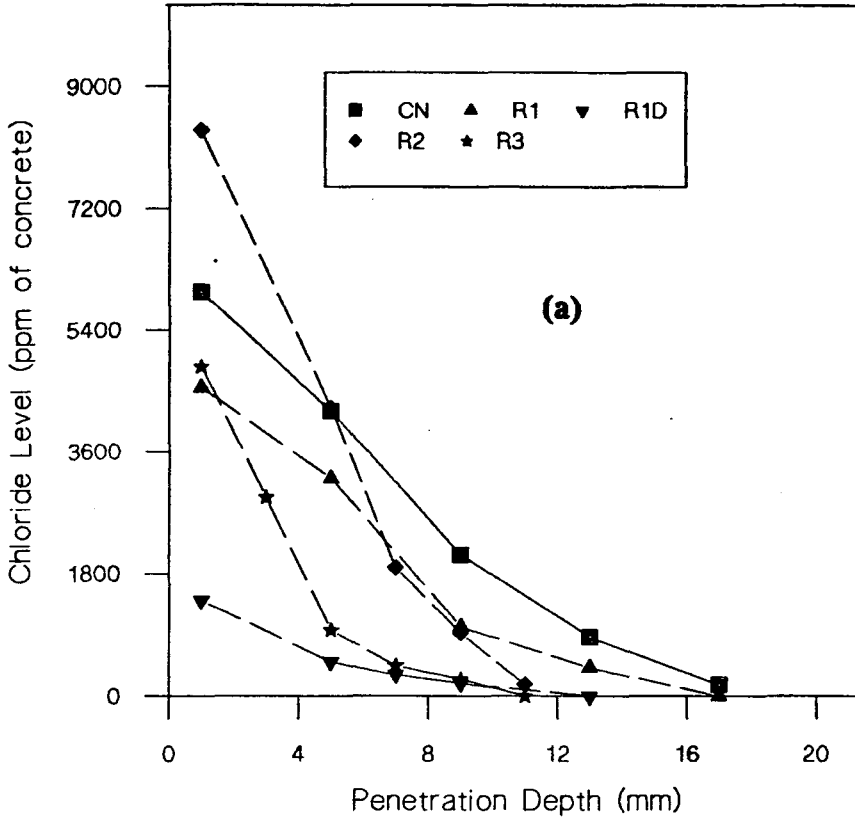
The results obtained from Series I testing are presented in Figure 7.1.

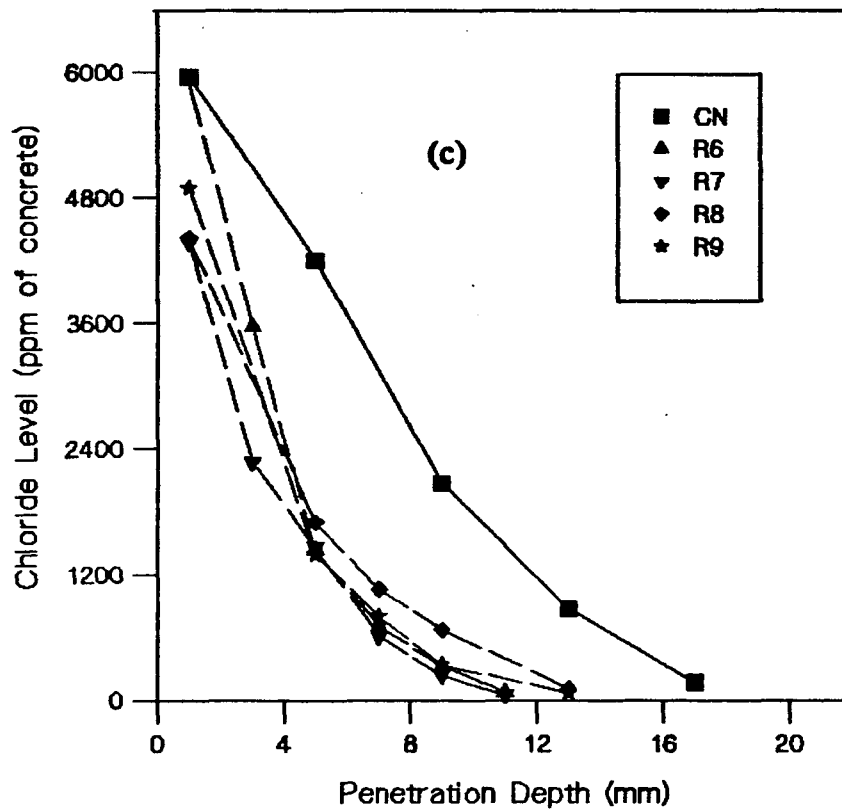
Reported in Tables 7.3 through 7.9, respectively, are the results obtained (for the Control and modified concretes) from Series II, III, IV, and V; results for the Control concrete are presented as absolute values, and modified concrete results are presented relative to the corresponding results of the Control mix, as percentage ratios.

All results presented represent an average value for the specimens tested.

Finally, presented in Figures 7.2 through 7.9 are bse images obtained at various magnifications for all mixes tested, with the exception of R6 and R7 (which were not tested due to practical difficulties). The micrographs presented show, unless otherwise stated, features which could be found throughout the microstructure.

Figure 7.1 Diffusion test results (Series I).





Mix	W/C	
CN	0.35	---
R1	0.35	5% SF + 10% ACR
R1D*	0.35	5% Sf + 10% ACR
R2	0.35	0% SF + 2% BUTST
R3	0.35	10% SF + 1% BUTST + 1% SOYO
R4	0.35	30% SF + 1% SOYO
R5	0.35	20% PFA + 5% SF + 1% SOYO
R6	0.35	65% FGGBS + 1% SOYO
R7	0.35	65% GGBS + 2% BUTST
R8	0.35	35% GGBS + 30% FGGBS + 2% BUTST
R9	0.35	35% GGBS + 30% FGGBS

* see 7.2

Table 7.3 Results of capillary rise and porosity testing (Series II)

Mix ref.	Time ^a								Porosity ^d (%)
	1hr	4hr	7hr	1d	3d	7d	14d	21d	
CN	Weight gain ^b (g)								13.0
	6.2	12.0	16.3	29.3	44.4	47.1	48.2	48.9	
	WGR ^c								PR ^e
R1	<u>22</u>	<u>21</u>	<u>19</u>	<u>17</u>	<u>16</u>	<u>20</u>	<u>24</u>	<u>27</u>	<u>62</u>
R1D	<u>39</u>	<u>31</u>	<u>28</u>	<u>23</u>	<u>21</u>	<u>25</u>	<u>29</u>	<u>32</u>	<u>60</u>
R2	<u>17</u>	<u>15</u>	<u>14</u>	<u>13</u>	<u>12</u>	<u>15</u>	<u>19</u>	<u>21</u>	<u>38</u>
R3	<u>17</u>	<u>15</u>	<u>14</u>	<u>12</u>	<u>12</u>	<u>15</u>	<u>18</u>	<u>21</u>	<u>36</u>
R4	<u>36</u>	<u>30</u>	<u>28</u>	<u>26</u>	<u>27</u>	<u>34</u>	<u>40</u>	<u>43</u>	<u>70</u>
R5	<u>38</u>	<u>30</u>	<u>26</u>	<u>23</u>	<u>22</u>	<u>27</u>	<u>31</u>	<u>35</u>	<u>70</u>
R6	<u>35</u>	<u>29</u>	<u>26</u>	<u>23</u>	<u>22</u>	<u>26</u>	<u>30</u>	<u>33</u>	<u>87</u>
R7	<u>13</u>	<u>13</u>	<u>13</u>	<u>13</u>	<u>14</u>	<u>19</u>	<u>24</u>	<u>27</u>	<u>68</u>
R8	<u>18</u>	<u>17</u>	<u>15</u>	<u>15</u>	<u>15</u>	<u>20</u>	<u>25</u>	<u>28</u>	<u>74</u>
R9	63	<u>56</u>	<u>54</u>	<u>51</u>	<u>50</u>	<u>57</u>	62	64	112*

a time after testing commenced (hr:- hours; d:- days).

b weight gain relative to the initial weight of specimens.

c percentage ratio of weight gain of mix relative to that of the Control.

d effective porosity (of 105°C-dried specimens).

e percentage ratio of porosity result for mix relative to that of the Control.

Table 7.4 Results of capillary rise testing and MAT (Series IIIA)

Mix ref.	Time ^a						
	1hr	7hr	1d	3d	14d	18d	21d
	Weight gain ^b (g)						
CN	0.3	0.8	1.35	2.05	3.8	4.9	5.4
	WGR ^c						
R1	233*	169*	137	107	92	102	100
R1D	567*	400*	322*	268*	203*	210*	202*

a time after testing commenced.

b weight gain relative to the initial weight of specimens.

c percentage ratio of weight gain of mix relative to that of the control.

Measurements were not made on other modified concretes as they were not thought to be informative (see 6.3.2).

Table 7.5 Results of capillary rise testing, MAT, and saturation (Series IIIB)

Mix ref.	Time ^a								
	1hr	7hr	1d	3d	7d	14d	18d	21d	23d [#]
	Weight gain ^b (g)								
CN	0.6	1.1	1.6	2.3	3.2	4.1	5.5	5.6	7.2
	WGR ^c								
R1	108	105	94	89	84	81	83	85	79
R1D	125\$	123\$	119\$	107\$	98\$	94\$	98\$	101\$	105\$
R2	<u>34</u>	<u>33</u>	<u>33</u>	<u>34</u>	<u>34</u>	<u>33</u>	<u>31</u>	<u>31</u>	<u>37</u>
R3	<u>26</u>	<u>29</u>	<u>27</u>	<u>28</u>	<u>29</u>	<u>28</u>	<u>29</u>	<u>30</u>	<u>35</u>
R4	<u>50</u>	<u>50</u>	<u>47</u>	<u>48</u>	<u>52</u>	<u>53</u>	<u>55</u>	<u>57</u>	<u>71</u>
R5	<u>42</u>	<u>41</u>	<u>41</u>	<u>48</u>	<u>45</u>	<u>44</u>	<u>43</u>	<u>46</u>	<u>49</u>
R6	<u>50</u>	<u>50</u>	<u>50</u>	<u>48</u>	<u>52</u>	<u>52</u>	<u>50</u>	<u>54</u>	92
R7	<u>48</u>	<u>47</u>	<u>50</u>	<u>51</u>	<u>50</u>	<u>53</u>	<u>55</u>	<u>57</u>	141*
R8	<u>33</u>	<u>45</u>	<u>44</u>	<u>41</u>	<u>44</u>	<u>44</u>	<u>43</u>	<u>44</u>	95
R9	158*	147*	137	126	114	105	93	95	177*

a time after testing commenced.

b weight gain relative to the initial weight of specimens.

c percentage ratio of weight gain of mix relative to that of the Control.

after saturation.

\$ data are not directly comparable with control since specimens were not dried to original weight; drying was extremely slow and the water uptake during Series IIIA was large.

Table 7.6 Results of resistivity testing (Series IIB)

Mix ref.	RS _{bs} # (Ωm)	RS _{ss} \$ (Ωm)
CN	173	160
RSR@		
R1	<u>381</u>	<u>373</u>
R1D	<u>451</u>	<u>452</u>
R2	<u>632</u>	<u>622</u>
R3	<u>870</u>	<u>831</u>
R4	<u>181</u>	<u>177</u>
R5	<u>481</u>	<u>486</u>
R6	<u>581</u>	<u>516</u>
R7	<u>540</u>	<u>404</u>
R8	<u>530</u>	<u>462</u>
R9	<u>488</u>	<u>334</u>

resistivity measured before specimens were subjected to saturation (converted to equivalent value at 20°C (A3.1)).

\$ resistivity measured after specimens were subjected to saturation (converted to equivalent value at 20°C (A3.1)).

@ percentage ratio of the resistivity of mix relative to that of the control.

Table 7.7 Results of severe drying testing (Series IIIB)

Mix ref.	Time ^a						
	3hr	6hr	1d	5d	14d	21d	35d
CN	Weight loss ^b (g)						
	4.5	6.1	11.1	19.9	28.1	30.0	36.4
	WLR ^c						
R1	<u>79</u>	<u>74</u>	<u>73</u>	<u>83</u>	<u>72</u>	<u>74</u>	<u>76</u>
R1D	---	---	---	---	---	---	---
R2	<u>87</u>	<u>84</u>	<u>86</u>	<u>72</u>	<u>83</u>	<u>83</u>	<u>87</u>
R3	<u>74</u>	<u>74</u>	<u>73</u>	<u>72</u>	<u>73</u>	<u>80</u>	<u>79</u>
R4	107	105	100	97	96	96	96
R5	93	<u>87</u>	<u>82</u>	<u>81</u>	<u>76</u>	<u>82</u>	<u>85</u>
R6	100	96	94	93	94	96	99
R7	140*	135*	126*	119*	116*	117*	116*
R8	113*	112*	110	106	105	106	107
R9	97	102	101	102	103	104	108

a time after testing commenced.

b weight loss relative to the initial weight of specimens.

c percentage ratio of weight loss of mix relative to that of the Control.

Table 7.8 Results of permeability testing (Series IV)

Mix ref.	Total chloride content (ppm of concrete)		
	Penetration depth band (mm)		
	2-4	12-14	22-24
CN	2021	441	75
	CIR [#]		
R1	<u>44</u>	<u>53</u>	184*
R1D	<u>50</u>	<u>55</u>	126
R2	<u>54</u>	<u>71</u>	81
R3	<u>45</u>	85	109
R4	137	246*	901*
R5	106	162*	431*
R6	90	291*	953*
R7	99	189	450*
R8	87	188*	693*
R9	81	<u>59</u>	135

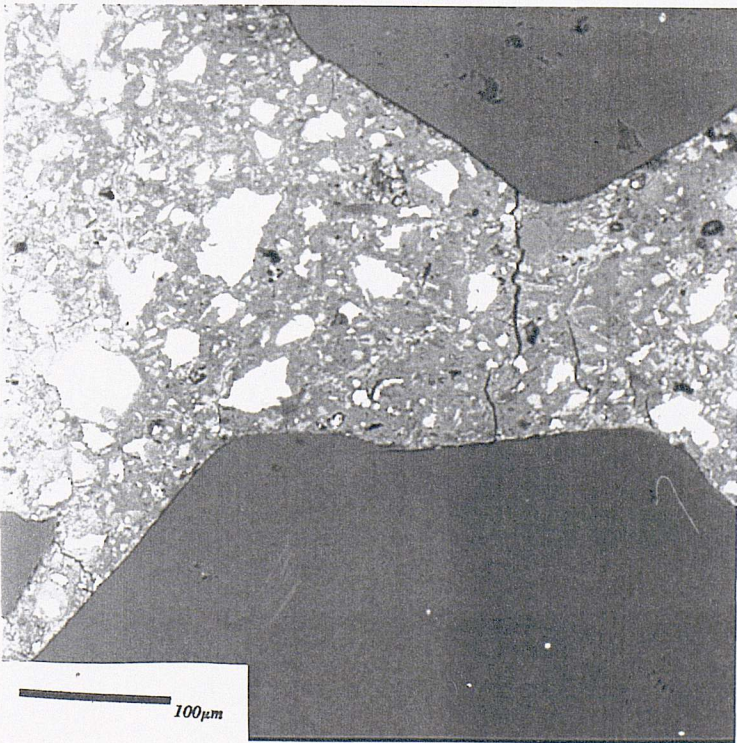
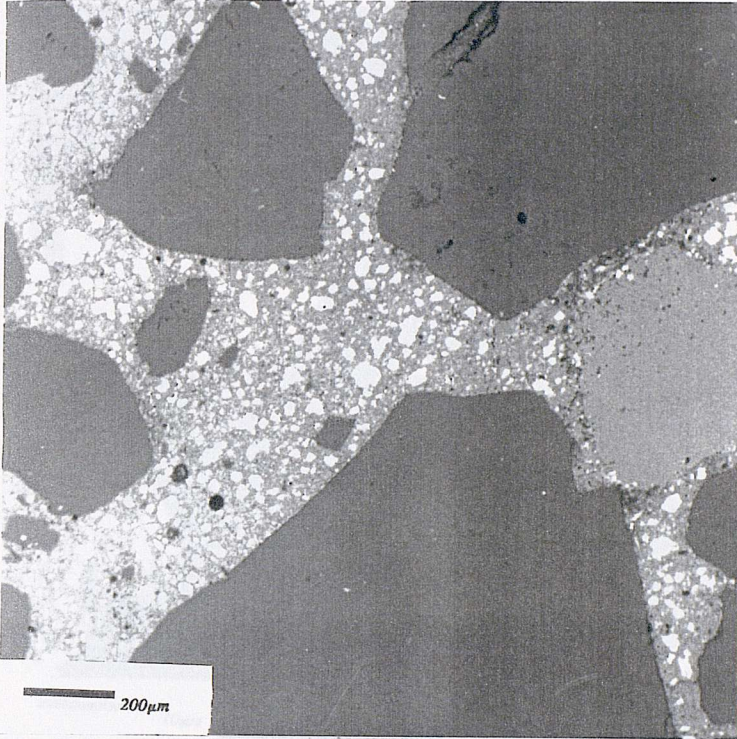
percentage ratio of result for modified mix relative to the corresponding result for the control.

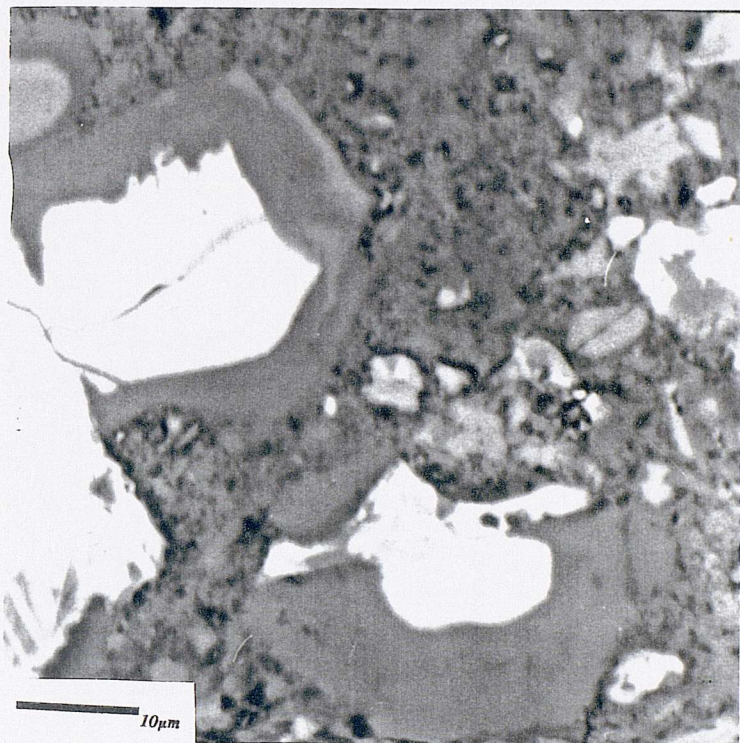
Table 7.9 Results of compressive strength testing (Series V)

Mix ref.	Compressive strength (MPa)	
	3d	28d
CN	48	70
	SR [#]	
R1	58*	58*
R2	69*	76*
R3	77*	89
R4	56*	69*
R5	66*	71*
R6	39*	76*
R7	25*	64*
R8	32*	69*
R9	39*	83*

percentage ratio of the compressive strength relative to the control.

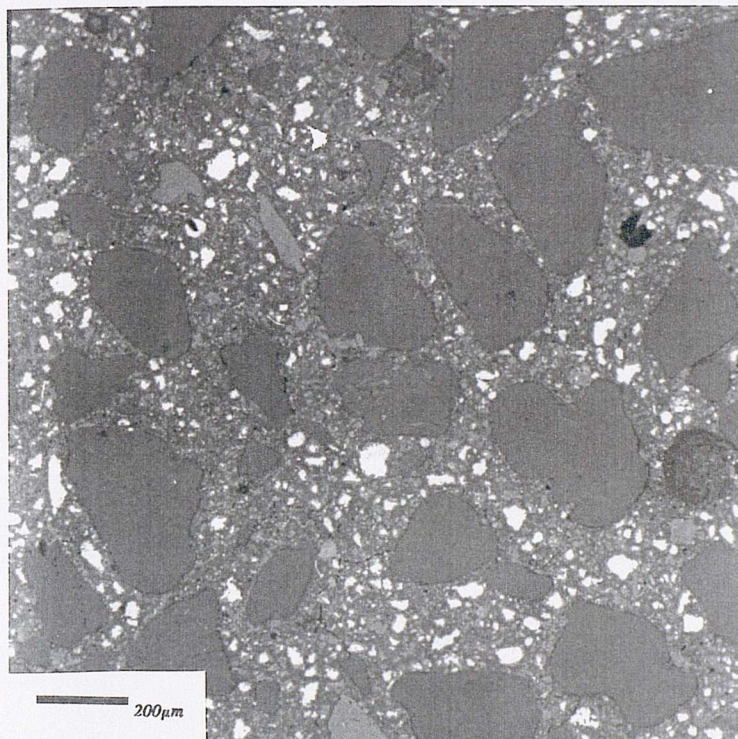
Figure 7.2 Bse images (mix CN (Control), w/c 0.35).



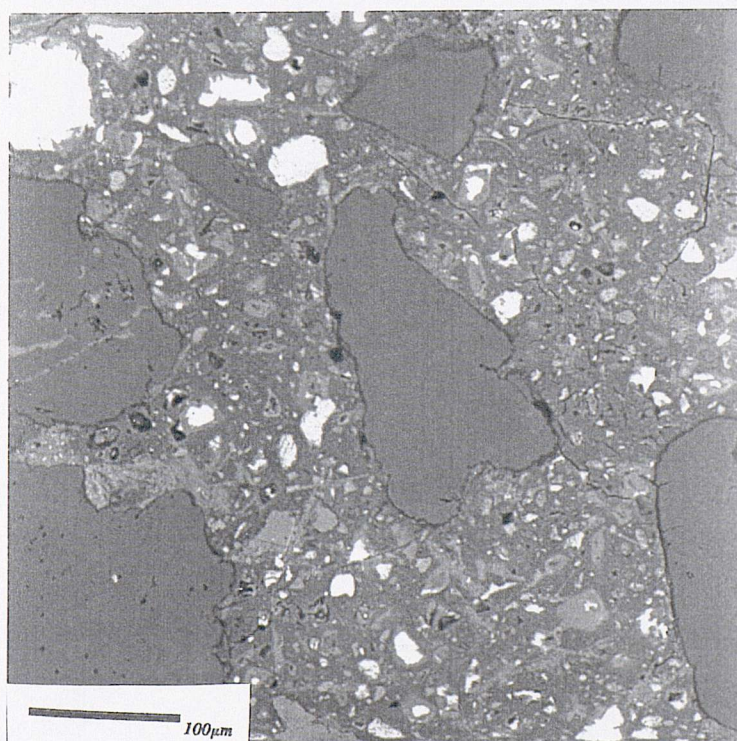


(c) microstructure at high magnification

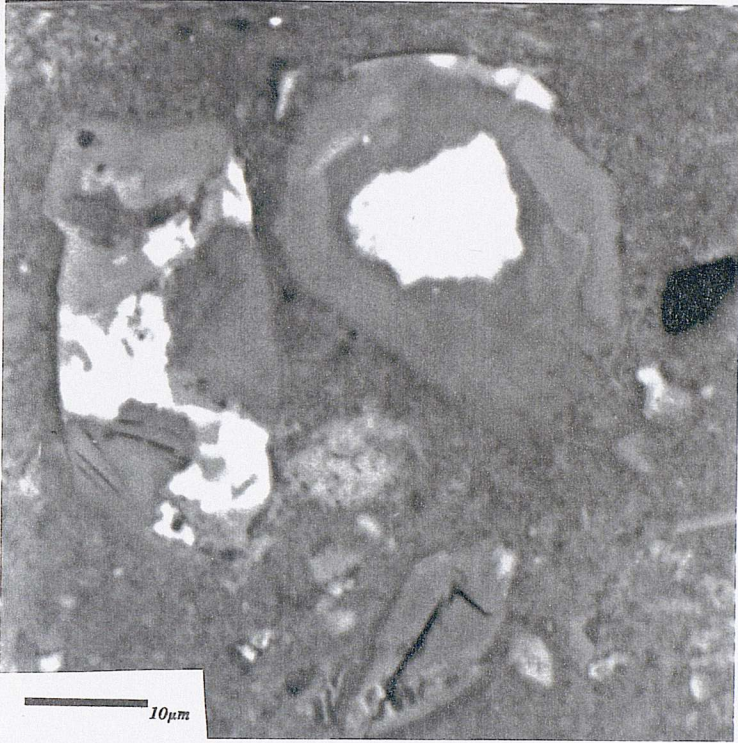
Figure 7.3 Bse images (mix R1 (5% SF and 10% Acrylic), w/c 0.35).



(a) general view of microstructure

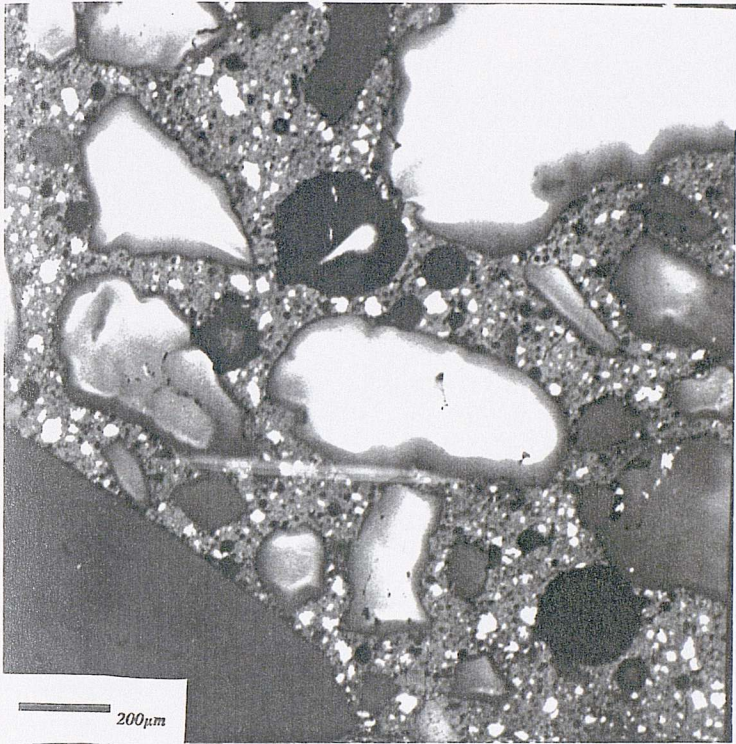


(b) microstructure at low magnification



(c) microstructure at high magnification

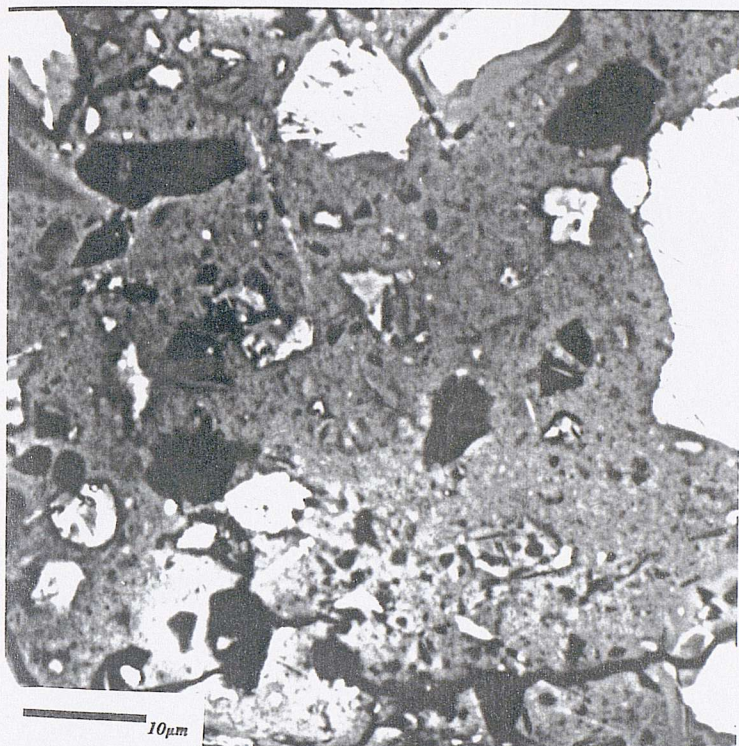
Figure 7.4 Bse images (mix R2 (10% SF and 2% Butyl stearate), w/c 0.35).



(a) general view of microstructure

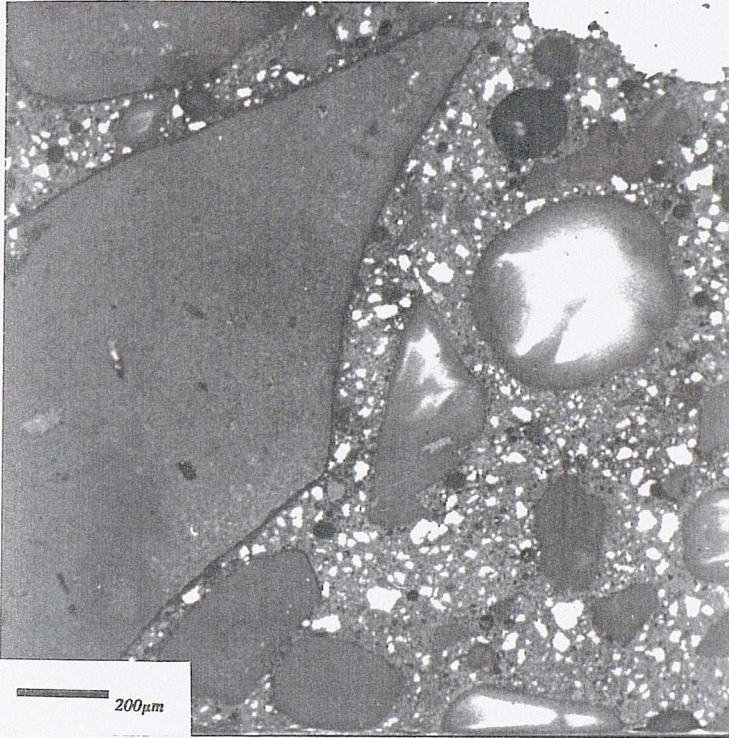


(b) microstructure at low magnification

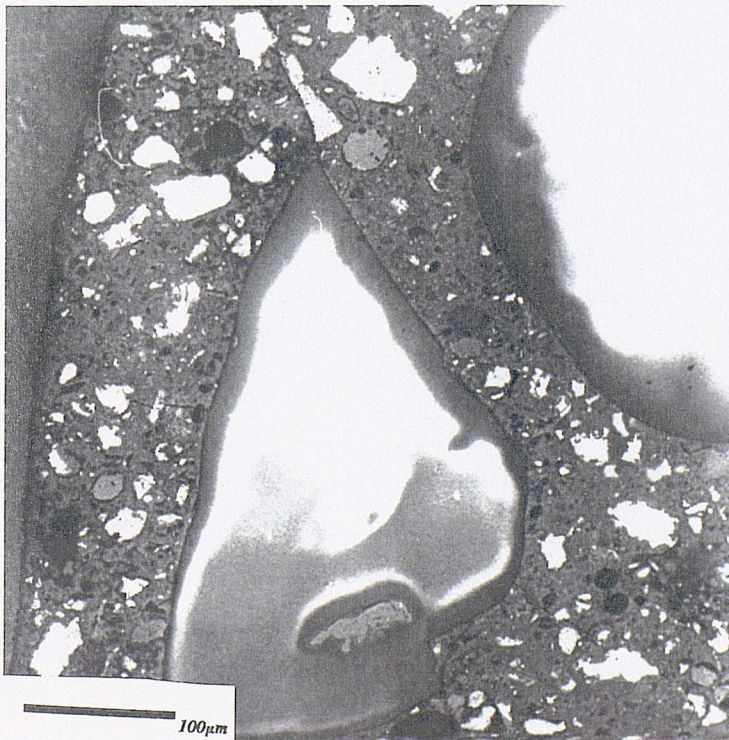


(c) microstructure at
high magnification

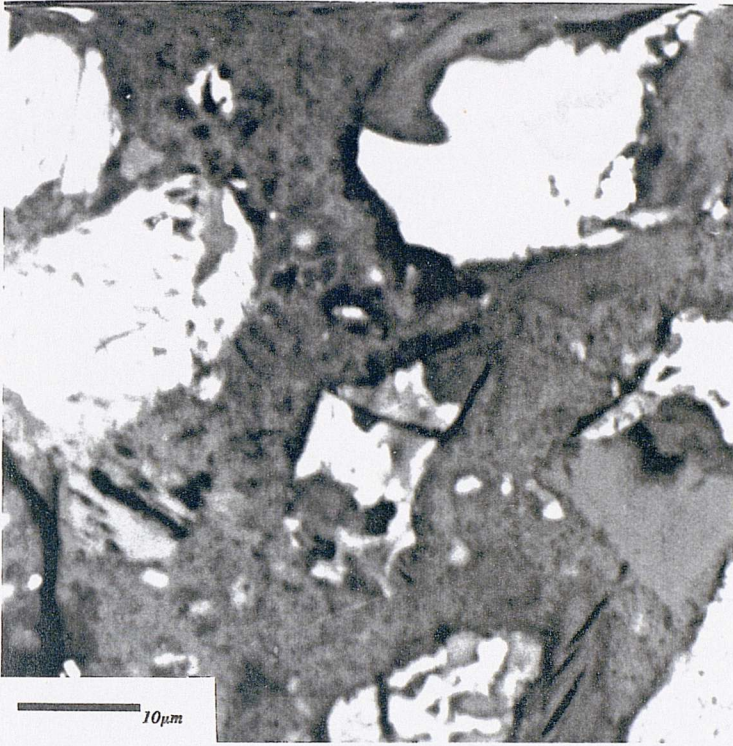
Figure 7.5 Bse images (mix R3 (10% SF, 1% Butyl stearate, and 1% Soyabean oil), w/c 0.35).



(a) general view of microstructure



(b) microstructure at low magnification

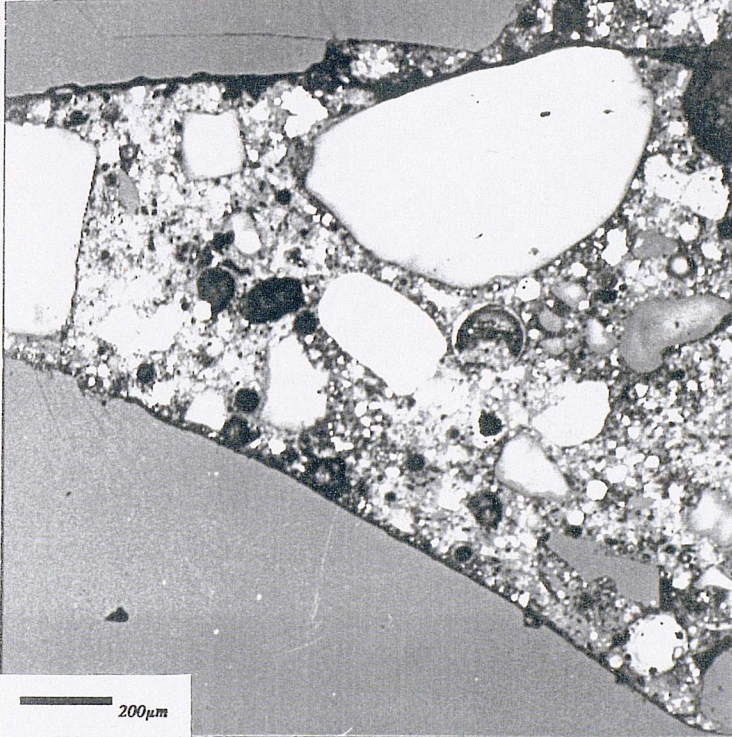


(c) low porosity area
(high magnification)

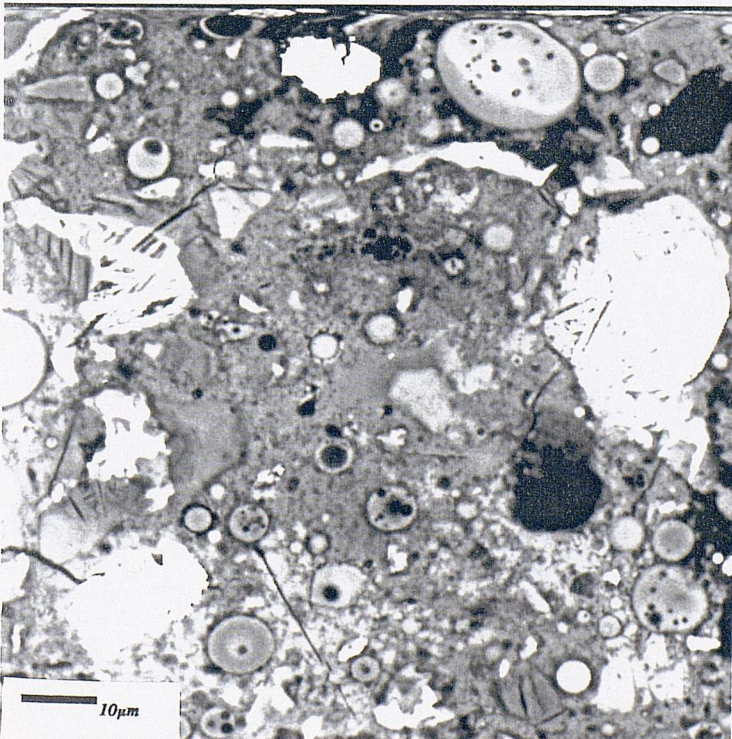


(d) high porosity area
(high magnification)

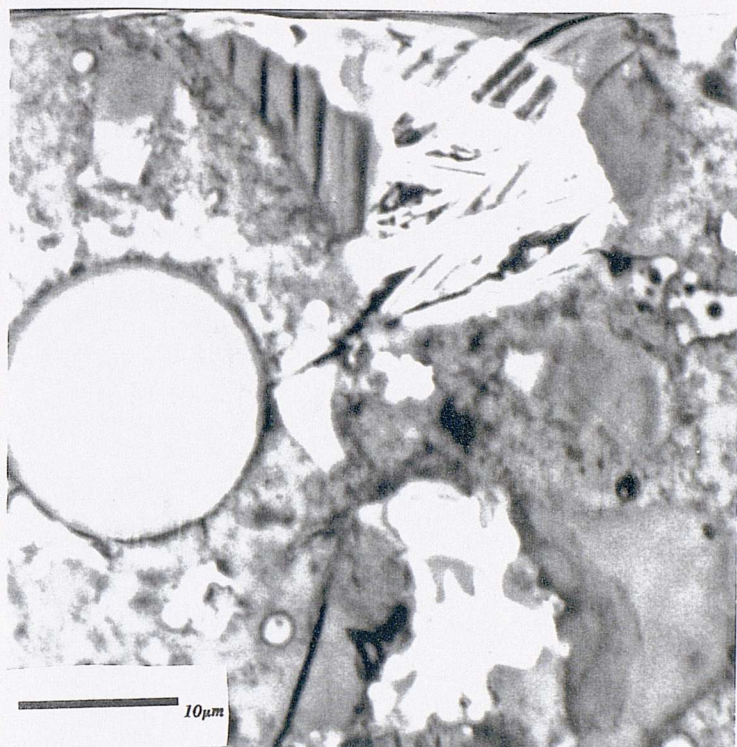
Figure 7.6 Bse images (mix R4 (30% PFA and 1% Soyabean oil, w/c 0.35).



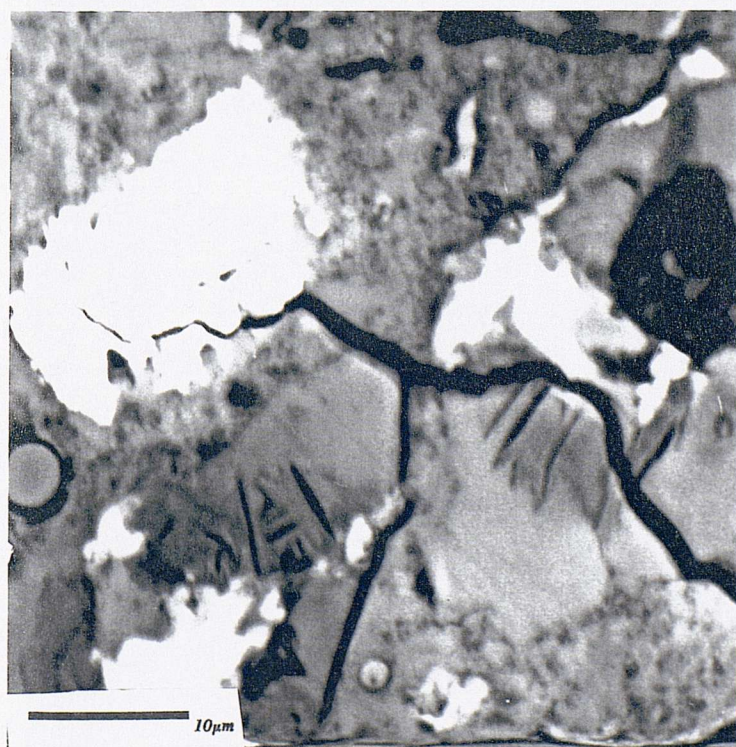
(a) general view of microstructure



(b) extent of PFA hydration

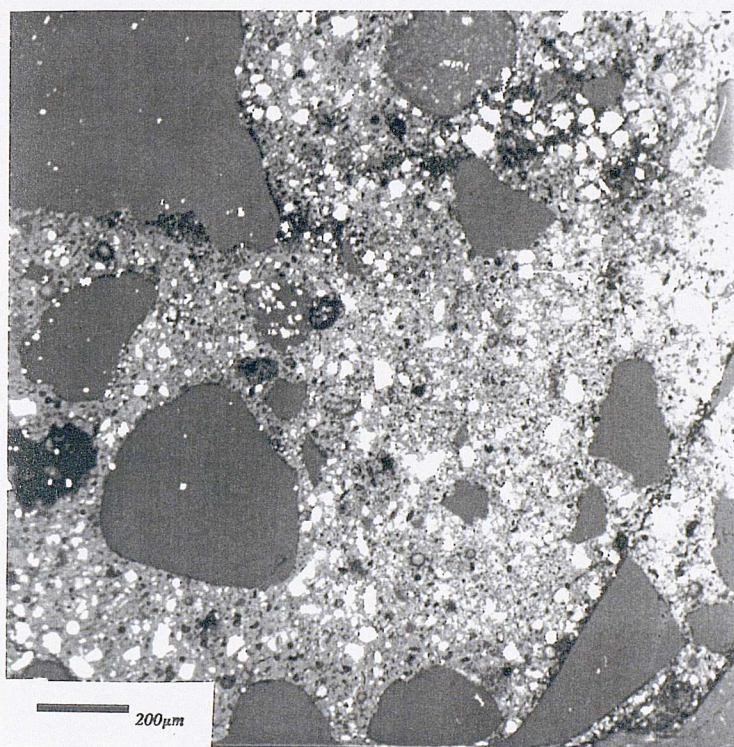


(c) microstructure at
high magnification

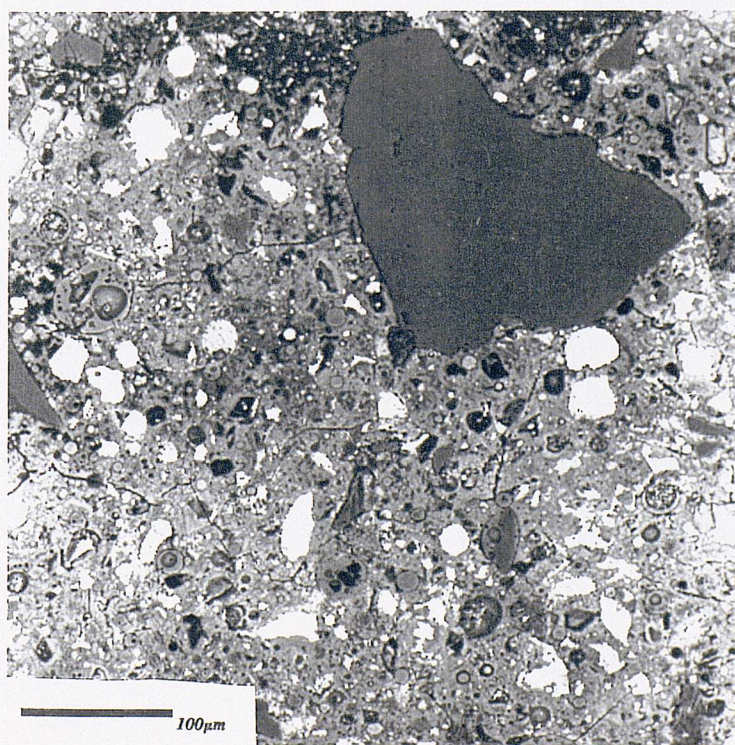


(d) microstructure at
high magnification

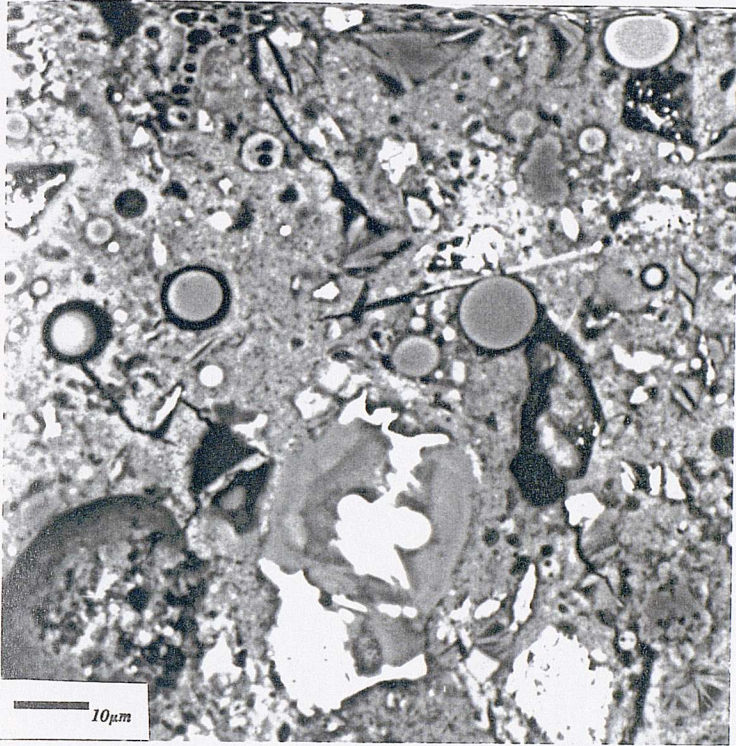
Figure 7.7 Bse images (mix R5 (5% SF, 20% PFA, and 1% Soyabean oil), w/c 0.35)



(a) general view of microstructure



(b) microstructure at low magnification

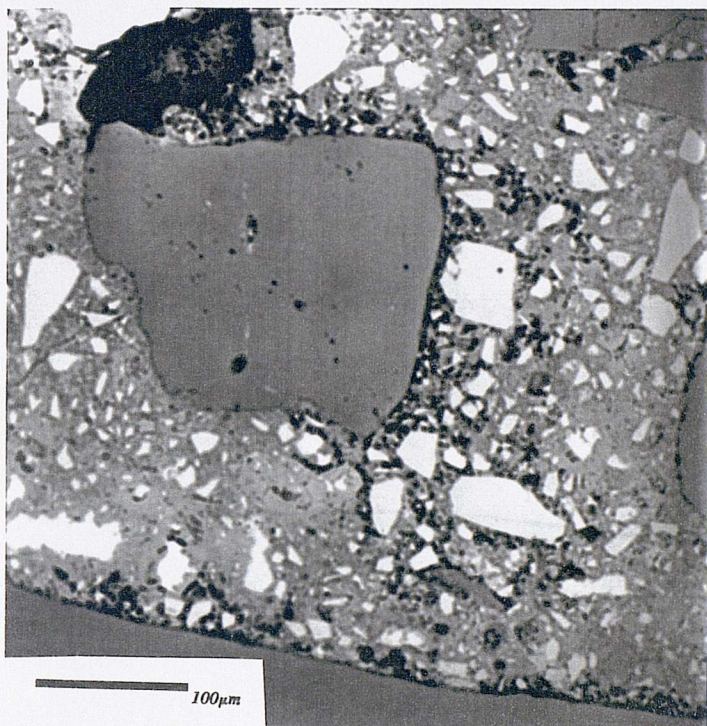


(c) extent of PFA hydration

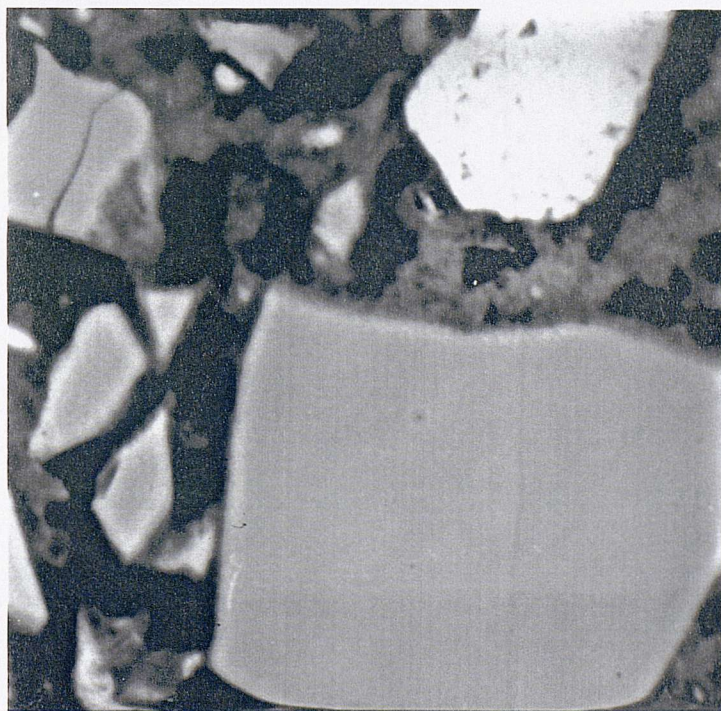


(d) microstructure at high magnification

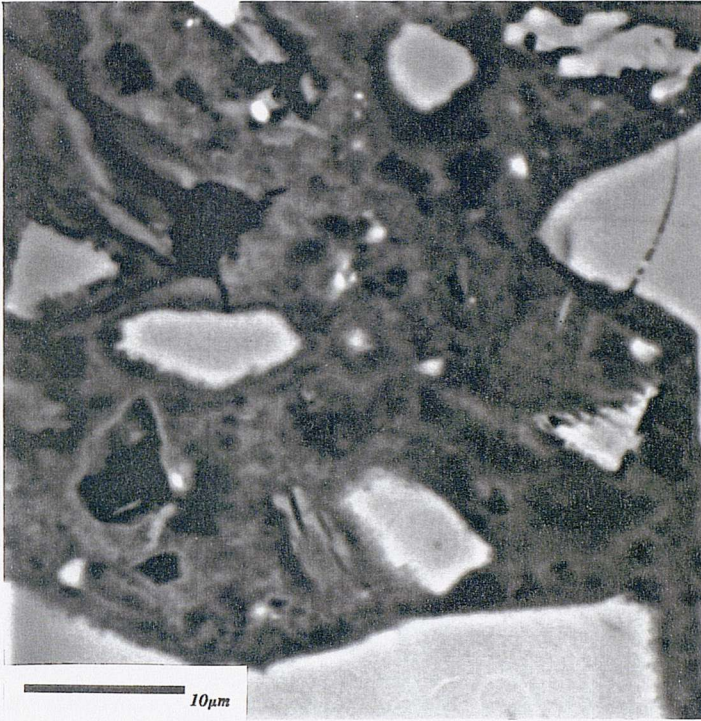
Figure 7.8 Bse images (mix R8 (35% GGBS, 30% FGGBS, and 2% Butyl stearate, w/c 0.35)



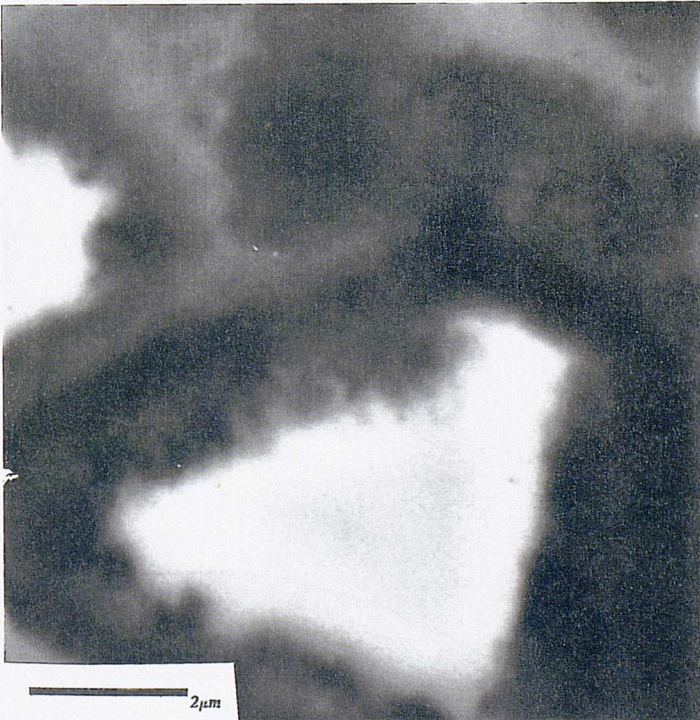
(a) microstructure at low magnification



(b) high porosity area (high magnification)

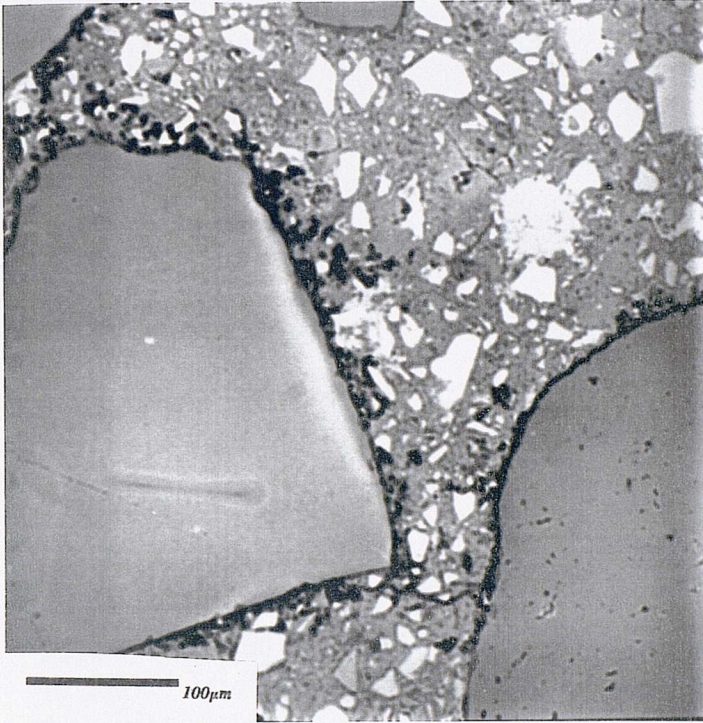


(c) low porosity area
(high magnification)

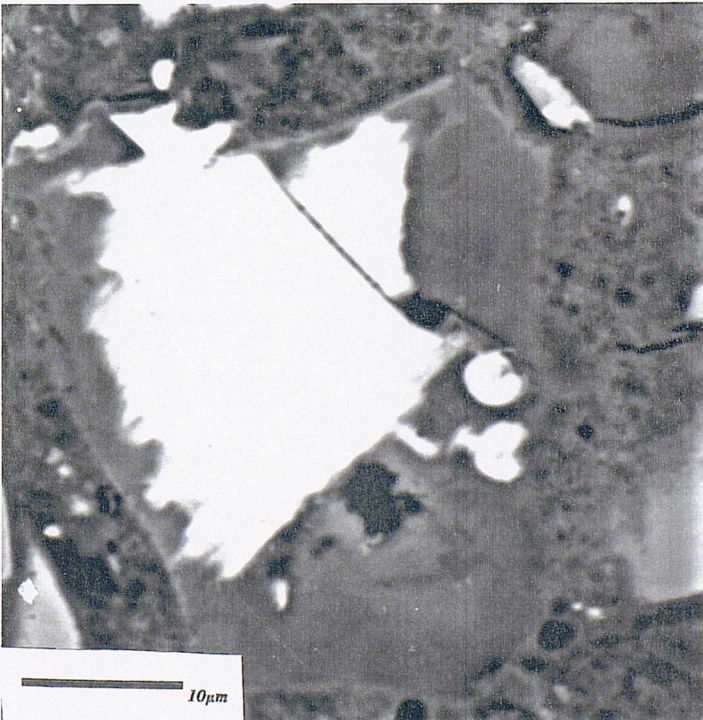


(d) well hydrated
slag grain
(fairly high
magnification)

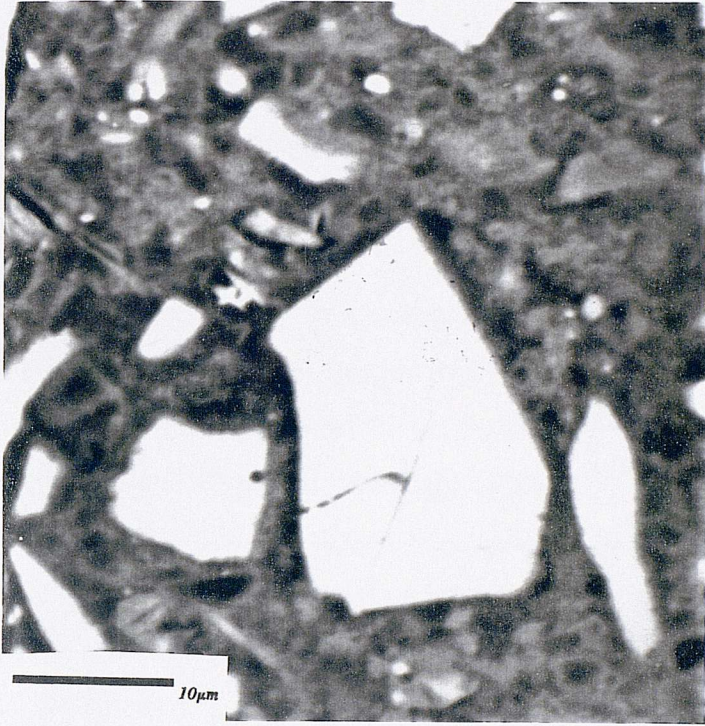
Figure 7.9 Bse images (mix R9 (35% GGBS and 30% FGGBS, w/c 0.35).



(a) microstructure at low magnification



(b) microstructure at high magnification



(c) microstructure at
high magnification

7.4 Discussion

7.4.1 Acrylic-modified mix

Before proceeding, to discuss the performance of the acrylic modified mix in the hardened state, it is important to remark on the properties of the mix in the fresh state.

Following compaction, it was standard practice to allow the bleed water to evaporate off the trowelled surface of specimens, by leaving the specimens standing in laboratory air, before covering them with wet burlap and polythene sheets. This process was observed to lead to plastic shrinkage cracking on the R1 specimens, after only 10 minutes of air exposure. It is generally believed that plastic shrinkage cracking is likely to occur when the rate of water evaporation is such that water loss from the exposed surface cannot be compensated by rising bleed water. No such cracking was observed in any of the other concretes prepared at this stage, nor those prepared before (in Phase 2), and this suggests that the cracking cannot be attributed to the specimens being subjected to excessively harsh drying. Moreover, since no cracking was observed when silica fume and the acrylic latex were used separately (in Phase 2), it is likely that the phenomenon is associated with some combined effect of the two materials. It is reported (Dennis 1988) that in latex-modified mortars, and if water is lost from the surface quicker than it can be replaced from the mortar below, polymer particles coalesce at the surface of the mortar thereby forming a polymer skin "skinning effect", and surface cracking occurs almost simultaneously. The incorporation of silica fume in OPC concrete is known (e.g. Jahren 1983) to reduce bleeding substantially. It is conceivable, therefore, that the incorporation of silica fume in the latex-modified concrete promotes the cracking and skinning process. Practical experience with latex-modified mortars (Dennis 1988) indicates that the skinning effect renders re-trowelling ineffective in closing the drying cracks (any attempt to re-trowel a skinned surface leads to further cracking), and this was actually experienced when an attempt was made to re-trowel one of the R1 specimens (this specimen was discarded afterwards).

In view of the above, mix R1 would be impractical for conventional in situ construction, and this calls into question the value of testing the hardened concrete. Nonetheless, a decision was made to proceed with testing. This was because it was felt that it would still be possible to compare the performance of the acrylic-modified mix under conditions of sealed curing as against air curing, by comparing corresponding results for specimens R1 and R1D (see 7.1 and 7.2). Comparing chloride penetration for specimens R1 and R1D (in Figure 7.1a) shows that dry curing improves diffusion resistance substantially. Indeed, R1D seems to be the least penetrable of all mixes tested. This trend, however, is not mirrored in the results of other tests. The results in Table 7.4 show that the rate of water uptake in specimens R1D is appreciably higher than that of R1. This indicates that any beneficial effect of air drying on polymer film formation was largely negated by the associated adverse effects, viz: i) increasing the volume of empty pore space, ii) increasing the strength of capillary forces, iii) reduced cement hydration, hence, pore structure coarsening, and iv) increasing the intensity of microcracking. The results in Table 7.3 show that oven-dried R1 and R1D specimens, in contrast to specimens tested as received, are of markedly superior absorption resistance to the Control specimens, this being most certainly due to polymer film formation aided by oven drying. It is interesting to note that the effect of dry curing, in terms of a reduction of cement hydration, is nonetheless still apparent: the initial water uptake of specimens R1D is almost double that of R1, the difference exhibiting a tendency to narrow steadily with the progress of testing. Permeability test results show (see Table 7.8 and Figure 7.10) that chloride had penetrated specimens R1 and R1D in amounts substantially lower than in the Control at shallow (2-4mm) and intermediate penetration depths (12-14mm). However, at greater depths, the chloride level is almost double that of the Control in the case of R1 specimens and marginally higher in the case of R1D. One possible explanation for this may be that i) the total volume of penetrable porosity in R1 and R1D is markedly lower than that of the Control, but ii) some proportion of that porosity is of larger size, compared to the penetrable porosity of the Control concrete, or that microcracking was (in R1 and R1D) more intense than in the Control. SEM lends support to the first proposition (compare Figures 7.2c and 7.3c), but not to the second. It should be noted, however, that SEM

Mix	W/C	
CN	0.35	---
R1	0.35	5% SF + 10% ACR
R1D*	0.35	5% Sf + 10% ACR

* see 7.2

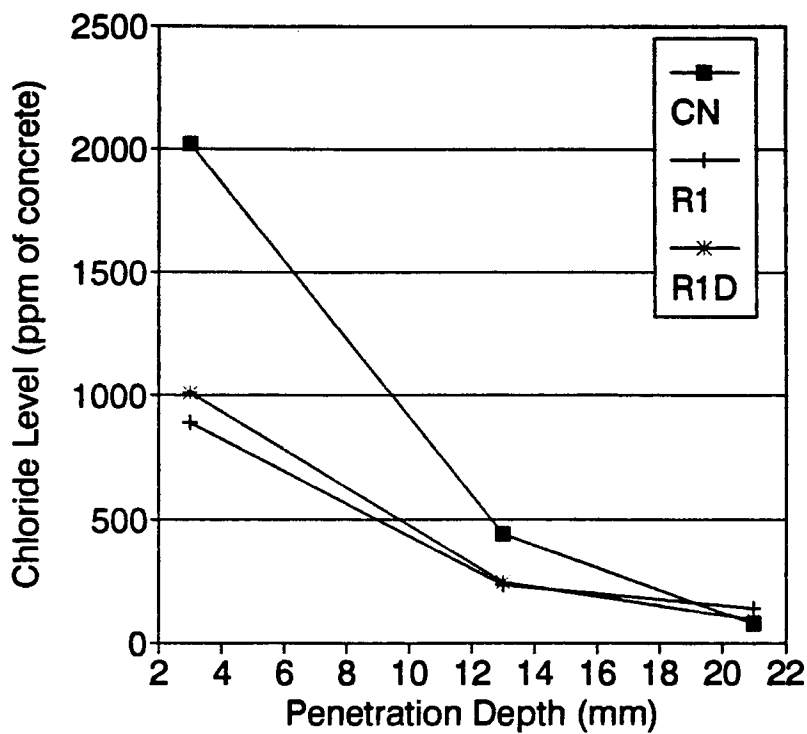


Figure 7.10 Pressure-induced chloride penetration (acrylic-modified concretes).

analysis is performed on relatively small samples and it is conceivable that these may not be entirely representative of the water permeability test specimens. It is worth noting that differences in chloride ingress between R1D and R1 specimens are relatively small and only manifest at the deep part of the penetration front. This, however, demonstrates how the adverse effects associated with air drying (the R1D specimens) were negated by the presence of polymer films (unmodified OPC concrete treated identically to R1D would exhibit much higher permeability than the parallel sealed-cured concrete).

It is interesting to observe that R1D performs substantially better than R1 in resisting chloride ion diffusion (Figure 7.1a), yet shows similar performance in resisting pressure-induced water flow (Figure 7.10). One possible explanation is that the process of polymer film formation involves, as well as the physical coalescence of polymer microparticles (Figure 6.49), chemical reactions which result in alterations to pore solution composition. Another is that the formation of polymer films on pore walls alters the electrochemical interactions between the diffusing ions and pore walls. These propositions appear plausible since the induced effects, whilst affecting ion diffusion (see 3.6.2), would be expected to have little influence on pressure-induced water flow. A third possibility is that polymer films, which form across pore walls, hinder ion diffusion, but rupture under the applied water pressure (7 bar) in the permeability test. The hypothesis above may be evaluated by performing the following tests: i) determining the conductivity of pore solutions expressed from parallel specimens of R1 and R1D before and following diffusion testing, ii) comparing the relative performance of R1 and R1D under varying pressure levels (say from 1.5 to 10 bar) in the water permeability test.

7.4.2 Water repellent-modified mixes

7.4.2.1 General

The aim of testing the water repellent-modified mixes was two-fold. First, to investigate how the performance of cement replaced concretes containing water repellents compares with that of a practical OPC concrete of low water/cement ratio. For that purpose, the Control concrete (mix CN) was tested along with the modified concretes; results as reported in Section 7.3 are thus directly applicable in this context (in Tables 7.3 through 7.9, modified concrete results which indicate favourable performance are presented in highlighted underlined text and those which suggest adverse behaviour are emphasised by a highlighted asterisk). Second, to investigate whether the admixtures are compatible with cement replaced concretes, i.e. whether they increase the absorption resistance of cement replaced concrete without reducing its ability to resist chloride ion diffusion. Ideally, for this purpose, parallel cement replaced concretes containing no water repellents would be tested along with the modified concretes. However, this approach was not followed due to unanticipated practical difficulties, and it was decided to rely instead on an indirect approach, by using the results obtained for the cement replaced concretes of Phase 2 (i.e. mixes 4 (GGBS65(0.4)), 5 (PFA30(0.4)) and 6 (SF10(0.4)+), see 6.1.1.2.2).

7.4.2.2 Silica fume concretes

The results of diffusion testing (Figure 7.1a) show that R3 offered substantially higher resistance to chloride diffusion, compared with CN. In this respect, the performance of R3 parallels in large measure that of the unmodified silica fume mix of phase 2 (mix 6 (SF(0.4)+)) and, therefore, it is safe to conclude that butyl stearate and soyabean oil when used in combination had little influence on the ability of silica fume concrete to resist chloride diffusion. As for mix R2, it is apparent the chloride had not penetrated deeply, although chloride levels at shallow depths (<5mm) are higher than those of CN. Indeed, similar to R3, R2 exhibits essentially no chloride ingress at depths greater than 9mm.

The results in Table 7.2 show that water uptake in both the R2 and R3 specimens was extremely small, in comparison with CN, during the entire test duration, and even after "saturation" (this relates to the effective porosity after drying). The effectiveness of the water repellents used, in increasing the absorption resistance of silica fume concrete, can be gauged by comparing the graphs relating to R2 and R3 with that of mix 6 (see Figure 7.11). It may be argued, at first sight, that such comparison would be biased in favour of R2 and R3 since mix 6 was of higher (0.4 compared to 0.35) water/cement ratio. However, it is also to be recalled that mix 6 was dried less harshly (50°C & 11-14% RH as against 105°C) and was sealed-cured for a longer period (90 days as against 28 days) before testing. Figure 7.12 demonstrates the relative effects of these factors by comparing the absorption behaviour of the control concretes C1 and C2 (of Phase 2) with that of CN. It is immediately obvious that the graph relating to CN lies well above that of C2, and, in fact, above that of C1. This indicates that the effect of testing at an earlier age combined with more severe drying largely outstrips that of the change in water/cement ratio. It is therefore safe to conclude that the water repellents improve markedly the absorption resistance of silica fume concrete. It is also interesting to compare, as is demonstrated in Figure 7.11, the performance of R2 and R3 with that of mix 24 (of Phase 2, 0.35 w/c, see 6.1.1.2.7), prepared with Everdure Caltite, a widely specified waterproofer.

Mix	W/C	
6	0.4	10% SF
24	0.35	30 l/m ³ Everdure Calcite
R2	0.35	10% SF + 2% BUTST
R3	0.35	10% SF + 1% BUTST + 1% SOYO

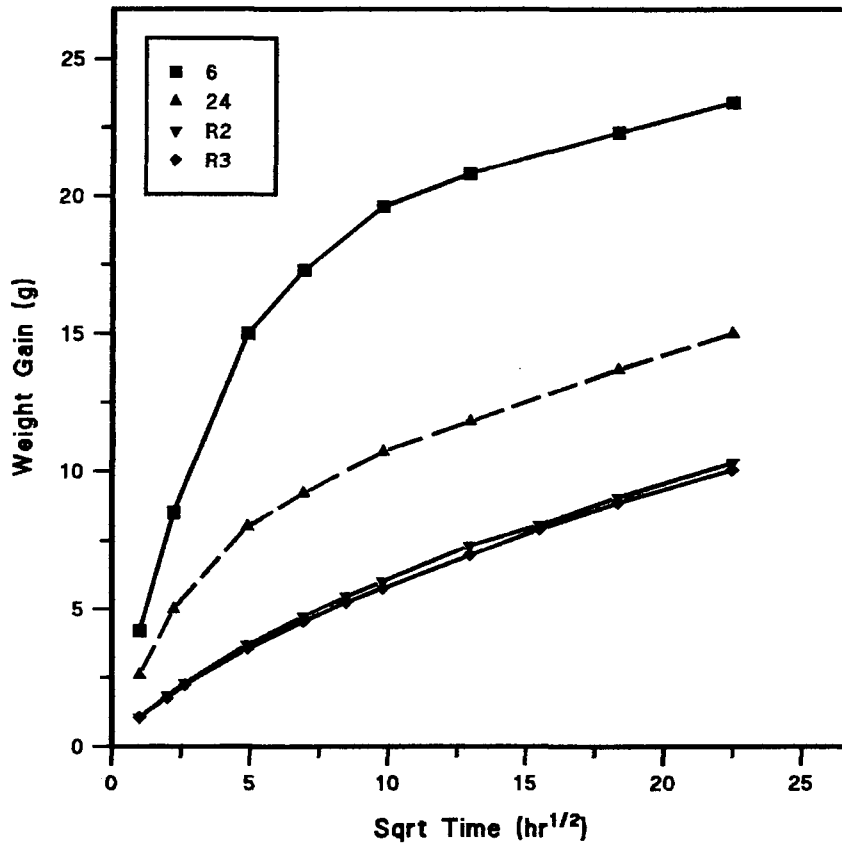


Figure 7.11 Absorption behaviour of silica fume concretes.

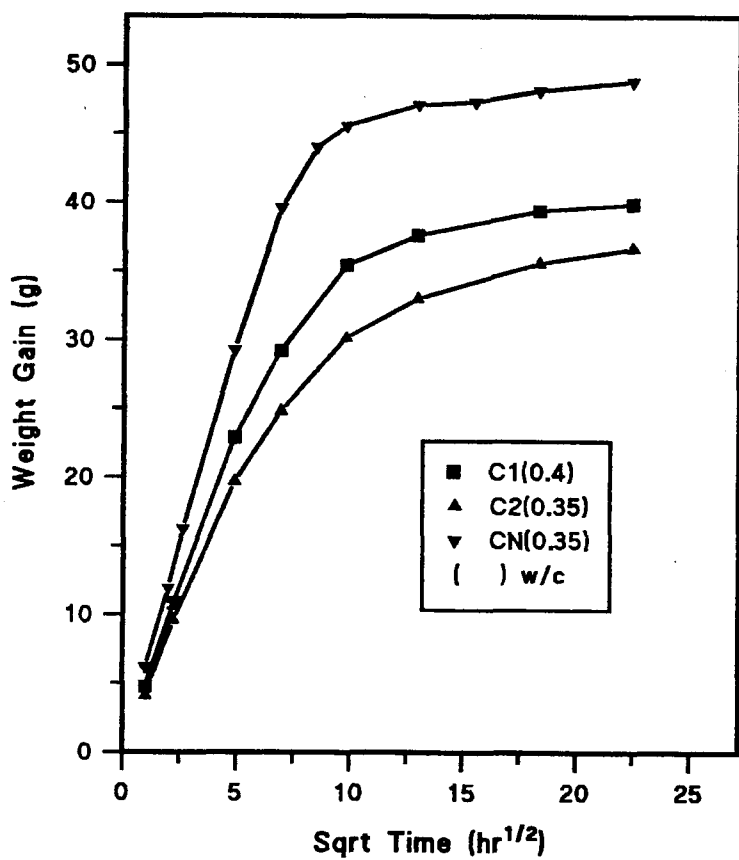


Figure 7.12 Absorption behaviour of control concretes.

It is worthwhile to consider at this stage the results of SEM on R2 and R3. At low magnifications R2 appears much less dense than CN (compare Figures 7.2a and b respectively with Figures 7.4a and b), due, primarily, to the presence of a large proportion of relatively large isolated porosity. The aggregate interface also seems inferior to that of CN, as some of the large voids appear to rest on the boundaries of the aggregate particles. However, at high magnifications (see Figure 7.4c) R2 appears to have a microstructure typical of silica fume concrete (see 6.3.5.3) and the large voids appear to be completely isolated by extremely dense paste. Comparing Figures 7.5a and b with Figures 7.2a and b reveals that R3 is also less dense than CN, though, apparently, to a lesser extent than R2. This is due, primarily, to the presence of highly porous areas which seem to form more frequently in the vicinity of the aggregate. Figure 7.5c shows that the paste in R3 is also typical of silica fume mixes, the highly porous areas (see Figure 7.5d) excepted. Finally, it is important to note that Ca(OH)_2 , which is apparently present in large quantities in CN, cannot be detected in images of both R2 and R3, and this furnishes indirect evidence that the admixtures do not hinder silica fume reaction.

There are other aspects of the performance of R2 and R3 that merit consideration. The results in Table 7.6 indicate that the electrical resistivity of R2 and R3 are more than 6-fold higher than that of CN and that this trend was apparent even after specimens were saturated. The results of severe drying (Table 7.7) suggest that R2 and R3 will dry, after a long wet cycle, to a somewhat lesser extent than CN, and this notably contrasts with the behaviour of the water repellent mixes of Phase 2 (see 6.3.2). Finally, permeability testing (Table 7.8 and Figure 7.13) confirms that R2 and R3 possess a smaller proportion of penetrable porosity than CN, this being characteristic of silica fume modified concrete (see 6.3.2 and 6.4), but that some proportion of this porosity, particularly in R3, and as SEM suggests, is of relatively large size, compared with the penetrable porosity of CN.

Mix	W/C	
CN	0.35	---
R2	0.35	10% SF + 2% BUTST
R3	0.35	10% SF + 1% BUTST + 1% SOYO

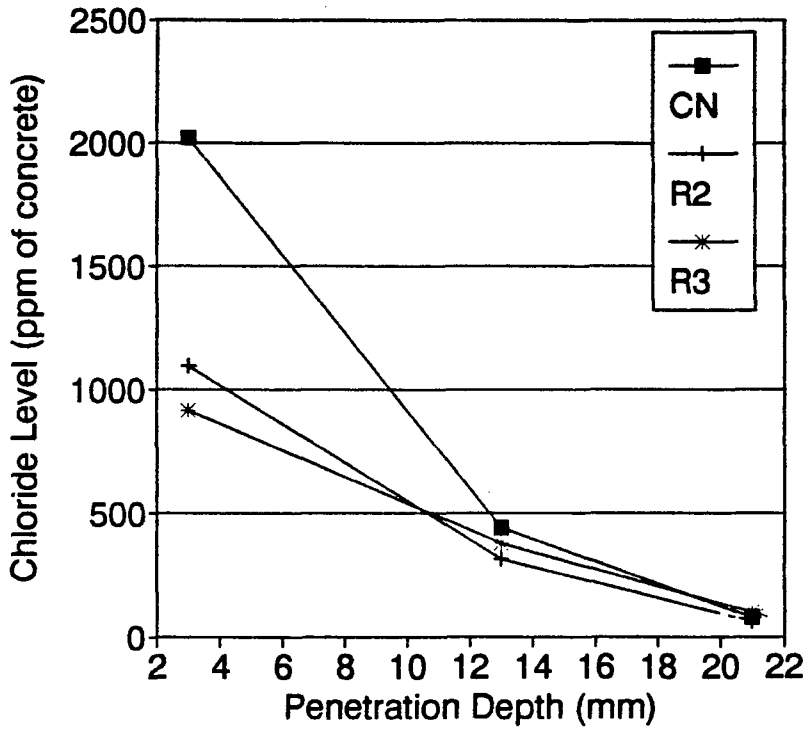


Figure 7.13 Pressure-induced chloride penetration (silica fume concretes).

7.4.2.3 PFA concretes

The results of diffusion testing (see Figure 7.1b) indicate that R4 offered higher resistance to chloride diffusion, compared with CN. It is apparent nonetheless that the reduction in chloride ingress is much less pronounced than that displayed by the silica fume concretes (R2 and R3) and the slag concretes (R6, R7, R8, and R9). However, it should be recalled that the unmodified PFA mix (5 (PFA30(0.4))) tested in Phase 2 was also bettered, by a large margin, by the silica fume and slag concretes (mixes 4 (GGBS65(0.4)) & 6 (SF10(0.4)+), see 6.3). It therefore seems safe to conclude that it is unlikely the soyabean oil had altered in any significant measure the diffusion resistance of the PFA concrete. It is interesting, but not surprising, to note also that the inclusion of 5% silica fume (in mix R5) gives rise to better diffusion resistance.

As for absorption resistance, Table 7.3 shows that the water uptake of R4 and R5 was markedly less than that of CN, and also that the effective porosity after drying was 30% lower. Figure 7.14 demonstrates that using soyabean oil at 1% markedly improves the absorption resistance of PFA concrete. It is also worth noting the effect of silica fume inclusion (in mix R5) in further reducing water uptake (at the later stages of the experiment). Finally, it is worth comparing the absorption behaviour of mixes R4 and R5 with that of mix 24 (see Figure 7.14, and 7.4.2.2).

Presented in Figures 7.6 and 7.7 are the results of SEM on R4 and R5. As seen in Figure 7.6a and Figures 7.7a and b, the paste in both R4 and R5 comprises areas of relatively large porosity dispersed within an otherwise dense paste; the presence of large porosity areas being notably more pronounced in R4. The high porosity areas seem to concentrate rather along the aggregate interfaces. It should be recalled at this point that the unmodified PFA concrete tested in Phase 2 also exhibited a tendency to form porous areas in the vicinity of the aggregate (see 6.3.5.3), though perhaps to a lesser extent. It is also worth remembering that a similar phenomenon was observed when a similar proportion of soyabean oil was used with OPC concrete (mix 15 (SOYO1(0.35)+), see 6.3.5.3).

Mix	W/C	
5	0.4	30% PFA
24	0.35	30 l/m ³ Everdure Caltite
R4	0.35	30% SF + 1% SOYO
R5	0.35	20% PFA + 5% SF + 1% SOYO

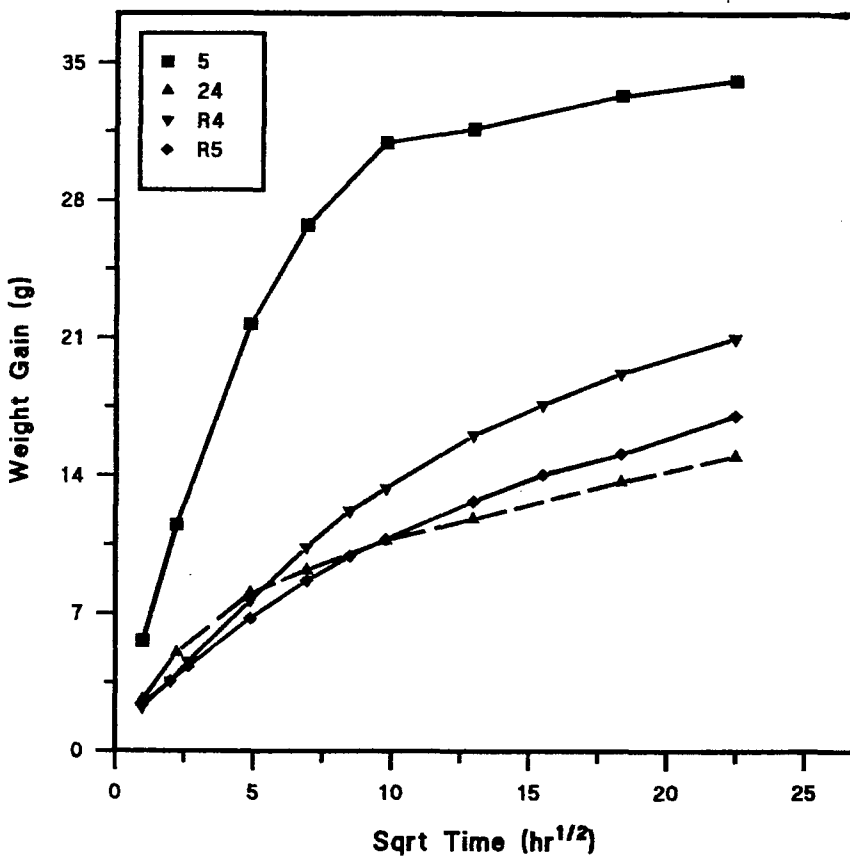


Figure 7.14 Absorption behaviour of PFA concretes.

The microstructure seen in Figure 7.6b seems to be typical of that of relatively mature PFA concrete, and there are no signs that the presence of soyabean oil hindered PFA hydration: the majority of PFA particles seem to have hydrated in varying degrees, and notably fewer, in comparison with the younger mix PFA30(0.4) of Phase 2, completely unaltered particles are seen. It is also interesting to observe that PFA hydration in R4 is more pronounced than in R5 (compare Figures 7.6b and 7.7c). This may be explained by the fact that the pozzolanic reaction of the silica fume, which precedes that of the PFA, results in a reduction in pore solution alkalinity and this retards PFA hydration. No clearly visible differences in porosity (the relatively large pores being excluded) are found when Figures 7.6b and 7.7c are compared. However, at high magnifications (compare Figures 7.6c and d with 7.7d) R5 appears slightly denser than R4.

Permeability test results also merit consideration. Table 7.8 shows that the amount of chloride which penetrated R4 was, at depth (20-22 mm), 9-fold higher than in CN. This is probably due, at least partly, to the presence of high porosity areas described above. The higher permeability of R4 can be illustrated also by considering, as Figure 6.15 demonstrates, that 500 ppm chloride (by weight of concrete) would penetrate in R4 to roughly twice the depth as in CN. Table 7.8 and Figure 7.15 show that R5 was also of higher permeability, in relation to CN, though to a lesser extent than R4. It is perhaps worth noting at this stage that the inclusion of 1% soyabean oil in OPC concrete (mix 15 of Phase 2 (SOYO1(0.35)+)) was also found to bring about an increase in permeability, and evidence was furnished that this was due, primarily, to the presence of areas of relatively high porosity (see 6.3.2).

Finally, it is worth considering the results obtained from compressive strength testing. As seen in Table 7.9, R4 exhibits a strength reduction (in relation to CN), at 28 days, of merely 30%. This is surprising, in view of the results (at 28 days) of Phase 2 testing (see Table 6.24), for: i) soyabean oil, when used at a similar dose in OPC concrete and in combination with an air detrainng agent (mix 15), was found to decrease compressive strength by a similar proportion, and ii) the unmodified PFA mix

Mix	W/C	
CN	0.35	---
R4	0.35	30% SF + 1% SOYO
R5	0.35	20% PFA + 5% SF + 1% SOYO

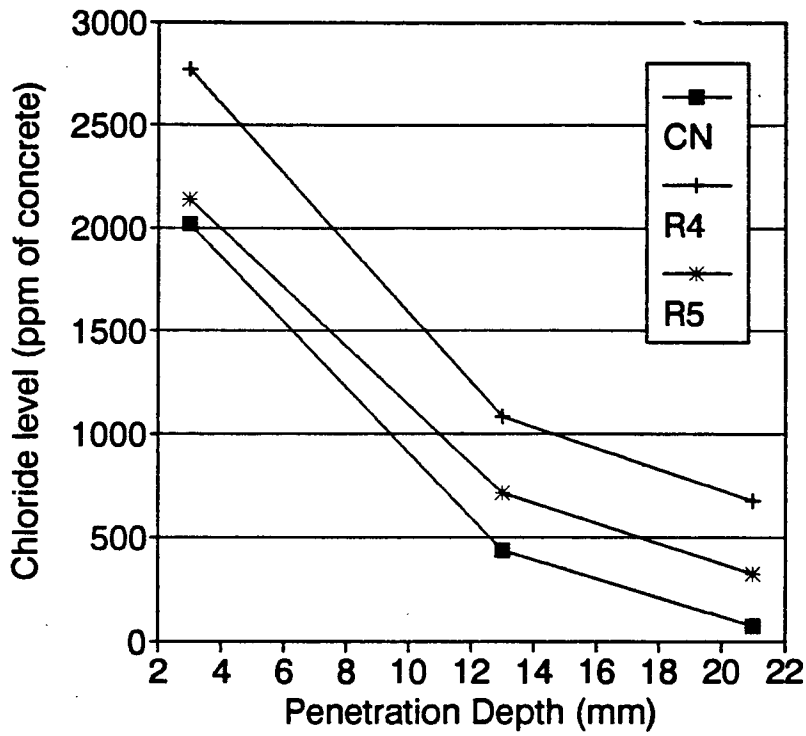


Figure 7.15 Pressure-induced chloride penetration (PFA concretes).

(PFA30(0.4)) also exhibited a similar reduction (relevant to the respective control) in strength. One explanation may be that the entrainment of air (by the soyabean oil (see 6.1.1.2.4)) in mix R4 was hindered due to the carbon present in the PFA. It is also possible that PFA hydration is accelerated by reducing the water/cement ratio (from 0.4 (mix PFA30(0.4)) to 0.35 (mix R4)), and/or using a superplasticizer (see Table 7.1). Finally, it may be that soyabean oil accelerates PFA hydration. Clearly, a detailed study of the effect of water repellents on PFA hydration is desirable.

7.4.2.4 Slag concretes

Comparing graphs relating to the water repellent-modified mixes (R6, R7, R8) with that of the unmodified mix (R9) and that of CN (Figure 7.1c) shows clearly that the water repellents have no unfavourable influence on the ability of slag concrete to resist chloride diffusion. Unfortunately, it is difficult to establish the effect of replacing a portion of the standard slag with a finer slag (see 7.1). It is nonetheless worth comparing the performance of mixes R7 and R8, which differ only in so far as 30% of the GGBS in R7 was replaced by an equivalent amount of FGGBS. It is found, perhaps surprisingly, that R7 was somewhat more resistant to chloride diffusion than R8.

As for absorption resistance, the data in Table 7.3 show that all three modified mixes were substantially superior to the control, and also that, in contrast to R9, the mixes have lower effective porosity than CN. Furthermore, comparison of the graphs relating to the modified concretes with that of R9 (see Figure 7.16) shows that the water repellents used increase markedly the absorption resistance of slag concrete. The same conclusion is arrived at when a similar comparison is made using the data in Table 7.5. Comparing the graph relating to R9 (in Figure 7.16) with that of the unmodified GGBS mix of Phase 2 (mix 4) suggests that the use of FGGBS had a relatively small influence on absorption resistance (see 7.4.2.2). However, it is perhaps worth comparing the performance of R9 against CN (Table 7.3), and contrasting this performance with that of mix GGBS65(0.4) against its respective control (see Table 6.16b). Comparing graphs relating to R7 and R8 shows no favourable effect for the FGGBS. Finally, it is worth comparing the absorption behaviour of mixes R6, R7, and R8 with that of mix 24 (see Figure 7.16, and 7.4.2.2).

Mix	W/C	
4	0.4	65% GGBS
24	0.35	30 l/m ³ Everdure Caltite
R6	0.35	65% FGGBS + 1% SOYO
R7	0.35	65% GGBS + 2% BUTST
R8	0.35	35% GGBS + 30% FGGBS + 2% BUTST
R9	0.35	35% GGBS + 30% FGGBS

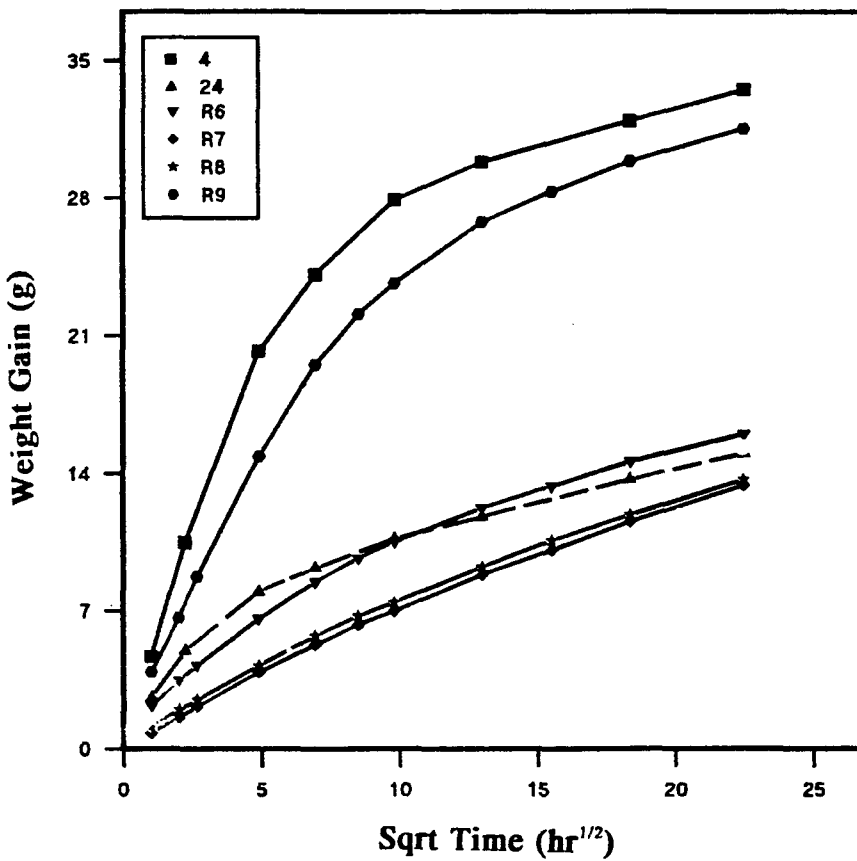


Figure 7.16 Absorption behaviour of slag concretes.

Presented in Figures 7.8 and 7.9 are the results of SEM on R8 and R9. As seen in Figure 7.8a, the majority of the paste in R8 is of comparable denseness to CN, except where areas of relatively large porosity are found; these seem to concentrate in the vicinity of the aggregate. Figure 7.9a shows that the same phenomenon is also manifest, though perhaps to a lesser extent, in the unmodified mix R9 and thus the phenomenon cannot be attributed solely to the presence of butyl stearate. It should be noted in this connection that both mixes R8 and R9 were of very high workability (A2.3) and exhibited relatively high bleeding on vibration. It seems likely, therefore, that using 1% superplasticizer (see Table 7.1) had to some extent contributed to the formation of the porous areas seen in R8. The porous and dense areas, respectively, are shown more clearly in Figures 7.8b and c. It is evident that slag had undergone relatively little hydration in porous areas. In contrast, much of the slag seen in Figure 7.8c is found to have undergone considerable hydration. Indeed rims reminiscent of prolonged hydration can be seen surrounding numerous slag particles (see also Figure 7.8c and d). When comparison is made between Figure 7.8c and Figures 7.9b and c, it becomes clear that butyl stearate had not altered the microstructure which is characteristic of relatively mature slag concrete.

There are other aspects of the performance of the slag concretes that merit consideration.

Electrical resistivity of the slag concretes, as seen in Table 7.6, is more than 3-fold higher than that of CN. It is also noteworthy that the resistivity of the modified concretes is found to be somewhat higher than that of R9, and that this margin widens after saturation.

As for permeability, Table 7.8 shows that the amount of chloride which penetrated R6, R7, and R8 specimens was, at depth (20-22 mm), considerably higher than in CN, or, indeed, in R9. This is also demonstrated in Figure 7.17, in which horizontal lines are additionally plotted so that comparison (between mixes) can also be made on the basis of the depth penetrated at any of the selected chloride concentration levels. Comparing

the performance of R9 against that of the unmodified concrete of Phase 2 (mix 4 (GGBS65(0.4))), which exhibited higher permeability than the control (see 6.3.2), suggests that permeability performance of slag concrete may be improved by replacing a proportion of standard slag with a finer slag. It is worth noting, however, that this was not the case in the presence of butyl stearate (compare the graphs relating to R7 and R8).

Finally, it is worth considering the results obtained from compressive strength testing (Table 7.9). Comparing the results of R9 with those relating to mix GGBS65(0.4) of Phase 2 (Table 6.24) reveals that, at 28 days, R9 performed, in relation to the respective control, distinctly better than GGBS65(0.4). This suggests that increasing the fineness of grinding of slag can improve performance. There is also the possibility, however, of a favourable influence of the superplasticizer used and/or the reduction in water/cement ratio (0.4 for GGBS65(0.4) against 0.35 for R9). Comparing R7 and R8 reveals that, in the presence of butyl stearate, the effect of FGGBS is only pronounced in so far as early-age (3 days) strength is concerned. It is also worth comparing at this stage the results of mix R7 with those of GGBS65(0.4). It is immediately obvious that, at 28 days, both concretes performed similarly (in relation to the respective control concretes), and it would appear, at first sight, that the inclusion of butyl stearate had no unfavourable influence on strength. However, this proposition is disputed by considering that, both at 3 days and 28 days, R8 had roughly 20% lower strength than R9. It is suggested, therefore, that the use of superplasticizer and/or reducing the water/cement ratio (from 0.4 for GGBS65(0.4) to 0.35 for R7) has a favourable influence on slag hydration. Finally, it is worth noting that R6 yielded comparable strength to R9. Clearly, a detailed study of the effect of water repellents on slag hydration is desirable.

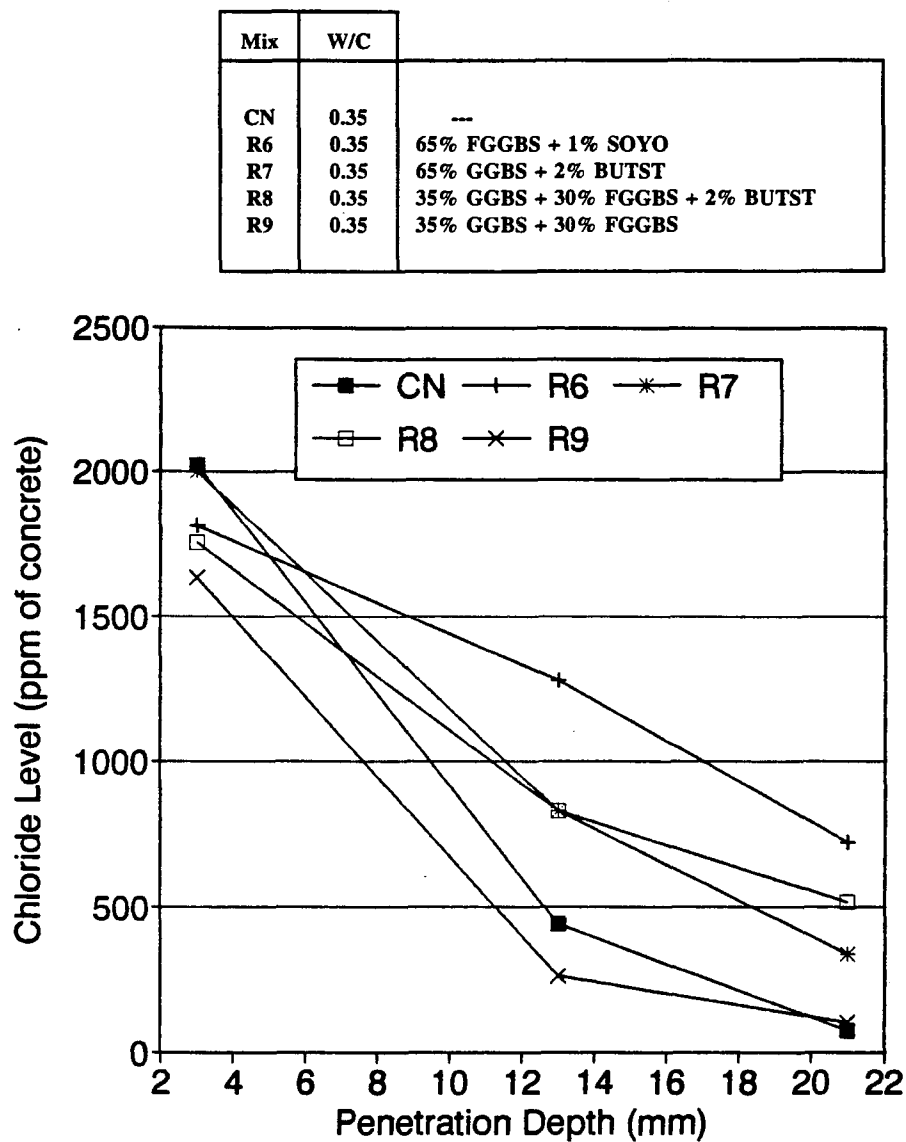


Figure 7.17 Pressure-induced chloride penetration (slag concretes).

7.5 Summary

The main findings of Phase 3 are as follows:

- Acrylic latex and silica fume are not compatible, as their use in combination leads to excessive early plastic shrinkage cracking.
- Dry curing (see 7.2) of polymer latex modified concretes sets into motion two conflicting effects (in connection with impenetrability to chlorides), viz.: drying promotes polymer film formation (favourable effect), but gives rise to a range of adverse effects (increases the volume of empty pore space, causes microcracking and pore structure coarsening, curtails cement hydration), and the net effect is determined by the more dominant of the two effects. The adverse effects associated with drying may be alleviated by water (fresh) immersion prior to exposure.
- Effective water repellents (butyl stearate and soyabean oil) are compatible with cement replacement materials in that they increase the absorption resistance of low (0.35) water/cement ratio cement replaced concrete substantially (they reduce dramatically the rate of water absorption and also the amount of water absorbed after a long period of water exposure) without reducing its ability to resist chloride ion diffusion.
- Introduction of 1-2% (by weight of cement) of effective water repellent in low (0.35) water/cement ratio cement replaced concrete leads, in varying degrees, to increased inhomogeneity of the cement paste (areas of high and low porosity appear on SEM micrographs). This gives rise to increased permeability to water, the effect being dramatic in the case of mixes without silica fume.
- Cement replaced concrete (particular mixes incorporating silica fume) modified with 1-2% effective water repellent exhibit substantially higher electrical resistivity than corresponding low (0.35) water/cement ratio OPC concrete. This is attributable to the

effect of the cement replacement material (reduced ion mobility and changes in pore solution composition), and also to the effect of the water repellent in increasing dramatically resistance to wetting of unsaturated concrete (see 2.2).

- Low (0.35) water/cement ratio OPC concrete containing silica fume and water repellent exhibits somewhat less rapid drying than the corresponding OPC concrete.
- All concretes tested developed compressive strengths of 45 MPa or higher at 28 days (standard cured); rapid early-age strength development is only achieved, however, in concretes incorporating silica fume. Evidence is furnished that the performance of GGBS (or FGGBS) and PFA concretes in regard to strength development improves with decreasing water/cement ratio.

Chapter 8 Concrete Specification in Chloride-Rich Environments

8.1 Introduction

Figure 8.1 illustrates how the performance of structures degrades with age (the process is commonly referred to as "deterioration"), and explains why current emphasis in design is given to maintaining the performance of structures above a given minimum level for a given specified period of time, termed the "design life". Accordingly, durability can be defined as the ability of a structure to withstand the conditions to which it is exposed and perform satisfactorily during its intended design life.

Various physical, chemical, and electrochemical phenomena can cause concrete structures to deteriorate. The ACI "Guide for durable concrete" recognizes five classes of concrete deterioration, according to the factors which can cause deterioration, as follows (ACI Committee 201 1977):

- freezing and thawing;
- aggressive chemical exposure;
- abrasion;
- corrosion of steel and other metals embedded in concrete;
- chemical reactions in aggregates (alkali silica and alkali carbonate reaction).

It is now universally agreed that corrosion of reinforcement induced by chloride contamination is by far the most serious and widespread form of deterioration. Mehta recently (1991) prepared a state-of-the-art report on concrete durability, and noted that failure analysis reports from around the world show that, in order of decreasing importance, the following causes of deterioration need most attention: corrosion of reinforcing steel (primarily chloride-induced), frost action in cold climates, chemical effects on hydrated cement pastes from external agents (viz., water containing carbon dioxide, sulphates or chlorides), physical-chemical effects such as alkali-aggregate reaction, and salt weathering.

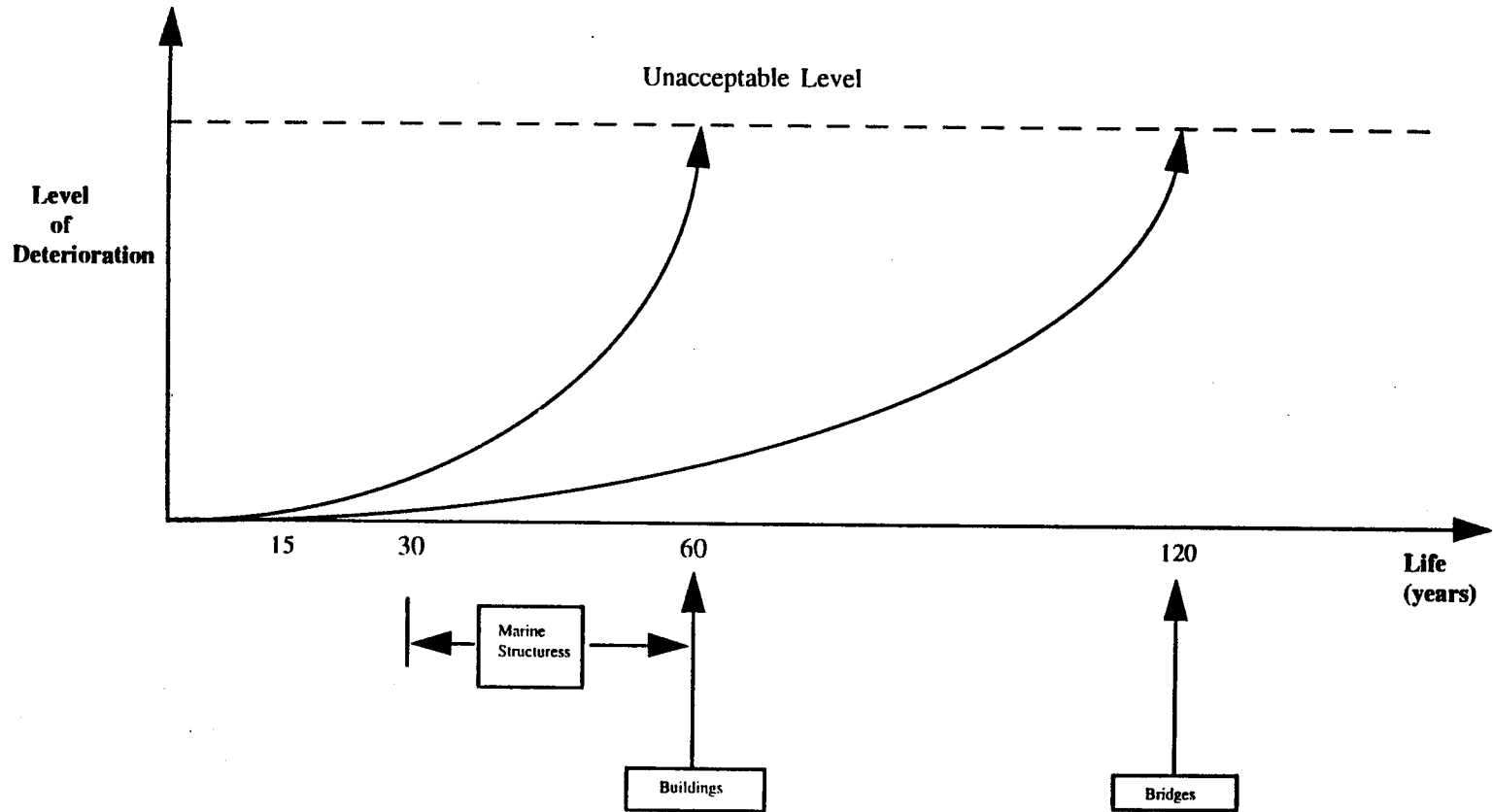


Figure 8.1 Design life and durability.

Deterioration can be broadly viewed as a two stage process, described by: i) the initiation time, which represents the time required for deterioration to start, and ii) the propagation time, defined as the time required for material degradation to reduce the performance of structures below the minimum allowable level. Therefore, improved durability can be achieved when measures are taken to prolong the initiation and/or the propagation time of relevant deterioration process(es); a relevant deterioration process is that which may contribute to lack of durability.

The ultimate objective of most durability research is to enable specifications to be made for more durable construction in particular environments of interest. This research has been concerned with using admixtures to increase the resistance of concrete to chloride ion penetration, so that the initiation period for reinforcement corrosion in chloride-rich exposure environments can be prolonged. Due to time constraints and limited resources, the experimental work was limited to investigating the resistance to chloride penetration of concrete **on first exposure**, i.e effects associated with age and exposure were not explored. Clearly, before any new admixtures can be specified, an assessment of the effect of the admixture on the **long-term** protective qualities of the concrete and wide range of engineering properties would be required. An appraisal of long-term protection can best be made by carrying out field trials, and this would require preliminary design specifications for construction in particular chloride-rich environments to be prepared.

In the majority of chloride-rich environments more than one deterioration mechanism can, and usually does, act simultaneously or consecutively. Design specifications must therefore be prepared with due regard not only to reinforcement corrosion but also to all other deterioration mechanisms that are relevant under the intended conditions of exposure.

The rates of most of the main deterioration processes attacking concrete structures are controlled by the rate of transport of particular species through concrete, which, in turn, is a complex function of: i) the actual conditions to which concrete is subjected when placed in a structure of given exposure (microclimate), ii) the nature of the transport mechanism(s) involved, and iii) the resistance afforded by concrete to transport.

As a general rule, an admixture, to be effective when used in a particular environment, must modify concrete such that it becomes more resistant (less penetrable) to all mechanisms responsible for the transport of the species of interest. One important finding of the experimental investigation conducted was that whilst an admixture may improve concrete resistance to one transport process, it may, at the same time, have an adverse effect on resistance to another process. Thus, before any admixture can be specified to reduce chloride penetration, the exposure environment will have to be defined.

It was felt that this chapter should be devoted to specification recommendations, for this approach is clearly (in the light of the aforementioned): i) the most appropriate way by which to put into context the findings of the experimental work, ii) is a prerequisite for field-testing, and iii) will help identify areas where further work is needed.

8.2 World climate

Many areas in the world have similar climates and are usually considered to fall into the same climatic regime. In Figure 8.2 and Table 8.1 details of a simplified system (Fookes et al. 1986), which is based on four broad climate types, are given. Broad details of a more accurate system are given in Figure 8.3.

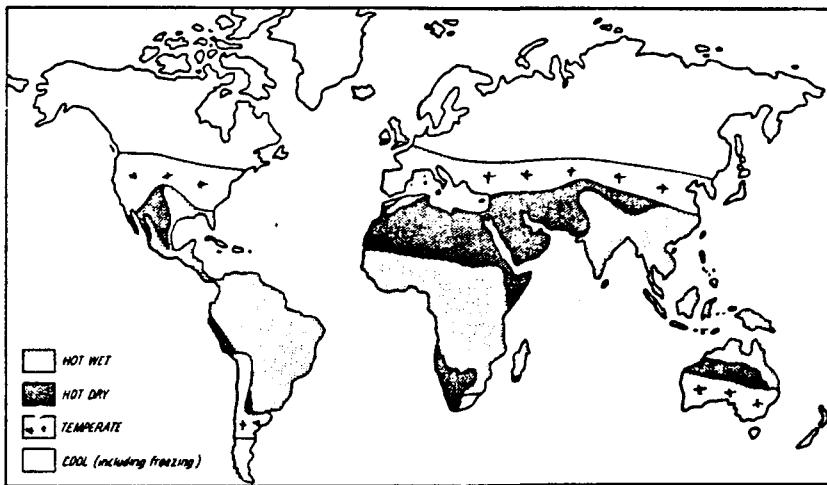
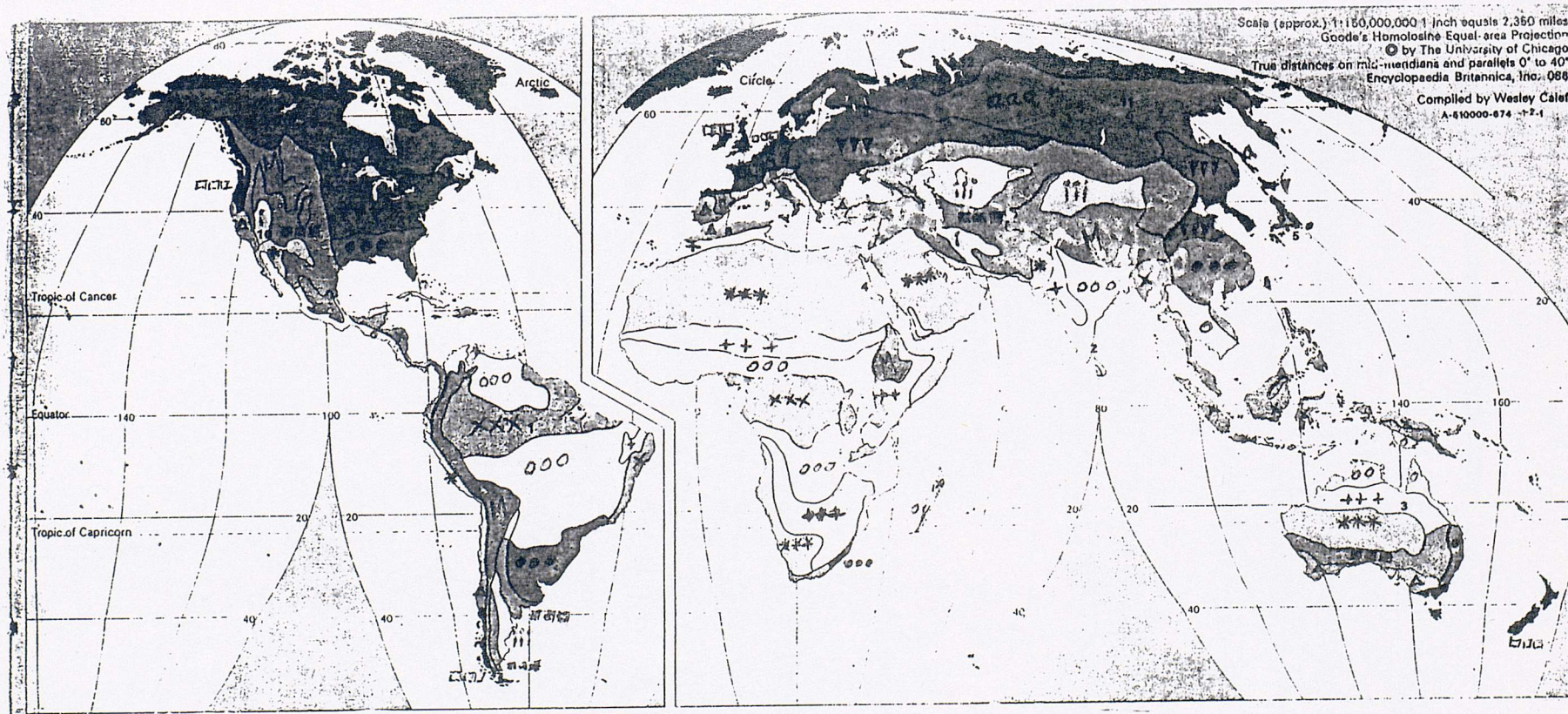


Figure 8.2 World climatic regions.

Table 8.1 Main characteristics of four broad climate types.

Climate type	Main characteristics
Cool with freezing	<ul style="list-style-type: none"> • usually with marked summer/winter temperature differences • average temperature less than 10°C with summer temperatures not exceeding 20°C • relative humidity not often below 40% and usually above 50% • moderate precipitation • sometimes windy
Temperate	<ul style="list-style-type: none"> • fairly marked summer/winter difference • seldom freezes, annual average temperature between 10 and 20°C • fairly high relative humidity • moderate to heavy rainfall • sometimes windy
Hot dry	<ul style="list-style-type: none"> • mainly hot desert climate • no freeze/thaw action but fairly marked day/night (up to 20°C) and summer/winter temperature difference, annual average temperature higher than 20°C with summer maximum usually exceeding 45°C • intense solar radiation (minimum cloud cover) • relative humidity very frequently around 60%, sometimes fairly low and sometimes reaching 100% (coastal) • very little rainfall • frequent dry winds
Hot wet	<ul style="list-style-type: none"> • mainly tropical climate • no freeze/thaw action with only moderate or small summer/winter temperature differences, annual average temperatures usually not exceeding 30°C • moderate to high relative humidity, usually over 60% • sometimes windy with at least one rainy season (moderate to heavy rainfall)



Climote Regions


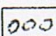
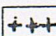






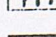
-  **Rainy tropical** At most, one or two dry months; all months warm or hot
-  **Wet and dry tropical** A well-developed dry season with one or two rainy seasons; all months warm or hot
-  **Semiarid tropical** Light precipitation, rapid evaporation; all months warm or hot
-  **Hot arid** Negligible precipitation, rapid evaporation; all months warm or hot
-  **Humid subtropical** Precipitation in all seasons with maximum in summer; long warm summers, cool winters
-  **Temperate marine** Numerous rainy days in all seasons with moderate total precipitation, higher precipitation in highland areas; warm summers, cool winters
-  **Semiarid mid-latitude** Light precipitation; warm or hot summers, cool or cold winters
-  **Arid mid-latitude** Extremely light precipitation; warm or hot summers, cool or cold winters
-  **Subarctic** Light precipitation; short cool summers, long very cold winters
-  **Arctic margin** Extremely light precipitation; very short cold summers, extremely long cold winters

Figure 8.3 World climate - more detailed

8.3 Specification recommendations

8.3.1 General

As mentioned before, the main concern of this chapter is to propose preliminary specifications for more durable concrete in particular chloride-rich exposure environments.

Concrete structures are nowadays built in a wide range of environments rich in chloride, the most common of which, and for this purpose the focus of this work, are the following:

- the marine environment;
- chloride-contaminated soils;
- environments where deicing salts are used or carried.

Before proceeding, it must be stressed that "There is a difference between the production of durable concrete and the design of structures that will be durable; the first is an essential part of the second but by no means all of it" (Somerville 1986). Indeed, design guides nowadays place emphasis not only on the material aspect of design, but also equally on the elements of architectural and structural design and processes of execution, and further stress the importance of considering inspection and maintenance procedures, including preventative maintenance, at the design stage; a good example is the CEB Design Guide for "Durable Concrete Structures" (CEB General Task Group 20 1992).

8.3.2 Structures in the marine environment

8.3.2.1 Classification of exposure conditions

Reinforced concrete is nowadays used in the construction of a wide variety of structures in the marine environment. Exposure conditions will undoubtedly vary widely, but can nevertheless be broadly classed according to the four basic exposure zones shown in Figure 8.4.

- **Atmospheric zone**

In the atmospheric zone, structures are not subjected directly to seawater, but receive, on an occasional or frequent basis depending on local conditions, salt from wind-blown seawater mist.

- **Splash zone**

The splash zone is that part of a structure which is situated above the mean high-tide level and is subjected to direct wetting by seawater due to wave action. The zone may be considered to extend up to the highest level reached by the waves with a statistical period of return of six months (Liu 1991). Thus, the conditions of exposure will vary from the top of the zone where the concrete only very occasionally comes into direct contact with seawater during storm conditions, to the bottom of the zone which is frequently exposed to the action of waves.

- **Tidal zone**

The tidal zone is that part of a structure which extends between the mean high-tide and low-tide levels and is thus submerged by seawater on a regular and predictable basis (usually every 12 hours and 25 minutes). The tidal zone is also influenced by lunar and diurnal effects (BS 6349: Part 1: 1984).

- **Submerged zone**

The submerged zone is that part of a structure which remains continuously immersed in seawater.

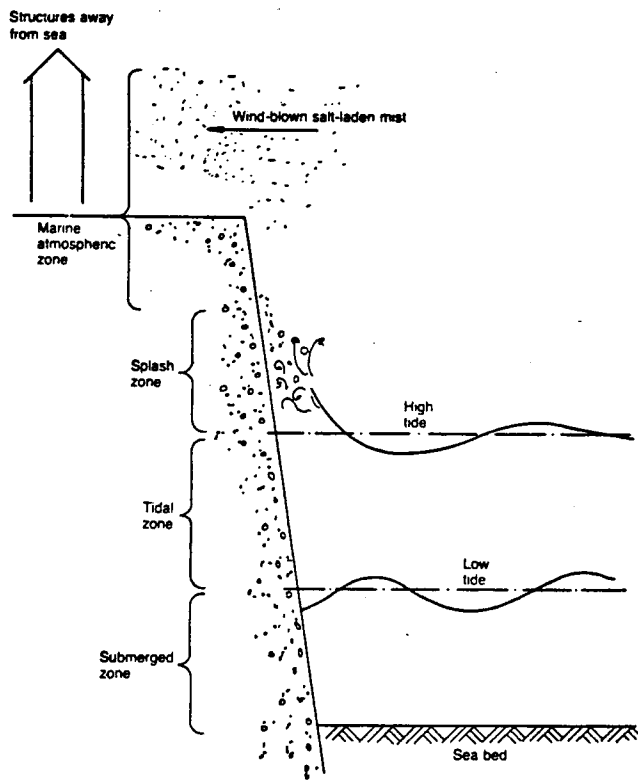


Figure 8.4 Marine exposure zones.

Additionally, marine structures can be divided into structures situated in seawater, and coastal structures (i.e. those situated inland near the shore); all four exposure zones may exist in a structure of the first category, whereas coastal structures will only be subjected to atmospheric exposure.

8.3.2.2 Relevant deterioration mechanisms

The problem of chloride-induced reinforcement corrosion in structures built in seawater has received considerable attention in the last few decades. It is now well established that the risk of corrosion relates broadly to location in relation to the four basic marine exposure zones; this is conceptually illustrated in Figure 8.5.

Corrosion has rarely been a problem in the submerged zone even though chlorides were often found to have penetrated in critical quantities to the level of the reinforcing steel (Browne & Baker 1983, Leeming 1989, Liu 1991). This can be explained (Chapter 2) by the low concentration of oxygen in seawater and the slow rate at which it can diffuse through the highly saturated concrete to the steel. Although the very slow rate of corrosion will probably increase in warm waters, it is thought (Fookes et al. 1986) unlikely that it would be a problem within the design life of most structures. It is concluded, therefore, that it is not necessary to adopt measures to slow down chloride penetration in the submerged zone, other than to provide OPC concrete of good quality (water/cement ratio of 0.45 or less, as suggested by most codes of practice (Mehta 1988)).

Other deterioration mechanisms that can be considered relevant under the conditions of exposure in the atmospheric, splash, and tidal zones include:

- Freezing and thawing: conditions are most severe in the tidal zone and the lowermost part of the splash zone, where the concrete could undergo many, up to two or three hundred a year, repeated cycles of freezing and thawing, as it is alternately immersed in seawater or exposed to air at freezing temperatures. The attack can be

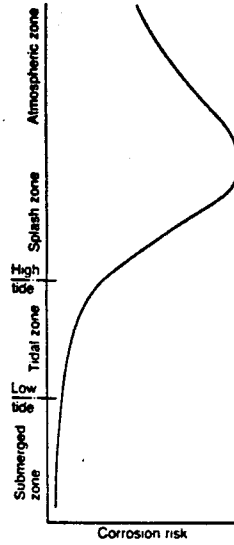


Figure 8.5 Variation of corrosion risk across marine exposure zones (CEB General Task Group 20 1992).

progressive unless precautions are taken.

- Aggressive chemical attack by seawater salts: the attack is mainly that of magnesium sulphate and is often not characterized by the expansion found in concretes exposed to sulphate solutions, but takes more the form of erosion or loss of constituents of the concrete mass (Lea 1970).
- Physical attack (salt weathering): the formation and growth of salts in the pores of concrete creates expansive forces leading to cracking and disintegration. The attack can be progressive, and is greatly aggravated when large fluctuations in day/night temperatures exist (crystalline salts have much higher coefficients of thermal expansion than the cement paste; solubility changes with temperature also cause problems).

Finally, abrasion by waves and floating objects (e.g. hard ice, gravel, etc.) affects concrete in the tidal and splash zones.

8.3.2.3 Regional climate and deterioration rate of marine structures

The regional climate often has a marked effect on the rate at which marine structures deteriorate. Unfortunately, this relation has not been recognised by the majority of codes of practice. For instance, the Australian Code of Practice (AS3600) makes no account for climate variations despite the fact that the climate in Australia can range from temperate to hot arid. In this connection, Browne (1991) notes that his experience with marine structures indicates that extra protection (i.e. using admixtures (mineral, chemical), application of coatings, using epoxy-coated reinforcement) would be essential to meet a 30 year or more design life, particularly in hot dry and hot wet zones.

It is interesting to observe that nearly two decades ago, in a review of the durability problems of the Middle East, Fookes and Collis (1975) warned that British (or other western) specifications fall well short of the requirements of the hot dry environment of the Middle East (see Table 8.2), and that reliance on these specifications was partly to blame for the extensive failures that have occurred. In a more recent publication, Fookes et al. (1986) illustrated how the regional climate relates to the frequency of occurrence of various forms of deterioration in marine atmospheric, splash and tidal zones (see Table 8.3). It should be stressed at this point that experience from the field indicates very clearly that in a hot wet climate structures generally deteriorate, as a result of chloride-induced reinforcement corrosion, at a much faster rate than in temperate or cool with freezing climates (Leeming 1989, Sagues et al. 1990, Browne 1991), and that this is not borne out in Table 8.3.

Table 8.2 Some aspects of concrete deterioration as related to climate regime (temperate vs. hot dry) and time (Fookes & Collis 1975)

Feature	Possible effects	Time before effects may be observed in hot, arid maritime climates						
		Temperate climates shown				for comparison		
		hours	days	weeks	months	years	decades	
Plastic shrinkage (including plastic settlement)	Cracking, localized loss of bond and/or actual cover to reinforcement	████████						
Initial drying shrinkage	Crazing and/or cracking, reduced effective/actual cover to reinforcement		████████████████████					
Initial thermal contraction	Cracking in depth, localized loss of cover to reinforcement			████████████████████				
Salt hydration	Cracking in depth, loss of cover to reinforcement			████████████████████				
Drying shrinkage	Cracking in depth, localized loss of cover to reinforcement			████████████████████				
Sulphate attack external	expansion and cracking, surface disintegration, general loss of effective and actual cover to reinforcement				████████████████████			
Unsound aggregates	Surface disintegration and general loss of effective and actual cover to reinforcement				████████████████████			
Salt crystallization	Surface disintegration and general loss of effective and actual cover to reinforcement				████████████████████			
Reactive Silicious aggregate	Pop-outs, expansion and cracking, loss of effective and actual cover to reinforcement					████████████████████		
Carbonation	Reduction in alkalinity, loss of effective cover to reinforcement					████████████████████		
Sulphate attack internal	Expansion and cracking, loss of effective and actual cover to reinforcement					████████████████████		
Reactive carbonate aggregate	Expansion and cracking, loss of effective and actual cover to reinforcement						████████████████████	
Loss of effective or actual cover to reinforcement	Reinforcement corrosion, cracking and spalling					████████████████████		
Excessive chloride concentrations	Accelerated reinforcement corrosion, cracking and spalling				████████████████████			

Table 8.3 General aspects of reinforced concrete deterioration and their occurrence in different climates

Feature	Possible effects	Approximate age at which feature becomes visible	Major factors	Occurrence rating in particular climate Scale: 1 lowest - 5 highest			
				Cool inc. freezing	Temperate	Hot dry	Hot wet
Defects of workmanship (e.g. honey combing, movement of formwork)	Loss of effective cover, porous concrete, loss of strength	First day	inexperienced operative, lack of supervision, inadequate specification	---	---	---	---
Bleeding and plastic settlement	Cracking, localised loss of bond, loss of effective cover	First day	Gap-graded fines Unsuitable mix design, deep sections, excessive retardation	3 ---	3/4 ---	4/5 ---	2/3 ---
Plastic shrinkage	Cracking or crazing loss of effective cover	First day	Porous aggregate, drying winds Inadequate protection	1/3 ---	3/4 ---	4/5 ---	2 ---
Initial thermal contraction	cracking at restrained locations	First month but depends on location	Rapid cooling after hardening (thermal chill) Unsuitable casting sequence, hot concrete, excessive cement content unsuitable cement type, very large sections, high expansion aggregate	1/2 ---	2/3 ---	3 ---	1/2 ---
Structural distress	cracking due to movement, cracking at restrained locations, loss of effective cover	At any time, but most commonly in early months	Long-term cyclic temperature movements Faulty design, weak concrete, premature loading, impact or earthquake damage	1/2	2/3	3/4	1
Drying shrinkage not controlled by reinforcement	Deep cracks, loss of effective cover	First months to first year	temperature/moisture gradients	2/3	3/4	5	2
Excess internal chloride	Severe cracking and spalling	A few months to several years	Contaminated aggregate, salt water for mix and/or curing Inappropriate admixture, unsuitable cement, very rich mixes	1/2	1/2	4/5	1/2
Chloride ingress	Corrosion of reinforcement leading to severe cracking and spalling	First few years	Temperature/moisture gradients	2/4	2	4	2
Frost damage	Spalling of concrete, loss of effective cover, loss of section	At any age	Freezing and thawing, porous concrete, saturation of surface	4/5	1/2	-	-
Physical salt weathering	Disintegration of surface, loss of effective cover to steel and loss of section	First few years	Difficult environment (e.g. subject to wind blown salty sands), unsuitable mix design, poor curing	1/2	1/2	4/5	1/3
External sulphate attack	Disintegration of surface, loss of effective cover to steel and loss of section	First few years	Sulphate rich environment (e.g. coastal sulphate swamps, seawater sulphates), unsuitable cement, inappropriate mix design	1/2	1/2	2	2
Reactive aggregate	Severe cracking	A few months to many years	Unsuitable aggregate, unsuitable cement, very rich mixes, high humidity	1	1	1	1/2

8.3.2.4 Recommendations

8.3.2.4.1 Structures situated in seawater

In the atmospheric, splash and tidal zones, chlorides penetrate the surface of concrete by absorption (during wetting and drying cycles) and then ion diffusion assists in transporting the ions to the depth of the reinforcing steel. Accordingly, concrete in these zones should have high resistance to absorption, and also to chloride ion diffusion. Once a critical level of chlorides reach the steel, the corrosion rate of reinforcement in the splash and atmospheric zones will almost certainly be a function of the concrete electrical resistivity and temperature. Hence, it is desirable for the concrete to have high electrical resistivity as well, so that corrosion propagation would be slow should the reinforcement eventually become depassivated. Testing in Phase 3 showed that using effective water repellents in low (0.35) water/cement ratio cement replaced concrete, except in the case of mix R4, results in substantially better performance in respect of all the desired properties, when comparison is made with a corresponding plain OPC concrete.

These concretes should find wide application in hot dry parts of the world (e.g Middle East, Parts of Australia, etc. (see Figure 8.2)), where the marine environment is extremely aggressive with respect to reinforcement corrosion to the extent that even structures made with high quality OPC concrete have been found to deteriorate in less than 10 to 15 years (Al-Rabiah et al. 1988, Sagues et al. 1990). In the tidal and splash zones, the problem is probably aggravated by chemical and physical attack of the concrete by seawater salts along with abrasion, which can in combination lead to partial loss of effective cover (see Table 8.2). Under these conditions, the water repellent-modified cement replaced concretes are also likely to fare better than equivalent OPC concrete, mainly for two reasons: i) they should have higher resistance to the penetration of seawater salts into the surface during wetting and drying cycles, and ii) cement replaced concrete is inherently more resistant to chemical attack (Lea 1970, Neville 1981).

Another case which deserves mention is that of structures in parts of the world where the climate is characterized by long very cold winters (subarctic regions, see Figure 8.3). Under these conditions concrete situated above low tide may suffer severe deterioration from freezing and thawing. As explained before, the attack is most severe in the tidal zone and the lowermost part of the splash zone. On the other hand, the embedded reinforcement would corrode at fairly low rates after depassivation due to the generally low temperatures and the restricted oxygen diffusion in the highly saturated concrete. Freeze-thaw damage can be progressive and in combination with the abrasive action of waves and hard floating ice can lead to loss of effective cover thereby accelerating the onset of corrosion of the reinforcing steel (ACI Committee 357 1985, Mehta 1991). This explains why Mehta (1991) and Lea (1970) regard freezing and thawing rather than reinforcement corrosion as the main deterioration causing mechanism in subarctic regions. Priority must therefore be given to providing adequate protection against excessive freeze-thaw damage. Experience indicates that durable structures can be made using OPC concrete provided that the water/cement ratio is low (0.4 or less), an adequate depth of cover is provided, and an air-entraining agent is used so that the hardened concrete has a proper air-void system (Leeming 1989, Gerwick 1990). It may be desirable nonetheless to use a water repellent-modified cement replaced concrete in the upper splash zone and the atmospheric zone of structures for which a fairly long service life is required. It is anticipated that such concrete would also offer good resistance to freeze-thaw attack. This is because the concrete has fairly high absorption resistance and is unlikely, therefore, to become critically saturated frequently under the conditions of exposure (deterioration due to freezing and thawing will only occur if a high degree of saturation, which is in the region of 85% (Fagerlund 1975) is attained); this should be verified by small-scale field testing.

8.3.2.4.2 Coastal structures

The deterioration of reinforced concrete can occur in structures up to a few miles inland from the coast. It normally arises from corrosion of the reinforcement, not attack of the concrete itself, and is caused by seawater mist carried inland by the wind. The chlorides gradually accumulate in the surface of the concrete by wetting and drying and diffuse inward towards the steel. Once a critical level of chlorides reach the steel, the corrosion rate of reinforcement will depend primarily on the concrete electrical resistivity and temperature.

The length of the corrosion initiation period is not only a function of the penetrability of concrete, but also the amount (per year) of airborne chloride that accumulates on the concrete surface. The latter will vary considerably depending on local conditions. For a particular coast, it will depend, in the main, on: i) distance from the shore, ii) height above sea level, and iii) orientation of the structural member in relation to the direction of the prevailing wind.

It is apparent from the foregoing that requirements for durable concrete in coastal structures will vary fairly widely. One specific case is examined next.

Figure 8.6 illustrates the effect of water/cement ratio on the penetration of wind-blown chloride into OPC concrete specimens exposed for three years near the Mediterranean Sea (30m from the shore and 15m above sea level, the climate being, according to Figure 8.3, dry subtropical). It is immediately obvious that chloride penetration with time is progressive and even with a water/cement ratio as low as 0.4, chlorides penetrated in critical levels to a depth of 25mm after just three years of exposure. Under these conditions, using a water repellent modified cement replaced concrete is recommended when a long design life is required. It may be worth noting that in the same publication, it was reported that according to a preliminary investigation (during the first summer) the average amount of airborne chloride decreased to 30% of its value at 30m at 100m distance from the shore, was nearly constant for a further 400 meters,

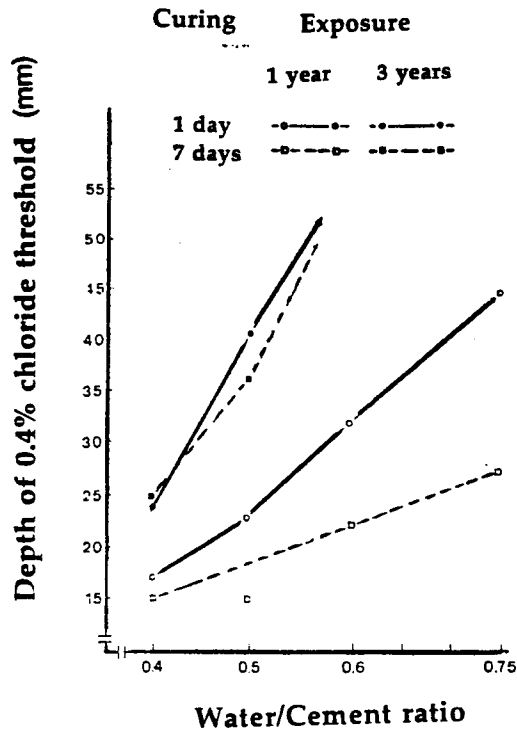


Figure 8.6 Effect of water/cement ratio and curing regime on depth of penetration of 0.4 percent Cl^- threshold after 1 and 3 years' exposure (Jaegermann 1990).

was further reduced from about 500 to 1400m, and became negligible thereafter. Unfortunately, the corresponding effect on chloride penetration in concrete was not investigated.

8.3.3 Structures in chloride-contaminated soils

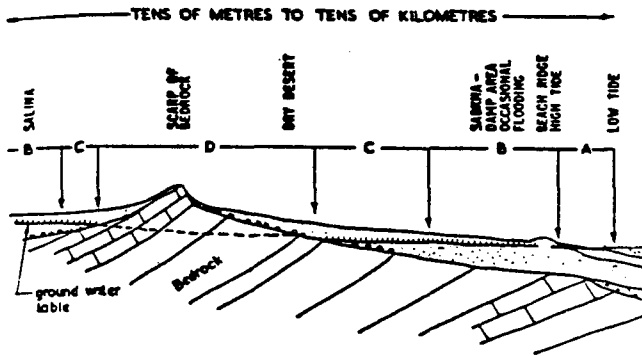
8.3.3.1 Foundations of coastal structures

8.3.3.1.1 Background

In many parts of the world's extensive hot drylands (e.g. Middle East, parts of Australia, etc.) conditions underground in coastal areas can be extremely aggressive to foundations. Consider the common situation depicted in Figure 8.7. The ground level in Zone B is sufficiently close to the water table for capillary rise moisture to reach the surface and on evaporation deposit the salts (seawater salts and other salts from the local ground) it contained in solution creating a salt crust with extremely high levels of chlorides and sulphates (see Table 8.4). A similar situation can also arise on reclaimed land adjacent to the sea (Figure 8.8): when the finished level of reclaimed land is within the capillary zone, then the effects of evaporation can concentrate seawater salts above the water table producing a salt crust in a relatively short time. Salt enrichment effects also apply where the ground level is reduced (by excavation say) until it lies within the capillary zone, or where fill material is employed to make up levels, when due to the higher suction characteristics of the fill material the capillary zone may reach higher than in the original undisturbed ground.

Table 8.4 Typical experimental chemical compositions of seawater and salt crust (Sabkha) waters (Fookes et al. 1985).

	Sample location		
	Open sea water	Arabian Gulf	Salt crust (Sabkha)
Parts per million of:			
Ca ²⁺	420	420	1250
Mg ²⁺	1320	1550	4000
Na ⁺	10700	20650	30000
K ⁺	380	660	1300
SO ₄ ²⁻	2700	3300	9950
Cl ⁻	19300	35000	56600
HCO ₃ ⁻	75	170	150



Zone	Natural Characteristics
A	Intertidal Near surface chemistry in equilibrium with seawater
B	Sabkha or Salina Ground surface within groundwater capillary range Salts concentrate at surface by evaporation
C	Ground surface may have high salt content but above capillary rise thus hence dry unless wetted by rain , watering or broken services
D	Ground surface may have high salt content but well above capillary rise hence dry unless wetted by rain, watering or broken services

Figure 8.7 Idealized cross-section of a coastal desert terrain showing relationship of salty soils to the local groundwater table (Fookes & Collis 1976).

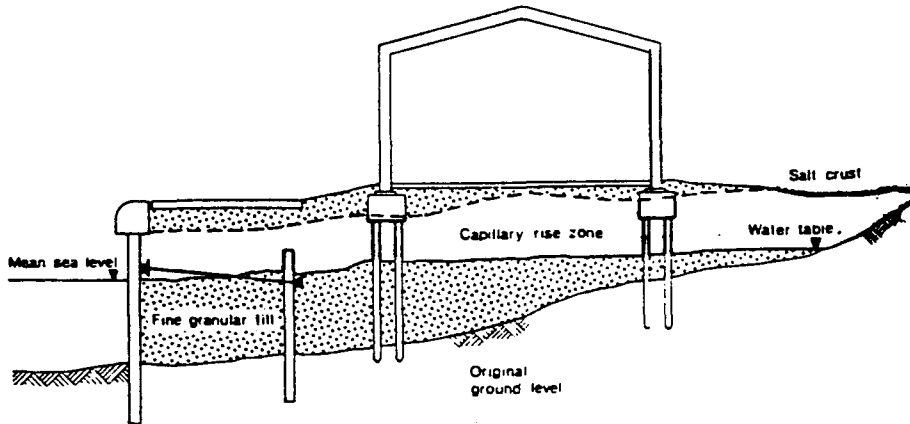


Figure 8.8 Capillary rise in a reclaimed area (Fookes & Collis 1981).

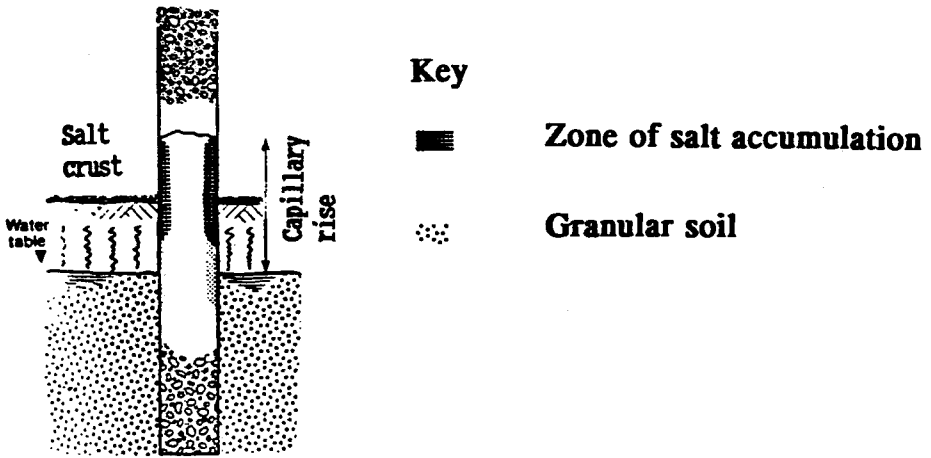
8.3.3.1.2 Recommendations

Figure 8.9a depicts a typical situation that concrete piles encounter when situated in a salt enrichment zone. As groundwater from the soil rises (by capillary suction) through the concrete towards the drying faces above ground, a point will be reached where the water supply rate is equal to the evaporation rate. At this point, all the soluble salts contained in the water will be deposited into the pores of the concrete. Thereafter, a situation will exist where evaporation of water at the drying face continually draws groundwater into the concrete. This process (known as "wick action", (see 3.3)) thus leads to a progressive build up of salt concentrations in the concrete, particularly at the evaporation region. Movement of ions (including chloride) into and within the concrete can also occur by diffusion.

The deterioration mechanisms that can be considered relevant under the conditions described above include the following:

- Corrosion of embedded reinforcement induced by the chlorides in groundwater.
- Concrete disintegration at the drying face (see Figure 8.9b) due to crystallization of groundwater salts and sulphate attack. It is perhaps worth noting that the attack by sulphates has seldom been observed to lead to cracking, but to erosion of the concrete constituents (Matta 1993), this being possibly due to the large quantities of associated chlorides inhibiting sulphoaluminate expansion.

It would seem essential, based on the foregoing, that concrete have the highest possible resistance to water absorption by capillarity, to water vapour diffusion, and also chloride ion diffusion. It is also desirable that it be of high electrical resistivity. Testing in Phase 3 showed that, of all mixes tested, mix R3 is the closest to satisfying these requirements. Additionally, as explained before (8.3.2.4.1), such concrete should fare better than equivalent OPC concrete in so far as sulphate attack and salt weathering is concerned. There is the possibility, however, that the water repellent material would be leached by the continuous through-flow of groundwater. The wick action process can be simulated in the laboratory (a test apparatus has been developed at Imperial College,



(a)

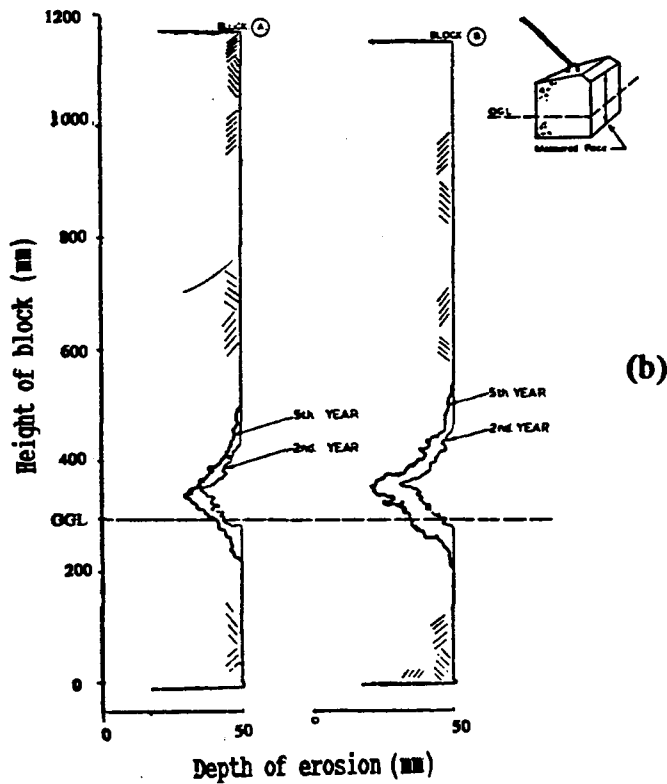


Figure 8.9 (a) Concrete pile in a salt enrichment zone.
(b) Concrete deterioration observed on face of fairly good quality concrete in salt enrichment zone observed over several years.

Buenfeld & S-Daoudi 1994), and it is recommended that such tests be carried out before proceeding with field testing.

8.3.3.2 Undersea tunnels

There has been much concern recently about the durability of undersea tunnels. These structures are normally designed for a service life in excess of 100 years, yet deterioration, due in the main to chloride-induced reinforcement corrosion, has been observed well within 15 years (Mehta 1991).

Undersea tunnels will usually be surrounded by saline groundwater while the interior is dry. A schematic representation of the transport mechanisms operating under these conditions is given in Figure 8.10. Inflow of groundwater occurs in response to the applied pressure head (sometimes as large as 100m) and the capillary suction forces, and evaporation of water at the inside face of the tunnel maintains the flow of aggressive groundwater through the concrete (see 8.3.3.1.2). Ion diffusion also assists in transporting ions into and within the concrete. Wetting and drying can also take place at the internal faces of the structure due to leakage through construction joints. These processes combined lead to a progressive increase of salt concentrations in the concrete.

The deterioration mechanisms that can be considered relevant under the conditions described above include the following:

- Corrosion of embedded reinforcement induced by chlorides.
- Concrete disintegration at the interior faces due to crystallization of groundwater salts and sulphate attack.

Case history studies of tunnels indicates that even high quality OPC concrete would not provide the embedded reinforcement with adequate protection against corrosion for more than a fraction of the intended design life (Ecob & King 1990, Ecob et al. 1990). It is anticipated that using the proprietary waterproofer Everdure Caltite should produce more durable concrete. This is because the system was found (Phase 2 testing) to be capable of dramatically reducing capillary absorption and also reduced pressure-induced flow (note that this was not the case with any of the concretes tested in Phase 3).

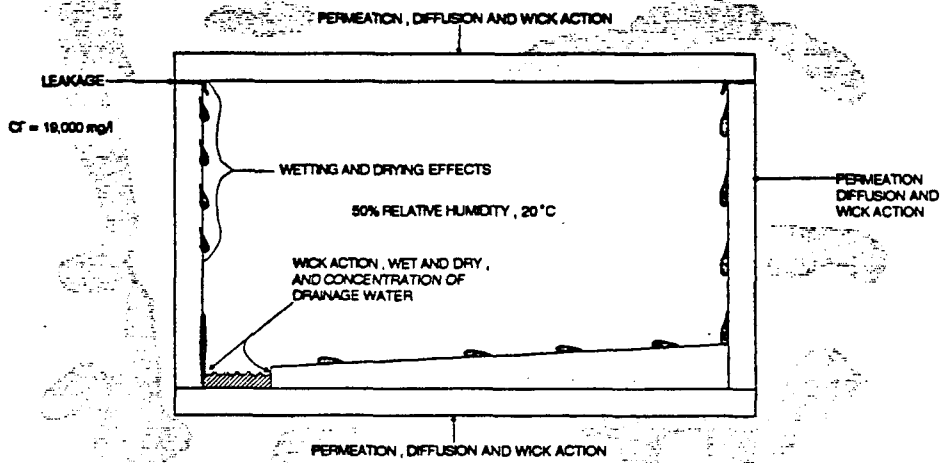


Figure 8.10 Schematic representation of transport mechanisms operating in an undersea tunnel.

It should be stressed that the resistance to pressure-induced chloride penetration of the Everdure Caltite concrete may not be sufficiently high for deeply submerged tunnels. Furthermore, the resistance afforded by the saturated modified concrete to chloride ion diffusion is only marginally better than that of equivalent OPC concrete. Since the use of silica fume was found (Phase 2) to be the most effective means of reducing permeability and chloride diffusion, it is suggested that future testing should investigate the performance of Everdure Caltite in silica fume modified concrete.

The results of testing in Phases 2 and 3 suggest that drying at 50°C and 11% RH renders concrete modified with acrylic latex substantially more resistant than the corresponding high-quality OPC concrete to pressure-induced water flow, absorption of water by capillarity, water vapour diffusion, and also chloride ion diffusion. There may therefore be scope for exploiting this effect in the production of precast segmental tunnel linings. It is of course essential that the acrylic concrete segments be immersed in fresh water before being exposed in situ, as this would help to eliminate the adverse effects associated with the heat-treatment (see 7.4.1).

8.3.4 Structures affected by deicing salts

Deicing salts are commonly used in large quantities during the winter in countries where the climate is cool with freezing (Figure 8.2) to improve traction on roads, bridges, runways, and are usually carried by traffic to parking garages. Chlorides from this source have frequently been found to rapidly contaminate concrete leading to premature corrosion of the reinforcing steel and extensive deterioration (Peterson 1980, Vassie 1985, Litvan & Bickley 1987, Manning 1987, OECD Scientific Experts Group 1989, Wallbank 1989).

Figure 8.11 illustrates how various superstructure and substructure components of highway bridges usually become contaminated with chloride. Chloride penetrates the surface of concrete by absorption (during wetting and drying cycles) and then ion diffusion assists in transporting the ions to the depth of the reinforcing steel. Once a critical level of chlorides reach the steel, the corrosion rate of the reinforcement will almost certainly be a function of the concrete electrical resistivity. Accordingly, the concrete should have high resistance to absorption and chloride ion diffusion, and also have high electrical resistivity. This can be achieved, as found in Phase 3, by using effective water repellents in low water/cement ratio cement replaced concrete.

Another deterioration mechanism that requires attention is freezing and thawing. The top surfaces of bridge decks are mostly at risk, where the attack is aggravated by accumulation of snow and direct application of deicing chemicals. The mechanism of attack, which manifests not as cracking (normal freezing and thawing) but in the form of surface scaling, is not as yet fully elucidated. Mather (1979) offered the following simplified view in regard to the role of the deicers in the attack process: "The deicer melts the snow or ice, which is often ponded by adjacent ice. The resulting liquid is absorbed, and because of the lowered freezing point, remains liquid. As more ice melts, the melt water becomes diluted until its freezing point rises to near the freezing point of water. Freezing then occurs. Thus, freezing and thawing occur as often as without the use of deicers, or even more often since a possibly insulating layer of ice

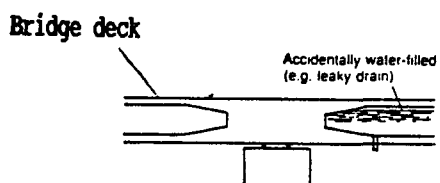
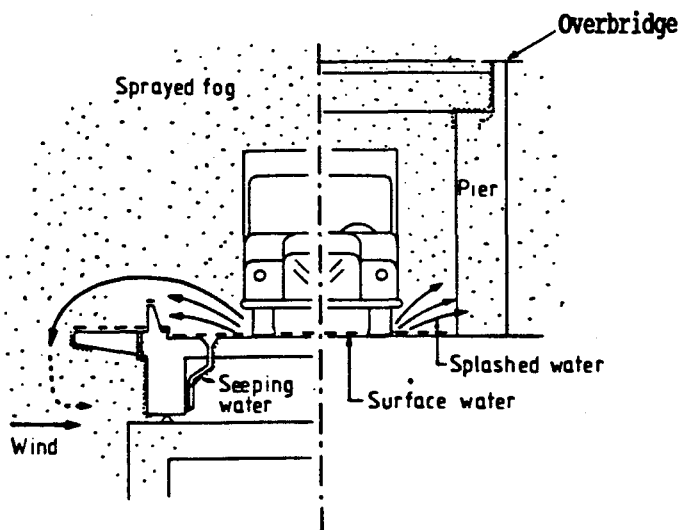


Figure 8.11 How bridge components become contaminated with deicing salts.

has been destroyed. In consequence, deicers can be said to increase saturation, possibly to increase the number of cycles of freezing and thawing". The attack process may be much more complex, however. Recently (1992), the CEB General Task Group 20 reviewed the relevant literature and proposed the following: "The application of deicing agents to a concrete surface covered with ice will cause a substantial drop in temperature at the concrete surface (temperature shock) during thawing of the ice. The difference in temperature between the surface area and the interior of the concrete gives rise to a state of internal stresses likely to induce cracking in the region of the outer layer of the concrete. Another significant effect is the change in the freezing behaviour of the pore water due to the deicing agents penetrating the outside of the concrete. As explained, the freezing point of the pore water will be lower when the pore radius is smaller. The diffusion processes in the pore water will further cause the content of the deicing agents to be reduced with decreasing radius. This will lead to a less noticeable dependence of the freezing point on the pore radius. Moreover, the content of the deicing agents will decrease with increasing distance from the surface of the concrete. The result of both these effects is that in the region of larger pores, as well as greater depths, water freezes within a smaller temperature range, which causes the redistribution of water (note that this would normally help to relieve the stresses that cause deterioration) to be considerably reduced. As a consequence, both of the change in temperature and of the change in the content of deicing agents with increasing distance from the concrete surface, it may happen that certain concrete layers suffer freezing at different times (Figure 8.12). In this case, scaling may result". The concretes recommended above would probably fare better than equivalent OPC concrete as they are less likely to become critically saturated due to their substantially higher absorption resistance. However, whether this is the case and, indeed, whether the resistance to scaling is adequate, particularly in subarctic regions (Figure 8.4), will have to be established first through laboratory testing then by small-scale field testing.

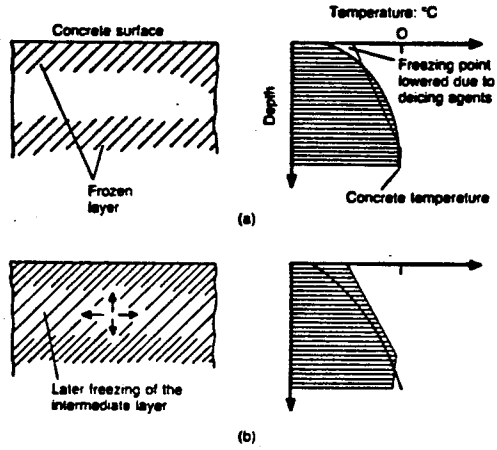


Figure 8.12 Scaling due to variations in the timing of freezing of layers:
 a) intermediate layer is initially unfrozen;
 b) intermediate layer freezes later, causing scaling.

8.4 Summary

The main aim of this chapter was to prepare preliminary specifications for more durable concrete for construction in particular (the most commonly encountered) chloride-rich exposure environments. The discussions in the preceding sections warrant the tentative recommendation given Table 8.5.

Emphasis in concrete mix design is currently shifting towards performance specifications. Therefore, the table should not be used directly for specification, but to aid in mix development.

Table 8.5 Preliminary specifications for concrete in chloride-rich exposure

Transport mechanisms	Examples	Design life	Regional climate	Concrete specification	Comments
<p>Absorption (drying and wetting)</p> <p>Ion diffusion</p>	<p>Atmospheric, Splash and Tidal zones of structures built in seawater</p>	<p>Usually 30-60 years</p>	<p>Temperate or Cool with freezing (excluding subarctic)</p>	<p>Design life of 40 years or less:</p> <p>0.35 w/c OPC concrete</p> <p>Design life of 60 years:</p> <p>OPC concrete (w/c 0.35) incorporating cement replacement material(s) (either 65% GGBS, or PFA and silica fume at 20% and 5% respectively) and effective water repellent</p> <p>or,</p> <p>if rapid early-age strength development is required, OPC concrete (w/c 0.4) with 10% silica fume replacement</p>	<p>(1)</p>
			<p>Subarctic</p>	<p>0.35 w/c air-entrained OPC concrete</p>	<p>(2)</p>
			<p>Hot wet</p> <p>or</p> <p>Hot dry</p>	<p>Design life of 30 years or less:</p> <p>OPC concrete (w/c 0.35) incorporating cement replacement material(s) (either 65% GGBS, or PFA and silica fume at 20% and 5% respectively) and effective water repellent</p> <p>or,</p> <p>if rapid early-age strength development is required, OPC concrete (w/c 0.4) with 10% silica fume replacement</p> <p>Design life of 60 years:</p> <p>OPC concrete (w/c 0.35) with silica fume replacement (10%) and effective water repellent</p>	<p>(3)</p>

table 8.5
cont'd ...

	Bridges affected by delcing salts	120 years	Freezing	OPC concrete (w/c 0.35) incorporating silica fume (10% replacement) and effective water repellent	(4)
Absorption (Wick action) Ion diffusion	Foundations of coastal structures	varies	Hot dry	OPC concrete (w/c 0.35) incorporating silica fume (10% replacement) and effective water repellent	(5)
Pressure-induced flow Absorption (drying and wetting, wick action) Ion diffusion	Undersea Tunnels (deeply submerged)	usually more than 100 years	not relevant	OPC concrete (w/c 0.35) modified with Everdure Caltite or, for precast segmental construction, OPC concrete (w/c 0.3) modified with acrylic latex (10% polymer solids by weight of cement)	(6)

• Comments

- (1): • in the less common case where a design life of 100 years or more is required (e.g. bridges), it may be prudent to use 0.35 w/c OPC concrete incorporating silica fume (10% in replacement) and effective water repellent.
- (2): • in the less common case where a design life of 100 years or more is required (e.g. bridges), it may be prudent to use, in the upper splash zone and the atmospheric zone, 0.35 w/c OPC concrete incorporating 10% silica fume replacement and effective water repellent;
• resistance of concrete to freeze-thaw action should be investigated.
- (3): • in the less common case where a design life of 100 years or more is required (e.g. bridges), additional protection (in the form of coatings, or epoxy coated reinforcement) may still be required.
- (4): • resistance of concrete to surface scaling must be investigated;
• extra protection (in the form of coatings, or epoxy-coated reinforcement) for the bridge deck and any substructure elements subjected to direct salt run-off or splash may still be required.
- (5): • laboratory wick action testing is required;
• where a fairly long design life is required it may still be necessary to apply membrane coatings to all concrete surfaces in contact with the contaminated soil.

- (6):
- it is worth investigating the performance of Everdure Calite in silica fume concrete.
 - it may still be necessary to employ extra protection: preferably by using epoxy-coated (fluidised bed dipping technique (FBD), Ecob et al. 1990) reinforcement.
 - acrylic modified tunnel linings require special treatment before exposure: following a period of normal curing, the segments should be subjected to drying (at 50°C and fairly low RH), then water (fresh) immersion.

Chapter 9 Conclusions

The main purpose of this research, as set out in 1.2.1, has been achieved. Admixtures that increase the resistance of concrete to chloride penetration have been identified, their effect on the various chloride transport processes has been assessed and has generally been explained, and specifications have been proposed for more durable concrete for construction in a wide range of chloride-rich exposure environments.

Considerable research has been conducted in the last few decades to devise ways of protecting new construction in chloride-rich exposure environments against chloride-induced corrosion of the embedded reinforcement. A literature survey into the methods devised to date was undertaken (Chapter 4). It was found that almost all methods suffer various shortcomings, and the development of more effective techniques is still a pressing need for the construction industry. An under-researched approach appeared to be the use of admixtures to increase the resistance of concrete to chloride ion penetration, so that the onset of corrosion is delayed.

Chlorides may penetrate concrete by absorption or pressure induced flow of water or by chloride ion diffusion (Chapter 3). A literature survey (5.1) revealed that, in addition to cement replacement materials, there are a wide range of basic materials and a few proprietary admixtures that may affect the rate of these processes when added to concrete.

A preliminary investigation (Chapter 5) was carried out to identify the materials which merit detailed investigation, and their dose levels. Those found to be of interest were then subjected to detailed testing in the second phase of the experimental programme (Chapter 6). The main findings are as follows.

- Using cement replacement materials at normal replacement levels is the most effective means of increasing the chloride ion diffusion resistance of OPC concrete.

- Addition of 3% or less (by weight of cement) of a material capable of increasing the angle of contact of surfaces with water to more than 90° (water repellent), such as certain stearates, fatty acids, and natural oils, is the most effective means of reducing water absorption; this dramatically reduces the rate of water absorption and also reduces the amount of water absorbed after a long period of water exposure. SEM did not identify any changes in the cement paste microstructure, as a result of the addition of most of these materials, that would be expected to produce such a dramatic reduction in absorption. This supports the idea that the principal effect of these materials is to provide a hydrophobic lining to pore walls, since this is one form of modification that would not be expected to produce effects visible in the SEM. Most water repellent materials tend to reduce resistance to pressure-induced water flow and chloride ion diffusion and may also increase the rate of carbonation. Furthermore, the materials often cause a reduction in compressive strength. This is not entirely due to the propensity of these materials to entrain air and hence cannot be eliminated by using an air-detraining agent. Removal of entrained air negates the capacity of water repellents to improve workability.
- Low water permeability may be achieved by the use of bentonite, cellulose acetate, or silica fume. Silica fume is preferred as it already has a history of use and it was the only material that was effective in reducing transport, that did not result in a reduction in strength.
- Certain polymer latices (at around 10% polymer solids by weight of cement) are very effective (in reducing chloride penetration) if the modified concrete is normally cured, then dried sufficiently, immersed afterwards in fresh water, before being exposed in situ. Drying helps promote polymer film formation; the optimum drying conditions will depend on the type of polymer used. The very low penetrability exhibited by polymer-modified concretes is principally due to polymer film formation. Polymer films are not visible in bse images, but are detectable in the SEM on fracture and etched fracture surfaces.

- Only two of the four proprietary waterproofers investigated, namely Everdure Caltite and Conplast Prolapin, are effective in reducing absorption, but they are bettered in this respect by several water repellents. They, however, and in contrast with the majority of water repellents, do not influence permeability adversely. In fact, Everdure Caltite has a favourable effect. SEM did not identify any change in cement paste microstructure, as a result of the addition of the Everdure Caltite system, which could account for the dramatic reduction in absorption, or the reduction in water permeability. This supports the manufacturers claim that: i) the water repellent component of the admixture provides a hydrophobic lining to pore walls, and ii) the asphaltic component (organic and therefore undetectable in the SEM) physically blocks pores.

In most exposure environments where chloride-induced corrosion is a problem, chlorides penetrate the concrete by absorption (during drying and wetting cycles) and then ion diffusion assists in transporting the ions to the depth of the reinforcing steel. Since it was not possible to better the chloride ion diffusion resistance of concretes containing normal replacement levels of GGBS, PFA, or silica fume, by using OPC and an admixture, the final phase of the experimental programme concentrated on using effective water repellents (butyl stearate and soyabean oil) to improve absorption resistance in cement replaced concrete (Chapter 7). The water repellents were found to be compatible with cement replaced concrete in that they improved absorption resistance substantially and did not reduce resistance to chloride ion diffusion. Microstructural examination (SEM) revealed that water repellents render the cement paste less homogeneous, causing the formation of areas of relatively high and low porosity. All concretes tested developed compressive strengths of 45 MPa or higher at 28 days (standard cured); rapid early-age strength development was only achieved, however, in concretes incorporating silica fume.

The findings of the experimental work and a review of relevant research and field experience allow preliminary specifications to be prepared for more durable concrete for construction in a wide range of chloride-rich environments (Table 8.5).

Chapter 10 Recommendations For Further Research

- Due to time constraints and limited resources, this study has been mainly concerned with the resistance to chloride penetration on first exposure. Before any new admixtures can be specified, an assessment of the effect of the admixture on the long-term protective qualities of the concrete and a wide range of engineering properties would be required. Preliminary specifications have been proposed for a range of chloride-rich exposure environments (Chapter 8). The next step is to carry out small-scale field trials to assess the long-term protective qualities of the suggested concretes. However, before such tests are carried out, it would be desirable to conduct further laboratory research with a view to optimize the properties of these concretes. One area of concern is the tendency of water repellents, when introduced in OPC or cement replaced concretes, to increase the porosity of the interfacial zone between the aggregate and the cement paste. This tendency may be due to the non-uniform distribution of the water repellent (which is not miscible with water) within the concrete mix during mixing and/or the tendency of the water repellent to separate out of the paste during compaction (vibration). It is felt that this may be resolved by employing modern emulsification techniques to produce a stable mixture of very fine water repellent particles dispersed uniformly in water (emulsion); the mixture can then be introduced in concrete.

- Regularly, throughout this project, queries arose concerning the relative influence of different types of pore space on the various transport processes. A fundamental investigation of the effects of "gel porosity", capillary porosity, interfacial zone porosity, entrapped and entrained air voids and microcracks is required in order to make further progress in producing low penetrability concretes.

- Evidence was furnished which supports the idea that chloride ion diffusion in concrete is controlled not only by physical effects (i.e. related to the characteristics of pore space) but also by chemical and electrochemical effects. Most emphasis in past

research has been given to the physical effects. A fundamental investigation of the role of the physical, chemical, and electrochemical effects is required if more effective admixtures (for reducing the rates of chloride ion diffusion in concrete) are to be developed.

References

ACI COMMITTEE 201 (1977) "Guide for Durable Concrete," ACI 201.2R-77, Published by the ACI.

ACI COMMITTEE 222 (1985) "Corrosion of metals in concrete," ACI Journal, Vol. 82, January-February, pp. 3-32.

ACI COMMITTEE 357 (1985) "ACI State-of-the-Art report - Offshore concrete structures for the arctic," Concrete International, Vol. 7, August, pp. 23-33.

ACI COMMITTEE 548 (1986) "Guide for use of polymers in concrete," ACI Journal, Vol. 83, September-October, pp. 798-827.

ACI COMMITTEE 212 (1989) "Chemical admixtures for concrete," ACI Materials Journal, Vol. 86, May-June, pp. 297-327.

ACI FORUM (1987) "Influence of chlorides in reinforced concrete," GIBSON, F.W. editor "Corrosion, concrete, and chlorides." Published by the ACI (SP-102), pp. 143-153.

ACI WORKSHOP COMMITTEE (1988) "Epoxy-coated reinforcement," Concrete International, Vol. 10, December, pp. 81-84.

AITKEN, C.T. and LITVAN, G.G. (1989) "laboratory investigation of concrete sealers," Concrete International, Vol. 11, November, pp. 37-42.

ALDRED, J.M. (1988) "HIP concrete; Hydrophobic pore blocking ingredient improves concrete durability," Concrete International, Vol. 10, November, pp. 53-57.

ALDRED, J.M. (1989) "The short-term and long-term performance of concrete incorporating dampproofing admixtures," Proceedings of the Third CANMET/ACI International Conference - Supplementary papers- "Superplasticizers and other chemical admixtures in concrete" (Ottawa; Canada), pp. 1-19.

AL-QASER, A.N.F. GRIFFITHS, D.L. and MNGABHAI, R.J. (1990) "Diffusion of various ions from sea water into polymer modified cement paste," PAGE, C.L. TREADAWAY, K.W.J. BAMFORTH, P.B. editors "Corrosion of reinforcement in concrete." Published for the Society of Chemical Industry by Elsevier Science Publishers Ltd., pp. 246-257.

AL-RABIAH, A.R. BAGGOT, R. and RASHEEDUZZAFAR (1988) "Construction and durability considerations for King Fahd Causeway - A case study," MALHOTRA, V.M. editor, Proceedings of the Second International Conference on "Concrete in the marine environment" (St. Andrews by-the-sea; Canada), Published by the ACI (SP-109), pp. 1-29.

AL-SULAIMANI, G.J. (1989) "Effect of epoxy coating of reinforcing bars on their bond behaviour with surrounding concrete," Proceedings of the Third International Conference on "Deterioration and repair of reinforced concrete in the Arabian Gulf" (Bahrain), Vol. 1, pp. 369-380.

AMERICAN PETROLEUM INSTITUTE (1952) "Recommended practice for determining permeability of porous media," Third Edition (API RP 27) (September).

ANDERSSON, K. ALLARD, B. BENGTSSON, M. and MAGNUSSON, B. (1989) "Chemical composition of cement pore solutions," Cement and Concrete Research, Vol. 19, No. 3, pp. 327-332.

ANDERSON, P.J. (1990) "Control and monitoring of concrete production," PhD Thesis, Academy of Technical Sciences, Technical University of Denmark.

ARMAGHANI, J. ROMANO, D. BERGIN, M. and MOXLEY, J. (1993) "High performance concrete in Florida bridges," Zia, P. editor. "High performance concrete in sever environments." Published by the ACI (SP-140), pp. 1-24.

ARYA, C. BUENFELD, N.R. and NEWMAN, J.B. (1987) "Assessment of simple methods of determining the free chloride ion content of cement paste," Cement and Concrete Research, Vol. 17, No. 6, pp. 907-918.

ARYA, C. BUENFELD, N.R. and NEWMAN, J.B. (1990) "Factors influencing chloride-binding in concrete," Cement and Concrete Research, Vol. 20, No. 2, pp. 291-300.

ATKINS, P.W. and BERAN, J.A. (1990) "General chemistry," Published by Scientific American Books, Second edition.

ATKINSON, A. and NICKERSON, A.K. (1984) "The diffusion of ions through water-saturated cement," Journal of Materials Science, Vol. 19, pp. 3068-3078.

ATKINSON, A. and NICKERSON, A.K. (1988) "Diffusion and sorption of cesium, strontium, and iodine in water-saturated cement," Nuclear Technology, Vol. 81, pp. 100-113.

BABAEI, K. and HAWKINS, N.M. (1988) "Evaluation of bridge deck protective strategies," Concrete International, Vol. 10, December, pp. 56-66.

BAILEY, J.E. and HAMPSON, C.J. (1982) "The chemistry of the aqueous phase of Portland Cement," Cement and Concrete Research, Vol. 12, No. 2, pp. 227-236.

BAKKER, R.F.M. (1983) "Permeability of blended cement concretes," MALHOTRA, V.M. editor, First International Conference on "The use of fly Ash, silica fume, & other mineral by-products in concrete." Vol. I, Published by the ACI (SP-79), pp. 589-605.

BAKKER, R.F.M. (1985) "Diffusion within and into concrete," A paper presented at the Thirteenth Annual Convention of the Institute of Concrete Technology at the University of Technology (Loughborough)(March).

BAKKER, R.F.M. (1988) "Chapter 3: Initiation period," SCHIESSL, P. editor, A Rilem Report "Corrosion of steel in concrete." Published by Chapman and Hall Ltd.

BAMFORTH, P.B. POCOCK, D.C. and ROBERY, P.C. (1985) "The sorptivity of concrete," Conference "Our world in concrete and structures" (Singapore)(27-28 August).

BAMFORTH, P.B. (1987) "The relationship between the permeability coefficients for concrete obtained using liquid and gas," Magazine of Concrete Research, Vol. 39, No. 138, pp. 3-11.

BARKER, A.P. (1990) "Conduction calorimetric studies of cements containing 5% additions," Cement and Concrete Research, Vol. 20, No. 2, pp. 219-226.

BAZANT, Z.P. and NAJJAR, L.J. (1971) "Drying of concrete as a nonlinear diffusion problem," Cement and Concrete research, Vol. 1, No. 5, pp. 461-473.

BAZANT, Z.P. (1979) "Physical model for steel corrosion in concrete sea structures - theory," Journal of the Structural Division (ASCE), Vol. 105, pp. 1137-1153.

BAZANT, Z.P. and RAFTSHOL, W.J. (1982) "Effect of cracking in drying and shrinkage specimens," Cement and Concrete Research, Vol. 12, No. 2, pp. 209-226.

BEAUDOIN, J.J RAMACHANDRAN, V.S. FELDMAN, R.F. (1990) "Interaction of chloride and C-S-H," Cement and Concrete Research, Vol. 20, No. 6, pp. 875-883.

BEEBY, A.W. (1978) "Corrosion of reinforcing steel in concrete in its relation to cracking," The structural Engineer, Vol. 56A, No. 3, pp. 77-81.

BEN-OTHTMAN, B. and BUENFELD, N.R. (1990) "Oxygen permeability of structural lightweight aggregate concrete," DHIR, R.K. and GREEN, J.W. editors. Proceedings of the International Conference on "Protection of concrete" (Dundee; Scotland, UK), Published by E. & F.N. Spon, pp. 725-736.

BEN-OTHTMAN (1994) "Durability of lightweight aggregate concrete," PhD Thesis, University of London, Imperial College.

BERKE, N.S. PFEIFER, D.W. and WEIL, T.G. (1988) "Protection against chloride-induced corrosion; A review of data and economics on microsilica and calcium nitrate," Concrete International, Vol. 10, December, pp. 45-55.

BERKE, N.S. and ROSENBERG, A. (1990) "Calcium nitrate corrosion inhibitor in concrete," VAZQUEZ, E. editor. Proceedings of the International Rilem Symposium "Admixtures for concrete: Improvement of properties" (Barcelona), Published by Chapman and Hall Ltd. (London), pp. 251-268.

BHARGAVA, J. and REHNSTROM, M. (1978) "Electrochemical aspects of electrical resistance gages for concrete," Swedish Council for Building Research (Stokholm), p. 35.

BROWNE, R.D. (1982) "Design prediction of the life for reinforced concrete in marine and other chloride environments," Durability of Building Materials, Vol. 1, pp. 113-125.

BROWNE, R.D. and BAKER, A.F. (1983) "The performance of structural concrete in a marine environment," CRANE, A.P. editor "Corrosion of reinforcement in concrete construction", Published by Ellis Horwood Limited (England), pp. 111-147.

BROWNE, R.D. (1991) "The corrosion of steel in concrete," A Short Course offered at Oxford University "Durability of Reinforced Concrete Structures" (22-24 September).

BUENFELD, N.R. (1984) "Permeability of concrete in a marine environment," PhD Thesis, University of London, Imperial College.

BUENFELD, N.R. and NEWMAN, J.B. (1987) "Examination of three methods for studying ion diffusion in cement pastes, mortars and concrete," Materials and Structures, Vol. 20, pp. 3-10.

BUENFELD, N.R. and S-DAOUDI, T.S. (1994) Private communication.

BUILDING RESEARCH ESTABLISHMENT (1978) "The structural condition of integrid buildings of prestressed concrete," Published by HMSO (London).

BUILDING RESEARCH ESTABLISHMENT (1988) "Design of normal concrete mixes," No BR 106, Published by the Department of the Environment.

BYFORS, K. (1987) "Influence of silica fume and flyash on chloride diffusion and pH values in cement paste," Cement and Concrete Research, Vol. 17, No. 1, pp. 115-130.

CADY, P.D. WEYERS, R.E. and MANSON, J.A. (1987) "Field performance of deep polymer impregnation," Journal of Transportation Engineering, Published by the American Society of Civil Engineers, Vol. 113, No. 1, January, pp. 1-15.

CAIRNS, J. and ABDULLAH, R. (1989) "Bond strength of epoxy coated reinforcement," Proceedings of the Third International Conference on "Deterioration and repair of reinforced concrete in the Arabian Gulf" (Bahrain), Vol. 1, pp. 353-367.

CALLEJA, J. (1981) "Durability," Proceedings of the 7th International Conference on "Cement chemistry" (Madrid), Volume II-2, p. 8.

CANHAM, I. PAGE, C.L. and NIXON, P.J. (1987) "Aspects of the pore solution chemistry of blended cements related to the control of alkali silica reaction," Cement and Concrete Research, Vol. 17, No. 5, pp. 839-844.

CARLES-GIBERGUES, A. OLLIVIER, J.P. and HANNA, B. (1989) "Ultrafine admixtures in high strength pastes and mortars," MALHOTRA, V.M. editor, Proceedings of the Third International Conference on " Fly ash, silica fume, slag, and natural pozzolans in concrete" (Trodheim; Norway), Published by the ACI (SP-114), Vol. I, pp. 117-129.

CARTER, P. (1991) "Sealing to improve durability of bridge infrastructure concrete," Concrete International, Vol. 12, July, pp. 33-66.

CAVALIER, P.G. and VASSIE, P.R. (1981) "Investigation and repair of reinforcement corrosion in a bridge deck," Proceedings of the Institution of Civil Engineers, Vol. 70, Part 1, August, pp. 461-480.

CEB GENERAL TASK GROUP 20 (1992) "Durable concrete structures - Design guide," Published by Thomas Telford Services Ltd. (London).

CHANDRA, S. and FLODIN, P. (1987) "Interactions of polymers and organic admixtures on Portkand Cement hydration," Cement and Concrete Research, Vol. 17, No. 6, pp. 875-890.

CHATTERJI, S. (1982) "Probable mechanisms of crack formation at early ages of concretes: A literature survey," Cement and Concrete Research, Vol. 12, No. 3, pp. 371-376.

CHENG-YI, H. and FELDMAN, R.F. (1985) "Hydration reactions in Portland cement-silica fume blends," Cement and Concrete Research, Vol. 15, No. 4, pp. 585-592.

CHORINSKY, E.G. (1987) "Polymers in cement mortars 1950-1987 in Germany," STAYNES, B.W. editor, Fifth International Congress on Polymers in Concrete "The production performance & potential of polymers in concrete" (England; Brighton)(22-24 September), pp. 23-25.

CLEAR K.C. (1976) "Time to corrosion of reinforcing steel in concrete slabs; Volume 3: Performance after 830 daily salt application" Report No. FHWA/RD-76/70, Published by the Federal Highway administration (Washington D.C.).

CLEAR, K.C. (1982) "Time-to-corrosion of reinforcing steel in concrete slabs," Report No. FHWA/RD-82/028, Published by the Federal Highway Administration (Washington D.C.).

COLLEPARDI, M. FRATESI, R. MARICONI, G. COPPOLA, L. and CORRADETTI, C. (1990) "Use of nitrate as corrosion inhibitor admixture in reinforced concrete structures immersed in sea-water," VAZQUEZ, E. editor, Proceedings of the International Rilem Symposium "Admixtures for concrete: Improvement of properties" (Barcelona), Published by Chapman and Hall Ltd. (London), pp. 279-288.

CONCRETE SOCIETY (1988) "Permeability testing of site concrete - A review of methods and experience," Technical Report No. 31, Published by the Concrete Society (London).

CONCRETE SOCIETY (1990) "The use of GGBS and PFA in concrete," Concrete Society Technical Report, Published by the Concrete Society (Slough; UK).

COPELAND, L.E. and BRAGG, R.H. (1955) "Self-desiccation in Portland-Cement pastes," ASTM Bulletin, February, pp. 34-39.

CORNET, I. and BRESLER, B. (1981) "Galvanized steel in concrete: Literature review and assessment of performance in galvanized reinforcement for concrete - II," International lead Zinc Research Organization Inc., May.

CRANK, J. (1975) "The mathematics of diffusion," Second edition, Published by Clarendon Press (Oxford).

CRC TECHNICAL COMMITTEE (1974) "Corrosion of reinforcement in concrete; A state-of-the-art report," Materials and Structures, Vol. 9, No. 51, pp. 187-206.

CROFT, J.B. (1967) "The influence of soil mineralogical composition on cement stabilization," Geotechnique, Vol. 17, No. 2, pp. 119-135.

CZERNIN, W. (1980) "Cement chemistry and physics for civil engineers," Published by George Godwin Ltd., Second edition (London), p. 91.

DAY, R.L. and MARSH, B.K. (1988) "Measurement of porosity in blended cement pastes," Cement and Concrete Research, Vol. 18, No. 1, pp. 63-73.

DECTER, M.H. SHORT, N.R. PAGE, C.L. and HIGGINS, D.D. (1989) "Chloride ion penetration into blended cement pastes and concrete," MALHOTRA, V.M. editor. Proceedings of the Third International Conference on " Fly ash, silica fume, slag, and natural pozzolans in concrete" (Trodheim; Norway), Published by the ACI (SP-114), Vol. II, pp. 1399-1411.

DENNIS, R. (1988) "Polymer dispersions or lattices," HEWLETT, P.C. editor "Cement admixtures: Uses and applications." Published by Longman Scientific & Technical, Second edition, pp. 130-143.

DENNO, G.M. (1990) Private communication.

DENNO, G.M. (1991) Private communication.

DETWILER, R.J. and MEHTA, P.K. (1989) "Chemical and physical effects of silica fume on the mechanical behaviour of concrete," ACI Materials Journal, Vol. 86, November-December, pp. 609-614.

DETWILER, R.J. KJELLEN, K.O. and GJØRV, O.E. (1991) "Resistance of chloride intrusion of concrete cured at different temperatures," ACI Materials Journal, Vol. 88, January-February, pp. 19-24.

DHIR, R.K. HEWLETT, P.C. and CHAN, Y.N. (1989) "Near surface characteristics of concrete: intrinsic permeability," Magazine of Concrete Research, Vol. 41, No. 147, pp. 87-97.

DHIR, R.K. JONES, M.R. AHMED, H.E.H. and SENEVIRATNE, A.M.G. (1990) "Rapid estimation of chloride diffusion coefficient in concrete," Magazine of Concrete Research, Vol. 42, No. 152, pp. 177-185.

DHIR, R.K. JONES, M.R. and SENEVIRATNE, A.M.G. (1991) "Diffusion of chlorides into concrete: influence of PFA quality," Cement and Concrete Research, Vol. 21, No. 6, pp. 1092-1102.

DIAB, H. BENTUR, A. HEITNER-WIRGUIN, C. and BEN-DOR, L. (1988) "The diffusion of Cl⁻ ions through Portland cement and Portland cement-polymer systems," Cement and Concrete Research, Vol. 18, No. 5, pp. 715-722.

DICKIE, R. (1986) "Chemical studies of the of the organic coating-steel interface after exposure to an aggressive environment," DICKIE, R. and FLOYD, F. editors, ACS Symposium Series 322 "Polymeric materials for corrosion control." Published by the American Chemical Society, p. 136.

ECOB, C.R. and KING, E.S. (1990) "Aggressive underground environments: Factors affecting durability and specification of appropriate protective systems," DHIR, R.K. and GREEN, J.W. editors, Proceedings of the International Conference on "Protection of concrete" (University of Dundee; Scotland; UK), Published by E. & F.N. Spon, pp. 751-763.

ECOB, C.R. KING, E.S. ROSTAM, S. and VINCENTSEN, L.J. (1990) "Epoxy coated reinforcement cages in precast concrete segmental tunnel linings - Durability," PAGE, C.L. TREADAWAY, K.W.J. BAMFORTH, P.B. editors "Corrosion of reinforcement in concrete." Published for the Society of Chemical Industry by Elsevier Science Publishers Ltd, pp. 550-558.

EL-BELBOL, S.M.T. and BUENFELD, N.R. (1988) "An accelerated chloride ion diffusion test," Materials Research Society Symposium "Pore structure and permrability of cementitious materials (Boston)", Published by the Materials Research Society, November, pp. 110-123.

EL-BELBOL, S.M.T. (1991) "Acceleration of chloride ion diffusion in concrete," PhD Thesis, University of London, Imperial College.

EL-JAZAIRI, B. BERKE, N.S. and GRACE, W.R. (1990) "The use of calcium nitrate as a corrosion inhibiting admixture to steel reinforcement in concrete," PAGE, C.L. TREADAWAY, K.W.J. BAMFORTH, P.B. editors "Corrosion of reinforcement in concrete." Published for the Society of Chemical Industry by Elsevier Science Publishers Ltd., pp. 571-585.

ERLIN, B. and HIME, W. (1985) "Chloride-induced corrosion," Concrete International, Vol. 7, September, pp. 23-25.

EVERETT, L.H. and TREADAWAY K.J.W. (1980) "Deterioration due to corrosion in reinforced concrete," Information Paper No. 12/80, Published by the Building Research Establishment (Garston).

FAGERLUND, G. (1975) "The significance of critical degree of saturation at freezing of porous and brittle materials," "Durability of concrete." Published by the ACI (SP-47), Vol. 2, pp. 13-65)

FAGERLUND, G. (1982) " On the capillarity of concrete," Nordic Concrete Research, Publication No. 1 (December)(Oslo).

FARRAY, A.L.A. BIJEN, J.M. and DE HANN, Y.M. (1989) "The reaction of fly ash in concrete; A critical examination," Cement and Concrete Research, Vol. 19, No. 2, pp. 235-246.

FELDMAN, R.F. and CHENG-YI, H. (1985) "Properties of portland cement-silica fume pastes; I. Porosity and surface properties," Cement and Concrete Research, Vol. 15, No. 5, pp. 765-774.

FELDMAN, R.F. (1986) "Pore structure, permeability, and diffusivity as related to durability," 8th International Symposium on "The chemistry of cement" (Rio), Vol. I, pp. 336-356.

FOOKES, P.G. and COLLIS, L. (1975) "Problems in the Middle East," Concrete, Vol. 9, July, pp. 12-17.

FOOKES, P.G. and COLLIS, L. (1976) "Cracking and the Middle East," Concrete, Vol. 10, February, pp. 14-19.

FOOKES, P.G. POLLOCK, D.J. and KAY, E.A. (1981) "Middle East concrete (2); Rates of deterioration," Concrete, Vol. 15, September, pp. 12-19.

FOOKES, P.G. FRENCH, W.J. and RICE, S.M.M. (1985) "The influence of ground and groundwater on construction in the Middle East," The Quarterly Journal of Engineering Geology, Vol. 18, pp. 101-128.

FOOKES, P.G. SIMM, J.D. and BARR, J.M. (1986) "Marine concrete performance in different climatic environments," International Conference on "Marine concrete" (London)(22-24 September), Published by the Concrete Society (London).

FORRESTER, J.A. (1970) "A conduction calorimeter for the study of cement hydration," Cement Technology, May/June, pp. 95-99.

FOWLER, D.W. and PAUL, D.R. (1978) "Corrosion protection of reinforcing provided by polymer-impregnated concrete," ACI Journal, Vol. 75, October, pp. 520-525.

FRANCOIS, R. and ARLIGUIE, G. (1991) "Reinforced concrete: Correlation between cracking and corrosion," MALHOTRA, W.M. editor, Proceedings of the Second Canment International Conference on "Concrete Durability" (Canada), Published by the ACI (SP-126), Vol. II, pp. 1221-1238.

FRACZEK, J. (1987) "A review of electrochemical principles as applied to corrosion of steel in a concrete or grout environment," GISBON, F.W. editor "Corrosion, concrete, and chlorides." Published by the ACI (SP-102), pp. 13-24.

FRONDISTOU-YANNAS, S.A. and SHAH, S.P. (1972) "Polymer latex modified mortar," ACI Journal, Vol. 69, January, pp. 61-65.

FULTON, F.S. (1969) "Concrete Technology; A South African Handbook," Published by the Portland Cement Institute (Johannesburg), Fourth edition.

FUNKE, W. (1988) "Organic coatings in corrosion protection," WILSON, A. NICHOLSON, J. and PROSSER, H. editors "Surface coatings - 2," Published by Elsevier Science Publishers Ltd. (London).

GARBOCZI, E.J. (1990) "Permeability, diffusivity, and microstructural parameters: A critical review," Cement and Concrete Research, Vol. 20, No. 4, pp. 591-601.

GAUTEFALL, O. and HAVDAHL, J. (1989) "Effect of condensed silica fume on the mechanism of chloride diffusion into hardened cement paste," MALHOTRA, V.M. editor, Proceedings of the Third International Conference on " Fly ash, silica fume, slag, and natural pozzolans in concrete" (Trodheim: Norway). Published by the ACI (SP-114), Vol. I, pp. 157-174.

GÉGOUT, P. REVERTÉGAT, E. and MOINE, G. (1992) "Action of chloride ions on hydrated cement pastes: Influence of the cement type and long time effect of the concentration of the chlorides," Cement and Concrete Research, Vol. 22, Nos. 2/3, pp. 451-457.

GERHARTZ (1), W. YAMAMOTO, S. and KAUDY, L. (1987) "Ullmann's encyclopedia of industrial chemistry," Vol. A23, Published by VCH Publishers Ltd. (Cambridge; UK), pp. 607-623.

GERHARTZ (2), W. YAMAMOTO, S. and KAUDY, L. (1987) "Ullmann's encyclopedia of industrial chemistry," Vol. A7, Published by VCH Publishers Ltd. (Cambridge; UK), pp. 116-118.

GERHARTZ (3), W. YAMAMOTO, S. and KAUDY, L. (1987) "Ullmann's encyclopedia of industrial chemistry," Vol. A6, Published by VCH Publishers Ltd. (Cambridge; UK), pp. 10-12.

GERHARTZ (4), W. YAMAMOTO, S. and KAUDY, L. (1987) "Ullmann's encyclopedia of industrial chemistry," Vol. A7, Published by VCH Publishers Ltd. (Cambridge; UK), pp. 341-367.

GERHARTZ (5), W. YAMAMOTO, S. and KAUDY, L. (1987) "Ullmann's encyclopedia of industrial chemistry," Vol. A7, Published by VCH Publishers Ltd. (Cambridge; UK), pp. 341-367.

GERHARTZ (6), W. YAMAMOTO, S. and KAUDY, L. (1987) "Ullmann's encyclopedia of industrial chemistry," Vol. A15, Published by VCH Publishers Ltd. (Cambridge; UK), pp. 334-345.

GERHARTZ (7), W. YAMAMOTO, S. and KAUDY, L. (1987) "Ullmann's encyclopedia of industrial chemistry," Vol. A20, Published by VCH Publishers Ltd. (Cambridge; UK), pp. 298-304.

GERHARTZ (8), W. YAMAMOTO, S. and KAUDY, L. (1987) "Ullmann's encyclopedia of industrial chemistry," Vol. A10, Published by VCH Publishers Ltd. (Cambridge; UK), pp. 224-254.

GERHARTZ (9), W. YAMAMOTO, S. and KAUDY, L. (1987) "Ullmann's encyclopedia of industrial chemistry," Vol. A16, Published by VCH Publishers Ltd. (Cambridge; UK), pp. 360-374.

GERHARTZ (10), W. YAMAMOTO, S. and KAUDY, L. (1987) "Ullmann's encyclopedia of industrial chemistry," Vol. A9, Published by VCH Publishers Ltd. (Cambridge; UK), pp. 297-325.

GERHARTZ (11), W. YAMAMOTO, S. and KAUDY, L. (1987) "Ullmann's encyclopedia of industrial chemistry," Vol. A3, Published by VCH Publishers Ltd. (Cambridge; UK), pp. 176-185.

GERHARTZ (12), W. YAMAMOTO, S. and KAUDY, L. (1987) "Ullmann's encyclopedia of industrial chemistry," Vol. A10, Published by VCH Publishers Ltd. (Cambridge; UK), pp. 1-22.

GERHARTZ (13), W. YAMAMOTO, S. and KAUDY, L. (1987) "Ullmann's encyclopedia of industrial chemistry," Vol. A23, Published by VCH Publishers Ltd. (Cambridge; UK), pp. 706-719.

GERWICK, B.C. (1990) "International experience on the performance of marine concrete," Concrete International, Vol. 12, May, pp. 47-53.

GJØRV, O.E. (1968) "Durability of reinforced concrete wharves in Norwegian harbours," Ingeniørforlaget (Oslo), pp. 153.

GJØRV, O.E. VENNESLAND, Ø. and EL-BUSAIDY, A.H.S (1977) "Electrical resistivity of concrete in the oceans," Presented at the 9th Annual Offshore Technology Conference (Houston; Texas)(2-5 May), pp. 581-587.

GJØRV, O.E. and VENNESLAND, Ø. (1979) "Diffusion of chloride ions from seawater into concrete," Cement and Concrete Research, Vol. 9, No. 2, pp. 229-238.

GLAVIND, M. and STANG, H. (1991) "A geometrical packing model as a basis for composing cement paste containing clay for high strength concrete," Proceedings of the Third International Symposium on "Brittle matrix composites" (Warsaw), Published by Elsevier Applied Science (London), pp. 508-518.

GLASSER, F.P. LUKE, K. and ANGUS, N.J. (1988) "Modification of cement pore fluid composition by pozzolanic additives," Cement and Concrete Research, Vol. 18, No. 2, pp. 165-178.

GLOVER, G.M. and RAASK, E. (1972) "Water diffusion and microstructure of hydrated cement pastes," Materials and Structures, Vol. 5, No. 29, pp. 315-322.

GOÑI, S. and ANDRADE, C. (1990) "Synthetic concrete pore solution chemistry and rebar corrosion rate in the presence of chlorides," Cement and Concrete Research, Vol. 20, No. 4, pp. 525-539.

GOTO, S. and ROY, D.M. (1981) "The effect of w/c ratio and curing temperature on the permeability of hardened cement paste," Cement and Concrete Research, Vol. 11, No. 4, pp. 575-579.

GOUDA, V.K. (1970) "Corrosion and corrosion inhibition of reinforcing steel; 1: Immersed in alkaline solution," British Corrosion Journal, Vol. 5, pp. 198-205.

GRAYSON (1), M. and ECKROTH, D. (1978) "Kirk-Othmar encyclopedia of chemical technology," Vol. 19, Published by John Wiley & Sons, Third edition, p. 608.

GRAYSON (2), M. and ECKROTH, D. (1978) "Kirk-Othmar encyclopedia of chemical technology," Vol. 8, Published by John Wiley & Sons, Third edition, pp. 900-930.

GRAYSON (3), M. and ECKROTH, D. (1978) "Kirk-Othmar encyclopedia of chemical technology," Vol. 5, Published by John Wiley & Sons, Third edition, pp. 89-117.

GREGG, S.J. and SING, K.S.W. (1982) "Adsorption, surface area, and porosity," Published by the Academic Press (London), Second edition, pp. 248-282.

GRIM, R.E. and GUVEN, N. (1978) "Bentonites: Geology, mineralogy and uses," Published by Elsevier Science Publishers Ltd. (New York).

GRUBE, M. and LAWRENCE, C.D. (1984) "Diffusion of oxygen through saturated concrete," Proceedings of a Seminar (PP/397) at Oxford University, Published by the Cement and Concrete Association (England), 13-14 September.

GUTTERIDGE, W.A. and DALZIEL, J.A. (1990) "Filler cement: The effect of the secondary component on the hydration of portland cement," Cement and Concrete Research, Vol. 20, No. 5, pp. 778-782.

HALL, C. (1989) "Water sorptivity of mortars and concretes: A review," Magazine of Concrete Research, Vol. 41, No. 147, pp. 51-61.

HANDY, R.L. (1958) "Cementation of soil minerals with portland cement or alkalis," Highway Research Board (Bulletin 198), pp. 55-64.

HANKINS, P.J. (1985) "The use of surface coatings to minimize carbonation in the Middle east," Proceedings of the First International Conference on "Deterioration and repair of reinforced concrete in the Arabian Gulf", Vol. 1, pp. 273-285.

HANSEN, J.H. and VILLASDEN, C. (1989) "Design of surface coatings for protection of reinforced concrete structures," Proceedings of the Third International Conference on "Deterioration and repair of concrete in the Arabian Gulf" (Bahrain), Vol. 1, pp. 647-664.

HANSSON, I.L.H and HANSSON, C. M. (1983) "Electrical resistivity measurements of Portland Cement based materials," Cement and Concrete Research, Vol. 13, No. 5, pp. 675-683.

HANSSON, I.L.H and HANSSON, C. M. (1985) "Ion-conduction in cement-based materials," Cement and Concrete Research, Vol. 15, No. 1, pp. 201-212.

HAUSMANN, D.A. (1967) "Steel corrosion in concrete - How does it occur?," Materials Protection, Vol. 6, pp. 19-23.

HEARN, N. (1992) "Saturated permeability of concrete as influenced by cracking and self-sealing," PhD Thesis, Cambridge University.

HEWLETT, P.C. EDMEADES, R.W. and HOLDSWORTH, R.L. (1988) "Integral waterproofers for concrete," HEWLETT, P.C. editor "Cement admixtures: Uses and applications." Published by Longman Scientific & Technical Group UK Limited, Second edition, pp. 55-66.

HIME, W. and ERLIN, B. (1987) "Some chemical and physical aspects of phenomena associated with chloride-induced corrosion," GISON, F.W. editor "Corrosion, concrete, and chlorides," Published by the ACI (SP-102), pp. 1-12.

HO, D.W.S and LEWIS, R.K. (1987) "The water sorptivity of Concretes: The influence of constituents under continuous curing," Durability of Building Materials, Vol. 4, pp. 241-252.

HOBBS, D.W. (1988) "Carbonation of concrete containing pfa," Magazine of Concrete Research, Vol. 40, No. 143, pp. 69-78.

HOFFMANN, D.W. (1984) "Changes in structure and chemistry of cement mortars stressed by a sodium chloride solution," Cement and Concrete Research, Vol. 14, No. 1, pp. 49-56.

HOPE, B.B. and IP, A.K.C. (1989) "Corrosion inhibitors for use in concrete," ACI Materials Journal, Vol. 86, November-December, pp. 602-608.

HORRIGMOE, G. (1985) "Effect of pore water and its diffusion in concrete," BAZANT, Z. editor "Mechanics of geomaterials." Published by John Wiley & Sons Ltd., pp. 349-367.

HOSEK, J. (1966) "Properties of cement mortars modified by polymer emulsion," ACI Journal, Vol. 63, December, pp. 1411-1423.

HOSEK, J. and SEREDA, P.J. (1968) "Effect of organic surface agents on properties of hydrated cement compacts," Materials and Structures, Vol. 1, Jan.-Feb., pp. 7-12.

HUDEK, P. (1987) "Deterioration of aggregates - The underlying causes," SCANLON, J.M. editor, Katharine and Bryant Mather International Conference "Concrete Durability." Published by the ACI (SP-100), Vol. II, pp. 1325-1342.

JAEGERMANN, C. (1990) "Effect of water/cement ratio and curing on chloride penetration into concrete exposed to Mediterranean climate," ACI Materials Journal, Vol. 87, July-August, pp. 333-339.

JAHREN, P. (1983) "Use of silica fume in concrete," MALHOTRA, V.M. editor, First International Conference on "The use of fly ash, silica fume. & other mineral by-products in concrete." Vol. I, Published by the ACI (SP-79), pp. 589-605.

JAWED, I. and SKALNY, J. (1978) "Alkalies in cement: A review; Effects of alkalies on the hydration and performance of Portland cement," Cement and Concrete Research, Vol. 8, No. 1, pp. 37-52.

JENKINS, A.D. (1972) "Polymer science; A materials science handbook', Published by the North-Holland Publishing Company Ltd. (London).

JUMPER, C.H. (1931) "Tests on integral and surface waterproofing for concrete," Journal of the American Concrete Institute - Proceedings, Vol. 48, pp. 209-241.

JUN-YUAN, H. SCHEETZ, B.E. and ROY, D.M. (1984) "Hydration of fly ash-Portland cements," Cement and Concrete Research, Vol. 14, No. 4, pp. 505-512.

JUSTNES, H. OYE, B.A. and DENNINGTON, S.P. (1990) "Protecting concrete against chloride ingress by latex additions," DHIR, R.K. and GREEN, J.W. editors, Proceedings of the International Conference on "Protection of concrete" (University of Dundee; Scotland; UK), Published by E. & F.N. Spon, pp. 751-763.

KAYYALI, O.A. and HAQUE, M.N. (1988) "Chloride penetration and the ratio of $[Cl^-]/[OH^-]$ in the pores of cement paste," Cement and Concrete Research, Vol. 18, No. 6, pp. 895-900.

KELHAM, S. (1988) "A water absorption test for concrete," Magazine of Concrete Research, Vol. 40, No. 143, pp. 106-110.

KILLOH, D.C. PARROTT, L.J. and PATEL, R.G. (1989) "Influence of curing at different relative humidities on the hydration and porosity of a Portland/fly ash cement paste," MALHOTRA, V.M. editor, Proceedings of the Third International Conference on " Fly ash, silica fume, slag, and natural pozzolans in concrete" (Troedheim; Norway), Published by the ACI (SP-114), Vol. I, pp. 157-174.

KIRKHAM, D. and POWERS, W.L. (1972) "Advanced soil physics," Published by Wiley-Interscience (New York), pp. 1-45.

KLINKENBERG, L.J. (1941) "The permeability of porous media to liquids and gases," Drilling and Production Practice, Published by the American Petroleum Institute (New York), pp. 200-214.

KOLLEK, J.J. (1989) "The determination of the permeability of concrete to oxygen by the Cembureau method - A recommendation," Materials and Structures, Vol. 22, pp. 225-230.

KONDO, R. STATAKA, M. and USHIYAMA, H. (1974) "A review of the 28th General Meeting of the Cement and Concrete Association of Japan," pp. 41-43.

KOTZ, J.C. and PURCELL, K.F. (1991) "Chemistry and chemical reactivity," Published by Saunders College Publishing, Second edition.

KRONLÖF, A. (1994) "Effect of very fine aggregate on concrete strength," Materials and Structures, Vol. 27, pp. 15-25.

KROSCWITZ (1), J. and HOWE-GRANT, M. (1992) "Kirk-Othmar encyclopedia of chemical technology," Vol. 8, Published by John Wiley & Sons, Fourth edition, pp. 108-118.

KROSCWITZ (2), J. and HOWE-GRANT, M. (1992) "Kirk-Othmar encyclopedia of chemical technology," Vol. 6, Published by John Wiley & Sons, Fourth edition, pp. 381-409.

KROSCWITZ (3), J. and HOWE-GRANT, M. (1992) "Kirk-Othmar encyclopedia of chemical technology," Vol. 8, Published by John Wiley & Sons, Fourth edition, pp. 432-445.

KROSCWITZ (4), J. and HOWE-GRANT, M. (1992) "Kirk-Othmar encyclopedia of chemical technology," Vol. 3, Published by John Wiley & Sons, Fourth edition, pp. 689-724.

KUHLMANN, L.A. (1990) "Styrene-butadiene latex-modified concrete: The ideal concrete repair material?," Concrete International, Vol. 12, October, pp. 59-65.

KUMAR, A. KOMARNENI, S. and ROY, D.M. (1987) "Diffusion of Cs⁺ and Cl⁻ through sealing materials," Cement and Concrete Research, Vol. 17, No. 1, pp. 53-160.

LAVELLE, J.A. (1988) "Acrylic latex-modified Portland cement," ACI Materials Journal, Vol. 85, January-February, pp. 41-48.

LAWRENCE, C.D. (1966) "Changes in composition of the aqueous phase during hydration of cement pastes and suspensions," Symposium on "Structure of Portland cement paste and concrete." Published by the Highway Research Board (Washington), pp. 378-391.

LAWRENCE, C.D. (1984) "Transport of oxygen through concrete," GLASSER, F.P. editor, British Ceramic Society Meeting on "Chemistry and chemically-related properties of concrete" (London)(April).

LEA, F.M. (1970) "The chemistry of cement and concrete," Published by Edward Arnold Publishers limited, Third edition.

LEEK, D.S. and POOLE, A.B. (1990) "The Breakdown of the passive film on high yield mild steel by chloride," PAGE, C.L. TREADAWAY, K.W.J. BAMFORTH, P.B. editors "Corrosion of reinforcement in concrete." Published for the Society of Chemical Industry by Elsevier Science Publishers Ltd, pp. 65-73.

LEEMING, M.B. (1989) "Concrete in the oceans programme - Coordinating report on the whole programme," Technical Report No. 25 (OTH 87 248). Published by the Department of Transport (UK).

LEIDHEISER, H. (1987) "Coatings," MANSFELD, F. editor "Corrosion mechanisms." Published by Marcel Dekker (New York).

LI, S. and ROY, D.M. (1986) "Investigation of relations between porosity, pore structure, and Cl⁻ diffusion of fly ash and blended cement pastes," Cement and Concrete Research, Vol. 16, No. 5, pp. 749-759.

LITVAN, G. and BICKLEY, J. (1987) "Durability of Parking Structures: Analysis of field survey," SCANLON, J.M. editor, Katharine and Bryant Mather International Conference "Concrete Durability." Published by the ACI (SP-100), Vol. II, pp. 1503-1521.

LIU, P.C. (1991) "Damage to concrete structures in a marine environment," Materials and Structures. Vol. 24, pp. 302-307.

LORPRAYOON, V. and ROSSINGTON, D.R. (1981) "Early hydration of cement constituents with organic admixtures," Cement and Concrete Research, Vol. 11, No. 2, pp. 267-277.

LOWE, I.R.G. HUGHES, B.P. and WALKER, J. (1971) "The diffusion of water in concrete at 30°C," Cement and Concrete Research, Vol. 1, No. 5, pp. 547-557.

MACINNIS, C. and NATHAWAD, Y.R. (1980) "The effects of a deicing agent on the absorption and permeability of various concretes," SEREDA, P.J. and LITVAN, G.G. editors, ASTM Special Technical Publication No. 691 "Durability of building materials and components" (Philadelphia), pp. 485-496.

MANNING, D. (1987) "A rational approach to corrosion protection of the concrete components of highway bridges," SCANLON, J.M. editor, Katharine and Bryant Mather International Conference on "Concrete Durability." Published by the ACI (SP-100), Vol. II, pp. 1527-1545.

MARSH, B.K. DAY, R.L. and BONNER, D.G. (1985) "Pore structure characteristics affecting the permeability of cement paste containing fly ash," Cement and Concrete Research, Vol. 15, No. 6, pp. 1027-1038.

MASLOW, P. (1974) "Chemical materials for construction," Published by The Structures Publishing Company.

MASO, J.C. (1980) "The bond between aggregates and hydrated cement pastes," 7th International Symposium on "The chemistry of cement" (Paris), Vol. I, pp. VII-1/3-15.

MATHER, B. (1979) "Concrete need not deteriorate," Concrete International, Vol. 1, September, pp. 32-37.

MARKLEY (1), K.S. (1961) "Fatty acids; Their chemistry, properties, production, and uses," Part 1, Published by Interscience Publishers Ltd. (London), Second edition.

MARKLEY (2), K.S. (1961) "Fatty acids; Their chemistry, properties, production, and uses," Part 2, Published by Interscience Publishers Ltd. (London), Second edition.

MATTA, Z.G. (1993) "Deterioration of concrete structures in the Arabian Gulf," Concrete International, Vol. 15, July, pp. 33-36.

McCARTER, W.J. EZIRIM, H. and EMERSON, M. (1992) "Absorption of water and chloride into concrete," Magazine of Concrete Research, Vol. 44, No. 158, pp. 31-37.

MEHTA, P.K. (1977) "Effect of cement composition on corrosion of reinforcing steel in concrete," ASTM publication (STP-629) "Corrosion of steel in concrete" (Philadelphia), pp. 12-19.

MEHTA, P.K. and MANMOHAN, C. (1980) "Pore distribution and permeability of hardened cement pastes," 7th International Symposium on "The chemistry of cement" (Paris), Vol III, pp. VII-1 - VII-5.

MEHTA, P.K. (1988) "Durability of concrete exposed to marine environments - A fresh look," MALHOTRA, V.M., Proceedings of the Second International Conference on "Concrete in the marine environment" (St. Andrews by-the-sea; Canada), Published by the ACI (SP-109), pp. 1-29.

MEHTA, P.K. (1991) "Durability of concrete - Fifty years of progress?," MALHOTRA, W.M. editor, Proceedings of the Second International Conference on "Concrete Durability" (Canada), Published by the ACI (SP-126), Vol. I, pp. 1-50.

MEHTA, P.K. and MONTEIRO, P.J.M. (1993) "Concrete: structure, properties, and materials," Second edition, Published by Prentice-Hall (New Jersey).

MIDGLEY, H.G. and ILLSTON, J.M. (1983) "Some comments on the microstructure of hardened cement pastes," Cement and Concrete Research, Vol. 13, No. 2, pp. 197-206.

MIDGLEY, H.G. and ILLSTON, J.M. (1984) "The penetration of chlorides into hardened cement pastes," Cement and Concrete Research, Vol. 14, No. 4, pp. 546-558.

MIKHAIL, R.Sh. (1983) "Microstructure and thermal analysis of solid surfaces," Published by John Wiley & Sons Ltd. (New York), pp. 22-72.

MONTEIRO, P.J.M. and MEHTA, P.K. (1986) "Improvement of the aggregate-cement paste transition zone by grain refinement of hydration products," Proceedings of the Eighth International Symposium on "The chemistry of cement" (Rio de Janeiro), Vol. 3, pp. 443-437.

MONFORE, G.E. and VERBECK, G.J. (1960) "Corrosion of prestressing wire in concrete," ACI Proceedings, Vol. 57, No. 5, pp. 491-516.

MOUKWA, M. and AITCIN, P.C. (1988) "The effect of drying on cement pastes pore structure as determined by mercury porosimetry," Cement and Concrete Research, Vol. 18, No. 5, pp. 745-752.

MOUKWA, M. (1989) "Penetration of chloride ions from sea water into mortars under different exposure conditions," Cement and Concrete Research, Vol. 19, No. 6, pp. 894-904.

NEVILLE, A.M. (1981) "Properties of Concrete," Published by Longman Group Limited (England), Third edition.

NOBLE, D.F. (1977) "Reactions and strength development in Portland Cement-Clay mixtures," Highway Research Record No. 198, pp. 39-56.

NURENBERGER, U. (1988) "Chapter 6," Series of otto-Graf-Institut No. 79 (Stuttgart).

NYAME, B.K. and ILLSTON, J.M. (1980) "Capillary pore structure and permeability of hardened cement paste," 7th International Symposium on "The chemistry of cement" (Paris), Vol. III, pp. VII-181 - VII-186.

ODOM, I.E. (1984) "Smectite clay minerals: Properties and uses," Phil. Transactions of the Royal Society of London, Vol. A311, pp. 391-409.

OECD SCIENTIFIC EXPERTS GROUP (1989) "Durability of concrete bridges," Report published by the OECD Publications Service.

OHAMA, Y. (1987) "Principle of latex modification and some typical properties of latex-modified mortars and concretes," ACI Materials Journal, Vol. 84, November-December, pp. 511-518.

ORCHARD, D.F. (1979) "Concrete technology: Properties of materials (Volume 1)," Published by Applied Sciences Publishers Ltd. (London), Fourth edition.

OSHIRO, T. and TANIGAWA, S. (1988) "Effect of surface coating on the durability of concrete exposed to a marine environment," MALHOTRA, V.M. editor, Proceedings of the Second International Conference on "Concrete in the marine environment" (St. Andrews by-the-sea; Canada), Published by the ACI (SP-109), pp. 179-198.

PAGE, C.L. SHORT, N.R. and EL TARRAS, A. (1981) "Diffusion of chloride ions in hardened cement pastes," Cement and Concrete Research, Vol. 11, No. 3, pp. 395-406.

PAGE, C.L. and VENNESLAND, Ø. (1983) "Pore solution Composition and chloride binding capacity of silica-fume cement pastes," Materials and structures, Vol. 16, No. 91, pp. 19-25.

PAGE, C.L. (1988) "Chapter 2: Basic principles of corrosion," SCHIESSL, P. editor, A Rilem Report "Corrosion of steel in concrete." Published by Chapman and Hall Ltd.

PAGE (1), C.L. LAMBERT, P. and VASSIE, P.R.W. (1991) "Investigation of reinforcement corrosion; 1. The pore electrolyte phase in chloride-contaminated concrete," Materials and Structures, Vol. 24, pp. 243-252.

PAGE (2), C.L. LAMBERT, P. and VASSIE, P.R.W. (1991) "Investigation of reinforcement corrosion; 2. Electrochemical monitoring of steel in chloride contaminated concrete," Materials and Structures, Vol. 24, pp. 351-358.

PAPADAKIS, V.G. VAYENAS, C.G. and FARDIS, M.N. (1991) "Physical and chemical characteristics affecting the durability of concrete," ACI Materials Journal, Vol. 88, March-April, pp. 186-196.

PARKHOMENKO, E.I. (1967) "Electrical properties of rock," Published by Plenum Press (New York).

PARROTT, L.J. (1987) "A review of carbonation in reinforced concrete," Carried out by the Cement and Concrete Association under a British Research Establishment contract.

PCA (1991) "Solidification and stabilization of wastes using Portland Cement," Published by the Portland Cement Association, pp. 12-14.

PEER, L.B.B. (1990) "Water flow in unsaturated concrete," PhD Thesis, Cambridge University.

PETERSON, C.A. (1980) "Survey of parking structure deterioration and distress," Concrete International, Vol. 2, March, pp. 53-61.

PERENCHIO, W.F. (1988) "Durability of concrete treated with silanes," Concrete International, Vol. 10, November, pp. 34-40.

PLEE, D. LEBEDENKO, F. OBRECHT, F. LETELLIER, M. and VAN DAMME, H. (1990) "Microstructure, permeability, and rheology of bentonite-cement slurries," Cement and Concrete Research, Vol. 20, No. 1, pp. 45-61.

POLLARD, S.J.T. MONTGOMERY, D.M. SOLLARS, C.J. and PERRY, R. (1991) "Organic compounds in the cement-based stabilization/solidification of hazardous mixed wastes - Mechanistic and process considerations," Journal of Hazardous Materials, Vol. 28, pp. 313-327.

POMEROY, C.D. (1976) "An assessment of the commercial prospects for fibre- and polymer-modified concretes," Cement and Concrete Research, Vol. 28, No. 96., pp. 121-129.

POPOVICS, S. (1987) "Strength losses of polymer-modified concretes under wet conditions," FOWLER, D.W. editor "Polymer modified concrete", Published by the ACI (SP-99), pp. 165-189.

POWERS, T.C. COPELAND, L.E. HAYES, J.C. and MANN, H.M. (1954) "Permeability of portland cement paste," Journal of the American Concrete Institute, Vol. 51, November, pp. 285-298.

POWERS, T.C. COPELAND, L.E. and MANN, H.M. (1959) "Capillary continuity and discontinuity in cement pastes," Journal of the Portland Cement Association, Vol. 1, No. 2, pp. 38-48.

POWERS, T.C. (1968) "The properties of fresh concrete," Published by John Wiley & Sons Inc. (New York).

RAHARINAIVO, A. BREVET, P. GRIMALDI, G. and PANNIER, G. (1986) "Relationships between concrete deterioration and reinforced steel corrosion," Durability of Building Materials, Vol. 4, pp. 97-112.

RAMACHANDRAN, V.S. (1971) "Possible states of chloride in the hydration of tricalcium silicate in the presence of calcium chloride," Materials and Structures, Vol. 4, No. 19, pp. 3-11.

RAMACHANDRAN, V.S. (1973) "Action of triethanolamine on the hydration of tricalcium aluminate," Cement and Concrete Research, Vol. 3, No. 1, pp. 41-54.

RAMACHANDRAN (1976) "Hydration of cement -- Role of triethanolamine," Cement and Concrete Research, Vol. 6, No. 5, pp. 623-632.

RAVINA, D. (1980) "Optimized determination of PFA (fly ash) fineness with reference to pozzolanic activity," Cement and Concrete Research, Vol. 10, pp. 573-580.

REGOURD, M. (1980) "Characterization and thermal activation of slag cements," 7th International Symposium on "The chemistry of cement" (Paris), Vol. 2III, pp. 105-111.

RIXON, M.R. and MAILVAGANAM, N.P. (1986) "Chemical admixtures for concrete," Published by E. & F.N. Spon Ltd. (London), Second edition.

ROBERTS, M.H. (1962) "Effect of calcium chloride on the durability of pre-tensioned wire in pre-stressed concrete," Magazine of Concrete Research, Vol. 14, pp. 143-154.

ROPER, H. and BAWEJA, D. (1991) "Carbonation-chloride interactions and their influence on corrosion rates of steel in concrete," MALHOTRA, W.M. editor, Proceedings of the Second Canment International Conference on "Concrete Durability" (Canada), Published by the ACI (SP-126), Vol. I, pp. 295-315.

ROSE (1), D.A. (1963) "Water movement in porous materials: Part 1 - Isothermal vapour transfer," British Journal of Applied Physics, Vol. 14, pp. 256-261.

ROSE (2), D.A. (1963) "Water movement in porous materials: Part 2 - The separation of the components of water movement," British Journal of Applied Physics, Vol. 14, pp. 491-496.

ROY, D.M. (1989) "Fly ash and silica fume; Chemistry and hydration," MALHOTRA, V.M. editor, Proceedings of the Third International Conference on " Fly ash, silica fume, slag, and natural pozzolans in concrete" (Trodheim; Norway), Published by the ACI (SP-114), Vol. I, pp. 117-129.

ROY, D.M. and IDORN, G.M. (1982) "Hydration, structure, and properties of blastfurnace slag cements, mortars, and concrete," ACI Journal, Vol. 79, November-December, pp. 444-456.

SAGOE-CRENTSIL, K.K. and GLASSER, F.P. (1990) "Analysis of the steel:concrete interface," PAGE, C.L. TREADAWAY, K.W.J. BAMFORTH, P.B. editors "Corrosion of reinforcement in concrete", Published for the Society of Chemical Industry by Elsevier Science Publishers Ltd, pp. 74-86.

SAGUES, A. POWERS, R. and ZAYED, A. (1990) "Marine environemnt corrosion of epoxy-coated reinforcing steel," PAGE, C.L. TREADAWAY, K.W.J. BAMFORTH, P.B. editors "Corrosion of reinforcement in concrete." Published for the Society of Chemical Industry by Elsevier Science Publishers Ltd., pp. 539-549.

SAKUTA, M. URANO, T. IZUMI, I. SUGIYAMA, M. and TANAKA, K. (1987) "Measures to restrain rate of carbonation in concrete," SCANLON, J.M. editor, Katharine and Bryant Mather International Conference on "Concrete Durability." Published by the ACI (SP-100), Vol. II, pp. 1962-1977.

SALPARANTA, L. (1990) "Epoxy-coated concrete reinforcements," PAGE, C.L. TREADAWAY, K.W.J. BAMFORTH, P.B. editors "Corrosion of reinforcement in concrete", Published for the Society of Chemical Industry by Elsevier Science Publishers Ltd., pp. 559-570.

SARGA, A. JOKELA, J. and METSO, J. (1984) "Zinc-coated concrete reinforcement," Research Report 306, Published by the Technical Research Centre of Finland.

SARKAR, S.L. (1991) "High strength concrete and its microstructure," GHOSH, S.N. editor "Cement and concrete science and technology: Progress in cement and concrete." Published by ABI Books Pvt. Ltd. (New Delhi; India), Vol. 1, Part 1, pp. 380-416.

SCHIESSL, P. (1987) "Influence of the composition of concrete on the corrosion protection of the reinforcement," SCANLON, J.M. editor, Katharine and Bryant Mather International Conference on "Concrete durability." Published by the ACI (SP-100), Vol. II, pp. 1633-1650.

SCHULTE, Ch. MADER, H. and WITTMAN, F.H. (1978), Cement and Concrete Research, Vol. 8, No. 3, pp. 359-368.

SCRIVENER, K.L. (1984) "The development of microstructure during the hydration of Portland cement," PhD Thesis, University of London, Imperial College.

SCRIVENER, K.L. and PRATT, P.L. (1987) "The characterisation and quantification of cement and concrete microstructures," Proceedings of the 1st Rilem International Congress, Vol. 1, pp. 61-68.

SCRIVENER, K.L. (1989) "The microstructure of concrete," SKALNY, J.P. editor "Materials science of concrete." Published by the American Ceramic Society.

SEDGWICK, J. (1991) "Strong but sensitive," The Atlantic Monthly, Vol. 267, No. 4, pp. 70-82.

SEMERAD, E. KREMNITZER, P. LACOM, W. HOLUB, F. and SATTLER, P. (1987) "Polymer modified mortar: influence of polymer addition on macroscopic and microscopic properties," STAYNES, B.W. editor, Fifth International Congress on Polymers in Concrete "The production performance & potential of polymers in concrete" (Brighton; England), pp. 223-228.

SERGI, G. YU, S.W. and PAGE, C.L. (1992) "Diffusion of chloride and hydroxide ions in cementitious materials exposed to a saline environment," Magazine of Concrete Research, Vol. 44, No. 158, pp. 63-69.

SHALON, R. and RAPHAEL, M. (1964) "Corrosion of reinforcing steel in hot countries," Rilem Bulletin (Paris), No. 24, pp. 29-45.

SHAW, D.J. (1966) "Introduction to colloid and surface chemistry," Published by Butterworth (London).

SHIMADA, H. and NISHI, S. (1983) "Sea water corrosion attack on concrete blocks embedding zinc galvanized steel bars," CRANE, A.P. editor "Corrosion of reinforcement in concrete construction." Published by Ellis Horwood Limited (England), pp. 407-418.

SHINDOU, T. NAITOU, T. and TSURUTA, K. (1986) "Study on durability of polymer-impregnated concrete (PIC) in the marine environment," International Conference on "Marine concrete" (London), Published by the Concrete Society (UK), September.

SHORT, N.R. PAGE, C.L. and GLASS, G.K. (1991) "A galvanic sensor for monitoring corrosion of steel in carbonated concrete," Magazine of Concrete Research, Vol. 43, No. 156, pp. 149-154.

SMITH, R.C. (1973) "Materials of construction," Published by McGraw Hill Company, Second edition.

SMOAK, W.G. (1976) "Development and field evaluation of a technique for polymer impregnation of new concrete bridge deck surfaces," Report No. FHWA-RD-76-95, Published by the Federal Highway Administration (Washington D.C.).

SMOLCZYK, H.R. (1984) "State of knowledge on chloride diffusion in concrete," Betonwerk+Fertigteil-Technik, HEFT 12, pp. 837-843.

SOMERVILLE, G. (1986) "The design life of concrete structures," The Structural Engineer, Vol. 64, No. 2, pp. 60-71.

SOPLER, B. (1973) "Corrosion of reinforcement in concrete - Part Series D," Report No. FCB 73-4, Published by the Norwegian Institute of Technology (University of Trondheim).

SØRENSEN, B. and JENSEN, P.B. (1990) "The corrosion properties of stainless steel reinforcement," PAGE, C.L. TREADAWAY, K.W.J. and BAMFORTH, P.B. editors "Corrosion of reinforcement in concrete." Published for the Society of Chemical Industry by Elsevier Science Publishers Ltd., pp. 601-610.

SOROKA, I. and STERN, N. (1976) "Calcareous fillers and the compressive strength of portland cement," Cement and Concrete Research, Vol. 6, No. 3, pp. 367-376.

STRATFULL, R.F. (1968) "How chloride affect concrete used with reinforcing steel," Material Protection, Vol. 7, No. 3, pp. 29-34.

SUZUKI, K. OHNO, Y. PRAPARANTANATRON, S. and TAMURA, H. (1990) "Mechanism of steel corrosion in cracked concrete," PAGE, C.L. TREADAWAY, K.W.J. and BAMFORTH, P.B. editors "Corrosion of reinforcement in concrete.", Published for the Society of Chemical Industry by Elsevier Science Publishers Ltd, pp. 19-28.

SWAMY, R.N. KOYAMA, S. ARIA, T. and MIKAMI, N. (1988) "Durability of steel reinforcement in marine environment," MALHOTRA, V.M. editor, Proceedings of the Second International Conference on "Concrete in the marine environment" (St. Andrews by-the-sea: Canada), Published by the ACI (SP-109), pp. 147-161.

SWAMY, R.N. (1990) "Resistance to chlorides of galvanized rebars", PAGE, C.L. TREADAWAY, K.W.J. and BAMFORTH, P.B. editors "Corrosion of reinforcement in concrete." Published for the Society of Chemical Industry by Elsevier Science Publishers Ltd., pp. 586-600.

SWAMY, R.N. and TANIKAWA, S. (1990) "Surface coatings to preserve concrete durability", **DHIR, R.K. and GREEN, J.W. editors, Proceedings of the International Conference on "Protection of concrete"** (University of Dundee; Scotland; UK), Published by E. & F.N. Spon, pp. 149-165.

TAYLOR, H.F.W. (1987) "A method for predicting alkali ion concentrations in cement pore solutions," Advances in Cement Research, Vol. 1, No. 1, pp. 5-17.

TAYLOR, H.F.W. (1990) "Cement chemistry," Published by Academic Press Limited.

THEISSING, E.M. WARDENIER, P. and deWIND, G. (1975) "The combination of sodium chloride and calcium chloride by some hardened cement pastes", Published by the Stevin Laboratory, Delf University of Technology (Delf).

THOOR (1), T.J.W. (1971) "Materials and technology," Vol. V, Published by Longman Group Ltd. (London), pp. 193-250.

THOOR (2), T.J.W. (1971) "Materials and technology," Vol. V, Published by Longman Group Ltd. (London), pp. 1-57.

THOOR (3), T.J.W. (1971) "Materials and technology," Vol. V, Published by Longman Group Ltd. (London), pp. 253-281.

THOOR (4), T.J.W. (1971) "Materials and technology," Vol. IV, Published by Longman Group Ltd. (London), pp. 37-73.

THOOR (5), T.J.W. (1971) "Materials and technology," Vol. IV, Published by Longman Group Ltd. (London), pp. 79-101.

TREADAWAY, K.W.J. (1988) "Chapter 4: Corrosion period," SCHIESSL, P. editor, A Rilem Report "Corrosion of steel in concrete," Published by Chapman and Hall Ltd.

TREADAWAY, K.W.J. COX, R.N. and BROWN, B.L. (1989) "Durability of corrosion resisting steels in concrete", Proceedings of the Institute of Civil Engineers, Part 1, Vol. 86, April, pp. 305-331.

TREECE, R.A. and JIRSA, J.O. (1989) "Bond strength of epoxy-coated reinforcing bars", ACI Materials Journal, Vol. 86, No. 2, pp. 167-174.

TREMPER, B. BEATON, J.L. and STRATFULL, R.F. (1958) "Causes and repair of deterioration to a California bridge due to corrosion of reinforcing steel in a marine environment; Part II", An H.R.B. Bulletin 182, Washington D.C., pp. 18-41.

TRITTHART, J. (1989) "Chloride binding in cement; II. The influence of the hydroxide concentration in the pore solution of hardened cement paste on chloride binding," Cement and Concrete Research, Vol. 19, No. 5, pp. 683-691.

TRITTHART, J. (1992) "Changes in pore water composition and total chloride content at different levels of cement paste plates under different storage conditions", Cement and Concrete Research, Vol. 22, No. 1, pp. 129-138.

TUUTTI, K. (1982) "Corrosion of steel in concrete", Research Report FO 4, Published by the Swedish Cement and Concrete Institute (Stockholm).

USHIYAMA, H. and GOTO, S. (1974) "Diffusion of various ions in hardened cement pastes", Proceedings of the 6th International Congress on "The chemistry of cement" (Moscow), Vol. 2-1, pp. 331-337.

VALENTA, O. (1970) "The permeability and durability of concrete in aggressive conditions," Proceedings of the 10th International Congress on Large Dams (Montreal), pp. 103-117.

VASSIE, P. (1985) "Reinforcement corrosion and the durability of concrete bridges," Proceedings of the Institution of Civil Engineers, Part 1, Vol. 78, October, pp. 1253-1256.

VIRMANI, Y.P. CLEAR, K.C. and PASKO, T.J. (1983) "Time-to-corrosion of reinforcing steel in concrete slabs; calcium nitrate admixture or epoxy coated reinforcing bars as corrosion protection system", Report No. FHWA/RD-83/012, Published by the Federal Highway administration (Washington D.C.), p. 71.

VOLLHARDT, K.P.C. and SCHORE, N.E. (1987) "Organic chemistry," Published by W.H. Freeman and Company (New York), Second edition.

VUORINEN, J. (1985) "Application of diffusion theory to permeability tests on concrete; Part II: Pressure-saturation test on concrete and coefficient of permeability," Magazine of Concrete Research, Vol. 37, No. 132, September, pp. 145-161.

WALLBANK, E.J. (1989) "The performance of concrete in bridges; A survey of 200 bridges," A report prepared for the Department of Transport by G. Maunsell and Partners, Published by Her Majesty's Stationary Office (London).

WARLOW, W.J. PYE, P.W. (1978) "Osmosis as a cause of blistering of in situ resin flooring on wet concrete", Magazine of Concrete Research, Vol. 20, No. 104, pp. 152-156.

WEAVER, C.E. and POLLARD, L.D. (1973) "The chemistry of clay minerals," Published by Elsevier Science Publishers Ltd. (New York).

WEINBURG, R. KHORASANI, R. SCHWEER, C. and WILS, S. (1988) "Solidification of oily organic wastes," ORIO, A.A. editor. 3rd International Conference on "Environmental Contamination." (Venice), pp. 54-56.

WEI, W. ROTHWELL, G.W. and DAVIRS, H. (1990) "Investigation of the gas and vapour resistance of surface coatings on concrete and effects of weathering on their carbonation protective performance", PAGE, C.L. TREADAWAY, K.W.J. and BAMFORTH, P.B. editors "Corrosion of reinforcement in concrete." Published for the Society of Chemical Industry by Elsevier Science Publishers Ltd., pp. 397-408.

WEYERS, R.E. and CADY, P.D. (1987) "Deterioration of concrete bridge decks from corrosion of reinforcing steel", Concrete International, Vol. 9, January, pp. 15-21.

WHITE, A.H. and BATEMAN, J.H. (1926) "Soaps as integral waterproofers for concrete", Journal of the American Concrete Institute - Proceedings, Vol. 22, pp. 535-559.

WHITING, D. (1981) "Rapid measurement of the chloride permeability of concrete" Public Roads Magazine, Vol. 45, No. 3, pp. 101-112.

WHITTINGTON, H.W. McCARTER, J. and FORDE, M.C. (1981) "The conduction of electricity through concrete", Magazine of Concrete Research, Vol. 33, No. 114, pp. 48-60.

WINSLOW, D. and Liu, D. (1990) "The pore structure of paste in concrete", Cement and Concrete Research, Vol. 20, No. 2, pp. 227-235.

WONG, K.H. WEYERS, E. and CADY, P.D. (1983) "The retardation of reinforcing steel corrosion by alkyl-alkoxy silane", Cement and Concrete Research, Vol. 13, No. 6, pp. 778-788.

WOOD, J.G.M. WILSON, J.R. and LEEK, D.S. (1989) "Improved testing for chloride ingress resistance of concretes and relation of results to calculated behaviour", Paper Presented at the 3rd international Conference on "Deterioration and repair of reinforced concrete in the Arabian Gulf." (21-24 October).

YAMAMOTO, Y. and KOBAYASHI, M. (1982) "use of mineral fines in high strength concrete; Water requirement and strength," Concrete International, Vol. 4, No. 7, pp. 33-40.

YEOMANS, S.R. (1991) "Comparative studies of galvanized and epoxy coated steel reinforcement in concrete", Malhotra, V.M. editor, Proceedings of the Second Canadian International Conference on "Durability of concrete" (Canada), Published by the ACI (SP-126), Vol. I, pp. 355-370.

YING-YU, L. and QUI-DONG, W. (1987) "The mechanism of carbonation of mortars and the dependence of carbonation on pore structure," SCANLON, J.M. editor, Proceedings of the Katherine and Bryant Mather International Conference on "Concrete Durability", Published by the ACI (SP-100), Volume II, pp. 1915-1943.

YOUNG, J.F. (1972) "A review of the mechanisms of set-retardation in portland cement pastes containing organic admixtures," Cement and Concrete Research, Vol. 2, No. 4, pp. 415-433.

YOUNG, J.F. (1988) "A review of the pore structure of cement paste and concrete and its influence on permeability" WHITING, D. and WALITT, A. editors "Permeability of concrete", Published by the ACI (SP-108), pp. 1-18.

YOUNG, R.J. and LOVELL, P.A. (1991) "Introduction to polymers," Published by Chapman & Hall (London), Second edition.

YU, S.W. and PAGE, C.L. (1991) "Diffusion in cementitious materials: 1. Comparative study of chloride and oxygen diffusion in hardened cement pastes", Cement and Concrete Research, Vol. 21, No. 4, pp. 581-558.

ZHANG, M. and GJØRV, O.E. (1991) "Effect of silica fume on pore structure and chloride diffusivity of low porosity cement pastes," Cement and Concrete Research, Vol. 21, No. 6, pp. 1006-1014.

Appendices

Appendix 1 Materials

A1.1 General

The following materials were used in fabricating all mixes:

Cement

The cement used was a typical Ordinary Portland Cement, complying with the requirements of BS12. It was supplied by Blue Circle Industries PLC. The composition and properties of the cement are given in Table A1.1.

Table A1.1 Chemical composition and properties of Northfleet OPC

Ingredient	Proportion by weight (%)	Ingredient	Proportion by weight (%)
SiO₂	20.36	Fe₂O₃	3.01
Al₂O₃	5.14	Na₂O	0.14
CaO	64.58	K₂O	0.78
MgO	1.14	SO₃	2.84
Loss on ignition	: 1.15		
Free lime	: 0.79		
Specific surface (m²/kg)	: 380		
Specific Gravity	: 3.15		

Aggregates

Thames Valley river aggregates, supplied by Greenham limited, were used for both the fine and coarse (gravel) aggregates.

The fine aggregates used had a water absorption of 1.8% and a saturated surface dry specific gravity of 2.59. The corresponding values for the coarse aggregate were 2.47% and 2.52, respectively. Sieve analysis revealed the percentage of fine aggregate passing the 600 micron sieve to be 74%.

Water

Tap water at approximately 20°C was used as mix water

A listing of all admixtures used in this work is given in Table A1.2, which includes details of the suppliers, and the product trade names.

Table A1.2 Material Suppliers

Class	Materials	Source	Trade name
Cement replacement materials	Ground granulated blastfurnace slag (GGBS) Pulverized fuel ash (PFA) Silica fume (SF)	Appleby Group/ Scunthorpe Boral Pozzolan Ltd. Elkem Materials Limited	--- Pozzolan EMSAC 500S
Fine particulate materials	Kieselguhr Bentonite Whiting Talc Pumice powder Hydrated lime Iron oxide powder	BDH Limited BDH Limited BDH Limited BDH Limited FSA Chemicals FSA Chemicals BDH Limited	Kieselguhr white GPR Bentonite powder technical Calcium carbonate precipitated heavy GPR Talc fine powder --- --- Iron(II) oxide calcined GP (ferric oxide)
Water repellents	Sodium stearate Sodium oleate Calcium stearate Magnesium stearate Aluminum stearate Butyl stearate Oleic acid Caprylic acid Soyabean oil Corn oil linseed oil Tar emulsion Asphalt emulsion	BDH Limited BDH Limited BDH Limited BDH Limited BDH Limited BDH Limited BDH Limited BDH Limited Sainsbury's Sainsbury's BDH Limited Tando Chemicals Limited Colas Limited	Sodium stearate purified Sodium oleate 'dry' (so called) technical Calcium stearate technical Magnesium stearate GPR Aluminum stearate technical Butyl stearate Oleic acid GPR n-Octanoic acid GPR Soya oil Corn oil Oil of linseed --- ---

table A1.2
continued

Class	Materials	Source	Trade name
Polymer latices	EVA SBR Acrylic	Vinamul Limited Doverstrand Fosroc	Vinamul 3281 Revinex 29Y40 FCC 866
Amino alcohol derivatives	Diethyl ethanolamine Dimethyl ethanolamine	BDH limited Aldrich Chemicals Co. Ltd.	2-Diethylaminoethanol GPR N,N-Dimethylethanolamine
Proprietary waterproofers	Everdure Caltite Conplast prolapin Sikal Setcrete1	Cementaids Limited Fosroc Sika Limited Don Construction Chemicals Ltd.	Everdure Caltite Conplast Prolapin powder Sikal Setcrete1
Miscellaneous	Iron powder Sodium silicate Potassium silicate Cellulose acetate fibre Aluminum powder Magnesium carbonate Iron(II) sulphate Triethanolamine	BDH Limited BDH Limited BDH Limited BDH Limited BDH Limited BDH Limited BDH Limited BDH Limited	Iron powder, reduced by hydrogen GPR Sodium silicate solution (water glass) Potassium silicate solution Cellulose acetate GPR Aluminum powder fine Magnesium carbonate hydrated basic, light GPR Iron(II) sulphate dried GPR (ferrous sulphate) Triethanolamine GPR
Others	Superplasticizer Tri-n-butyl phosphate Silicone	Fosroc BDH Limited BDH Limited	Conplast SP-450 Tri-n-butyl phosphate GPR Silicone antifoaming agent

A1.2 Cement replacement materials

Ground granulated blastfurnace slag

Ground granulated blastfurnace slag (GGBS) is fine powder resulting from drying and grinding granulated blastfurnace slag. The major oxide components of slag are CaO (C), SiO₂ (S), Al₂O₃ (A), and magnesia (M). Rapid quenching of molten slag in water results in the formation of a slag glass consisting of a network of calcium, silicon, aluminum and magnesium ions in disordered combination with oxygen. In addition to this glass, small quantities of crystalline phases may be present. These may include merwinite (C₃MS₂) or minerals in the melilite series (an amorphous series of which two principal members are gehlenite (C₂AS) and akermanite (C₂MS₂)). Generally, the glass content and fineness of grinding of slag are good indicators of its hydraulic reactivity. However, the factors governing slag reaction in slag-cement systems are numerous and complex interactions between these factors exist (Lea 1970, Roy & Idorn 1982, Concrete Society 1990, Taylor 1990). Various hydraulic factors have nevertheless been proposed to relate slag composition to its hydraulicity. BS6699 contains a requirement that the ratio (C+M+Al)/S be greater than 1 (on the premise that hydraulicity increases with increasing C+M+Al and decreases with increasing S (Regourd 1980)) and, for optimum hydraulicity, that C/S should be at a maximum of 1.4 (Concrete Society 1990).

The GGBS used in this study complies with the requirements of BS6699. The chemical composition and properties are given in Table A1.3.

Table A1.3 Chemical composition and properties of GGBS

Ingredient	Proportion by weight (%)	Ingredient	Proportion by weight (%)
SiO₂	35.37	S²⁻	0.93
Al₂O₃	13.06	SO₃	0.17
CaO	39.18	Na₂O	0.22
MgO	9.30	K₂O	0.48
Fe₂O₃	0.56	C	0.12
MnO	0.48	Cl⁻	0.014
TiO₂	0.71		
Glass count	: 98		
Loss on ignition	: 0.78		
Insoluble residue	: 0.81		
Specific surface (m²/kg)	: 390		
Specific Gravity	: 2.9		

Pulverized fuel ash

Pulverized fuel ash (PFA), commonly known also as fly ash, is solid material extracted by electrostatic means from the flue gases of furnaces fired with pulverized bituminous coal. The product consists essentially of spherical particles of aluminosilicate glass containing some iron, calcium, magnesium and alkali metals in the glass structure, together with small quantities of crystalline materials such as quartz, mullite, and oxides of iron; the glass is responsible for the reactivity of PFA with alkali and calcium hydroxides (pozzolanic reaction), the crystalline constituents being relatively unreactive (Lea 1970, Roy 1989, Taylor 1990). In order to ensure that sufficient glass is present in PFA, the standard specifications of a number of countries place a minimum limit upon the SiO₂+Al₂O₃+Fe₂O₃ content, usually 70 percent (Concrete Society 1990). In general, bituminous coals give ashes low in CaO. Another variety of fly ashes produced from lignite or sub-bituminous coal give ashes higher in CaO. These contain substantially less glass (of a higher Ca content) and a different suite of minerals, some

of which (C_3A , C_2S , C , C_4AF , C_4A_3S , and other sulphates) are reactive (unlike low-CaO fly ash, high-CaO fly ash has hydraulic properties of its own)(Roy 1989, Taylor 1990). The PFA used in Europe and Japan is mostly of the low CaO variety. The American designations (according to ASTM C618) of Class F and Class C fly ash, though based on contents of $SiO_2+Al_2O_3+Fe_2O_3$ above and below 70%, respectively, correspond approximately to low- and high-CaO fly ash.

In addition to the glass content, the reactivity of low-CaO fly ash depends on its fineness (reactivity generally increases with fineness (Ravina (1980)). Thus, BS 3892 specifies three zones of fineness, based on the percentage (by weight) retained on the 45 μ m sieve.

PFA particles occur in a variety of shapes and surface characteristics. Most are solid spheres, but often irregular residual coal fragments (carbon) are present, imperfectly rounded ellipsoids, vesicular solids of irregular shape, and various hollow or partly hollow spheres. The content of "cenospheres" (thin-walled hollow particles without interior particles) tends to be quite small in most fly ashes, but there may be a more appreciable content of "plerospheres" (hollow spheres with smaller spheres enclosed)(Roy 1989).

The PFA used in this study was a low-calcium PFA, complying with the requirements of BS3892 (Table A1.4).

Table A1.4 Chemical composition and properties of PFA

Ingredient	Proportion by weight (%)	Ingredient	Proportion by weight (%)
SiO₂	49.1	TiO₂	0.92
Al₂O₃	26.4	SO₃	0.59
Fe₂O₃	10.9	Na₂O	1.24
CaO	1.28	K₂O	3.59
MgO	1.64	Cl	0.009
Loss on ignition : 3.67%			
Material passing 45µm sieve : 91.8%			
Specific Gravity : 2.1			

Silica fume

Silica fume, also commonly known as microsilica or condensed silica, is a byproduct of the production of silicon or silicon alloys. The particles are spherical, typically around 1000-2000 Å in diameter (the N₂ specific area is normally in the range 15-25 m²/g), and consist largely of SiO₂-rich (greater than 86%) glass (Roy 1989). Crystalline impurities include KCl, quartz, metallic iron and iron silicide (Taylor 1990). The high pozzolanic reactivity, in comparison with PFA, of silica fume is largely due to its extremely fine size. It is worth mentioning, however, that the pozzolanic reactivity of silica fume was found to depend more on the chemical composition and nature of impurities than on the fineness or SiO₂ content (Taylor 1990); for instance, Taylor mentions that the presence of a surface layer of carbon greatly decreases reactivity.

The silica fume used in this study is a typical silica fume (Table A1.5).

Table A1.5 Chemical composition and properties of silica fume

Ingredient	Proportion by weight (%)	Ingredient	Proportion by weight (%)
SiO ₂	94.0	CaO	0.3
Al ₂ O ₃	1.0	MgO	0.6
Fe ₂ O ₃	1.0	Na ₂ O	0.3
C (total)	1.5	K ₂ O	0.8
		SO ₃	0.3
<p>Average particle size : 1500 Å</p> <p>% Material retained on 45µm sieve : 0.15</p> <p>Specific surface (BET) (m²/g) : greater than 15</p> <p>Dry solids (% by weight) : 50% (±2%)</p> <p>Specific Gravity (of solids) : 2.2</p> <p>Bulk density (kg/m³) : 1350-1410</p>			

A1.3 Fine particulate materials

Cement made from portland cement clinker ground with sand was occasionally used in the early part of this century, mainly for mass concrete construction in dams. During the second world war various countries became interested in the use of fine particulate materials as a means of economy in the use of cement (Lea 1970). It is anticipated that forthcoming European standards may allow the inclusion of up to 5% of fine particulate material as a filler in cement.

Much literature has been published regarding the use of fine particulate materials (including fine natural and crushed sand) in concrete, and their effects on cement hydration and concrete properties in the fresh and hardened states have drawn much attention in both experimental and theoretical research (Powers 1968, Fulton 1969, Soroka & Stern 1976, Neville 1981, Yamamoto & Kobayashi 1982, Monteiro & Mehta 1986, Carles-Gibergues et al. 1989, Detwiler & Mehta 1989, Barker 1990, Anderson 1990, Gutteridge & Dalziel 1990, Taylor 1990, Glavind & Stang 1991, Kronlöf 1994). A review of this literature reveals that the inclusion of fine particulate materials can have the following effects:

- i) a marked improvement in rheological properties, such as cohesiveness and workability;
- ii) a reduction in bleeding rate (by promoting better packing they prevent the formation of water flow channels between cement and aggregate particles). Less space would thus be available in the paste/aggregate interfacial zone for large crystallized hydration products, making the zone denser. Water would also mix more homogeneously with cement, promoting hydration evenly throughout the paste, and possibly leading to an increase in the degree of hydration;
- iii) fine particulate materials act as nucleation sites for the cement hydration products. This effect will cause grain refinement of the hydration products, i.e. instead of a few

large and oriented grains there will be many small ones of a more random orientation (noteworthy is that grain refinement leads to improved mechanical behaviour in crystalline materials such as metals and ice);

iv) by acting as nucleation sites, fine particulate materials increase the crystallization rate of calcium hydroxide, and, consequently, the rate of cement hydration (see Appendix 4);

v) some fine particulate materials are not entirely inert chemically: they react with the cement compounds, and possibly interfere with the hydration process.

The literature reveals almost universal agreement, however, that the beneficial effects (improved workability, mechanical properties, increased resistance to molecular transport) of fine particulate materials are only pronounced in lean mixes or in mixes where the fine aggregate is deficient in fines.

It is worth mentioning that fine particulate materials may interfere with air entrainment, and a larger dose of air entraining agent would thus be required to achieve a certain level of air entrainment (Orchard 1979, Neville 1981).

Kieselguhr

The term kieselguhr (or diatomaceous earth) refers to sedimentary rocks that are mainly composed of the skeletons of single-celled microorganisms (diatoms). The skeletons are composed primarily of opal-like amorphous silica, with crystalline inclusions of β -cristobalite (Lea 1970).

Worldwide, the processing methods for crude kieselguhr differ only slightly from one another (Gerhartz (1) et al. 1987). The most important principle is minimization of mechanical damage to the diatom skeletons, to maintain the high porosity of kieselguhr.

The processing steps are shown in Figure A1.1.

The kieselguhr used in this study was a dried kieselguhr. The material normally has high porosity (it absorbs three to four times its own weight of liquid before becoming saturated), low density, fairly high surface area, and the particles are quite irregular in shape (Grayson (1) et al. 1978). The chemical and physical properties are given in Table A1.6.

Table A1.6 Chemical composition and properties of kieselguhr

Ingredient	Proportion by weight (%)	Ingredient	Proportion by weight (%)
SiO₂	89.0	CaO	1.1
Al₂O₃	3.5	MgO	0.2
Fe₂O₃	1.5	Na₂O & K₂O	0.8
Crystalline content of amorphous silica : less than 3 %			
Average particle size : 14 μm			
% Material passing 53 μm sieve : 100			
Specific Gravity : 2.2			

Kieselguhr is generally regarded as a high-silica natural pozzolan. However, despite its high pozzolanic reactivity, its use in concrete (at the normal pozzolan dose levels of 15-30% replacement by weight of cement) is much restricted by its physical properties, which greatly increase the water demand (Lea 1970, Taylor 1990). It is also noteworthy that Neville (1981) reports that it is calcined kieselguhr which exhibits pozzolanic properties, whilst others (Fulton 1969, Orchard 1979) report that calcination[#] may or may not be necessary.

[#] during calcination (heat treatment in gas or oil-fired rotary kiln at 800-1000°C) calcium carbonate is transformed into CaO, and CO₂ is released.; the process also removes deleterious organic impurities and converts any harmful clay impurities into inert or pozzolanic material (Gerhartz (1) et al. (1987)).

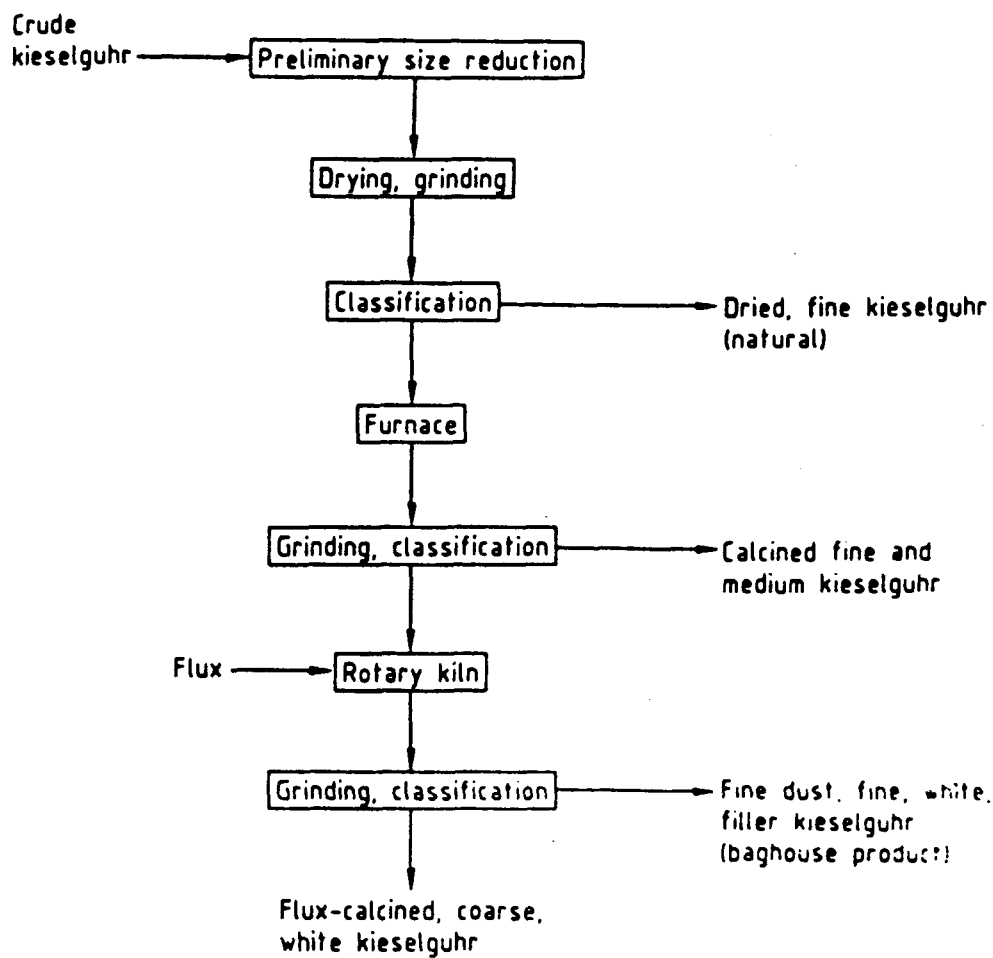


Figure A1.1 Kieselguhr processing.

Bentonite

Bentonite is clay material composed principally of a smectite mineral (montmorillonite). The bentonite used in this study was a sodium montmorillonite (sodium bentonite) (specific gravity 2.16).

The various properties of clays have been investigated intensively during the last three decades, and many new applications have been introduced, especially in the environmental and chemical areas. A wide range of textbooks and technical publications describe the properties of clays in considerable detail (Weaver & Pollard 1973, Grim & Guven 1978, Odom 1984, Gerhartz (2) et al. 1987, Gerhartz (3) et al. 1987, Kroschwitz (2) et al. 1992). Work concerned with the effect of a variety clays on cement hydration has also been published (Handy 1958, Croft 1967, Noble 1967, Plee et al. 1990). The following discussion is based on a review of the above mentioned literature.

A two dimensional schematic presentation of the structure of montmorillonite is shown in Figure A1.2. Montmorillonite (classified as a 2:1 phyllosilicate) has a layer lattice structure, and differs from the theoretical formula in that the lattice is always unbalanced by substitutions of cations within the clay structure. When substitutions of some of the aluminum or silica occur by cations of lower valence, a negative charge deficiency results. This charge deficiency is partly balanced by substitutions within the sheet of the unit layer, and the remainder is balanced outside of the structure by layers of hydrated cations adsorbed between the unit layers and around their edges. These cations (calcium, magnesium, sodium) are loosely bound and may be easily exchanged. The cation exchange capacity of montmorillonite is fairly high, ranging from 50 to 120 millequivalents per 100 g of dry clay. It is also worth noting that clay minerals are considered as useful adsorbents in environmental technology because of their ability to bind heavy metal ions by cation exchange.

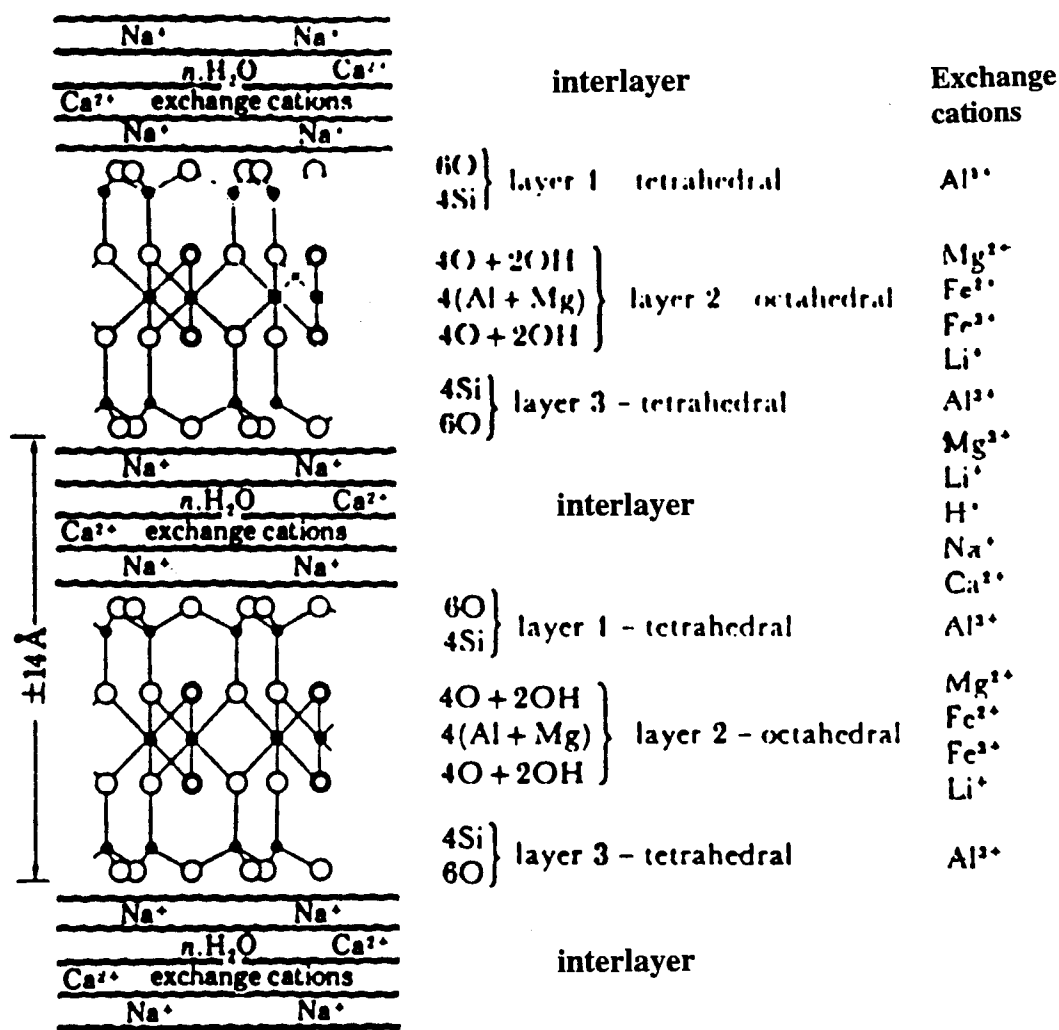


Figure A1.2 Structure of smectite clay minerals.

Bentonite crystals may be as large as 2 μm and as small as 0.2 μm with an average size of about 0.5 μm . However, even when dispersed in water, the crystals tend to occur in aggregates rather than single crystals, thus the effective particles size is considerably larger than the actual particle size and surface area is considerably reduced. Bentonites containing sodium as the predominant exchangeable ion yield the smallest effective particle size and the largest surface area in clay-water systems because their natural crystal size tends to be small and swelling pressure tends to disrupt interlocked crystals.

Depending on their behaviour when in contact with water, bentonites can be divided into two groups: i) those which show considerable swelling (volume can increase up to 15 times), and ii) those which show only a small degree of swelling. Bentonites with intermediate properties are also known. Whether bentonite is high-swelling or low-swelling depends on the nature of the predominant exchangeable cations: in the latter calcium and magnesium (calcium bentonite) are predominant, whilst in the former (sodium bentonite) sodium predominates.

Three major factors likely to influence the properties of sodium-bentonite/cement systems are: a dramatic pH rise, a supersaturation of Ca^{2+} ions, and, less important, a non negligible K^+ ion concentration. The expected consequences are as follows. The high Ca^{2+} concentration is expected to yield a calcium-exchanged bentonite. This effect should be further enhanced by the large ionic strength, which is a well known flocculation factor, due to the compression of the electrical double layers (these help keep colloids in suspension (Gerhartz (4) et al. 1987)). Moreover, the pH of the OPC pastes (greater than 12.6) is precisely in the range where bentonites are known to coagulate (forming aggregates (a system of clay particles and water)).

In a clay/water system the very polar water molecules are attracted strongly to negative faces or positive edges of clay particles. The adsorbed water molecules, in turn, attract other water molecules, and these, in turn, attract yet other water molecules. On drying (at ordinary temperatures), loss of water from a clay-water system leads to drying

shrinkage. Initially, the volume shrinkage is about equal to the volume of the water evaporated. The water lost during shrinkage is called shrinkage water and is that which separates the clay particles. Beyond a given moisture content, however, there is either very little shrinkage. The critical point at which shrinkage stops is reached when the moisture films around the particle become so thin that the particles tend to touch one another and shrinkage can go no further. Drying at 105°C, however, removes all water including adsorbed water and interlayer (see Figure A1.2) water (except the water of crystallinity) and shrinkage is fairly large.

Finally, regarding the effect of clay on cement hydration, it has been reported (see references above) that the hydration of cement grains may be restricted by encapsulation of the cement by very fine grained clay.

Whiting

Whiting is a calcarious (high CaCO_3) filler. The name is broadly used to describe finely divided meticulously milled carbonates that are derived from high calcium or dolomitic limestone, marble, shell, or chemically precipitated calcium carbonate. The material used in this study was of the precipitated variety.

Whiting has a specific gravity of 2.7 and is only slightly soluble in water (0.15 g/l at 25°C). The average particle size is 0.2 μm , and all material is finer than 15 μm .

Whiting is not entirely chemically inert when introduced in concrete: it has been reported (Sokora & Stern 1976, Neville 1981, Taylor 1990) to react with the aluminate phase (C_3A), producing a calcium carboaluminate compound ($3\text{CaO}\cdot\text{Al}_2\text{O}_3\cdot\text{CaCO}_3\cdot 11\text{H}_2\text{O}$), thus competing with gypsum (see A4.1). SEM reveals that, in pastes with a high proportion of the filler, calcium hydroxide is concentrated into large masses which form bridges between the grains of the filler (Taylor 1990); this contrasts with the smaller and more evenly dispersed crystals formed in the absence of

filler.

Talc

Talc is a hydrated magnesium silicate which can be represented by the formula $3\text{MgO}\cdot 4\text{SiO}_2\cdot \text{H}_2\text{O}$, although the ratios of MgO, SiO_2 , and H_2O may vary slightly.

Talc is inert in most chemical reagents and despite being insoluble in water, it exhibits a relatively high (9-9.5) alkaline pH (Grayson (1) & Eckroth et al. 1978, Kroschwitz (1) et al. 1992). All material is finer than 100 μm .

Ground pumice

Pumice is a light coloured foamed volcanic rock glass of mainly acid character (> 65% SiO_2 , rhyolite)(Gerhartz (5) et al. 1987).

Ground pumice (also known as pumicite) is regarded as a natural pozzolan of moderate reactivity (it is less reactive than Kieselguhr), and is used at 15-30% replacement by weight of cement (Orchard 1979, Neville 1981). The hydration reactions of volcanic natural pozzolans have been reviewed by Taylor (1990).

The pumice powder used has a specific gravity of 2.2 and an average particle size of 63 μm .

Hydrated lime

When a relatively pure limestone (greater than 95% CaCO_3) is heated at a sufficiently high temperature (about 800°C), the calcium carbonate is decomposed into carbon dioxide and calcium oxide (quick lime). Hydrated lime, which is essentially $\text{Ca}(\text{OH})_2$ powder, is then produced by reaction of the quick lime with about twice the amount of stoichiometric water (Lea 1970, Gerhartz (6) et al. 1987).

Hydrated lime is a white powder, with a specific gravity of 2.3. It is much finer than cement (specific surface area of $1500 \text{ m}^2/\text{kg}$ (Blaine)). The material is only sparingly soluble in water (solubility decreases from about 1.85 g/l at 0°C to 0.71 g/l at 100°C), and is even less soluble in the cement paste pore solution due to the presence of alkali hydroxides (see A4.1). Hydrated lime is generally regarded (Fulton 1969, Lea 1970) as chemically inert in respect of its reactivity with cement compounds. However, the material reacts readily with acidic materials. In particular, it reacts with atmospheric carbon dioxide, in the presence of moisture, to form tiny crystals of calcium carbonate (Atkins & Berman 1992). It is also worth noting that hydrated lime reacts with pozzolans producing calcium silicates and aluminates (Gerhartz (6) et al. 1987).

Iron oxide

Red iron oxide powder (Fe_2O_3), produced by calcination of yellow iron oxide, is commonly used as a pigment in concrete (Orchard 1979, Gerhartz (7) et al. 1987)). The material used has a specific gravity of 5.2 and an average particle size of $0.1 \mu\text{m}$.

A1.4 Water repellents

Aliphatic alcohols

Aliphatic alcohols are discussed in various textbooks of general (Kotz and Purcell 1987, Atkins & Beran 1990) and organic (Vollhardt & Schore 1994) chemistry.

Alcohols are characterized by the presence of a hydroxyl group (-OH) covalently bonded to a saturated carbon atom. They follow the general structural form R-OH, although several important alcohols (e.g. glycerine) contain more than one hydroxyl group. Alcohols can act as weak Brønsted acids (RO⁻) and strong bases convert alcohols into their conjugate bases (e.g. with NaOH solution, ROH forms RONA).

Alcohols were not introduced directly to concrete, but are believed to form as a result of the interaction of esters (butyl stearate, vegetable oils) with concrete. Details of two alcohols which are of interest to this study are given in Table A1.7.

Table A1.7 Physical properties of two aliphatic alcohols

Material (Common name)	IUPAC # name	Structure	Solubility in water (g/l at 23°C)	Boiling point (°C)
Butyl alcohol	1-Butanol	CH ₃ CH ₂ CH ₂ CH ₂ OH	.80	117.3
Glycerine (glycerol)	1,2,3-propantriol	$ \begin{array}{c} \text{CH}_2\text{OH} \\ \\ \text{HCOH} \\ \\ \text{CH}_2\text{OH} \end{array} $	infinite	---

also referred to as systematic name.

Fatty acids

An excellent review of fatty acids is given by Markley ((1) 1961). Other literature was also reviewed (Lea 1970, Thoor (1) 1971, Rixon & Mailvaganam 1986, Gerhartz (8) et al. 1987, Vollhardt & Shore 1994).

Naturally-occurring fatty acids are monobasic aliphatic acids in which a hydrocarbon chain is linked at one end to a carboxyl (-COOH) group; they take the structural form R-COOH. The total number of carbon atoms in the molecule can be as high as thirty, but the most commonly-occurring fatty acids contain not less than ten and not more than twenty-two carbon atoms. Broadly speaking, fatty acids fall into two main categories: saturated and unsaturated. In the saturated acids, each carbon atom, other than that in the terminal (-COOH) group and the terminal (CH₃) group, is linked to two carbon and two hydrogen atoms. Thus, all four valencies of each carbon atom are satisfied. Hence, the saturated fatty acids are resistant to oxidation and rancidity. By contrast, the unsaturated fatty acids contain carbon atoms, in pairs, which are linked to only one hydrogen atom instead of two, the remaining valency of each of these carbon atoms unsatisfied or "unsaturated", and a double bond, or "ethylenic linkage", results between these pairs of carbon atoms. The unsaturated fatty acids are classified according to the number of ethylenic linkages they contain, e.g. mono, di, tri-ethylenic. They are more reactive than the saturated acids and their susceptibility to rancidity, oxidation, polymerization, etc. increases as the degree of unsaturation increases.

When introduced in concrete, fatty acids react with the alkalis and calcium hydroxide present in the pore solution precipitating, ultimately, as water-insoluble calcium soaps ((RCOO)₂Ca). Initially, the reaction proceeds slowly, but as the pH of the pore solution rises with continued cement hydration (see A4.1), the reaction becomes more rapid. Noteworthy also is that the reaction rate increases with increasing temperature.

As regards possible reactions with the cement compounds, unsaturated fatty acids, although not affecting tricalcium silicate hydration, have been found to interfere with ettringite formation by virtue of formation of reaction complexes involving the double bond (oleic acid possibly forms calcium aluminoleate)(Rixon & Mailvaganam 1986).

The lowest molecular weight fatty acids exhibit appreciable solubility in water compared to the corresponding hydrocarbons due to the presence in the former of the polar (hydrophillic) carboxyl group. As the hydrocarbon chain increases, however, the ability of the carboxyl to bring about solubility of the fatty acid in water diminishes appreciably; nevertheless, as will be discussed next, it will still have the effect of orienting fatty acid molecules with respect to water.

High molecular weight fatty acids are characteristically long-chain molecules containing a polar (hydrophillic) group (-COOH) at one end of a non-polar (hydrophobic) hydrocarbon chain (R). The fatty acid molecules therefore become concentrated at the air/liquid interfaces with their hydrophillic groups in the liquid and their hydrophobic parts out of it, and this construction reduces the surface tension of the water. During mixing of concrete, a large number of discrete air bubbles are formed, but these are mostly destroyed due to the high surface tension of water. Thus, by reducing the surface tension of water, fatty acids stabilize the air bubbles leading to air entrainment. It should be noted, however, that fatty acids cannot be expected to entrain air as efficiently as water-soluble soaps, mainly because fatty acids have fairly low solubilities in water, thus the fatty acid molecules do not spread as efficiently in the mix water as the soap molecules.

The properties of the saturated fatty acids which are of interest to this study are compiled in Table A1.8 and those of the unsaturated acids are given in Table A1.9. It should be noted that only oleic and caprylic acid were introduced to concrete directly, the other materials are of interest as they are essential constituents of some of the materials investigated (butyl stearate, vegetable oils).

Table A1.8 Composition and properties of saturated fatty acids

	Common name		
	Caprylic	Palmitic	Stearic
IUPAC name	Octanoic	Hexadecanoic	Octadecanoic
Structure	$C_7H_{15}COOH$	$C_{15}H_{31}COOH$	$C_{17}H_{35}COOH$
Molecular weight	144.21	256.42	284.47
Density (g/cm³) (at 20°C)	0.91	0.85 (at 62°C)	0.847 (at 69°C)
Minimum Assay (%)	97.5	---	---
Melting point (°C)	16.7	63.1	69.6
Boiling point (°C)	240	351	376
Solubility in (g/100 g water)			
- at 20°C	0.068	0.00072	0.00029
- at 60°C	0.113	0.0012	0.0005
Neutralization # value	389.1	218.8	207.5

neutralization value is equal to the amount of alkali (milligrams KOH) required to neutralize 1 g of fatty acid divided by the molecular weight of the acid.

Table A1.9 Composition and properties of unsaturated fatty acids

	Common name		
	Oleic	Linoleic	Linolenic
IUPAC name	cis-9-Octadecenoic	cis,cis-9,12-Octadecadienoic	cis,cis,cis-9,12,15,-Octadecatrienoic
Structure	$C_{17}H_{33}COOH$ (one double bond)	$C_{17}H_{31}COOH$ (two double bonds)	$C_{17}H_{29}COOH$ (three double bonds)
Molecular weight	282.47	280.45	278.44
Density at 20°C (g/cm³)	0.891	0.902	0.916
Minimum Assay (%)	65-70	---	---
Melting point (°C)	13.4-16.3	-5.0	-11.0
Boiling point at 1.33 KPa (°C)	223	224	2245
Solubility at 20°C (g/100 g water)	insoluble	insoluble	insoluble
Iodine value #	90	181	274
Neutralization value	199	200	202

Iodine value is a measure of the degree of unsaturation of the fatty acid (expressed as percentage iodine absorbed by the fatty acid). There is no iodine present in fatty acids, but the test measures the amount of iodine (I₂) which can be absorbed by the unsaturated acids (one of the properties of unsaturated organic compounds is their ability to form addition compounds with halogens).

Vegetable oils and butyl stearate

Vegetable oils and butyl stearate belong to a class of aliphatic organic materials known as esters. An excellent review of esters is given by Markley ((2) 1961). Other literature was also reviewed (Lea 1970, Thoor (1) and (2) 1971, Rixon & Mailvaganam 1986, Gerhartz (8) et al. 1987).

Butyl stearate, a synthetic material, has the structural formula RCOOR' ($\text{C}_{17}\text{H}_{35}\text{COOC}_4\text{H}_9$) and is the product of a reaction between a fatty acid (stearic acid) and an alcohol (butyl alcohol). Vegetable oils, on the other hand, are natural materials which comprise the triesters of long-chain fatty acids with the polyhydric alcohol glycerol, and are often called triglycerides. They have the structural formula shown in Figure A1.3, where R1, R2, and R3 may be the same or different fatty acid radicals. The complexity of the triglycerides arises from variations in: i) the number, kind, and mode of arrangement of the individual fatty acids which are attached to the glycerol skeleton to form specific triglycerides, and ii) the number and relative proportions of such triglycerides which are mixed or mutually dissolved to form the specific oil.

Oils and butyl stearate have a lower density than water and are almost completely insoluble in it. Perhaps the most important reaction that butyl stearate and oils undergo when used in concrete is hydrolysis in the presence of the alkali and calcium hydroxides (saponification) to give the parent alcohol and a salt, or salts in the case of the oils, of the constituent fatty acid(s). The fatty acid salt(s) eventually precipitate(s) as water insoluble calcium soap(s) $((\text{RCOO})_2\text{Ca})$. The alcohol can itself react with calcium hydroxide: e.g. glycerol forms calcium glycerite, which is water-soluble. Initially, saponification proceeds slowly, but as the pH of the pore solution rises with continued cement hydration, the reaction becomes more rapid. Noteworthy also is that the saponification rate increases with increasing temperature.

Details regarding the composition and properties of the esters used are compiled in Table A1.10.

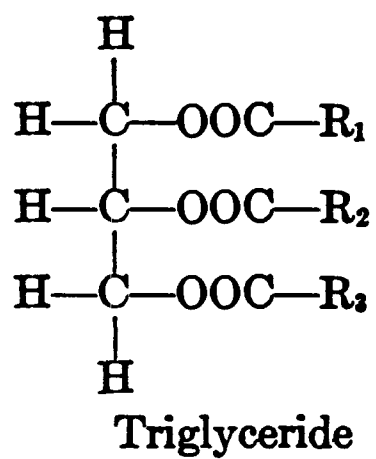


Figure 1.3 Structure of vegetable oils.

Table A1.10 Composition and properties of esters

		Butyl stearate	Soyabean oil	Corn oil	Linseed oil
Fatty acid composition (%)	Stearic	100	2-6	2-5	3-5
	Palmitic	---	7-11	8-12	5-7
	Oleic	---	15-33	19-49	16-26
	Linoleic	---	43-56	34-62	14-24
	Linolenic	---	5-11	trace	50-65
Molecular weight		340.59	#	#	#
Density (g/cm³) (at 20°C)		0.857	0.88	0.89	0.930
Assay (%)		50 ^{\$}	95 minimum	95 minimum	99
Melting point (°C)		19.5	---	---	---
Saponification value #		n/a	189-195	187-193	188-196

saponification value is a measure of the mean molecular weight of the fatty acids present in the oil. The process of saponification is the hydrolysis of triglycerides into glycerol and the potassium salt of the fatty acids, using a solution of potassium hydroxide in alcohol. This process measures the amount of alkali which is required to combine with fatty acids liberated by the hydrolysis of the fat, and from this the equivalent weight and molecular weight of the fatty acids can be determined. The saponification value is expressed as the number of milligrams of potassium hydroxide required to saponify one gram of oil.

\$ the material is supplied as emulsion of butyl stearate in water (contains surface active agents (surfactants) which promote emulsification (see: Grayson (2) & Eckroth 1978, Gerhartz (10) et al. 1992)).

Soaps

There is a large volume of literature which deals with the nature and characteristics of soaps (White & Bateman 1926, Jumper 1931, Markley (2) 1961, Thoor (3) 1971, Rixon & Mailvaganam 1986, Gerhartz (9) et al. 1987, Aldred 1989, Kroschwitz (3) et al. 1992).

The term "soap" is generally used to denote the salts of fatty acids. The majority of commercial soaps comprise the alkali metal, alkaline earth metal, aluminum, heavy metal, or ammonium, salts of fatty acids. They follow the general structural formula $(RCOO)_xM$, where x is the valence of the metal M (x equals 1 in the case of the ammonium salt).

There are two broad classes of soaps, namely water-soluble and water-insoluble. The fatty acid salts of ammonium and the alkali metals, with the exception of lithium, constitute the water-soluble class; the salts of aluminum, alkaline earth and heavy metals are of the water insoluble type.

In an aqueous solution, water-soluble soaps dissociate yielding simple cations (e.g. Na^+) and the corresponding fatty acid anion ($RCOO^-$); the latter has a hydrophobic (non polar hence water repelling) hydrocarbon tail (R) and a polar head (COO^-) which is soluble in water (hydrophilic). At liquid/gas interfaces, the fatty acid anions become oriented so that their hydrophilic heads are in the water phase and the hydrophobic tails are in the air phase. In effect, the hydrophobic tails tend to be squeezed through the surface breaking the electrostatic attraction between the water molecules and reducing the surface tension, thus promoting foaming (air entrainment).

Generally, potassium and ammonium soaps are more readily soluble in water than sodium soaps. Soaps of saturated acids become less readily soluble as the number of carbon atoms (including that of the $COOH$ group) in the hydrocarbon chain increases from 8 to 18; for example, sodium laurate (C:12) is rapidly soluble, whereas sodium

stearate (C:18) requires the application of heat to dissolve. The soaps derived from unsaturated acids are more readily soluble than the corresponding saturated-acid soaps.

Another important characteristic of water-soluble soaps is their ability to promote the emulsification of water-insoluble materials (e.g. oils, asphalt and other hydrocarbons, polymers, etc.) in water. When a soap is dissolved in distilled water at an extremely low concentration, the soap ions within the bulk of the solution retain random movement but, as the concentration of the soap in the solution is progressively increased, the surface-active anions begin to aggregate in clusters, or "micelles", in which the hydrophobic tails are directed inwards towards one another and the hydrophilic head groups are directed towards the surrounding water. These micelles, which are of colloidal dimensions, are capable of holding water-insoluble substances within (the nonpolar tails interact with the nonpolar oil phase).

Water-soluble soaps cause air entrainment when introduced in concrete, thus dosages exceeding 0.2% w/w_{cement} are not usually recommended due to the likelihood of significant strength loss. They react with the calcium hydroxide in the pore solution and precipitate, eventually, as water-insoluble calcium soaps ((RCOO)₂Ca); this is analogous to the soaps forming scum in hard water. As for their effect on cement hydration, it is conceivable that, at concentrations corresponding to micelle formation, the soaps adhere to the cement grains preventing wetting hence delaying hydration; this effect is unlikely to persist, however, as it is counterbalanced by the effect of calcium ions (precipitation as calcium soaps). Soaps of unsaturated acids may also interfere with ettringite formation by virtue of complex formation (as explained before).

Water-insoluble soaps are characterized by water repellency, extremely small particle size and high specific surface area, solubility in some organic solvents, purity of metal content, and good lubrication power. Since they are solid and insoluble in water, they remain as minute water repellent particles within the concrete. Thus, their value is in large measure a function of the degree of dispersion in concrete.

Details concerning the composition and properties of water-soluble and water-insoluble soaps used are given in Tables A1.11 and A1.12, respectively.

Table A1.11 Composition and properties of water-soluble soaps

	Material	
	Sodium stearate	Sodium oleate
Structure	$C_{17}H_{35}COONa$	$C_{17}H_{33}COONa$
Molecular weight	306.46	304.45
Form	granules	granules
Colour	milky white	yellow
Solubility in water	soluble on heating	soluble without heating

Table A1.12 Composition and properties of water-insoluble soaps

	Material		
	Aluminum stearate	Calcium stearate	Magnesium stearate
Structure	$(C_{17}H_{35}COO)_3Al$	$(C_{17}H_{35}COO)_2Ca$	$(C_{17}H_{35}COO)_2Mg$
Molecular weight	876	606	590
Form	powder	powder	powder
Color	white	white	white
Metal (%)	3.2	6.4	4.5
Specific gravity	1.01	1.12	1.03
Free fatty acid (%)	3.0	0.5	0.5
Melting range (°C)	110-150	145-160	145
Fineness	98% finer than 75 μm sieve	100% finer than 45 μm sieve	100% finer than 45 μm sieve

Mineral oil

Mineral oils are distilled from petroleum and shale deposits. This group includes a wide range of materials, such as: paraffin oil, fuel oils, and a large variety of lubricating oils. In contrast to vegetable oils, mineral oils are not esters, but simple hydrocarbons (Thoor (4) 1971). According to Lea (1970), mineral oils contain no constituents which react chemically with set cements, though they seriously affect the early-age hydration. The mineral oil used in this study was not a simple hydrocarbon, however. The material is a chemical release agent used in preparing concrete specimens, to prevent concrete from adhering to the mould surfaces. The material comprises a small amount of a tall oil fatty acid dispersed in a carrier oil (a mineral oil known as light gas oil). When the concrete is placed, the calcium hydroxide liberated by the hydration of cement reacts with the fatty acid distributed over the mould's surface to form a calcium soap, which forms a barrier to give the release. Similarly, when the material is incorporated in concrete, the fatty acids would react with the alkalis and calcium hydroxide in the pore solution and precipitate, eventually, as calcium salts $((RCOO)_2Ca)$.

Asphalt and tar emulsions

There is a large volume of literature which deals with the nature and characteristics of coal tar, asphalt, and their emulsions (Thoor (5) 1971, Smith 1973, Maslow 1974, Gerhartz (11) et al. 1987, Kroschwitz (4) et al. 1992).

Coal tar and asphalt are bituminous materials similar in appearance. Although sometimes used for the same purposes, the two are fundamentally different. Manufactured from a variety of residuals left over from the distillation of petroleum oil, asphalt is a complex mixture of mainly paraffinic and naphthenic hydrocarbons (alkanes and cycloalkanes), and only minor amounts of aromatic constituents. On the other hand, nearly all of the multitude of chemical constituents of coal tar (primarily a product of the carbonization of bituminous coal) are aromatic hydrocarbons of the benzene-ring

type.

Asphalt and coal tars cannot be incorporated directly in concrete as they exist as solids at ambient temperatures and are immiscible with water. They can be introduced, however, in the form of solid microparticles (particle size ranges from 1-25 μm , with an average of 5 μm) suspended in water, i.e. in the form of emulsions. The particles are held in suspension in water by a thin film of water containing a stabilizing agent(s). Water will not ordinarily mix with the tar or asphalt particles in any form, but merely keeps the particles separated. On evaporation of the water, the emulsion is broken and the particles fuse together (coalesce) to form a continuous adherent coating on adjoining solid surfaces. The application of heat (temperatures in the range 50-120°C) aids this process as it leads to softening of the tar/asphalt particles.

Emulsion processes of asphalt vary and the emulsions are made in rapid-, medium-, and slow-setting types for diverse applications in the road-building industry. The rapid-setting and medium-setting grades, which are stabilized by the use of cationic surfactants (cation-active agents), are not suitable for use in concrete: they are acidic and have low stability, the emulsion breaking on contact with solid surfaces. The slow-setting grades, on the other hand, have sufficient stability so that a finely divided material such as cement may be mixed without breaking the emulsion. They are not acidic, and are stabilized by the use of various stabilizing agents (soap (an anionic surfactant), soap/bentonite, or bentonite). The emulsion used in this study was a slow-setting type stabilized by the use of bentonite (total amount of solids = 55%).

The coal tar emulsion used comprised 43.25% (w/w) coal tar dispersed in 39% water by the use of stabilizing agents (17% clay and 0.75% anionic surfactants). It is expected that the surfactant component causes air entrainment in concrete.

A1.5 Polymer latices

A polymer is a substance composed of molecules which have long sequences of one or more species of atoms or groups of atoms linked to each other by primary, usually covalent, bonds. They are formed by linking together monomer molecules through chemical reactions, the process by which this is achieved being known as polymerization. Homopolymers are derived from one species of monomer, whilst a copolymer is derived from more than one species of monomer (Young & Lovell 1991).

Different types of polymers have been used in concrete. These can be broadly divided into three groups: latices, liquid resins, and water soluble polymers. This study was concerned with latices since they are the most widely used (ACI Committee 548 1986). A latex generally contains 50% by weight of very small (usually 0.05 to 1.0 μm in diameter) spherical particles of high molecular weight polymers held in suspension in water by the use of surface-active agents. Latices are usually formed by emulsion polymerization of monomers (Young and Lovell 1991). Most commercial latices are copolymer systems and often contain various modifiers.

Not all latices are compatible with cement, and to select an emulsion primarily intended for the production of paint or adhesives to act as an admixture in concrete would be an error (Maslow 1974). Latices used as admixtures in OPC systems are specifically formulated so that they remain stable (i.e. the particles remain in suspension and do not aggregate) in a mortar/concrete environment; the destabilizing effect arises from contact with a fine material (cement) and from the presence of multivalent cations (Ca^{2+} , Al^{3+}) in the pore solution.

Another aspect relating to the compatibility of latices with cement is their susceptibility to alkaline hydrolysis. SBR and acrylic latices are known to have good resistance to alkaline hydrolysis (Maslow 1974, Chorinsky 1987). PVA latices, on the other hand, are known to be particularly sensitive: they swell and undergo hydrolysis to form polyvinyl alcohol which is soluble in water thus subject to leaching (Frondistou-Yannas

& Shah 1972).

Three latices specially formulated for use with cement were used in this study (Table A1.13): i) ethylene vinylacetate copolymer (EVA), ii) styrene butadiene rubber copolymer (SBR), and iii) acrylic copolymer.

Table A1.13 Composition and properties of polymer latices

	Latex		
	EVA	SBR	Acrylic
Appearance	milky white liquid	milky white liquid	milky white liquid
Total solids (%)	55	46-48	46-48
Stabilizing system	polyvinyl alcohol	surfactant	surfactant
Particle size (μm)	1-3	0.2	0.15
pH	4.0 *	10.5-11.5	8.8-10
Density (g/cm^3)	1.01	1.01	1.06
MFFT ($^{\circ}\text{C}$) #	0	1-4	10-12

* acid pH is due to the use of polyvinyl alcohol as stabilizing agent.

minimum film formation temperature.

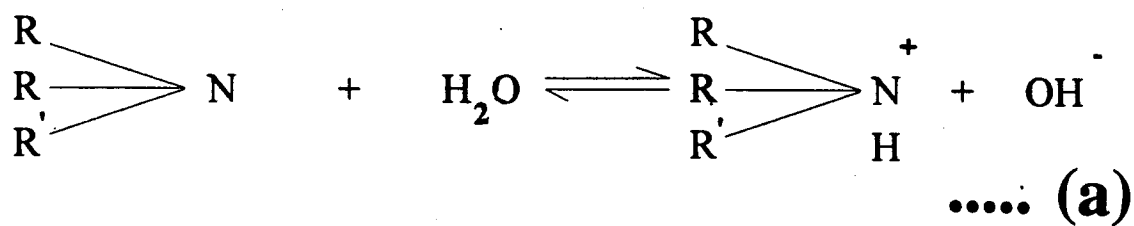
A1.6 Amino alcohol derivatives

Amino alcohols are usually designated as alkanoamines. Ethanolamines (aminoethanols) and propanolamines (aminopropanol) are by far the most widely available compounds. The amino alcohol derivatives used in this study are derivatives of monoethanolamine (2-aminoethanol, which has the structural formula $\text{H}_2\text{N}-\text{CH}_2\text{CH}_2-\text{OH}$), and are usually known as N-alkylated ethanolamines (Gerhartz (12) et al. 1987). Table A1.14 includes details regarding their structure and properties.

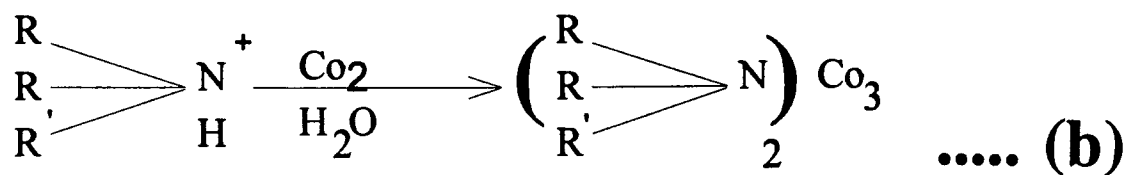
Table A1.14 Composition and properties of amino alcohol derivatives

	Common name	
	Diethyl ethanolamine	Dimethyl ethanolamine
IUPAC name	N,N-diethylaminoethanol	N,N-dimethylaminoethanol
Structure	$(\text{CH}_3)_2\text{N}-\text{CH}_2\text{CH}_2\text{OH}$	$(\text{C}_2\text{H}_5)_2\text{N}-\text{CH}_2\text{CH}_2\text{OH}$
Molecular weight	117.2	89.1
Nature	liquid	liquid
Density at 20°C (g/cm³)	0.887	0.886
Minimum Assay (%)	99	99
Boiling point (°C)	134	162
Solubility (g/100 g water) at 25°C	infinite	infinite

Regarding the use of amino alcohol derivatives in concrete, Sakuta et al. (1987) proposed that they have the capacity to bind both carbon dioxide (and other acidic gases) and chloride ions. In theory, the reactions can proceed as illustrated in Figure A1.4.



Followed by:



or,

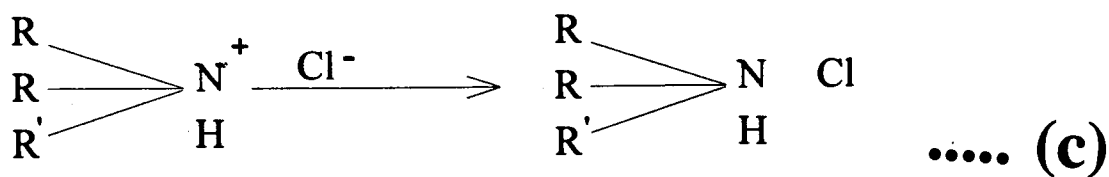


Figure A1.4 Binding of carbon dioxide and chloride ions by amino alcohol derivative.

Clearly, reaction (a) would not proceed from left to right in the cement paste pore solution due to the presence high OH^- concentrations. However, during carbonation, OH^- is neutralised, and reaction (b) can proceed. Hydroxyl ions are also subject to leaching during chloride ingress (see 3.6.2), thus it is conceivable that reaction (c) will proceed.

Sakuta et al. (1987) investigated carbonation rate and chloride penetration in 0.5 water/cement ratio mortar specimens modified with 4% amino alcohol derivative. Testing included the following: i) accelerated carbonation testing, ii) drying (7 days at 20°C & 60%RH) followed by 14 days of immersion in a saturated NaCl solution, then spraying with indicator to determine depth of chloride penetration. They concluded that their results demonstrate that amino alcohol derivatives reduce carbonation and chloride penetration rate due to the capacity of the materials to absorb carbon dioxide and chlorides. It should be noted, however, that whilst the results they obtained are indeed favourable, they do not demonstrate conclusively that the effect is due to binding of the aggressive species, since it may well have been, at least in part, a consequence of pore structure refinement.

A1.7 Miscellaneous

Iron powder

Commercially available iron powders vary widely in properties (particle shape, size distribution), depending on the nature of the manufacturing process (carbonyl process, atomization, reduction of oxides, electrolytic process, mechanical comminution). The powder used in this study was reduced from iron oxides, the process producing irregular spongy particles. The material has an average particle size of 51 μm , and a specific gravity of 7.9.

Sodium and potassium silicates

Commercial alkali silicates are generally specified according to: i) source of alkali (sodium, potassium, lithium), ii) ratio of silica (SiO_2) to alkali metal oxide (M_2O), and iii) water content of the silicate. The water content of silicate solutions is customarily defined indirectly by giving the density of the solution, which together with the silica to alkali-metal oxide ratio, defines a unique composition for the silicate solution. Solutions of sodium and potassium silicates with $\text{SiO}_2/\text{M}_2\text{O} \geq 1.5$ are colourless, water white, and viscous (Gerhartz (13) et al. 1987). Table A1.15 includes details regarding the properties of the silicate solution used.

Sodium silicate has not been widely used as an integral waterproofer in concrete, due to its pronounced adverse effect on compressive strength (Fulton 1969). It is widely used for surface application.

Table A1.15 Composition and properties of sodium and potassium silicates

	Material	
	Sodium silicate (water glass)	Potassium silicate
SiO₂ (%)	30	23
M₂O (%)	12	11
Solids (%)	45	35
Density at 20°C (g/cm³)	1.50	1.33
pH	11.2	11.8

Cellulose acetate

Cellulose acetate, a synthetic plastic, is an organic ester of cellulose (a high molecular weight polymer of glucose). Fibres of cellulose acetate have a bright, lustrous appearance, are often irregular in cross-sections, and have a high water absorption capacity. Absorption of water by the fibres causes swelling roughly proportional to the increase in moisture (Grayson (3) & Eckroth 1978). The fibre used has a specific gravity of 1.3.

The absorption of water by the fibres gives rise to a reduction in the effective water/cement ratio of the concrete mix. This would lead to a decrease in workability.

The water initially absorbed by the fibres would probably be released into the concrete pores as they dry with the progress of hydration; this may alleviate the effects of self desiccation.

Aluminum powder

Aluminum powder belongs to a class of admixtures commonly known in the literature as gas forming admixtures (ACI Committee 212 1989). Such materials are usually incorporated in concrete to counteract settlement and bleeding, causing the concrete to retain more nearly the volume at which it was cast. They function by generating gas bubbles in the fresh mix during and immediately following placement and prior to setting of cement. Metallic aluminum, in powder form, is one such material, which generates small bubbles of hydrogen gas by reacting with the alkalis released as the cement hydrates. The rate and duration of gas evolution is dependent on the type of cement (alkali content), water/cement ratio, and fineness and particle shape of the aluminum powder. The addition rate may vary from 0.006 to 0.02 percent by weight of cement under normal conditions. At these levels, the aluminum powder, causes a slight expansion in plastic concrete or mortar and thus reduces or eliminates voids caused by plastic settlement. When large amounts of aluminum are used, expansion is greatly increased resulting in a lightweight, low strength concrete (Smith 1973). The effect on compressive strength depends to a large extent on the restraint offered to expansion.

It is worth mentioning that gas forming admixtures "are not considered to be acceptable air-entraining admixtures , since they do not necessarily provide an air-void system that will provide adequate resistance to freezing and thawing" (ACI Committee 212 1989).

No literature could be found that relates to the benefits in respect of resistance to the ingress of aggressive species, if any, that the use of aluminum powder imparts to the hardened concrete.

The powder has an average particle size of 100 μm . The minimum assay is 90%.

Magnesium carbonate

Many salts precipitate additional phases when added to Portland cement. If the hydroxide of the added cation is less soluble than calcium hydroxide, either it or a basic complex salt is precipitated. Precipitation will leave in solution all or part of the added anion and an equivalent amount of Ca^{2+} . The calcium salt of the added anion, if of sufficiently low solubility, is similarly precipitated. Magnesium carbonate, when introduced in very finely divided form, is thus likely to precipitate $\text{Mg}(\text{OH})_2$ and CaCO_3 . The reactions result in removal of Ca^{2+} from solution, accelerating the hydration of the alite (C_3S) phase, and leading to more rapid setting (see Appendix 4). Taylor (1990) maintains, however, that the chemistry underlying accelerating effects produced by salts that yield precipitates is not well understood, and more than one mechanism probably operates. He postulates that increased hydration may also be due to the increased permeability of the protective layer formed on the cement grains during the dormant period (see Appendix 4).

No literature could be found that relates to the effects of magnesium carbonate on molecular and ion transport in concrete. It is worth noting, however, that the beneficial effects of the precipitates ($\text{Mg}(\text{OH})_2$ and CaCO_3) in causing pore blocking may be countered by the long-term adverse effects associated with accelerated cement hydration. Because of their low solubility and diffusivity, cement hydration products cannot diffuse to a significant distance from the cement grain in the time allowed by rapid hydration. As a consequence, they will tend to precipitate closer to the cement grains, thus producing little pore blocking. The thick hydration products surrounding the cement grains may also impede subsequent hydration. Thus, although more hydration products will be formed initially, it is likely that, in the long-term, the concrete will have a coarser pore structure. An analogous effect is caused by high curing temperatures, as observed by Detwiler et al. (1991).

Triethanolamine

Triethanolamine (TEA) is an amino alcohol (an alkanolamine). It can be regarded as a derivative of ammonia (NH_3) in which the three hydrogen atoms have been replaced by a $-\text{CH}_2\text{CH}_2-\text{OH}$ group to form $\text{N}(\text{CH}_2\text{CH}_2-\text{OH})_3$. TEA is a viscous colourless liquid at room temperature and is totally miscible with water (Gerhartz (12) et al. 1987). Some physical properties of triethanolamine are compiled in Table A1.16.

Table A1.16 Physical properties of triethanolamine

	Common name
	Triethanolamine (TEA)
IUPAC name	2,2',2''-nitrilotriethanol
Molecular weight	149.2
Density at 20°C (g/cm³)	1.122-1.128
Minimum Assay (%)	97
Melting point (°C)	21.6
Boiling point (°C)	336.1

TEA is added in some admixture formulations to decrease the retarding effect on cement hydration (e.g. water reducers), and rarely, if ever, as a sole ingredient. Ramachandran (1976) conducted an extensive investigation of the chemistry of its action on OPC hydration. Following additions of 0 to 1.0% (w/w_{cement}) TEA, studies were made of the hydration characteristics of the following systems (water/cement ratio 0.5 and 1.0): i) C_3A , ii) C_3A + gypsum, iii) C_3S , vi) C_2S , and v) Portland cement. They found that TEA in amounts greater than 0.1% has a pronounced influence on the hydration of the varying phases: it accelerated the hydration of the C_3A and C_3A +gypsum systems and extended the induction period of the hydration of the C_3S , the effect being more pronounced the higher the TEA dose rate. Ramachandran also

investigated the initial and final setting characteristics of portland cement mortars treated with 0 to 0.5% TEA (see Table A1.17), and the compressive strength of cement mortars (triethanolamine introduced at 0-1.0%)(see Figure A1.5). For the reduction in strength associated with large amounts of TEA, they proposed the following explanations: i) rapid early hydration may create a dense zone of hydration product around the grains, which retards subsequent hydration; ii) formation of hydration product with higher density may promote a more porous pore structure; iii) cement that has set in a few minutes has obviously not been mixed thoroughly, and consequently will be a non-uniform distribution of hydration products within the structure that will prevent the development of full strength; iv) rapid formation of ettringite may alter the initial matrix and disturb subsequent bonding characteristics; v) rapid setting may promote initial cracks, also heat development and cooling may also initiate shrinkage cracks.

Finally, it is worth noting that no literature could be found that relates to the effects of TEA on molecular and ion transport in concrete.

Table A1.17 Initial and final setting characteristics of cement mortars with added TEA.

TEA (%)	Initial setting time	Final setting time
0	4.3 hours	8.3 hours
0.01	4.7 hours	8.1 hours
0.025	4.9 hours	8.1 hours
0.05	4.8 hours	8.4 hours
0.1	2 min	24 hours
0.5	6 min	---

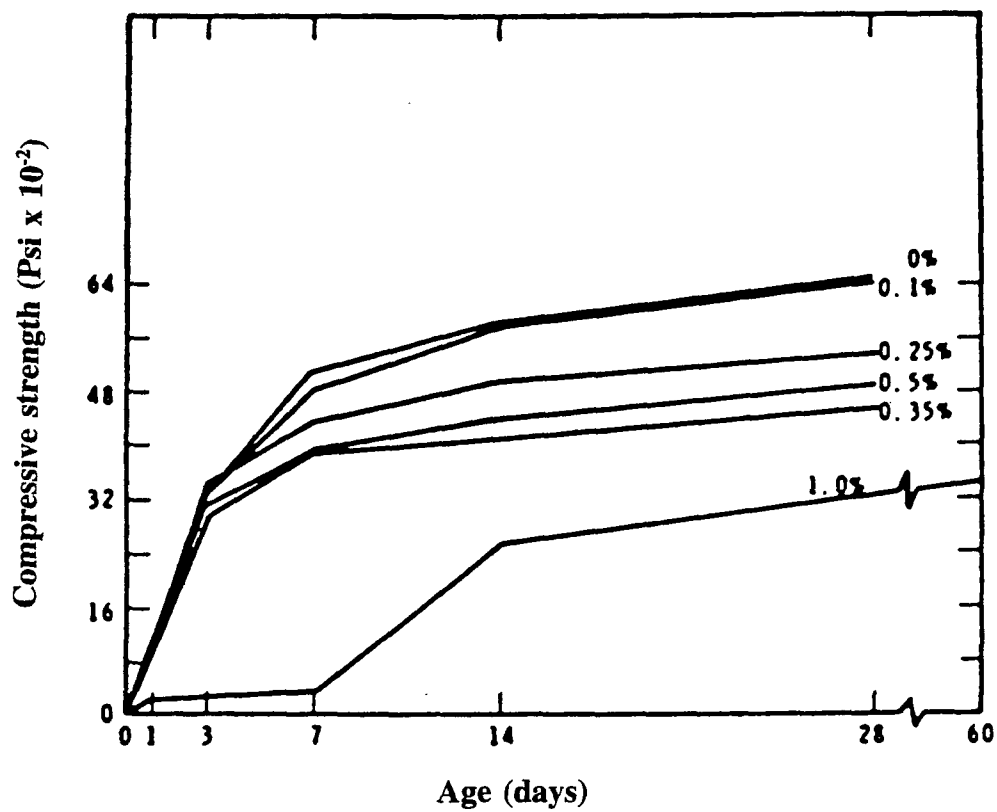


Figure A1.5 Effect of TEA dosage rate on compressive strength of modified mortar.

Appendix 2 Details of Concrete Mixes

A2.1 Phase 1 mixes

A2.1.1 Control mix

The control concrete was designed to have a free water/cement ratio of 0.45 and a cement content of 400kg/m³. Mix design was basically carried out according to the procedure outlined in a Building Research Establishment report on the design of normal concrete mixes (1988). The mix had a 35:65 ratio of fine to coarse aggregate; the theoretical batch proportions are summarized in Table A1.2.

Table A2.1 Control mix batch proportions

	Amount (kg/m ³)
Cement	400
Water (Total)	216
Coarse aggregate^a	1109
Fine aggregate^b	603
Total (theoretical density)	2329

a moisture content = 0.1%

b moisture content = 0.3%

In the fresh state the control concrete appeared to have excellent cohesion and sufficient workability (55mm slump)

A2.1.2 Modified mixes

The modified mixes were fabricated using the materials listed in Appendix 1, and as outlined in Chapter 5. Details of theoretical batch proportions are given in Table A2.2.

The results of slump testing are reported in Table A2.3. As is widely recognised (Neville 1981), slump was found to bear no unique relationship to workability; therefore, comments regarding to the observed ease of compaction relative to the control mix are also included. Moreover, note is made of whether segregation was observed and of excessive bleeding occurring upon compaction.

Table A2.2 Theoretical batch proportions of modified mixes (Phase 1)

Mix Ref.	Cement (kg/m ³)	Coarse Aggr. (kg/m ³)	Fine Aggr. (kg/m ³)	Water (Total) (kg/m ³)	Admixture (kg/m ³)	Secondary material (kg/m ³)
GGBS40	240	1109	603	216	160	---
GGBS70	120	1109	603	216	280	---
PFA30	280	1109	603	216	120	---
SF5	380	1109	603	196	40	---
SF10	360	1109	603	176	80	---
KIES5	400	1109	603	216	20	---
KIES10	400	1109	603	216	40	---
BEN2	400	1109	603	216	8	---
BEN5	400	1109	603	216	20	---
BEN10	400	1109	603	216	40	(1)a
WHIT5	400	1109	603	216	20	---
WHIT10	400	1109	603	216	40	---
TALC5	400	1109	603	216	20	---
TALC10	400	1109	603	216	40	---
PUM2	400	1109	603	216	8	---
PUM5	400	1109	603	216	20	---
LIME5	400	1109	603	216	20	---
LIME5	400	1109	603	216	60	---
HL30	400	1109	603	216	120	---
MSAND5	400	1109	603	216	20	---
MSAND10	400	1109	603	216	40	---
IRO0.125	400	1109	603	216	0.5	---
IRO0.25	400	1109	603	216	1	---
IRO2	400	1109	603	216	8	---
SODST0.2	400	1109	603	216	0.8	---
CALST1	400	1109	603	216	4	---
CALST3	400	1109	603	216	12	---
MAGST0.5	400	1109	603	216	2	---
MAGST1	400	1109	603	216	4	---
MAGST3	400	1109	603	216	12	---
ALST0.25	400	1109	603	216	1	---
ALST0.5	400	1109	603	216	2	---
ALST1	400	1109	603	216	4	---
SODO0.2	400	1109	603	216	0.8	---
SODO0.4	400	1109	603	216	1.6	---
BUTST2	400	1109	603	216	8	---
BUTST3	400	1109	603	216	12	---
OLEICA1	400	1109	603	216	4	---
OLEICA2	400	1109	603	216	8	---
CAPA0.5	400	1109	603	216	2	---
CAPA2	400	1109	603	216	8	---

table A2.2 continued

Mix Ref.	Cement (kg/m ³)	Coarse Aggr. (kg/m ³)	Fine Aggr. (kg/m ³)	Water (Total) (kg/m ³)	Admixture (kg/m ³)	Secondary material (kg/m ³)
SOYO1	400	1109	603	216	4	---
SOYO5	400	1109	603	216	20	---
SOYOE0.5	400	1109	603	216	2	(2)a
SOYOE1	400	1109	603	216	4	(2)a
SOYOE3	400	1109	603	216	12	(2)b
SOYOE10	400	1109	603	216	40	(2)c
CORNO1	400	1109	603	216	4	---
CORNO5	400	1109	603	216	20	---
LINSO0.5	400	1109	603	216	2	---
LINSO1	400	1109	603	216	4	---
LINSO2	400	1109	603	216	8	---
MINO0.5	400	1109	603	216	2	(3)a
MINO1	400	1109	603	216	4	(3)a
TAR10	400	1109	603	213	8	---
TAR20	400	1109	603	210	16	---
TAR50	400	1109	603	200	40	---
ASPH15	400	1109	603	207	15	---
ASPH30	400	1109	603	198	30	---
EVA5	400	1109	603	200	36	(4)a
SBR5	400	1109	603	192	43	---
ACR5	400	1109	603	196	40	---
ACR10	400	1109	603	176	80	---
AMINO13	400	1109	603	216	12	---
AMINO23	400	1109	603	216	12	---
CAL30	400	1109	603	186	30	---
CONP1	400	1109	603	216	4	---
CONP3	400	1109	603	216	12	---
SIK9	400	1109	603	216	9	---
SIK18	400	1109	603	216	18	---
SET6	400	1109	603	216	6	---
SET15	400	1109	603	216	15	---

table A2.2 continued

Mix Ref.	Cement (kg/m ³)	Coarse Aggr. (kg/m ³)	Fine Aggr. (kg/m ³)	Water (Total) (kg/m ³)	Admixture (kg/m ³)	Secondary material (kg/m ³)
IRON2	400	1109	603	216	8	---
IRON10	400	1109	603	216	40	---
SODSIL1	400	1109	603	216	4	---
SODSIL5	400	1109	603	216	20	(5)a
SODSIL10S	400	1109	603	216	40	(5)b
SODSIL10SZ	400	1109	603	216	40	(6)a
POTSIL1	400	1109	603	216	4	---
POTSIL3	400	1109	603	216	12	---
CEL1	400	1109	603	216	4	---
CEL5	400	1109	603	216	20	---
AL0.1	400	1109	603	216	0.4	---
AL0.2	400	1109	603	216	0.8	---
ALR0.05	400	1109	603	216	0.2	---
ALR0.2	400	1109	603	216	0.8	---
MAGC1	400	1109	603	216	4	---
MAGC2	400	1109	603	216	8	---
FORM1	400	1109	603	216	(1)	---
FORM2	400	1109	603	216	(2)	---
FORM3	400	1109	603	216	(3)	---
TEA0.025	400	1109	603	216	0.1	---
TEA0.1	400	1109	603	216	0.4	---
TEA0.25	400	1109	603	216	1	---
TEA0.5	400	1109	603	216	2	---

Admixture

- (1): iron(II) sulphate: 4; calcium carbonate: 8.
 (2): iron(II) sulphate: 2; calcium carbonate: 8.
 (3): iron(II) sulphate: 8; calcium carbonate: 12.

Secondary materials

- (1): superplasticizer (SP-450)

a: 8

- (2): emulsification promoting agent (kiesulguhr)

a: 1

b: 2

c: 4

(3): emulsification promoting agent (sodium oleate)

a: 0.05

(4): air-detraining agent (silicone)

a: 0.13

(5): sugar

a: 0.2

b: 0.6

(6): zinc sulphate

a: 8

Table A2.3 Results of slump testing and general comments

Mix	Slump	Comments	Mix	Slump	Comments	Mix	Slump	Comments
GGBS40	45		SODO L 0.2	115	(3)	AMINO13	200	(3)
GGBS70	70	(2)	SODOL0.4	110	(3)	AMINO23	75	(2)
PFA30	65	(2)	BUTST2	70	(2)			
SF5	30		BUTST3	55	(2)			
SF10	20	(1)				CAL30	75	(2)
			OLEICA1	125	(3)	CONP1	65	
			OLEICA2	130	(3)	CONP3	45	
KIES5	35		CAPA0.5	160	(3)	SIK9	80	(2)
KIES10	0	(1)	CAPA2	75	(2)	SIK18	120	(3)
BEN2	25					SET6	45	
BEN5	25		SOYO1	95	(3)	SET15	85	(2)
BEN10	0	(1)(6)	SOYO5	90	(3)			
WHIT5	38		SOYOE0.5	50	(2)			
WHIT10	58		SOYOE1	60	(2)	IRON2	47	
TALC5	40		SOYOE3	60	(2)	IRON10	47	
TALC10	35		SOYOE10	60	(2)	SODSIL1	30	
PUM2	50		CORNO1	125	(3)	SODSIL5	20	
PUM5	55		CORNO5	80	(3)	SODSIL10S	20	(6)
LIME5	65		LINSO0.5	80	(3)	SODSIL10SZ	20	(6)
LIME15	25		LINSO1	95	(3)	POTSIL1	30	
LIME30	0		LINSO2	95	(3)	POTSIL3	0	(1)
MSAND5	20		MINO0.5	75	(2)	CEL1	50	
MSAND10	30		MINO1	65	(2)	CEL5	0	
IRO0.125	50					AL0.1	40	
IRO0.25	40		TAR10	45		AL0.2	47	
IRO2	60		TAR20	63	(2)	ALR0.05	65	
			TAR50	65	(2)	ALR0.2	75	
			ASPH15	65	(2)	MAGC1	50	
			ASPH30	130	(3)	MAGC2	30	
SODST0.2	20					FORM1	80	
CALST1	45		EVA5	>255	(4)(5)	FORM2	70	
CALST3	50		SBR5	>255	(4)(5)	FORM3	60	
MAGST0.5	40		ACR5	60	(1)(5)	TEA0.025	40	
MAGST1	50	(2)	ACR10	>255	(4)(5)	TEA0.1	65	(2)
MAGST3	57	(2)				TEA0.25	95	(2)
ALST0.25	70	(3)				TEA0.5	95	(2)
ALST0.5	90	(3)						
ALST1	115	(3)						

Comments

- (1): very stiff and difficult to compact.
(2): easier to compact than control.
(3): much easier to compact than control.
(4): segregation observed.
(5): excessive bleeding upon compaction.
(6): sticky mix.

A2.2 Phase 2 mixes

A2.2.1 Control mixes

The control concrete (mix C1 (C(0.4))) was designed to have a free water/cement ratio of 0.40 and a cement content of 400kg/m³. Mix design was basically carried out according to the procedure outlined in a Building Research Establishment report on the design of normal concrete mixes (1988). The mix had a 40:60 ratio of fine to coarse aggregate. The corrected mix proportions, derived from analysis of batch proportions and the fresh density, are reported in Table A2.4.

Table A2.4 Mix details (control "C1")

	Amount (Kg/m³)
Cement	397
Water (Free)	159
Coarse aggregate (SSD)	1079
Fine aggregate (SSD)	720
fresh density	2355

The volume of paste in 1 m³ of mix C1 was calculated from the information in Table A2.4. This was used as the paste content for the other control mixes (mixes: C2 (C(0.35)) & C3 (C(0.3)+)). A simple calculation, assuming similar air contents pertaining to all mixes, revealed the cement contents (kg/m³) for C2 (0.35 water/cement ratio) and C3 (0.3 water/cement ratio) to be of the order of 426 and 461, respectively.

The corrected mix proportions, derived from analysis of batch proportions and the fresh density, for mixes C2 and C3 are reported in Tables A2.5 and A2.6, respectively.

Table A2.5 Mix details (control "C2")

	Amount (Kg/m³)
Cement	427
Water (Free)	149
Coarse aggregate (SSD)	1078
Fine aggregate (SSD)	719
fresh density	2373

Table A2.6 Mix details (control "C3")

	Amount (Kg/m³)
Cement	456
Water (Free)	137
Coarse aggregate (SSD)	1065
Fine aggregate (SSD)	711
Superplasticizer[@] (Sp-450)	4.11
fresh density	2373

@ A trial was made to produce this mix without the use of a superplasticizer; however, the resulting mix was very stiff and adequate compaction could not be assured.

A2.2.2 Modified mixes

Modified mixes were fabricated using the materials listed in Appendix 1, and as outlined in Chapter 6.

The corrected mix proportions, derived from analysis of batch proportions and the fresh density, are given in Table A2.7.

Presented in Table A2.8 are the results of slump testing; also included are general comments about the workability of mixes.

Table A2.7 Details of modified mixes (Phase 2)

Mix Ref.	Cement (kg/m ³)	Coarse Aggr. (kg/m ³)	Fine Aggr. (kg/m ³)	Water (Free) (kg/m ³)	Admix- ture (kg/m ³)	Secondary material (kg/m ³)	Fresh Density (kg/m ³)
GGBS70(0.4)	139	1079	720	159	258	---	2355
PFA30(0.4)	275	1068	712	157	118	---	2330
SF10(0.4)+	358	1081	721	119	80	(1)a	2355
KIES3(0.4)	397	1078	719	159	11.91	---	2364
BEN10(0.4)+	384	1043	696	154	38.4	(1)b	2318
WHIT5(0.4)	395	1073	715	158	19.7	---	2360
IRO2(0.4)	397	1078	719	159	7.9	---	2360
MAGST2(0.35)+	421	1064	709	147	8.42	(2)a	2350
ALST0.5(0.35)+	426	1077	718	149	2.13	(2)a	2373
BUTST3(0.4)	387	1053	702	155	11.62	---	2309
CAPA0.25(0.35)+	425	1074	716	158	1.06	(2)a	2375
SOYO1(0.35)+	425	1074	716	149	4.25	(3)a	2372
LINSO1(0.35)+	421	1064	709	157	4.21	(2)b	2355
TAR25(0.35)+	421	1065	710	138	19.74	(2)c	2355
ASPH20(0.35)	415	1050	700	134	19.46	---	2318
EVA10(0.3)+	437	1022	682	96	79.50	(2)d	2318
SBR5(0.35)+	411	1064	709	120	43.86	(4)c	2349
SBR10(0.3)+	432	1038	692	80	91.9	(2)e	2336
ACR10(0.3)+	445	1041	694	89	88.79	(4)c	2360
AMINO22(0.35)	422	1066	711	148	8.44	---	2355
CAL30(0.35)+	426	1076	717	119	29.92	(5)a	2372
CONP3(0.35)	422	1067	711	148	12.66	---	2360
SIK9(0.4)	395	1073	715	158	8.95	---	2350
SET6(0.4)	392	1066	711	157	5.93	---	2333
IRON10(0.4)	396	1075	717	158	39.6	---	2385
CEL2(0.4)	393	1067	712	157	7.85	---	2336
FORM2(0.4)	396	1077	718	159	(1)	---	2360
TEA0.025(0.4)	394	1071	714	158	0.1	---	2336
TEA0.1(0.4)	397	1079	719	159	0.4	---	2355
LPV325(0.4)	324	1162	775	130	---	---	2390
LPV245(0.4)+	245	1229	820	99	---	(1)c	2400

Admixture

(2): iron sulphate: 1.98; calcium carbonate: 1.98.

Secondary materials

(1): superlasticizer (SP-450)

a: 3.58

b: 3.97

c: 5.89

(2): air detraining agent (tri-*n*-butyl phosphate)

a: 0.21

b: 0.28

c: 0.55

d: 0.80

e: 0.65

(3): emulsification promoting agent (kieselguhr)

a: 2.12

(4): air-detraining agent (silicone)

a: 1.59

b: 0.40

c: 0.63

d: 1.31

(5): superplasticizer (Superplastet)

a: 4.26

Table A2.8 Results of slump testing and general comments

Mix ref.	Slump (mm)	Comments	Mix ref.	Slump (mm)	Comments
C(0.4)	NS	(3)	ASPH20(0.35)	NS	(3)
C(0.35)	NS	(3)	EVA10(0.3)+	NS	(1)
C(0.3)	NS	(2)	SBR5(0.35)+	35	(3)
			SBR10(0.3)+	50	(3)
			ACR10(0.3)+	50	(3)
GGBS70(0.4)	35	(3)	AMINO22(0.35)	NS	(2)
PFA30(0.4)	75	(3)	CAL30(0.35)+	NS	(3)
SF10(0.4)+	45	(3)	CONP3(0.35)	NS	(3)
KIES3(0.4)	NS	(3)	SIK9(0.4)	NS	(3)
BEN10(0.4)+	NS	(2),(5)	SET6(0.4)	NS	(2)
WHIT5(0.4)	NS	(3)	IRON10(0.4)	NS	(3)
IRO2(0.4)	NS	(3)	CEL2(0.4)	NS	(3)
MAGST2(0.35)+	NS	(3)	FORM2(0.4)	NS	(3)
ALST0.5(0.35)+	NS	(3)	TEA0.025(0.4)	35	(3)
BUTST3(0.4)	45	(3)	TEA0.1(0.4)	90	(3)
CAPA0.25(0.35)+	NS	(3)	LPV325(0.4)	NS	(3)
SOYO1(0.35)+	NS	(3)	LPV245(0.4)+	NS	(1),(4)
LINSO1(0.35)+	NS	(3)			
TAR25(0.35)+	NS	(3)			

Slump

NS: no slump concrete; defined, according to (refer to relevant code), as having a slump not exceeding 25mm.

Comments

- (1): very stiff and very difficult to compact.
- (2): stiff and difficult to compact.
- (3): no problems encountered in compaction.
- (4): excessive bleeding upon compaction.
- (5): sticky mix.

N.B. despite variations in the ease of compaction, all mixes were compacted satisfactorily.

A2.3 Phase 3 mixes

A2.3.1 Control mix

The control concrete was essentially that used in Phase 2, with the exception that a superplasticiser was used to improve workability. Details of the mix theoretical batch proportions are given in Table A2.9.

Table A2.9 Control mix batch proportions

	Amount (Kg/m ³)
Cement	427
Water (Total)	189
Coarse aggregate^a	1052
Fine aggregate^b	706
SP-450	4.26
Total (theoretical density)	2378

a moisture content = 0.1%.

b moisture content = 0.3%.

A2.3.2 Modified mixes

The modified mixes were fabricated from the materials listed in Appendix 1, and as outlined in Chapter 7. Details of theoretical batch proportions are given in Table A2.10.

Presented in Table A2.11 are the results of slump testing; also included are general comments about the workability of mixes.

Table A2.10 Details of modified mix theoretical batch proportions (Phase 3)

Materials	Amount (kg/m ³)								
	Mix ref.								
	R1	R2	R3	R4	R5	R6	R7	R8	R9
Cement	405	383	383	298	320	149	149	149	149
Water (Total)	126	147	147	189	168	189	189	189	189
Coarse Aggregate	1052	1052	1052	1052	1052	1052	1052	1052	1052
Fine aggregate	706	706	706	706	706	706	706	706	706
SF	42.6	85.2	85.2	---	42.6	---	---	---	---
PFA	---	---	---	128	85.2	---	---	---	---
GGBS	---	---	---	---	---	---	277	149	149
FGGBS	---	---	---	---	---	277	---	128	128
Acrylic	85.2	---	---	---	---	---	---	---	---
Soyabean oil	---	---	4.26	4.26	4.26	4.26	---	---	---
Butyl stearate	---	8.52	4.26	---	---	---	8.52	8.52	---
SP-450	---	6.39	6.39	4.26	4.26	4.26	4.26	4.26	4.2

Table A2.11 Results of slump testing and general comments.

Mix ref.	Slump (mm)	Comments
CN	30	(1)
R1	100	(2)
R2	55	(2)
R3	45	(2)
R4	80	(2)
R5	45	(1)
R6	70	(2)
R7	120	(3)
R8	120	(3)
R9	150	(3)

(1): mix easily compacted.

(2): mix fairly easy to compact.

(3): flowing concrete.

Appendix 3 Calculations

A3.1 Calculation of resistivity

The resistivity of the concrete, at the temperature of measurement, is calculated using the equation:

$$RS_t = \frac{A}{L} (R-C) * 10^{-3} \quad \text{(A3.1)}$$

in which,

- RS_t = resistivity at temperature $t^\circ\text{C}$ (Ωm);
- t = temperature at which test was undertaken ($^\circ\text{C}$);
- R = measured resistance (Ω);
- A = cross-sectional area of specimen (mm^2);
- L = specimen length (mm); and
- C = correction for resistance of NaOH solution (Ω).

This value of resistivity is corrected to the equivalent value at 20°C (RS (Ωm)) by assuming a temperature coefficient of resistivity for concrete of $0.025/^\circ\text{C}$ (Buenfeld 1986), as follows:

$$RS = RS_t (1 + 0.025 (t - 20)) \quad \text{(A3.2)}$$

A3.2 Calculation of intrinsic (oxygen-based) permeability coefficient

Corrections for gas slippage, based on the method proposed by Dhir and his co-workers require, to be sufficiently accurate, that each specimen be tested at no less than 8 distinct pressure levels (see 3.5.3 and Figure A3.1). This would have been very time consuming to carry out on all specimens available for testing. Moreover, the effort was considered unjustifiable as it was felt that such corrections were unnecessary, because the object of testing was to establish relative rather than absolute performance. Instead, the approach outlined below was followed.

The outflow rate (Q) is plotted against $P_1^2 - P_2^2 / P_2$ (for the three values of P_1 , and $k_{g(D)}$) can be calculated from the slope of the resulting straight line (all parameters are as defined earlier (3.6.3)):

$$k_{g(D)} = \frac{2\mu l \text{ slope}}{A} \quad (\text{A3.3})$$

Substituting in the value of μ at 20°C ($2.02 \cdot 10^{-5}$ Ns/m²) and converting to more convenient units:

$$k_{g(D)} = 6.733 \cdot 10^{-15} \frac{l}{A} \text{ slope} \quad (\text{A3.4})$$

in which:

$k_{g(D)}$ is in m^2

L is in mm ;

A in mm^2 ;

P_1 and P_2 in bars; and

Q in Cm^3/min .

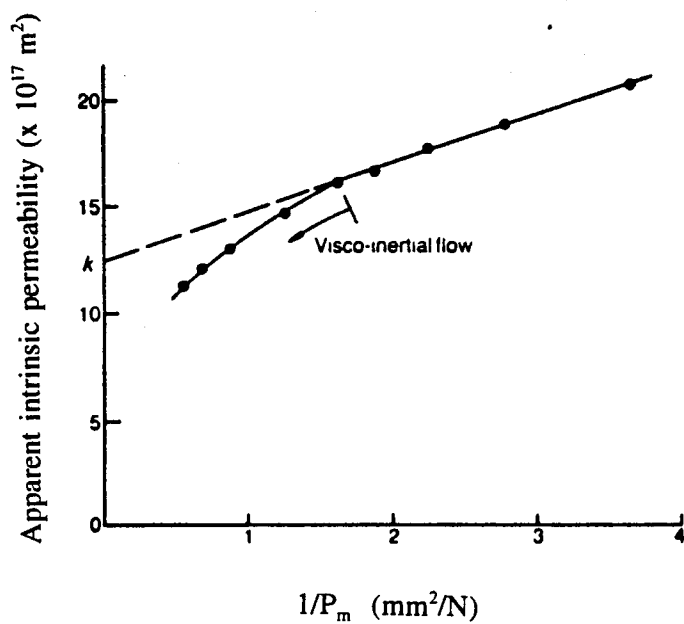


Figure A3.1 Correcting oxygen permeability coefficient for gas slippage (Dhir et al. 1989).

Appendix 4 Ordinary Portland cement hydration, development of microstructure, and effect of organics

A4.1 OPC hydration and development of microstructure

This section presents a review of OPC hydration and the development of microstructure, the purpose of which is to allow easy comprehension of the discussions in A4.2 and other parts of this thesis. The review is based largely on work by Scrivener (1984, 1989), and other reviews (Lea 1970, Neville 1981, Taylor 1990, Mehta & Monterio 1993).

The name Portland Cement is used to describe a material produced by intimately mixing together CaO-, silica-, alumina-, and iron oxide-bearing materials, burning them at a clinkering temperature, and grinding the resulting clinker. Ordinary Portland Cement is composed of four major phases (see Table A4.1). The cement also contains other minor compounds, small amounts of sulphates (gypsum ($\text{CaSO}_4 \cdot 2\text{H}_2\text{O}$) and alkali sulphates) and unreacted lime.

Table A4.1 Phase composition of Ordinary Portland Cement

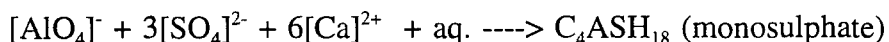
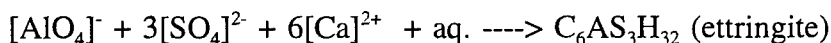
Phase	Composition (%)	Formula #	Nomenclature #
Alite	50-70	Ca_3SiO_5	C_3S
Belite	15-30	Ca_2SiO_5	C_2S
Aluminate	5-10	$\text{Ca}_3\text{Al}_2\text{O}_6$	C_3A
Ferrite	5-15	$\text{Ca}_2\text{AlFeO}_5$	C_4AF

the abbreviation are used merely for convenience since the phases are not normally present in pure form; cement chemists nomenclature: **CaO**: C; **SiO₂**: S; **Al₂O₃**: A; **Fe₂O₃**: F; **MgO**: M; **SO₃**: S; **H₂O**: H.

When portland cement comes into contact with water, its components react and different hydration products are formed. The reaction rate is dependent upon the phase composition of the cement, its fineness, the presence of admixtures (in particular

Since OPC is composed of a heterogeneous mixture of several compounds, the hydration process consists of simultaneously occurring reactions of the anhydrous compounds with water. All these compounds, however, do not hydrate at the same rate, as will be seen next.

The aluminate reacts rapidly with water and forms metastable hydrates which convert rapidly to hydrogarnet (C_3AH_6). This almost instantaneous reaction is accompanied by the liberation of a large amount of heat and rapid setting and, unless slowed down by some means, the Portland cement will be useless for most construction purposes. This is generally accomplished by the addition of gypsum. Therefore, for practical purposes, it is not the hydration of the aluminate alone, but its hydration in the presence of gypsum which is important. The relevant chemical reactions of C_3A aluminate phase may be expressed as follows:

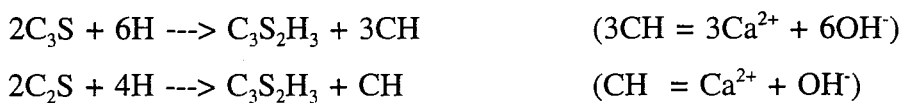


Ettringite is usually the first hydrate to crystallize because of the high sulphate/aluminate ratio in the solution phase during the first hour of hydration. In normally retarded OPC, the precipitation of ettringite contributes to stiffening (loss of consistency), setting (solidification of the paste), and early strength development. Later, after the depletion of the sulphate in the solution and when the aluminate concentration increases again, due to increased hydration of the aluminate and perhaps the ferrite phase, the ettringite becomes unstable and is gradually converted into monosulphate.

It should be stressed that the hydration reactions of the aluminate phase are more complicated than suggested above. Indeed, the aluminate and ferrite phases yield a multitude of hydration products (AFt (Al_2O_3 - Fe_2O_3 -tri) and AFm (Al_2O_3 - Fe_2O_3 -mono)) which are, despite having variable chemical compositions, structurally similar to ettringite and the monosulphate hydrate, respectively.

Several theories have been proposed to explain the mechanism of retardation of C_3A by gypsum. According to one theory, since gypsum and the alkali sulphates go into solution quickly, the solubility of C_3A is depressed by the presence hydroxyl, alkali, and sulphate ions. Another postulates that the retardation is due to ettringite forming a partly protective coating on the aluminate phase thus hindering further dissolution.

The hydration of the alite and belite phases produces a family of calcium silicate hydrates which are structurally similar but vary in morphology, calcium/silica ratio, and the content of chemically combined water. These simply referred to as C-S-H. Making the approximate assumption that $C_3S_2H_3$ is the final product of hydration of both C_3S and C_2S , the reactions of hydration can be written (though merely as a guide) as follows:



The main phases that contribute to strength development are alite and belite. Alite reacts relatively quickly and is mainly responsible for strength development in the first four weeks. Belite, on the other hand, reacts more slowly, contributing to strength at later ages (mainly from four weeks onwards).

The hydration reaction of OPC is exothermic and a characteristic rate of heat curve can be identified. This exotherm lends itself to study by isothermal conduction calorimetry (Forrester 1970), and the curve produced typically takes the form illustrated in Figure A4.1. The curve suggests that hydration process may be divided into five stages of initial rapid reaction, an induction period (the so-called "dormant period", acceleration and deceleration periods, and finally the period of slow reaction. The process can be best understood with reference to Figure A4.2, which summarises the microstructural development of OPC during hydration of a typical polymineralic clinker grain. The first stage (initial peak (1), see Figure A4.1) is attributable to a combination of exothermic wetting and the early-stage reactions, with the cement give a gelatinous coating and

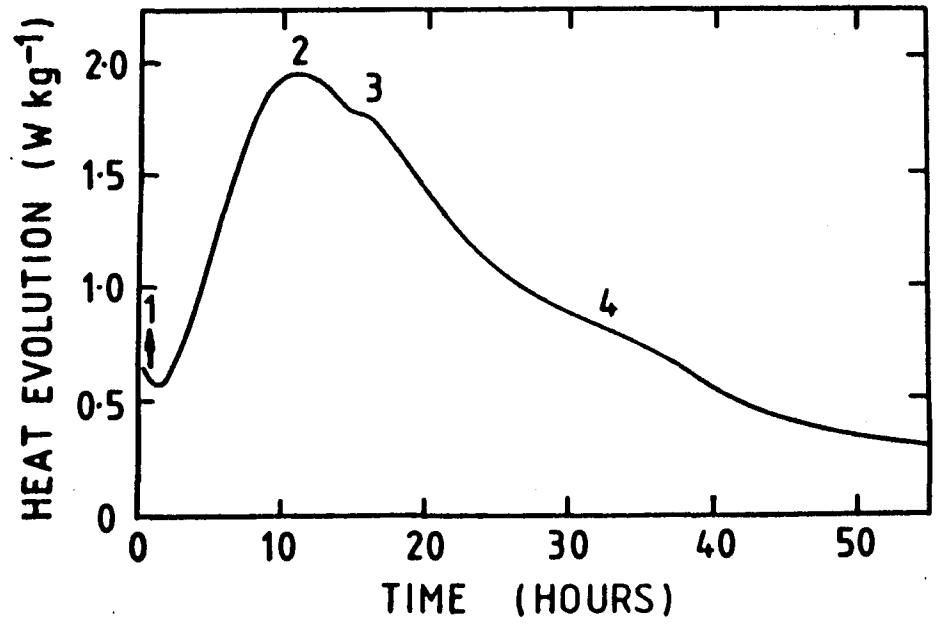


Figure A4.1 Rate of heat evolution at 20°C for a typical Portland cement (Taylor 1990).

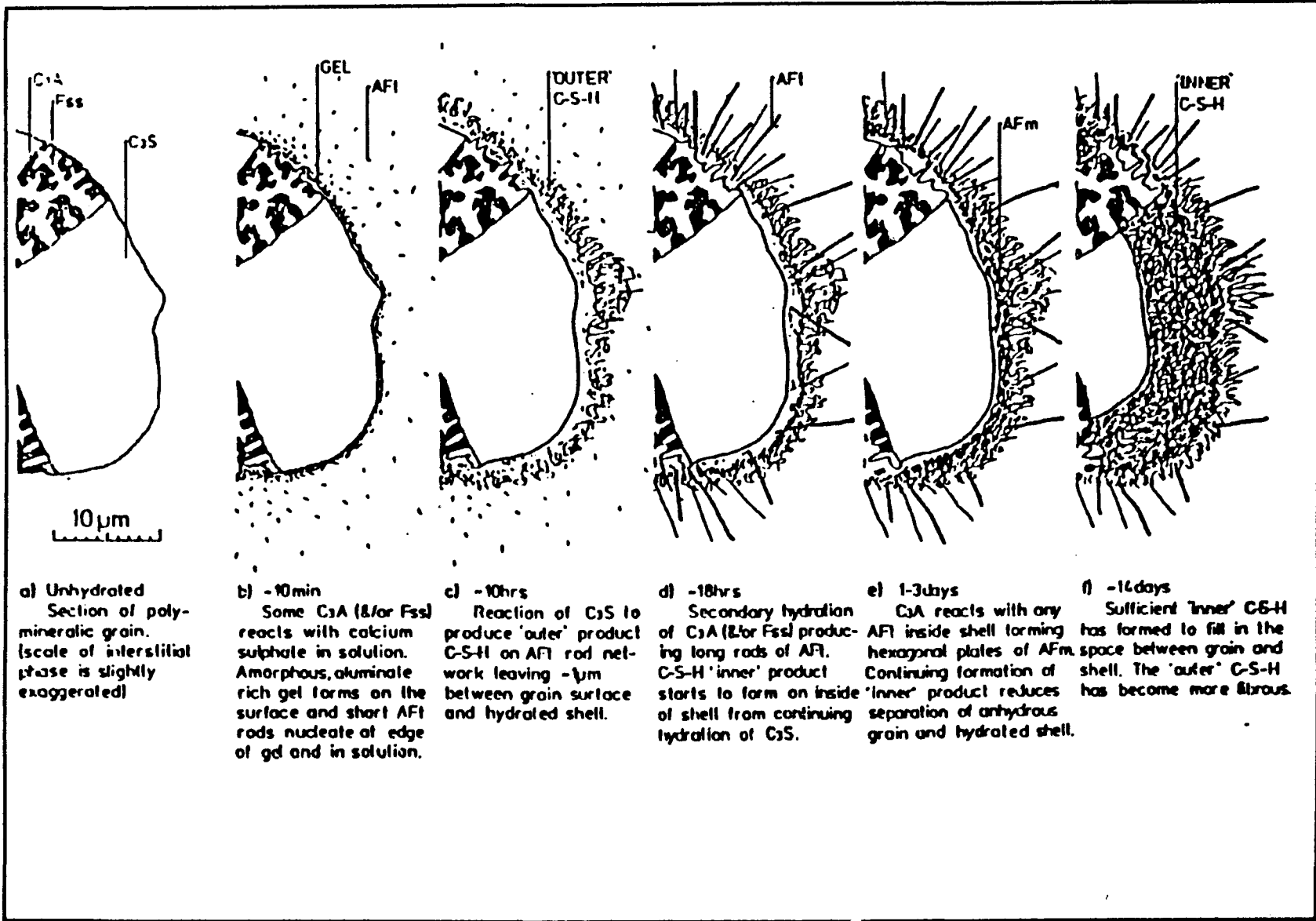


Figure A4.2 Microstructural development of Portland cement (Scrivener 1984).

rods of AFt phase (Figure A4.2b). Rehydration of hemihydrate to give gypsum may contribute. The induction period is associated with low reactivity. A number of mechanisms may be responsible for suppressing hydration. They involve a first stage product acting as a protective but temporary barrier, formation of a semi-permeable membrane, a rate controlling reaction involving C-S-H nucleation and intergrowth, or temporary poisoning of calcium hydroxide nuclei. The acceleration stage (Figure A4.2c) is associated with rapid reaction of the alite phase and is characterized by rapid growth of C-S-H and CH. During this stage the reaction proceeds by dissolution and precipitation. The CH forms massive crystals in the originally water-filled space, and nucleation sites still appear to be relatively few in number. The C-S-H forms a thickening layer (hydration shell) around the cement grains, engulfing the first stage AFt rods. The shells grow outwards and when peak (2) is reached they are some 0.5-1 μm thick; this corresponds approximately to the completion of setting. During the deceleratory period, a renewed growth of AFt crystals takes place (Figure 7.6d). Their formation is associated with a shoulder on the heat evolution curve (3). During the final part of the deceleratory period, there is a drop in sulphate concentration and a conversion of AFt to AFm (Figure A4.2e), which is detected as a small 4th peak. With the decreasing permeability of the shells, CSH begins to deposit also on their insides, and its surface advances inwards more quickly than that of the alite retreats. Grains smaller than about 5 micrometer appear to react completely before the end of day 1, and before much of the material has deposited inside the shells. With larger grains, the spaces between shell and core fill up, and at about 7 days they will have disappeared; at this stage the shells are typically about 8 μm thick and consist mainly of material that has been deposited on their inner surface (see Figure A4.2f). After the spaces between shells and cores have filled up, reaction is slow and, in contrast to that formed earlier, appears to occur by a topochemical mechanism. In old cement pastes three regions can be distinguished around the relics of the larger fully reacted grains, viz.: (i) an outer layer some 1 micrometer thick that has formed through solution in originally water-filled space, (ii) a middle layer some 8 μm thick that has been deposited, also through solution, on the inside of the shell and thus in space originally occupied by the cement grain, and (iii) a central core, that has formed topochemically.

The compositional features of the fluids in contact with hydrating OPC paste systems during the early stages of hydration, as well as from pore fluids extracted from cement pastes at advanced stages of hydration, have been addressed in various publications (Lawrence 1966, Bailey & Hampson 1982, Canham et al. 1987, Taylor 1987, Glasser et al. 1988, Andersson et al. 1989, Taylor 1990). Figure A4.3 shows typical results obtained during the early period of hydration (Lawrence 1966). Relatively high concentrations of Ca^{2+} , K^+ , Na^+ , SO_4^{2-} and OH^- are quickly reached, and the solution is characterized by supersaturation with respect to $\text{Ca}(\text{OH})_2$. Between 2 and 12 hours, in the sample given, the concentrations change relatively little, indicating an approximate balance between continued dissolution of the cement phases and the precipitation of products. At 12-16 hours, the concentrations of Ca^{2+} and SO_4^{2-} fall sharply, and the solution thereafter is essentially one of the alkali hydroxides. With pastes of normal Portland cements more than about 1 day old, the only ions present in concentrations above a few mmol/l are K^+ , Na^+ , and OH^- (note that the solubility of $\text{Ca}(\text{OH})_2$ is depressed by the presence of the alkali). Most studies show that the concentrations of these ions, hence the solution pH, increase with time (provided no leaching or ingress of ions is allowed), and approach a limit after 28 to 90 days (see Figure A4.4). Typical concentrations after 180 days for pastes of water/cement ratio of 0.5 are 0.08 mol/l for Na^+ and 0.24 mol/l for K^+ for a low alkali cement (0.16% Na_2O , 0.43% K_2O) and 0.16 mol/l for Na^+ and 0.55 mol/l for K^+ for a high alkali cement (0.24% Na_2O , 1.12% K_2O). The corresponding OH^- concentrations are 0.32 mol/l and 0.71 mol/l, respectively.

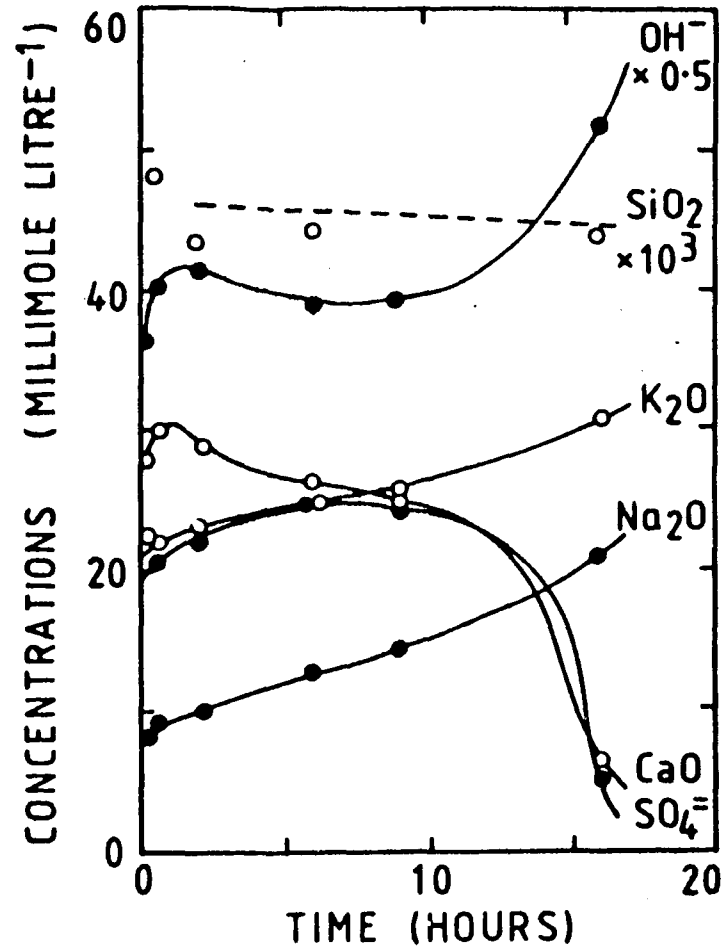


Figure A4.3 Concentrations in the pore solution of a Portland cement paste (0.5 water/cement ratio).

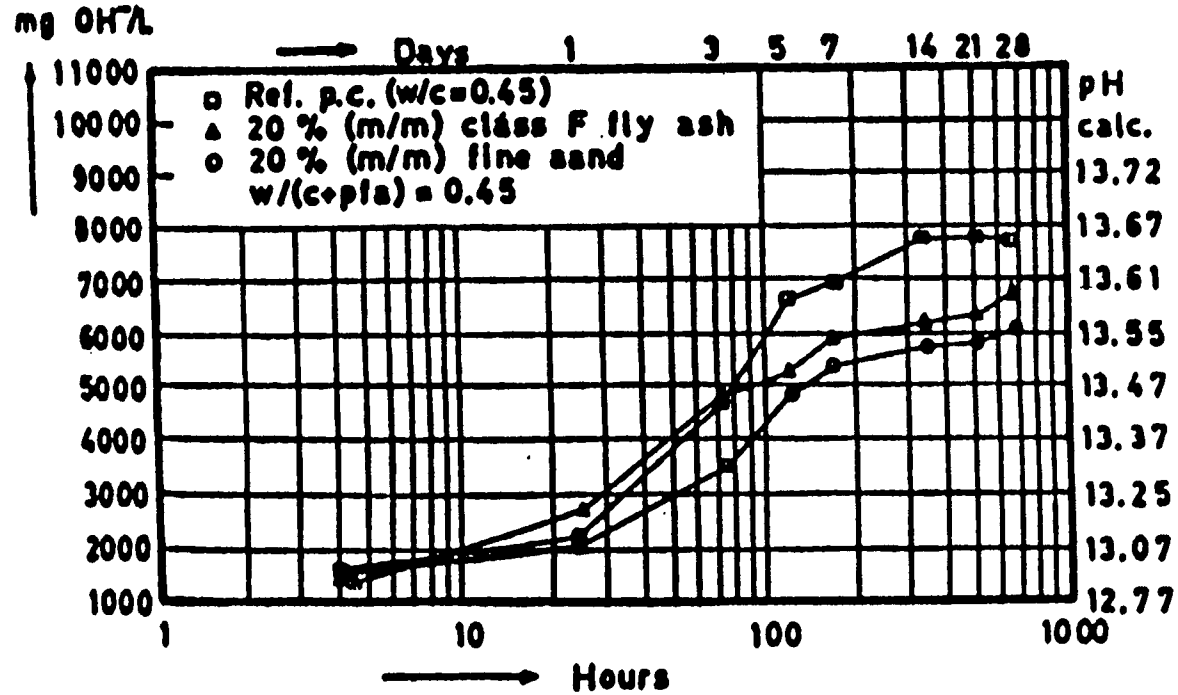


Figure A4.4 The development of the OH⁻ concentration in the pore solution of Portland cement paste and pfa-modified pastes (Fraay et al. 1989).

A4.2 Effect of organics on OPC hydration

The hydration of cement is relatively complex (A4.1) and becomes additionally so in the presence of admixtures. The effect of organic materials on OPC hydration has received much attention during the last three decades due to its relevance to the manufacture of various commercial admixtures (water-reducing, retarding and air entraining agents, polymer latices)(Lea 1970, Young 1972, Ramachandran 1976, Lorprayoon & Rossington 1981, Rixon & Mailvaganam 1986, Chandra & Flodin 1987, Semerad et al. 1987), and to cement-based stabilization of hazardous organic wastes (Weinburg et al. 1988, PCA 1991, Pollard et al. 1991). However, despite these efforts, there still remains much uncertainty as regards the mechanism(s) by which many of these materials affect cement hydration.

Clearly, as in the case of inorganic materials, organic materials that alter cement hydration do so by interfering with the various processes involved in cement hydration and the development of its microstructure (see A4.1).

A variety of conceptual models have been proposed to explain the interference mechanisms of organics on cement hydration. The effect of many organics on cement hydration is in effect a complex interplay of various phenomena, viz.: adsorption, complexation, precipitation, and nucleation control. The purpose of this section is to briefly examine these processes (the review is based entirely on the literature cited above).

Organic compounds can adsorb onto the surfaces of the anhydrous cement compounds, hindering dissolution by water, thus retarding their hydration. Adsorption may be simply physical, where, for example, a water-repelling material will simply coat the cement particles to minimize its contact with water. The possible mechanisms of chemisorption are illustrated in Figure A4.5. In Figure A4.5a, the carboxyl group (-COOH) of the molecule (e.g. lignosulphonate derivative, hydroxylated carboxylic acid) is adsorbed at the surface of Ca^{2+} ions, whilst the unionised OH groups forms a hydrogen bond with

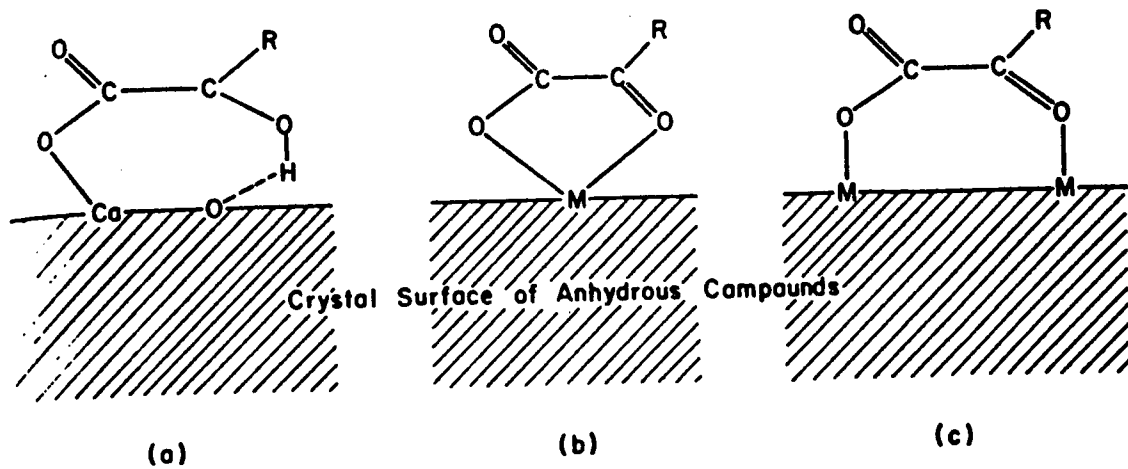


Figure A4.5 Possible adsorption mechanisms of organic admixtures onto cement surfaces (Young 1972)

oxygen ions on the surface. In an alkaline solution, however, some compounds which cause retardation will have no hydroxyl groups and thus hydrogen bonding need not be postulated in every case. Calcium, aluminum, iron, or silicon ions are all potentially capable of chelating with organic compounds. Thus, the most important mechanism of chemisorption is likely to be chelation to the surface (Figures A4.5b and c).

There is evidence that C_3S and C_2S adsorb organic molecules from aqueous solutions much less strongly than C_3A , and that the mechanism is that of physical adsorption. Indeed, the adsorption of retarders onto cement could be considered as being wholly due to adsorption onto C_3A . However, since the majority of retarding admixtures act primarily by retarding the hydration of C_3S , some amount of the retarder must remain associated with C_3S to provide retardation.

There are anomalies, however, that cannot be explained in terms of adsorption onto anhydrous cement. First, in the case of some retarders, it was found that surface adsorption is possible without retardation. Second, some organic materials were found to accelerate the initial hydration of the cement before retardation begins. Finally, adsorption of organics onto C_3A is much reduced in the presence of gypsum. Thus, there is no strong case for adsorption onto anhydrous surfaces being the sole mechanism of retardation.

The conditions in cement pastes are also thought favourable for complexing to occur between organics and the aluminate, ferrite and silicate ions, and this may be the reason why some organics accelerate the initial hydration of the cement before retardation begins. This is because complex formation, by preventing early precipitation of hydration products, promotes the dissolution of more of the cement compounds before hydration barriers are set up and admixtures removed from solution. Although complexing of the calcium ion can occur, these complexes have low stability and are unlikely to contribute appreciably to the supersaturation of calcium hydroxide during the acceleration phase, which is associated with C_3S hydration.

Insoluble products are often formed when organics are exposed to the strongly alkaline environment of a cement paste and these may precipitate onto the cement grains forming a barrier to water transport, thus retarding subsequent hydration. There are reported cases, however, where the organic was completely removed from the cement paste by harmless precipitation (e.g. oxalic acid). It is also worth noting that the removal of Ca^{2+} through formation of insoluble calcium salts contributes to the solution of calcium ions from the cement compounds (examples of organics which act as accelerators include formic acid).

The self retarding feature of C_3S hydration is often attributed to the inhibition of the nucleation of crystalline $\text{Ca}(\text{OH})_2$ by soluble silica which is present in small quantities. The silicate ions adsorb onto the $\text{Ca}(\text{OH})_2$ nuclei, and growth does not proceed until some level of supersaturation is reached during the induction period of hydration. Similar observations are noted in the presence of many organics which cause retardation, namely: i) the extension of the induction period, ii) the increase in the level of $\text{Ca}(\text{OH})_2$ supersaturation before crystallization begins, and iii) the higher rate of heat liberation in the acceleration period of cement hydration. It is perfectly conceivable, therefore, that the retardation of C_3S hydration and the length of the dormant period is determined primarily by the effects of the admixtures on the nucleation of calcium hydroxide. Finally, there is also the possibility that the extension of the dormant period is due to the organic molecules, or the products of their reaction in the highly alkaline solutions, adsorbing onto the CSH formed by C_3S , hindering nucleation, thus retarding further hydration of the C_3S .

Finally, it is worth noting that the action of organic admixtures in concrete is complicated by the fact that, in addition to the effects discussed above, they may act as flocculants, dispersants, wetting agents, etc. (see Table A4.2).

Table A4.2 Effects of selected chemicals on hydration process of OPC-PFA systems (PCA 1991)

Chemical or Material	Flocculant	Dispersant	Wetting Agent	Chelating Agent	Matrix Disruptor	Retarder	Accelerator	Destroys Reaction
Carboxylic acids		X				X		.
Carbonyls		X				X		.
Amides			X				Allows for better mixing	
Amines	X						X	.
Alcohols			X			X		.
Sulfonates		X				X		
Glucose/sugar				X		X		.
Chlorinated hydrocarbons					X	X		X
Oil								>25-30%§
Calcium chloride					>4%‡		<2%‡	>4%§
Iron†	X				X		X	
Tin					X	X		
Lead					X	X		.
Borates					X	X		.
Magnesium	X				X	X		
Gypsum (hydrate)						X		.
Gypsum (anhydrate)							X	.
Silica	X					X†		

* At high concentrations

† Ratio of Fe⁺² to Fe⁺³ important

‡ Only in certain forms

§ By weight